Stroke

CENTENNIAL COLLECTION 100

Stroke in Children: Key Advances in the Field and the Next 20 Years

Adam Kirton, MD; Lori C. Jordan, MD, PhD

In 2003, the IPSS (International Pediatric Stroke Study) group was founded, raising awareness of stroke in children among the medical community and launching a new era of collaboration and progress.[1] Enrollment in and expansion of this stroke registry for children continues today https://lab.research.sickkids.ca/ipss/about/. Over the last 20 years, significant improvements have occurred in nearly all aspects of pediatric stroke care. This article will highlight some seminal achievements and focus on where the field may be headed over the next 20 years. While there are too many accomplishments to discuss here, we have tried to highlight randomized controlled trials as well as major topical areas below.

SICKLE CELL DISEASE

Predating the IPSS, work focused on preventing stroke in children with sickle cell disease, an especially high-risk group; without stroke risk screening and preventative treatment, 1 in 10 children with sickle cell disease will have a stroke before 19 years of age.[2] A major advance occurred in 2016 when the TWiTCH trial (TCD With Transfusions Changing to Hydroxyurea) showed that children receiving monthly red cell transfusions for primary stroke prevention based on elevated transcranial doppler blood flow velocities were able to transition from transfusions to oral hydroxyurea if significant intracranial stenosis was not present.[3] However, after a stroke has occurred, the recommended stroke prevention therapy, regular blood transfusion, is frequently not accessible to children in low and middle-income countries[4] where >50% of the children with sickle cell disease live. The next 20 years will focus on less burdensome stroke care for children with sickle cell disease and care that is globally available. In low and middle-income countries, primary and secondary stroke prevention trials (SPRING [Stroke Prevention in Nigeria] and SPRINT [Secondary Stroke Prevention in Children With Sickle Cell Disease in Nigeria]) have been completed using oral hydroxyurea,[5,6] and additional early phase and expanded access trials are in process with newer oral agents, including pyruvate kinase activators[7,8] and a hemoglobin S polymerization inhibitor.[9] Potentially curative therapies such as stem cell transplantation and gene therapy are fascinating but reducing toxicities and costs will be important to allow wider accessibility.[10]

ARTERIOPATHY RANDOMIZED CONTROLLED TRIALS

Cerebral arteriopathy, a frequent cause of stroke in children, and its relation to infection have been an active area of research with 2 large observational studies completed (VIPS I and II).[11,12] Two multicenter clinical trials are in progress that aim to determine if high-dose methylprednisolone in children with focal cerebral arteriopathy can improve or stabilize disease and reduce arterial ischemic stroke recurrence (the PASTA trial [Pediatric Arteriopathy Steroid Aspirin] and the FOCAS trial [Focal Cerebral Arteriopathy Steroid]).[13,14] The genetics of more diverse arteriopathies are not well understood but rapid progress suggests these will be important targets in the coming decades.

Key Words: child ■ forecasting ■ research ■ stroke ■ therapeutics

The American Heart Association celebrates its 100th anniversary in 2024. This article is part of a series across the entire AHA Journal portfolio written by international thought leaders on the past, present, and future of cardiovascular and cerebrovascular research and care. To explore the full Centennial Collection, visit https://www.ahajournals.org/centennial.

The opinions expressed in this article are not necessarily those of the editors or of the American Heart Association.

Correspondence to: Lori C. Jordan, MD, PhD, 2200 Children's Way, DOT 11212, Nashville, TN 37232. Email lori.jordan@vumc.org

For Sources of Funding and Disclosures, see page 184.

Stroke is available at www.ahajournals.org/journal/str

Nonstandard Abbreviations and Acronyms

DINOSAUR	Darbepoetin for Ischemic Neonatal Stroke to Augment Regeneration
FOCAS	Focal Cerebral Arteriopathy Steroid
HEAL	High-Dose Erythropoietin for Asphyxia and Encephalopathy
I-ACQUIRE	Multi-site Randomized Controlled Trial of Intensive Infant Rehabilitation
IPSS	International Pediatric Stroke Study
PASTA	Paediatric Arteriopathy Steroid Aspirin
SPORT	Stimulation for Perinatal Stroke Optimizing Recovery Trajectories
SPRING	Stroke Prevention in Nigeria
SPRINT	Secondary Stroke Prevention in Children With Sickle Cell Disease in Nigeria
TIPS	Thrombolysis in Pediatric Stroke
TWiTCH	TCD With Transfusions Changing to Hydroxyurea

RECANALIZATION THERAPIES FOR ACUTE STROKE

With increased awareness of pediatric stroke and the development of more robust systems of care for children, emergent acute stroke therapies are increasingly possible. A recent case-control study found that outcomes were better in carefully selected children 2 to 18 years of age treated with mechanical thrombectomy for large vessel occlusion.[15] Thrombolysis remains an ongoing challenge in children with acute stroke; a prior pediatric safety and dose-finding trial of alteplase for stroke (TIPS [Thrombolysis in Pediatric Stroke]) closed due to low enrollment.[16] With increased pediatric stroke awareness, further studies seem feasible, but the adult stroke community's ongoing transition to the thrombolytic tenecteplase is complex for those who treat children given that pediatric pharmacokinetic data and dosing guidance are lacking.[17] Simple extrapolation of adult care to children with stroke is a pitfall. Future work should include a focus on defining clinical and radiographic biomarkers to refine selection criteria for acute recanalization strategies including those used in adults (eg, collateral status, salvageable penumbra) but also those unique to children (eg, mechanism of stroke, young age).

NEUROCRITICAL CARE

Advances in neonatal and pediatric neurocritical are expected to continue to improve outcomes. In neonatal stroke, trials are underway that suggest the safety and feasibility of both hormonal therapies (erythropoiesis-stimulating agents) such as the DINOSAUR trial (Darbepoetin for Ischemic Neonatal Stroke to Augment Regeneration)[18] and early stem cell therapies[19,20] though these will need to overcome challenges learned from related trials such as HEAL (High-Dose Erythropoietin for Asphyxia and Encephalopathy).[21] Advances in neuromonitoring coupled with carefully designed observational studies of seizures after neonatal and childhood stroke and trials in related conditions such as newborns with symptomatic seizures after brain injury[22] are quickly refining the management of stroke-induced seizures while the predictors and consequences of remote symptomatic epilepsy are increasingly understood.[23] Progress is anticipated in acute cerebral monitoring of high-risk populations such as children undergoing cardiac surgery or extracorporeal membrane oxygenation where the potential exists to reduce acquired brain injury and improve outcomes.

NEUROREHABILITATION AND NEUROMODULATION

Despite improvements in acute care and prevention, strokes will continue to occur in children, mandating amplification of ongoing progress in rehabilitation. Evidence-based guidelines have improved clarity regarding both valid and invalid therapies for neurological disabilities in children,[24] facilitating informed decision-making for clinicians and families. Efforts have facilitated the development of frameworks towards more rigorous clinical trials; however, trials to date, including a recent one in Scandinavia,[25] continue to confirm that response rates to rehabilitation therapies are highly heterogeneous with modest effect sizes, suggesting new approaches are required. Advances in understanding brain development following stroke are informing new approaches in the motor system,[26] including noninvasive neuromodulation strategies that have reached phase 3 efficacy trials (SPORT [Stimulation for Perinatal Stroke Optimizing Recovery Trajectories]).[27] The complexity of differences between individuals will see personalized rehabilitation approaches remain an important goal of future efforts. Attention to other modulators of brain development that might dictate recovery from early stroke is required, including many potentially modifiable factors such as sleep, education, environment, socioeconomic factors, and epileptic encephalopathy, all of which may be under-recognized.

FAMILY-CENTERED CARE, MENTAL HEALTH, AND INFORMATION SHARING

Improving the overall care and support of children and families affected by stroke must remain a priority. The mental health consequences of stroke in children are increasingly understood including posttraumatic stress disorder and other long-term morbidities for the entire

family.[28] Some emotional consequences seem amenable to simple interventions such as counseling and educational tools for the misplaced parental and caregiver guilt that often accompanies a diagnosis of neonatal stroke,[29] but increased awareness and training are required. How stroke in childhood affects a person's entire lifespan remains poorly understood but long-term adult outcome studies are underway.[30] Access to information (and misinformation) remains a challenge for both affected families and health care professionals. These and other elements of family-centered care will continue to expand via the efforts of global partnerships between diverse experts and those with lived experience.[31]

INTERNATIONAL, MULTIDISCIPLINARY COLLABORATIONS

As a relatively rare disease, future progress in childhood stroke will depend on furthering the international collaborations that have defined the field to date. Collaborations must engage parallel networks of related fields with a passion for helping children with cerebrovascular diseases, the diversity of which continues to expand including interventional neuroradiology, neurosurgery, neurogenetics, neurorehabilitation, neonatology, neurocritical care, hematology, infectious disease, and others. Recent examples include the International Pediatric Stroke Organization[32] which brings together multidisciplinary health professionals, scientists and patient advocates and the incorporation of pediatric-specific clinical trials for both infant rehabilitation (I-ACQUIRE)[33] and acute childhood stroke treatment into the powerful machinery of StrokeNet. Networks will also need to evolve and adapt to embrace emerging research concepts (eg, big data, open neuroscience, artificial intelligence) to amplify what has been amazing progress in the last few decades. Hope for improved outcomes for children with stroke has never been higher.

ARTICLE INFORMATION

Affiliations

Departments of Pediatrics and Clinical Neurosciences, Alberta Children's Hospital Research Institute, University of Calgary, Canada (A.K.). Department of Pediatrics, Division of Pediatric Neurology, Vanderbilt University Medical Center, Nashville, TN (L.C.J.).

Sources of Funding

None.

Disclosures

None.

REFERENCES

1. Golomb MR, Fullerton HJ, Nowak-Gottl U, Deveber G; International Pediatric Stroke Study Group. Male predominance in childhood ischemic stroke: findings from the international pediatric stroke study. *Stroke*. 2009;40:52–57. doi: 10.1161/STROKEAHA.108.521203
2. Ohene-Frempong K, Weiner SJ, Sleeper LA, Miller ST, Embury S, Moohr JW, Wethers DL, Pegelow CH, Gill FM. Cerebrovascular accidents in sickle cell disease: rates and risk factors. *Blood*. 1998;91:288–294.
3. Ware RE, Davis BR, Schultz WH, Brown RC, Aygun B, Sarnaik S, Odame I, Fuh B, George A, Owen W, et al. Hydroxycarbamide versus chronic transfusion for maintenance of transcranial doppler flow velocities in children with sickle cell anaemia-TCD With Transfusions Changing to Hydroxyurea (TWiTCH): a multicentre, open-label, phase 3, non-inferiority trial. *Lancet*. 2016;387:661–670. doi: 10.1016/S0140-6736(15)01041-7
4. Lagunju IA, Brown BJ, Sodeinde OO. Chronic blood transfusion for primary and secondary stroke prevention in Nigerian children with sickle cell disease: a 5-year appraisal. *Pediatr Blood Cancer*. 2013;60:1940–1945. doi: 10.1002/pbc.24698
5. Abdullahi SU, Jibir BW, Bello-Manga H, Gambo S, Inuwa H, Tijjani AG, Idris N, Galadanci A, Hikima MS, Galadanci N, et al. Hydroxyurea for primary stroke prevention in children with sickle cell anaemia in Nigeria (SPRING): a double-blind, multicentre, randomised, phase 3 trial. *Lancet Haematol*. 2022;9:e26–e37. doi: 10.1016/S2352-3026(21)00368-9
6. Abdullahi SU, Sunusi S, Abba MS, Sani S, Inuwa HA, Gambo S, Gambo A, Musa B, Covert Greene BV, Kassim AA, et al. Hydroxyurea for secondary stroke prevention in children with sickle cell anemia in Nigeria: a randomized controlled trial. *Blood*. 2023;141:825–834. doi: 10.1182/blood.2022016620
7. ClinicalTrials.gov. A Phase 2 Open-label Study to Evaluate the Activity of Etavopivat on Transcranial Doppler Velocities in Pediatric Patients With Sickle Cell Disease Who Are at Increased Risk for Primary Stroke. 2023. Accessed September 10, 2023. https://clinicaltrials.gov/study/NCT05953584
8. Xu JZ, Conrey A, Frey I, Gwaabe E, Menapace LA, Tumburu L, Lundt M, Lequang T, Li Q, Glass K, et al. A phase 1 dose escalation study of the pyruvate kinase activator mitapivat (AG-348) in sickle cell disease. *Blood*. 2022;140:2053–2062. doi: 10.1182/blood.2022015403
9. ClinicalTrials.gov. Expanded Access Protocol for Pediatric Patients With Sickle Cell Disease Who Have No Alternative Treatment Options. 2021. Accessed September 10, 2023. https://classic.clinicaltrials.gov/ct2/show/NCT04724421
10. Kassim AA, Leonard A. Debating the future of sickle cell disease curative therapy: haploidentical hematopoietic stem cell transplantation vs gene therapy. *J Clin Med*. 2022;11:4775. doi: 10.3390/jcm11164775
11. Fullerton HJ, Wintermark M, Hills NK, Dowling MM, Tan M, Rafay MF, Elkind MS, Barkovich AJ, deVeber GA; VIPS Investigators. Risk of recurrent arterial ischemic stroke in childhood: a prospective international study. *Stroke*. 2016;47:53–59. doi: 10.1161/STROKEAHA.115.011173
12. Fullerton HJ, Hills NK, Elkind MS, Dowling MM, Wintermark M, Glaser CA, Tan M, Rivkin MJ, Titomanlio L, Barkovich AJ, et al; VIPS Investigators. Infection, vaccination, and childhood arterial ischemic stroke: results of the VIPS study. *Neurology*. 2015;85:1459–1466. doi: 10.1212/WNL.0000000000002065
13. ClinicalTrials.gov. High Dose Steroids in Children With Stroke (PASTA). 2021. Accessed September 10, 2023. https://clinicaltrials.gov/study/NCT04873583
14. Park Y, Fullerton HJ, Elm JJ. A pragmatic, adaptive clinical trial design for a rare disease: the FOcal Cerebral Arteriopathy Steroid (FOCAS) trial. *Contemp Clin Trials*. 2019;86:105852. doi: 10.1016/j.cct.2019.105852
15. Bhatia KD, Chowdhury S, Andrews I, Goetti R, Webster R, Troedson C, Dale RC, Muthusami P, Parra-Farinas C, Dlamini N, et al. Association between thrombectomy and functional outcomes in pediatric patients with acute ischemic stroke from large vessel occlusion. *JAMA Neurol*. 2023;80:910–918. doi: 10.1001/jamaneurol.2023.2303
16. Rivkin MJ, deVeber G, Ichord RN, Kirton A, Chan AK, Hovinga CA, Gill JC, Szabo A, Hill MD, Scholz K, et al. Thrombolysis in Pediatric Stroke Study. *Stroke*. 2015;46:880–885. doi: 10.1161/STROKEAHA.114.008210
17. Sun LR, Wilson JL, Waak M, Kiskaddon A, Goldenberg NA, Jordan LC, Barry M. Tenecteplase in acute stroke: what about the children? *Stroke*. 2023;54:1950–1953. doi: 10.1161/STROKEAHA.123.042951
18. ClinicalTrials.gov. Darbepoetin for Ischemic Neonatal Stroke to Augment Regeneration (DINOSAUR). 2021. Accessed November 3, 2023. https://clinicaltrials.gov/study/NCT03171818
19. Wagenaar N, de Theije CGM, de Vries LS, Groenendaal F, Benders M, Nijboer CHA. Promoting neuroregeneration after perinatal arterial ischemic stroke: neurotrophic factors and mesenchymal stem cells. *Pediatr Res*. 2018;83:372–384. doi: 10.1038/pr.2017.243
20. Baak LM, Wagenaar N, van der Aa NE, Groenendaal F, Dudink J, Tataranno ML, Mahamuud U, Verhage CH, Eijsermans R, Smit LS, et al. Feasibility and safety of intranasally administered mesenchymal stromal cells

after Perinatal Arterial Ischaemic Stroke in the Netherlands (PASSION): a first-in-human, open-label intervention study. *Lancet Neurol*. 2022;21:528–536. doi: 10.1016/S1474-4422(22)00117-X
21. Wu YW, Comstock BA, Gonzalez FF, Mayock DE, Goodman AM, Maitre NL, Chang T, Van Meurs KP, Lampland AL, Bendel-Stenzel E, et al; HEAL Consortium. Trial of erythropoietin for hypoxic-ischemic encephalopathy in newborns. *N Engl J Med*. 2022;387:148–159. doi: 10.1056/NEJMoa2119660
22. Glass HC, Soul JS, Chang T, Wusthoff CJ, Chu CJ, Massey SL, Abend NS, Lemmon M, Thomas C, Numis AL, et al. Safety of early discontinuation of antiseizure medication after acute symptomatic neonatal seizures. *JAMA Neurol*. 2021;78:817–825. doi: 10.1001/jamaneurol.2021.1437
23. Fox CK, Jordan LC, Beslow LA, Armstrong J, Mackay MT, deVeber G. Children with post-stroke epilepsy have poorer outcomes one year after stroke. *Int J Stroke*. 2018;13:820–823. doi: 10.1177/1747493018784434
24. Jackman M, Sakzewski L, Morgan C, Boyd RN, Brennan SE, Langdon K, Toovey RAM, Greaves S, Thorley M, Novak I. Interventions to improve physical function for children and young people with cerebral palsy: international clinical practice guideline. *Dev Med Child Neurol*. 2022;64:536–549. doi: 10.1111/dmcn.15055
25. Klevberg GL, Zucknick M, Jahnsen R, Eliasson AC. Development of hand use with and without intensive training among children with unilateral cerebral palsy in Scandinavia. *Dev Neurorehabil*. 2023;26:163–171. doi: 10.1080/17518423.2023.2193256
26. Kirton A, Metzler MJ, Craig BT, Hilderley A, Dunbar M, Giuffre A, Wrightson J, Zewdie E, Carlson HL. Perinatal stroke: mapping and modulating developmental plasticity. *Nat Rev Neurol*. 2021;17:415–432. doi: 10.1038/s41582-021-00503-x
27. ClinicalTrials.gov. Stimulation for Perinatal Stroke Optimizing Recovery Trajectories (SPORT). Accessed September 10, 2023. https://clinicaltrials.gov/ct2/show/NCT03216837
28. Lehman LL, Maletsky K, Beaute J, Rakesh K, Kapur K, Rivkin MJ, Mrakotsky C. Prevalence of symptoms of anxiety, depression, and post-traumatic stress disorder in parents and children following pediatric stroke. *J Child Neurol*. 2020;35:472–479. doi: 10.1177/0883073820909617
29. Bemister TB, Brooks BL, Dyck RH, Kirton A. Predictors of caregiver depression and family functioning after perinatal stroke. *BMC Pediatr*. 2015;15:75. doi: 10.1186/s12887-015-0397-5
30. Rohner A, Gutbrod K, Kohler B, Lidzba K, Fischer U, Goeggel-Simonetti B, Regenyi M, Steinlin M, Bigi S. Health-related quality of life in young adults following pediatric arterial ischemic stroke. *Stroke*. 2020;51:952–957. doi: 10.1161/STROKEAHA.119.027622
31. IPSO Kid Stroke Connections. 2023. Accessed September 10, 2023. https://community.internationalpediatricstroke.org/
32. International Pediatric Stroke Organization (IPSO). 2019. Accessed November 3, 2023. https://internationalpediatricstroke.org/
33. Perinatal Arterial Stroke: A Multi-site RCT of Intensive Infant Rehabilitation (I-ACQUIRE). Access November 3, 2023. https://www.nihstrokenet.org/trials/i-acquire/home

Imaging of Hemorrhagic Stroke in Children

James L. Leach, MD[a,*], Betul E. Derinkuyu, MD[a], John Michael Taylor, MD[b], Sudhakar Vadivelu, DO[c]

KEYWORDS

• Children • Hemorrhagic • Stroke • Computed tomography • MR imaging • Brain • Angiography • DSA

KEY POINTS

- Nearly half of pediatric stroke cases are hemorrhagic, in contrast to adults where most stroke presentations are ischemic.
- There are substantial differences in etiology of hemorrhagic stroke in the preterm neonate, term neonate, and older child.
- Vascular malformations predominate as a cause of hemorrhagic stroke in children and adolescents while germinal matrix-intraventricular hemorrhage, venous thrombosis, and coagulopathies are more common in neonates.
- Neuroimaging plays the key role in diagnosis. Identification of hemorrhage patterns associated with common etiologies in each age group and application of rapid vascular imaging is critical for directing patient management.

INTRODUCTION

This study aims to provide a practical overview of the causes and imaging findings in childhood hemorrhagic stroke (HS). HS is a clinical term, which typically refers to an acute, nontraumatic, neurologic presentation associated with intracranial hemorrhage (ICH). It traditionally encompasses spontaneous intraparenchymal hemorrhage (IPH) with or without intraventricular extension, isolated intraventricular hemorrhage (IVH), and nontraumatic subarachnoid hemorrhage (SAH). Despite its common usage, the term "hemorrhagic stroke" remains confusing. It has occasionally been used to imply hemorrhagic transformation of arterial ischemic stroke and is often used to describe hemorrhagic cerebral venous thrombosis (CVT). Notably, some authors exclude one or both conditions under the general "hemorrhagic stroke" definition.[1] For the purposes of this review, HS will be defined as those acute clinical scenarios where nontraumatic spontaneous ICH is the dominant feature. Since a broadening spectrum of CVT is an increasingly recognized underlying cause of IPH and HS across the pediatric age cohort (particularly in neonates), it will be reviewed in this article. Hemorrhagic transformation of arterial ischemic stroke and hypoxic ischemic encephalopathy typically does not present with ICH as the dominant or sole imaging finding[2] and is not specifically discussed in this study.

Although stroke (ischemic and hemorrhagic) in childhood is uncommon compared to stroke in adults (estimated incidence of 2–13 per 100,000

[a] Division of Pediatric Neuroradiology, Department of Radiology, Cincinnati Children's Hospital Medical Center, University of Cincinnati College of Medicine, Cincinnati, OH, USA; [b] Division of Neurology, Department of Pediatrics, Cincinnati Children's Hospital Medical Center, University of Cincinnati College of Medicine, Cincinnati, OH, USA; [c] Division of Pediatric Neurosurgery, Department of Neurosurgery, Cincinnati Children's Hospital Medical Center, University of Cincinnati College of Medicine, Cincinnati, OH, USA
* Corresponding author. Cincinnati Children's Hospital Medical Center, University of Cincinnati College of Medicine, 3333 Burnet Avenue, Cincinnati, OH 45229.
E-mail address: james.leach@cchmc.org

Neuroimag Clin N Am 34 (2024) 615–636
https://doi.org/10.1016/j.nic.2024.08.023

children per year), pediatric stroke can result in significant long-term disability and mortality.[3,4] In contrast to adults where ischemic stroke predominates (85%), nearly half of all pediatric stroke is hemorrhagic.[4–6] Notably, the importance of HS relative to ischemic stroke varies across different age groups within the pediatric population. While ischemic stroke predominates in the first year of life, hemorrhagic stroke is more common between the ages of 1 and 14 years. In the latter half of the second decade of life, as adult physiology and stroke risk factors set in, ischemic stroke predominates. Most patients with HS are critically ill with up to 73% requiring intensive care unit admission.[7] Delayed diagnosis or misdiagnosis of HS negatively affects outcome due to the potential for progressive bleeding over time and increased risk of rebleeding with rapid clinical deterioration and neurologic injury.[8] Early and accurate neuroimaging assessment with prompt diagnosis is crucial for guiding interdisciplinary management and informing acute treatment.

ETIOLOGY OF HEMORRHAGIC STROKE IN CHILDREN

Multiple clinical studies have addressed the underlying causes of HS in children[9,10] with marked variability between cohorts and definitions. Most studies have excluded neonates, and many exclude CVT. Moreover, some studies only include IPH, while others include all subtypes of ICH.[9–14] What is clear from these studies is that etiologies and imaging patterns are quite different in the neonatal period versus older children and that preterm neonates differ significantly from term neonates (**Box 1**).[1,10,13] In preterm neonates, HS is more commonly related to venous thrombosis, coagulopathy, and the spectrum of hemorrhagic germinal matrix pathologies, which includes germinal matrix-intraventricular hemorrhage (GM-IVH) and periventricular hemorrhagic infarction (PVHI). In term neonates CVT, medullary venous thrombosis (MVT), subpial hemorrhage (SPH), coagulopathies, and hemorrhagic transformation of arterial ischemic stroke are more common causes of nontraumatic ICH, with vascular malformations and aneurysms much less commonly seen. In many cases of neonatal HS, no cause can be identified.[13,16] In older children and adolescents, vascular malformations strongly predominate as a cause of ICH (60%), most commonly cerebral arteriovenous malformations (AVM) and cerebral cavernous malformations (CCM).[9,10] Importantly, cerebral arteriovenous shunt lesions, including cerebral AVM and pial arteriovenous fistulae (pAVFs), are the leading cause of hemorrhagic stroke in the first two decades of life. Since these high-flow vascular lesions are surgically or endovascularly treatable and carry a high risk of life-threatening recurrent hemorrhage, they should be recognized early in the diagnostic evaluation of children with HS. Cerebral aneurysms have similar implications, though these are significantly less common as a cause of HS in children.

IMAGING EVALUATION

When a child presents with an abrupt onset of a neurologic deficit, ischemic or hemorrhagic stroke is often the presumed diagnosis. While stroke mimics (postictal state or migraine) are more common in children than in adults,[17] rapid neuroimaging is essential to guide therapy and to exclude ICH as a cause.

The choice of imaging modality for children with an acute neurologic deficit should be driven by clinical presentation, age, modality availability, and likely cause. Many pediatric stroke guidelines recommend brain MR imaging as an initial imaging modality especially in suspected arterial ischemic stroke, as computed tomography (CT) is less sensitive for the detection of early ischemic abnormalities.[18,19] Round-the-clock availability for MR imaging in pediatric patients is not universal; MR imaging often requires sedation or anesthesia in young children and entails longer preparation and imaging times. Given the higher prevalence of HS in children compared to adults, exclusion of ICH as an etiology of stroke symptoms is a critical first step in evaluating these patients.

Noncontrast head CT is the initial study of choice in emergency settings (particularly in unstable patients) because of its near universal availability, rapid image acquisition, high sensitivity for acute hemorrhage[20,21] and ability to perform in almost all patients without sedation (particularly important in the pediatric population).[22,23] CT angiography (CTA) and/or CT-venography (CTV) can be performed immediately after the identification of spontaneous ICH. CTA has a high sensitivity and specificity (90%–100%) in identifying vascular malformations and other potential causes of ICH[24] although as discussed later may be negative in the acute stage because of local mass effect and/or vasospasm. CT utilizes ionizing radiation, and even with modern dose reduction techniques, there is concern for use in children.[25] In the acute clinical scenario, time is of the essence and rapid diagnosis of a vascular cause is of paramount clinical importance. Head CT followed by CTA/CTV (if indicated) should be considered as the first-choice examination.

Box 1
Common etiologies of hemorrhagic stroke by age group in children

Neonatal: Preterm (0–28 days, < 34–36 week gestation)

- Germinal matrix-intraventricular hemorrhage-periventricular hemorrhagic infarction spectrum (GMH-IVH-PVHI)
- Cerebellar hemorrhage
- Cerebral venous thrombosis with associated parenchymal hemorrhage
  - Medullary Vein Thrombosis (MVT)
- Hematologic/coagulopathy
  - Coagulopathy (iatrogenic/ECMO), hemophilia, and vitamin K deficiency, thrombocytopenia
- Diffuse hypoxic ischemic injury with associated parenchymal hemorrhage
- Arterial ischemic infarction with associated parenchymal hemorrhage
- Unknown

Neonatal: Term/near term (0–28 days, >34–36 week gestation)

- Cerebral venous thrombosis with associated parenchymal hemorrhage
  - Dural sinus thrombosis without or with cortical, deep, or MVT
  - Isolated cortical venous thrombosis
  - MVT
- Arterial ischemic infarction with associated parenchymal hemorrhage
- GMH-IVH-PVHI
- SPH
- Hematologic/coagulopathy
  - Coagulopathy (iatrogenic and ECMO), hemophilia, vitamin K deficiency, and thrombocytopenia
- Unknown

Childhood

- Vascular
  - Arteriovenous malformation
  - Cavernous malformation
  - Aneurysm
  - Arteriovenous fistula
- Hematologic/cardiac
  - Coagulopathy (iatrogenic and ECMO), hemophilia, and thrombocytopenia
- Cerebral venous thrombosis with associated parenchymal hemorrhage
  - Dural sinus thrombosis without or with cortical, deep, or MVT
  - Isolated cortical venous thrombosis
- Arterial ischemic infarction with associated parenchymal hemorrhage
- Neoplastic

Etiologies are listed in rough order as most common to least common in each age group based upon published data.[9,10,12–15] More cases of HS are of unknown etiology in neonates than in older children. Details regarding the estimated etiology prevalence in each group is provided in the text.

In a clinically stable patient, as an initial follow-up examination when a cause is not identified by CT/CTA/CTV, or when the findings of CT/CTA/CTV require further clarification, MR imaging is very useful given its higher sensitivity for brain parenchymal abnormalities and ability to differentiate high flow from low flow vascular pathology. Besides conventional noncontrast sequences,

additional MR imaging techniques are helpful. Gradient-recalled echo (GRE) or susceptibility-weighted imaging (SWI) should always be performed given high sensitivity for hemorrhage (particularly subacute and chronic hemorrhage)[26] as well as sensitivity for intraluminal thrombus (arterial and venous). Noncontrast time-of-flight (TOF), contrast-enhanced magnetic resonance angiography (MRA), and MR venography (MRV) should also be considered. MRA coverage should be tailored to cover the hemorrhagic area and surrounding regions. Contrast-enhanced MR imaging (optimally using volumetric-isotropic techniques that allow multiplanar reformations) is important to assess vascular malformations with complex flow and to optimally assess for venous thrombus. Time-resolved 4 dimensional contrast-enhanced MRA (4D MRA) can be very useful to detect arteriovenous shunt lesions, but often it has limitations related to spatial resolution and temporal resolution depending upon the sequence and magnet field strength and may be more limited in sensitivity in the acute setting.[27] Arterial spin labeling (ASL) is a more recent technique that can detect focal areas that characterize arteriovenous shunt lesions. ASL has shown excellent sensitivity for high-flow vascular lesions in the initial workup of IPH in children. In one report of 121 children with nontraumatic IPH studied by catheter-directed digital subtraction angiography (DSA), ASL imaging showed a high sensitivity (90%), specificity (97%), and accuracy (92%) for the detection of arteriovenous shunt lesions.[27] Its performance was better than conventional contrast-enhanced MR imaging without ASL, 4D MRA, and CTA for the detection of an arteriovenous shunt lesion. Incorporation of ASL (always performed precontrast administration) is highly recommended in the MR imaging workup of children with spontaneous ICH. It is important to note that MR imaging and CT/CTA/CTV can provide complementary information regarding causes of HS and are often both performed in the pediatric cohort.[23]

Catheter-directed DSA remains the reference standard imaging technique for intracranial vascular evaluation, with superior sensitivity and specificity for the detection of vascular etiology in children with HS,[1] and an excellent safety profile when performed by experienced operators in specialized pediatric centers.[28] Catheter-directed DSA can detect subtle arteriovenous shunt lesions or aneurysms that escape detection by CT and MR imaging given its unsurpassed temporal and spatial resolution, and it is, therefore, an essential diagnostic study in children with HS. Moreover, detailed angioarchitectural and hemodynamic data uniquely available from catheter-directed DSA analysis are vital for guiding the formulation and execution of a definitive treatment plan in children with HS.[29] The timing of performing catheter-directed DSA performance in a child with ICH depends upon the clinical stability of the patient, intracranial pressure, neurologic status, results of previous noninvasive imaging, and timing of planned endovascular or surgical therapy. If imaging evaluations are negative in the acute phase of HS, delayed imaging including repeat catheter-directed DSA should be strongly considered, as well as comprehensive hematologic workup. Vasospasm, transient thrombosis, and compression of blood vessels by adjacent hematoma may transiently mask the underlying vascular lesion in the acute setting.[30,31] The timing of the follow-up evaluation depends upon the suspected etiology but is typically performed within 1 to 3 months.

In neonates, head ultrasound (HUS) is a useful and easily performed screening study for the diagnosis of GM-IVH or a large IPH that is typically associated with PVHI.[32,33] HUS is often the first screening test obtained in preterm neonates and in term neonates with neurologic deficits or seizures. While MR imaging is more sensitive for the detection of ICH and brain parenchymal ischemia, HUS can identify clinically significant GMH-IVH, PVHI, and ventriculomegaly without the need for patient transport from the neonatal intensive care unit or sedation.[32] Commonly, serial HUS are performed in preterm infants to identify clinically significant hemorrhagic and ischemic injuries, with brain MR imaging performed at term equivalent age (TEA) for more detailed brain parenchymal assessment or to answer clinically relevant questions (eg, suspected CVT in a term neonate).[34,35]

The imaging patterns and findings of the more common causes of spontaneous (nontraumatic) ICH in children are reviewed.

Neonatal Hemorrhagic Stroke

The majority of spontaneous ICH cases with identifiable cause in this age group are related to GMH-IVH and PVHI in the preterm neonate, and CVT or coagulopathy in the term neonate.[15] As stated, in many neonates with HS no definite cause can be found.[12,13] Neonatal HS is distinct from HS in any other period of life due to specific developmental risk factors, unique developmentally specific pathophysiologic mechanisms, and lifelong consequences.[15] The common HS etiologies of preterm and term neonates are listed in **Box 1**.

Germinal matrix-intraventricular hemorrhage

GMH-IVH is a multifactorial brain injury seen predominantly in preterm newborns before the

germinal matrix completely involutes (approximately the 34th week of gestation). It is especially common in those younger than 32 weeks of gestation (very preterm). GMH is thought to occur when perinatal stress triggers a sudden or marked alteration of blood flow or venous pressure in the rich, immature, and fragile vascular network of the subependymal germinal matrix. GMH may secondarily disrupt the ependyma and extend into the lateral ventricles, resulting in IVH. Most cases occur within the first week of life of preterm neonates, particularly in the first 72 hours.[15,36,37] The main risk factors for GMH-IVH are low gestational age, low birth weight, and perinatal distress. GMH can occur anywhere along the germinal matrix, most common in the caudothalamic groove region. GM-IVH has traditionally been graded using the Papile system (Grade I—isolated GMH, Grade II—GMH and IVH without ventriculomegaly, Grade III—GMH and IVH with ventriculomegaly, and Grade IV—associated IPH [now termed PVHI]).[38] High-grade GMH-IVH is usually symptomatic and associated with abnormal neurodevelopmental outcomes such as posthemorrhagic hydrocephalus, cerebral palsy, epilepsy, and severe cognitive impairment.[15] While HUS is the most common imaging study performed to assess GMH-IVH, MR imaging is more sensitive and specific.[39] In a recent study, up to 50% of neonates with a normal HUS show mild GMH-IVH (Grades I–II) on MR imaging at TEA. Conversely, up to 60% of neonates with a normal brain MR imaging had grade I or II GMH-IVH identified on HUS.[40] While MR imaging may have higher sensitivity and specificity, GMH-IVH is typically diagnosed by HUS, which is routinely done at birth in premature neonates and then through the first few weeks of life. HUS has excellent sensitivity for higher grades of GM-IVH and clinically important ventriculomegaly. The characteristic findings of subependymal hyperechoic globular thickening detected during the first week of life (usually remaining visible for a few weeks) and mixed echogenicity within the lateral ventricles (with or without enlargement) have been well described[34,41,42] (**Fig. 1**). Imaging findings of GMH-IVH on MR imaging are best delineated using SWI, which is highly sensitive for IVH, IPH, and SAH.[40]

Periventricular hemorrhagic infarction

Grade IV GMH-IVH is currently termed PVHI and is thought to be a type of hemorrhagic periventricular venous infarction precipitated by impairment of deep medullary venous drainage resulting from compression of the terminal (thalamostriate) vein distributions by adjacent subependymal germinal matrix hemorrhage.[43,44] Notably, deep medullary vein thrombosis (MVT) may also occur without GMH (see later discussion). PVHI can occur in any grade (I–III) of GMH-IVH but is most common with grade III.[41] The critical venous structures involved in the pathogenesis of PVHI are the superior thalamostriate vein (superior terminal vein) tributary of the internal cerebral vein (ICV), which drains the internal capsule and corpus striatum, and the inferior thalamostriate vein (inferior terminal vein) tributary of the basal vein of Rosenthal, which drains the periventricular temporal lobe.[45] The unusual "U-shaped" morphology of the superior thalamostriate vein in the caudothalamic groove region, near the foramen of Monro, is believed to predispose to venous obstruction by adjacent subependymal hemorrhage resulting in thrombosis and the ensuing complications that result from impairment of deep medullary venous drainage.[46]

PVHI occurs in 4% to 11% of preterm newborns, is most commonly unilateral (90%), adjacent to regions of GMM-IVH (84% grade III), and typically within the periventricular white matter of the parietal and posterior frontal regions.[47,48] PVHI continues to have a high mortality (40%) with over two-thirds of survivors having severe motor and cognitive deficits.[47,49,50] The location of the PVHI correlates well with functional outcome. Those neonates with PVHI involving the superior and middle terminal vein territory (caudate and central corona radiata in the parietal/posterior frontal regions) are more likely to have severe hemiplegia.[45] Diffusion tensor imaging (DTI) of the internal capsule can be useful for the prediction of motor outcomes.[51] When a GMH or PVHI-like pattern is identified after 32 weeks, it is more likely to be an epiphenomenon of other injuries such as primary venous thrombosis.[42]

PVHI has a very typical imaging pattern (see **Fig. 1**). On HUS, PVHI is typically diagnosed as a focal unilateral or less commonly asymmetric bilateral fan-shaped periventricular white matter hyperechogenicity often extending from a region of GMH.[41,42] Over time, the echogenicity decreases and the resulting periventricular encephalomalacia results in a porencephalic cyst communicating with the ventricle. On MR imaging, PVHI signal depends upon the age of the hemorrhage with typical marked susceptibility effect on SWI. In the acute stage, surrounding edema is common with variable diffusion restriction. Engorged and/or thrombosed medullary veins can be identified on SWI but may be obscured by adjacent IPH.[14] As on HUS, evolution of the IPH occurs often with resultant typical porencephaly.

Medullary vein thrombosis

MVT is an increasingly recognized cause of IPH and brain injury in preterm and term neonates[52–55]

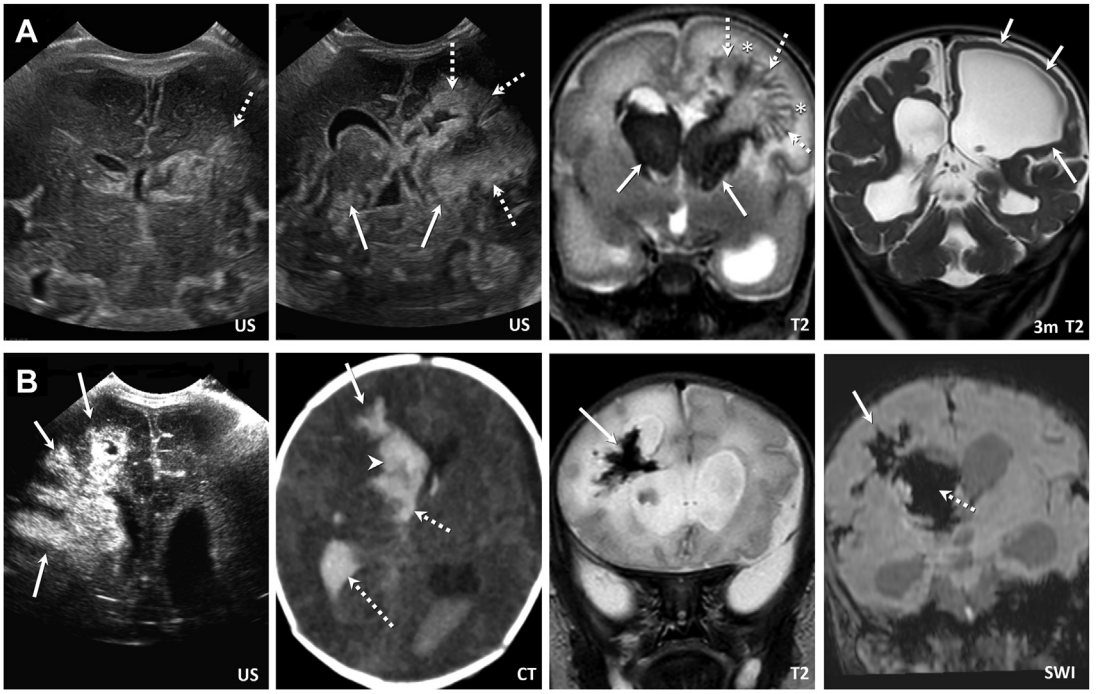

Fig. 1. Hemorrhagic germinal matrix spectrum pathology (germinal matrix hemorrhage-intraventricular hemorrhage [GMH-IVH]-periventricular hemorrhagic infarction [PVHI]). (*A*) A 28 week gestation premature neonate. Initial head ultrasound (US) at day of life (DOL) 1 demonstrates mixed echogenicity IVH and a large area of hyperechogenicity compatible with PVHI in the left periventricular white matter (dashed *arrows*). Brain MR imaging performed the next day. Coronal T2-weighted image (T2) demonstrates predominantly hypointense intraventricular hemorrhage (*solid arrows*) and fan-shaped intraparenchymal hemorrhage extending along thrombosed medullary veins (*dashed arrows*). Adjacent edema in the brain parenchyma is noted (*). Coronal T2-weighted image 3 months later (3m T2) demonstrates typical porencephaly related to PVHI (*solid arrows*). (*B*) Former 34 week gestational neonate, DOL 5 with increased irritability and difficulty feeding. US demonstrates large flame-shaped echogenicity in the right periventricular white matter consistent with PVHI (*solid arrows*). Head CT (CT) demonstrates extensive IVH (*dashed arrows*), GMH (*arrowhead*), and irregular PVHI (*solid arrow*). Thrombosed medullary veins with adjacent parenchymal hemorrhage are well demonstrated on T2-weighted coronal (T2) and susceptibility-weighted coronal (SWI) brain MR imaging performed the next day (*solid arrows*). Large GMH and adjacent IVH are noted (*dashed arrow*).

and can occur in isolation, with GM-IVH (PVHI, described in earlier discussion), with dural sinus thrombosis or with SPH (as described in later discussion). The medullary venous system can be divided into the *superficial ventriculofugal system* (draining the subcortical white matter toward cortical veins on the brain surface) and the *deep ventriculopetal system* (draining toward the subependymal and deep veins). Anastomotic veins can bridge these 2 systems, and drainage patterns can overlap.[53] The deep medullary veins are a part of the deep venous system draining the white matter and striatum and originate 1 to 2 cm deep to the pial surface.[53] They have radial orientation perpendicular to the lateral ventricles with drainage to the subependymal veins and subsequently via the ICV and basal vein of Rosenthal to the vein of Galen. Imaging findings of MVT are best identified on MR imaging. MVT should be considered in the setting of a fan-shaped area of edema and hemorrhagic signal extending from the ventricular margin into the deep white matter and/or basal ganglia (**Fig. 2**A). IPH (petechial, small punctate, and larger hematomas) can be seen in most cases. Multifocal deep white matter and corpus callosum edema/infarction can also be present depending on the drainage territory of the involved vein(s).[52,53] The SWI sequence outlines the engorged/thrombosed medullary veins in a typical radial pattern extending into the deep white matter. As the medullary veins are not typically identified with venographic techniques or contrast administration, confirmation of occlusion of the medullary veins is often not possible.[56] Because of this some authors have used the term medullary vein engorgement to describe this appearance.[53] MRV and contrast

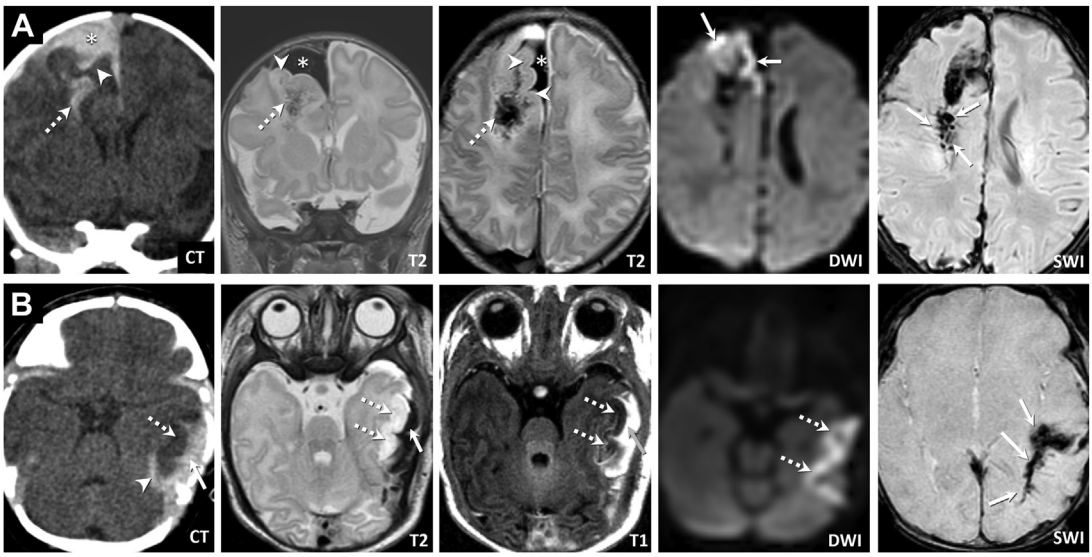

Fig. 2. Subpial hemorrhage (SPH) and medullary venous congestion/thrombosis (MVT). (*A*) A 2 day old male infant, 38 weeks' gestation age at delivery. Left arm and leg jerking consistent with seizure. Head CT demonstrates a sizable hemorrhage along the surface of the right frontal lobe (*) focally distorting the adjacent brain parenchyma. Irregular subcortical hemorrhage is present (*dashed arrow*). Intervening cortex is hypodense consistent with edema (*arrowhead*). Coronal and axial T2-weighted images (T2) show similar superficial hemorrhage (*) displacing the brain parenchyma with cortical edema (*arrowhead*) and irregular subcortical hemorrhage with morphology consistent with engorged or thrombosed medullary veins (*dashed arrows*). Localized cortical diffusion restriction of the cortex is noted (DWI, *arrows*). Thrombosed ependymal and medullary veins are more readily demonstrated on SWI (SWI *arrows*). CTA was performed without evidence of vascular malformation, DVA, or cortical venous thrombosis. Hematologic workup documented a prothrombotic Factor V Leiden mutation. (*B*) A 2 day old male infant, term gestation with prolonged traumatic delivery followed by seizure activity postnatally. Localized superficial subpial hemorrhage noted along left temporal lobe on CT (*arrow*), with displaced edematous cortex (*dashed arrows*), and subcortical hemorrhage (*arrowhead*). On MR imaging (T1 and T2), the subpial hemorrhage was T2 hypointense, and T1 hyperintense (*arrows*), compatible with early subacute hemorrhage with displaced edematous brain (*dashed arrows*). Diffusion restriction compatible with cortical infarction is noted (DWI, *dashed arrows*). On SWI, adjacent thrombosed/engorged medullary veins were noted (SWI, *arrows*).

administration, however, are important to identify any associated CVT in these cases. Edema (cytotoxic and vasogenic) and IPH are seen in most cases (98%) with resultant encephalomalacia on follow-up imaging.[52,53]

Subpial hemorrhage

SPH is a form of ICH more commonly seen in term neonates, characterized by bleeding into a potential space between the glia limitans (outermost layer of the astrocytic foot processes in the neocortex) and the pia mater, distinct from the subarachnoid space.[57,58] SPH is thought to represent up to 15% of ICH in the neonatal period.[59] Many risk factors (birth trauma, neonatal asphyxia, fetal head molding with venous compression, and venous thrombosis) have been suggested but the exact pathophysiology is still uncertain. It has been proposed that a primary injury to the glia limitans with rupture of intracortical vessels results in subpial pooling of hemorrhage and elevation of the pia mater, which secondarily causes mechanical compression of traversing venous structures resulting in venous thrombosis, venous hypertension, and focal cortical infarction.[58,60] While HUS and CT can identify the characteristic hemorrhage pattern, MR imaging can more completely characterize SPH and associated brain injuries.[58] Localized hemorrhagic signal is identified closely opposed to the superficial cortex, often elliptical in shape with the long axis tangential to the brain surface. A key feature is that the cortex is deformed and displaced away from the elevated layer of pia mater by the hemorrhagic collection[58] (see **Fig. 2**). There is often cortical and subcortical injury identified as increased T2/FLAIR (fluid-attenuated inversion recovery) signal and associated cortical diffusion restriction complicated by parenchymal hemorrhage (up to 67%).[61] The intense susceptibility effect on SWI images can mask the

characteristic subpial location of the hemorrhage, which is better assessed on T2-weighted images. Notably, SAH may coexist with SPH.[61] Temporal lobe involvement is the most common location for SPH (52%–82% of cases).[61,62] In many cases (76%–100%), imaging findings suggesting deep and/or superficial MVT or congestion are identified[53,62] (see **Fig. 2**B). While earlier reports suggested that cortical vein thrombosis might be a common etiology in temporal lobe SPH, confirmatory evidence of this is rare.[56,61] In the absence of associated parenchymal infarction and/or parenchymal hemorrhage, SPH can resolve without imaging sequelae.[61] Neurologic deficits relate to the location and extent of parenchymal injury. While many patients (60%–70%) have normal neurologic examination at discharge and generally good neurologic outcomes, long-term effects such as language delays, mild hemiparesis, and epilepsy can result.[61,62]

Cerebral Venous Thrombosis

Thrombosis of the dural venous sinuses and/or cortical veins (CVT) is a common cause of spontaneous ICH in children. Also, as noted earlier, venous thrombosis or hypertension is thought to be at least a contributory factor in the pathogenesis of GM-IVH, the likely cause of PVHI, and an important pathogenic factor in some cases of neonatal SPH. Its incidence is probably underestimated but is approximately 0.4 to 1.1 cases/100,000/y in children overall, 6.4/100,000/y in neonates and infants, 0.6 to 0.8/100,000/y in younger children, and 1.2/100,000/y in adolescents.[63–68] There is a high prevalence (up to 43% of pediatric HS cases) in the neonatal period.[63] In neonates and younger children, there is a male predominance.[64–68] Conversely, in adolescents and adults, CVT is much more common in female individuals.[68,69]

Clinical presentation is variable and often nonspecific including seizures, encephalopathy, and altered levels of consciousness. Focal neurologic findings are more common in patients with parenchymal sequelae of CVT (localized edema, venous infarction, or IPH).[70] As in adults, CVT in neonates, infants, and children is often multifactorial in etiology. A predisposing condition can be identified in up to 95% of cases including febrile illness, dehydration, head and neck infection (sinusitis and oto-mastoiditis), genetic and acquired prothrombotic states, bacterial meningitis, anemia, and L-asparaginase therapy for acute lymphocytic leukemia (ALL).[63,70,71]

Imaging findings of CVT are well documented[56,72–74] (**Figs. 3** and **4**). Clues to the diagnosis of CVT as a cause of IPH include hyperdense (thrombus-filled) dural venous sinuses or cortical veins on noncontrast CT, filling defects in dural venous sinuses and cortical veins on CTV and postcontrast MR imaging sequences (including postcontrast MRV), and absent or decreased flow-related enhancement of dural venous sinuses on noncontrast MRV. SWI sequences are critical on MR imaging for directly identifying thrombosed venous segments and associated venous engorgement[75] and can be a key clue to venous thrombosis as an etiology for parenchymal hemorrhage (see **Fig. 3**B).

While imaging studies may show no parenchymal abnormality, parenchymal sequelae are commonly found on imaging, occurring in 30% to 60% of cases, with an increased prevalence in neonates.[64,76] Parenchymal changes can represent vasogenic edema, parenchymal infarction, and parenchymal hemorrhage. Up to 76% of the parenchymal abnormalities in neonates and infants and 33% of those in older children are hemorrhagic.[76] Thalamic, basal ganglia, deep white matter, and IVHs (related to deep venous occlusion) are more common in neonates than in older children and adults with CVT.[55,77,78] Multiple patterns may coexist.

The pathophysiology of parenchymal abnormalities in CVT is thought to be related to venous hypertension, which causes a secondary decrease in local perfusion pressure resulting in cellular energy depletion (potentially complicated by parenchymal infarction), and blood–brain barrier disruption that features vasogenic edema, and varying degrees of mural integrity failure affecting microvascular networks in the brain parenchyma.[76–79] Recruitment of collaterals after venous occlusion is thought to be critical in preventing parenchymal sequelae. Adaptive collateral venous drainage can be achieved through microvascular anastomoses[80] or variations in cortical venous anatomy.[81] Cortical venous or medullary venous involvement[82,83] limits access of affected brain parenchyma to collateral venous drainage pathways. Consequently, parenchymal sequelae (including parenchymal hemorrhage) are more common with cortical vein involvement (associated with dural sinus thrombosis or isolated cortical venous thrombosis).[82,84–86]

Common parenchymal hemorrhage patterns include lobar hemorrhage (particularly involving the frontal and temporal lobes) with a multilobular or flame-shaped morphology, hemorrhage associated with venous infarction manifesting cortical diffusion restriction, and localized subcortical hemorrhage.[72] Multiple patterns can be seen in the same patient. Bilateral frontal parenchymal hemorrhages (superior sagittal sinus thrombosis

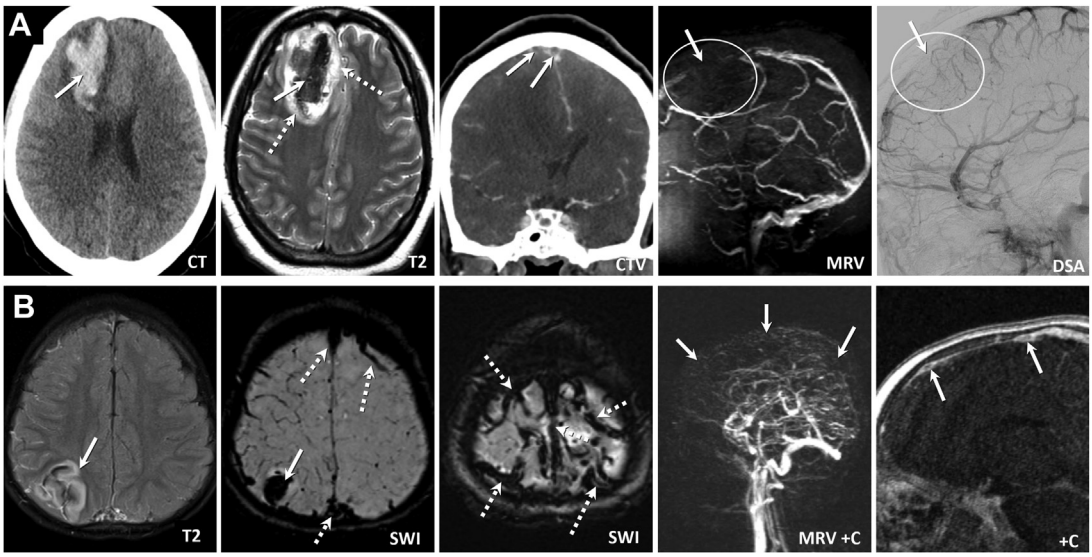

Fig. 3. Cerebral venous thrombosis. (*A*) An 18 year old female patient with aplastic anemia presenting with headache. Focal parenchymal hemorrhage noted in the right frontal lobe on the initial CT (*arrows*) with mild surrounding edema. On MR imaging, T2-weighted images (T2) demonstrate localized T2 hypointense hemorrhage (*arrow*) with moderate surrounding edema (*dashed arrows*). CT venogram (CTV) was performed documenting filling defects within the superior sagittal sinus (SSS) and superficial cortical veins (*arrows*). TOF MR-venogram (MRV) demonstrates the lack of flow-related enhancement in the SSS (*arrow*) and the lack of visualization of cortical veins (outlined by circle) consistent with thrombosis. Because of the size of the hemorrhage, a catheter-directed digital subtraction angiogram was performed to exclude an arteriovenous shunt lesion. This documented segmental occlusion of the SSS (*arrow*) and associated cortical veins (outlined by circle) consistent with thrombosis. (*B*) A 2 year old male patient with focal seizures. MR imaging of the brain was performed. On T2-weighted images (T2), a focal area of cortical and subcortical edema is noted in the right parietal lobe (*arrow*). On SWI, a focal area of susceptibility effect is noted consistent with focal parenchymal hemorrhage in the immediate subcortical region (*arrow*). The SSS and enlarged cortical veins exhibit extensive magnetic susceptibility blooming compatible with dural sinus and cortical vein thrombosis (*dashed arrows*). Absence of enhancement of the SSS and cortical veins noted on postcontrast MRV (MRV +C, *arrows*), with cortical vein filling defects on postcontrast sagittal T1 images (+C, *arrows*). Hematologic workup revealed a prothrombin G20210A mutation.

pattern); lateral temporal lobe parenchymal hemorrhage and edema (transverse sinus thrombosis pattern); unilateral or bilateral thalamic, caudate, and/or deep white matter edema with associated hemorrhage (deep venous system pattern) should prompt strong consideration of CVT as an etiology and should be evaluated with contrast administration and/or venographic techniques[56,72] (see **Figs. 3** and **4**).

Vascular Malformations

Vascular malformations, including cerebral AVMs, pAVFs, and cavernous malformations, are the most common overall cause of HS (particularly IPH) in children beyond the neonatal period.[9,10] Vascular malformations are identified as the underlying cause of nontraumatic ICH in 44% to 87% of nonperinatal pediatric cases.[4,10,11,87–91] In a child presenting with nontraumatic IPH, imaging exclusion of a vascular malformation as a cause should be a top priority. A separate article is devoted to vascular malformations; here, we discuss their HS implications.

Cerebral arteriovenous malformations

Cerebral AVMs are thought to be the cause of up to 50% of cases of spontaneous IPH in children.[10] In comparison to adults, hemorrhagic presentation (75% vs 60%) and deep location (38% vs 18%) are more common in children.[4,92,93] Adjusting for the increased hemorrhagic presentation in children, the long-term cumulative risk of brain AVM hemorrhage in children is similar to adults (approximately 2%–4% per year)[4] but mortality related to brain AVMs is higher in children.[92] Brain AVM hemorrhage patterns can be variable depending upon nidus location, venous drainage pattern, and associated aneurysms. Deep venous drainage (most common with deep AVM location), single draining vein and infratentorial location have been shown to correlate with an increased risk of hemorrhage in pediatric brain AVMs.[94] A recent study found that

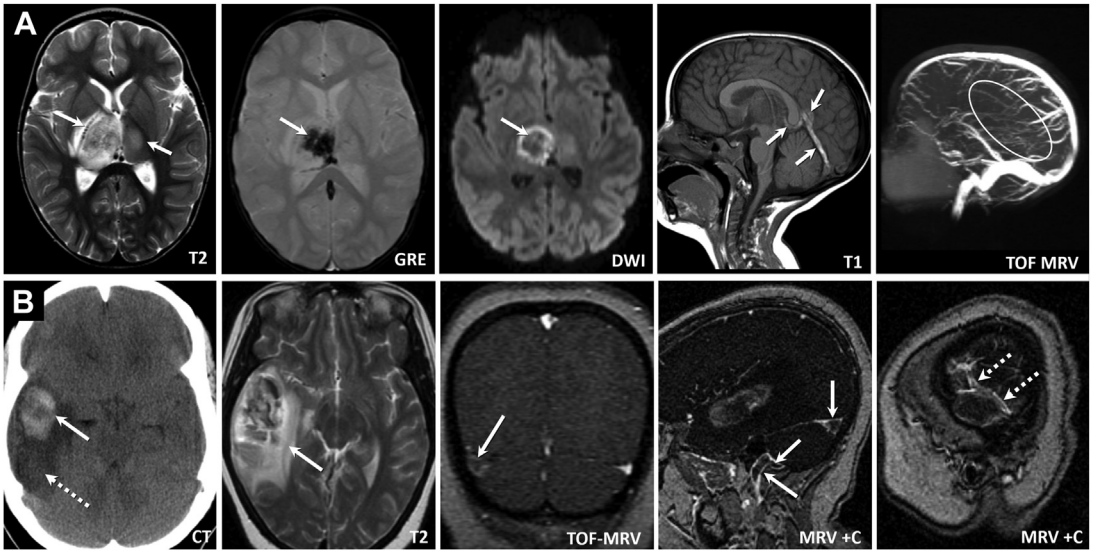

Fig. 4. Cerebral venous thrombosis. (*A*) Thalamic edema and hemorrhage with thrombosis of the deep venous system. Three year old female patient with lethargy and altered mental status. T2-weighted axial MR image (T2) at the level of foramen of Monro demonstrates marked edema and swelling of the right thalamus, with milder edema in the left thalamus (*arrows*). On gradient recalled echo (GRE) sequence, marked ill-defined feathery blooming effect is noted in the medial right thalamus (*arrow*), consistent with hemorrhage. Peripheral diffusion restriction is noted on DWI (*arrow*). T1 hyperintense thrombus noted in the straight sinus, vein of Galen, and proximal internal cerebral veins (*arrows*) consistent with thrombus. TOF MRV demonstrates lack of any flow-related enhancement in the deep venous system consistent with thrombosis (region outlined by circle). (*B*) Thrombosis of the transverse sinus and vein of Labbe'. A 14 year old female patient with headache and new onset seizure. CT demonstrated focal hemorrhage in the right temporal lobe (*arrow*) with moderate surrounding edema (*dashed arrows*). On MR imaging, edema with central mixed signal consistent with hemorrhage is noted (*arrows*). On TOF-MRV, thrombosis of the right transverse sinus is noted (*arrow*). On postcontrast MRV (MRV+C), extensive filling defects are noted throughout the transverse sinus, sigmoid sinus and jugular bulb (*arrows*) as well as the vein of Labbe' (*dashed arrows*).

AVM with associated flow-related aneurysms (perinidal and intranidal) were more likely hemorrhagic at presentation (94% vs 59%), have smaller nidal size, and have a higher annual hemorrhage risk if not obliterated compared to those AVMs without associated aneurysms.[95]

ICH occupying multiple intracranial compartments (IPH, IVH, and SAH) is common with AVM rupture. Approximately 50% of AVM-associated ICHs are isolated IPH, 30% to 38% are IPH with IVH or SAH, and 20% are isolated SAH.[96] Noncontrast CT findings suggesting AVM as a source of hemorrhage include dilated blood density tubular structures. IPH is typically oblong within the brain parenchyma suggesting a high-pressure vascular rupture. On CTA, AVM nidus morphology/location, dilated supplying arteries, and venous drainage pattern can be identified with high sensitivity[97] (**Fig. 5**). In the acute setting, the AVM nidus may not be readily visible on CTA (related to hematoma compression, vasospasm, and transient thrombosis), especially if small and compact, but enlarged feeding arteries and draining veins can be identified and are an important clue to AVM diagnosis. Intranidal, perinidal, and feeding (afferent) artery aneurysms, while detectable by CTA (and should be searched for), are better seen by catheter-directed DSA.[97] MR imaging (particularly with the use of ASL flow techniques) should be considered in stable patients. As described earlier, focal increase in ASL signal has a high sensitivity for arteriovenous shunt lesions in the setting of IPH, outperforming CTA in some studies.[27] Flow-related enhancement of ectatic vessels near the location of hemorrhage and/or draining veins on TOF MRA suggests an underlying arteriovenous shunt lesion. If no vascular cause is found on imaging, delayed imaging follow up is important.[30,31]

Pial arteriovenous fistulae

pAVFs consist of a monofocal arteriovenous shunt zone constituted by a solitary pial vein or venous pouch that is arterialized by one or more pial arterial feeders, predisposing it to marked degrees of venous ectasia, variceal dilatation, and hemorrhage. The vast majority of pAVFs is congenital

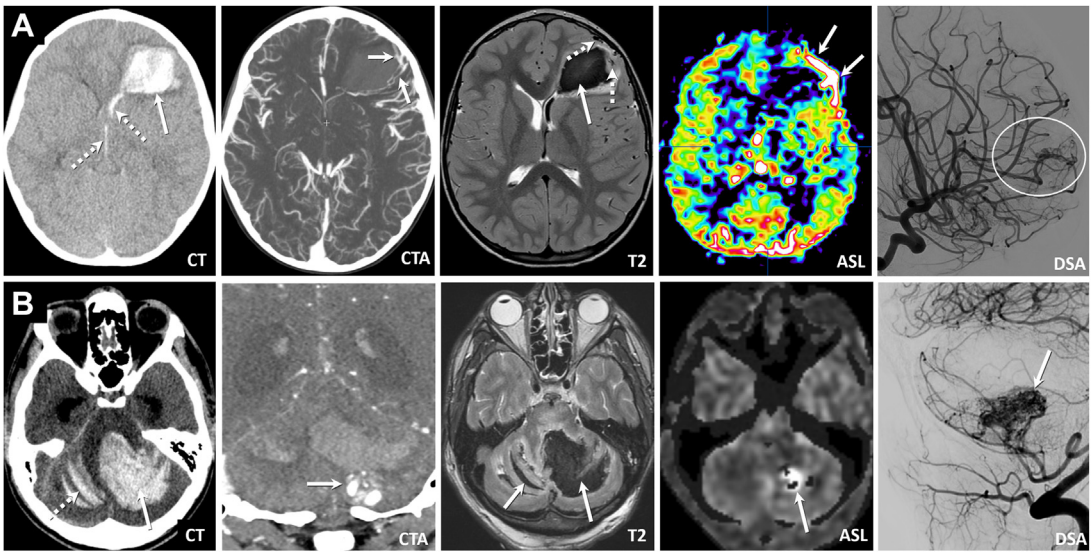

Fig. 5. Arteriovenous malformation with associated hemorrhage. (*A*) A 7 year old female patient with acute onset of headache, confusion, and vomiting. CT demonstrated a left frontal lobe parenchymal hemorrhage (*arrow*) tapering toward the ventricle with intraventricular extension (*dashed arrow*). Minimal surrounding edema. Immediately performed CTA demonstrated splaying of normal cerebral vascularity with an asymmetrically enlarged vessel along the lateral margin of the hemorrhage suspicious for an arteriovenous shunt lesion (*arrows*). MR imaging was performed and T2-weighted images demonstrated a T2-hypointense hemorrhage (*arrow*) with prominent vessels along the left frontal lobe surface (*dashed arrows*). ASL images demonstrated focal increased ASL signal in superficial vessels along the lateral margin of the hemorrhage consistent with high flow arteriovenous shunting (*arrows*). Catheter-directed digital subtraction angiogram (DSA) revealed arteriovenous shunting through a nidal AVM along the dorsal lateral aspect of the hematoma (outline), supplied by frontal branches of the left middle cerebral artery, with venous drainage to a frontal cortical vein (corresponding to the enlarged vascularity seen by CTA and high flow on ASL). (*B*) A 15 year old male patient with sudden headache, vomiting, and unresponsiveness, glasgow coma scale 3/15 on arrival to hospital. CT revealed a large cerebellar hemorrhage (*arrow*) with intraventricular extension, and extensive subarachnoid hemorrhage (*dashed arrows*). Immediately performed CTA demonstrated abnormally ectatic vessels (*arrows*) localized along the inferior margin of the hematoma suggesting a nidal AVM. The hemorrhage was hypointense on MR (T2, *arrows*) with localized high flow signal on ASL along the inferior hematoma consistent with shunting (ASL, *arrow*). Catheter-directed DSA demonstrated a nidus supplied by branches of the left posterior inferior cerebellar artery (*arrow*). Despite emergency posterior fossa decompression and embolization, the patient did not regain neurologic function and expired.

and present in infancy or early childhood, in contradistinction to cerebral AVMs that typically present in older children. Although some angioarchitectural features of pAVFs overlap with vein of Galen malformations (VOGM), intracranial hemorrhagic complications are exceedingly rare in patients with VOGM prior to adolescence. Consequently, VOGM is generally not considered in the differential diagnosis of pediatric hemorrhagic stroke.

pAVFs are predisposed to rupture, making them an important cause of pediatric HS. The markedly elevated pial venous pressures associated with pAVFs leads to secondary complications of venous hypertension including subependymal white matter injury, cortical atrophy, parenchymal calcification, encephaloclastic changes, high-flow occlusive venopathy, and communicating hydrocephalus.[98,99] Hemorrhage can occur at presentation in approximately 20% to 25% of cases.[100,101] Hemorrhagic presentation is more common in older children/adults but can occur at any age. Hemorrhage patterns are often mixed, with varying degrees of IPH, IVH, and SAH depending upon the location of the shunt and bleeding point (**Fig. 6**). Successful endovascular treatment has been reported in up to 90% of cases.[100] There is a common (25%–30%) association with hereditary hemorrhagic telangiectasia and RASA1 gene mutations.[100,102]

Cavernous malformation

Up to 25% of all CCM manifest in childhood and are thought to be the cause of up to 9% of HS presentations in children.[9,10] Approximately 20% of all CCMs are associated with developmental venous anomaly (DVA), more commonly within the posterior fossa.[103,104] When multiple CCMs are identified on imaging in a patient not previously

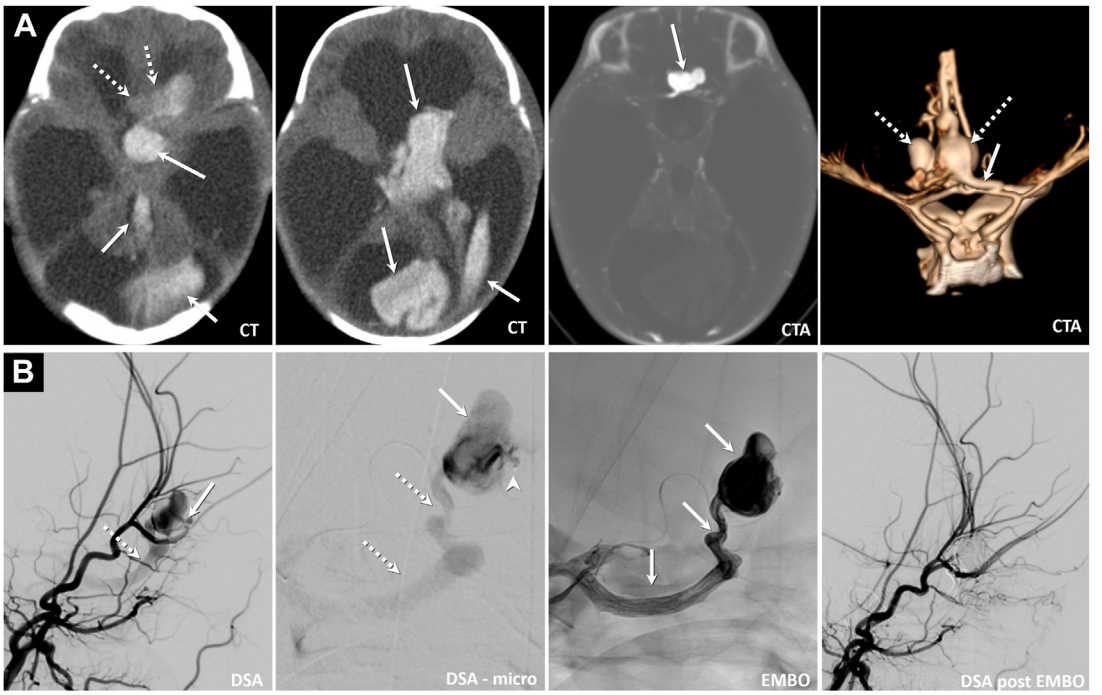

Fig. 6. Pial arteriovenous fistula. A 2 day old infant with hydrocephalus. (*A*) Hemorrhage after shunt placement. CT demonstrates large amount of intraventricular hemorrhage (*arrows*). Subtle lobular regions of mild hyperdensity seen along the inferior frontal lobe adjacent to the hemorrhage concerning for a vascular lesion (*dashed arrows*). Immediate CTA demonstrates a lobular venous aneurysm (*arrows*) in the inferior frontal region corresponding to the areas of mild hyperdensity seen on CT. 3D reconstruction (3D-CTA) demonstrates a single arterial feeder arising from the left anterior cerebral artery (*arrow*) and associated lobular venous aneurysm (*dashed arrows*). (*B*) Catheter-directed DSA documents the feeder artery originating from the anterior cerebral artery (*arrow*) with rapid venous drainage into the right superficial middle cerebral vein on the right (dashed *arrow*). Microcatheter injection (DSA-micro) at the fistulous point (*arrowhead*) demonstrates direct connection to the venous aneurysm (*arrow*) and rapid flow into middle cerebral vein (dashed *arrow*). Embolization (EMBO) was performed with onyx (onyx cast-arrows), totally occluding the fistula and venous drainage (post-EMBO).

treated with cranial radiotherapy, a genetic cause (familial CCM) should be considered.[105]

On CT imaging, CCM appearance depends upon internal hemorrhagic product evolution, associated extralesional hemorrhage, and associated calcification. On MR imaging, CCM have a typical pattern of a multilobular circumscribed lesion with a T2 hypointense rim that blooms on SWI/GRE sequences. Centrally the sinusoidal spaces have differing signal intensities depending upon the stage of internal blood products[106] (**Fig. 7**). Often definitive diagnosis on CT is not possible with the imaging differential being localized parenchymal hemorrhage, AVM, or tumor. Recognizing the typical MR imaging appearance of a CCM, associated DVA (if present), and additional CCM (suggesting a familial CM syndrome) is often a useful finding when diagnosing CCM as a cause for ICH. With extensive intralesional or extralesional hemorrhage, the typical imaging features may not be present and may only become manifest on delayed imaging, or as a diagnosis of exclusion when careful repeat MR imaging and catheter-directed DSA fail to identify another cause.

Hemorrhage related to CCM is a major cause of clinical symptoms and can occur within the CCM (intralesional) or outside the CCM in the adjacent brain parenchyma (extralesional). IVH can occur if the CCM is in a subependymal location. The most widely accepted definition of CCM hemorrhage is an acute or subacute onset of lesion referable symptoms in the context of imaging, pathologic, surgical, or CSF evidence of recent extralesional or intralesional hemorrhage.[107] Given that symptoms are lesion location dependent and that criteria for intralesional and extralesional hemorrhage are poorly defined, some authors have expanded this definition to include more detailed imaging-based criteria. Nikoubashman[108] in a study of pediatric CCM defined acute CCM hemorrhage on MR imaging as *intralesional*: acute or subacute internal hemorrhagic signal accompanied by lesion growth,

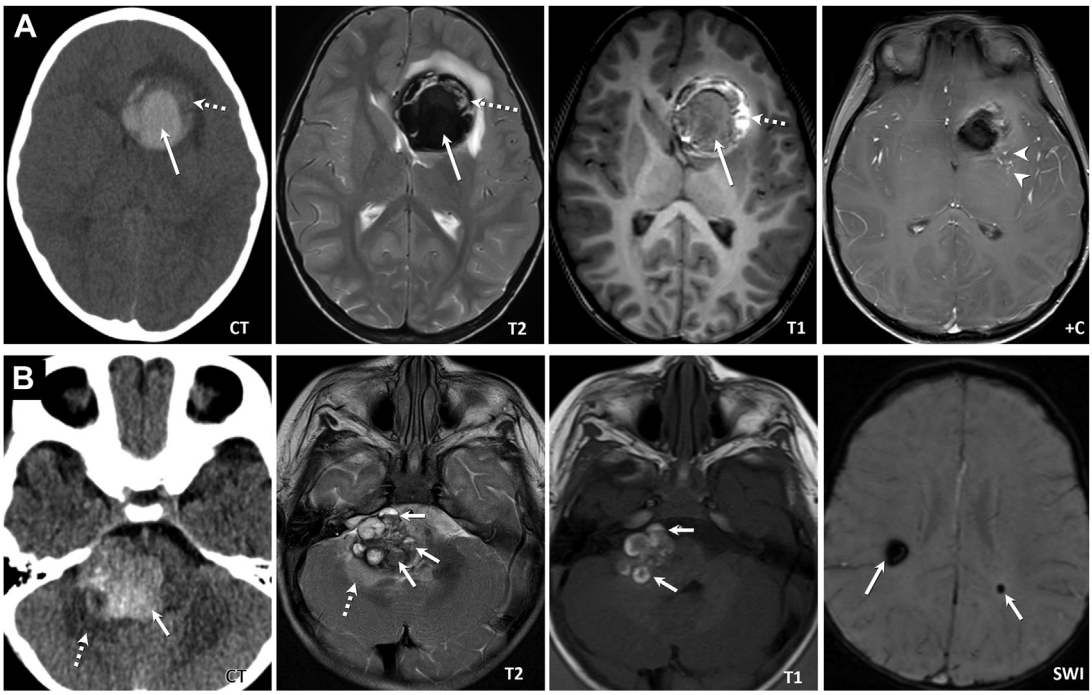

Fig. 7. Cavernous malformation. (*A*) A 5 year old female patient with increasing headache and lethargy. CT demonstrated a large (4 cm) hemorrhagic lesion in the left frontal lobe with surrounding edema (*dashed arrows*). The hemorrhage was lobular with high density centrally and medially and lower density laterally. Immediate CTA was performed, which did not demonstrate a shunting lesion or aneurysm. Subsequent MR imaging was performed to differentiate between cerebral cavernous malformation (CCM) and neoplasm. T2-weighted and T1-weighted images show a multilobular hemorrhagic lesion with central acute blood products (*arrows*) corresponding to the hyperdensity on CT and more peripheral, less-circumscribed subacute hemorrhage (*dashed arrows*) compatible with extralesional hemorrhage. An adjacent developmental venous anomaly was seen on postcontrast images (*arrowheads*). Findings were consistent with CCM complicated by intralesional and extralesional hemorrhage (documented surgically). (*B*) A 10 month old male patient with vomiting, right eye deviation, and lethargy. Head CT demonstrates a hyperdense lesion (*arrow*) in the right pons with mild surrounding edema (*dashed arrows*), and small calcifications. Immediate CTA did not show a shunting lesion or aneurysm. MR imaging demonstrates a multilobular popcorn like mass with dark T2 signal surrounding multiple circumscribed internal spaces (some with fluid levels, *arrows*). On T1, many of the areas exhibit isointense and hyperintense signal consistent with a mix of acute and subacute blood products. There is adjacent edema (*dashed arrow*). Imaging findings consistent with CCM. Multiple additional small CCM identified (*arrows*) in both cerebral hemispheres on SWI suggesting a familial CCM syndrome.

mass effect, or surrounding edema and *extralesional*: gross extralesional hemorrhage manifested as acute or subacute blood degradation products outside the confines of the CCM. Because of varying criteria and differences in cohorts, hemorrhage rates in CCM have been variably reported. In children, the overall annual hemorrhage rate of CCM is approximately 3%[109] or 4.5%/lesion/year,[108] with much higher annual rates in CCM initially presenting with hemorrhage (11%).[108] Prior CCM hemorrhage and brainstem location have universally been reported as the most significant risk factors for subsequent CCM hemorrhage.[109,110]

Imaging appearance has also been shown to correlate with annual hemorrhage risk: CCM with acute or subacute internal blood products—23%, CCM without acute or subacute blood products—3.4%, and dot-sized SWI or GRE lesions—1.3%.[108] Hemorrhage risk is highest in the first 3 years after initial hemorrhage.[109,110] While an associated DVA has been suggested as a risk factor for hemorrhage by some authors,[109] others have not found this association.[110–113] Lesions located within the brainstem or near eloquent cortex are more often symptomatic related to CCM expansion and extralesional hemorrhage.[113,114]

Intracranial Arterial Aneurysms

While intracranial arterial aneurysms (IAAs) rupture is a less common clinical presentation in children than in adults, they are responsible for 10% to

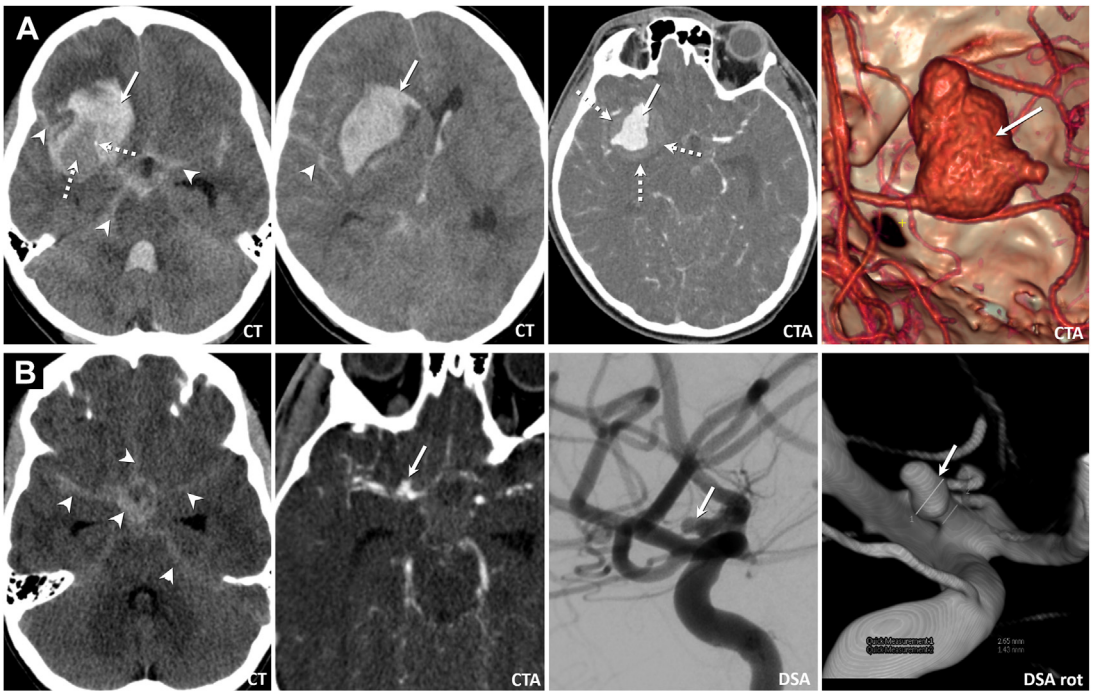

Fig. 8. Intracranial arterial aneurysm. (*A*) A 15 year old male patient who lost consciousness in the shower. CT shows a large parenchymal hemorrhage in the right frontal lobe (*arrow*) extending into the right lateral ventricle, extensive subarachnoid hemorrhage in the right sylvian fissure, basal cisterns, and cerebral sulci (*arrowheads*). In the right sylvian region, an area of intermediate-to-high density noted within the hemorrhage with an associated tiny calcification (*dashed arrows*). CTA demonstrates a giant (26 mm) lobular fusiform aneurysm arising from the right middle cerebral artery bifurcation intrinsically involving the superior M2 division (*arrow*), surrounded by hemorrhage (*dashed arrows*). (*B*) A 13 year old male patient with history of aortic coarctation presented with vomiting and acute headache. Head CT reveals diffuse SAH, more prominent in the right suprasellar cistern (*arrowheads*). Immediate CTA demonstrates a small aneurysm from the right carotid terminus at the origin of the right A1 segment. Catheter-directed DSA confirms the aneurysm and its angioarchitecture is further elucidated by reconstructed 3D images generated with rotational angiography (DSA rot).

15% of childhood HS and up to 60% of isolated spontaneous SAH in children.[6] Overall, pediatric IAAs present with ICH in 35% to 50% of identified cases.[115,116] Aneurysm rupture typically causes isolated SAH (80%) but can also cause IVH and IPH (20%).[6] Although flow-related mechanical stresses caused by arteriovenous shunt lesions often lead to aneurysm formation and rupture, in such cases, the underlying arteriovenous shunt lesion usually dominates the diagnostic picture.

Noncontrast CT is highly sensitive for SAH (93%–100%) particularly in the first 6 hours after headache onset.[117] Typically immediate CTA is performed after identification of nontraumatic SAH,[118] and it can identify the cause in 80% to 95% of patients.[119] When negative, catheter-directed DSA should be performed and can identify vascular pathology in up to 13% of CTA-negative cases. If both CTA and DSA are negative, follow-up CTA and or DSA are recommended (additional yield of 4%).[119] Pediatric IAAs arise more commonly in the posterior circulation and from the internal carotid artery terminus compared to adults (Fig. 8B). Giant (>25 mm) and fusiform aneurysms are more common in young children and infants[116,120,121] (Fig. 8A). While idiopathic IAAs are the most common type identified in children (as in adults), infectious and traumatic aneurysms are more common in children. The presence of multiple cerebral aneurysms (particularly when located distal to the circle of Willis) in a febrile patient (particularly if immunocompromised or with cardiac valve vegetations) should be considered highly suspicious for infectious aneurysms.

Coagulopathy-related Hemorrhagic Stroke

Disorders of coagulation (iatrogenic, hematologic, or hereditary) are a cause of pediatric HS in 12% to 30% of cases depending upon the age cohort evaluated, being more common in children aged less than 2 years.[9,10,12–14] Coagulopathy related to the treatment of congenital cardiac disease or

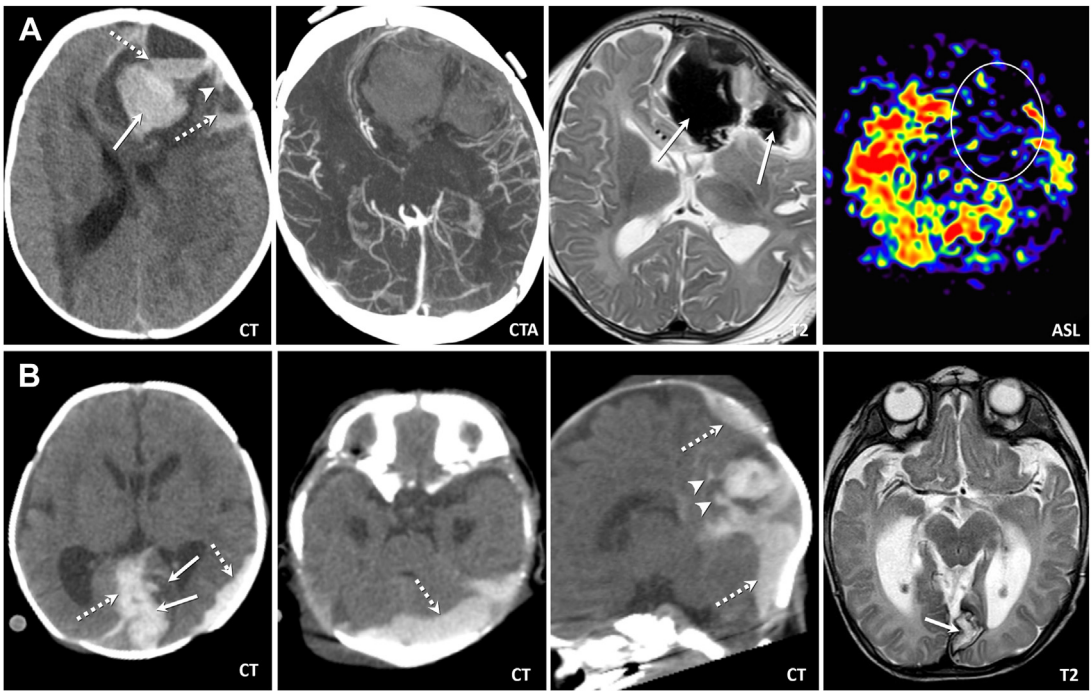

Fig. 9. Coagulopathy-related hemorrhage. (*A*) A 3 month old male patient with increased fussiness and vomiting. Head CT demonstrates a huge lobular left frontal lobe IPH (*arrow*) and adjacent subarachnoid hemorrhage (*arrowhead*). Multiple fluid–fluid levels are identified consistent with nonclotting blood products (*dashed arrows*). CTA was performed, which shows no evidence of shunting lesion, aneurysm, or dural sinus thrombosis. MR imaging performed after hemicraniectomy demonstrates T2 hypointense hemorrhage (*arrows*) with surrounding edema. MRA (not shown) and ASL images show no evidence of shunting (ASL, region outlined by circle). Detailed hematological studies identified a profound coagulopathy secondary to acquired vitamin K deficiency in the setting of autosomal recessive progressive familial intrahepatic cholestasis-type 4. Follow-up MR imaging/MRA/MRV as the clot retracted showed no vascular abnormalities. (*B*) An 11 day old female infant (38 weeks' gestation) with congenital diaphragmatic hernia and pulmonary hypoplasia, on ECMO for pulmonary hypertension and respiratory arrest. Dramatic hematocrit drop triggered imaging, which revealed a large left hemothorax and ICH on head CT. Head CT demonstrates extensive multicompartment ICH with localized parenchymal hemorrhage and adjacent edema in the left occipital lobe (*arrows*), extensive subdural hemorrhage (*dashed arrows* on axial and sagittal CT images) and adjacent subarachnoid hemorrhage (*arrowheads* on sagittal CT image). Follow-up MR (T2) 3 months later showed residual encephalomalacia with hemosiderin staining in the left occipital lobe, which is likely the sequelae of infarction with hemorrhagic transformation (T2, *arrow*). No abnormality on MRA, MRV, or ASL (not shown).

severe pulmonary disease (including therapeutic anticoagulation and extracorporeal membrane oxygenation [ECMO]) is more common in younger children, particularly in infants.[10] When HS is associated with congenital cardiac disease, up to 70% have a coagulation deficit, usually iatrogenic.[10] In neonates, alloimmune thrombocytopenia and vitamin K deficiency are also important causes of coagulopathy leading to HS.[122] Routine vitamin K supplementation for neonates has dramatically decreased vitamin K deficiency-related ICH; however, it remains a substantial cause (up to 50% of cases) in countries where supplementation is not standard.[123]

Coagulopathy-related ICH is often multicompartmental and dramatic on imaging. Fluid levels (indicating nonclotted blood products) can be seen both with IPH and extra-axial hemorrhage (Fig. 9). In a cardiac patient, on either anticoagulation or ECMO therapy with a new neurologic deficit or change in mental status, ICH is the diagnosis of exclusion and should be immediately assessed by CT imaging. In the setting of coagulopathy, usually, no vascular cause is identified by CTA or MR imaging/MRA. Nonetheless, it may be important to evaluate the possibility of an anatomic/vascular cause in the acute phase and with delayed follow-up imaging depending upon the clinical scenario. Detailed hematologic/coagulation studies are warranted when no cause of ICH can be documented by comprehensive imaging evaluation.

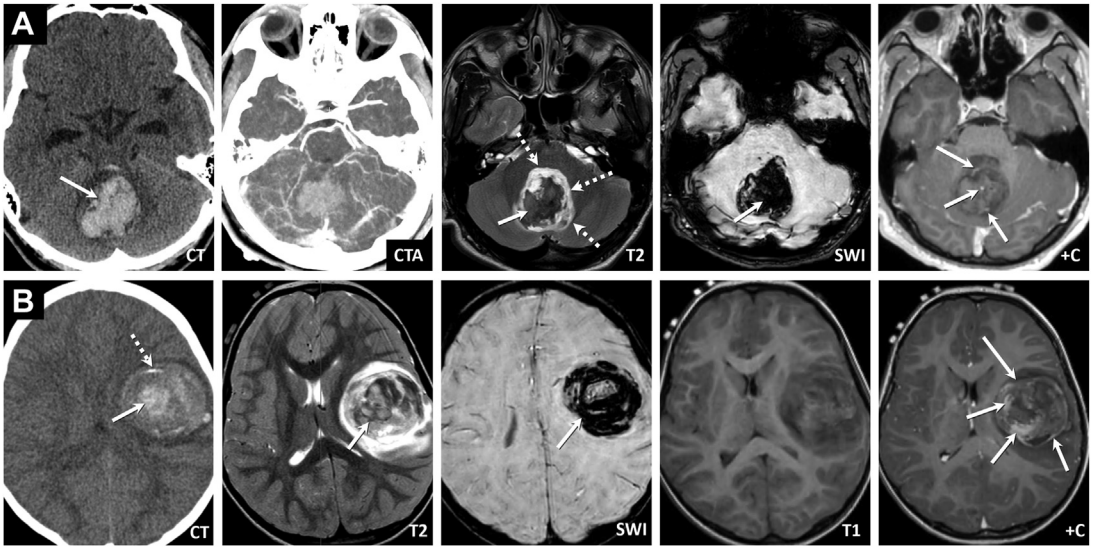

Fig. 10. Hemorrhagic tumor. (*A*) A 15 year old male patient with nausea, vomiting, and new seizure activity. CT demonstrates a localized hemorrhage in the central cerebellum (*arrow*) with minimal surrounding low density (CT). CTA was normal without evidence of aneurysm or shunting lesion (CTA). Follow-up MR imaging examination (T2, SWI, +C) demonstrates a localized hemorrhage (*arrow*) surrounded by irregular T2 hyperintense tissue (*dashed arrow*) suggesting hemorrhage into an underlying mass. There was an extensive susceptibility effect that obscures detail within the lesion on SWI (SWI, *arrow*). No other lesions on SWI. Postcontrast MR imaging demonstrates a small linear area of enhancement within the hemorrhagic region and along its periphery, which may represent vasculature or possibly tumor enhancement (+C, *arrows*). The typical lobular morphology of CCM was not present. ASL was negative for high flow (not shown). Hemorrhagic tumor was felt to be most likely. Low-grade glioneuronal neoplasm (BRAF–) was found on surgical resection. (*B*) An 8 year old female patient with vomiting and seizure activity. Noncontrast CT demonstrates localized hemorrhagic lesion in the left frontal parietal region (CT). Ill-defined intraparenchymal hemorrhage with more prominent hyperdensity centrally is seen on CT (*arrow*). A small calcification present along the ventral margin (*dashed arrow*). T2-weighted images on MR imaging demonstrate extensive T2 hypointense hemorrhage (T2, *arrow*) with blooming susceptibility on SWI images (SWI, *arrow*). The hemorrhage is very heterogeneous suggesting hemorrhage in an underlying lesion, and there is moderate surrounding edema (CT, *dashed arrows*). Postcontrast images demonstrate irregular enhancement within and along the margins of the lesion strongly supporting neoplasm (+C, *arrows*). Resection confirmed pilomyxoid astrocytoma.

Neoplasia

Neoplastic disorders presenting with ICH or having hemorrhage as a predominant imaging finding occurs in 3% to 18% of children with HS.[9,10] Up to 10% of intracranial tumors in children can present with ICH.[124] Tumor-related ICH has most commonly been reported with embryonal tumors and metastatic tumors (neuroblastoma, hepatoblastoma, rhabdomyosarcoma, leukemic infiltration, melanoma, and thyroid origin tumors), but it can also be seen with low-grade (pilocytic, pilomyxoid) and higher grade glial neoplasms.[124–128] In higher grade primary tumors and metastatic lesions, rapid tumor cell proliferation, vascular invasion, tumor neovascularization with fragile blood vessels, and tumor necrosis are likely causative. In pilocytic astrocytomas, dysplastic capillaries with "glomeruloid" morphology, vessel hyalinization, and intratumoral microaneurysms have been described.[129] When intratumoral hemorrhage involves only a part of the tumor, imaging diagnosis of tumor-related hemorrhage is typically straightforward. When intratumoral hemorrhage is diffusely noted throughout the tumor with the disruption of tumor architecture, the diagnosis may be more challenging. Tumoral hemorrhage may mimic CCM or bland IPH. A large amount of edema surrounding the hematoma, patchy hemorrhage occupying only a portion of an identified lesion, and internal "tumor like" enhancement or signal may provide clues (**Fig. 10**). Careful imaging follow-up as the hemorrhage resolves may sometimes be the only way to make the diagnosis.

Other conditions

Other conditions can be associated with HS in children, though less commonly than those entities covered thus far. These include a variety of noninflammatory steno-occlusive arteriopathies (moyamoya arteriopathies), inflammatory arteriopathies

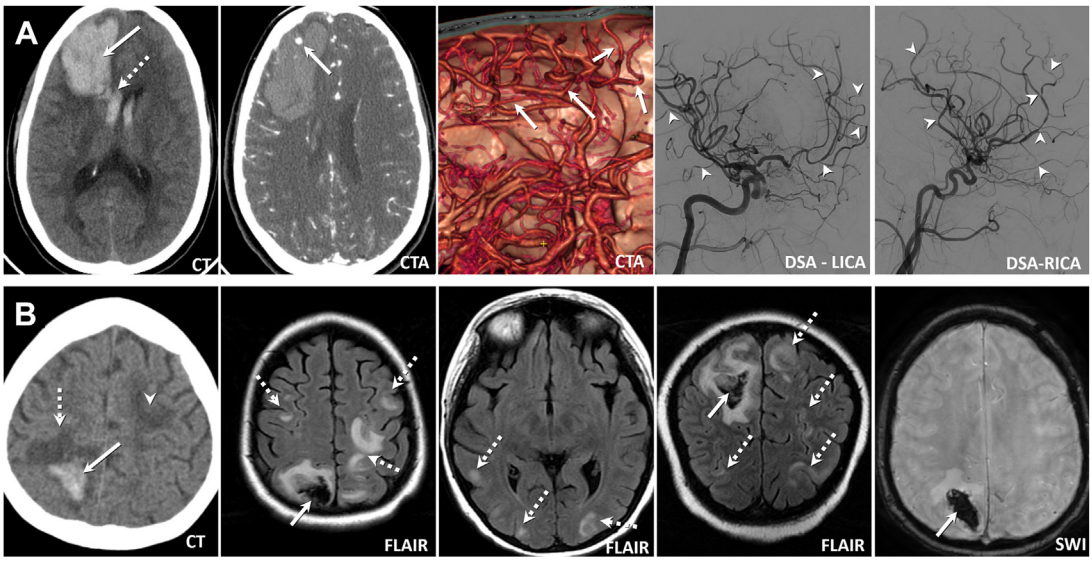

Fig. 11. Other causes. (*A*) Secondary central nervous system (CNS) vasculitis and pseudoaneurysm. A 15 year old female patient, newly diagnosed systemic lupus erythematosus (SLE) with acute onset of severe headache. CT demonstrates an IPH in the left frontal lobe (CT, *arrow*) with intraventricular extension (*dashed arrow*). CTA demonstrates a focal area of collection of extravascular contrast within the ventral margin of the hematoma without direct continuity to other vessels (CTA, *arrow*). The finding suggests a pseudoaneurysm or localized contrast extravasation ("spot-sign"). Luminal irregularity involving multiple vessels suggests vasculitis and/or vasospasm (*arrows* on 3D volume reconstruction image). Decompressive craniotomy was performed with clipping/exclusion of the pseudoaneurysm and partial hematoma evacuation. Subsequent catheter directed-DSA shows widespread, multifocal, segmental luminal constriction irregularly involving cortical branch arteries throughout the left internal carotid artery distribution (DSA-LICA) and right internal carotid artery distribution (DSA-RICA) (*arrowheads*) as well as posterior cerebral arteries (not shown) consistent with CNS vasculitis. Follow-up angiogram 4 months after immunosuppressive treatment (not shown) for presumed SLE-related vasculitis showed improvement in vessel narrowing with mild irregularity remaining. (*B*) Hemorrhagic posterior reversible encephalopathy syndrome (PRES). A 12 year old male patient with relapsed ALL after bone marrow transplant. Two seizures in the setting of marked hypertension. CT demonstrated localized hemorrhage within the right parietal lobe (CT, *arrow*) with moderate surrounding edema (CT, dashed *arrow*) and edema in the left frontal lobe (CT, *arrowhead*). MR imaging showed localized subcortical hemorrhage in the right parietal lobe with moderate surrounding edema. Axial and coronal T2 FLAIR images (FLAIR) show multifocal regions of cortical and subcortical edema throughout the brain parenchyma in a pattern consistent with PRES (*dashed arrows*) and focal T2 hypointensity indicative of hemorrhage (*arrow*). Localized marked susceptibility effect on SWI in the area of T2 FLAIR signal hypointensity (SWI, *arrow*) consistent with hemorrhage. No evidence of venous thrombosis on MRV, SWI, or postcontrast MR imaging (not shown). No abnormal flow-related enhancement on ASL imaging (not shown).

(primary and secondary central nervous system angiitis), and arteriopathies resulting from maladaptive responses to endothelial injury (posterior reversible encephalopathy syndrome and reversible cerebral vasoconstriction syndrome). These conditions typically present in school-age children and adolescents. The clinical context, MR imaging findings and catheter-directed DSA features aid in the differential diagnosis[87,130–134] (**Fig. 11**).

SUMMARY

HS is an important cause of neurologic morbidity and mortality in children and is more common than ischemic stroke between the ages of 1 and 14 years, a notable contradistinction relative to adult stroke epidemiology. Rapid neuroimaging is of the utmost importance in making the diagnosis of HS, identifying a likely etiology, and directing acute care. In the neonatal period, HS is usually due to GMH, PVHI, CVT (including MVT), SPH, and coagulopathy. In older children, HS is usually caused by vascular malformations, and less commonly IAA. The differential diagnosis of HS at any age is strongly guided by the pattern of hemorrhage within specific intracranial compartments. CT and MR imaging with flow-sensitive MR imaging (ASL, TOF MRA) and other noninvasive vascular imaging studies (CTA, MRA, and 3D-CEMRI) play a primary role in the initial diagnostic evaluation. Catheter-directed DSA is critical for definitive diagnosis and treatment planning.

CLINICS CARE POINTS

- Vascular malformations are the most common cause of hemorrhagic stroke in children after the neonatal period. When non-traumatic spontaneous intraparenchymal hemorrhage is identified in a child, immediate vascular imaging utilizing CTA (first choice given availability and speed) and/or MRI/MRA (if patient is stable and MRI immediately available) should be performed to exclude a shunting lesion and identify the likely cause. Catheter-directed DSA can be performed for more detailed assessment or if no cause is initially identified on non-invasive imaging given its high spatial and temporal resolution for vascular lesions.
- Cerebral venous thrombosis is an increasingly recognized cause of hemorrhagic stroke throughout childhood. Highest prevalence is in neonates with periventricular hemorrhagic infarction (PVHI), medullary vein thrombosis (MVT), and subpial hemorrhage all likely having venous occlusion as the underlying etiology. In older children, sequelae of infection and prothrombotic states are common causes for CVT.
- In pre-term neonates, most cases of spontaneous intracranial hemorrhage with identified cause are related to germinal matrix hemorrhage and associated pathology (intraventricular hemorrhage, PVHI). While head ultrasound is the primary initial diagnostic tool for initial diagnosis and to inform clinical care, MRI is often used for definitive diagnosis and for prognostic information, often at term equivalent age.
- When isolated non-traumatic subarachnoid hemorrhage occurs in a child, intracranial arterial aneurysm rupture is the diagnosis of exclusion. Immediate CTA is the diagnostic test of choice in this scenario and can identify a cause in 80-95% of patents. Digital subtraction angiography can be performed for further characterization and can identify vascular pathology in up to 13% of CTA negative cases.

REFERENCES

1. Ferriero DM, Fullerton HJ, Bernard TJ, et al. Management of stroke in neonates and children: a scientific statement from the American heart association/American stroke association. Stroke 2019;50(3):e51–96.
2. Beslow LA, Smith SE, Vossough A, et al. Hemorrhagic transformation of childhood arterial ischemic stroke. Stroke 2011;42(4):941–6.
3. Hollist M, Au K, Morgan L, et al. Pediatric stroke: overview and recent updates. Aging Dis 2021;12(4):1043–55.
4. Fullerton HJ, Wu YW, Zhao S, et al. Risk of stroke in children: ethnic and gender disparities. Neurology 2003;61(2):189–94.
5. Broderick J, Talbot GT, Prenger E, et al. Stroke in children within a major metropolitan area: the surprising importance of intracerebral hemorrhage. J Child Neurol 1993;8(3):250–5.
6. Jordan LC, Hillis AE. Hemorrhagic stroke in children. Pediatr Neurol 2007;36(2):73–80.
7. Fox CK, Johnston SC, Sidney S, et al. High critical care usage due to pediatric stroke: results of a population-based study. Neurology 2012;79(5):420–7.
8. Romero JM, Rojas-Serrano LF. Current evaluation of intracerebral hemorrhage. Radiol Clin North Am 2023;61(3):479–90.
9. Ciochon UM, Bindslev JBB, Hoei-Hansen CE, et al. Causes and risk factors of pediatric spontaneous intracranial hemorrhage-A systematic review. Diagnostics (Basel) 2022;12(6). https://doi.org/10.3390/diagnostics12061459.
10. Boulouis G, Stricker S, Benichi S, et al. Etiology of intracerebral hemorrhage in children: cohort study, systematic review, and meta-analysis. J Neurosurg Pediatr 2021;27(3):357–63.
11. Boulouis G, Blauwblomme T, Hak JF, et al. Nontraumatic pediatric intracerebral hemorrhage. Stroke 2019;50(12):3654–61.
12. Bruno CJ, Beslow LA, Witmer CM, et al. Haemorrhagic stroke in term and late preterm neonates. Arch Dis Child Fetal Neonatal Ed 2014;99(1):F48–53.
13. Cole L, Dewey D, Letourneau N, et al. Clinical characteristics, risk factors, and outcomes associated with neonatal hemorrhagic stroke: a population-based case-control study. JAMA Pediatr 2017;171(3):230–8.
14. Sandoval Karamian AG, Yang QZ, Tam LT, et al. Intracranial hemorrhage in term and late-preterm neonates: an institutional perspective. AJNR Am J Neuroradiol 2022;43(10):1494–9.
15. Srivastava R, Mailo J, Dunbar M. Perinatal stroke in fetuses, preterm and term infants. Semin Pediatr Neurol 2022;43:100988.
16. Armstrong-Wells J, Johnston SC, Wu YW, et al. Prevalence and predictors of perinatal hemorrhagic stroke: results from the kaiser pediatric stroke study. Pediatrics 2009;123(3):823–8.
17. Shellhaas RA, Smith SE, O'Tool E, et al. Mimics of childhood stroke: characteristics of a prospective cohort. Pediatrics 2006;118(2):704–9.

18. Pangprasertkul S, Borisoot W, Buawangpong N, et al. Comparison of arterial ischemic and hemorrhagic pediatric stroke in etiology, risk factors, clinical manifestations, and prognosis. Pediatr Emerg Care 2022;38(9):e1569–73.
19. Gerstl L, Weinberger R, Heinen F, et al. Arterial ischemic stroke in infants, children, and adolescents: results of a Germany-wide surveillance study 2015-2017. J Neurol 2019;266(12):2929–41.
20. Morgenstern LB, Hemphill JC 3rd, Anderson C, et al. Guidelines for the management of spontaneous intracerebral hemorrhage: a guideline for healthcare professionals from the American Heart Association/American Stroke Association. Stroke 2010;41(9):2108–29.
21. Dubosh NM, Bellolio MF, Rabinstein AA, et al. Sensitivity of early brain computed tomography to exclude aneurysmal subarachnoid hemorrhage: a systematic review and meta-analysis. Stroke 2016;47(3):750–5.
22. Sporns PB, Psychogios MN, Fullerton HJ, et al. Neuroimaging of pediatric intracerebral hemorrhage. J Clin Med 2020;9(5). https://doi.org/10.3390/jcm9051518.
23. Srinivasan VM, Gressot LV, Daniels BS, et al. Management of intracerebral hemorrhage in pediatric neurosurgery. Surg Neurol Int 2016;7(Suppl 44):S1121–6.
24. Jain A, Malhotra A, Payabvash S. Imaging of spontaneous intracerebral hemorrhage. Neuroimaging Clin N Am 2021;31(2):193–203.
25. Mirsky DM, Beslow LA, Amlie-Lefond C, et al. Pathways for neuroimaging of childhood stroke. Pediatr Neurol 2017;69:11–23.
26. Kidwell CS, Chalela JA, Saver JL, et al. Comparison of MRI and CT for detection of acute intracerebral hemorrhage. JAMA 2004;292(15):1823–30.
27. Hak JF, Boulouis G, Kerleroux B, et al. Arterial spin labeling for the etiological workup of intracerebral hemorrhage in children. Stroke 2022;53(1):185–93.
28. Lin N, Smith ER, Scott RM, et al. Safety of neuroangiography and embolization in children: complication analysis of 697 consecutive procedures in 394 patients. J Neurosurg Pediatr 2015;16(4):432–8.
29. Harrar DB, Sun LR, Goss M, et al. Cerebral digital subtraction angiography in acute intracranial hemorrhage: considerations in critically ill children. J Child Neurol 2022;37(8–9):693–701.
30. Hino A, Fujimoto M, Yamaki T, et al. Value of repeat angiography in patients with spontaneous subcortical hemorrhage. Stroke 1998;29(12):2517–21.
31. Ogilvy CS, Heros RC, Ojemann RG, et al. Angiographically occult arteriovenous malformations. J Neurosurg 1988;69(3):350–5.
32. Intrapiromkul J, Northington F, Huisman TA, et al. Accuracy of head ultrasound for the detection of intracranial hemorrhage in preterm neonates: comparison with brain MRI and susceptibility-weighted imaging. J Neuroradiol 2013;40(2):81–8.
33. Elkhunovich M, Sirody J, McCormick T, et al. The utility of cranial ultrasound for detection of intracranial hemorrhage in infants. Pediatr Emerg Care 2018;34(2):96–101.
34. Dudink J, Jeanne Steggerda S, Horsch S. State-of-the-art neonatal cerebral ultrasound: technique and reporting. Pediatr Res 2020;87(Suppl 1):3–12.
35. Hinojosa-Rodríguez M, Harmony T, Carrillo-Prado C, et al. Clinical neuroimaging in the preterm infant: diagnosis and prognosis. Neuroimage Clin 2017;16:355–68.
36. Roy B, Walker K, Morgan C, et al. Epidemiology and pathogenesis of stroke in preterm infants: a systematic review. J Neonatal Perinat Med 2022;15(1):11–8.
37. Elgendy MM, Puthuraya S, LoPiccolo C, et al. Neonatal stroke: clinical characteristics and neurodevelopmental outcomes. Pediatr Neonatol 2022;63(1):41–7.
38. Papile LA, Burstein J, Burstein R, et al. Incidence and evolution of subependymal and intraventricular hemorrhage: a study of infants with birth weights less than 1,500 gm. J Pediatr 1978;92(4):529–34.
39. Buchmayer J, Kasprian G, Giordano V, et al. Routine use of cerebral magnetic resonance imaging in infants born extremely preterm. J Pediatr 2022;248:74–80.e1.
40. Nataraj P, Svojsik M, Sura L, et al. Comparing head ultrasounds and susceptibility-weighted imaging for the detection of low-grade hemorrhages in preterm infants. J Perinatol 2021;41(4):736–42.
41. You SK. Neuroimaging of germinal matrix and intraventricular hemorrhage in premature infants. J Korean Neurosurg Soc 2023;66(3):239–46.
42. Parodi A, Govaert P, Horsch S, et al. Cranial ultrasound findings in preterm germinal matrix haemorrhage, sequelae and outcome. Pediatr Res 2020;87(Suppl 1):13–24.
43. Gould SJ, Howard S, Hope PL, et al. Periventricular intraparenchymal cerebral haemorrhage in preterm infants: the role of venous infarction. J Pathol 1987;151(3):197–202.
44. Volpe JJ. Intracranial hemorrhage: germinal matrix-Intraventircular hemorrhage of the premature infant. Neurology of the Newborn. 5th edition. Philadelphia, PA: Saunders/Elsevier; 2008. chap 11.
45. Dudink J, Lequin M, Weisglas-Kuperus N, et al. Venous subtypes of preterm periventricular haemorrhagic infarction. Arch Dis Child Fetal Neonatal Ed 2008;93(3):F201–6.
46. Tortora D, Severino M, Malova M, et al. Differences in subependymal vein anatomy may predispose preterm infants to GMH-IVH. Arch Dis Child Fetal Neonatal Ed 2018;103(1):F59–65.
47. Cizmeci MN, de Vries LS, Ly LG, et al. Periventricular hemorrhagic infarction in very preterm infants:

characteristic sonographic findings and association with neurodevelopmental outcome at age 2 years. J Pediatr 2020;217:79–85.e1.
48. Soltirovska Salamon A, Groenendaal F, van Haastert IC, et al. Neuroimaging and neurodevelopmental outcome of preterm infants with a periventricular haemorrhagic infarction located in the temporal or frontal lobe. Dev Med Child Neurol 2014;56(6):547–55.
49. Bassan H, Feldman HA, Limperopoulos C, et al. Periventricular hemorrhagic infarction: risk factors and neonatal outcome. Pediatr Neurol 2006;35(2):85–92.
50. Bassan H, Limperopoulos C, Visconti K, et al. Neurodevelopmental outcome in survivors of periventricular hemorrhagic infarction. Pediatrics 2007;120(4):785–92.
51. Roze E, Benders MJ, Kersbergen KJ, et al. Neonatal DTI early after birth predicts motor outcome in preterm infants with periventricular hemorrhagic infarction. Pediatr Res 2015;78(3):298–303.
52. Pin JN, Leonardi L, Nosadini M, et al. Deep medullary vein thrombosis in newborns: a systematic literature review. Neonatology 2023;120(5):539–47.
53. Khalatbari H, Wright JN, Ishak GE, et al. Deep medullary vein engorgement and superficial medullary vein engorgement: two patterns of perinatal venous stroke. Pediatr Radiol 2021;51(5):675–85.
54. Benninger KL, Benninger TL, Moore-Clingenpeel M, et al. Deep medullary vein white matter injury global severity score predicts neurodevelopmental impairment. J Child Neurol 2021;36(4):253–61.
55. Christensen R, Krishnan P, deVeber G, et al. Cerebral venous sinus thrombosis in preterm infants. Stroke 2022;53(7):2241–8.
56. Lai LM, Sato TS, Kandemirli SG, et al. Neuroimaging of neonatal stroke: venous focus. Radiographics 2024;44(2):e230117.
57. Pinto C, Cunha B, Pinto MM, et al. Subpial hemorrhage : a distinctive neonatal stroke pattern. Clin Neuroradiol 2022;32(4):1057–65.
58. Barreto ARF, Carrasco M, Dabrowski AK, et al. Subpial hemorrhage in neonates: what radiologists need to know. AJR Am J Roentgenol 2021;216(4):1056–65.
59. Friede RL. Subpial hemorrhage in infants. J Neuropathol Exp Neurol 1972;31(3):548–56.
60. Marín-Padilla M. Developmental neuropathology and impact of perinatal brain damage. I: hemorrhagic lesions of neocortex. J Neuropathol Exp Neurol 1996;55(7):758–73.
61. Zhuang X, Jin K, Li J, et al. Subpial hemorrhages in neonates: imaging features, clinical factors and outcomes. Sci Rep 2023;13(1):3408.
62. Cain DW, Dingman AL, Armstrong J, et al. Subpial hemorrhage of the neonate. Stroke 2020;51(1):315–8.
63. Heller C, Heinecke A, Junker R, et al. Cerebral venous thrombosis in children: a multifactorial origin. Circulation 2003;108(11):1362–7.
64. deVeber G, Andrew M, Adams C, et al. Cerebral sinovenous thrombosis in children. N Engl J Med 2001;345(6):417–23.
65. Carvalho KS, Bodensteiner JB, Connolly PJ, et al. Cerebral venous thrombosis in children. J Child Neurol 2001;16(8):574–80.
66. Lynch JK, Nelson KB. Epidemiology of perinatal stroke. Curr Opin Pediatr 2001;13(6):499–505.
67. Devianne J, Legris N, Crassard I, et al. Epidemiology, clinical features, and outcome in a cohort of adolescents with cerebral venous thrombosis. Neurology 2021;97(19):e1920–32.
68. Otite FO, Vanguru H, Anikpezie N, et al. Contemporary incidence and burden of cerebral venous sinus thrombosis in children of the United States. Stroke 2022;53(12):e496–9.
69. Ferro JM, Canhão P, Stam J, et al. Prognosis of cerebral vein and dural sinus thrombosis: results of the international study on cerebral vein and dural sinus thrombosis (ISCVT). Stroke 2004;35(3):664–70.
70. Dlamini N, Billinghurst L, Kirkham FJ. Cerebral venous sinus (sinovenous) thrombosis in children. Neurosurg Clin N Am 2010;21(3):511–27.
71. Cornelius LP, Elango N, Jeyaram VK. Clinico-etiological factors, neuroimaging characteristics and outcome in pediatric cerebral venous sinus thrombosis. Ann Indian Acad Neurol 2021;24(6):901–7.
72. Leach JL, Fortuna RB, Jones BV, et al. Imaging of cerebral venous thrombosis: current techniques, spectrum of findings, and diagnostic pitfalls. Radiographics 2006;26(Suppl 1):S19–41. discussion S42-3.
73. Bracken J, Barnacle A, Ditchfield M. Potential pitfalls in imaging of paediatric cerebral sinovenous thrombosis. Pediatr Radiol 2013;43(2):219–31.
74. Canedo-Antelo M, Baleato-González S, Mosqueira AJ, et al. Radiologic clues to cerebral venous thrombosis. Radiographics 2019;39(6):1611–28.
75. Idbaih A, Boukobza M, Crassard I, et al. MRI of clot in cerebral venous thrombosis: high diagnostic value of susceptibility-weighted images. Stroke 2006;37(4):991–5.
76. Teksam M, Moharir M, Deveber G, et al. Frequency and topographic distribution of brain lesions in pediatric cerebral venous thrombosis. AJNR Am J Neuroradiol 2008;29(10):1961–5.
77. Berfelo FJ, Kersbergen KJ, van Ommen CH, et al. Neonatal cerebral sinovenous thrombosis from symptom to outcome. Stroke 2010;41(7):1382–8.
78. Wu YW, Hamrick SE, Miller SP, et al. Intraventricular hemorrhage in term neonates caused by sinovenous thrombosis. Ann Neurol 2003;54(1):123–6.

79. Usman U, Wasay M. Mechanism of neuronal injury in cerebral venous thrombosis. J Pakistan Med Assoc 2006;56(11):509–12.
80. Kanaiwa H, Kuchiwaki H, Inao S, et al. Changes in the cerebrocortical capillary network following venous sinus occlusion in cats. Surg Neurol 1995; 44(2):172–9. discussion 179-80.
81. Dinç Y, Özpar R, Hakyemez B, et al. The relationship between early neurological deterioration, poor clinical outcome, and venous collateral score in cerebral venous sinus thrombosis. Neurological Sciences and Neurophysiology 2021;38(3):158–65.
82. Ritchey Z, Hollatz AL, Weitzenkamp D, et al. Pediatric cortical vein thrombosis: frequency and association with venous infarction. Stroke 2016;47(3): 866–8.
83. Cervós-Navarro J, Kannuki S, Matsumoto K. Neuropathological changes following occlusion of the superior sagittal sinus and cerebral veins in the cat. Neuropathol Appl Neurobiol 1994;20(2):122–9.
84. Liu L, Zhou C, Jiang H, et al. Cortical vein involvement and its influence in a cohort of adolescents with cerebral venous thrombosis. Thromb J 2023; 21(1):78.
85. Coutinho JM, Gerritsma JJ, Zuurbier SM, et al. Isolated cortical vein thrombosis: systematic review of case reports and case series. Stroke 2014;45(6): 1836–8.
86. Liang J, Chen H, Li Z, et al. Cortical vein thrombosis in adult patients of cerebral venous sinus thrombosis correlates with poor outcome and brain lesions: a retrospective study. BMC Neurol 2017; 17(1):219.
87. Liu J, Wang D, Lei C, et al. Etiology, clinical characteristics and prognosis of spontaneous intracerebral hemorrhage in children: a prospective cohort study in China. J Neurol Sci 2015;358(1–2):367–70.
88. Meyer-Heim AD, Boltshauser E. Spontaneous intracranial haemorrhage in children: aetiology, presentation and outcome. Brain Dev 2003;25(6):416–21.
89. Jordan LC, Johnston SC, Wu YW, et al. The importance of cerebral aneurysms in childhood hemorrhagic stroke: a population-based study. Stroke 2009;40(2):400–5.
90. Kumar R, Shukla D, Mahapatra AK. Spontaneous intracranial hemorrhage in children. Pediatr Neurosurg 2009;45(1):37–45.
91. El-Ghanem M, Kass-Hout T, Kass-Hout O, et al. Arteriovenous malformations in the pediatric population: review of the existing literature. Interv Neurol 2016;5(3–4):218–25.
92. Oulasvirta E, Koroknay-Pál P, Hafez A, et al. Characteristics and long-term outcome of 127 children with cerebral arteriovenous malformations. Neurosurgery 2019;84(1):151–9.
93. Pepper J, Lamin S, Thomas A, et al. Clinical features and outcome in pediatric arteriovenous malformation: institutional multimodality treatment. Childs Nerv Syst 2023;39(4):975–82.
94. Ai X, Ye Z, Xu J, et al. The factors associated with hemorrhagic presentation in children with untreated brain arteriovenous malformation: a meta-analysis. J Neurosurg Pediatr 2018;23(3):343–54.
95. Lu A, Winkler E, Morshed R, et al. 196 increased hemorrhage risk with brain AVM-associated aneurysms in children. Neurosurgery 2023;69:32.
96. Dinc N, Won SY, Quick-Weller J, et al. Prognostic variables and outcome in relation to different bleeding patterns in arteriovenous malformations. Neurosurg Rev 2019;42(3):731–6.
97. Zwanzger C, López-Rueda A, Campodónico D, et al. Usefulness of CT angiography for characterizing cerebral arteriovenous malformations presenting as hemorrhage: comparison with digital subtraction angiography. Radiologia (Engl Ed) 2020;62(5):392–9. Utilidad de la angio-TC para la caracterización de malformaciones arteriovenosas cerebrales con presentación hemorrágica comparada con la angiografía por sustracción digital.
98. Li J, Ji Z, Yu J, et al. Angioarchitecture and prognosis of pediatric intracranial pial arteriovenous fistula. Stroke Vasc Neurol 2023;8(4):292–300.
99. Requejo F, Jaimovich R, Marelli J, et al. Intracranial pial fistulas in pediatric population. Clinical features and treatment modalities. Childs Nerv Syst 2015;31(9):1509–14.
100. Lim J, Kuo CC, Waqas M, et al. A systematic review of non-galenic pial arteriovenous fistulas. World Neurosurg 2023;170:226–35.e3.
101. Hetts SW, Keenan K, Fullerton HJ, et al. Pediatric intracranial nongalenic pial arteriovenous fistulas: clinical features, angioarchitecture, and outcomes. AJNR Am J Neuroradiol 2012;33(9):1710–9.
102. Walcott BP, Smith ER, Scott RM, et al. Pial arteriovenous fistulae in pediatric patients: associated syndromes and treatment outcome. J Neurointerventional Surg 2013;5(1):10–4.
103. Linscott LL, Leach JL, Jones BV, et al. Developmental venous anomalies of the brain in children – imaging spectrum and update. Pediatr Radiol 2016;46(3):394–406. quiz 391-3.
104. Abdulrauf SI, Kaynar MY, Awad IA. A comparison of the clinical profile of cavernous malformations with and without associated venous malformations. Neurosurgery 1999;44(1):41–6. discussion 46-7.
105. Jaman E, Abdallah HM, Zhang X, et al. Clinical characteristics of familial and sporadic pediatric cerebral cavernous malformations and outcomes. J Neurosurg Pediatr 2023;32(4):506–13.
106. Zabramski JM, Wascher TM, Spetzler RF, et al. The natural history of familial cavernous malformations: results of an ongoing study. J Neurosurg 1994; 80(3):422–32.

107. Al-Shahi SR, Berg MJ, Morrison L, et al. Hemorrhage from cavernous malformations of the brain: definition and reporting standards. Angioma Alliance Scientific Advisory Board. Stroke 2008;39(12):3222–30.
108. Nikoubashman O, Di Rocco F, Davagnanam I, et al. Prospective hemorrhage rates of cerebral cavernous malformations in children and adolescents based on MRI appearance. AJNR Am J Neuroradiol 2015; 36(11):2177–83.
109. Gross BA, Du R, Orbach DB, et al. The natural history of cerebral cavernous malformations in children. J Neurosurg Pediatr 2016;17(2):123–8.
110. Gross BA, Du R. Hemorrhage from cerebral cavernous malformations: a systematic pooled analysis. J Neurosurg 2017;126(4):1079–87.
111. Flemming KD, Kumar S, Brown RD, et al. Predictors of initial presentation with hemorrhage in patients with cavernous malformations. World Neurosurg 2020;133:e767–73.
112. Jeon JS, Kim JE, Chung YS, et al. A risk factor analysis of prospective symptomatic haemorrhage in adult patients with cerebral cavernous malformation. J Neurol Neurosurg Psychiatry 2014;85(12): 1366–70.
113. Santos AN, Rauschenbach L, Saban D, et al. Natural course of cerebral cavernous malformations in children: a five-year follow-up study. Stroke 2022;53(3):817–24.
114. Paddock M, Lanham S, Gill K, et al. Pediatric cerebral cavernous malformations. Pediatr Neurol 2021;116:74–83.
115. Hetts SW, Narvid J, Sanai N, et al. Intracranial aneurysms in childhood: 27-year single-institution experience. AJNR Am J Neuroradiol 2009;30(7): 1315–24.
116. Xu R, Xie ME, Yang W, et al. Epidemiology and outcomes of pediatric intracranial aneurysms: comparison with an adult population in a 30-year, prospective database. J Neurosurg Pediatr 2021; 28(6):685–94.
117. Perry JJ, Stiell IG, Sivilotti ML, et al. Sensitivity of computed tomography performed within six hours of onset of headache for diagnosis of subarachnoid haemorrhage: prospective cohort study. BMJ 2011;343:d4277.
118. Levinson S, Pendharkar AV, Gauden AJ, et al. Modern imaging of aneurysmal subarachnoid hemorrhage. Radiol Clin North Am 2023;61(3):457–65.
119. Heit JJ, Pastena GT, Nogueira RG, et al. Cerebral angiography for evaluation of patients with CT angiogram-negative subarachnoid hemorrhage: an 11-year experience. AJNR Am J Neuroradiol 2016;37(2):297–304.
120. Aeron G, Abruzzo TA, Jones BV. Clinical and imaging features of intracranial arterial aneurysms in the pediatric population. Radiographics 2012;32(3): 667–81.
121. Clarke JE, Luther E, Oppenhuizen B, et al. Intracranial aneurysms in the infant population: an institutional case series and individual participant data meta-analysis. J Neurosurg Pediatr 2022;1–11.
122. Tan AP, Svrckova P, Cowan F, et al. Intracranial hemorrhage in neonates: a review of etiologies, patterns and predicted clinical outcomes. Eur J Paediatr Neurol 2018;22(4):690–717.
123. Xie LL, Jiang L. Arterial ischemic stroke and hemorrhagic stroke in Chinese children: a retrospective analysis. Brain Dev 2014;36(2):153–8.
124. Laurent JP, Bruce DA, Schut L. Hemorrhagic brain tumors in pediatric patients. Childs Brain 1981; 8(4):263–70.
125. Teshigawara A, Kimura T, Ichi S. Critical cerebellar hemorrhage due to pilocytic astrocytoma in a child: a case report. Surg Neurol Int 2021;12:448.
126. Yadav SS, Lawande MA, Patkar DA, et al. Rare case of hemorrhagic brain metastasis from hepatoblastoma. J Pediatr Neurosci 2012;7(1):73–4.
127. Sidi-Fragandrea V, Hatzipantelis E, Panagopoulou P, et al. Isolated central nervous system recurrence in a child with stage IV neuroblastoma. Pediatr Hematol Oncol 2010;27(5):387–92.
128. Gokce M, Aytac S, Altan I, et al. Intracerebral metastasis in pediatric acute lymphoblastic leukemia: a rare presentation. J Pediatr Neurosci 2012; 7(3):208–10.
129. Donofrio CA, Gagliardi F, Callea M, et al. Pediatric cerebellar pilocytic astrocytoma presenting with spontaneous intratumoral hemorrhage. Neurosurg Rev 2020;43(1):9–16.
130. Ge P, Zhang Q, Ye X, et al. Clinical features, surgical treatment, and long-term outcome in children with hemorrhagic moyamoya disease. J Stroke Cerebrovasc Dis 2018;27(6):1517–23.
131. Maldonado-Soto AR, Fryer RH. Reversible cerebral vasoconstriction syndrome in children: an update. Semin Pediatr Neurol 2021;40:100936.
132. Ducros A, Fiedler U, Porcher R, et al. Hemorrhagic manifestations of reversible cerebral vasoconstriction syndrome: frequency, features, and risk factors. Stroke 2010;41(11):2505–11.
133. Hefzy HM, Bartynski WS, Boardman JF, et al. Hemorrhage in posterior reversible encephalopathy syndrome: imaging and clinical features. AJNR Am J Neuroradiol 2009;30(7):1371–9.
134. Chen TH. Childhood posterior reversible encephalopathy syndrome: clinicoradiological characteristics, managements, and outcome. Front Pediatr 2020;8:585.

EDITORIAL

Modified Pediatric ASPECTS

Building Tools for Future Pediatric Stroke Studies

Sarah Lee, MD, and Christine K. Fox, MD, MAS

Neurology® 2021;97:570-571. doi:10.1212/WNL.0000000000012543

Correspondence
Christine K. Fox
christine.fox@ucsf.edu

The Alberta Stroke Program Early CT Score (ASPECTS) is a quick and reliable semiquantitative tool to estimate the size of an acute ischemic infarct on a noncontrast head CT.[1] Ten brain regions in the middle cerebral artery territory are evaluated, with 1 point subtracted for each infarcted region; total scores range from 0 to 10. Lower ASPECTS, indicating larger infarct burden, has been associated with higher risk of hemorrhagic transformation and worse outcomes in adult patients with stroke[2] and is one criterion considered in the assessment of eligibility for thrombectomy. A version of this scoring system, the modified pediatric ASPECTS (modASPECTS), was developed to measure infarct size in children using diffusion-weighted sequences on MRI.[3] For modASPECTS, 30 regions are scored, including areas of the anterior and posterior cerebral artery territories in addition to the middle cerebral artery territory.[4] One point is added for each area involved, resulting in a score from 0 to 30, with higher scores indicating more areas of infarct.

RELATED ARTICLE

Research Article
Association of Pediatric ASPECTS and NIH Stroke Scale, Hemorrhagic Transformation, and 12-Month Outcome in Children With Acute Ischemic Stroke
Page 575

In this issue of *Neurology*®, Beslow et al.[5] report a retrospective study of children enrolled in 2 pediatric stroke registries that aimed to measure the association between modASPECTS and clinical stroke severity, hemorrhagic transformation, and outcome. This study is clinically relevant because clinicians have become increasingly interested in extending hyperacute reperfusion therapies to children but need a validated tool for estimating infarct size that can be reliably used in pediatric-specific stroke studies. The authors found that modASPECTS correlates with initial pediatric NIH Stroke Scale (PedNIHSS) measurements, hemorrhage on the acute MRI, and 12-month measurements of the Pediatric Stroke Outcome Measure. Their findings support the face validity of the tool by demonstrating its correlation with clinical outcomes.

The correlation between modASPECTS and PedNIHSS scores in the current study was modest ($\rho = 0.4$), although slightly stronger in the subset of children who had imaging and neurologic examination scored from the same day. How well should modASPECTS correlate with PedNIHSS score? Diffusion-weighted imaging (DWI) is sensitive to small infarcts, and a modASPECTS region is given a point if any part of that region has restricted diffusion—features of scoring that may decrease this correlation. The authors postulated that lack of a stronger correlation may reflect the predilection of children to have a stroke in the basal ganglia, resulting in severe clinical symptoms despite small infarct size. At the opposite end of the spectrum, small punctate infarcts in multiple vascular territories as can be seen in the context of an embolic stroke may lead to a high modASPECTS with a relatively benign clinical examination.

ASPECTS is a major factor in adult treatment selection within 6 hours, but patients presenting between 6 and 24 hours—a more realistic window for pediatric strokes—also require evidence of a mismatch between irreversibly infarcted tissue and penumbral tissue at risk. Another interpretation offered for the less-than-robust correlation found in this study is that children with a healthy system of collateral vessels might have substantial clinical-imaging mismatch after stroke. If this explanation is borne out, it supports the possibility that children could be good candidates for reperfusion therapies. The clinical-imaging mismatch approach was successful in the DWI or CTP Assessment With Clinical Mismatch in the Triage of Wake-Up and Late Presenting Strokes Undergoing Neurointervention With Trevo (DAWN) randomized trial,

From the Division of Child Neurology (S.L.), Department of Neurology, Stanford University, CA; and Departments of Neurology and Pediatrics (C.K.F.), University of California San Francisco.

Go to Neurology.org/N for full disclosures. Funding information and disclosures deemed relevant by the authors, if any, are provided at the end of the article.

which demonstrated the benefit of thrombectomy in a 6- to 24-hour time window for adult patients with a relatively small ischemic core compared to a high NIHSS score.[6]

The study in the current issue had several limitations. ModASPECTS was scored by the same people on the same imaging studies used to evaluate the presence of hemorrhage. The unblinded method introduces a potential source of bias that a longitudinal approach with serial scans, as the authors suggest, would mitigate. In addition, while higher modASPECTS and hemorrhage were associated in the overall cohort, the association was no longer significant in the subset of children >2 years of age with anterior circulation stroke presenting within 24 hours—the subset who would theoretically be candidates for thrombectomy. An inherent limitation of childhood stroke studies is that symptom recognition, clinical diagnosis, and imaging are often delayed. In the current study, more than half of the MRIs that were scored were performed at least a day after stroke ictus, outside the accepted adult treatment windows when infarcts presumably have been completed.

MRI is often the imaging study of choice for children who have a stroke, so a pediatric stroke scoring system using this modality is sensible. However, DWI-ASPECTS, a scoring system to quantify infarct size on MRI in adults, has such a low interrater agreement in some studies that relevance for patient selection has been questioned.[7] While modASPECTS appears to have excellent interrater reliability in prior studies and correlates well with infarct volume in both neonates and older children with stroke,[4,8] it is not yet in widespread clinical use. Whether modASPECTS assessments can be reproduced with fidelity across providers in multiple disciplines at a large number of centers merits further investigation.

The efficacy and safety of early reperfusion therapies in children are uncertain. To conduct studies of hyperacute stroke interventions in children, reliable tools for quick stratification and selection of children must be developed. Adaptation of the NIHSS to the PedNIHSS for use in children was one step along the way. How PedNIHSS or modASPECTS might be best used for pediatric patient selection for hyperacute stroke treatment is not yet clear. Future studies of these and other child-specific tools are of paramount importance to the field of pediatric stroke. Despite some limitations, the results from Beslow et al. continue to lay important groundwork for future pediatric stroke studies by improving our understanding of a potentially important tool for estimating infarct size on MRI in children.

Study Funding

The authors report no targeted funding.

Disclosure

S. Lee and C.K. Fox report no disclosures relevant to the manuscript. Go to Neurology.org/N for full disclosures.

References

1. Barber PA, Demchuk AM, Zhang J, Buchan AM. Validity and reliability of a quantitative computed tomography score in predicting outcome of hyperacute stroke before thrombolytic therapy: ASPECTS Study Group: Alberta Stroke Programme Early CT Score. *Lancet.* 2000;355(9216):1670-1674.
2. Davoli A, Motta C, Koch G, et al. Pretreatment predictors of malignant evolution in patients with ischemic stroke undergoing mechanical thrombectomy. *J Neurointerv Surg.* 2018;10(4):340-344.
3. Wusthoff CJ, Kessler SK, Vossough A, et al. Risk of later seizure after perinatal arterial ischemic stroke: a prospective cohort study. *Pediatrics.* 2011;127(6):e1550-e1557.
4. Beslow LA, Vossough A, Dahmoush HM, et al. Modified pediatric ASPECTS correlates with infarct volume in childhood arterial ischemic stroke. *Front Neurol.* 2012;3:122.
5. Beslow LA, Vossough A, Ichord RN, et al. Association of pediatric ASPECTS and NIH Stroke Scale, hemorrhagic transformation, and 12-month outcome in children with acute ischemic stroke. *Neurology.* 2021;97(12):e1202-e1209.
6. Nogueira RG, Jadhav AP, Haussen DC, et al. Thrombectomy 6 to 24 hours after stroke with a mismatch between deficit and infarct. *N Engl J Med.* 2018;378:11-21.
7. Fahed R, Lecler A, Sabben C, et al. DWI-ASPECTS (diffusion-weighted imaging-Alberta Stroke Program Early Computed Tomography Scores) and DWI-FLAIR (diffusion-weighted imaging-fluid attenuated inversion recovery) mismatch in thrombectomy candidates: an intrarater and interrater agreement study. *Stroke.* 2018;49(1):223-227.
8. Mackay MT, Slavova N, Pastore-Wapp M, et al. Pediatric ASPECTS predicts outcomes following acute symptomatic neonatal arterial stroke. *Neurology.* 2020;94(12):e1259-e1270.

Monitoring Cerebral Perfusion Changes after Revascularization in Patients with Moyamoya Disease by Using Arterial Spin-labeling MR Imaging

Seunghyun Lee, MD • *Tae Jin Yun, MD* • *Roh-Eul Yoo, MD* • *Byung-Woo Yoon, MD* • *Koung Mi Kang, MD* • *Seung Hong Choi, MD* • *Ji-hoon Kim, MD* • *Jeong Eun Kim, MD* • *Chul-Ho Sohn, MD* • *Moon Hee Han, MD*

From the Institute of Radiation Medicine, Seoul National University Medical Research Center, Seoul, Republic of Korea (S.L., T.J.Y., R.E.Y., K.M.K., S.H.C., J.H.K., C.H.S., M.H.H.); Department of Radiology (S.L., T.J.Y., R.E.Y., K.M.K., S.H.C., J.H.K., C.H.S., M.H.H.), Clinical Research Center for Stroke, Clinical Research Institute (B.W.Y.), Department of Neurology (B.W.Y.), and Department of Neurosurgery (J.E.K.), Seoul National University Hospital, 101 Daehangno, Jongno-gu, Seoul 03080, Republic of Korea. Received March 2, 2017; revision requested April 26; final revision received January 30, 2018; accepted February 28. **Address correspondence to** T.J.Y. (e-mail: *radiologyyun@gmail.com*).

Conflicts of interest are listed at the end of this article.

Radiology 2018; ▪▪:1–9 • **https://doi.org/10.1148/radiol.2018170509** • **Content code:** NR

Purpose: To determine whether arterial spin-labeling (ASL) magnetic resonance (MR) imaging could be used to identify changes in cerebral blood flow (CBF), collateral blood flow, and anastomosis site patency after revascularization in patients with moyamoya disease.

Materials and Methods: This retrospective study was conducted in 145 patients with moyamoya disease who underwent middle cerebral artery (MCA)–superficial temporal artery anastomosis. Preoperative, early postoperative, and late postoperative ASL and digital subtraction angiography images were analyzed. In the MCA territory, absolute CBF (hereafter, CBF_{MCA}) and normalized CBF values adjusted to nonanastomosis side (hereafter, $nCBF_{MCA}$) and to cerebellum (hereafter, $nCBF_{Cbll}$) were calculated. Collateral grading in the MCA territory was assessed according to Alberta Stroke Program Early CT Score methodology, and anastomosis site patency were also assessed. Changes in CBF were compared by using one-way analysis of variance with Bonferroni correction for multiple comparisons. Intermodality agreement was determined by κ statistics.

Results: Significant increases in CBF_{MCA}, $nCBF_{MCA}$, and $nCBF_{Cbll}$ were found after revascularization (preoperative and postoperative values of CBF_{MCA}, 35.2 mL/100 g per minute ± 7.8 [mean ± standard deviation] and 51.5 mL/100 g per minute ± 12.0; $nCBF_{MCA}$, 0.73 mL/100 g per minute ± 0.14 and 1.01 mL/100 g per minute ± 0.18; $nCBF_{Cbll}$, 0.74 mL/100 g per minute ± 0.12 and 1.12 mL/100 g per minute ± 0.16; all $P < .001$). Agreements for collateral grading and anastomosis patency between ASL MR imaging and digital subtraction angiography were moderate to good, with weighted κ values of 0.77 (95% confidence interval: 0.73, 0.81) and 0.57 (95% confidence interval: 0.37, 0.76), respectively.

Conclusion: ASL MR imaging can be used to identify perfusion changes in patients with moyamoya disease after revascularization as a noninvasive monitoring tool.

Online supplemental material is available for this article.

Moyamoya disease is a cerebrovascular disease characterized by stenosis or occlusion of the distal portion of the internal carotid arteries with the development of collateral vessels (1,2). Digital subtraction angiography (DSA) is the current reference standard for assessing the extent of moyamoya disease, the presence of collateral vessels, and postoperative anastomosis patency (3). However, DSA is inherently invasive, relatively time consuming, and costly.

By incorporating arterial spin-labeling (ASL) technique, it is possible to quantitatively estimate cerebral blood flow (CBF) at the tissue level by using proton labeling within arterial water (4,5). The primary advantage of ASL is that it is noninvasive and does not expose patients to ionizing radiation or contrast agents (2,5). In addition, although arterial transit artifact is known as a disadvantage for quantitative measurement, it contains important information about late-arriving flow (3). Currently, ASL magnetic resonance (MR) imaging can help grade collateral flow and may complement DSA findings (3,6).

We hypothesized that ASL can be used to quantitatively assess changes in CBF before and after revascularization, that collateral flow grading can be evaluated with ASL imaging, and that ASL parameters reflect impaired anastomosis patency. Therefore, the objective of our study was to determine whether ASL MR imaging can help identify changes in CBF, collateral blood flow, and anastomosis site patency in patients with moyamoya disease after revascularization.

Materials and Methods

Our institutional review board approved this study. Informed consent requirement was waived because of its retrospective nature.

Patient Selection

From January 2010 to March 2016, 295 patients with moyamoya disease who had undergone middle cerebral artery (MCA)–superficial temporal artery anastomosis at

Abbreviations

ASL = arterial spin labeling, CBF = cerebral blood flow, CBF_{MCA} = CBF values of the MCA territory, DSA = digital subtraction angiography, MCA = middle cerebral artery, $nCBF_{CbII}$ = normalized CBF values adjusted to cerebellum, $nCBF_{MCA}$ = normalized CBF values adjusted to nonanastomosis side

Summary

Arterial spin-labeling MR imaging can be used to identify perfusion changes in patients with moyamoya disease after direct revascularization.

Implication for Patient Care

Arterial spin-labeling perfusion-weighted MR imaging can identify perfusion changes after revascularization in patients with moyamoya disease without exposing the patients to ionizing radiation or contrast agents.

our institution were screened for enrollment by using our radiology report database. The inclusion criteria were as follows: *(a)* both ASL perfusion MR images and DSA images were available at baseline and at follow-up (41 patients were excluded), *(b)* ASL perfusion MR imaging was performed with the standard protocol (25 patients were excluded), *(c)* ASL perfusion MR imaging was of good quality (one patient was excluded), and *(d)* direct revascularization was performed because of moyamoya disease (83 patients were excluded). After excluding 150 patients who failed to meet the inclusion criteria, ASL and DSA images of the remaining 145 patients were analyzed. Among the 145 patients, 11 had undergone bilateral MCA–superficial temporal artery anastomosis surgery. There were 47 male patients (mean age, 34.2 years; range, 16–60 years) and 98 female patients (mean age, 39.0 years; range, 15–65 years) with an overall mean age of 37.4 years (range, 15–65 years).

ASL and DSA Image Acquisition

The standard imaging regimen for patients with moyamoya disease at our institution is defined as baseline ASL imaging and DSA within 2 months before surgery for diagnosis of moyamoya disease, early postoperative ASL imaging within 1 week after surgery to screen for acute complications of surgery without performing DSA, and late postoperative ASL imaging and DSA within 7 months after surgery for routine follow-up.

For these 145 patients, baseline and late postoperative ASL imaging and DSA were performed at 40.0 days ± 6.0 (standard deviation) before surgery and 196.7 days ± 12.6 after surgery. Only 79 patients were imaged for early postoperative follow-up at 10.4 days ± 7.9 after the surgery without DSA imaging. The most common cause of early postoperative imaging (n = 79) was a clinical suspicion of hyperperfusion syndrome (n = 55). The other causes were preoperative bleeding, hyperthyroidism, aneurysm, infarction, and a family history of moyamoya disease or stroke (n = 24). In 11 patients who underwent bilateral MCA–superficial temporal artery anastomosis surgery, follow-up DSA and ASL images after bilateral surgery were analyzed.

ASL perfusion MR images were acquired with 1.5-T or 3.0-T MR imagers (Signa HDxt, GE Healthcare, Milwaukee, Wis [n = 281]; or Discovery 750, GE Healthcare [n = 88]) by using an eight-channel or 32-channel head coil. For patients with moyamoya disease, the following sequences were performed based on the standard protocol of our institution: axial T2-weighted, axial T1-weighted, axial fluid-attenuated inversion-recovery, axial postcontrast T1-weighted MR angiography, and ASL perfusion sequences. For our study, only ASL images were assessed.

Raw ASL perfusion MR images were obtained before subtraction by using the following parameters at 1.5 T: repetition time msec/echo time msec, 1325.0/5.0; section thickness, 5 mm; number of signals acquired, three; number of sections, 32; readout of eight arms × 512 samples; field of view, 24 × 24 cm; matrix, 64 × 64; and voxel resolution, 3.8 × 3.8 × 5.0 mm. The following parameters were used at 3.0 T: 4446.0/9.9; section thickness, 6 mm; number of signals acquired, three; number of sections, 22; readout of eight arms × 512 samples; field of view, 24 × 24 cm; matrix, 64 × 64; and voxel resolution, 3.8 × 3.8 × 5.0 mm. With this sequence, pseudocontinuous spin labeling was performed for 1.5 seconds before a postlabeling delay of 1.5 seconds. CBF values were acquired by using an equation described previously (7).

Biplane angiography units (Integris Allura, Philips Healthcare, Best, the Netherlands; and Innova IGS 630, GE Healthcare) were used for DSA examinations, including anteroposterior and lateral projections with selective injection of the respective internal carotid, external carotid, and/or vertebral artery with nonionic monomeric iodine contrast medium (iopamidol, Pamiray 250; Dongkook Pharmaceutical, Seoul, Korea) by using a 5-F catheter.

Quantitative Analysis of CBF at ASL

On a picture archiving and communication system workstation, regions of interest were drawn manually in the most representative sections of each CBF map along the level of the basal ganglia on the operated side to determine absolute CBF values of the MCA territory (CBF_{MCA}) by a neuroradiologist (S.L., with 6 years of clinical experience in neuroradiology) (8). To adjust for interindividual variation among MR imagers and CBF, additional regions of interest were drawn within the MCA territory of the contralateral parenchyma at the same section level ($CBF_{opposite}$) and within the cerebellum (CBF_{CbII}) for CBF normalization. All values of CBF maps were measured in absolute units (mL/100 g per minute).

When normalizing absolute CBF_{MCA} values, symmetric regions of interest at the nonanastomosis side were used to minimize inhomogeneous perfusion effect because certain regions of interest at the level of the cerebellum were minimally affected by transit time error (9,10). Subsequently, normalized CBF values (hereafter, $nCBF_{MCA}$) were calculated by using the following equation: $nCBF_{MCA} = CBF_{MCA}/CBF_{opposite}$. Normalized CBF values adjusted to cerebellum ($nCBF_{CbII}$) were calculated as $nCBF_{CbII} = CBF_{MCA}/CBF_{CbII}$.

Collateral Flow Grading at ASL and DSA

Two neuroradiologists (S.L. and T.J.Y., with more than 10 years of clinical experience in neuroradiology) who were blinded to the findings of each modality reviewed ASL and DSA images for MCA territory abnormalities. Guided by the Alberta Stroke Program Early CT Score, or ASPECTS, study, ASL and DSA

images were divided into six anatomic sites based on regional vascular territories (M1–M3 and M4–M6) of the side operated or to be operated on (ie, six regions were evaluated in each patient for two time points) (11,12).

ASL images were graded by consensus on a scale from 0 to 3 as follows: 0, no or minimal ASL signal; 1, moderate ASL signal with arterial transit artifact; 2, high ASL signal with arterial transit artifact; and 3, normal signal without arterial transit artifact (3,6,12,13).

A similar scoring system was used for DSA images: 0, no collaterals visible to the ischemic site (absence of any capillary blush); 1, collaterals to the periphery of the ischemic site; 2, complete irrigation of the ischemic bed via collateral flow; and 3, normal antegrade flow (3,6,13).

Anastomosis Patency Grading at ASL and DSA

Two neuroradiologists (S.L. and T.J.Y.) who were blinded to the findings of each modality reviewed the ASL and DSA images to assess the anastomosis site after surgery in a consensus reading.

Anastomosis patency at ASL was visually analyzed with respect to the "bright vessel appearance" previously studied for arterial occlusion (7). Grading for patency was scored on a three-point scale as follows: 0, poor (bright signal intensity relative to the cortical signal intensity); 1, fair (similar signal intensity compared with cortical signal intensity); and 2, good (no signal intensity).

Visual assessment for anastomosis site patency at DSA was also scored on a three-point scale as follows: 0, poor (when neither anastomosis nor any of the recipient branches could be visualized); 1, fair (when anastomosis and only recipient branches immediately distal to the anastomosis or graft artery could be demonstrated); and 2, good (when the anastomosis and second arteries or more distal branches of the recipient vessels connected to the anastomosis or graft artery could be demonstrated) (14).

The scoring of anastomosis patency at ASL or DSA was then converted to a simple two-point system to calculate diagnostic accuracy: 0, poor or fair; and 1, good.

Statistical Analysis

All statistical analyses were performed with MedCalc software (version 12.1.0 for Microsoft Windows 2000/XP/Vista/7; MedCalc Software, Mariakerke, Belgium). For each parameter, normality of data were assessed with the Kolmogorov-Smirnov test.

An absolute CBF_{MCA} value measured at the operative side and two normalized CBF values, $nCBF_{MCA}$ and $nCBF_{Cbll}$, were assessed in 145 patients in both preoperative and late postoperative visits. Among 145 patients, 79 patients visited for early postoperative follow-up. To evaluate changes between baseline and late postoperative CBF values observed in 145 patients with moyamoya disease, paired *t* test was performed for changes in CBF_{MCA}, $nCBF_{MCA}$, and $nCBF_{Cbll.}$ We also used the paired *t* test to compare the difference in areas of drawn regions of interest. CBF values of three different times—preoperative, early postoperative, and late postoperative—were assessed in 79 patients with moyamoya disease who underwent imaging for early postoperative follow-up, and a time effect was examined by using repeated measured one-way analysis of variance. When a significant time effect was observed, posthoc comparisons between each visit were conducted with a Bonferroni correction. We also performed χ^2 test for comparison of the sex ratio and unpaired *t* test for a comparison of the mean age between the early postoperative imaging group and late postoperative imaging group.

Table 1: Comparison between Preoperative and Postoperative CBF Values in Patients (*n* = 145) Who Underwent MCA–STA Anastomosis Based on ASL Measurements

Parameter	Before Surgery	After Surgery	*P* Value
Period (d)*	40.0 ± 6.0	196.7 ± 12.6	…
Absolute CBF			
Anastomosis side	35.2 ± 7.8	51.5 ± 12.0	<.001
Nonanastomosis side	47.3 ± 6.9	46.1 ± 9.5	>.05
Cerebellum	48.4 ± 9.0	51.7 ± 11.9	>.05
Normalized CBF†			
Per cerebellum	0.74 ± 0.12	1.12 ± 0.16	<.001
Per nonanastomosis side	0.73 ± 0.14	1.01 ± 0.18	<.001

Note.—Data are means ± standard deviation. Absolute and normalized values of cerebral blood flow (CBF) before and after surgery were compared by using paired *t* test. MCA–STA = middle cerebral artery–superficial temporal artery.

* Mean period between arterial spin-labeling (ASL) and operation is preoperative or postoperative days from surgery.

† Normalized CBF (nCBF) values are calculated as follows: nCBF (per cerebellum) = $CBF_{anastomosis\ side}/CBF_{cerebellum}$ and nCBF (per nonanastomosis side) = $CBF_{anastomosis\ side}/CBF_{nonanastomosis\ side}$.

Collateral grading assessment was performed at six sites (M1–M6 territory) per patient at the preoperative and late postoperative stage by using both ASL and DSA. Thus, 12 matched-pair assessments existed for each patient. To assess the intermodality agreement between ASL and DSA regarding collateral flow, linear κ coefficient and the 95% confidence interval were estimated considering correlations among 12 pairs evaluated in each patient (15). Agreement between reviewers was expressed as κ value to account for the chance of agreement between the two reviewers. κ values were defined as follows: less than 0, negative agreement; 0–0.20, positive but poor agreement; 0.21–0.40, fair agreement; 0.41–0.60, moderate agreement; 0.61–0.80, good agreement; and greater than 0.81, excellent agreement.

McNemar two-tailed test was conducted to compare the sensitivity of ASL bright vessel appearance for the depiction of impaired anastomosis site patency by using DSA as the reference standard. Statistical significance was considered when the *P* value was less than .05.

Results

Mean absolute CBF values from ASL in the anastomosis side at preoperative and late postoperative follow-up were 35.2 mL/100 g per minute ± 7.8 and 51.5 mL/100 g per minute ± 12.0, respectively. All normalized CBF values ($nCBF_{MCA}$ and $nCBF_{Cbll}$) were increased at late postoperative follow-up (all $P < .001$) (Table 1).

Table 2: Contingency Table for Intermodality Agreement of Collateral Flow Grading (*n* = 1740)

	DSA*				
Full Four-Point Grade	Grade 0	Grade 1	Grade 2	Grade 3	Total
ASL†					
Grade 0	297 (84.6)	41 (7.1)	14 (4.2)	19 (4.0)	371
Grade 1	21 (6.0)	445 (77.4)	37 (11.0)	34 (7.1)	537
Grade 2	6 (1.7)	44 (7.7)	274 (81.8)	15 (3.1)	339
Grade 3	27 (7.7)	45 (7.8)	10 (3.0)	411 (85.8)	493
Total	351 (100)	575 (100)	335 (100)	479 (100)	1740

Note.—Data are the number of cases, with percentages in parentheses. Collateral grading was used for digital subtraction angiography (DSA) and arterial spin-labeling (ASL) imaging (baseline and late postoperative follow-up imaging) provided in M1–M6 territory per patient. ASL vs DSA: weighted κ, 0.765 (95% confidence interval: 0.724, 0.805). Linear-weighted κ values were calculated for intermodality consensus grading with common criteria as follows: poor agreement, 0–0.20; fair agreement, 0.20–0.40; moderate agreement, 0.40–0.60; good agreement, 0.60–0.80;
excellent agreement, 0.80–1.00.

* Grade 0, no visible collaterals to ischemic site; grade 1, collateral flow to periphery of ischemic site; grade 2, complete irrigation of ischemic bed via collateral flow; and grade 3, normal antegrade flow.

† Grade 0, no or minimal ASL signal; grade 1, moderate ASL signal with arterial transit artifact (ATA); grade 2, high ASL signal with ATA; and grade 3, normal perfusion without ATA.

Table 3: Diagnostic Accuracy of ASL for Detecting Impaired Anastomosis Site in All Patients (*n* = 145)

	DSA*		
Parameter	Impaired	Normal	Total
ASL*			
Impaired	11 (44)	0 (0)	11
Normal	14 (56)	120 (100)	134
Total	25 (100)	120 (100)	145

Note.—Data are the number of patients, with percentages in parentheses. Anastomosis patency was evaluated by using postoperative digital subtraction angiography (DSA) imaging and follow-up arterial spin-labeling (ASL) imaging. McNemar two-tailed test was conducted to compare sensitivity of ASL bright vessel appearance for detection of impaired anastomosis site patency by using DSA as reference standard. Diagnostic accuracy of ASL vs DSA: sensitivity of 44%, specificity of 100% (95% confidence interval: 5.830, 15.813; $P < .001$).

* Grading is converted to simple two-point system: impaired (grade 0 or 1) and normal (grade 2).

In the subgroup analysis, in which 79 patients underwent early postoperative imaging after surgery, no significant difference was found in the sex ratio ($P = .118$) and age ($P = .694$) between the early postoperative imaging group ($n = 79$) and the late postoperative follow-up group ($n = 66$). No difference was found in the mean baseline CBF values between the two groups (CBF_{MCA}, 35.3 mL/100 g per minute ± 8.1 vs 35.2 mL/100 g per minute ± 7.5; $nCBF_{MCA}$, 0.74 mL/100 g per minute ± 0.14 vs 0.73 mL/100 g per minute ± 0.15; $nCBF_{CbII}$, 0.75 mL/100 g per minute ± 0.12 vs 0.74 mL/100 g per minute ± 0.13; $P = .94$, $P = .67$, and $P = .78$, respectively). Hyperperfusion is usually defined as an increase of greater than 100% in CBF compared with the preoperative value. There were 13 patients with an increase of more than 100% in CBF in the early postoperative images (mean CBF change, 154.9%; range, 103.4%–234.3%; baseline CBF_{MCA} vs early postoperative CBF_{MCA}, 27.1 mL/100 g per minute ± 7.8 vs 68.5 mL/100 g per minute ± 23.2). Absolute and normalized CBF values at the anastomosis side were increased at 3 months after surgery compared with those preoperatively. They were then stabilized at late postoperative follow-up (all $P < .001$) (Table E1 [online]).

The κ values of intermodality agreement between ASL and DSA for collateral grading are summarized in Table 2. The overall agreement on collateral flow grading was good (κ, 0.77; 95% confidence interval: 0.73, 0.81). Collateral flow grading was interpreted as grade 0 in 297 cases (84.6%), grade 1 in 445 cases (77.4%), grade 2 in 274 cases (81.8%), and grade 3 in 411 cases (85.8%) by using ASL and DSA.

Anastomosis patency also showed moderate intermodality agreement between ASL and DSA (κ, 0.57; 95% confidence interval: 0.37, 0.76). Among 11 patients with fair or poor patency at ASL, all 11 patients also had impaired fair or poor flow at DSA. An analysis for the diagnostic accuracy of ASL demonstrated that the sensitivity of ASL bright vessel appearance for the depiction of anastomosis patency was only 44%. However, its specificity was perfect (100%) when DSA was used as a reference standard (Table 3).

The interobserver agreement on collateral grading and anastomosis site patency are shown in Table E2 (online). The interobserver agreement on collateral grading between the two reviewers for ASL and DSA findings was substantial (κ, 0.706). In the subgroup analysis, the κ values for interobserver agreement for each ASL and DSA showed excellent (κ, 0.819) and moderate agreement (κ, 0.589), respectively. The interobserver agreement on anastomosis site patency was almost perfect between the two readers regarding the presence of abnormal bright signal at ASL (κ, 0.876) and abnormal anastomosis site at DSA (κ, 0.907).

Representative images are shown in Figure 1 and Figure 2.

Discussion

Our study assessed whether ASL MR imaging can identify changes in CBF, collateral blood flow, and anastomosis site

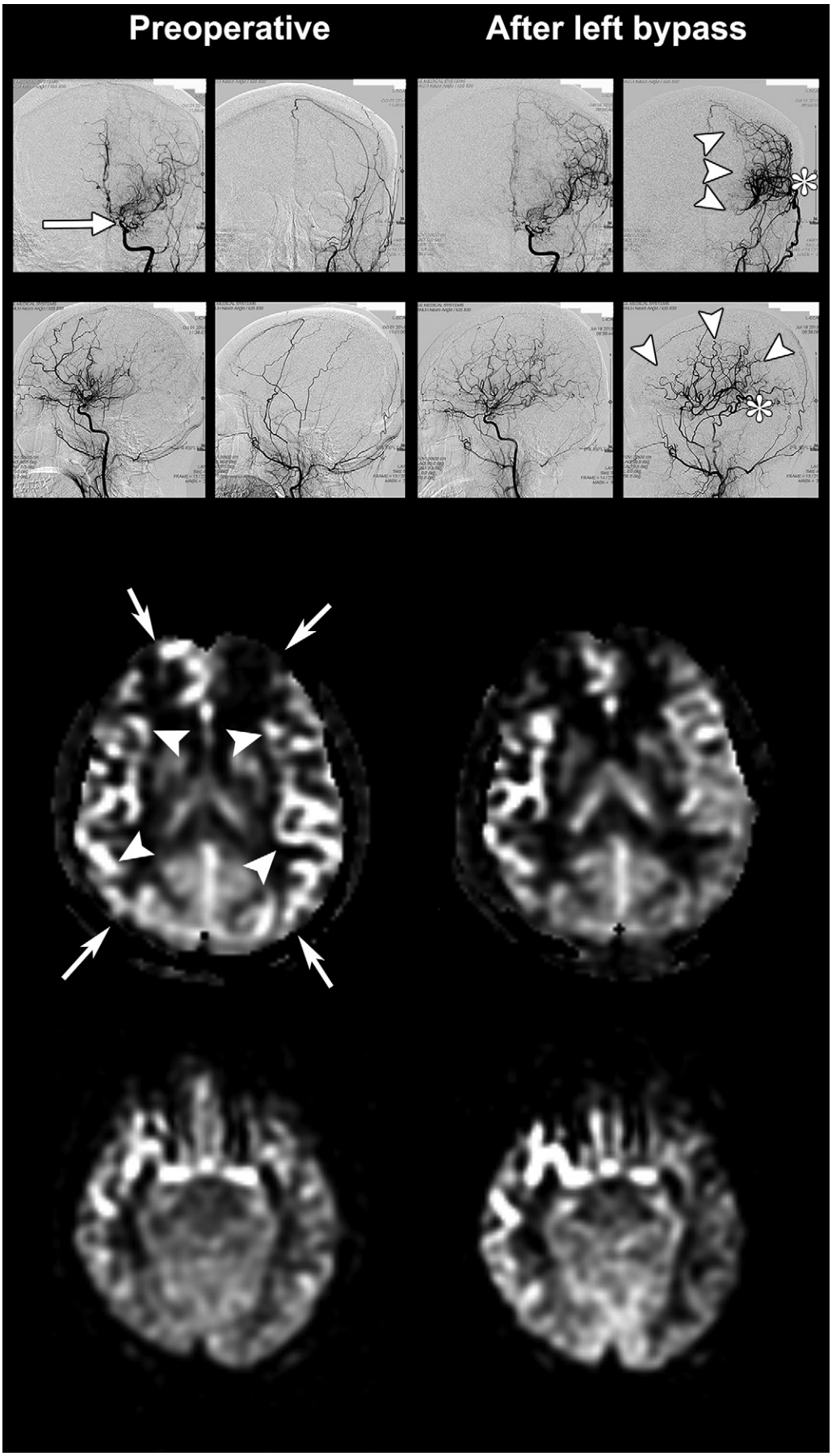

Figure 1: Representative digital subtraction angiography (DSA) and arterial spin-labeling (ASL) images in a 37-year-old woman who underwent left direct middle cerebral artery (MCA)–superior temporal artery (STA) anastomosis with good postoperative outcome. Preoperative DSA images show anterior and lateral projections from both internal and external carotid artery injections that demonstrate occlusion of bilateral proximal MCAs (arrow in first row) with reconstituted collateral flows. Follow-up DSA after left MCA–STA anastomosis shows abundant blood flow (arrowheads in first and second rows) with intact anastomosis site (* in first and second rows). Preoperative ASL images show decreased perfusion (arrows in third row) and arterial transit artifact (ATA) signals (arrowheads in third row) in bilateral MCA territories indicating late-arriving flow via collateral pathways. After left MCA–STA bypass surgery, postoperative ASL images show increased perfusion with decreased ATA signals in left MCA territories without ATA signal at each anastomosis site, indicating normalized flow and intact anastomosis site (fourth row). In this patient, encephalodurogaleosynangiosis was also performed at right side.

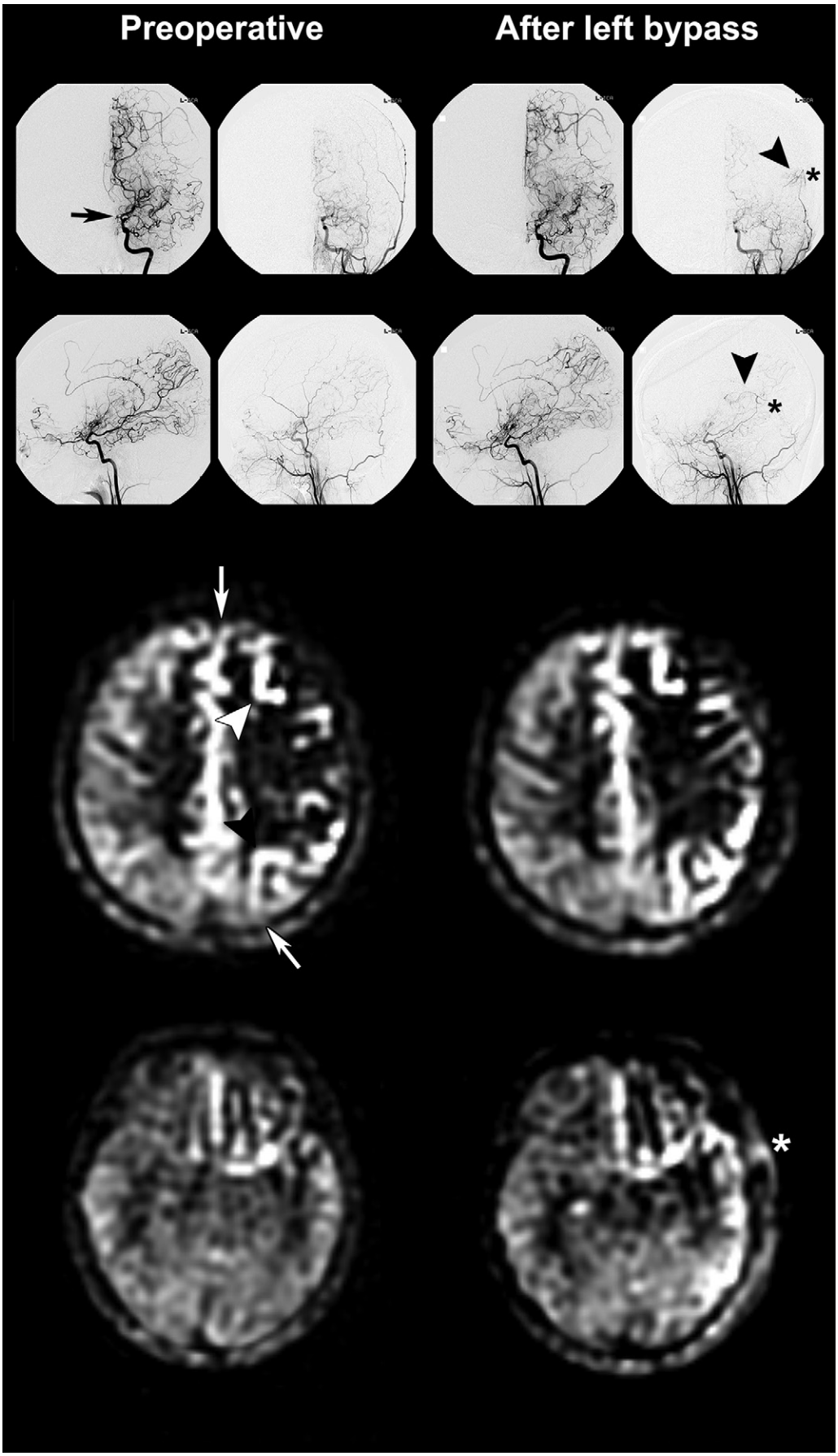

Figure 2: Representative digital subtraction angiography (DSA) and arterial spin-labeling (ASL) images in a 27-year-old woman who underwent left direct middle cerebral artery (MCA)–superior temporal artery (STA) anastomosis with poor postoperative outcome. Preoperative DSA images show anterior and lateral projections from left internal and external carotid artery injections that demonstrate occlusion of left distal internal carotid artery (arrow in first row) with reconstituted collateral flows. Follow-up DSA after left MCA–STA anastomosis shows impaired blood flow (arrowheads in first and second rows) from anastomosis site (* in first and second rows). Preoperative ASL images show decreased perfusion (arrows in third row) and arterial transit artifact (ATA) signals in left distal internal carotid artery territories (arrowheads in third row) indicating late-arriving flow via collateral pathways. After left MCA–STA bypass surgery, postoperative ASL images still show impaired perfusion and ATA signals in left MCA territory and prominent ATA signal in MCA–STA anastomosis site (* in fourth row) indicating flow stagnation in anastomosis site.

patency in patients with moyamoya disease after revascularization. Results demonstrated that ASL MR imaging can be used to identify perfusion changes after revascularization with excellent diagnostic performance compared with DSA findings.

Direct revascularization is the most widely used surgical method in adult patients with moyamoya disease despite its risk of hyper- or hypoperfusion (16,17). Thus, it is important to monitor perfusion changes in patients with moyamoya disease after revascularization. Several previous studies have examined the ability of ASL MR imaging to assess the hemodynamic status as a monitoring tool compared with nuclear medicine methods such as single-photon emission computed tomography (SPECT) and positron emission tomography (PET) (2,18,19). Goetti et al have also reported that ASL allows for the detection of perfusion changes by using dynamic-susceptibility perfusion MR imaging as reference (10). However, although quantitative CBF measurements in ASL have shown good correlation with other modalities, CBF in affected vascular territories may be underestimated because of delayed arterial arrival times (3). Thus, changes of quantitative CBF after revascularization need to be serially analyzed in a large number of patients by using ASL. In our study, we found that absolute CBF_{MCA} values were increased at early postoperative follow-up and stabilized at late postoperative follow-up compared with preoperative values in ASL imaging by using a large number of patients. An interesting result of our study was that normalized CBF values adjusted to the nonanastomosis side or cerebellum also showed similar patterns of improvement and stabilization after revascularization. These results imply that perfusion changes in patients who underwent direct revascularization could be successfully monitored by using ASL. Sugino et al reported that $nCBF_{MCA}$ values were increased (to 1.22 mL/100 g per minute $\pm$ 0.73) within 3 days after surgery and then normalized at 21 days postoperatively (8). Yun et al showed that $nCBF_{CbII}$ values tend to increase with longer follow-up intervals in the anastomosis side despite use of different methodologies (2). Cho et al (20) reported that hemodynamic status became stable at 6 months postoperatively by using SPECT evaluation after surgery, and neovascularization continuously increased during a long-term follow-up period of 54 months by using angiography. Their hypothesis was that direct revascularization rapidly augmented the CBF, whereas abnormal moyamoya vessels and major cerebral arteries slowly started to regress after at least 6 months following surgery. Our study also showed that the CBF in the early postoperative period rapidly increased and then slightly stabilized at the late postoperative period (approximately 6 months after surgery) compared with that of the preoperative period. Therefore, results of our study may reflect the natural course of perfusion changes in moyamoya disease after surgery. These clinical values could be used as predictors of complication after direct revascularization. They could facilitate early detection of hyper- or hypoperfusion to minimize the risk of surgical morbidity.

An important limitation of ASL perfusion MR imaging is that its results can be influenced by the presence of collateral moyamoya vessels, which may lead to underestimation of CBF values because of delayed arterial arrival times, or arterial transit artifact (3,10). There is recruitment of flow from collateral pathways of the circle of Willis or leptomeningeal anastomoses, which are maintained by the cerebrovascular reactivity in patients with moyamoya disease. Labeled blood flowing through these collateral pathways would have a delayed arrival at the brain tissue, resulting in a strong ASL signal within the cortical vessels. However, this disadvantage for quantification of CBF might be a benefit for visualizing collateral vessels (3). Patients with moyamoya disease may have significantly different outcomes based on their ability to recruit collateral pathways. Therefore, it is important to monitor collateral flow changes after revascularization (3,17). In several previous studies, collateral scoring based on arterial transit artifact of ASL perfusion MR imaging has shown good agreement with DSA in steno-occlusive disease (3,6,13). Our study also showed that collateral flow grading in each segmental territory of the MCA (M1–M6) had good agreement between ASL and DSA. Therefore, ASL may reflect similar results in patients with moyamoya disease, although DSA is still the reference standard for evaluating collateral scoring.

After direct revascularization, anastomosis site patency is the most important factor when monitoring patients with moyamoya disease. If neurologic deterioration or abrupt changes in CBF occur after surgical treatment, then surgeons should consider DSA to evaluate anastomosis site patency (20). However, ASL may provide important information by using bright vessel appearance. Yoo et al have shown that ASL bright vessel appearance occurs when there is an occluded arterial segment with sluggish blood flow because of arterial transit artifact (7). Our data showed that ASL and DSA had moderate intermodality agreement for evaluating anastomosis patency. For detecting impaired anastomosis patency by using ASL, the sensitivity was 44% and the specificity was 100%. The low sensitivity could be because of suboptimal image quality after revascularization surgery. However, given the high specificity of 100% for detecting impaired anastomosis, we speculate that the use of ASL as a screening tool would reduce the need for DSA. The low sensitivity of ASL might be an indicator of poor diagnostic performance.

Our study had several limitations that need to be taken into account when interpreting the data. First, accurate drawing of the MCA territory was challenging. ASL imaging has an overall low spatial resolution and requires postprocessing for accurate absolute CBF measurements; it is up to the observer to choose the region of interest in the MCA territory. Thus, in addition to quantifying absolute CBF values, we used another methodology to assess CBF by analyzing CBF values relative to the contralateral side and cerebellum. In addition, perfusion territory imaging with vessel selective ASL was not used. Therefore, we recorded the size of the region of interest to minimize variance in each patient. There was no difference in size of the region of interest at the MCA territory or the cerebellum. However, potential bias may have been introduced by including portions of the temporal and occipital lobes in the regions of interest.

Second, we did not have a standard of reference such as PET, SPECT, or perfusion CT available to validate quantitative CBF results from ASL. However, we focused on serial changes of CBF in each patient after revascularization. We used absolute CBF values adjusted by the cerebellum, which is supplied by the posterior circulation. In our study, we emphasized the clinical utility of ASL for evaluation of the collateral flow grading and anastomosis site patency, as well as the importance of the acquisition of

CBF. As mentioned previously, ASL could underestimate CBF because of the delayed arrival of the blood flow. Previous studies showed that the combination of multiple inversion time-pulsed technique of ASL and time-to-peak map in dynamic-susceptibility perfusion MR imaging to improve this drawback could help assess cerebral hemodynamics in patients with moyamoya disease (21–23). Therefore, the advancement in ASL technique might allow for better evaluation of CBF and support the clinical utility of ASL through further study.

Third, our study was performed by using MR imagers with two different magnetic field strengths. We therefore analyzed normalized CBF values to minimize possible bias associated with different field strengths as previously studied (7). In a subgroup analysis of the two different magnetic field strengths, the only significant effect was found for $nCBF_{MCA}$ at preoperative imaging ($P = .024$); the effect of different field strengths on $nCBF_{Cbll}$ was not significant in the preoperative and late postoperative stage ($P = .242$ and $P = .563$) (Table E3 [online]). Therefore, there was little difference of normalized CBF measurement in the cerebellum between 1.5-T and 3.0-T imagers. We also performed only pseudocontinuous spin labeling for 1.5 seconds before a postlabeling delay of 1.5 seconds. Wang et al (24) reported the multidelay ASL to be able to improve CBF quantification in patients with moyamoya disease.

Fourth, the percentage of ASL overestimation was 8.8% (153 of 1740) and the percentage of ASL underestimation was 9.2% (160 of 1740) in the collateral grading evaluation. The complete mismatch cases (2.6%, 46 of 1740) were reported in our study. These results could be explained by the difficulties of applying the DSA collateral grading system, initially developed for acute ischemic stroke, to a chronic cerebrovascular disease. ASL images can only show axial images, whereas DSA images are obtained by using anteroposterior and lateral projection methods. The difference in image projection could potentially have caused the observed discrepancy. A previous similar study (3) also described the nonvessel-selective ASL technique to be unable to distinguish slow antegrade flow from leptomeningeal or other retrograde collateral flow. Therefore, we used consensus reading for each modality to minimize variability related to measurement errors. However, the use of consensus opinion to assess the utility of ASL grading relative to DSA as reference standard might have led to an overestimation of the level of agreement that could be expected in clinical practice. In addition, we evaluated data for a large number of patients by using segmental territories in the MCA for intermodality agreement.

In conclusion, our results suggest that ASL MR imaging can be used to identify and monitor perfusion changes in patients with moyamoya disease after direct revascularization.

Author contributions: Guarantors of integrity of entire study, S.L., T.J.Y.; study concepts/study design or data acquisition or data analysis/interpretation, all authors; manuscript drafting or manuscript revision for important intellectual content, all authors; approval of final version of submitted manuscript, all authors; agrees to ensure any questions related to the work are appropriately resolved, all authors; literature research, S.L., T.J.Y.; clinical studies, all authors; statistical analysis, S.L., T.J.Y.; and manuscript editing, S.L., T.J.Y., R.E.Y., B.W.Y., K.M.K., S.H.C., J.H.K., C.H.S., M.H.H.

Disclosures of Conflicts of Interest: **S.L.** disclosed no relevant relationships. **T.J.Y.** disclosed no relevant relationships. **R.E.Y.** disclosed no relevant relationships. **B.W.Y.** disclosed no relevant relationships. **K.M.K.** disclosed no relevant relationships. **S.H.C.** disclosed no relevant relationships. **J.H.K.** disclosed no relevant relationships. **J.E.K.** disclosed no relevant relationships. **C.H.S.** disclosed no relevant relationships. **M.H.H.** disclosed no relevant relationships.

References

1. Suzuki J, Kodama N. Moyamoya disease—a review. Stroke 1983;14(1):104–109.
2. Yun TJ, Paeng JC, Sohn CH, et al. Monitoring cerebrovascular reactivity through the use of arterial spin labeling in patients with moyamoya disease. Radiology 2016;278(1):205–213.
3. Zaharchuk G, Do HM, Marks MP, Rosenberg J, Moseley ME, Steinberg GK. Arterial spin-labeling MRI can identify the presence and intensity of collateral perfusion in patients with moyamoya disease. Stroke 2011;42(9):2485–2491.
4. Detre JA, Leigh JS, Williams DS, Koretsky AP. Perfusion imaging. Magn Reson Med 1992;23(1):37–45.
5. Wolf RL, Detre JA. Clinical neuroimaging using arterial spin-labeled perfusion magnetic resonance imaging. Neurotherapeutics 2007;4(3):346–359.
6. Roach BA, Donahue MJ, Davis LT, et al. Interrogating the functional correlates of collateralization in patients with intracranial stenosis using multimodal hemodynamic imaging. AJNR Am J Neuroradiol 2016;37(6):1132–1138.
7. Yoo RE, Choi SH, Cho HR, et al. Tumor blood flow from arterial spin labeling perfusion MRI: a key parameter in distinguishing high-grade gliomas from primary cerebral lymphomas, and in predicting genetic biomarkers in high-grade gliomas. J Magn Reson Imaging. 2013;38(4):852-60.
8. Sugino T, Mikami T, Miyata K, Suzuki K, Houkin K, Mikuni N. Arterial spin-labeling magnetic resonance imaging after revascularization of moyamoya disease. J Stroke Cerebrovasc Dis 2013;22(6):811–816.
9. Yun TJ, Cheon JE, Na DG, et al. Childhood moyamoya disease: quantitative evaluation of perfusion MR imaging—correlation with clinical outcome after revascularization surgery. Radiology 2009;251(1):216–223.
10. Goetti R, O'Gorman R, Khan N, Kellenberger CJ, Scheer I. Arterial spin labelling MRI for assessment of cerebral perfusion in children with moyamoya disease: comparison with dynamic susceptibility contrast MRI. Neuroradiology 2013;55(5):639–647.
11. Barber PA, Demchuk AM, Zhang J, Buchan AM. Validity and reliability of a quantitative computed tomography score in predicting outcome of hyperacute stroke before thrombolytic therapy. ASPECTS Study Group. Alberta Stroke Programme Early CT Score. Lancet 2000;355(9216):1670–1674.
12. Kim JJ, Fischbein NJ, Lu Y, Pham D, Dillon WP. Regional angiographic grading system for collateral flow: correlation with cerebral infarction in patients with middle cerebral artery occlusion. Stroke 2004;35(6):1340–1344.
13. Chng SM, Petersen ET, Zimine I, Sitoh YY, Lim CC, Golay X. Territorial arterial spin labeling in the assessment of collateral circulation: comparison with digital subtraction angiography. Stroke 2008;39(12):3248–3254.
14. Tsuchiya K, Honya K, Fujikawa A, Tateishi H, Shiokawa Y. Postoperative assessment of extracranial-intracranial bypass by time-resolved 3D contrast-enhanced MR angiography using parallel imaging. AJNR Am J Neuroradiol 2005;26(9):2243–2247.
15. Yang Z, Zhou M. Weighted kappa statistic for clustered matched-pair ordinal data. Comput Stat Data Anal 2015;82:1–18.
16. Fujimura M, Mugikura S, Kaneta T, Shimizu H, Tominaga T. Incidence and risk factors for symptomatic cerebral hyperperfusion after superficial temporal artery-middle cerebral artery anastomosis in patients with moyamoya disease. Surg Neurol 2009;71(4):442–447.
17. Guzman R, Lee M, Achrol A, et al. Clinical outcome after 450 revascularization procedures for moyamoya disease: clinical article. J Neurosurg 2009;111(5):927–935.
18. Bokkers RP, Bremmer JP, van Berckel BN, et al. Arterial spin labeling perfusion MRI at multiple delay times: a correlative study with H(2)(15)O positron emission tomography in patients with symptomatic carotid artery occlusion. J Cereb Blood Flow Metab 2010;30(1):222–229.
19. Noguchi T, Kawashima M, Irie H, et al. Arterial spin-labeling MR imaging in moyamoya disease compared with SPECT imaging. Eur J Radiol 2011;80(3):e557–e562.
20. Cho WS, Kim JE, Kim CH, et al. Long-term outcomes after combined revascularization surgery in adult moyamoya disease. Stroke 2014;45:3025-3031.
21. Okada Y, Shima T, Nishida M, Yamane K, Yamada T, Yamanaka C. Effectiveness of superficial temporal artery-middle cerebral artery anastomosis in adult moyamoya disease: cerebral hemodynamics and clinical course in ischemic and hemorrhagic varieties. Stroke 1998;29(3):625–630.
22. Yun TJ, Sohn CH, Han MH, et al. Effect of delayed transit time on arterial spin labeling: correlation with dynamic susceptibility contrast perfusion magnetic resonance in moyamoya disease. Invest Radiol 2013;48(11):795–802.
23. Qiao PG, Han C, Zuo ZW, et al. Clinical assessment of cerebral hemodynamics in Moyamoya disease via multiple inversion time arterial spin labeling and dynamic susceptibility contrast-magnetic resonance imaging: a comparative study. J Neuroradiol 2017;44(4):273–280.
24. Wang R, Yu S, Alger JR, et al. Multi-delay arterial spin labeling perfusion MRI in moyamoya disease—comparison with CT perfusion imaging. Eur Radiol 2014;24(5):1135–1144.

Original Article | Pediatric Imaging

eISSN 2005-8330
https://doi.org/10.3348/kjr.2020.1464
Korean J Radiol 2021;22(9):1537-1546

Korean Journal of Radiology
KJR

Monitoring Cerebral Perfusion Changes Using Arterial Spin-Labeling Perfusion MRI after Indirect Revascularization in Children with Moyamoya Disease

Seul Bi Lee[1], Seunghyun Lee[1, 2], Yeon Jin Cho[1, 2], Young Hun Choi[1, 2], Jung-Eun Cheon[1, 2, 3], Woo Sun Kim[1, 2, 3]

[1]Department of Radiology, Seoul National University Hospital, Seoul, Korea; [2]Department of Radiology, Seoul National University College of Medicine, Seoul, Korea; [3]Institute of Radiation Medicine, Seoul National University Medical Research Center, Seoul, Korea

Objective: To assess the role of arterial spin-labeling (ASL) perfusion MRI in identifying cerebral perfusion changes after indirect revascularization in children with moyamoya disease.

Materials and Methods: We included pre- and postoperative perfusion MRI data of 30 children with moyamoya disease (13 boys and 17 girls; mean age ± standard deviation, 6.3 ± 3.0 years) who underwent indirect revascularization between June 2016 and August 2017. Relative cerebral blood flow (rCBF) and qualitative perfusion scores for arterial transit time (ATT) effects were evaluated in the middle cerebral artery (MCA) territory on ASL perfusion MRI. The rCBF and relative time-to-peak (rTTP) values were also measured using dynamic susceptibility contrast (DSC) perfusion MRI. Each perfusion change on ASL and DSC perfusion MRI was analyzed using the paired *t* test. We analyzed the correlation between perfusion changes on ASL and DSC images using Spearman's correlation coefficient.

Results: The ASL rCBF values improved at both the ganglionic and supraganglionic levels of the MCA territory after surgery ($p = 0.040$ and $p = 0.003$, respectively). The ATT perfusion scores also improved at both levels ($p < 0.001$ and $p < 0.001$, respectively). The rCBF and rTTP values on DSC MRI showed significant improvement at both levels of the MCA territory of the operated side (all $p < 0.05$). There was no significant correlation between the improvements in rCBF values on the two perfusion images ($r = 0.195$, $p = 0.303$); however, there was a correlation between the change in perfusion scores on ASL and rTTP on DSC MRI ($r = 0.701$, $p < 0.001$).

Conclusion: Recognizing the effects of ATT on ASL perfusion MRI may help monitor cerebral perfusion changes and complement quantitative rCBF assessment using ASL perfusion MRI in patients with moyamoya disease after indirect revascularization.

Keywords: *Children; Arterial spin-labeling; Moyamoya disease; Magnetic resonance imaging*

INTRODUCTION

Moyamoya disease (MMD) is a cerebrovascular disease characterized by steno-occlusive changes in the distal portion of the internal carotid arteries [1]. Progressive characteristics can lead to brain injuries due to multiple stroke events, resulting in significant brain disability and worse prognosis when present at younger ages [1]. Therefore, revascularization surgery should be considered for restoring cerebral perfusion and preventing neurocognitive decline [2].

Arterial spin-labeling (ASL) perfusion magnetic resonance imaging (MRI) is magnetically labeled by the radiofrequency (RF) pulse protons of arterial blood flowing into the brain as an endogenous tracer [3]. Labeled arterial blood water acts as a diffusible tracer for quantitatively estimating cerebral

Received: September 28, 2020 **Revised:** February 19, 2021 **Accepted:** March 12, 2021
Corresponding author: Seunghyun Lee, MD, Department of Radiology, Seoul National University College of Medicine, Seoul National University Hospital, 101 Daehak-ro, Jongno-gu, Seoul 03080, Korea.
• E-mail: seunghyun.lee.22@gmail.com

blood flow (CBF) in brain tissues without using gadolinium-based contrast agents [4]. ASL perfusion images can be generated by subtracting an image that labels arterial spin from one without such spin-labeling to suppress the signal from the static tissue [3-5]. The ASL technique has three main categories: continuous ASL (cASL), pulsed ASL (pASL), and pseudo-continuous ASL [5,6]. The cASL has a higher signal-to-noise ratio (SNR) than the pASL, but it cannot be used in clinical MRI scanners because it requires long and continuous RF transmission. In contrast with cASL, pASL has a labeling efficiency, as a short RF pulse with a thick slab is used to label arterial blood, but it allows a lower SNR than cASL. Pseudo-continuous ASL is a widely used ASL technique, and it divides the long continuous RF pulse into multiple short pulses, resulting in a high labeling efficiency in the clinical MRI scanner while maintaining a better SNR [5,6]. This pseudo-continuous ASL perfusion MRI can help predict clinical outcomes and evaluate surgical success in patients with MMD [4,7-10]. However, the arterial transit time (ATT) effect, which is the hyperintense focus of intravascular signals on ASL perfusion MRI, confounds CBF measurement and introduces an error into the estimate [11,12]. However, the ATT effect has essential information on delayed-arriving arterial flow via collateral vessels and may complement perfusion MRI even though it complicates quantitative CBF value calculation [13].

This study aimed to assess whether 1) ASL perfusion MRI can identify quantitative changes in CBF despite the presence of ATT effects, and 2) perfusion scores with ATT effects can help detect perfusion changes after indirect revascularization, compared with dynamic susceptibility contrast (DSC) perfusion MRI. Therefore, this study sought to assess the role of ASL perfusion MRI in identifying cerebral perfusion changes after indirect revascularization in children with MMD.

MATERIALS AND METHODS

The Institutional Review Board approved this study. The requirement for obtaining informed consent was waived because of its retrospective nature (IRB No. 2007-033-1139).

Patient Selection

We retrospectively reviewed 34 patients with MMD who underwent indirect revascularization surgery using encephaloduroarteriosynangiosis (EDAS) at our institution between June 2016 and August 2017. The inclusion criteria were as follows: 1) perfusion MRI with ASL and DSC technique at baseline and postoperative follow-up, 2) age of < 18 years at the time of diagnosis, and 3) no history of revascularization surgery. Four patients were excluded because of inadequate image quality of ASL and DSC perfusion (two labeling errors and two severe motions). Thirty patients were included in the study. Six patients in this study also participated in the previous report by Ha et al. [9]; however, the quantitative data for DSC perfusion MRI and the qualitative change in the ATT effect for ASL perfusion MRI were not analyzed in the previous study. The patient characteristics are summarized in Table 1. Age, sex, family history, and clinical symptoms of transient ischemic attacks, headache, and others were collected. Clinical status, including bilateral involvement of MMD and the presence of an old infarction, was also collected. The preoperative angiographic severity was assessed using the Suzuki staging system [14].

Image Acquisition

The standard imaging protocol for MMD patients at our institution was defined as follows: 1) baseline ASL and DSC perfusion imaging within 1 month before the first surgery for MMD diagnosis and 2) postoperative ASL and DSC perfusion imaging within 1 month before the second surgery on the opposite side. If there was no contralateral involvement of MMD, only perfusion imaging was performed after 6 months. Patients under seven years of age underwent MRI scans

Table 1. Patient Characteristics

Characteristics	Value
Age, year, mean ± SD	6.3 ± 3.0 (range, 2–13)
Sex, boys	13 (43.3)
Family history, present	3 (10.0)
Clinical symptoms	
Transient ischemic attack	19 (63.3)
Headache	4 (13.3)
Others	7 (23.3)
Bilateral involvements	30 (100.0)
Presence of old infarction	5 (16.7)
Preoperative Suzuki staging	
1	1 (3.3)
2	11 (36.7)
3	10 (33.3)
4	3 (10.0)
5	5 (16.7)

Data are number of patients with the percentage in parentheses unless specified otherwise. SD = standard deviation

https://doi.org/10.3348/kjr.2020.1464

Korean Journal of Radiology
KJR

under mild to moderate sedation using sedative drugs.

ASL perfusion MRI was performed using 1.5T MR scanners (Avanto, Siemens Healthineers) with a 12-channel head coil. Raw data acquisition of ASL perfusion MRI was performed before subtraction using the following parameters: repetition time/echo time (TR/TE), 4290.0/22.0 ms; section thickness, 10 mm; a generalized autocalibrating partially parallel acquisition acceleration factor, 2; number of sections, 30; readout, eight arms x 512 samples; field of view, 25 x 25 cm; matrix, 96 x 96. Pseudo-continuous spin-labeling with two-dimensional single-shot-gradient-echo echo-planar imaging readout was performed for 1.8 seconds before a post-spin-labeling delay of 1.5 seconds. The total scan duration for ASL perfusion MRI was 4.5 minutes.

DSC perfusion MRI was performed using a single-shot gradient-echo echo-planar imaging sequence during intravenous injection of the gadolinium-based contrast agent with the following parameters: TR/TE, 1500/30 ms; flip angle, 60°; field of view, 24 x 24 cm; 17 sections; matrix, 128 x 128; thickness, 5 mm; intersection gap, 1.5 mm. For each section, 50 images were obtained at intervals equal to the TR. Gadobutrol at a dose of 0.1 mmoL/kg and rate of 2 mL/s was injected with an MR-compatible power injector (Spectris, Medrad) four or five times. The total scan duration for DSC perfusion MRI was 2 minutes.

ASL Perfusion Image Analysis

On a picture archiving and communication system workstation (Infinitt; Infinitt Healthcare), regions of interest (ROIs) were drawn manually, covering the middle cerebral artery (MCA) territories of the operative side by a pediatric radiologist according to previous studies [4,15,16]. ROIs were drawn at the six locations for the Alberta Stroke Program Early CT score (ASPECTS), and a segmental assessment of the MCA vascular territory over the standard ganglionic and supraganglionic levels was performed (Fig. 1). CBF calculations for ASL images have been described previously [9]. All CBF map values were measured in absolute units (mL/100 g/min). The average CBF values at each level were derived based on the CBF values at the ganglionic and supraganglionic levels. To adjust for interindividual variation, additional ROIs were drawn within the cerebellum for CBF normalization. Subsequently, relative CBF (rCBF) values were calculated using the following equation: rCBF on ganglionic level = $CBF_{ganglionic}/CBF_{cerebellum}$; rCBF on supraganglionic level = $CBF_{supraganglionic}/CBF_{cerebellum}$.

Two pediatric radiologists reviewed the ASL images for ATT at the ganglionic and supraganglionic levels of the MCA territory, which were the same levels used in the quantitative analysis. Qualitative perfusion scoring on ASL utilizes a 4-point scale: 0, complete absence of parenchymal perfusion; 1, incomplete parenchymal perfusion (i.e., partially absent or conspicuously decreased perfusion with ATT effect); 2, delayed-but-complete parenchymal perfusion (i.e., ASL demonstrates complete parenchymal perfusion, but shows an ATT effect); 3, complete/normal perfusion (i.e., ASL shows approximately homogeneous parenchymal perfusion, without obvious ATT effect) [11,13,17,18]. These perfusion scores were recorded at six ASPECTS areas at the same location where the ROI was drawn for quantitative analysis. The average perfusion scores for the ganglionic and supraganglionic levels were used as the ASL perfusion scores.

DSC Perfusion Image Analysis

DSC perfusion images with CBF and time-to-peak (TTP) maps were generated using a commercially available

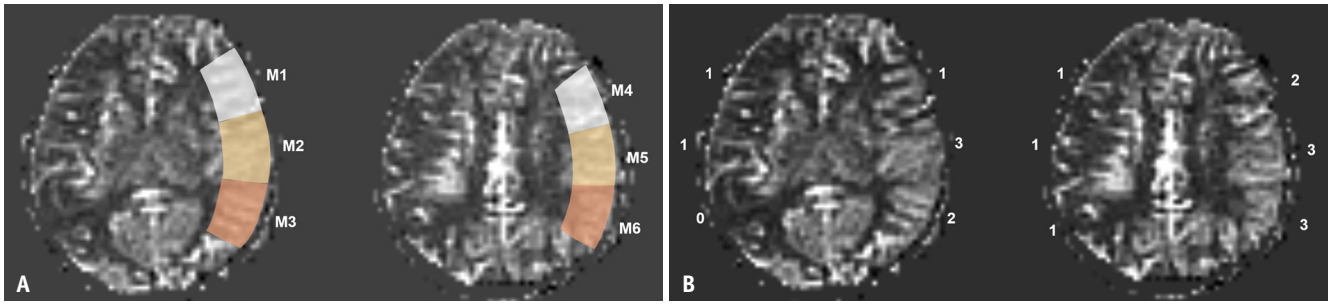

Fig. 1. Example of region of interest placement for ASL imaging assessment.
A. The region of interest manually drawn to cover the cortex of the operated side of the middle cerebral artery territories for each of the ganglionic and supraganglionic levels on ASL perfusion MRI and dynamic susceptibility contrast perfusion MRI. **B.** The qualitative perfusion scoring for ASL utilizes a 4-point scale: 0, complete absence of parenchymal perfusion; 1, incomplete parenchymal perfusion (i.e., partially absent or conspicuously decreased perfusion with ATT effect); 2, delayed-but-complete parenchymal perfusion (i.e., ASL demonstrates complete parenchymal perfusion, but shows ATT effect); 3, complete/normal perfusion (i.e., ASL shows approximately homogeneous parenchymal perfusion, without obvious ATT effect). ASL = arterial spin-labeling, ATT = arterial transit time

https://doi.org/10.3348/kjr.2020.1464

software package (Olea Sphere, Olea Medical) [19,20]. All CBF and TTP values were measured on each DSC perfusion map for the ganglionic and supraganglionic levels of the MCA territory and cerebellum using the same method utilized for the ASL CBF measurement by a pediatric radiologist. The rCBF values for the DSC images were calculated using the same CBF normalization method used for the ASL image. The relative TTP (rTTP) value was calculated using the following equation according to a previously reported method: $rTTP = TTP_{measured\ level} - TTP_{cerebellum}$ [21].

Statistical Analysis

Clinical characteristics and preoperative radiologic status were analyzed using descriptive statistics. The quantitative and qualitative perfusion changes on ASL perfusion MRI for the operated side were pre- and postoperatively assessed using a paired *t* test. Quantitative changes in DSC perfusion parameters were pre- and postoperatively assessed using a paired *t* test.

The changes in rCBF and rTTP values on DSC perfusion MRI were used as reference standards for postoperative perfusion changes after indirect revascularization [21,22]. We analyzed the correlation between the rCBF changes on the ASL and DSC images and the correlation between the ATT effect changes on ASL images and the rTTP changes on DSC images using Spearman's correlation test.

Interobserver agreement of the reviewers was expressed as the κ value for qualitative perfusion scoring on ASL perfusion MRI. The κ value was interpreted as follows: < 0, negative agreement; 0–0.20, positive but poor agreement; 0.21–0.40, fair agreement; 0.41–0.60, moderate agreement; 0.61–0.80, good agreement; > 0.81, excellent agreement.

All statistical analyses were performed using MedCalc software (version 12.1.0; MedCalc Software). Statistical significance was considered when the *p* value was < 0.05.

RESULTS

Patient Characteristics

This study enrolled 13 boys and 17 girls (mean age, 6.3 years [range, 2–13 years]). All patients underwent unilateral EDAS, and only one patient underwent a combination of EDAS and bifrontal encephalogaleoperiosteal synangiosis. Baseline and postoperative perfusion MRI were performed 3.5 ± 3.6 (mean ± standard deviation [SD]) days before surgery and 73.8 ± 56.7 days after surgery.

All patients had bilateral MMD, three (10%) had a family history of MMD, and none of the patients had moyamoya syndrome with associated diseases. Transient ischemic attack was the most common initial clinical symptom (63.3%), followed by a headache. Four children had an old infarction injury at the watershed zone, and one patient had a territorial cortical infarction on MRI preoperatively. None of the patients had a newly noted postoperative infarction. Preoperative angiographic findings with two or three grades of the Suzuki stage were common findings in our patients.

Perfusion Changes on ASL Perfusion MRI

The results of the quantitative and qualitative analyses of ASL perfusion MRI are summarized in Table 2. Postoperatively, the rCBF values improved at both the ganglionic and supraganglionic levels of the MCA territory on the operated side (mean ± SD of 1.04 ± 0.28 vs. 1.19 ± 0.44 and 0.92 ± 0.35 vs. 1.23 ± 0.51; $p = 0.040$ and $p = 0.003$). The qualitative perfusion scores for parenchymal perfusion and ATT also improved at both the ganglionic and supraganglionic levels (mean ± SD of 1.74 ± 0.74 vs. 2.54 ± 0.39 and 1.33 ± 0.63 vs. 2.12 ± 0.53; $p < 0.001$ and $p < 0.001$). The interobserver agreement for qualitative perfusion scoring for the two reviewers showed good agreement (κ = 0.797).

Perfusion Changes on DSC Perfusion MRI

The results of the quantitative analysis of the perfusion values on DSC perfusion MRI are summarized in Table 3.

Table 2. Perfusion Changes on ASL Perfusion MRI after Indirect Revascularization

Parameter	Preoperative	Postoperative	*P*
Relative CBF*			
Ganglionic level	1.04 ± 0.28	1.19 ± 0.44	0.040
Supraganglionic level	0.92 ± 0.35	1.23 ± 0.51	0.003
ASL perfusion scoring†			
Ganglionic level	1.74 ± 0.74	2.54 ± 0.39	< 0.001
Supraganglionic level	1.33 ± 0.63	2.12 ± 0.53	< 0.001

Values are presented as mean ± standard deviation. *Relative CBF values were calculated as follows: $CBF_{measured\ level}/CBF_{cerebellum}$, †The scoring of ASL perfusion was defined as follows: 0, complete absence of parenchymal perfusion; 1, incomplete parenchymal perfusion (i.e., partially absent or conspicuously decreased perfusion with ATT effect); 2, delayed-but-complete parenchymal perfusion (i.e., ASL demonstrates complete parenchymal perfusion, but shows ATT effect); and 3, complete/normal perfusion (i.e., ASL shows approximately homogeneous parenchymal perfusion, without obvious ATT effect). ASL = arterial spin-labeling, ATT = arterial transit time, CBF = cerebral blood flow

https://doi.org/10.3348/kjr.2020.1464

Korean Journal of Radiology
KJR

DSC perfusion MRI showed a significant increase in rCBF values (ganglionic; mean ± SD of 1.04 ± 0.20 vs. 1.18 ± 0.26, supraganglionic; mean ± SD of 0.95 ± 0.20 vs. 1.07 ± 0.22; both $p = 0.001$). The rTTP values showed a significant decrease at the ganglionic and supraganglionic levels of the MCA territory on the operated side (mean ± SD of 2.48 ± 1.52 vs. 1.54 ± 0.86 and 3.00 ± 1.82 vs. 1.73 ± 1.09; $p < 0.001$ and $p < 0.001$).

Correlation between the Change Degrees in ASL and DSC Perfusion Parameters

When evaluating the correlation between the degrees of improvement in ASL and DSC parameters, no significant correlation between the changes in rCBF values for ASL and DSC perfusion MRI was found ($r = 0.195$, $p = 0.303$). However, there was a significant correlation between the changes in perfusion scores for ASL and rTTP on DSC perfusion MRI ($r = 0.701$, $p < 0.001$). The correlation plots are shown in Figure 2. Representative good and poor postoperative cases are presented in Figures 3 and 4, respectively.

Table 3. Perfusion Changes on Dynamic Susceptibility Contrast Perfusion MRI after Indirect Revascularization

Parameters	Preoperative	Postoperative	*P*
Relative CBF*			
Ganglionic level	1.04 ± 0.20	1.18 ± 0.26	0.001
Supraganglionic level	0.95 ± 0.20	1.07 ± 0.22	0.001
Relative TTP†			
Ganglionic level	2.48 ± 1.52	1.54 ± 0.86	< 0.001
Supraganglionic level	3.00 ± 1.82	1.73 ± 1.09	< 0.001

Values are presented as mean ± standard deviation. *Relative CBF values were calculated as follows: $CBF_{measured\ level}/CBF_{cerebellum}$, †Relative TTP value was calculated as follows: $TTP_{measured\ level}$-$TTP_{cerebellum}$. CBF = cerebral blood flow, TTP = time-to-peak

DISCUSSION

Our study assessed whether ASL perfusion MRI can be used to monitor perfusion after indirect revascularization surgery in pediatric patients with MMD. ASL perfusion MRI showed an increase in quantitative rCBF values and improved qualitative perfusion scores for the MCA territory on the operated side after indirect revascularization. Compared with the DSC perfusion parameters, there was a significant correlation between the degree of change in the qualitative perfusion scores using the ATT effect and the rTTP improvement on DSC perfusion MRI.

MMD is a progressive steno-occlusive change in the intracranial vessels, and bypass surgery is currently

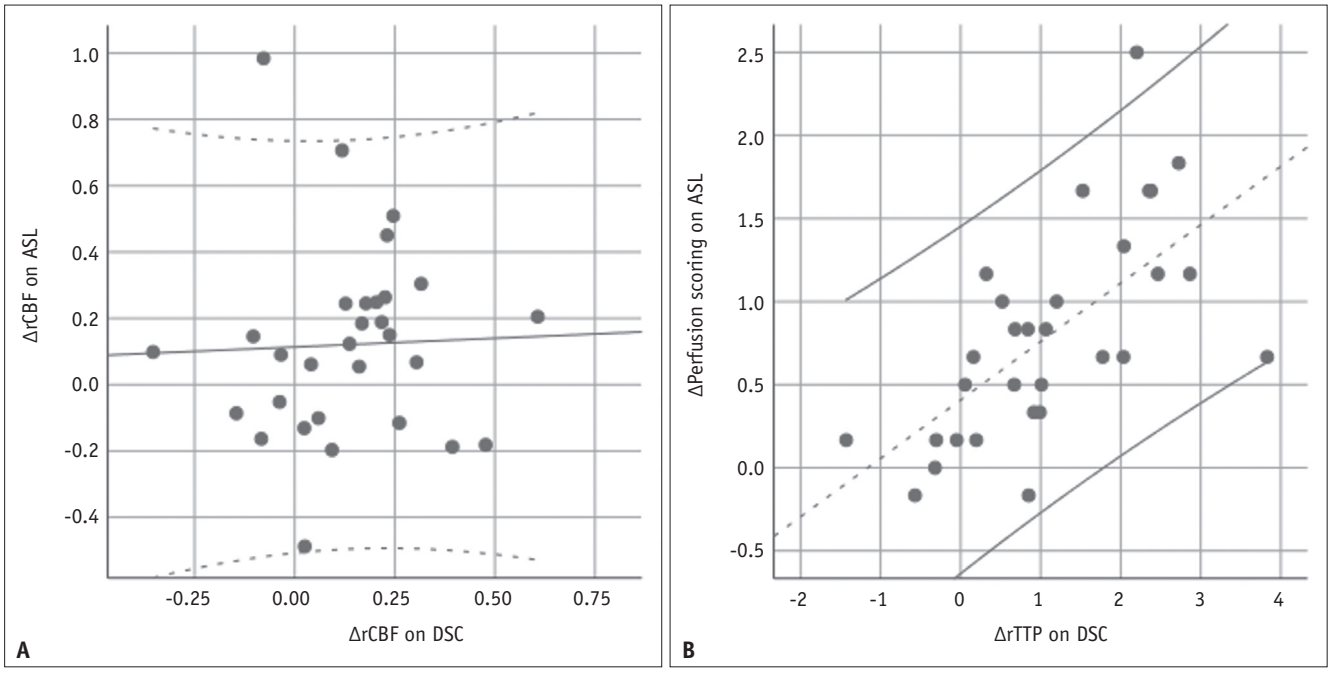

Fig. 2. Correlation plots for the change degrees after surgery for the ASL and DSC perfusion parameters.
A. There was no significant correlation between the mean improvement in rCBF assessed with DSC MRI and the mean improvement in rCBF assessed by ASL MRI ($r = 0.195$, $p = 0.303$). **B.** There was a significant correlation between the mean improvement in rTTP values on DSC MRI and the mean improvement in the arterial transit time perfusion score on ASL perfusion MRI ($r = 0.701$, $p < 0.001$). ASL = arterial spin-labeling, DSC = dynamic susceptibility contrast, rCBF = relative cerebral blood flow, rTTP = relative time-to-peak

https://doi.org/10.3348/kjr.2020.1464

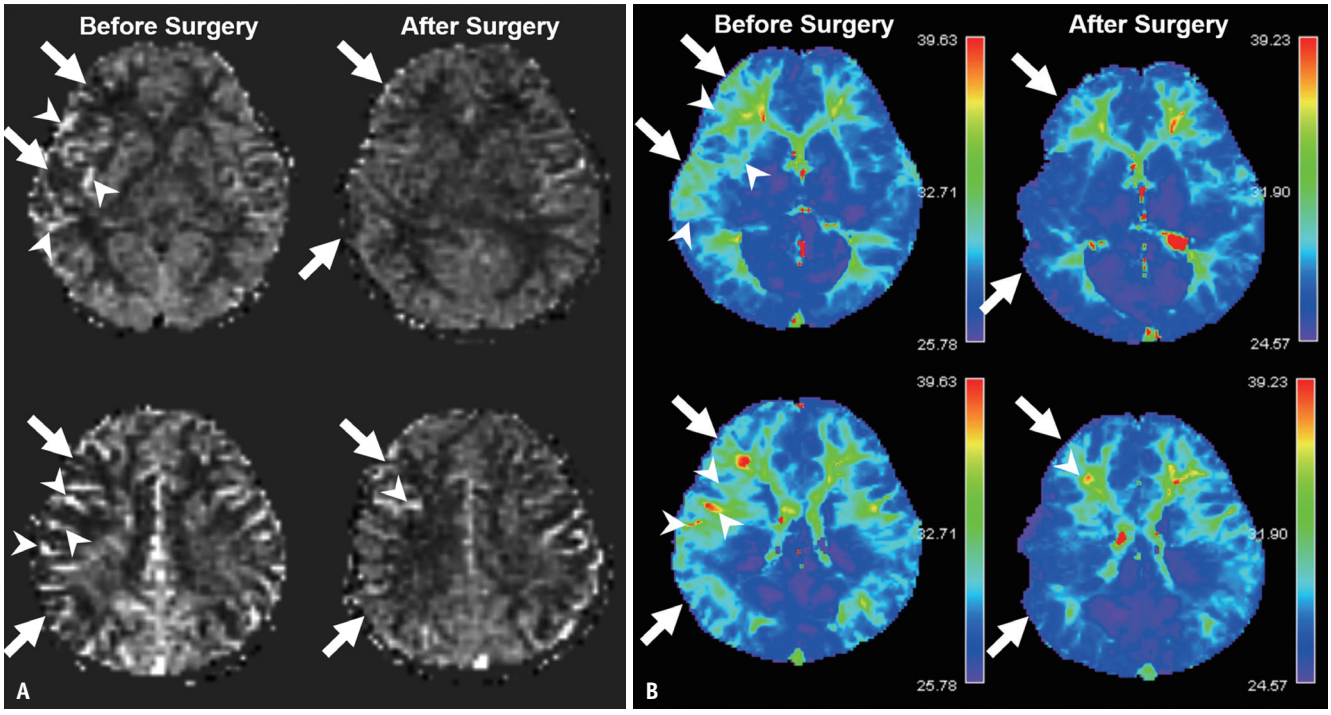

Fig. 3. Good postoperative case. A 6-year-old girl underwent right encephaloduroarteriosynangiosis with good postoperative outcomes. **A.** Preoperative ASL perfusion image showing ATT effects (arrowheads) and no parenchymal signal areas (arrows) at the ganglionic and supraganglionic levels of the right MCA territory. Postoperative ASL images show decreased ATT effects (arrowhead) and improved parenchymal signal intensity (arrows) at the same level in the right MCA territory. **B.** Preoperative TTP maps of dynamic susceptibility contrast perfusion MRI showing a delayed TTP area in the right MCA territory (arrows) with several foci having delayed transit times (arrowheads) corresponding to the ATT areas on ASL images. Postoperative TTP maps show an improved TTP area in the operative MCA territory. Only a subtle delayed TTP area remained at the supraganglionic level with a delayed transit time (arrowheads) corresponding to the ATT area on the ASL image. ASL = arterial spin-labeling, ATT = arterial transit time, MCA = middle cerebral artery, TTP = time-to-peak

regarded as its effective treatment [23]. EDAS is an indirect revascularization method in which the parietal branch of the superficial temporal artery, together with the surrounding connective tissue, is separated and sutured into the MCA territory [1]. Therefore, indirect revascularization involves grafted cortical blood vessel growth in ischemic vulnerable brain tissue from the cortical brain surface [1,23]. The effect of indirect revascularization is based on the extent of postsurgical neo-angiogenesis; thus, overall hemodynamic change monitoring is important [24].

For assessing cerebral hemodynamic changes, positron emission tomography (PET) and single-photon emission computed tomography (SPECT) have been useful for quantifying CBF and cerebrovascular reserve alterations. However, there are intrinsic disadvantages of serial examinations, radiation concerns, and poor spatial resolution [25,26]. For the MRI techniques, postoperative hemodynamic changes on DSC perfusion MRI may be well-correlated with clinical outcomes after revascularization surgery in children with MMD [12,21,22]. Yun et al. [21] reported that the rTTP value of DSC perfusion parameters is a useful marker for postoperative hemodynamic monitoring and clinical outcomes in pediatric patients with MMD. Lee et al. [22] also showed that the TTP perfusion map reflects the ischemic status of patients with MMD and the degree of ischemia reduction after revascularization surgery. As reported in previous studies, our study also showed that rCBF and rTTP values on DSC perfusion MRI improved after indirect revascularization surgery.

However, DSC perfusion MRI is technically more challenging in children because it requires a gadolinium contrast agent with high-flow bolus injection, despite the advantage of providing several quantified perfusion parameters [27]. Another critical limitation of DSC perfusion MRI is that confounding due to the presence of collateral vessels with the effects of arterial arrival delay may lead to rCBF underestimation and rTTP overestimation [4,28]. This drawback caused by delayed-arriving collateral flow can also occur during ASL perfusion MRI. However, ASL perfusion MRI may leverage this disadvantage to facilitate interpretations for collateral vessels; it also does not require the use of a gadolinium-based contrast agent, which is an

https://doi.org/10.3348/kjr.2020.1464

Korean Journal of Radiology
KJR

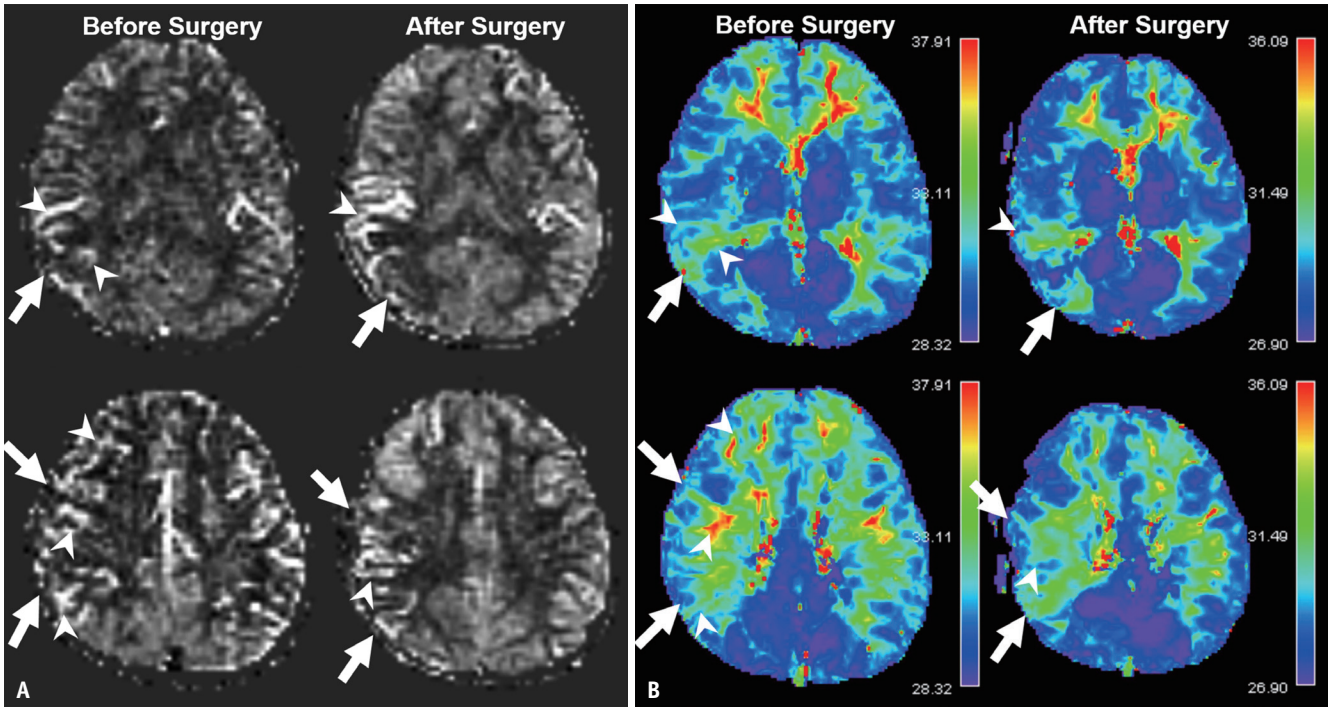

Fig. 4. Poor postoperative case. A 7-year-old boy underwent right encephaloduroarteriosynangiosis with poor postoperative outcomes. **A.** Preoperative ASL perfusion image showing ATT effects (arrowheads) and no parenchymal signal areas (arrows) at the ganglionic and supraganglionic levels of the right MCA territory. Postoperative ASL images show impaired perfusion (arrows) and ATT effects (arrowheads) in the right MCA territory, indicating flow stagnation in the cephaloduroarteriosynangiosis area. **B.** Preoperative TTP maps of dynamic susceptibility contrast perfusion MRI showing delayed TTP area in the right MCA territory (arrows) with profound delayed transit time (arrowheads) corresponding to those of the ATT areas on ASL images. Postoperative TTP maps show delayed TTP areas (arrows) in the operative MCA territory. Multiple delayed TTP areas (arrows) remained at the supraganglionic level with a delayed transit time (arrowheads) corresponding to the ATT area on the ASL image. ASL = arterial spin-labeling, ATT = arterial transit time, MCA = middle cerebral artery, TTP = time-to-peak

advantage [4,8,13]. ASL perfusion MRI has a characteristic feature: the ATT effect refers to labeled blood, which fails to reach the capillary bed and remains inside the artery, appearing as a strong bright signal intensity, which indicates collateral vascular flow [13]. Therefore, careful use of ASL images facilitates the assessment of postoperative hemodynamic status, in which collateral vessels possibly exist and are reduced in patients with MMD [4,29].

The ATT effect has two conflicting characteristics regarding CBF estimation: derived CBF may be underestimated due to a very long ATT when no labeled blood has reached the imaging volume or overestimated because the bright intravascular signal blood has slowly come to the precapillary arterioles [11,12,30]. However, Fahlström et al. reported that the ATT effects used for CBF calculations may have negligible overestimated effects when assessed using a vascular region-based CBF on a single delayed pseudo-continuous ASL perfusion MRI [11]. Our study showed that rCBF on ASL slightly improved after indirect revascularization surgery, but the difference in rCBF between the pre- and postoperative stages was low, and the standard variation was higher postoperatively. This phenomenon should be considered as the combined effect of high (due to the ATT effect) and low (due to the apparent perfusion deficit) CBF voxels [17].

In our study, there was no significant correlation between rCBF on ASL and the degree of improvement of rCBF on DSC perfusion MRI, although the rCBF values on ASL significantly increased in the MCA territory after revascularization surgery. The lack of correlation with DSC perfusion parameters may be related to CBF measurements based on ASL perfusion MRI and the ATT effects of the single-delay pseudo-continuous technique. However, regarding qualitative perfusion changes, we hypothesized that there was a decrease in collateral vessels at the operated side of the MCA territory after revascularization surgery, which may have improved the perfusion scores with ATT decrease. Recently, Ukai et al. [18] reported that severe ATT effects on ASL perfusion MRI may suggest a decrease in cerebrovascular reserve and a severe MMD stage. Our study showed an ATT effect reduction on ASL due to improved MCA territory perfusion through the newly grafted

https://doi.org/10.3348/kjr.2020.1464

EDAS flow and decreased delayed-arriving flow through the collateral vessels.

The qualitative ASL perfusion score was correlated with an improvement in rTTP on DSC perfusion MRI. Lee et al. reported the excellent diagnostic performance of the ATT effect in adult patients with MMD in evaluating collateral grading and anastomosis patency after direct revascularization [8]. However, there are few studies on the changes in ATT effects related to the DSC perfusion parameters before and after surgery in pediatric patients with MMD. Therefore, this study suggests the potential application of single-delay pseudo-continuous ASL perfusion MRI to postoperative perfusion status monitoring in pediatric patients with MMD. Additionally, single-delay pseudo-continuous ASL perfusion MRI is more advantageous than the multi-delay ASL technique in terms of SNR and scan time [31].

This study has some limitations. First, we only evaluated the perfusion status for the ganglionic and supraganglionic levels of the MCA territory. Perfusion changes in the basal collateral vessels in the basal ganglia region should also be evaluated in patients with MMD. However, we emphasized perfusion changes before and after the EDAS area using perfusion MRI data, even though the EDAS area did not exactly match these MCA territories. Potential bias may have been introduced in the ROIs by only including the ganglionic and supraganglionic levels of the MCA territories. Second, only a few patients with MMD were studied. However, our study included only a homogenous population of pediatric patients undergoing indirect revascularization, mostly EDAS, showing changes in perfusion between the pre- and postoperative stages. Third, we could not compare the data of ASL perfusion MRI and standard methods, including PET, SPECT, or perfusion CT, to validate the quantitative CBF results, because these examinations were not performed in our hospital. Since SPECT or PET was not used as a reference standard in this study, the interpretation of these quantitative results may have some limitations for both ASL and DSC perfusion MRI. However, rTTP on DSC has been used as a reference standard for postoperative perfusion improvement in previous studies [4,21,22]. Therefore, we compared the perfusion changes on ASL images with the rTTP value for DSC perfusion MRI after indirect revascularization. Finally, our study was conducted using an MR imager with a magnetic field strength of 1.5. Theoretically, 3T can offer an advantage over 1.5T related to the SNR. However, 1.5T is preferred over 3T for postoperative follow-up studies, and it has fewer susceptible artifacts. In previous studies, there was a slight difference between the normalized CBF measurements coordinated in the cerebellum between the 1.5T and 3T imagers [8].

In conclusion, recognizing the effects of ATT on ASL perfusion MRI may help monitor cerebral perfusion changes and complement quantitative CBF assessment in MMD patients after indirect revascularization.

Conflicts of Interest

The authors have no potential conflicts of interest to disclose.

Acknowledgments

Six patients in this study overlapped with a previous report (Ha JY et al. Korean J Radiol 2019;20:985-996) [9].

Author Contributions

Conceptualization: Seul Bi Lee, Seunghyun Lee. Data curation: Seul Bi Lee, Seunghyun Lee, Yeon Jin Cho, Young Hun Choi. Formal analysis: Seul Bi Lee, Seunghyun Lee. Funding acquisition: Seunghyun Lee. Investigation: Seul Bi Lee, Seunghyun Lee, Yeon Jin Cho, Young Hun Choi. Methodology: all authors. Project administration: Seunghyun Lee. Resources: all authors. Software: Seul Bi Lee, Seunghyun Lee. Supervision: Seunghyun Lee. Validation: all authors. Visualization: Seul Bi Lee, Seunghyun Lee. Writing—original draft: all authors. Writing—review & editing: all authors.

ORCID iDs

Seul Bi Lee
https://orcid.org/0000-0002-5163-3911
Seunghyun Lee
https://orcid.org/0000-0003-1858-0640
Yeon Jin Cho
https://orcid.org/0000-0001-9820-3030
Young Hun Choi
https://orcid.org/0000-0002-1842-9062
Jung-Eun Cheon
https://orcid.org/0000-0003-1479-2064
Woo Sun Kim
https://orcid.org/0000-0003-2184-1311

REFERENCES

1. Fung LW, Thompson D, Ganesan V. Revascularisation surgery

for paediatric moyamoya: a review of the literature. *Childs Nerv Syst* 2005;21:358-364
2. Zeifert PD, Karzmark P, Bell-Stephens TE, Steinberg GK, Dorfman LJ. Neurocognitive performance after cerebral revascularization in adult moyamoya disease. *Stroke* 2017;48:1514-1517
3. Zaharchuk G, Bammer R, Straka M, Shankaranarayan A, Alsop DC, Fischbein NJ, et al. Arterial spin-label imaging in patients with normal bolus perfusion-weighted MR imaging findings: pilot identification of the borderzone sign. *Radiology* 2009;252:797-807
4. Goetti R, O'Gorman R, Khan N, Kellenberger CJ, Scheer I. Arterial spin labelling MRI for assessment of cerebral perfusion in children with moyamoya disease: comparison with dynamic susceptibility contrast MRI. *Neuroradiology* 2013;55:639-647
5. Essig M, Shiroishi MS, Nguyen TB, Saake M, Provenzale JM, Enterline D, et al. Perfusion MRI: the five most frequently asked technical questions. *AJR Am J Roentgenol* 2013;200:24-34
6. Nezamzadeh M, Matson GB, Young K, Weiner MW, Schuff N. Improved pseudo-continuous arterial spin labeling for mapping brain perfusion. *J Magn Reson Imaging* 2010;31:1419-1427
7. Wang R, Yu S, Alger JR, Zuo Z, Chen J, Wang R, et al. Multi-delay arterial spin labeling perfusion MRI in moyamoya disease--comparison with CT perfusion imaging. *Eur Radiol* 2014;24:1135-1144
8. Lee S, Yun TJ, Yoo RE, Yoon BW, Kang KM, Choi SH, et al. Monitoring cerebral perfusion changes after revascularization in patients with moyamoya disease by using arterial spin-labeling MR imaging. *Radiology* 2018;288:565-572
9. Ha JY, Choi YH, Lee S, Cho YJ, Cheon JE, Kim IO, et al. Arterial spin labeling MRI for quantitative assessment of cerebral perfusion before and after cerebral revascularization in children with moyamoya disease. *Korean J Radiol* 2019;20:985-996
10. Quon JL, Kim LH, Lober RM, Maleki M, Steinberg GK, Yeom KW. Arterial spin-labeling cerebral perfusion changes after revascularization surgery in pediatric moyamoya disease and syndrome. *J Neurosurg Pediatr* 2019;23:486-492
11. Fahlström M, Lewén A, Enblad P, Larsson EM, Wikström J. High intravascular signal arterial transit time artifacts have negligible effects on cerebral blood flow and cerebrovascular reserve capacity measurement using single postlabel delay arterial spin-labeling in patients with moyamoya disease. *AJNR Am J Neuroradiol* 2020;41:430-436
12. Tortora D, Scavetta C, Rebella G, Bertamino M, Scala M, Giacomini T, et al. Spatial coefficient of variation applied to arterial spin labeling MRI may contribute to predict surgical revascularization outcomes in pediatric moyamoya vasculopathy. *Neuroradiology* 2020;62:1003-1015
13. Zaharchuk G, Do HM, Marks MP, Rosenberg J, Moseley ME, Steinberg GK. Arterial spin-labeling MRI can identify the presence and intensity of collateral perfusion in patients with moyamoya disease. *Stroke* 2011;42:2485-2491
14. Suzuki J, Kodama N. Moyamoya disease--a review. *Stroke* 1983;14:104-109
15. Helton KJ, Glass JO, Reddick WE, Paydar A, Zandieh AR, Dave R, et al. Comparing segmented ASL perfusion of vascular territories using manual versus semiautomated techniques in children with sickle cell anemia. *J Magn Reson Imaging* 2015;41:439-446
16. Lou X, Yu S, Scalzo F, Starkman S, Ali LK, Kim D, et al. Multi-delay ASL can identify leptomeningeal collateral perfusion in endovascular therapy of ischemic stroke. *Oncotarget* 2017;8:2437-2443
17. Bolar DS, Gagoski B, Orbach DB, Smith E, Adalsteinsson E, Rosen BR, et al. Comparison of CBF measured with combined velocity-selective arterial spin-labeling and pulsed arterial spin-labeling to blood flow patterns assessed by conventional angiography in pediatric moyamoya. *AJNR Am J Neuroradiol* 2019;40:1842-1849
18. Ukai R, Mikami T, Nagahama H, Wanibuchi M, Akiyama Y, Miyata K, et al. Arterial transit artifacts observed by arterial spin labeling in Moyamoya disease. *J Stroke Cerebrovasc Dis* 2020;29:105058
19. Potreck A, Seker F, Hoffmann A, Pfaff J, Nagel S, Bendszus M, et al. A novel method to assess pial collateralization from stroke perfusion MRI: subdividing Tmax into anatomical compartments. *Eur Radiol* 2017;27:618-626
20. Schmidt MA, Knott M, Hoelter P, Engelhorn T, Larsson EM, Nguyen T, et al. Standardized acquisition and post-processing of dynamic susceptibility contrast perfusion in patients with brain tumors, cerebrovascular disease and dementia: comparability of post-processing software. *Br J Radiol* 2020;93:20190543
21. Yun TJ, Cheon JE, Na DG, Kim WS, Kim IO, Chang KH, et al. Childhood moyamoya disease: quantitative evaluation of perfusion MR imaging--correlation with clinical outcome after revascularization surgery. *Radiology* 2009;251:216-223
22. Lee SK, Kim DI, Jeong EK, Kim SY, Kim SH, In YK, et al. Postoperative evaluation of moyamoya disease with perfusion-weighted MR imaging: initial experience. *AJNR Am J Neuroradiol* 2003;24:741-747
23. Acker G, Fekonja L, Vajkoczy P. Surgical management of moyamoya disease. *Stroke* 2018;49:476-482
24. Kim HG, Lee SK, Lee JD. Characteristics of infarction after encephaloduroarteriosynangiosis in young patients with moyamoya disease. *J Neurosurg Pediatr* 2017;19:1-7
25. Kuwabara Y, Ichiya Y, Sasaki M, Yoshida T, Masuda K, Ikezaki K, et al. Cerebral hemodynamics and metabolism in moyamoya disease--a positron emission tomography study. *Clin Neurol Neurosurg* 1997;99 Suppl 2:S74-S78
26. Noguchi T, Kawashima M, Irie H, Ootsuka T, Nishihara M, Matsushima T, et al. Arterial spin-labeling MR imaging in moyamoya disease compared with SPECT imaging. *Eur J Radiol* 2011;80:e557-e562

 https://doi.org/10.3348/kjr.2020.1464

27. Gaudino S, Martucci M, Botto A, Ruberto E, Leone E, Infante A, et al. Brain DSC MR perfusion in children: a clinical feasibility study using different technical standards of contrast administration. *AJNR Am J Neuroradiol* 2019;40:359-365
28. Calamante F, Gadian DG, Connelly A. Delay and dispersion effects in dynamic susceptibility contrast MRI: simulations using singular value decomposition. *Magn Reson Med* 2000;44:466-473
29. Tortora D, Severino M, Pacetti M, Morana G, Mancardi MM, Capra V, et al. Noninvasive assessment of hemodynamic stress distribution after indirect revascularization for pediatric moyamoya vasculopathy. *AJNR Am J Neuroradiol* 2018;39:1157-1163
30. Nael K, Meshksar A, Liebeskind DS, Coull BM, Krupinski EA, Villablanca JP. Quantitative analysis of hypoperfusion in acute stroke: arterial spin labeling versus dynamic susceptibility contrast. *Stroke* 2013;44:3090-3096
31. Donahue MJ, Achten E, Cogswell PM, De Leeuw FE, Derdeyn CP, Dijkhuizen RM, et al. Consensus statement on current and emerging methods for the diagnosis and evaluation of cerebrovascular disease. *J Cereb Blood Flow Metab* 2018;38:1391-1417

https://doi.org/10.3348/kjr.2020.1464

AJNR Am J Neuroradiol 24:741–747, April 2003

Postoperative Evaluation of Moyamoya Disease with Perfusion-Weighted MR Imaging: Initial Experience

Seung-Koo Lee, Dong Ik Kim, Eun-Kee Jeong, Si-Yeon Kim, Sang Heum Kim, Yon Kwon In, Dong-Seok Kim, and Joong-Uhn Choi

BACKGROUND AND PURPOSE: **Encephaloduroarteriosynangiosis (EDAS) has become the main treatment for moyamoya disease, a chronically progressive cerebrovascular occlusive disease in children. We aimed to assess the utility of perfusion-weighted MR imaging for evaluating hemodynamic changes before and after EDAS.**

METHODS: **Thirteen patients with angiographically confirmed moyamoya disease who underwent EDAS were investigated, and results were compared with those of a control group (n = 5). Perfusion MR imaging was performed before and after EDAS by using a T2*-weighted contrast material–enhanced technique. Relative cerebral blood volume (rCBV) and time to peak enhancement (TTP) maps were calculated. Relative ratios of rCBV and TTP in the middle cerebral artery (MCA) and basal ganglia were measured and compared with those of the posterior cerebral artery (PCA). Changes in hemodynamic parameters between pre- and post-EDAS perfusion maps were investigated.**

RESULTS: **The mean rCBV ratio of MCA to PCA in the patient group was slightly higher than that in the control group, without statistical significance. All 13 patients showed a delayed TTP in the MCA before EDAS compared with the control group ($P = .0006$), and the TTP after EDAS was significantly reduced ($P = .0002$). In the basal ganglia, shortening of the TTP was demonstrated before EDAS, but no significant change was observed after EDAS.**

CONCLUSION: **Perfusion-weighted MR imaging can be applied for evaluating postoperative changes in cerebral blood flow in moyamoya disease. Shortening of the TTP in the MCA of the hemisphere operated on is a marker for the development of collateral circulation from the external carotid artery to the internal carotid artery.**

Moyamoya disease is a chronically progressive cerebrovascular disease affecting the supraclinoid internal carotid arteries (ICAs) with prominent collateral arterial formation (1). Despite the fact that moyamoya disease is thought to affect primarily Japanese or Koreans, it also has been reported in other ethnic groups (2, 3). The etiology is still uncertain, and without proper treatment, children presenting with ischemic symptoms tend to show an aggravating natural course (4). Encephaloduroarteriosynangiosis (EDAS) is the treatment of choice because this procedure can reestablish cerebral perfusion by means of external carotid artery (ECA)-to-ICA bypass (5). Development of collateral vessels after surgery usually occurs in the middle cerebral artery (MCA) territory because of the distribution of the superficial temporal artery, which is the most commonly used supplier for EDAS. Although other advanced procedures for reconstruction of blood flow to the anterior cerebral artery (ACA) territory have been introduced recently (6–8), EDAS is still widely used in many institutes.

Conventional angiography is used to diagnose moyamoya disease (9), but single photon emission tomography (SPECT) is known to be the reference standard for evaluating the hemodynamic status of patients with moyamoya disease (10, 11). MR imaging also has been widely used in assessing moyamoya disease, because of its capacity to illustrate anatomic

Received September 17, 2001; accepted after revision November 8, 2002.

From the Department of Diagnostic Radiology and the Research Institute of Radiological Science (S.K.L., D.I.K., E.K.J, S.Y.K., S.H.K., Y.K.I.), and the Department of Neurosurgery (D.S.K., J.U.C.), BK21 Project for Medical Science, Yonsei University College of Medicine, Seoul, Korea.

Supported by a grant from the Korean Radiological Foundation and HMP-99-N-01–0001 of the Ministry of Health and Welfare, Korea.

Address reprint requests to Dong Ik Kim, MD, PhD, Department of Diagnostic Radiology, Yonsei University College of Medicine, 134 Shinchondong, Seodaemungu, Seoul, Korea 120–752; e-mail:.

detail and the vascular architecture (12, 13). Recently, T2*-weighted perfusion MR imaging has been found to be effective in estimating cerebral hemodynamics in moyamoya disease (14–17). These diagnostic maneuvers can be used to assess local hemodynamic changes after ICA-to-ECA bypass surgery (18–20). However, there is a paucity of reports describing the efficacy of perfusion-weighted MR imaging in postoperative evaluation. The purpose of this study was to assess the utility of perfusion MR imaging in illustrating the hemodynamic changes of an ischemic brain in moyamoya disease before and after EDAS.

Methods

Thirteen patients with childhood moyamoya disease who underwent EDAS between July 1999 and March 2002 were evaluated by using perfusion-weighted MR imaging before and after surgery. The subjects consisted of eight female and five male patients, with ages ranging from 2 to 27 years (mean, 8.5 years). They received preoperative diagnostic evaluation with technetium-99m ethyl cysteinate dimer SPECT and conventional angiography. On cerebral angiograms, all 13 patients showed stenosis, either partial or complete obstruction, in the supraclinoid portion of the ICAs. All showed patent posterior cerebral arteries (PCAs) and various degrees of leptomeningeal collateral vessels (eg, less than Suzuki grade V [21]). EDAS was performed according to the patients' clinical symptoms and angiographic findings. EDAS was performed in the left cerebral hemisphere in four patients, in the right cerebral hemisphere in three patients, and in both hemispheres in the remaining six patients.

All patients underwent preoperative perfusion-weighted MR imaging 3–7 days before EDAS and postoperative perfusion-weighted MR imaging 6–8 months after EDAS. Five children (three male, two female subjects; mean age, 9.3 years; age range,) were included in the control group because healthy volunteers were not available for perfusion study. Age-matched control subjects could not be recruited because they would have needed sedation, and ethical considerations prohibited this. The control subjects were referred for brain imaging with the complaint of simple headache or psychiatric problem. They were found to have no central nervous system disease radiologically and at follow-up studies. Informed consent was received from all participants or the participants' parents or legal guardian, and all procedures were performed under approval by the institutional board of clinical studies.

The MR examinations were conducted by using a 1.5-T system (Signa Horizon, GE Medical System, Milwaukee, WI, or Gyroscan Intera, Philips Medical Systems, Best, the Netherlands) with a quadrature head coil. Perfusion-weighted MR imaging was performed by using a single-shot gradient-echo echo-planar imaging sequence during an intravenous bolus injection of 0.2 mmol/kg gadopentetate dimeglumine (Magnevist; Schering AG, Berlin, Germany) with the following parameters: 1500/40/1 (TR/TE/excitations), 24-cm field of view, 5-mm section thickness with a 2-mm intersection gap, and 128 × 128 matrix. Six sections were chosen starting from the anteroposterior commisure line including the transthalamic level, and 40 dynamic perfusion images were obtained from each level. Contrast material was injected by using a power injector (Spectris; Medrad, Indianola, PA) after the fifth dynamic image, followed by flushing with normal saline, and image acquisition continued until all 40 phase images were obtained.

Data from the eight patients who were examined with the GE system were transferred to a personal computer, where the data were analyzed by using a program coded for Interactive Data Language (IDL 5.4 Win32; Research Systems Inc., Boulder, CO). The data of the other five patients examined with the Philips system were processed by Easyvision (Philips Medical Systems). For each pixel, the time-concentration or ΔR2* curve was obtained, which was calculated from the equation $\Delta R2^*(t) = [\ln(SI_0/SI(t))]$, where SI_0 is the average precontrast signal intensity and $SI(t)$ is the signal intensity at time t. The relative cerebral blood volume (rCBV) was calculated pixel by pixel from the time-relaxation curve obtained by dynamic imaging. The time interval to peak enhancement (TTP) maps were also calculated. The regions of interest in the bilateral MCA territory, PCA territory, and basal ganglia were drawn (Fig 1) and contained more than 20 pixels. The rCBV ratios and TTP differences of the MCA and of the basal ganglia to the PCA territory were calculated on the pre- and postoperative perfusion MR images. Statistical analysis was done between patients and control group by using the Student's t test for the independent samples. A paired t test was used to analyze the patient group for changes before and after EDAS. A P value of less than or equal to .05 was considered to indicate a statistically significant difference.

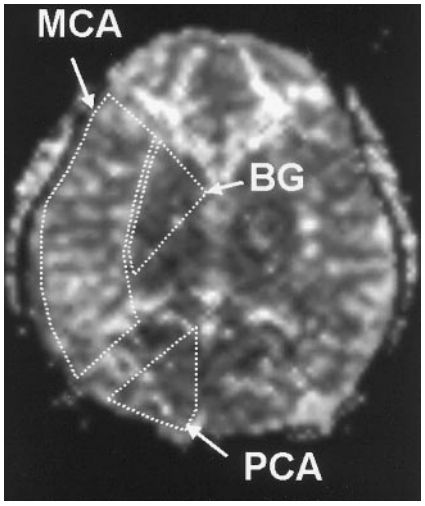

FIG 1. Regions of interest (*MCA*, *PCA*, and *BG*) are drawn on a TTP map. On the rCBV maps (not shown), the relative signal intensity ratios of the MCA and the BG to the PCA territory were obtained, whereas on the TTP maps the time differences in the MCA and BG were calculated and compared with that of the PCA territory.

rCBV Ratios and TTP Values in the Control Group and Patients

Parameter	Control Group (n = 5)	Patient Group (n = 13)	*P* Value*
rCBV ratio			
MCA to PCA	1.35 ± 0.14	1.31 ± 0.66	.950
BG to PCA	0.79 ± 0.12	0.78 ± 0.25	.756
TTP difference (sec)			
MCA to PCA	0	4.37 ± 2.25	.0006
BG to PCA	−0.76 ± 0.22	−1.08 ± 1.99	.765

Note.—Data are the mean ± SD.

* Two-tailed t test.

Results

The measured rCBV and TTP values in the control and patient groups are listed in the Table. The mean rCBV ratio of the MCA to PCA territory in the control group was 1.35 ± 0.14 in the MCA territory and 0.79 ± 0.12 in the basal ganglia. The TTP in the MCA territory was identical to that of the PCA ter-

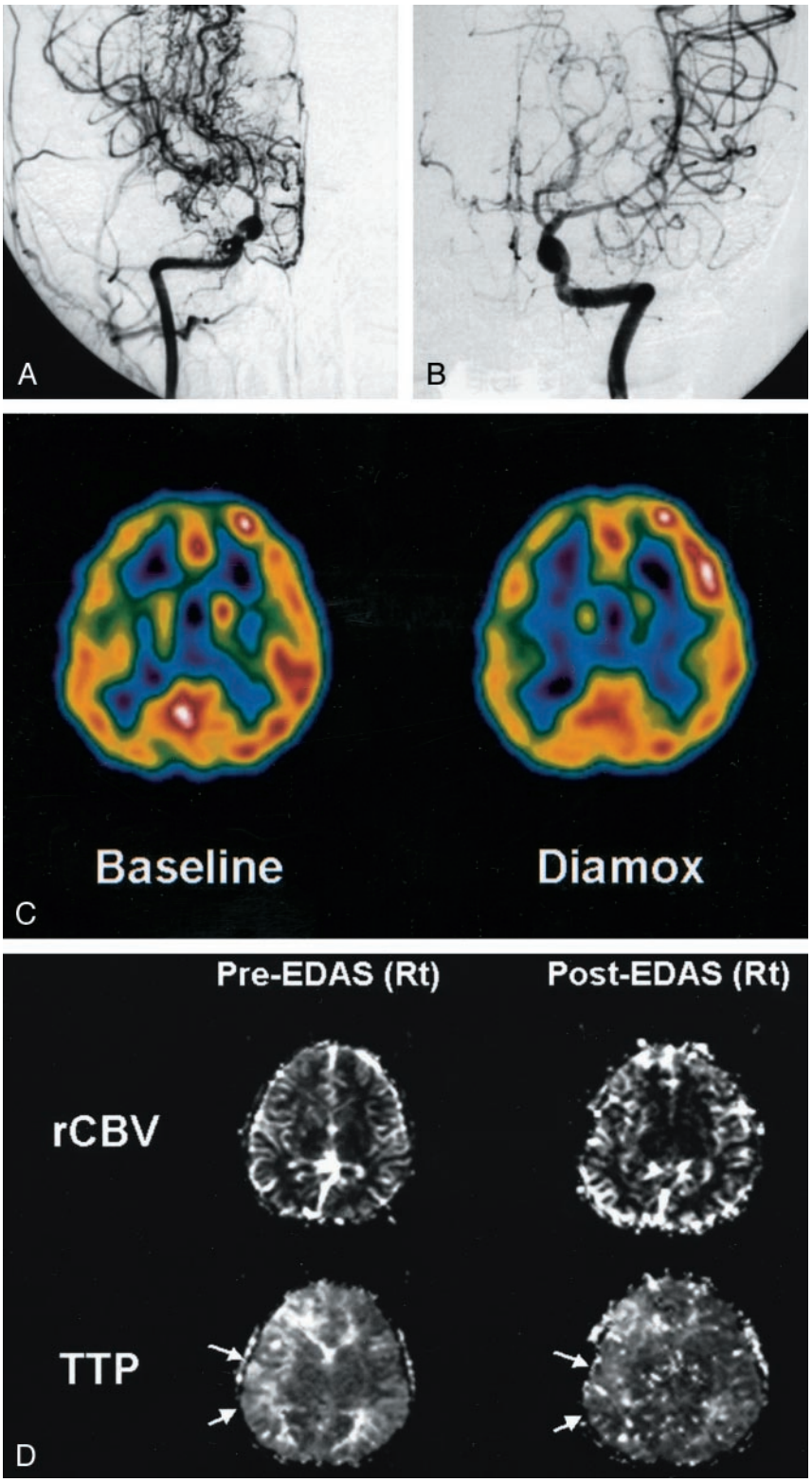

FIG 2. 9-year-old boy with moyamoya disease.

A, Anteroposterior angiogram of the right ICA shows an occlusion of the supraclinoid portion, with development of multiple basal collateral vessels (moyamoya vessels).

B, Left ICA angiogram depicts mild changes of the luminal caliber in the left MCA, but with preserved patency. Left ACA shows severe narrowing.

C, Technetium-99m ethyl cysteinate dimer SPECT scan (left scan) reveals decreased perfusion in both hemispheres, more prominent on the right side. After the acetazolamide (*Diamox*) injection (right scan), there is no evidence of a significant perfusion reduction.

D, Perfusion MR images show delayed TTP in the right hemisphere before EDAS (arrows in left TTP map) and a signal intensity reduction after EDAS (arrows in right TTP map), which means a restoration of rapid flow at the surgical site. Note, rCBV maps show nothing significant.

ritory, whereas the TTP in the basal ganglia was shorter than that in the PCA territory.

The mean rCBV ratio of MCA to PCA territory was slightly higher than that in the control group, without statistical significance ($P = .950$, t test for independent samples, two-tailed). In the basal ganglia, no definite change in rCBV was observed in the patient group when compared with the control group ($P = .756$). The TTP delay was striking in the MCA territory of the affected hemisphere in the patient group, with an average 4.37 seconds delay compared with the control group ($P = .0006$). Three of 13 patients showed an asymmetric delay in the TTP in both MCA territories. This corresponded well with

conventional angiography, which depicted a different degree of stenosis between both MCAs (Fig 2). In the basal ganglia, no significant TTP differences could be found between the two groups.

After surgery, the rCBV ratio in the MCA territory decreased in the case of the initial rCBV increase, but the overall change in the rCBV value was not statistically significant ($P = .281$, paired t test, two-tailed) (Fig 3A). The rCBV in the basal ganglia also did not depict any changes after surgery (Fig 3B). The TTP in the MCA territory operated on was significantly shortened after surgery ($P = .0002$), whereas the TTP in the basal ganglia was not (Fig 4). TTP shortening was demonstrated as a marked signal intensity reduction in the calculated maps after EDAS (Fig 2D). One patient underwent additional postoperative perfusion MR imaging before a second surgery on the contralateral side. The second perfusion MR imaging examination was performed 1 month after EDAS on the left side, and the patient then underwent a right EDAS. On the second perfusion MR image, the TTP shortening of the operated hemisphere was not definite, which suggested that neovascularization was not established at that time. Six months later, the patient was again evaluated with perfusion MR imaging and conventional angiography. On the follow-up conventional angiogram, neovascularization and prominent vascular staining were demonstrated from the ECA to the frontoparietal cerebral cortex. The results agreed well with those of perfusion MR imaging, which depicted shortened TTP at the left MCA territory after surgery (Fig 5).

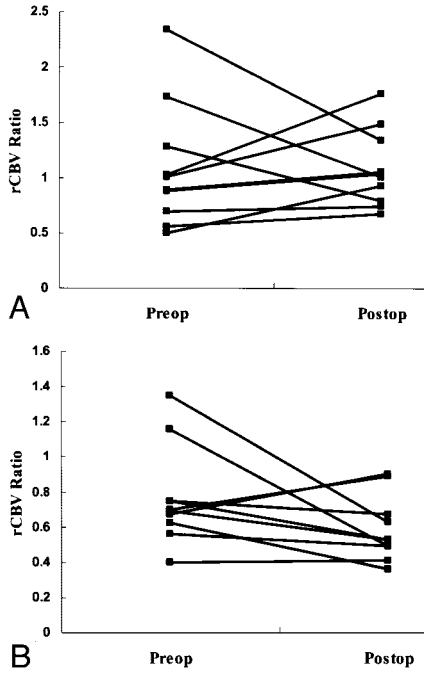

FIG 3. *A* and *B*, Graphs show changes in the rCBV ratios to the posterior circulation of the MCA territory (*A*) and the basal ganglia (*B*). The rCBV can be increased or decreased before (*Preop*) and after (*Postop*) surgery, which cannot characterize the rCBV patterns of moyamoya disease.

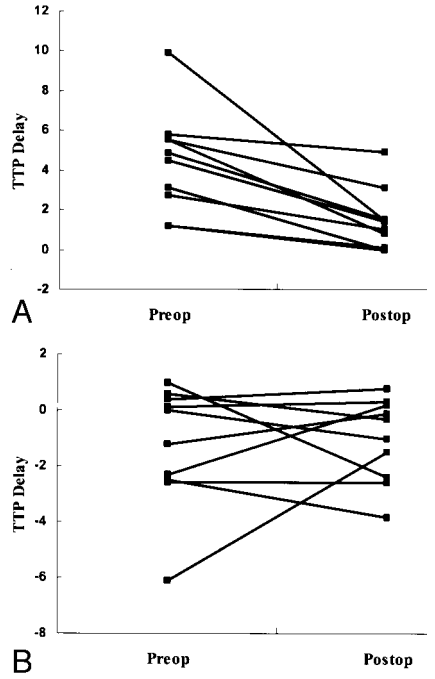

FIG 4. *A* and *B*, Graphs show changes in the TTP delay to the posterior circulation of the MCA territory (*A*) and basal ganglia (*B*). Note the markedly increased TTP in the MCA territory, with a significant reduction after surgery (*Postop*). There were no specific changes in the TTP values in the basal ganglia.

Discussion

As moyamoya disease forms many collateral vessels owing to the occlusion of major proximal intracranial arteries, the key role of imaging diagnosis has been focused on detecting collateral circulation, although the disease may induce an infarct or hemorrhage. CT was found to be useful in detecting the important diagnostic signs such as arterial occlusions and the formation of collateral vessels (22). However, a definite diagnosis is made with conventional angiography (9), which can depict the characteristic basal collateral vessels resembling a "puff of smoke" (ie, moyamoya vessels). Conventional angiography provides a detailed status of collateral development and stenosis of major cerebral arteries. In children, the moyamoya vessels change through six stages: 1) carotid fork stenosis; 2) progressive carotid stenosis with initial moyamoya collateral vessels and dilatations of cerebral arteries; 3) dilatation of moyamoya collateral vessels and disappearance of ACAs and MCAs; 4) thinning of moyamoya vessels; 5) contraction of moyamoya vessels and disappearance of PCAs; and 6) intracerebral vessels perfused from the ECA and/or vertebrae. On the basis of this grading system, the moyamoya vessels of all patients in this study were below grade 5. MR angiography has also played a role in detecting the collateral arteries, although many institutes prefer conventional angiography as a primary diagnostic tool.

Alterations in the local cerebral hemodynamic status are more important in understanding and plan-

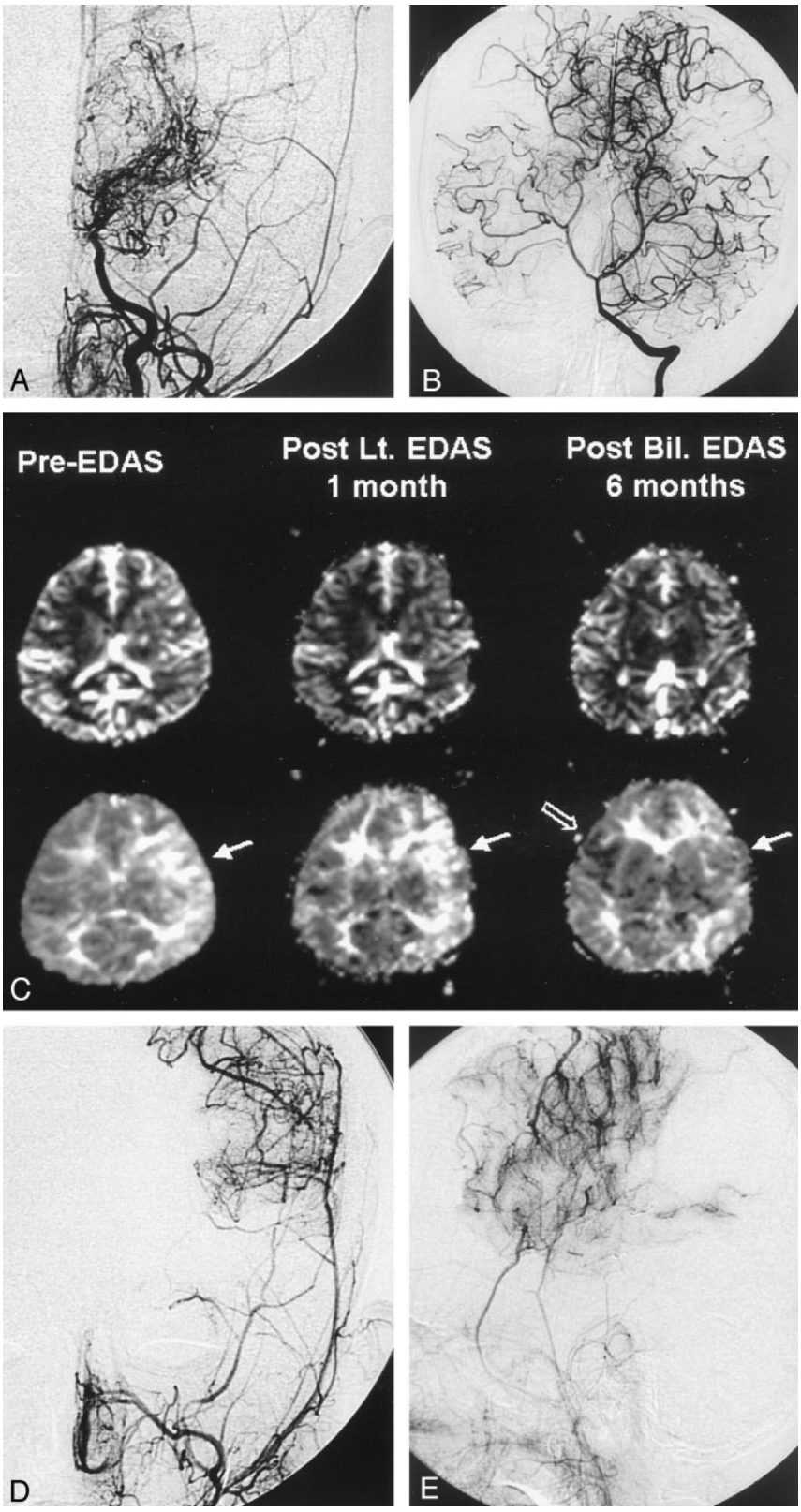

FIG 5. 7-year-old boy with moyamoya disease.

A, Preoperative left carotid angiogram shows an occlusion of the supraclinoid ICA with basal collateral vessels. No transdural collateral vessels from the superficial temporal or middle meningeal arteries are seen.

B, Vertebral artery angiogram shows prominent leptomeningeal collateral vessels supplying the bilateral hemispheres.

C, Serial perfusion-weighted MR images (rCBV, top row; TTP, bottom row) were obtained because the patient underwent bilateral EDAS procedures with a 1-month interval. One-month follow-up perfusion MR image shows a mild reduction in the TTP delay (arrow in middle TTP map), which means neovascularization is beginning to develop. The last perfusion MR image (right TTP map) shows near-complete normalization of the TTP in the left hemisphere (solid arrow) and a partial TTP shortening on the right side (open arrow).

D and *E*, Postoperative 7-month follow-up left ECA angiograms show successful neovascularization from the middle meningeal and superficial temporal arteries.

ning treatments for patients with moyamoya disease, which cannot be assessed with angiography alone. Scintigraphic methods, such as SPECT or positron emission tomography, are the reference standard for assessing cerebral hemodynamics because the tracer decay kinetics are well known, and the tracer distribution is proportional to the local cerebral blood flow. Previous studies have reported reduced regional cerebral blood flow in the frontal and temporal lobes and increased flow in the parietal and occipital lobes

and the basal ganglia (10, 23). These flow changes reflect the course of the disease, which starts from the ICA, MCA, and extends to the PCA. The posterior circulation usually supplies the ischemic frontotemporal lobes via the leptomeningeal collateral vessels, whereas the deep nuclei are supplied from the multiple basal collateral vessels. Such findings can be detected with perfusion-weighted echo-planar MR imaging. Yamada et al (17) demonstrated a reduced rCBV and a TTP delay at the anterior circulation in the case of a stenotic PCA. In contrast, the current study showed a TTP delay in all patients, even those with a normal PCA, whereas the rCBV changes varied. Angiography showed normal calibers of the PCAs and prominent leptomeningeal collateral vessels in all subjects. An asymmetric TTP delay between both MCA territories was also observed in three of 10 patients, in whom a different degree of stenosis was clearly depicted at conventional angiography. The TTP delay of the anterior circulation was proportional to the severity of the ICA stenosis. Therefore, this is a universal finding of moyamoya disease on perfusion MR images and can reflect the severity of the disease.

The goal of surgical treatment in moyamoya disease is to reestablish cerebral blood flow to the ischemic regions. EDAS is widely used in childhood moyamoya disease because it is a simple procedure and has a low risk of ischemia during temporary blocking of the cerebral blood flow in a conventional superficial temporal artery–MCA anastomosis (4, 24). Most surgical procedures have focused on increasing the blood flow primarily in the MCA territory and do not directly benefit the ACA territory (8). We measured the perfusion changes of only the MCA territory because of the nature of the surgical procedure. If a modified procedure that can reestablish the ACA flow is chosen for investigation, perfusion measurement must be done in the ACA territory in the future.

After EDAS, the superficial temporal artery or the adjacent middle meningeal artery participates in forming collateral pathways and can be detected with conventional angiography (25) or MR angiography (20). The effectiveness of EDAS must be assessed not only by visualizing the neovascularization but also by monitoring improved perfusion status with other diagnostic techniques. In this study, an alteration of the temporal parameters of perfusion-weighted MR imaging (eg, delay of TTP in the affected territory and reduction of TTP delay after surgical treatment, which corresponded with the rapid staining of cerebral arteries from ECA anastomosis) was shown. All patients who showed a decreased TTP delay in this study showed a fairly good outcome after surgery. Therefore, a reduction of the TTP in the MCA territory can indirectly reflect the improved perfusion status, although an accurate interpretation of the TTP in cerebral hemodynamics is still unclear.

TTP maps or angiography cannot assess perfusion at the cellular level, because they depict only the capillary blood flow. A cellular extraction of radiotracers can reflect such microhemodynamics, and a complete evaluation of postoperative patients must include postoperative scintigraphic studies. Although our protocol did not include postoperative SPECT, clinical improvement and angiographic evidence are enough to support satisfactory cerebral perfusion. Moreover, as conventional MR imaging can be performed easily during the postoperative period, it can be used as a primary follow-up diagnostic tool for evaluating the surgical outcome.

All hemodynamic parameters of perfusion-weighted imaging were relative values; therefore, the differences between the MCA and PCA territories could not be compared. The arterial input function of the MCA territory was impossible to obtain because the MCA was not identified in moyamoya disease. Actually, the real arterial input function of the cerebrum could not be assessed owing to the nature of the disease.

Previous studies with perfusion MR imaging or SPECT used a cerebral-to-cerebellar ratio or region-to-mean hemispheric blood volume to calculate regional cerebral blood flow (17, 26, 27). In the current study, the authors compared MCA territorial blood flow to occipital lobe-PCA territory because all patients showed patent PCAs at angiography. We could not use the occipital lobe instead of cerebellum as a standard because posterior fossa images were poor with echo planar imaging sequences due to susceptibility artifacts by the skull base and mastoid air cells. If ECA-to-ICA anastomosis occurs, the cerebral hemodynamics must be changed, including the mean hemispheric blood flow and volume. Therefore, the method in this study of using PCA and its territorial blood volume as a standard may be more ideal than the mean hemispheric blood volume in the pre- and postoperative evaluation with normal PCA flow. However, it is clear whether one should use another standard hemodynamic parameter if the patient has a stenotic or occluded PCA.

Lack of normal control values from healthy volunteers is a limitation of this study. We used control data from patients with simple headache or psychiatric conditions because we could not perform dynamic bolus injection of MR contrast material in healthy children. However, the control group children were found to have no central nervous system disease radiologically or clinically on follow-up.

The relatively broad age range of 2–27 years is another limitation. It may raise the question as to whether age-related hemodynamic changes would affect outcome. To our knowledge, TTP or rCBV change according to aging in the childhood period has not been reported. Oyama et al (28) reported that cerebral blood flow gradually decreases with aging in moyamoya disease; however, their patient population ranged from 16 to 58 years. We also could not get proper data from a healthy population to get standard hemodynamic features of children. This remains an unsolved problem in this study, and future investigation must be performed.

In summary, TTP perfusion maps can depict the preoperative hemodyamic status of patients with

moyamoya disease and postoperative changes as well. We postulate that perfusion MR imaging is a useful tool to evaluate cerebral blood flow in moyamoya disease.

Conclusion

Perfusion-weighted MR imaging can be applied for evaluating the postoperative changes in the cerebral blood flow in moyamoya disease. A shortening of the TTP in the MCA territory of the hemisphere operated on is a marker for the development of collateral circulation from the ECA to the ICA.

Acknowledgments

The authors wish to thank Sei Young Kim, MR technologist at the Severance Hospital, Yonsei University, for assistance with the MR examination and image preparation.

References

1. Suzuki J, Takaku A. **Cerebrovascular "moyamoya" disease: a disease showing abnormal net-like vessels in base of brain.** *Arch Neurol* 1969;20:288–299
2. Taveras JM. **Multiple progressive intracranial arterial occlusions: a syndrome of children and young adults**. *AJR Am J Roentgenol* 1969;106:235–268
3. Pecker J, Simon J, Guy G, Herry JF. **Nishimoto's disease: significance of its angiographic appearances.** *Neuroradiology* 1973;5:223–230
4. Choi JU, Kim DS, Kim EY, Lee KC. **Natural history of moyamoya disease: comparison of activity of daily living in surgery and nonsurgery groups**. *Clinic Neurol Neurosurg* 1997;99(suppl 2):S11–S18
5. Fujita K, Tamak N, Matsumoto S. **Surgical treatment of moyamoya disease in children: which is the more effective procedure, EDAS or EMS?** *Childs Nerv Syst* 1986;2:134–138
6. Iwama T, Hashimoto N, Miyake H, Yonekawa Y. **Direct revascularization to the anterior cerebral artery territory in patients with moyamoya disease: report of five cases.** *Neurosurgery* 1998;42:1157–1162
7. Matsushima T, Inoue TK, Suzuki SO, et al. **Surgical techniques and the results of a fronto-temporo-parietal combined indirect bypass procedure for children with moyamoya disease: a comparison with the results of encephalo-duro-arterio-synangiosis alone.** *Clin Neurol Neurosurg* 1997;99(suppl 2):S123–127
8. Kim SK, Wang KC, Kim IO, Lee DS, Cho BK. **Combined encephalo-duro-arterio-synangiosis and bifrontal encephalo-galeo-(periosteal)-synangiosis in pediatric moyamoya disease.** *Neurosurgery* 2002;50:88–96
9. Hasuo K, Tamura S, Kudo S, et al. **Moyamoya disease: use of digital subtraction angiography in its diagnosis.** *Radiology* 1985;157:107–111
10. Kuroda S, Houkin K, Kamiyama H, Abe H, Mitsumor K. **Regional cerebral hemodynamics in childhood moyamoya disease.** *Childs Nerv Syst* 1995;11:584–590
11. Miller JH, Khonsary A, Raffel C. **The scintigraphic appearance of childhood moyamoya disease on cerebral perfusion imaging.** *Pediatr Radiol* 1996;26:833–838
12. Yamada I, Matsushima Y, Suzuki S. **Moyamoya disease: diagnosis with three-dimensional time-of-flight MR angiography**. *Radiology* 1992;184:773–778
13. Yamada I, Suzuki S, Matsushima Y. **Moyamoya disease: comparison of assessment with MR angiography and MR imaging versus conventional angiography**. *Radiology* 1995;196:211–218
14. Tzika AA, Robertson RL, Barnes PD, et al. **Childhood moyamoya disease: hemodynamic MRI**. *Pediatr Radiol* 1997;27:727–735
15. Tsuchiya K, Inaoka S, Mizutani Y, Hachiya J. **Echo-planar perfusion MR of moyamoya disease**. *AJNR Am J Neuroradiol* 1998;19:211–216
16. Adams WM, Laitt RD, Li KL, Jackson A, Sherrington CR, Talbot P. **Demonstration of cerebral perfusion abnormalities in moyamoya disease using susceptibility perfusion- and diffusion-weighted MRI**. *Neuroradiology* 1999;41:86–92
17. Yamada I, Himeno Y, Nagaoka T, et al. **Moyamoya disease: evaluation with diffusion-weighted and perfusion echo-planar MR imaging**. *Radiology* 1999;212:340–347
18. Ohashi K, Fernandez-Ulloa M, Hall LC. **SPECT, magnetic resonance and angiographic features in a moyamoya patient before and after external-to-internal carotid artery bypass**. *J Nucl Med* 1992;33:1692–1695
19. Touho H, Karasawa J, Ohnishi H. **Preoperative and postoperative evaluation of cerebral perfusion and vasodilatory capacity with 99mTc-HMPAO SPECT and acetazolamide in childhood moyamoya disease**. *Stroke* 1996;27:282–289
20. Yoon HK, Shin HJ, Lee M, Byun HS, Na DG, Han BK. **MR angiography of moyamoya disease before and after encephaloduroarteriosynangiosis.** *AJR Am J Roentgenol* 2000;174:195–200
21. Suzuki J, Takaku A, Kodama N, Sato S. **An attempt to treat cerebrovascular moyamoya disease in children.** *Childs Brain* 1975;1:193–206
22. Takahashi M, Miyauchi T, Kowada M. **Computed tomography of moyamoya disease: demonstration of occluded arteries and collateral vessels as important diagnostic signs**. *Radiology* 1980;134:671–676
23. Takeuchi S, Tanaka R, Ishii R, Tsuchida T, Kobayashi K, Arai H. **Cerebral hemodynamics in patients with moyamoya disease: a study of regional cerebral blood flow by the 133Xe inhalation method**. *Surg Neurol* 1985;23:468–474
24. Karasawa J, Touho H, Ohnishi H, Miyamoto S, Kikuchi H. **Long-term follow-up study after extracranial-intracranial bypass surgery for anterior circulation ischemia in childhood moyamoya disease.** *J Neurosurg* 1992;77:84–89
25. Yamada I, Matsushima Y, Suzuki S. **Childhood moyamoya disease before and after encephalo-duro-arterio-synangiosis: an angiographic study.** *Neuroradiology* 1992;34:318–322
26. Hoshi H, Ohnishi T, Jinnouchi S, et al. **Cerebral blood flow study in patients with moyamoya disease evaluated by IMP SPECT**. *J Nucl Med* 1994;35:41–43
27. Yamada I, Murata Y, Umehara I, Suzuki S, Matsushima Y. **SPECT and MRI evaluations of the posterior circulation in moyamoya disease**. *J Nucl Med* 1996;37:1613–1617
28. Oyama H, Niwa M, Kida Y. **CBF change with aging in moyamoya disease [abstr].** *J Neurosurg Sci* 1998;42:33–36

ELSEVIER

Seminars in PEDIATRIC NEUROLOGY

Pediatric Moyamoya Biomarkers: Narrowing the Knowledge Gap

Laura L. Lehman,[*,†] Matsanga Leyila Kaseka,[‡,§] Jeffery Stout,[†,‖] Alfred P. See,[†,¶,#] Lisa Pabst,[**] Lisa R. Sun,[††] Sahar A. Hassanein,[‡‡] Michaela Waak,[§§] Arastoo Vossough,[‖‖] Edward R. Smith,[†,¶] and Nomazulu Dlamini[¶¶,##]

Moyamoya is a progressive cerebrovascular disorder that leads to stenosis of the arteries in the distal internal carotid, proximal middle cerebral and proximal anterior cerebral arteries of the circle of Willis. Typically a network of collaterals form to bypass the stenosis and maintain cerebral blood flow. As moyamoya progresses it affects the anterior circulation more commonly than posterior circulation, and cerebral blood flow becomes increasingly reliant on external carotid supply. Children with moyamoya are at increased risk for ischemic symptoms including stroke and transient ischemic attacks (TIA). In addition, cognitive decline may occur over time, even in the absence of clinical stroke. Standard of care for stroke prevention in children with symptomatic moyamoya is revascularization surgery. Treatment of children with asymptomatic moyamoya with revascularization surgery however remains more controversial. Therefore, biomarkers are needed to assist with not only diagnosis but also with determining ischemic risk and identifying best surgical candidates. In this review we will discuss the current knowledge as well as gaps in research in relation to pediatric moyamoya biomarkers including neurologic presentation, cognitive, neuroimaging, genetic and biologic biomarkers of disease severity and ischemic risk.
Semin Pediatr Neurol 43:101002

From the *Department of Neurology, Boston Children's Hospital, Boston, MA.
[†]Harvard Medical School, Boston, MA.
[‡]Department of Neurology, CHU Sainte-Justine, Montreal, Quebec, Canada.
[§]Université de Montréal, Montreal, Quebec, Canada.
[‖]Newborn Medicine, Boston Children's Hospital, Boston, MA.
[¶]Department of Neurosurgery, Boston Children's Hospital, Boston, MA.
[#]Department of Radiology, Boston Children's Hospital, Boston, MA.
**Department of Pediatrics, Division of Neurology, Nationwide Children's Hospital, Columbus, OH.
[††]Division of Pediatric Neurology, Division of Cerebrovascular Neurology, Department of Neurology, Johns Hopkins School of Medicine, Baltimore, MD.
[‡‡]Department of Pediatrics, Faculty of Medicine, Ain Shams University, Cairo, Egypt.
[§§]Department of Paediatric Intensive Care, Queensland Children's Hospital; Centre for Child Health Research, The University of Queensland, Brisbane, Australia.
[‖‖]Department of Radiology, Children's Hospital of Philadelphia, University of Philadelphia, Philadelphia, Pennsylvania.
[¶¶]Division of Neurology, Department of Paediatrics, The Hospital for Sick Children, Toronto, Canada.
[##]Faculty of Medicine, University of Toronto, Canada.
Address reprint requests to Laura L. Lehman, 300 Longwood Avenue, Fegan 11, Boston, MA 02115. E-mail: Laura.Lehman@Childrens.Harvard.edu

Introduction

Moyamoya is a progressive non-atherosclerotic cerebral arteriopathy that affects the distal internal carotid arteries (dICA), proximal middle cerebral arteries (MCA), and/or proximal anterior cerebral arteries (ACA) of the circle of Willis most commonly. The network of collaterals that develop to bypass the stenosis results in the characteristic angiographic 'puff of smoke' appearance described as 'moyamoya'. Moyamoya occasionally affects the posterior circulation (26%-37%) including proximal posterior cerebral arteries (PCA) and distal basilar artery.[1-3] Children with moyamoya frequently present with ischemic symptoms including stroke (31.5%-67.8%) and transient ischemic attacks (TIA) (13%-40.3%).[1,4,5] However, moyamoya can also present with headache (4%-6.3%), seizure (4.5%-9%), movement disorder (3.6%-4.2%), or occasionally hemorrhagic stroke (2.7%-2.8%).[1,4,5] Children with radiographic findings consistent with moyamoya but without an associated syndrome are labeled moyamoya disease while children with moyamoya associated with a known syndrome such as neurofibromatosis type 1 (NF1), sickle cell anemia or Down's syndrome are

https://doi.org/10.1016/j.spen.2022.101002

designated as moyamoya syndrome. With known associations between moyamoya and certain syndromes, more children are being diagnosed with moyamoya through screening magnetic resonance imaging (MRI) prior to development of symptoms.[6]

To date, there is no known therapy able to halt progression or reverse stenosis of the arteries in the circle of Willis. The current standard of care centers on both medical management as well as the use of revascularization surgery designed to improve cerebral blood flow (CBF) and lower stroke risk in children with moyamoya. Medical management can include antiplatelet such as aspirin, avoiding vasoconstrictive medications and maintaining cerebral perfusion/hemodynamics when under general anesthesia.

For children with symptomatic moyamoya, especially with TIA or history of stroke, revascularization surgery is recommended.[7] Indications for treatment of asymptomatic moyamoya remain in evolution. The Asymptomatic Moyamoya Registry (AMORE) is a multi-center prospective cohort study based in Japan of asymptomatic moyamoya in adults. This cohort study has revealed that asymptomatic moyamoya is not necessarily a benign disease, as 20% of cases suffered silent infarctions at follow-up and 40% of cases had altered cerebral hemodynamic function with altered cerebral vascular reactivity.[8] Such multi-center cohort studies are not yet available in children, although a growing body of literature supports the premise that asymptomatic moyamoya has a high likelihood of progression with concomitant risk to patients. Lin et al. found in a single-center cohort study that 45% of asymptomatic children became symptomatic over a mean follow up period of 5 years with 12% suffering a stroke.[9] Kaseka et al. found that 24% of children with asymptomatic moyamoya had ischemic events over median follow up of 3.76 years and 46% had radiologic progression over median follow up of 4.83 years.[4] However, predictors of progression in children with asymptomatic moyamoya are lacking.

Biomarkers are needed not only to assist in identifying children with moyamoya (diagnostic biomarkers) but also to assist in determining disease severity and ischemic risk (prognostic biomarkers). Given the challenges inherent in stratification of ischemic risk, a toolkit of biomarkers that aid in the identification of suitable operative candidates and quantifies therapy response are needed. Biomarkers that determine when or whether these asymptomatic children should have revascularization surgery is of utmost importance. Many biomarkers have been studied including neurologic, cognitive, radiographic, genetic and biologic. In this article we will review the current literature on these biomarkers in the context of limitations and future therapeutics.

Neurologic Presentation as Biomarker

Moyamoya has many phenotypes and is heterogeneous in presentation, progression, and radiographic findings. Moyamoya disease behaves differently than moyamoya syndrome.[1,4] Children present differently both radiographically and symptomatically depending on underlying syndromes associated with moyamoya.

Recent cohort studies found the proportion of patients presenting with stroke, TIA, headache, seizure or asymptomatically differed depending on whether the child had moyamoya disease or moyamoya syndrome and between syndromic forms as patients with Down syndrome, NF1 and sickle cell disease displayed distinct clinical phenotypes.[1,4] Children with Down syndrome were more likely to present with a stroke and bilateral disease.[10] Whereas children with NF1 were more likely to present with unilateral disease and less likely to suffer a stroke at follow-up compared to children with sickle cell disease. Patients with NF1 or sickle cell disease were more likely to be asymptomatic at diagnosis compared to idiopathic moyamoya (moyamoya disease), which may be related to screening neuroimaging in children with NF1 and sickle cell disease.[1,4] Of note NF1 and sickle cell disease may have arteriopathy that does not meet the definition of moyamoya and may therefore not have the same increased risk of stroke as those who have moyamoya syndrome. Kaseka and colleagues examined clinical and radiologic features to determine if they correlated with long term outcome. Stroke at presentation or being asymptomatic at presentation were correlated with Pediatric Stroke Outcome Measure.[4] All other symptoms were not significant.

Many studies have also demonstrated that children of younger age (<2 years old) are more likely to have a stroke at presentation.[11-14] Younger children also have faster progression of their stenosis and poorer long term prognosis.[11,14] Whether children's stroke risk or need for surgery can be gauged by their clinical presentation alone still needs further investigation. For example, whether children who are symptomatic are at greater risk for future stroke than asymptomatic children is not fully delineated. Categorizing the child's moyamoya based on neurologic presentation alone is not enough to determine who would benefit from revascularization surgery.

Cognitive Biomarkers

Moyamoya in children is frequently associated with cognitive impairment. The natural history of many children with moyamoya without revascularization surgery is development of neurocognitive decline and disability by adulthood.[15] Multiple studies demonstrate that most children with moyamoya, in the absence of cortical infarct, have baseline normal range overall intellectual abilities with selective impairment of various cognitive subdomains.[16-18] Hsu et al. described a cohort of 13 children with moyamoya presenting with TIA in which 2 of the children had single domain cognitive impairments and an additional 3 patients had impairment of multiple cognitive domains, largely localizable to frontotemporal dysfunction.[18] Two recent studies have demonstrated an association between regional hemodynamics and cognitive outcome. In a study of 30 children with moyamoya, fronto-

parietal and white matter hemodynamics were shown to be associated with executive function and processing speed.[38] Kazumata et al. demonstrated that in 21 children with moyamoya disease and no apparent brain lesions, there was a significant difference in working memory compared to verbal comprehension and that regional cerebral blood flow in the left dorsolateral prefrontal cortex as well as bilateral medial frontal cortices were associated with lower IQ, perceptual reasoning and processing speed without any association with angiographic severity of disease.[16] This suggests that the chronic ischemia and hypoperfusion due to moyamoya vasculopathy leads to selective cognitive impairment, even in the absence of infarction. Other studies have demonstrated the changes in neurocognitive profiles before and after surgical treatment of moyamoya and demonstrated post-operative improvements in performance IQ, functional memory, attention, and impulsivity.[17,19] The specific areas of improvement in these studies post-operatively overall support benefit to frontal lobe function following revascularization surgery.

Understanding which cognitive domains are at highest risk for deficits in children with moyamoya, particularly in those without infarction or neurologic symptoms, may serve as a prognostic biomarker for moyamoya disease and inform the need for intervention. Given the relatively limited long-term studies of cognitive outcomes and the logistical challenges of obtaining full neuropsychological testing over time, multi-site research studies are needed to address these gaps. Areas that require more investigation include long-term outcome studies of cognition in adulthood following childhood moyamoya diagnosis, baseline cognitive function and trajectory in children with moyamoya without stroke and the role of comorbid genetic conditions and factors on cognitive outcomes.

Cerebral Perfusion as Biomarker

Cerebral blood flow (CBF) is tightly regulated to provide necessary oxygen and nutrients to different regions of the brain according to their needs. In moyamoya, collaterals develop so as to bypass the occlusion and maintain CBF and cerebral perfusion pressure (CPP). In addition, CPP is maintained at a relative constant by numerous mechanisms which include a drop in vascular resistance and vasodilatation, mediated by cerebral autoregulation. As a consequence of disease progression and falling CPP, tissue oxygen extraction fraction is maximized followed by disruption in tissue metabolism and ischemic brain injury.[20,21] Measuring cerebral hemodynamics is thus an important aspect of moyamoya assessment and management. Different imaging techniques have been used and are being explored to provide the best approximation of the CBF. Xenon CT perfusion, O^{15} based PET, or HMPAO SPECT techniques are quantitative and the gold standard non-invasive techniques for assessment of cerebral perfusion. However, these techniques have high capital costs, limited availability, need for radioisotope injection, difficult to implement in younger children. Here we highlight imaging techniques with wider availability, suitability for use in children and lower cost.

The "Ivy Sign" defined as leptomeningeal or sulcal hyperintense signals on unenhanced fluid-attenuated inversion recovery (FLAIR) MRI along the cerebral sulci is frequently observed in moyamoya patients. The ivy sign is thought to represent dilated leptomeningeal branches on the surface of the brain with slow flow. On contrast MRI, its correlate is increased sulcal vascularity and enhancement. Previous studies have shown that its presence correlates with the severity of symptoms at presentation and a decreased cerebral vascular reserve and the recurrence ischemic symptoms in idiopathic moyamoya patients.[22-24] Data regarding the significance and impact of the ivy sign in pediatric moyamoya patients, especially non-Asian and non-idiopathic ones, is scarce. A recent, multicenter study reviewing the characteristics of the ivy sign in a pediatric North American and Israeli cohort showed a correlation between the ivy sign and clinical outcomes. The authors found that post-operative reduction of the ivy sign was associated with lower rate of postoperative stroke.[25] However, its utility as a predictor of ischemic symptom occurrence remains uncertain.

Arterial Spin Label (ASL) perfusion imaging provides non-invasive assessment of cerebral blood flow without the need for contrast injection. ASL use does present some limitations for moyamoya patients. Indeed, standard ASL techniques such as pulsed and pseudocontininuous ASL are affected by prolonged arterial arrival times secondary to the arteriopathy, resulting in delayed brain parenchyma arrival and associated macrovascular signal and artifactual areas of decreased CBF map signal.[26,27] Two adaptations of ASL permit more accurate quantification of CBF in the face of delayed parenchymal arrival. First, multi-delay ASL provides information about arrival time in addition to more accurately quantifying CBF as demonstrated by comparison with PET perfusion imaging.[28] Second, velocity-selective ASL (VSASL) i relies on imaging principles not affected by variations in arterial arrival time. Bolar et al. have demonstrated excellent agreement between VSASL- and DSA- based scoring of CBF in standard vascular territories and that the CBF, coefficient of variation, a marker of perfusion variability, between moyamoya patients with preserved perfusion and healthy controls is similar when measured with VSASL, but different when assessed with single-delay pulsed ASL.[29] However, as pointed out by the authors, one important limitation of ASL is that it does not distinguish between native collaterals and surgical collaterals. Furthermore, normative data of ASL perfusion imaging are minimal in children.[30,31]

Cerebrovascular Reactivity (CVR) is an estimate of the net hemodynamic balance between supply, demand and vascular tone. In the context of fixed arterial stenosis, there is often maximized autoregulatory and vasodilatory response that cannot be further increased by additional vasodilatory stimulation. Additionally, in cases of upstream stenosis, asymmetrical changes in response to increased tissue demand may result in a phenomenon termed "steal."[32] MRI-based CVR can be estimated by detecting changes in blood oxygenation levels resulting from a stimulus that induces vasodilation (eg breath hold, carbogen breathing, or acetazolamide administration).[33] The most accurate quantification of CVR results

from the use of a graded hypercapnic challenge using a breathing circuit,[34] but breath holding may be better suited for wide deployment in clinical settings. In children with moyamoya, steal detected using a breath hold protocol has been associated with a higher risk of future ischemic injury and cognitive impairment.[35-38] In adults with moyamoya, changes in CVR are correlated with new collateral formation, and CVR at baseline is somewhat predictive of the same.[39-42]

Arterial Anatomy as Biomarker

Catheter angiogram (DSA) is important for the definitive diagnosis of moyamoya, presurgical planning and Suzuki grading. The Suzuki grade, however, has not been shown to be a valid predictor of ischemic risk as a stand-alone test. Recently, Rosi et al. found that the presence of hypovascular territories correlated with a symptomatic presentation and ischemic changes on pre-operative brain MRI.[43] The persistence of hypovascular territories at follow-up angiogram was found to correlate with incidence of post-operative ischemic symptoms.[43] Although, posterior choroidal artery collaterals have been found to correlate with the risk of cerebral hemorrhage in adult idiopathic moyamoya, the role of collaterals in pediatric moyamoya remains unknown.[44] DSA following revascularization surgery has demonstrated the reduction of abnormal collaterals as soon as 3 to 6 months post-surgery in both children and adults with moyamoya.[45] Native formation of transdural collaterals is observed at a high rate in children. Characterizing these native transdural collaterals with catheter angiography in order to protect them during revascularization surgery has been shown to reduce surgical risk.[46] Rosi et al. did not observe a correlation between the pattern of collateralization, the clinical presentation and the outcome of pediatric moyamoya.[43] Additionally, DSA is an invasive procedure associated with risks. Developing a reliable non-invasive measure of brain vascularization and perfusion is therefore warranted.

MRI vessel wall imaging is a high-resolution black blood imaging technique that assesses endothelial disruption via evidence of enhancement and/or thickening within the vessel wall, although the molecular and cellular mechanisms of this enhancement are not yet definitively known. It can assist in not only better classifying a stenotic arteriopathy of uncertain cause, but it could also inform the likelihood of progression and stroke recurrence. Some moyamoya patients may demonstrate vessel wall enhancement. More specifically, a concentric enhancement has been associated with inflammatory arteriopathies and moyamoya, while eccentric pattern of enhancement has been associated with dissection and cardioembolic causes.[47,48] In adult moyamoya patients, the presence of vessel wall enhancement was associated with an increased risk of ischemic event occurrence and progression within 6 months and a change of vessel wall enhancement has been associated with recent neurological symptoms.[49-51] Data in pediatric moyamoya is however lacking.

Transcranial dopplers (TCD) ultrasonography is an attractive option for future use as a diagnostic and prognostic biomarker in moyamoya because of its excellent safety profile, cost effectiveness, portability, ability to provide anatomic and hemodynamic information, and capacity to be performed in resource-limited settings. While TCD has a clear role in screening children with sickle cell disease for stroke risk stratification and selection for chronic transfusion therapy, the role of TCD in other childhood moyamoya populations has not been established.[52] According to the American Heart Association Stroke Council, TCD may be used to evaluate and monitor children with moyamoya, though there are no validated TCD criteria for diagnosis or data on risk stratification by TCD.[53,54] In adults with moyamoya, TCD has been used to identify disease stage, estimate degree of stenosis, predict postoperative infarction, visualize arterial emboli, and measure wall shear stress at the sites of vascular stenosis.[55-60] Studies in adult moyamoya have shown a characteristic change in cerebral blood flow velocities over time as the disease progresses, with cerebral blood flow velocities increasing initially and then decreasing with advancing disease stage.[55,56,58,61] Despite the mounting evidence for a role of TCD in adult moyamoya, data in children remain limited. Future studies focusing on the ability of TCD to screen high-risk pediatric populations outside of sickle cell, to predict risk and rate of progression in childhood moyamoya, and to measure cerebrovascular reactivity in moyamoya are needed.

Silent White Matter Ischemia as a Biomarker

Silent white matter infarcts found on conventional neuroimaging is a hallmark imaging finding in children with moyamoya. Diffusion Tensor Imaging (DTI) is a MRI technique used to examine white matter tract alterations not seen using conventional MR imaging techniques. In adults with moyamoya white matter alterations have been found using DTI even when conventional imaging was negative for white matter injury or stroke.[62,63] These white matter alterations found using DTI in adults with moyamoya in the lateral prefrontal, cingulate, and inferior parietal regions were significantly associated with deficits in processing speed, executive functioning and working memory.[62] Children with moyamoya without stroke or white matter injury also have alterations in the white matter tracts specifically, in white matter tracts located within the watershed regions using diffusion MR imaging techniques.[64] These findings are concerning for ongoing hypoperfusion in children with moyamoya prior to stroke or white matter injury being seen on conventional MRI. These diffusion MR imaging techniques could be used in the future as an imaging biomarker to assist in surgical decision making. Whether white matter alterations occur to the same extent in symptomatic versus asymptomatic children with moyamoya is unknown.

Genetic Biomarkers

There is increasing evidence of a genetic contribution to moyamoya, with a recent population based study in Korea

finding a 132 fold increase in incidence risk for individuals with an affected first degree relative. In recent years, the availability of genomic analysis methods has moved beyond gentic linkage studies and permitted the identification of genes in a subset of cases. Notably, in 2011, through linkage analysis followed by exome sequencing of 72 Japanese patients, Kamada and colleagues identified a major founder susceptibility variant at p.R4859K of the ring finger protein 213 gene (*RNF213),* and Liu and colleagues identified a missense variant p.R4810K in a group of 8 Japanese families.[65,66] Subsequent studies identified additional pathogenic *RNF213* mutations in other East Asian moyamoya populations.[66] The identification of *RNF213* as a susceptibility gene for moyamoya has driven better phenotype-genotype correlation. For instance, Miyatake et al. identified that a c.14576G>A mutation is associated with early onset and severe disease.[67] However, despite these developments, most cases of idiopathic moyamoya remain genetically unexplained, especially in non-Asian populations. Beyond the coding sequence, single nucleotide polymorphisms in the promoter region of matrix metalloproteinases, tissue inhibitors of metalloproteinases (TIMPs), platelet-derived growth factor (PDGF) and transforming growth factor beta (TGFβ) have associated with moyamoya disease in some patient cohorts and suggest a multigenic contribution to risk.[70,73]

While the previously described *RNF213* founder effect is present in Korean, Japanese, and Han Chinese populations, these variants are not observed in the non-Asian population. Although *RNF213* is also identified in the non-Asian population, whole exome sequencing of non-Asian moyamoya trios have further broadened the candidate gene list of associations with moyamoya, although they are not as robustly replicated as the *RNF213* studies. These variants are observed in genes that have not been previously associated with moyamoya: *CHD4*, *CNOT3*, *DIAPH1*, *EVL*, *ZXDC*, *OBSCN*. *CHD4* encodes a helicase and *CNOT3* encodes a portion of a transcription complex, both of these that functions in chromatin remodeling through histone acetylation.[71,72,74] *DIAPH1* encodes a RhoA GTPase that lengthens actin filaments. *ZXDC* encodes a zinc finger protein that facilitates transcription of HMC class II.

Aside from the presenting phenotype, genetic biomarkers may also associate with physiologic responses such as the response to treatment. It has been reported that *RNF213* polymorphism is associated with better collateral formation after an indirect pial synangiosis in Japanese idiopathic moyamoya.[68] The description of the various *RNF213*-related phenotypes has refined follow-up planning and facilitated identification of early surgical candidates. Polymorphisms of vascular endothelial growth factor (VEGF) are also associated with pediatric moyamoya and may also predict poor response to surgical revascularization.[75,76] Of note, 50% of probands with *DIAPH1* variants also had thrombocytopenia which required transfusion before surgery.[72] These genotypic differences have had variable reports on long term response to revascularization surgery, with some groups finding worsened cognitive outcome, potentially due to severity of presenting disease, and other groups finding no differences in functional neurologic grading scales after surgery.[77,78] Genes identified in syndromic forms have also shed some light on the pathophysiology of moyamoya, but additional research is warranted to identify other susceptibility genes and develop pathway-targeted treatments.[69]

Biologic Biomarkers: Blood, Urine and CSF Biomarkers

Protein biomarkers have been shown to be useful in brain tumors focusing on the hypothesis that extracellular matrix (ECM) remodeling and angiogenesis were necessary in many CNS disorders. The proteins examined included vascular endothelial growth factor (VEGF) and matrix metalloproteinases (MMPs). VEGF and MMPs are elevated in the CSF and serum of patients with moyamoya and have also been found in urine in children with moyamoya.[79-90] In some CNS disorders such as arteriovenous malformations (AVM) and tumors, tissue can be taken for biomarker confirmation with biomarker staining. Unfortunately in moyamoya it is not possible to harvest tissue for confirmation. However, there is research matching CSF to urine or serum.[79,84,91,92] In addition, there are longitudinal data that demonstrate that the urinary biomarker profile changes in direct response to changes in disease status after treatment, as corroborated by radiographic studies and also with precedent in the literature.[79,84,91-95]

Specifically, in moyamoya disease and other vascular diseases, evidence exists that levels of MMPs and VEGF are elevated in the setting of chronic ischemia. Once successful revascularization occurs and the ischemia is reduced, the ischemic stimulus driving the upregulation of MMP and VEGF is decreased, with concomitant reduction in the levels of these markers.[79,87,90,93,96-98] As documented in previous work, the CNS levels of these molecules are directly related to urinary levels, with previous reports linking source tissue, CSF, serum and urine.[84,91,92,94,99-101] The working model is that the end-organ (brain) experiences chronic ischemia from the moyamoya arteriopathy and is elaborating these angiogenic factors at baseline in order to develop compensatory collateral development. Once surgical revascularization occurs, transient elevations in these factors enhance surgical collateral growth until the ischemia is corrected. This process is well-documented by postoperative imaging studies, showing improved perfusion and surgical collaterals on angiogram at which point the ischemic stimulus no longer exists, and the production of pro-angiogenic molecules decreases. −These changes occur in parallel to radiographic normalization of imaging biomarkers.[25,46,79]

Recent *in vivo* and *in vitro* data as well as clinical studies suggest that although moyamoya is not considered an inflammatory disease, inflammation may play an important role in its pathophysiology. For example, Ohkubo and colleagues have demonstrated that pro-inflammatory cytokines activate the transcription of *RNF213* and that *RNF213* is a downstream effector of the PI3 kinase-AKT pathway in

endothelial angiogenesis.[102,103] Furthermore, the association between moyamoya and conditions known to have a pro-inflammatory state such as sickle cell disease, trisomy 21 and hyperthyroidism is well recognized.[104-106] Deciphering the inflammatory signature of moyamoya arteriopathy in CSF, serum and urine will aid the identification of poor prognostic factors and the development of targeted therapies.

Diagnostic specificity can be improved by looking at a broader range of molecules and multiplexing several proteins in combination to create a biomarker "fingerprint" that is unique to a given disease, as has been done for other CNS vascular and tumor cohorts, including moyamoya disease.[84,91-93,95] In particular, molecules that regulate mechanisms of vascular morphogenesis and arteriogenesis (including, but not limited to, axon guidance factors, for example) may be useful as future areas of investigation to enhance the functionality of biomarker profiling in moyamoya disease.

Conclusion

The field of pediatric moyamoya is in need of specific biomarkers which would assist in diagnosis, treatment decisions, prognostication and development of future therapeutics. Biomarkers could also help to monitor known patients following treatment to better ascertain response to therapy. One way to monitor moyamoya may be to determine if there is a link between protein-based biomarkers (in the urine or serum) and imaging biomarkers (such as transdural collaterals, CVR, DTI or ivy sign on MRI).[25,46,79]

The rarity of moyamoya disease makes widespread screening of the general population to identify de novo cases an unrealistic goal. Utility would be greater in screening a defined, at-risk population, such as patients with Down syndrome, sickle cell disease or patients with known family histories of moyamoya.[7,80,107-110] This targeted approach could reduce risk of scanning, decrease cost of screening and aid in better detection of disease. Another major difficulty in treating moyamoya disease is the lack of effective methods to detect novel or progressive disease prior to the onset of disabling stroke.

Biomarkers in moyamoya disease could aid in stratification of risk and operative strategy in already identified moyamoya patients, with biomarker-based risk reassessment on an ongoing basis. Using biologic biomarkers that change in response to ischemia and imaging biomarkers that can demonstrate ischemic risk may allow clinicians to better select operative candidates . This could be especially useful in the growing number of asymptomatic or early-stage moyamoya disease cases that are presently without a clear clinical management strategy.

Development of a prognostic biomarker toolset would bring something entirely new and needed to the armamentarium of clinicians treating patients with moyamoya disease. Biomarker "fingerprints" for moyamoya may also have specific case use scenarios; for example, one fingerprint might be applied for screening for moyamoya, while a different group of biomarkers might help to stratify ischemia and follow response to surgery. Finally, the role of biomarkers may extend beyond diagnostic or prognostic adjuncts and actually inform the development of novel, biologically-based therapies. This approach of combining a specific therapy with immediate feedback on efficacy, theranostics, has rapidly expanded in medicine.

In conclusion,further research is needed to identify which biomarkers or combination of biomarkers could be used for early identification, predictors of ischemic risk, determination of surgical candidates and long-term prognostication in children with moyamoya. Prospective multi center studies are needed to examine these biomarkers and further understand and guide management of children with moyamoya.

Declaration of Competing Interest

The authors declare that they have no known competing financial interests or personal relationships that could have appeared to influence the work reported in this paper.

References

1. Gatti JR, Torriente AG, Sun LR: Clinical presentation and stroke incidence differ by moyamoya etiology. J Child Neurol 36(4):272-280, 2021
2. Kimiwada T, Hayashi T, Shirane R, et al: Posterior cerebral artery stenosis and posterior circulation revascularization surgery in pediatric patients with moyamoya disease. J Neurosurg Pediatr 21(6):632-638, 2018
3. Hishikawa T, Tokunaga K, Sugiu K, et al: Assessment of the difference in posterior circulation involvement between pediatric and adult patients with moyamoya disease. J Neurosurg 119(4):961-965, 2013
4. Kaseka ML, Slim M, Muthusami P, et al: Distinct clinical and radiographic phenotypes in pediatric patients with Moyamoya. Pediatr Neurol 120:18-26, 2021
5. Scott RM, Smith JL, Robertson RL, et al: Long-term outcome in children with moyamoya syndrome after cranial revascularization by pial synangiosis. J Neurosurg 100(2 Suppl Pediatrics):142-149, 2004
6. Rea D, Brandsema JF, Armstrong D, et al: Cerebral arteriopathy in children with neurofibromatosis type 1. Pediatrics 124(3):e476-e483, 2009
7. Ferriero DM, Fullerton HJ, Bernard TJ, et al: Management of stroke in neonates and children: A scientific statement from the American heart association/American stroke association. Stroke 50(3):e51-e96, 2019
8. Kuroda S, Group AS: Asymptomatic moyamoya disease: Literature review and ongoing AMORE study. Neurol Med Chir (Tokyo) 55 (3):194-198, 2015
9. Lin N, Baird L, Koss M, et al: Discovery of asymptomatic moyamoya arteriopathy in pediatric syndromic populations: Radiographic and clinical progression. Neurosurg Focus 31(6):E6, 2011
10. See AP, Ropper AE, Underberg DL, et al: Down syndrome and moyamoya: Clinical presentation and surgical management. J Neurosurg Pediatr 16(1):58-63, 2015
11. Hackenberg A, Battilana B, Hebeisen M, et al: Preoperative clinical symptomatology and stroke burden in pediatric moyamoya angiopathy: Defining associated risk variables. Eur J Paediatr Neurol 35:130-136, 2021
12. Law-Ye B, Saliou G, Toulgoat F, et al: Early-onset stroke with moyamoya-like syndrome and extraneurological signs: A first reported paediatric series. Eur Radiol 26(8):2853-2862, 2016

13. Jackson EM, Lin N, Manjila S, et al: Pial synangiosis in patients with moyamoya younger than 2 years of age. J Neurosurg Pediatr 13 (4):420-425, 2014
14. Kim SK, Seol HJ, Cho BK, et al: Moyamoya disease among young patients: Its aggressive clinical course and the role of active surgical treatment. Neurosurgery 54(4):840-844, 2004. discussion 844-846
15. Imaizumi T, Hayashi K, Saito K, et al: Long-term outcomes of pediatric moyamoya disease monitored to adulthood. Pediatr Neurol 18(4):321-325, 1998
16. Kazumata K, Tokairin K, Sugiyama T, et al: Association of cognitive function with cerebral blood flow in children with moyamoya disease. J Neurosurg Pediatr: 1-7, 2019
17. Lee JY, Phi JH, Wang KC, et al: Neurocognitive profiles of children with moyamoya disease before and after surgical intervention. Cerebrovasc Dis 31(3):230-237, 2011
18. Hsu YH, Kuo MF, Hua MS, et al: Selective neuropsychological impairments and related clinical factors in children with moyamoya disease of the transient ischemic attack type. Childs Nerv Syst 30(3):441-447, 2014
19. Kim W, Lee EY, Park SE, et al: Neuropsychological impacts of indirect revascularization for pediatric moyamoya disease. Childs Nerv Syst 34 (6):1199-1206, 2018
20. Ikezaki K, Matsushima T, Kuwabara Y, et al: Cerebral circulation and oxygen metabolism in childhood moyamoya disease: A perioperative positron emission tomography study. J Neurosurg 81(6):843-850, 1994
21. Derdeyn CP, Videen TO, Yundt KD, et al: Variability of cerebral blood volume and oxygen extraction: Stages of cerebral haemodynamic impairment revisited. Brain 125(Pt 3):595-607, 2002
22. Mori N, Mugikura S, Higano S, et al: The leptomeningeal "ivy sign" on fluid-attenuated inversion recovery MR imaging in Moyamoya disease: A sign of decreased cerebral vascular reserve? AJNR Am J Neuroradiol 30(5):930-935, 2009
23. Seo KD, Suh SH, Kim YB, et al: Ivy sign on fluid-attenuated inversion recovery images in Moyamoya disease: Correlation with clinical severity and old brain lesions. Yonsei Med J 56(5):1322-1327, 2015
24. Nam KW, Cho WS, Kwon HM, et al: Ivy sign predicts ischemic stroke recurrence in adult Moyamoya patients without revascularization surgery. Cerebrovasc Dis: 1-8, 2019
25. Montaser AS, Lalgudi Srinivasan H, Staffa SJ, et al: Ivy sign: A diagnostic and prognostic biomarker for pediatric moyamoya. J Neurosurg Pediatr: 1-9, 2021
26. Calamante F, Ganesan V, Kirkham FJ, et al: MR perfusion imaging in Moyamoya Syndrome: Potential implications for clinical evaluation of occlusive cerebrovascular disease. Stroke 32(12):2810-2816, 2001
27. Zaharchuk G, Do HM, Marks MP, et al: Arterial spin-labeling MRI can identify the presence and intensity of collateral perfusion in patients with moyamoya disease. Stroke 42(9):2485-2491, 2011
28. Fan AP, Khalighi MM, Guo J, et al: Identifying hypoperfusion in Moyamoya disease with arterial spin labeling and an [(15)O]-water positron emission tomography/magnetic resonance imaging normative database. Stroke 50(2):373-380, 2019
29. Bolar DS, Gagoski B, Orbach DB, et al: Comparison of CBF measured with combined velocity-selective arterial spin-labeling and pulsed arterial spin-labeling to blood flow patterns assessed by conventional angiography in pediatric Moyamoya. AJNR Am J Neuroradiol 40(11): 1842-1849, 2019
30. Hales PW, Kawadler JM, Aylett SE, et al: Arterial spin labeling characterization of cerebral perfusion during normal maturation from late childhood into adulthood: Normal 'reference range' values and their use in clinical studies. J Cereb Blood Flow Metab 34(5):776-784, 2014
31. Biagi L, Abbruzzese A, Bianchi MC, et al: Age dependence of cerebral perfusion assessed by magnetic resonance continuous arterial spin labeling. J Magn Reson Imaging 25(4):696-702, 2007
32. Fisher JA, Venkatraghavan L, Mikulis DJ: Magnetic resonance imaging-based cerebrovascular reactivity and hemodynamic reserve. Stroke 49 (8):2011-2018, 2018
33. Juttukonda MR, Donahue MJ: Neuroimaging of vascular reserve in patients with cerebrovascular diseases. Neuroimage 187:192-208, 2019
34. Pinto J, Bright MG, Bulte DP, et al: Cerebrovascular reactivity mapping without gas challenges: A methodological guide. Front Physiol 11:608475, 2020
35. Fierstra J, Sobczyk O, Battisti-Charbonney A, et al: Measuring cerebrovascular reactivity: What stimulus to use? J Physiol 591(23):5809-5821, 2013
36. Dlamini N, Shah-Basak P, Leung J, et al: Breath-hold blood oxygen level-dependent MRI: A tool for the assessment of cerebrovascular reserve in children with Moyamoya disease. AJNR Am J Neuroradiol 39(9):1717-1723, 2018
37. Dlamini N, Slim M, Kirkham F, et al: Predicting Ischemic risk using blood oxygen level-dependent MRI in children with Moyamoya. AJNR Am J Neuroradiol 41(1):160-166, 2020
38. Choi EJ, Westmacott R, Kirkham FJ, et al: Fronto-parietal and white matter haemodynamics predict cognitive outcome in children with Moyamoya independent of stroke. Transl Stroke Res 2022
39. Watchmaker JM, Frederick BD, Fusco MR, et al: Clinical use of cerebrovascular compliance imaging to evaluate revascularization in patients with Moyamoya. Neurosurgery 84(1):261-271, 2019
40. Gupta A, Chazen JL, Hartman M, et al: Cerebrovascular reserve and stroke risk in patients with carotid stenosis or occlusion: A systematic review and meta-analysis. Stroke 43(11):2884-2891, 2012
41. Silvestrini M, Vernieri F, Pasqualetti P, et al: Impaired cerebral vasoreactivity and risk of stroke in patients with asymptomatic carotid artery stenosis. JAMA 283(16):2122-2127, 2000
42. Marshall RS, Festa JR, Cheung YK, et al: Cerebral hemodynamics and cognitive impairment: Baseline data from the RECON trial. Neurology 78(4):250-255, 2012
43. Rosi A, Riordan CP, Smith ER, et al: Clinical status and evolution in moyamoya: Which angiographic findings correlate? Brain Communications 1(1), 2019
44. Hori S, Kashiwazaki D, Yamamoto S, et al: Impact of interethnic difference of collateral Angioarchitectures on prevalence of hemorrhagic stroke in Moyamoya disease. Neurosurgery 2018
45. Yamamoto S, Kashiwazaki D, Uchino H, et al: Ameliorative effects of combined revascularization surgery on abnormal collateral channels in Moyamoya disease. J Stroke Cerebrovasc Dis 30(4):105624, 2021
46. Storey A, Michael Scott R, Robertson R, et al: Preoperative transdural collateral vessels in moyamoya as radiographic biomarkers of disease. J Neurosurg Pediatr 19(3):289-295, 2017
47. Lindenholz A, van der Kolk AG, Zwanenburg JJM, et al: The use and pitfalls of intracranial vessel wall imaging: How we do it. Radiology 286(1):12-28, 2018
48. Dlamini N, Yau I, Muthusami P, et al: Arterial wall imaging in pediatric stroke. Stroke 49(4):891-898, 2018
49. Kathuveetil A, Sylaja PN, Senthilvelan S, et al: Vessel wall thickening and enhancement in high-resolution intracranial vessel wall imaging: A predictor of future Ischemic events in Moyamoya disease. AJNR American journal of neuroradiology 41(1):100-105, 2020
50. Muraoka S, Araki Y, Taoka T, et al: Prediction of intracranial arterial stenosis progression in patients with Moyamoya vasculopathy: Contrast-enhanced high-resolution magnetic resonance vessel wall imaging. World neurosurgery 116:e1114-e1121, 2018
51. Muraoka S, Taoka T, Kawai H, et al: Changes in vessel wall enhancement related to the recent neurological symptoms in patients with Moyamoya disease. Neurol Med Chir (Tokyo) 61(9):515-520, 2021
52. Adams RJ, McKie VC, Hsu L, et al: Prevention of a first stroke by transfusions in children with sickle cell anemia and abnormal results on transcranial Doppler ultrasonography. N Engl J Med 339(1):5-11, 1998
53. Roach ES, Golomb MR, Adams R, et al: Management of stroke in infants and children: a scientific statement from a special writing group of the American heart association stroke council and the council on cardiovascular disease in the young. Stroke 39(9):2644-2691, 2008
54. LaRovere KL: Transcranial doppler ultrasound in children with stroke and cerebrovascular disorders. Curr Opin Pediatr 27(6):712-718, 2015
55. Lee YS, Jung KH, Roh JK: Diagnosis of moyamoya disease with transcranial doppler sonography: Correlation study with magnetic resonance angiography. J Neuroimaging 14(4):319-323, 2004

56. Takase K, Kashihara M, Hashimoto T: Transcranial doppler ultrasonography in patients with moyamoya disease. Clin Neurol Neurosurg 99(Suppl 2):S101-S105, 1997
57. Wang JZ, Zhang S, Wei X, et al: Transcranial color Doppler sonography as an alternative tool for evaluation of terminal internal carotid artery steno-occlusion in moyamoya disease. J Clin Ultrasound 50 (1):33-40, 2022
58. Cho H, Jo KI, Yu J, et al: Low flow velocity in the middle cerebral artery predicting infarction after bypass surgery in adult moyamoya disease. J Neurosurg 126(5):1573-1577, 2017
59. Shulman JG, Snider S, Vaitkevicius H, et al: Direct visualization of arterial emboli in Moyamoya syndrome. Front Neurol 8:425, 2017
60. Lee WJ, Jung KH, Lee KJ, et al: Sonographic findings associated with stenosis progression and vascular complications in moyamoya disease. J Neurosurg 125(3):689-697, 2016
61. Kwag HJ, Jeong DW, Lee SH, et al: Intracranial hemodynamic changes during adult moyamoya disease progression. J Clin Neurol 4(2):67-74, 2008
62. Kazumata K, Tha KK, Tokairin K, et al: Brain structure, connectivity, and cognitive changes following revascularization surgery in adult Moyamoya disease. Neurosurgery 85(5):E943-e952, 2019
63. Kazumata K, Tokairin K, Ito M, et al: Combined structural and diffusion tensor imaging detection of ischemic injury in moyamoya disease: Relation to disease advancement and cerebral hypoperfusion. J Neurosurg 134(3):1155-1164, 2020
64. Ahtam B, Feldman Henry A, Solit Marina, et al: Diffusion tensor imaging suggests decreased axonal myelination in children with Moyamoya without Stroke. Stroke 2022(53)
65. Kamada F, Aoki Y, Narisawa A, et al: A genome-wide association study identifies RNF213 as the first Moyamoya disease gene. Journal of human genetics 56(1):34-40, 2011
66. Liu W, Morito D, Takashima S, et al: Identification of RNF213 as a susceptibility gene for moyamoya disease and its possible role in vascular development. PloS one 6(7):e22542, 2011. -e22542
67. Miyatake S, Miyake N, Touho H, et al: Homozygous c.14576G>A variant of RNF213 predicts early-onset and severe form of moyamoya disease. Neurology 78(11):803-810, 2012
68. Ito M, Kawabori M, Sugiyama T, et al: Impact of RNF213 founder polymorphism (p.R4810K) on the postoperative development of indirect pial synangiosis after direct/indirect combined revascularization surgery for adult Moyamoya disease. Neurosurg Rev 2022
69. Guey S, Tournier-Lasserve E, Herve D, et al: Moyamoya disease and syndromes: From genetics to clinical management. Appl Clin Genet 8:49-68, 2015
70. Roder C, Peters V, Kasuya H, et al: Polymorphisms in TGFB1 and PDGFRB are associated with Moyamoya disease in European patients. Acta Neurochir (Wien) 152(12):2153-2160, 2010
71. Pinard A, Guey S, Guo D, et al: The pleiotropy associated with de novo variants in CHD4, CNOT3, and SETD5 extends to moyamoya angiopathy. Genet Med 22(2):427-431, 2020
72. Kundishora AJ, Peters ST, Pinard A, et al: DIAPH1 variants in non-east Asian patients with sporadic Moyamoya disease. JAMA Neurol 78 (8):993-1003, 2021
73. Kang HS, Kim SK, Cho BK, et al: Single nucleotide polymorphisms of tissue inhibitor of metalloproteinase genes in familial moyamoya disease. Neurosurgery 58(6):1074-1080, 2006. discussion 1074-1080
74. Shoemaker LD, Clark MJ, Patwardhan A, et al: Disease variant landscape of a large multiethnic population of Moyamoya patients by exome sequencing. G3 (Bethesda) 6(1):41-49, 2015
75. Park YS, Jeon YJ, Kim HS, et al: The role of VEGF and KDR polymorphisms in moyamoya disease and collateral revascularization. PLoS One 7(10):e47158, 2012
76. Mertens R, Graupera M, Gerhardt H, et al: The genetic basis of Moyamoya disease. Transl Stroke Res 13(1):25-45, 2022
77. Ge P, Ye X, Liu X, et al: Association between p.R4810K variant and long-term clinical outcome in patients with Moyamoya disease. Front Neurol 10:662, 2019
78. Nomura S, Yamaguchi K, Akagawa H, et al: Genotype-phenotype correlation in long-term cohort of Japanese patients with Moyamoya disease. Cerebrovasc Dis 47(3-4):105-111, 2019
79. Sesen J, Driscoll J, Moses-Gardner A, et al: Non-invasive urinary biomarkers in Moyamoya disease. Front Neurol 12:661952, 2021
80. Scott RM, Smith ER: Moyamoya disease and moyamoya syndrome. N Engl J Med 360(12):1226-1237, 2009
81. Kaur B, Tan C, Brat DJ, et al: Genetic and hypoxic regulation of angiogenesis in gliomas. J Neurooncol 70(2):229-243, 2004
82. Gururangan S, Friedman HS: Recent advances in the treatment of pediatric brain tumors. Oncology (Williston Park) 18(13):1649-1661, 2004. discussion 1662, 1665-1646, 1668
83. Purow B, Fine HA: Progress report on the potential of angiogenesis inhibitors for neuro-oncology. Cancer Invest 22(4):577-587, 2004
84. Smith ER, Zurakowski D, Saad A, et al: Urinary biomarkers predict brain tumor presence and response to therapy. Clin Cancer Res 14 (8):2378-2386, 2008
85. Lim M, Cheshier S, Steinberg GK: New vessel formation in the central nervous system during tumor growth, vascular malformations, and Moyamoya. Curr Neurovasc Res 3(3):237-245, 2006
86. Fujimura M, Watanabe M, Narisawa A, et al: Increased expression of serum Matrix Metalloproteinase-9 in patients with moyamoya disease. Surg Neurol 72(5):476-480, 2009. discussion 480
87. Kusaka N, Sugiu K, Tokunaga K, et al: Enhanced brain angiogenesis in chronic cerebral hypoperfusion after administration of plasmid human vascular endothelial growth factor in combination with indirect vasoreconstructive surgery. J Neurosurg 103(5):882-890, 2005
88. Malek AM, Connors S, Robertson RL, et al: Elevation of cerebrospinal fluid levels of basic fibroblast growth factor in moyamoya and central nervous system disorders. Pediatr Neurosurg 27(4):182-189, 1997
89. Nanba R, Kuroda S, Ishikawa T, et al: Increased expression of hepatocyte growth factor in cerebrospinal fluid and intracranial artery in moyamoya disease. Stroke 35(12):2837-2842, 2004
90. Kang HS, Kim JH, Phi JH, et al: Plasma matrix metalloproteinases, cytokines and angiogenic factors in moyamoya disease. J Neurol Neurosurg Psychiatry 81(6):673-678, 2010
91. Fehnel KP, Penn DL, Duggins-Warf M, et al: Dysregulation of the EphrinB2-EphB4 ratio in pediatric cerebral arteriovenous malformations is associated with endothelial cell dysfunction in vitro and functions as a novel noninvasive biomarker in patients. Exp Mol Med 52(4):658-671, 2020
92. Smith ER, Manfredi M, Scott RM, et al: A recurrent craniopharyngioma illustrates the potential usefulness of urinary matrix metalloproteinases as noninvasive biomarkers: Case report. Neurosurgery 60(6):E1148-E1149, 2007. discussion E1149
93. Pricola Fehnel K, Duggins-Warf M, Zurakowski D, et al: Using urinary bFGF and TIMP3 levels to predict the presence of juvenile pilocytic astrocytoma and establish a distinct biomarker signature. J Neurosurg Pediatr 18(4):396-407, 2016
94. Akino T, Han X, Nakayama H, et al: Netrin-1 promotes medulloblastoma cell invasiveness and angiogenesis, and demonstrates elevated expression in tumor tissue and urine of patients with pediatric medulloblastoma. Cancer research 74(14):3716-3726, 2014
95. Baxter PA, Su JM, Onar-Thomas A, et al: A phase I/II study of veliparib (ABT-888) with radiation and temozolomide in newly diagnosed diffuse pontine glioma: A pediatric brain tumor consortium study. Neuro Oncol 22(6):875-885, 2020
96. Saitoh Y, Kato A, Hagihara Y, et al: Gene therapy for ischemic brain diseases. Curr Gene Ther 3(1):49-58, 2003
97. Ramos C, Napoleao P, Selas M, et al: Prognostic value of VEGF in patients submitted to percutaneous coronary intervention. Dis Markers 2014:135357, 2014
98. Semenova AE, Sergienko IV, Masenko VP, et al: The influence of rosuvastatin therapy and percutaneous coronary intervention on angiogenic growth factors in coronary artery disease patients. Acta Cardiol 64(3):405-409, 2009
99. Chan LW, Moses MA, Goley E, et al: Urinary VEGF and MMP levels as predictive markers of 1-year progression-free survival in cancer patients treated with radiation therapy: A longitudinal study of protein kinetics throughout tumor progression and therapy. J Clin Oncol 22(3):499-506, 2004
100. Coticchia CM, Curatolo AS, Zurakowski D, et al: Urinary MMP-2 and MMP-9 predict the presence of ovarian cancer in women with normal CA125 levels. Gynecologic oncology 123(2):295-300, 2011

101. Moses MA, Wiederschain D, Loughlin KR, et al: Increased incidence of matrix metalloproteinases in urine of cancer patients. Cancer research 58(7):1395-1399, 1998
102. Bang OY, Fujimura M, Kim SK: The pathophysiology of moyamoya disease: An update. Journal of stroke 18(1):12-20, 2016
103. Ohkubo K, Sakai Y, Inoue H, et al: Moyamoya disease susceptibility gene RNF213 links inflammatory and angiogenic signals in endothelial cells. Scientific reports 5:13191, 2015
104. Huggard D, Kelly L, Ryan E, et al: Increased systemic inflammation in children with Down syndrome. Cytokine 127:154938, 2020
105. Conran N, Belcher JD: Inflammation in sickle cell disease. Clin Hemorheol Microcirc 68(2-3):263-299, 2018
106. Ahn JH, Jeon JP, Kim JE, et al: Association of hyperthyroidism and thyroid autoantibodies with Moyamoya disease and its stroke event: A population-based case-control study and meta-analysis. Neurol Med Chir (Tokyo) 58(3):116-123, 2018
107. Smith ER: Moyamoya Biomarkers. J Korean Neurosurg Soc 57(6):415-421, 2015
108. Smith ER, McClain CD, Heeney M, et al: Pial synangiosis in patients with moyamoya syndrome and sickle cell anemia: Perioperative management and surgical outcome. Neurosurg Focus 26 (4):E10, 2009
109. See AP, Ropper AE, Underberg DL, et al: Down syndrome and moyamoya: Clinical presentation and surgical management. J Neurosurg Pediatr: 1-6, 2015
110. Kainth DS, Chaudhry SA, Kainth HS, et al: Prevalence and characteristics of concurrent down syndrome in patients with moyamoya disease. Neurosurgery 72(2):210-215, 2013. discussion 215

JNS PEDIATRICS

CLINICAL ARTICLE

J Neurosurg Pediatr 29:458–466, 2022

Ivy sign: a diagnostic and prognostic biomarker for pediatric moyamoya

***Alaa S. Montaser, MD, PhD,[1,2] Harishchandra Lalgudi Srinivasan, FRCS,[3] Steven J. Staffa, MS,[4] David Zurakowski, MS, PhD,[4] Anna L. Slingerland, BS,[1] Darren B. Orbach, MD, PhD,[1,5] Moran Hausman-Kedem, MD,[6,7] Jonathan Roth, MD,[3,7] and Edward R. Smith, MD[1]**

[1]Department of Neurosurgery, Boston Children's Hospital, Harvard Medical School, Boston, Massachusetts; [2]Department of Neurosurgery, Mayo Clinic, Jacksonville, Florida; [3]Department of Neurosurgery, Dana Children's Hospital, Tel Aviv Sourasky Medical Center, Tel Aviv, Israel; [4]Departments of Anesthesiology and Surgery, Boston Children's Hospital, Harvard Medical School, Boston, Massachusetts; [5]Department of Radiology, Boston Children's Hospital, Harvard Medical School, Boston, Massachusetts; [6]Pediatric Neurology Institute, Dana-Dwek Children's Hospital, Tel Aviv Sourasky Medical Center, Tel Aviv, Israel; and [7]Sackler Faculty of Medicine, Tel Aviv University, Tel Aviv, Israel

OBJECTIVE Ivy sign is a radiographic finding on FLAIR MRI sequences and is associated with slow cortical blood flow in moyamoya. Limited data exist on the utility of the ivy sign as a diagnostic and prognostic tool in pediatric patients, particularly outside of Asian populations. The authors aimed to investigate a modified grading scale with which to characterize the prevalence and extent of the ivy sign in children with moyamoya and evaluate its efficacy as a biomarker in predicting postoperative outcomes, including stroke risk.

METHODS Pre- and postoperative clinical and radiographic data of all pediatric patients (21 years of age or younger) who underwent surgery for moyamoya disease or moyamoya syndrome at two major tertiary referral centers in the US and Israel, between July 2009 and August 2019, were retrospectively reviewed. Ivy sign scores were correlated to Suzuki stage, Matsushima grade, and postoperative stroke rate to quantify the diagnostic and prognostic utility of ivy sign.

RESULTS A total of 171 hemispheres in 107 patients were included. The median age at the time of surgery was 9 years (range 3 months–21 years). The ivy sign was most frequently encountered in association with Suzuki stage III or IV disease in all vascular territories, including the anterior cerebral artery (53.7%), middle cerebral artery (56.3%), and posterior cerebral artery (47.5%) territories. Following surgical revascularization, 85% of hemispheres with Matsushima grade A demonstrated a concomitant, statistically significant reduction in ivy sign scores (OR 5.3, 95% CI 1.4–20.0; p = 0.013). Postoperatively, revascularized hemispheres that exhibited ivy sign score decreases had significantly lower rates of postoperative stroke (3.4%) compared with hemispheres that demonstrated no reversal of the ivy sign (16.1%) (OR 5.5, 95% CI 1.5–21.0; p = 0.008).

CONCLUSIONS This is the largest study to date that focuses on the role of the ivy sign in pediatric moyamoya. These data demonstrate that the ivy sign was present in approximately half the pediatric patients with moyamoya with Suzuki stage III or IV disease, when blood flow was most unstable. The authors found that reversal of the ivy sign provided both radiographic and clinical utility as a prognostic biomarker postoperatively, given the statistically significant association with both better Matsushima grades and a fivefold reduction in postoperative stroke rates. These findings can help inform clinical decision-making, and they have particular value in the pediatric population, as the ability to minimize additional radiographic evaluations and tailor radiographic surveillance is requisite.

https://thejns.org/doi/abs/10.3171/2021.11.PEDS21384

KEYWORDS moyamoya disease; pediatric moyamoya; ivy sign; vascular disorders

The ivy sign is a radiographic finding consisting of a bright signal in the cortical sulci and subarachnoid space on specific MRI sequences, which was first described on T1-weighted postcontrast studies, then subsequently on FLAIR images.[1–4] Previously called leptomeningeal contrast enhancement or leptomeningeal high signal intensity,[5,6] it was initially recognized decades ago in a small series of 3 children with moyamoya disease in Japan.[1] While the presence of the ivy sign has since been identified in multiple conditions in which there is slow cor-

ABBREVIATIONS ACA = anterior cerebral artery; AIS = arterial ischemic stroke; MCA = middle cerebral artery; PCA = posterior cerebral artery; PiPeD = pial pericranial dural; TIA = transient ischemic attack.

SUBMITTED July 25, 2021. **ACCEPTED** November 4, 2021.

INCLUDE WHEN CITING Published online December 31, 2021; DOI: 10.3171/2021.11.PEDS21384.

* A.S.M. and H.L.S. contributed equally to this work and share first authorship.

tical blood flow, it is most commonly associated with moyamoya (both the syndrome and disease) and is most commonly identified on FLAIR sequences. The prevalence of the ivy sign in patients with moyamoya varies widely among series, reported to be between 20% and 90%, with this variability often attributed to inhomogeneity of the populations under study[6–9] and the underlying etiology.[10] Importantly, the presence of the ivy sign can diminish or completely vanish with normalization of cerebral blood flow, as has been reported after surgical revascularization.[11,12]

The ivy sign has acquired relevance in the clinical practice of patients with moyamoya for several reasons.[3,5,6,11,13–16] First, it can help to diagnose the presence of moyamoya, given the ease of identifying the ivy sign on routine axial FLAIR MRI studies. Second, it has utility in providing visualization of the severity and anatomical distribution of cerebral ischemia, including providing data on the potential efficacy of surgical revascularization if reduction of ivy sign occurs postoperatively. Third, the ease of acquiring a FLAIR sequence as part of routine MRI means that it may reduce (or completely obviate) the need for other studies to assess cerebral perfusion (such as SPECT/PET), thereby reducing the cost, time, and risk (of radiation and sedation) of the moyamoya evaluation—a point particularly relevant to children.[7,13,16–18]

The ease of acquisition and ready reproducibility of the ivy sign makes it an appealing target as a potential radiographic biomarker to provide diagnostic and prognostic insight. However, the relative rarity of moyamoya, especially in the pediatric population (where, ironically, the need for less-invasive testing is most impactful), means that high-volume studies have been challenging to complete. Herein, we present the largest study (of which we are aware) to date reporting on the presence and utility of the ivy sign in the diagnosis and prognosis of pediatric moyamoya.[19]

Methods

This study was approved by the IRB at each respective hospital.

Patient Population

We retrospectively reviewed the medical records of a consecutive cohort of pediatric patients with moyamoya disease or moyamoya syndrome who underwent surgery at one of two large tertiary referral centers in the US and Israel between July 2009 and August 2019.[16,20,21] We included patients who were 21 years or younger at the time of surgery and who had relevant imaging studies available at the time of this paper preparation. All patients were treated with indirect revascularization procedures.[22,23]

Data Collection

The medical records of the identified cohort were reviewed, and the following data were extracted using a standardized data collection form: age at presentation, sex, associated medical conditions, whether the patient had received cranial irradiation for a tumor, clinical presentation, disease laterality, radiographic evidence of stroke, presence of the ivy sign on axial FLAIR studies (as reviewed with the neuroradiology department), presence of transdural collaterals on DSA at the time of diagnosis (as defined by our previous study),[12] Suzuki grade, indications for surgery, type of surgical technique, intraoperative blood loss, intra- and postoperative complications, clinical and radiographic outcome (including radiographic evidence of stroke on postoperative imaging), and follow-up duration.[24]

The presence of transient ischemic attack (TIA) and/or clinically and radiologically defined arterial ischemic stroke (AIS) was recorded. The radiographic outcome after surgery was determined by evaluating the most recent MRI study, including FLAIR sequences, to assess the presence of the ivy sign (quantified using the method described below) and by evaluating the most recent DSA to assess the engraftment, evidenced by ingrowth of collateral branch vessels and quantified by the Matsushima grade (in middle cerebral artery [MCA] territories, when relevant).[25,26]

Neuroimaging Analysis

Ivy Sign Score

Ivy sign was defined as a linear, high signal intensity along the cortical sulci in the cerebral hemispheres on FLAIR sequences; all pre- and postoperative images were matched in acquisition type (2D to 2D and 3D to 3D) to control for technical variability.[2,11,27] All MRI studies were reviewed by neuroradiologists and study authors, and reports detailing the ivy sign and the diagnosis of moyamoya were generated as part of routine clinical practice.

Each hemisphere was divided into 3 segments in a craniocaudal orientation: 1) from the level of the basal cisterns downward to the skull base, 2) from the level of the basal cistern to the level of the foramen of Monro, and 3) from the level of the foramen of Monro to the vertex (Fig. 1 and Table 1).[28] Furthermore, each segment was divided into vascular territories according to the main vascular supply: anterior cerebral artery (ACA), MCA, and posterior cerebral artery (PCA) territories. Two caudal segments included 3 vascular territories (ACA, MCA, and PCA), while the rostral-most segment included only 2 vascular territories (ACA and MCA); hence, each hemisphere would have 8 vascular territories.

Each vascular territory was graded as 0 or 1 for the absence or presence of ivy sign in that region. Thereby, the overall ivy sign grade of a given hemisphere could range from 0 to 8. This hemispheric ivy sign grade was used to simplify risk assessment.

In addition to the hemispheric grade, a more refined analysis of each territory was further carried out to perform a more granular assessment of specific regions. In this secondary analysis, the grading for each of the 8 territories noted above was expanded from a binary score (0/1 = absent/present) to a more detailed 0- to 3-point grading system, whereby 0 indicated the absence of ivy sign; 1 indicated that the ivy sign was identified in less than one-third of the cortical surface in the territory of interest; 2 indicated that the ivy sign was seen in one-third to two-thirds of the cortical surface; and 3 indicated that the ivy sign

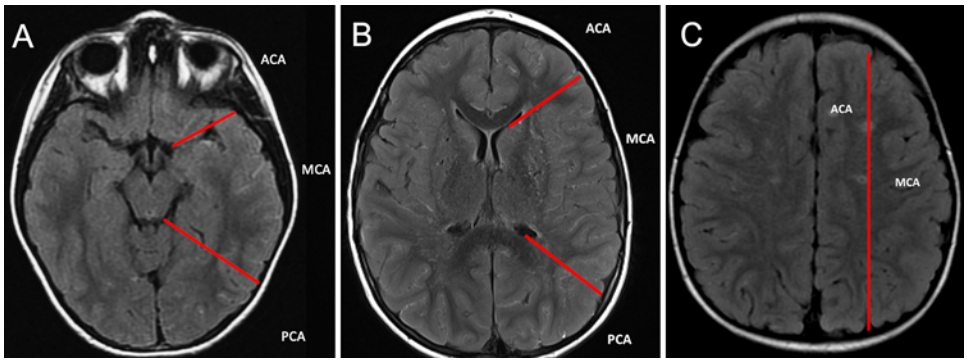

FIG. 1. Axial MR images showing the subhemispheric regions according to the vascular territories used to calculate the ivy sign score. The cuts are taken at the midbrain (**A**), the level of the foramen of Monro (**B**), and the centrum semiovale (**C**), with the sections divided as shown by the *red lines*. Figure is available in color online only.

was seen in more than two-thirds of the cortical surface in the territory of interest (Fig. 1). The difference in scoring between ACA/MCA and PCA territories (Table 1) is due to the size of the relative area of parenchyma perfused by each vessel. Both the hemispheric grade (0–8) and the more granular scoring of each territory were recorded for the preoperative MRI studies and compared with a follow-up MRI study obtained 6 to 12 months postoperatively. Ivy sign reversal was recorded for each patient.

Infarction

Regarding hemispheres with radiological evidence of infarction, ivy sign scoring along the physically adjacent infarcted cortex was considered uninterpretable. However, if the cortex overlying the infarcted area (e.g., subcortical infarction) was spared, then the ivy sign score was recorded accordingly.

Digital Subtraction Angiography

Similar to MRI, DSA findings were also reported by neuroradiologists and/or interventional neuroradiologists in a nonblinded fashion as part of the routine clinical practice, and, subsequently, the Suzuki stage was recorded. Follow-up DSA studies were reviewed to assess the engraftment at the site of the surgery for indirect revascularization procedures, evidenced by ingrowth of collateral branch vessels; the Matsushima grade was recorded for each hemisphere.[23,29,30]

Correlation of Ivy Sign Score and DSA Findings

We sought to ascertain the correlation of angiography-proven disease (Suzuki stage) with preoperative ivy sign score, of the individual arterial territories and per hemisphere as well. We tested the correlation between the degree of revascularization (as evidenced by postoperative engraftment and Matsushima grade) and the postoperative ivy sign score.

Statistical Analysis

All continuous data are presented as median and IQR, and categorical data are presented as frequencies and percentages. Overall analyses as well as stratified analyses were performed by arterial territory and by preoperative

TABLE 1. Patient demographics, radiographic characteristics, surgical intervention, and ivy sign scoring in different arterial vascular territories

	Value
No. of hemispheres	171
No. of patients	107
Median age (range)	9 yrs (3 mos–21 yrs)
Sex	
M	36
F	71
Preop infarction (n = 90/171)	
ACA	24
MCA	57
PCA	9
Suzuki stage	
I or II	30
III or IV	90
V or VI	35
Op side	
Bilat	61
Unilat	46
Op type	
Pial synangiosis	123
PiPeD	24
Myosynangiosis	14
Other indirect	10
Arterial territory*	
ACA	0–3
MCA	0–3
PCA	0–2

Values represent the number of patients or hemispheres unless indicated otherwise.
* Refers to the delineation of anatomical regions that correlate with arterial supply, as described in Fig. 1. Arterial territory numbers indicate the ivy sign score ranges for the grading system of each vascular territory.

ivy sign score. Comparisons of categorical data between subgroups were performed using Fisher's exact test. The analyses of changes in continuous ivy sign data by territory from preoperative to postoperative assessment were performed using the nonparametric Wilcoxon signed-rank test. Comparison of ivy sign by preoperative Suzuki stage was done using the Kruskal-Wallis test. Receiver operating characteristic curve analysis was implemented to determine the association between ivy sign overall and by territory versus stroke risk, with Youden's J index examined to determine the cut point that maximizes the sum of sensitivity and specificity. Multivariable, generalized estimating equation logistic regression modeling was implemented to analyze risk factors for preoperative stroke in the MCA territory, while accounting for nesting of hemispheres within patients. Results from the generalized estimating equation modeling are presented as adjusted odds ratios with corresponding 95% confidence intervals and p values. A two-tailed $p < 0.05$ was considered statistically significant. All statistical analyses were performed using Stata version 16.0 (StataCorp LLC).

Results

Patient Demographics and Radiographic Characteristics

A total of 171 hemispheres in 107 patients were included in this study, with a median age of 9 years (range 3 months–21 years), including 36 males and 71 females. The median follow-up for postoperative MRI was 6 months, and for postoperative angiography it was 12 months. Radiographic evidence of AIS at presentation MRI, not including watershed infarcts, was identified in 90 hemispheres (53%). Preoperative diagnostic DSA was available for 155 hemispheres (91%) and demonstrated Suzuki grade I or II in 30 hemispheres (19%), Suzuki grade III or IV in 90 hemispheres (58%), and Suzuki grade V or VI in 35 hemispheres (23%) (Table 1).

The ivy sign was more frequently encountered in association with Suzuki stage III or IV in all vascular territories. In all hemispheres with Suzuki grade III or IV (n = 90/171), the ivy sign was encountered in 53.7%, 56.3%, and 47.5% of ACA, MCA, and PCA territories, respectively. This association was statistically significant in the PCA territory ($p = 0.02$) and showed a trend toward the MCA territory ($p = 0.12$) but was not associated with the ACA territory ($p = 0.56$).

Ivy Sign and Surgical Revascularization

Surgical revascularization led to a decrease or reversal of ivy sign in each anatomically correlated area separately (Fig. 2 and Table 2), as well as a decrease or reversal of the total ivy sign score in the individual hemisphere. The preoperative median ivy sign score in the ACA territory was 1 (IQR 0, 2), and the postoperative median score in the same territory was 0 (IQR 0, 1). The preoperative median ivy sign score in the MCA territory was 2 (IQR 1, 2), and the postoperative median score in the same territory was 1 (IQR 0, 2). The preoperative median ivy sign score in the PCA territory was 1 (IQR 0, 2), and the postoperative median score in the same territory was 0 (IQR 0, 1). The total median preoperative ivy sign score in a hemisphere was 4 (IQR 1, 6), and the postoperative total ivy sign score was 1 (IQR 0, 4). For patients who had a reduction in the ivy sign score postoperatively, the stroke risk on follow-up was 3.4% over the study period, while for those patients who did not demonstrate a reduction in the ivy sign score after surgery, the stroke rate was almost fivefold higher at 16.1%. This underscores the prognostic utility of the ivy sign score on postoperative MRI.

After surgical revascularization, there was a significant correlation between better engraftment and reduction in ivy sign as measured by the ivy sign score; 85% of hemispheres with a Matsushima grade A demonstrated a decrease or reversal of ivy sign (OR 5.3, 95% CI 1.4–20.0; $p = 0.013$) (Fig. 3). This link between the degree of engraftment (as quantified by the Matsushima grade) and concomitant change in the ivy sign score held true, with a poorer Matsushima grade correlating with lower rates of ivy sign reversal. A decrease or reversal of ivy sign was observed in 57.1% of hemispheres with a Matsushima grade B and only in 47.1% of hemispheres with a Matsushima grade C.

Ivy Sign and Postoperative Stroke Rate

Overall, patients who did not show improvement in ivy sign scores postoperatively had higher rates of subsequent stroke than did those patients who showed a decrease or reversal of ivy sign after revascularization. In contrast, patients who demonstrated a reduction or reversal of ivy sign postoperatively had significantly lower stroke risk over time. Ivy sign was evaluated in the entire hemisphere, even if just one vascular territory (most commonly the MCA) was targeted for revascularization. This is important, as MCA revascularization can provide blood supply to other (PCA and ACA) territories and furthers the utility of this imaging technique as a territory-specific marker of surgical response.

In the ACA territory, none of the hemispheres (n = 0/57) with a decrease in or reversal of ivy sign experienced a postoperative stroke, and 6.4% (n = 6/94) of hemispheres that demonstrated no improvement of ivy sign had strokes ($p = 0.084$) (Table 3). In the PCA territory, none of the hemispheres (n = 0/34) with a decrease or reversal of ivy sign experienced a postoperative stroke, and 5.1% (n = 6/117) of hemispheres that demonstrated no improvement of ivy sign had strokes ($p = 0.338$). In the area that is most commonly treated—the MCA territory—the most striking correlation was observed. In the MCA territory, 2.3% (n = 2/86) of hemispheres that showed improvement in ivy sign had strokes, while 10.8% (n = 7/65) of hemispheres with no improvement in ivy sign experienced strokes ($p = 0.039$).

A decrease in or reversal of the total ivy sign score in the MCA territory was significantly associated with lower rates of postoperative stroke (2.3%) compared with hemispheres that demonstrated no reversal of the ivy sign (10.8%) ($p = 0.039$). While not of a large enough number to achieve significance, it was noted that a decrease of or reversal in the total ivy sign score in the ACA and PCA territories was also associated with lower rates of postoperative infarcts. Overall, improvement of the ivy sign in an individual hemisphere as a whole was significantly

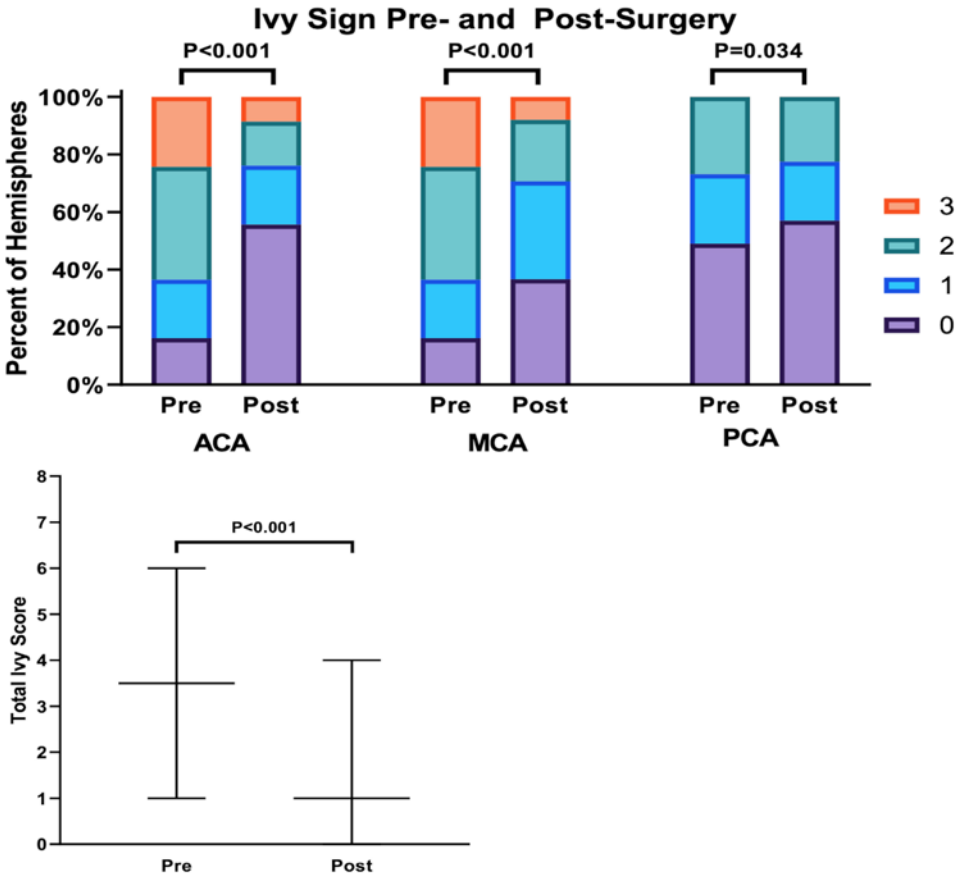

FIG. 2. Pre- and postoperative ivy sign scores in each vascular territory. **Upper:** Bar graph showing a significant reduction in the ivy sign score in the ACA and MCA territories after surgery, with a concomitant trend in the PCA territory. **Lower:** Graph showing change in the pre- and postoperative ivy sign scores for the combined entire hemisphere, with a significant reduction ($p < 0.001$) of approximately 2 points present postrevascularization.

associated with lower rates of postoperative stroke (3.4%) compared with hemispheres that demonstrated no reversal of the ivy sign (16.1%) (OR 5.5, 95% CI 1.5–21.0; $p = 0.008$) (Fig. 4).

Discussion

The ivy sign is well described in the literature for adult patients with moyamoya, yet reports specific to the pediatric population are very limited. Many ivy sign studies that mention children are composed of mixed pediatric and adult populations, with the majority derived from East Asian countries, likely encompassing a relatively homogeneous subset of the disease. Here, we present a new standardized grading system to quantify the ivy sign in children. We report the prevalence of the ivy sign at diagnosis, how the ivy sign changed in response to surgery, and evidence supporting its utility as a prognostic tool related to postoperative radiographic outcomes and stroke rates. The novelty in this study is derived from its specific focus on the pediatric age group, investigation of a predominantly non-Asian population, and large number of patients, which affords more rigorous statistical analysis of the data. The anatomical layout used in this study for ivy sign scoring shares many concepts with precedent reports,[3] but with some modifications to allow for ease of use and reproducibility.

TABLE 2. Impact of surgical revascularization on ivy sign score

	Preop Median Score (IQR)	Postop Median Score (IQR)	p Value
ACA	1 (0, 2)	0 (0, 1)	<0.001
MCA	2 (1, 2)	1 (0, 2)	<0.001
PCA	1 (0, 2)	0 (0, 1)	0.034
Total score	4 (1, 6)	1 (0, 4)	<0.001

These data are the aggregate scores from all patients in the study (107 patients and 171 hemispheres). The p values were calculated using the Wilcoxon signed-rank test.

Is the Ivy Sign a Useful Diagnostic Tool?

The ivy sign has been reported to be seen reliably in patients with moyamoya, including pediatric populations, but there are limited data that objectively link this MRI finding with other measures of disease severity.[16,19,27,31,32] Our data reveal that the degree of ivy sign (as measured

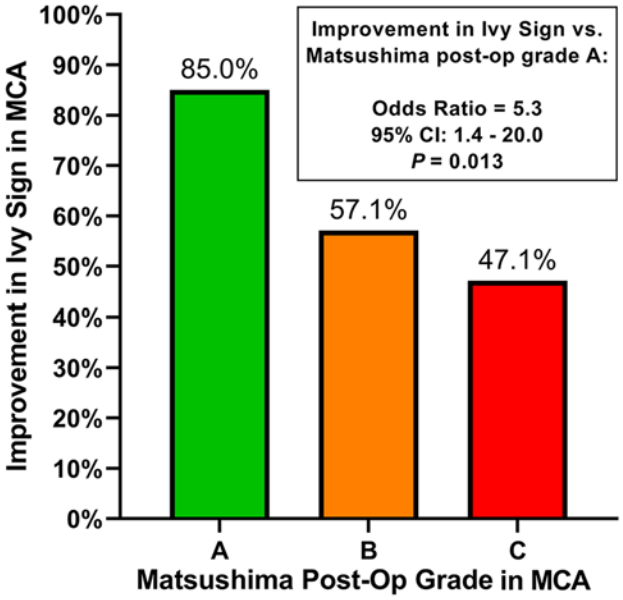

FIG. 3. Postoperative ivy sign as a function of the Matsushima grade. Bar graph showing that a better Matsushima grade correlated with a significantly greater percent improvement (reduction) in ivy sign. This demonstrates a direct link between the angiographic findings and the MR image–based ivy sign score, suggesting that increased angiographic response (more surgical collaterals as measured by the Matsushima grade) may lead to reduced ivy sign (better brain perfusion as measured by the ivy sign score) after surgery. Figure is available in color online only.

by our scoring system) correlates with the degree of disease severity seen on preoperative angiograms (as measured by the Suzuki stage). In our series, the ivy sign was most commonly seen in Suzuki stage III or IV disease (53.7%, 56.3%, and 47.5% in ACA, MCA, and PCA territories, respectively). This finding makes sense hemodynamically, as Suzuki stage III or IV represents the most unstable blood supply in the progression of moyamoya.[33,34] In Suzuki stage I or II, the compromise to blood flow is minimal, with relatively stable circulation, which contrasts sharply to Suzuki stage V or VI, often referred to as a "burnt out" end stage of the disease. Furthermore, the majority of patients with moyamoya are symptomatic and diagnosed at Suzuki stage III or IV disease. In combination, the findings from our research underscore the ability

TABLE 3. Correlation between ivy sign score improvement and the risk of postoperative stroke

	Postop Infarct Rate		
	Ivy Sign Improved	Ivy Sign Did Not Improve	p Value
ACA	0/57 (0)	6/94 (6.4)	0.084
MCA	2/86 (2.3)	7/65 (10.8)	0.039
PCA	0/34 (0)	6/117 (5.1)	0.338

Data are presented as n (%), where the numerator represents the actual number of postoperative infarctions, and the denominator represents the number of hemispheres with improved or unimproved ivy sign. The p values were calculated using Fisher's exact test.

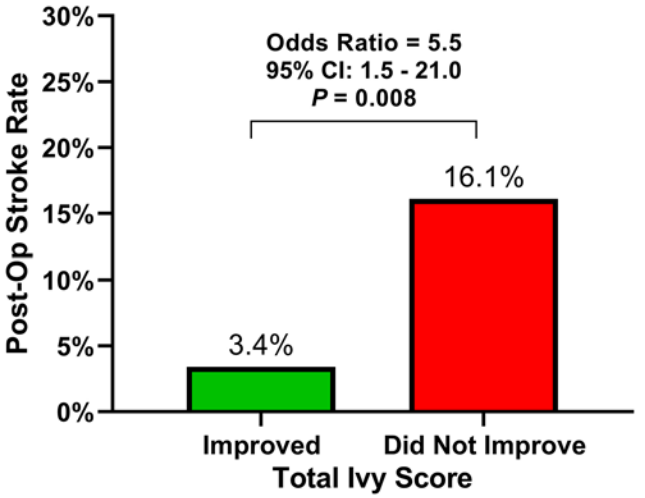

FIG. 4. Bar graph showing the correlation between ivy sign score reduction after surgery and postoperative stroke risk on follow-up. Figure is available in color online only.

of the ivy sign to identify brain "at risk" of ischemia and to link these MRI findings directly with angiography-proven disease.

Is the Ivy Sign a Useful Radiographic Prognostic Tool?

The results of this study indicate that the ivy sign has utility as a predictor of postrevascularization angiographic outcome. The data we present demonstrate that the ivy sign significantly diminishes (as measured by our scoring system) with successful revascularization surgery (as measured by Matsushima grade and the postoperative stroke rate) (Fig. 5). Our results are in concordance with those of previous reports.[5,11,13,18,35] Kawashima et al.[11] reported improvement of the ivy sign on the ipsilateral side of revascularization surgery in 21 of 22 patients. Hamano et al.[35] noted a preoperative ivy sign in 112 of 144 hemispheres with moyamoya and reported reversal of the ivy sign postoperatively in all hemispheres. Our research provides a more objective quantification of the use of the ivy sign in this specific population.

In our series, we found that surgical revascularization led to improvement of the ivy sign score, both in the specific vascular territory that was treated and in the ipsilateral hemisphere as a whole (Fig. 2 and Table 2). Our results represent robust findings in a large volume of pediatric moyamoya cases treated with indirect anastomosis, confirm diagnostic utility, and add new prognostic tools directly relevant to clinical practice.

Additionally, we noted that a decrease of the total ivy sign score was significantly associated with a better Matsushima grade postoperatively. Following surgical revascularization, 85% of hemispheres with Matsushima grade A demonstrated a statistically significant improvement of the ivy sign (OR 5.3, 95% CI 1.4–20.0; p = 0.013) (Fig. 3). Improvement of the ivy sign was also observed in 57.1% of hemispheres with Matsushima grade B, and in 47.1% of hemispheres with Matsushima grade C. The importance of this finding is that it adds support for the decreased use

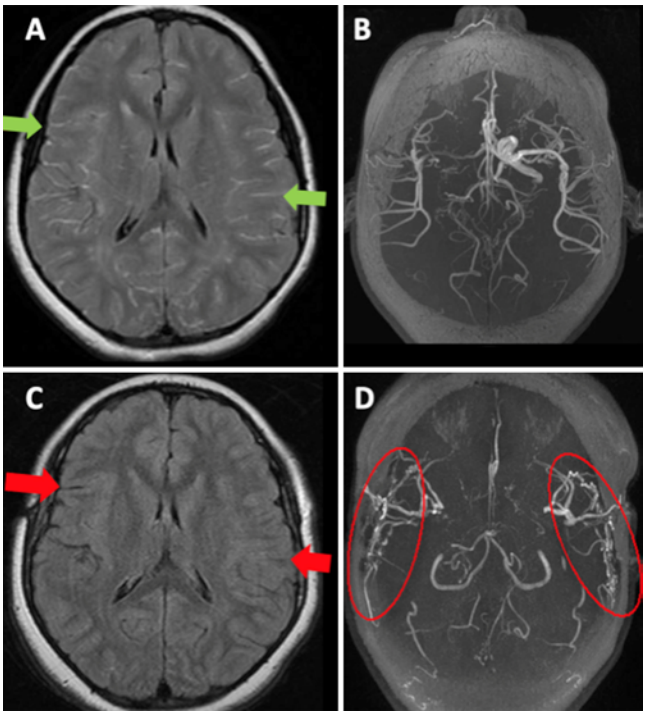

FIG. 5. A and B: Preoperative axial FLAIR MR image (A) demonstrating the ivy sign bilaterally (*green arrows*), and preoperative axial time-of-flight MR angiogram maximum intensity projection (MIP) image (B) demonstrating paucity of arterial supply in the MCA territories (more on the right side). **C and D:** Postoperative FLAIR MR image (C) showing complete improvement of the ivy sign (*red arrows*), correlated with robust postoperative engraftment (*red ovals*) as shown in the postoperative time-of-flight MR angiogram MIP image (D). Figure is available in color online only.

of postoperative angiography in patients who demonstrate good changes in the ivy sign. There is precedent for this practice in the literature, and our work here adds evidence that can more objectively inform decision-making to reduce the cost, radiation, and risk of postoperative angiography.[36]

Is the Ivy Sign Useful Clinically?

The use of the ivy sign for preoperative assessment and as a postoperative prognostic is appealing, as it represents a simple, easy-to-interpret, and uniform tool that could reduce—or even eliminate—the risks associated with the use of other tests, which is particularly important in the pediatric population. While catheter angiography remains critical for moyamoya diagnosis and surgical planning in order to identify (and avoid) transdural collaterals, the use of the ivy sign as a marker of preoperative ischemia and postoperative revascularization may reduce the need for studies such as CT perfusion and postoperative angiography.[12,36] For instance, adoption of the ivy sign as a radiographic biomarker of brain perfusion could eliminate radiation exposure and the additional time and cost associated with CT perfusion with acetazolamide challenge. The standardization of how FLAIR images are acquired can reduce operator-specific variability or technical challenges that may differ by institution for certain studies, such as arterial spin labeling. Postoperatively, ivy sign scoring may reduce the need for catheter angiograms. In combination, a greater use of the ivy sign pre- and postoperatively can lead to fewer tests, lower costs, and reduced risk from radiation and sedation associated with multiple imaging modalities. The ivy sign serves as a prognostic radiographic biomarker for postoperative TIA and stroke risk. Our data suggest that a decrease of the total ivy sign score in a given hemisphere was significantly associated with lower rates of postoperative infarct. Importantly, to our knowledge, this study demonstrates that indirect revascularization in a single (MCA) territory can result in ivy sign improvement in the entire hemisphere, underscoring the robustness of this approach in children and adding to the perfusion data reported elsewhere.[37] We observed that 3.4% of hemispheres that demonstrated ivy sign improvement had strokes, while 16.1% of hemispheres with no reversal of ivy sign had strokes. Conversely, the lack of ivy sign reversal postoperatively was associated with a fivefold increased risk of stroke following surgical revascularization.

Limitations and Future Directions

Although the current study included a large number of pediatric patients with moyamoya, the sample size would benefit from larger cohorts to improve the generalizability of the results. Our sample size was also too small to power a study able to differentiate the impact of individual subtypes of surgical techniques on the persistence of ivy sign and stroke risk, such as contrasting between procedures including pial synangiosis, pial pericranial dural (PiPeD) revascularization, myosynangiosis, and other operative approaches. However, we do have some data reporting on the comparative efficacy of ACA revascularization techniques, comparing a single-institution series of pericranial grafts with a series of burr holes,[38] which demonstrated that burr holes were markedly inferior for angiographic ingrowth of collaterals compared with the pericranial technique (28% collateral growth with burr holes vs 91% pericranium/PiPeD). Further supporting the value of future studies that compare the effectiveness of different surgical techniques, these same series revealed that the ivy sign was markedly diminished or completely absent in 32% to 50% of patients within 6 months after ACA pericranial operations, suggesting that the pericranium provides comparable efficacy to the superficial temporal artery in pial synangiosis.

Another limitation of this study is the lack of blinded reviewers, making bias and generalizability potential issues. We hope that by simplifying the scoring system and partnering with radiologists, the approach as outlined here may become more readily applicable in the future. It is important to acknowledge technical limitations to ivy sign acquisition, including noting that the ivy sign is globally present as an artifact in children sedated with propofol and that there may be subtle differences in ivy sign visualization across scanners from different companies, limiting the applicability in certain subsets of patients.[39] Lastly, future studies could address the interesting approach of a head-to-head comparison of the ivy sign to other imaging modalities, such as arterial spin labeling MRI or CT perfusion scans with acetazolamide challenge.

Conclusions

The current study is the largest to date that specifically focuses on the role of the ivy sign in pediatric moyamoya. These data demonstrate that ivy sign is present in about half of pediatric patients with moyamoya with Suzuki stage III or IV disease, when blood flow is most unstable. Following indirect anastomosis, we have demonstrated that reversal of the ivy sign provides both radiographic and clinical utility as a prognostic biomarker, given the statistically significant association with both better Matsushima grades and a fivefold reduction in postoperative stroke rates. These findings can help to inform clinical decision-making and have particular value in the pediatric population, given the potential ability to minimize the need for additional radiographic evaluations in children.

Acknowledgments

We acknowledge Kids@Heart and the Marcus Chae Moyamoya Fund.

References

1. Ohta T, Tanaka H, Kuroiwa T. Diffuse leptomeningeal enhancement, "ivy sign," in magnetic resonance images of moyamoya disease in childhood: case report. *Neurosurgery*. 1995;37(5):1009-1012.
2. Maeda M, Tsuchida C. "Ivy sign" on fluid-attenuated inversion-recovery images in childhood moyamoya disease. *AJNR Am J Neuroradiol*. 1999;20(10):1836-1838.
3. Mori N, Mugikura S, Higano S, et al. The leptomeningeal "ivy sign" on fluid-attenuated inversion recovery MR imaging in Moyamoya disease: a sign of decreased cerebral vascular reserve? *AJNR Am J Neuroradiol*. 2009;30(5):930-935.
4. Komatsu K, Mikami T, Suzuki H, et al. Geometrical complexity of cortical microvascularization in moyamoya disease. *World Neurosurg*. 2017;106:51-59.
5. Komiyama M, Nakajima H, Nishikawa M, Yasui T, Kitano S, Sakamoto H. Leptomeningeal contrast enhancement in moyamoya: its potential role in postoperative assessment of circulation through the bypass. *Neuroradiology*. 2001;43(1):17-23.
6. Fujiwara H, Momoshima S, Kuribayashi S. Leptomeningeal high signal intensity (ivy sign) on fluid-attenuated inversion-recovery (FLAIR) MR images in moyamoya disease. *Eur J Radiol*. 2005;55(2):224-230.
7. Vuignier S, Ito M, Kurisu K, et al. Ivy sign, misery perfusion, and asymptomatic moyamoya disease: FLAIR imaging and (15)O-gas positron emission tomography. *Acta Neurochir (Wien)*. 2013;155(11):2097-2104.
8. Jung MY, Kim YO, Yoon W, Joo SP, Woo YJ. Characteristics of brain magnetic resonance images at symptom onset in children with moyamoya disease. *Brain Dev*. 2015;37(3):299-306.
9. Savolainen M, Pekkola J, Mustanoja S, et al. Moyamoya angiopathy: radiological follow-up findings in Finnish patients. *J Neurol*. 2020;267(8):2301-2306.
10. Kaseka ML, Slim M, Muthusami P, et al. Distinct clinical and radiographic phenotypes in pediatric patients with moyamoya. *Pediatr Neurol*. 2021;120:18-26.
11. Kawashima M, Noguchi T, Takase Y, Nakahara Y, Matsushima T. Decrease in leptomeningeal ivy sign on fluid-attenuated inversion recovery images after cerebral revascularization in patients with Moyamoya disease. *AJNR Am J Neuroradiol*. 2010;31(9):1713-1718.
12. Storey A, Michael Scott R, Robertson R, Smith E. Preoperative transdural collateral vessels in moyamoya as radiographic biomarkers of disease. *J Neurosurg Pediatr*. 2017;19(3):289-295.
13. Ideguchi R, Morikawa M, Enokizono M, Ogawa Y, Nagata I, Uetani M. Ivy signs on FLAIR images before and after STA-MCA anastomosis in patients with moyamoya disease. *Acta Radiol*. 2011;52(3):291-296.
14. Kaku Y, Iihara K, Nakajima N, et al. The leptomeningeal ivy sign on fluid-attenuated inversion recovery images in moyamoya disease: positron emission tomography study. *Cerebrovasc Dis*. 2013;36(1):19-25.
15. Nam KW, Cho WS, Kwon HM, et al. Ivy sign predicts ischemic stroke recurrence in adult moyamoya patients without revascularization surgery. *Cerebrovasc Dis*. 2019;47(5-6):223-230.
16. Scott RM, Smith ER. Moyamoya disease and moyamoya syndrome. *N Engl J Med*. 2009;360(12):1226-1237.
17. Kawashima M, Noguchi T, Takase Y, Ootsuka T, Kido N, Matsushima T. Unilateral hemispheric proliferation of ivy sign on fluid-attenuated inversion recovery images in moyamoya disease correlates highly with ipsilateral hemispheric decrease of cerebrovascular reserve. *AJNR Am J Neuroradiol*. 2009;30(9):1709-1716.
18. Lee JK, Yoon BH, Chung SY, Park MS, Kim SM, Lee DS. The usefulness of the ivy sign on fluid-attenuated intensity recovery images in improved brain hemodynamic changes after superficial temporal artery-middle cerebral artery anastomosis in adult patients with moyamoya disease. *J Korean Neurosurg Soc*. 2013;54(4):302-308.
19. Yu J, Du Q, Xie H, Chen J, Chen J. What and why: the current situation and future prospects of "ivy sign" in moyamoya disease. *Ther Adv Chronic Dis*. 2020;11:2040622320960004.
20. Ferriero DM, Fullerton HJ, Bernard TJ, et al. Management of stroke in neonates and children: a scientific statement from the American Heart Association/American Stroke Association. *Stroke*. 2019;50(3):e51-e96.
21. Fukui M. Guidelines for the diagnosis and treatment of spontaneous occlusion of the circle of Willis ('moyamoya' disease). Research Committee on Spontaneous Occlusion of the Circle of Willis (Moyamoya Disease) of the Ministry of Health and Welfare, Japan. *Clin Neurol Neurosurg*. 1997;99(suppl 2):S238-S240.
22. Montaser A, Driscoll J, Smith H, et al. Long-term clinical and radiographic outcomes after pial pericranial dural revascularization: a hybrid surgical technique for treatment of anterior cerebral territory ischemia in pediatric moyamoya disease. *J Neurosurg Pediatr*. 2021;28(3):351-359.
23. Smith ER, Scott RM. Spontaneous occlusion of the circle of Willis in children: pediatric moyamoya summary with proposed evidence-based practice guidelines. A review. *J Neurosurg Pediatr*. 2012;9(4):353-360.
24. Suzuki J, Takaku A. Cerebrovascular "moyamoya" disease. Disease showing abnormal net-like vessels in base of brain. *Arch Neurol*. 1969;20(3):288-299.
25. Matsushima Y, Aoyagi M, Fukai N, Tanaka K, Tsuruoka S, Inaba Y. Angiographic demonstration of cerebral revascularization after encephalo-duro-arterio-synangiosis (EDAS) performed on pediatric moyamoya patients. *Bull Tokyo Med Dent Univ*. 1982;29(1):7-17.
26. Matsushima T, Inoue T, Katsuta T, et al. An indirect revascularization method in the surgical treatment of moyamoya disease—various kinds of indirect procedures and a multiple combined indirect procedure. *Neurol Med Chir (Tokyo)*. 1998;38(suppl):297-302.
27. Yoon HK, Shin HJ, Chang YW. "Ivy sign" in childhood moyamoya disease: depiction on FLAIR and contrast-enhanced T1-weighted MR images. *Radiology*. 2002;223(2):384-389.
28. Lin YH, Kuo MF, Lu CJ, et al. Standardized MR perfusion scoring system for evaluation of sequential perfusion changes

and surgical outcome of moyamoya disease. *AJNR Am J Neuroradiol*. 2019;40(2):260-266.
29. Matsushima Y, Inaba Y. The specificity of the collaterals to the brain through the study and surgical treatment of moyamoya disease. *Stroke*. 1986;17(1):117-122.
30. Matsushima T, Inoue T, Suzuki SO, Fujii K, Fukui M, Hasuo K. Surgical treatment of moyamoya disease in pediatric patients—comparison between the results of indirect and direct revascularization procedures. *Neurosurgery*. 1992;31(3):401-405.
31. Sivrioglu AK, Saglam M, Yildiz B, Anagnostakou V, Kizilkilic O. Ivy sign in moyamoya disease. *Eurasian J Med*. 2016;48(1):58-61.
32. Lin N, Baird L, Koss M, et al. Discovery of asymptomatic moyamoya arteriopathy in pediatric syndromic populations: radiographic and clinical progression. *Neurosurg Focus*. 2011;31(6):E6.
33. Kim SJ, Son TO, Kim KH, et al. Neovascularization precedes occlusion in moyamoya disease: angiographic findings in 172 pediatric patients. *Eur Neurol*. 2014;72(5-6):299-305.
34. Cho A, Chae JH, Kim HM, et al. Electroencephalography in pediatric moyamoya disease: reappraisal of clinical value. *Childs Nerv Syst*. 2014;30(3):449-459.
35. Hamano E, Kataoka H, Morita N, et al. Clinical implications of the cortical hyperintensity belt sign in fluid-attenuated inversion recovery images after bypass surgery for moyamoya disease. *J Neurosurg*. 2017;126(1):1-7.
36. Rosi A, Riordan CP, Smith ER, Scott RM, Orbach DB. Clinical status and evolution in moyamoya: which angiographic findings correlate? *Brain Commun*. 2019;1(1):fcz029.
37. Mirone G, Cicala D, Meucci C, et al. Multiple burr-hole surgery for the treatment of moyamoya disease and quasi-moyamoya disease in children: preliminary surgical and imaging results. *World Neurosurg*. 2019;127:e843-e855.
38. Scott RM, Smith JL, Robertson RL, Madsen JR, Soriano SG, Rockoff MA. Long-term outcome in children with moyamoya syndrome after cranial revascularization by pial synangiosis. *J Neurosurg*. 2004;100(2 Suppl Pediatrics):142-149.
39. Harreld JH, Sabin ND, Rossi MG, et al. Elevated cerebral blood volume contributes to increased FLAIR signal in the cerebral sulci of propofol-sedated children. *AJNR Am J Neuroradiol*. 2014;35(8):1574-1579.

Disclosures

The authors report no conflict of interest concerning the materials or methods used in this study or the findings specified in this paper.

Author Contributions

Conception and design: Smith, Montaser, Lalgudi Srinivasan, Roth. Acquisition of data: Montaser, Lalgudi Srinivasan, Orbach, Hausman-Kedem. Analysis and interpretation of data: Smith, Montaser, Lalgudi Srinivasan, Staffa, Zurakowski, Orbach, Hausman-Kedem, Roth. Drafting the article: Smith, Montaser, Lalgudi Srinivasan, Roth. Critically revising the article: Smith, Montaser, Lalgudi Srinivasan, Slingerland, Roth. Reviewed submitted version of manuscript: Slingerland, Roth. Approved the final version of the manuscript on behalf of all authors: Smith. Statistical analysis: Staffa, Zurakowski. Administrative/technical/material support: Slingerland. Study supervision: Smith, Roth.

Correspondence

Edward R. Smith: Boston Children's Hospital, Harvard Medical School, Boston, MA. edward.smith@childrens.harvard.edu.

Novel Indirect Revascularization Technique with Preservation of Temporal Muscle Function for Moyamoya Disease Encephalo-Duro-Fascio-Arterio-Pericranial-Synangiosis: A Case Series and Technical Note

Kei Noguchi, Takachika Aoki, Kimihiko Orito, Soushou Kajiwara, Kana Fujimori, Motohiro Morioka

■ BACKGROUND: **Direct and/or indirect bypass surgery is the established approach for preventing stroke in patients with moyamoya disease. However, conventional indirect revascularization, including encephalo-myo-synangiosis, has some disadvantages associated with the mass effect of the temporal muscle under the bone flap and postsurgical depression in the temporal region. We devised a novel indirect revascularization method, using only the temporal fascia, to address the aforementioned disadvantages.**

■ METHODS: **A skin incision was performed along the superficial temporal artery. The temporal fascia was cut such that the base of the fascia flap was on the posterior side. The fascia and temporal muscles were dissected separately. After turning over the fascia, the muscle was cut such that the base of the muscle flap was on the anterior side. Craniotomy, direct bypass, and encephalo-duro-synangiosis were performed conventionally. Only the temporal fascia was used for indirect revascularization and duraplasty. The muscle was replaced in the anatomically correct position after replacing the bone flap.**

■ RESULTS: **We performed the aforementioned surgery on 18 (13 women and 5 men) consecutive patients (21 cerebral hemispheres) enrolled between 2012 and 2016. The average age was 28.7 years. The mean follow-up period was 31.6 months. In 17 patients (94%), the symptoms and cerebral blood flow improved. Digital subtraction angiography showed satisfactory angiogenesis from the temporal fascia. Depression in the temporal region and atrophy of the temporal muscle were negligible.**

■ CONCLUSIONS: **This surgical technique provides good clinical and cosmetic outcomes. It may also be one of the good surgical treatments available for symptomatic moyamoya disease.**

Moyamoya disease is characterized by idiopathic progressive arterial stenosis or occlusion of the circle of Willis and development of an abnormal fragile vascular network, frequently causing stroke in children or young adults. The symptoms are transient ischemic attacks, cerebral infarction, and hemorrhage.[1-4] To prevent future instances of stroke, direct and/or indirect bypass surgical procedures have been established for patients with moyamoya disease.[5-11] Encephalo-myo-synangiosis (EMS), using the temporal muscle, is one of the major indirect procedures. EMS was first described by Karasawa et al.,[12] and many studies have reported the effectiveness of EMS as an indirect procedure for treating moyamoya disease.[6,13] However, the conventional methods of indirect revascularization, including EMS and similar techniques, such as encephalo-duro-arterio-myo-synangiosis, have some serious disadvantages. First, these techniques lead to a mass effect of the temporal muscle under the bone flap, and some studies have reported the calcification or acute swelling of the muscle flap under the bone flap, causing focal neurologic deficits and convulsive seizure.[14-16] Second, insertion of the temporal muscle under the bone flap and wide temporal bone window to prevent the compression of the vascularized temporal muscle flap causes postsurgical depression in the temporal region.

Key words
- Combined revascularization
- Cosmetic
- Moyamoya disease
- Surgical treatment
- Technical note
- Temporal muscle

Abbreviations and Acronyms
CBF: Cerebral blood flow
DSA: Digital subtraction angiography
EMS: Encephalo-myo-synangiosis
MCA: Middle cerebral artery
MRI: Magnetic resonance imaging
mRS: Modified Rankin Scale
SPECT: Single photon emission computed tomography
STA: Superficial temporal artery

Department of Neurosurgery, Kurume University School of Medicine, Fukuoka, Japan

To whom correspondence should be addressed: Takachika Aoki, M.D., Ph.D. [E-mail: takachi@med.kurume-u.ac.jp]

Citation: World Neurosurg. (2018) 120:168-175.
https://doi.org/10.1016/j.wneu.2018.08.171

*Journal homepage: **www.WORLDNEUROSURGERY.org***

*Available online: **www.sciencedirect.com***

These are serious issues because there are many young children and female patients with moyamoya disease. To solve these problems, we devised a new surgical method of indirect revascularization that uses only the temporal fascia, and not the temporal muscle.

MATERIALS AND METHODS

Patient Population

This surgical method was used to treat 18 consecutive patients (13 women and 5 men) with moyamoya disease (21 cerebral hemispheres) who visited our institute between April 2012 and March 2016. The average age was 28.7 ± 16.7 years (range, 3–56 years). Eleven patients (61%) were treated only on the right side, and 4 patients (22%) were treated only on the left side. Both hemispheres were treated in 3 patients (17%). In one of these cases, both hemispheres were treated in a single step. Clinical presentations included transient ischemic attacks in 11 patients (61%), ischemic stroke in 3 patients (17%), hemorrhagic stroke in 2 patients (11%), and periodic headaches in 2 patients (11%). Fifteen patients (83%) had a preoperative modified Rankin Scale (mRS) score of 0–1, 2 patients (11%) had a score of 2, and 1 patient (6%) had a score of 4. Patient characteristics and clinical presentation are shown in **Table 1**. All patients were symptomatic and showed reduced cerebral blood flow (CBF) in the affected side, detected using single photon emission computed tomography (SPECT). All cases were diagnosed as moyamoya disease using well-established and generally accepted diagnostic criteria.[17,18] We obtained informed consent in all cases, and the institutional review board approved the study protocol (number 17183). In patients younger than 18 years of age, informed consent was obtained from the parent or guardian.

Table 1. Demographic Data and Clinical Presentation (N = 18)

Characteristic	Value
Mean age ± SD (range) (years)	28.7 ± 16.7 (range, 3–56)
Sex	
Female	13 (72)
Male	5 (28)
Total number of hemispheres treated	21
Unilateral treatment	15 (83)
Treatment for right side only	11 (61)
Treatment for left side only	4 (22)
Bilateral treatment	3 (17)
Clinical presentation	
Periodic headache	2 (11)
TIA	11 (61)
Ischemic stroke	3 (17)
Hemorrhagic stroke	2 (11)
Preoperative mRS score	
0–1	15 (83)
2	2 (11)
4	1 (6)

Values are numbers (%) unless indicated otherwise.
TIA, transient ischemic attack; mRS, modified Rankin Scale.

Surgical Outcome

After performing the surgery, we followed-up the patients and recorded their clinical presentations. All adverse events experienced by the patients were recorded without exception. Magnetic resonance imaging (MRI) and magnetic resonance angiography were performed within 3 days of surgery to evaluate the surgical complications and confirm the bypass patency; SPECT was performed within 3 days of surgery and a period of 6 months to 1 year after surgery to assess the improvement in CBF. The mRS scores were evaluated 1 year after surgery. To evaluate angiogenesis, we performed digital subtraction angiography (DSA) within 6–12 months of surgery. To evaluate cosmetic outcome for the patients for whom the surgery was performed on only one cerebral hemisphere and more than 2 years had passed since the surgery, we compared the thickness of the temporal muscle on the bone flap of the operative side and that of the nonoperative side at the level of the foramen of Monro in MRI axial slices.

Surgical Technique

The patient was placed in a supine position with the head rotated between 30° and 60° to the opposite side of the surgical site in a Mayfield headrest. The temporal region was kept horizontal using a shoulder pillow. A skin incision was made along the parietal branch of the superficial temporal artery (STA) and extended forward in a gently curving arc. After dissecting the parietal branch of the STA, an additional skin incision was made and extended backward from a point where it intersected the temporal line (**Figure 1A**). The frontal branch of the STA was dissected from the inner side of the skin flap in cases where it was necessary. This skin incision provided us with a wide access to the temporal fascia and frontal periosteum (**Figure 1B**), and we could use frontotemporal craniotomy to perform indirect revascularization for a wide region. The temporal fascia was cut such that the base of the vascularized fascia flap was on the posterior side, and the temporal fascia and the temporal muscle were dissected separately. After turning over the temporal fascia (**Figure 1C**), the temporal muscle was cut such that the base of the vascularized fascia flap was on the anterior side. The temporal fascia on the temporal line was sutured with the reconstructed temporal muscle after replacing the bone flap. The frontal periosteum was also cut to create a vascularized flap with its base directed toward the anterior side (**Figure 1D**). After turning over these vascularized flaps, a wide craniotomy was carefully performed so as not to damage the middle meningeal artery. The dura mater was cut open to form dural flaps, while retaining the main branch of the middle meningeal artery. A suitable cortical recipient artery (more

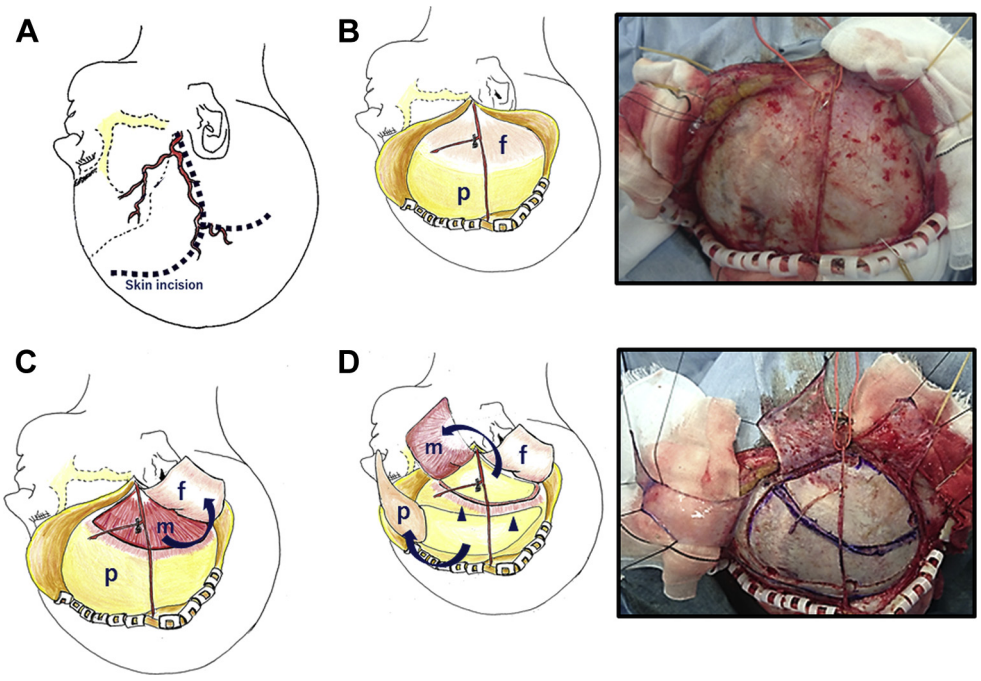

Figure 1. Intraoperative photographs and schematic drawings demonstrating the surgical procedures. The skin incision is performed along the superficial temporal artery (STA), and an additional incision is performed in the posterior direction to obtain wide access to the temporal fascia (**A** and **B**). The temporal fascia is incised in the posterior direction toward the base. The temporal fascia and temporal muscle are dissected separately, and the fascia is turned to the posterior side (**C**). The temporal muscle is incised in the anterior direction toward the base and turned to the anterior side. The periosteum is also incised in the anterior direction toward the base. The base of the vascularized flap of the temporal fascia is made at the posterior side, and those of the temporal muscle and periosteum are made at the anterior side (**D**). The temporal fascia on the temporal line is left on the bone flap to suture with the temporal muscle during closing of the cranium (*arrowheads* in **D**). A wide craniotomy and encephalo-duro-synangiosis are performed conventionally. An STA–middle cerebral artery combined bypass is performed (**E**). Only the temporal fascia and periosteum are laid on the brain surface and used for duraplasty and indirect revascularization (**F**). After placing the bone flap back in the original position (**G**), the temporal muscle is placed in the anatomically correct position and sutured with the left temporal fascia on the temporal line (**H**). f, temporal fascia; m, temporal muscle; p, periosteum.

(Continues)

than 0.5 mm) was identified, and STA-middle cerebral artery (MCA) anastomosis was performed (end-to-side anastomosis, with 10-0 nylon sutures) (Figure 1E). The bypass patency was confirmed using Doppler ultrasound and indocyanine green video angiography. The external surfaces of the dural flaps were inverted on the brain surface (encephalo-duro-synangiosis). The vascularized flaps of the temporal fascia and the frontal periosteum were laid on the frontotemporal brain surface and sutured with the dural edge. These vascularized flaps were used for indirect revascularization and duraplasty (Figure 1F). In this way, we successfully performed indirect revascularization for frontotemporal lesions in a wide region. We did not perform EMS, the vascularized flap of the temporal muscle was returned to the anatomically correct position after replacing the frontotemporal bone flap, and it was sutured with the left temporal fascia on the frontotemporal bone flap (Figures 1G and H). The temporal fascia and the temporal muscle were positioned such that upward and downward surfaces were reversed. The skin incision was closed conventionally.

RESULTS

The indirect revascularization technique was used in 18 cases (21 cerebral hemispheres). Of the 21 cerebral hemispheres, 20 (95%) were treated with STA-MCA direct bypass (single and double bypass in 12 and 8 cases, respectively). One patient (5%) could not be treated with direct revascularization because there was no suitable recipient artery. In all the patients treated with direct revascularization, we confirmed bypass patency using magnetic resonance angiography. We followed-up all the patients for a mean period of 31.6 ± 15.7 months. No deaths were reported within the mean follow-up period. Seventeen patients (94%) never experienced recurrent ischemic symptoms or stroke during the follow-up period. These patients also had improved CBF, as assessed using SPECT. One year after the surgery, the mRS score improved in 3 cases (17%), remained unchanged in 14 cases (78%), and deteriorated in 1 case (5%). Only 1 patient

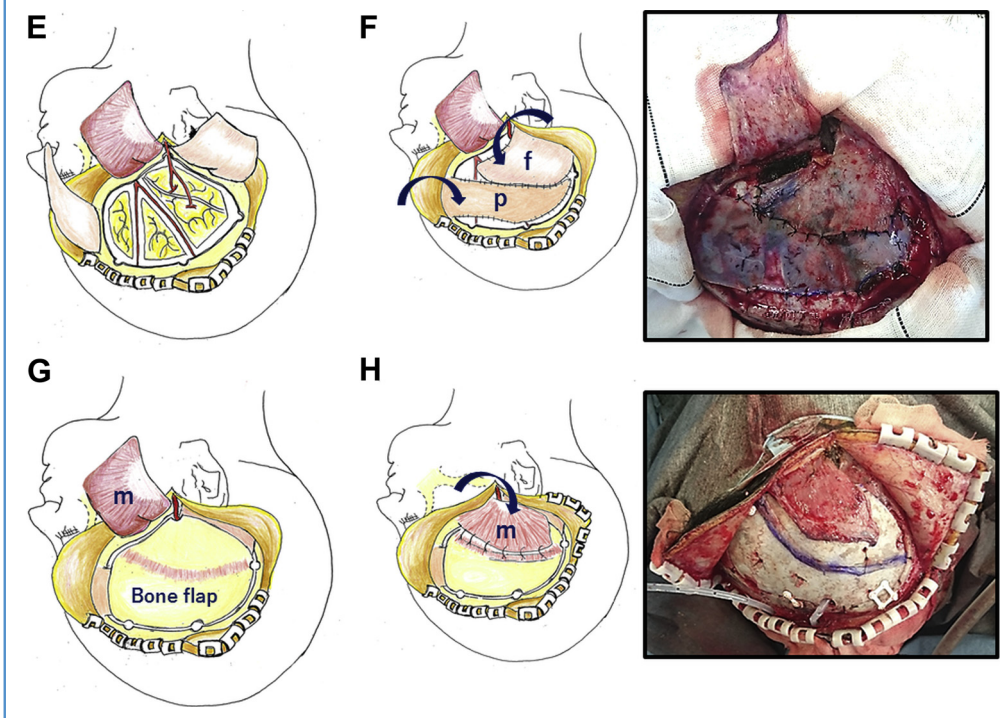

Figure 1. (Continued).

not treated with direct bypass experienced frontal cortical infarction on the operative side 6 months after surgery. In this case, no improvement was observed in CBF. One year after surgery, the mRS score for this case deteriorated from 0 to 1. This was the only case in which a deterioration in mRS score was observed. One patient exhibited small wound dehiscence 6 months after surgery and needed reoperation for wound closure. The summary of each case and surgical outcomes are shown in **Table 2**.

Using DSA, we observed abundant angiogenesis from the dura mater, temporal fascia, and periosteum in 17 cases (94%). Only 1 case had a poor angiogenesis. This was the same case as that which exhibited a frontal cortical infarction on the operative side 6 months after surgery. No angiogenesis from the indirect bypass vascularized donors (dura mater, periosteum, etc.) was observed 6 months after surgery, but a remarkable angiogenesis occurred over 6 months after surgery in this case.

This indirect revascularization technique also had excellent cosmetic outcomes. The surgery was performed on only 1 cerebral hemisphere in 9 cases. In these cases, more than 2 years had passed since the surgery. The operative side, which contained the temporal lesion, did not exhibit a depression, and the shape of the head remained symmetric in all cases. The mean temporal muscle thickness on the bone flap on the operative side was 5.6 $\pm$ 1.5 mm, and the mean temporal muscle thickness on the nonoperative side was 6.4 $\pm$ 1.6 mm at the level of the foramen of Monro in MRI axial slices. There was no statistically significant difference between the 2 groups ($P = 0.4$, Student t test) (**Figure 2** and **Table 3**).

DISCUSSION

In this study, we report a novel indirect revascularization technique for the treatment of moyamoya disease. This technique provides good outcome, both clinically and cosmetically, with excellent angiogenesis.

Various indirect procedures and their effectiveness in treating moyamoya disease have been reported in the literature. These techniques include EMS, omental transplantation, encephalo-duro-arterio-synangiosis, encephalo-galeo-synangiosis, encephalo-duro-arterio-myo-synangiosis, and encephalo-duro-myo-arterio-pericranial-synangiosis.[8,10,19-24] These surgical techniques are essentially based on similar theories stating that vascularized tissues placed on the brain surface may trigger angiogenesis. Although the temporal muscle has recently been used as a source of angiogenesis, there is no report showing obvious angiogenesis from the muscle itself. Further, the vascularized temporal muscle flap within the skull substantially increases the risk of brain compression, which occasionally induces cerebral ischemia or brain shift. In fact, some studies have reported complications in which the temporal muscle flap gets swollen during the acute stage after surgery, and calcified and hypertrophied in the chronic stage after surgery, and these can cause focal neurologic deficits and convulsive seizure.[14-16] One of the reasons for this complication is considered to be the compression of the vascularized temporal muscle at the site of insertion into the skull. Therefore, it is necessary to construct a wider bone window at the site of temporal muscle insertion to avoid these complications.[14] A study has reported that shaving the bone flaps to half of their original thickness is a good way to remove this compression.[25] However,

Table 2. Summary of Cases and Surgical Outcomes

Case Number	Age (Years), Sex	Clinical Form	Pre-mRS Score	Side	Direct Bypass	CBF	Angiogenesis	Follow-Up Period (Months)	Postoperative Course	Post-mRS Score
1	24, F	TIA	0	Rt.	STA-MCA single bypass	Improved	+	60	Uneventful	0
2	34, F	Cerebral infarction	2	Rt.	STA-MCA single bypass	Improved	+	59	Uneventful	1
3	48, M	TIA	0	Rt.	STA-MCA double bypass	Improved	+	52	Uneventful	0
4	39, M	TIA	0	Rt.	STA-MCA double bypass	Improved	+	48	Uneventful	0
5	50, F	Cerebral Infarction	2	Lt.	STA-MCA single bypass	Improved	+	47	Uneventful	1
6	5, M	TIA	0	Rt.	STA-MCA single bypass	Improved	+	47	Uneventful	0
7	12, F	Periodic headache	0	Rt.	STA-MCA single bypass	Improved	+	43	Uneventful	0
8	42, F	Cerebral hemorrhage	4	Rt.	STA-MCA double bypass	Improved	+	33	Uneventful	3
9	5, F	TIA	0	Lt.	None	Unchanged	Poor	33	Cerebral infarction	1
				Rt.	STA-MCA double bypass	Improved	Poor	29	In Lt. frontal lobe 6 months after surgery	
10	21, F	TIA	0	Rt.	STA-MCA double bypass	Improved	+	28	Uneventful	0
11	56, F	TIA	0	Lt.	STA-MCA double bypass	Improved	+	23	Small wound dehiscence 6 months after surgery	0
12	7, F	TIA	0	Lt.	STA-MCA single bypass	Improved	+	22	Uneventful	0
				Rt.	STA-MCA single bypass	Improved	+	18		
13	31, F	Periodic headache	0	Rt.	STA-MCA single bypass	Improved	+	18	Uneventful	0
14	3, F	TIA	0	Rt.	STA-MCA single bypass	Improved	+	17	Uneventful	0
15	21, M	TIA	0	Lt.	STA-MCA double bypass	Improved	+	16	Uneventful	0
16	35, F	TIA	0	Bilateral	STA-MCA single bypass	Improved	+	14	Uneventful	0
17	36, M	Cerebral hemorrhage	1	Lt.	STA-MCA double bypass	Improved	+	14	Uneventful	1
18	48, F	Cerebral infarction	1	Rt.	STA-MCA single bypass	Improved	+	11	Uneventful	1

mRS, modified Rankin Scale; CBF, cerebral blood flow; F, female; Rt., right; STA, superficial temporal artery; MCA, middle cerebral artery; +, abundant angiogenesis from dura mater, temporal fascia, and periosteum; M, male; TIA, transient ischemic attack; Lt., left; Poor, no observable angiogenesis from dura mater, temporal fascia, or periosteum.

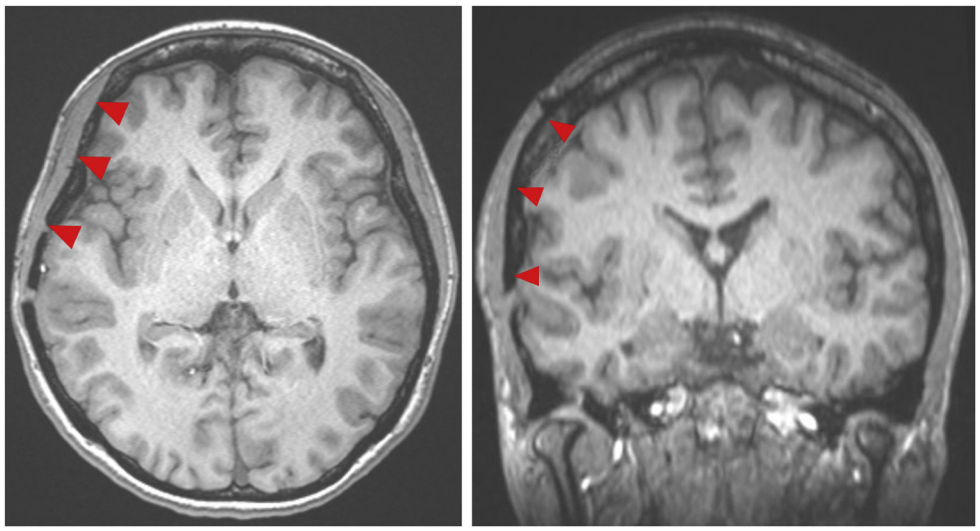

Figure 2. Magnetic resonance imaging (MRI) performed 3 years after surgery on a 24-year-old woman (left: MRI T1-weighted axial image, right: MRI T1-weighted coronal image). This case is the same case described in Figure 3 (case 1 in Table 2). The temporal muscle is retained in the anatomically correct position outside the skull (*arrowheads*). A depression in the temporal region and atrophy of the temporal muscle are barely visible, and the head shape is almost symmetric.

this method may make the bone flap fragile. With respect to cosmetic outcomes, the insertion of the temporal muscle under the bone flap and wide temporal bone window can cause varying degrees of postsurgical depression in the temporal region. There is also a risk of compromising the symmetry of the head. This is a serious issue because half of the patients with moyamoya disease are young girls. Our surgical technique, on the other hand, has no risk of such cosmetic complications because the temporal muscle is retained in the anatomically correct position outside the skull (Figure 2).

The vascularized temporal muscle flap is usually perfused by the middle and deep temporal artery branches arising from the maxillary artery.[26] On the other hand, the vascularized temporal fascia flap is perfused by the fascial branch of the middle temporal artery and the anterior auricular branches of the STA.[26,27] The highly vascular inner side of the temporal fascia was visible intraoperatively, and it is conceivable that these vessels contributed to the angiogenesis from the temporal fascia. The anterior auricular branch of the STA is usually inconspicuous. However, after using the temporal fascia as a vascularized flap, this vessel was clearly visible and was detectable using DSA (Figure 3). We confirmed angiogenesis in this case by angiography of the external carotid artery and its branches. The angiogenesis from the temporal fascia could be detected appreciably using the conventional approach of EMS.

We performed the surgeries using the indirect revascularization technique, with STA-MCA direct bypass to improve the symptoms of cerebral ischemia as quickly as possible after treatment.[28,29] This combined revascularization is known to yield better results than a single direct or indirect bypass operation.[1,30] Indirect revascularizations may take several months to develop neovascularity,[12,31] and angiogenesis from indirect revascularization is occasionally insufficient for adult patients.[23,32,33]

We performed wide frontotemporal craniotomy for indirect revascularization of the frontal lobe with a vascularized periosteum flap. Many studies have reported the importance of indirect revascularization of the frontal lobe.[34-37] Kuroda et al.[23] reported the encephalo-duro-myo-arterio-pericranial-synangiosis technique. They also reported the importance of improving the

Table 3. Comparison of Mean Temporal Muscle Thickness of the Operative Versus Nonoperative Side 2 Years After Surgery

	Operative Side	Nonoperative Side
Case Number*	Temporal Muscle Thickness (mm)	Temporal Muscle Thickness (mm)
1	4.1	5.8
2	4.7	6.1
3	9.3	10.5
4	6.3	6.9
5	4.6	5.0
6	4.5	5.3
7	5.9	6.5
8	4.7	4.7
10	6.5	7.0
Mean ± SD	5.6 ± 1.5	6.4 ± 1.6
P value†		0.4

*The case numbers are the same as those in Table 2.
†Student *t* test.

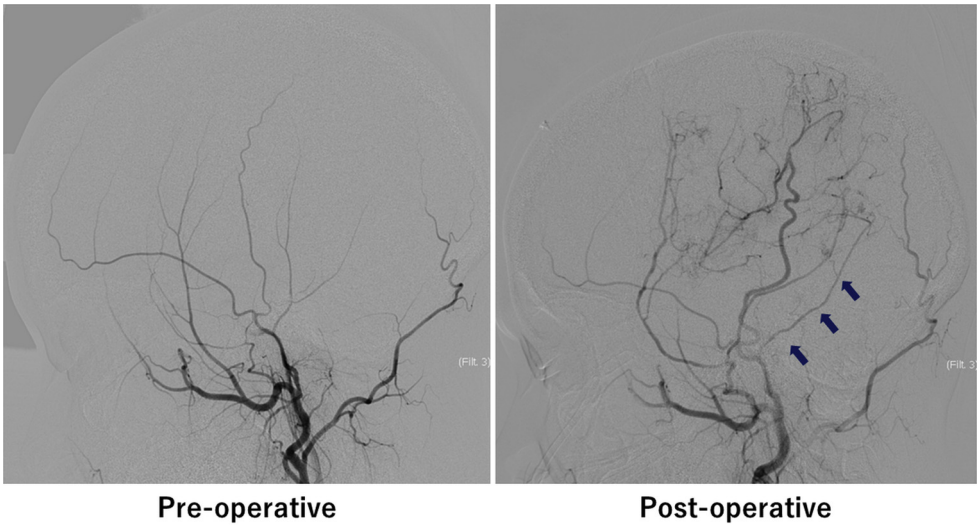

Figure 3. Pre- and postoperative digital subtraction angiography (DSA) of a 24-year-old woman (left: preoperation, right: postoperation). This case is the same case described in **Figure 2** (case 1 in **Table 2**). The vascularized temporal fascia flap is perfused by the anterior auricular branches of the superficial temporal artery (*arrows*). This vessel is usually inconspicuous. However, after using temporal fascia as a vascularized flap, this vessel is clearly visible and detectable using DSA. Angiogenesis from this vessel was sufficient.

disturbed cerebral hemodynamics in the frontal lobe using encephalo-duro-pericranial-synangiosis. Our technique is similar to the one reported by Kuroda et al. with respect to the indirect bypass performed to increase CBF in the frontal lobe. We obtained good outcomes in the patients in this study. Meanwhile, the improvement in mRS scores might be because of the direct bypass. However, postoperative DSA revealed an excellent angiogenesis, except for 1 case. Therefore, our surgical procedure is considered similar to EMS in terms of angiogenetic effect.

In this study, only 1 patient had a frontal cortical infarction on the operative side 6 months after surgery. This particular case did not involve STA-MCA direct bypass because we were unable to find a suitable MCA recipient. This case demonstrated no angiogenesis not only from the temporal fascia but also from other vascularized donor tissues, including the dura mater and periosteum. Therefore, we considered that the lack of angiogenesis after indirect bypass in this case was not because of our technical procedures. In our experience, this is the first case of a child not exhibiting angiogenesis after indirect bypass, and the underlying reason was unclear.

We observed small wound dehiscence 6 months after surgery in 1 case, and reoperation was needed for wound closure. The patient was a heavy smoker and had diabetes mellitus; these factors contributed greatly to the risk of wound complications.[38,39] Further, the titanium bone plate embedded just under the wound at the intersection point could also be considered as one of the causes. The galeal blood supply is important to prevent wound-related complications,[38] especially for extracranial-intracranial bypass surgery. There was no other case of wound complication because we took care not to embed the titanium bone plate just under the wound at the intersection point.

CONCLUSIONS

We report a novel combined revascularization technique with selective insertion of the temporal fascia preserving the temporal muscle functions. This technique has the same angiogenetic effect as the usual indirect bypass and provides good short- and midterm cosmetic outcomes. We consider this surgical technique to be one of the good surgical treatments currently available for symptomatic moyamoya disease. Nevertheless, this study had an insufficient number of patients and too short a follow-up period to confirm the clinical outcome. The long-term clinical outcomes of this study should therefore be further investigated.

REFERENCES

1. Kawaguchi T, Fujita S, Hosoda K, Shose Y, Hamano S, Iwakura M, et al. Multiple burr-hole operation for adult moyamoya disease. *J Neurosurg*. 1996;84:468-476.

2. Houkin K, Kamiyama H, Abe H, Takahashi A, Kuroda S. Surgical therapy for adult moyamoya disease. Can surgical revascularization prevent the recurrence of intracerebral hemorrhage? *Stroke*. 1996;27:1342-1346.

3. Kronenburg A, Esposito G, Fierstra J, Braun KP, Regli L. Combined bypass technique for contemporary revascularization of unilateral MCA and bilateral frontal territories in moyamoya vasculopathy. *Acta Neurochir*. 2014;suppl 119:65-70.

4. Ohtaki M, Uede T, Morimoto S, Nonaka T, Tanabe S, Hashi K. Intellectual functions and regional cerebral haemodynamics after extensive omental transplantation spread over both frontal lobes in childhood moyamoya disease. *Acta Neurochir (Wien)*. 1998;140:1043-1053.

5. Kuroda S, Houkin K. Moyamoya disease: current concepts and future perspectives. *Lancet Neurol*. 2008;7:1056-1066.

6. Kinugasa K, Mandai S, Kamata I, Sugiu K, Ohmoto T. Surgical treatment of moyamoya disease: operative technique for encephalo-duro-arterio-myo-synangiosis, its follow-up, clinical results, and angiograms. *Neurosurgery*. 1993;32:527-531.

7. Patel NN, Mangano FT, Klimo P Jr. Indirect revascularization techniques for treating moyamoya disease. *Neurosurg Clin N Am*. 2010;21:553-563.

8. Touho H. Cerebral ischemia due to compression of the brain by ossified and hypertrophied muscle used for encephalomyosynangiosis in childhood moyamoya disease. *Surg Neurol*. 2009;72:725-727.

9. Endo M, Kawano N, Miyaska Y, Yada K. Cranial burr hole for revascularization in moyamoya disease. *J Neurosurg*. 1989;71:180-185.

10. Ishii R. [Surgical treatment of moyamoya disease]. *No Shinkei Geka*. 1986;14:1059-1068 [in Japanese].

11. Elazab EE, Abdel-Hameed FA. The arterial supply of the temporalis muscle. *Surg Radiol Anat*. 2006;28:241-247.

12. Karasawa J, Kikuchi H, Furuse S, Sakaki T, Yoshida Y. [A surgical treatment of Moyamoya disease: encephalo-myo-synangiosis]. *Neurol Med Chir*. 1977;17:29-37 [in Japanese].

13. Ishikawa T, Houkin K, Kamiyama H, Abe H. Effects of surgical revascularization on outcome of patients with pediatric moyamoya disease. *Stroke*. 1997;28:1170-1173.

14. Suzuki J, Takaku A. Cerebrovascular "moyamoya" disease. Disease showing abnormal net-like vessels in base of brain. *Arch Neurol*. 1969;20:288-299.

15. Houkin K, Kuroda S, Ishikawa T, Abe H. Neovascularization (angiogenesis) after revascularization in moyamoya disease. Which technique is most useful for moyamoya disease? *Acta Neurochir (Wien)*. 2000;142:269-276.

16. Macyszyn L, Attiah M, Ma TS, Ali Z, Faught R, Hossain A, et al. Direct versus indirect revascularization procedures for moyamoya disease: a comparative effectiveness study. *J Neurosurg*. 2017;126:1523-1529.

17. Cho WS, Kim JE, Kim CH, Ban SP, Kang HS, Son YJ, et al. Long-term outcomes after combined revascularization surgery in adult moyamoya disease. *Stroke*. 2014;45:3025-3031.

18. Mizoi K, Kayama T, Yoshimoto T, Nagamine Y. Indirect revascularization for moyamoya disease: is there a beneficial effect for adult patients? *Surg Neurol*. 1996;45:541-549.

19. Suzuki J, Kodama N. Moyamoya disease–a review. *Stroke*. 1983;14:104-109.

20. Fujimura M, Kaneta T, Shimizu H, Tominaga T. Cerebral ischemia owing to compression of the brain by swollen temporal muscle used for encephalo-myo-synangiosis in moyamoya disease. *Neurosurg Rev*. 2009;32:245-249.

21. Fukui M. Guidelines for the diagnosis and treatment of spontaneous occlusion of the circle of Willis ('moyamoya' disease). Research Committee on Spontaneous Occlusion of the Circle of Willis (Moyamoya Disease) of the Ministry of Health and Welfare, Japan. *Clin Neurol Neurosurg*. 1997;99(suppl 2):S238-S240.

22. Smith ER, Scott RM. Spontaneous occlusion of the circle of Willis in children: pediatric moyamoya summary with proposed evidence-based practice guidelines. A review. *J Neurosurg Pediatr*. 2012;9:353-360.

23. Kuroda S, Houkin K, Ishikawa T, Nakayama N, Iwasaki Y. Novel bypass surgery for moyamoya disease using pericranial flap: its impacts on cerebral hemodynamics and long-term outcome. *Neurosurgery*. 2010;66:1093-1101.

24. Takemura S, Sato S, Kuroki A, Saito S, Kayama T. [New ideas for indirect revascularization surgery for moyamoya disease]. *No Shinkei Geka*. 1999;27:987-992 [in Japanese].

25. Goltsman D, Munabi NC, Ascherman JA. The association between smoking and plastic surgery outcomes in 40,465 patients: an analysis of the ACS-NSQIP datasets. *Plast Reconstr Surg*. 2017;139:503-511.

26. Scott RM, Smith ER. Moyamoya disease and moyamoya syndrome. *N Engl J Med*. 2009;360:1226-1237.

27. Takanari K, Araki Y, Okamoto S, Sato H, Yagi S, Toriyama K, et al. Operative wound-related complications after cranial revascularization surgeries. *J Neurosurg*. 2015;123:1145-1150.

28. Nakagawa Y, Shimoyama M, Kashiwaba T, Suzuki Y, Gotoh S, Miyasaka K, et al. [Reconstructive operation of moyamoya disease and its problems]. *No Shinkei Geka*. 1981;9:305-314 [in Japanese].

29. Houkin K, Nakayama N, Kuroda S, Ishikawa T, Nonaka T. How does angiogenesis develop in pediatric moyamoya disease after surgery? A prospective study with MR angiography. *Childs Nerv Syst*. 2004;20:734-741.

30. Miyamoto S, Yoshimoto T, Hashimoto N, Okada Y, Tsuji I, Tominaga T, et al. Effects of extracranial-intracranial bypass for patients with hemorrhagic moyamoya disease: results of the Japan Adult Moyamoya Trial. *Stroke*. 2014;45:1415-1421.

31. Kim DS, Huh PW, Kim HS, Kim IS, Choi S, Mok JH, et al. [Surgical treatment of moyamoya disease in adults: combined direct and indirect vs. indirect bypass surgery]. *Neurol Med Chir (Tokyo)*. 2012;52:333-338 [in Japanese].

32. Karasawa J, Kikuchi H, Furuse S, Kawamura J, Sakaki T. Treatment of moyamoya disease with STA-MCA anastomosis. *J Neurosurg*. 1978;49:679-688.

33. Takao Y, Kazunari O. [Blood flow measurement and clinical usefulness of the temporal fascial scar tissue flap and the periosteal scar tissue flap in posterior canal wall reconstructed tympanoplasty for the mastoid cavity problem in the postoperative ear]. *Nippon Jibiinkoka Gakkai Kaiho*. 2014;117:788-793 [in Japanese].

34. Karasawa J, Kikuchi H, Kawamura J, Sakai T. Intracranial transplantation of the omentum for cerebrovascular moyamoya disease: a two-year follow-up study. *Surg Neurol*. 1980;14:444-449.

35. Sakamoto T, Kawaguchi M, Kurehara K, Kitaguchi K, Furuya H, Karasawa J. Risk factors for neurologic deterioration after revascularization surgery in patients with moyamoya disease. *Anesth Analg*. 1997;85:1060-1065.

36. Choi IJ, Cho SJ, Chang JC, Park SQ, Park HK. Angiographic results of indirect and combined bypass surgery for adult moyamoya disease. *J Cerebrovasc Endovasc Neurosurg*. 2012;14:216-222.

37. Park JH, Yang SY, Chung YN, Kim JE, Kim SK, Han DH, et al. Modified encephaloduroarteriosynangiosis with bifrontal encephalogaleoperiosteal synangiosis for the treatment of pediatric moyamoya disease. Technical note. *J Neurosurg*. 2007;106:237-342.

38. Imai H, Miyawaki S, Ono H, Nakatomi H, Yoshimoto Y, Saito N. The importance of encephalo-myo-synangiosis in surgical revascularization strategies for moyamoya disease in children and adults. *World Neurosurg*. 2015;83:691-699.

39. Matsushima Y, Fukai N, Tanaka K, Tsuruoka S, Inaba Y, Aoyagi M, et al. A new surgical treatment of moyamoya disease in children: a preliminary report. *Surg Neurol*. 1981;15:313-320.

Conflict of interest statement: This work was supported by Grants-in-Aid for Scientific Research from the Ministry of Education, Sports, Science, and Culture of Japan (MEXT/JSPS KAKENHI grant numbers JP 15K10322 and 16K15143).

Received 28 June 2018; accepted 22 August 2018

Citation: World Neurosurg. (2018) 120:168-175.
https://doi.org/10.1016/j.wneu.2018.08.171

Journal homepage: ***www.WORLDNEUROSURGERY.org***

Available online: ***www.sciencedirect.com***

Special Considerations for Cross-Sectional Imaging in the Child with Neurovascular Disease

Vivek Pai, MD[a,b], Pradeep Krishnan, MD[a,b], Manohar Shroff, MD, FRCPC, DABR[a,b,*]

KEYWORDS

• Pediatric stroke • Arteriovenous Malformation • Cerebral venous sinus thrombosis

KEY POINTS

- An individualized evaluation for the need and type of sedation or general anesthesia is the critical first step in acquisition of diagnostic-quality imaging.
- MR imaging is the preferred choice of evaluation of children with suspected stroke; however, despite its poor sensitivity, CT plays a major role if MR imaging is unavailable or contraindicated.
- Utilization of the full potential of MR imaging is necessary when evaluating intracranial arteriovenous shunts, such that angioarchitecture and high-risk features are delineated before endovascular treatment.
- Anatomic variants of the major intracranial arteries are common and seldom of clinical significance, although in certain conditions detection of these is imperative to make an informed decision before conventional angiography and neurointervention.
- Imaging of sinovenous thrombosis is riddled with pitfalls, which need to be systematically excluded when interpreting cross-sectional studies.

INTRODUCTION

Broadly, pediatric neurovascular diseases can be divided into vaso-occlusive lesions, hemorrhagic lesions, drivers of hydrovenous dysfunction, and drivers of neonatal cardiopulmonary failure.[1] Compared with adults, pediatric neurovascular diseases are uncommon with an annual incidence of 2.5 to 3.1 per 100,000 population in children aged less than 15 years.[1] These disorders have varied presentations often limiting accurate clinical evaluation.[2] This limitation is further confounded by the age of these patients, with some lesions presenting as early as the neonatal period. Cross-sectional neuroimaging plays a central role in the noninvasive evaluation of patients with suspected and previously known neurovascular lesions. This review provides an overview of pediatric neurovascular diseases and currently available, commonly used diagnostic imaging techniques.

Sedation: A Radiological Perspective

A major consideration before neuroimaging is assessment of the need for and type of sedation (drug-induced central nervous system depression) or general anesthesia (drug-induced loss of

[a] Division of Neuroradiology, Department of Diagnostic and Interventional Radiology, The Hospital for Sick Children, 170 Elizabeth Street, Toronto, Ontario M5G 1E8, Canada; [b] Department of Medical Imaging, University of Toronto, 263 McCaul Street, 4th Floor, Toronto, Ontario M5T 1W7, Canada
* Corresponding author. Division of Neuroradiology, Department of Diagnostic and Interventional Radiology, The Hospital for Sick Children, 170 Elizabeth Street, Toronto, Ontario M5G 1E8, Canada.
E-mail address: manohar.shroff@sickkids.ca

Neuroimag Clin N Am 34 (2024) 491–515
https://doi.org/10.1016/j.nic.2024.08.021

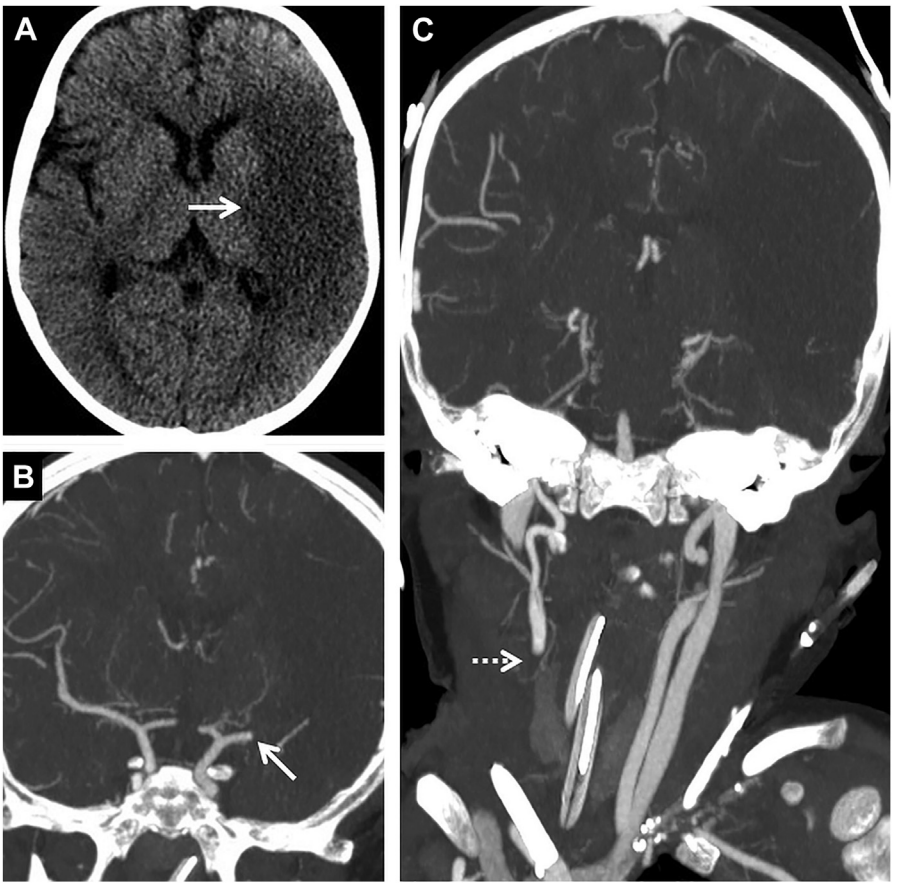

Fig. 1. Pediatric arterial ischemic stroke. CT imaging in a 1-year-old referred due to concerns of acute stroke following extracorporeal cardiopulmonary resuscitation. Axial CT image (*A*) reveals a large, wedge-shaped area of hypoattenuation (*arrow*), with loss of gray-white matter differentiation, involving the left middle cerebral artery (MCA) territory distribution, in keeping with an infarction. Coronal maximum intensity pixel projection (MIP) reconstruction of a CT angiography (CTA) (*B*) confirms the abrupt loss of contrast opacification along the left M1-MCA segment (*arrow*) in keeping with thrombo-occlusion. (*C*) Coronal MIP reconstruction of the CTA (including the neck vessels) demonstrates absent opacification of the proximal right common carotid artery (*dotted arrow*) secondary to ligation (commonly performed after extracorporeal membrane oxygenation).

consciousness, resulting in an unarousable state, even following noxious stimuli).[3,4] Achieving immobility during imaging is crucial because motion artifacts limit evaluation or obscure the pathologic condition. A nondiagnostic study may trigger patient and/or family anxiety as well as warrant repeat imaging, with consequent financial implications, loss of man-hours, and logistical issues.[5]

Decision for sedation or general anesthesia (S/GA) is made on a case-by-case basis, with age being the primary determinant. Generally, patients aged between 6 months and 6 years require some form of S/GA, depending on the imaging test.[5] The upper age limit may vary across institutions, some considering 5 years as the cutoff,[6] and also on the level of cooperation, comorbidities present, and neurologic status of the child. Infants younger than 6 months may be imaged using a "feed-and-sleep" technique, although anesthesia may be indicated in clinically unstable patients.[6]

The need for S/GA is reduced in older children, but concomitant comorbidities (behavioral issues, involuntary movements) often necessitate S/GA.[5] In anxious patients, without comorbidities, nonpharmacologic methods may be useful (eg, familiarization with mock computed tomography [CT]/magnetic resonance [MR] imaging drills, allowing a family member into the imaging suite, application of soft restraints, and use of MR-compatible audiovisual projection goggles).[5,7] Desensitization with mock MR imaging drills is shown to reduce the need for GA by 16.8% in children

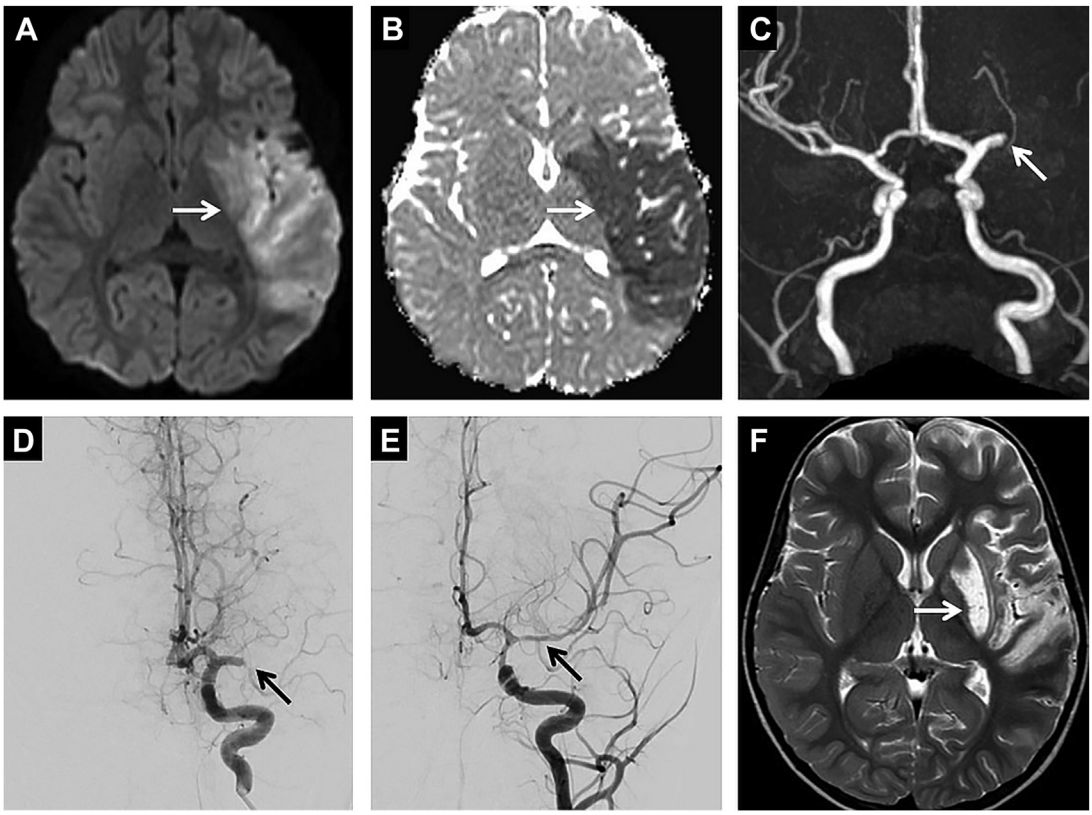

Fig. 2. Pediatric arterial ischemic stroke. MR imaging in a 3-year-old patient, with a complex cardiac anomaly, presenting with acute right-sided hemiplegia. Axial DWI (*A*) and apparent diffusion coefficient map (*B*) reveal a wedge-shaped area of restricted diffusion (*arrows* in *A, B*) involving the left MCA territory. MIP reconstruction of the TOF-MRA (circle of Willis) (*C*) confirms abrupt loss of flow signal in the left M1-MCA segment (*arrow*), in keeping with a thrombo-occlusion. TOF-MRA of the neck was also performed but did not demonstrate a tandem occlusion (not shown). anteroposterior (AP) projection of the left internal carotid artery (ICA) run before mechanical thrombectomy (*D*) confirms the left M1-MCA thrombo-occlusion (*arrow*). AP projection of the left ICA run following mechanical thrombectomy (*E*) demonstrates recanalization of the left MCA (*arrow*), with vasospasm that was treated with intra-arterial calcium channel blockers. Axial T2-weighted (T2W) image (*F*) obtained after 6 weeks reveals an area of encephalomalacia in the left MCA territory (*arrow*) in keeping with interval evolution of the presenting infarction.

aged between 3 and 8 years.[7] Psychological support provided by Child Life Specialists can also reduce the need for S/GA.[5,8]

The type of imaging is also another determinant when deciding if S/GA is warranted. With the advent of multidetector CT technology, multivolume data collection for each complete gantry rotation is now possible with a resultant increase in table speeds and rate of data acquisition, the latter being 3-to 5-fold faster than the previous generations of CT scanners, thus reducing the need for S/GA.[9–11] On the other hand, MR imaging, which is more time and motion sensitive, may warrant imaging under GA, to reduce callback rates. Sammons and colleagues[12] reported a success rate of 100% among patients undergoing neuroimaging under GA (n = 111 children; 56% with neurodevelopmental disabilities).

Ensuring that fasting guidelines are met is of prime importance to eliminate aspiration of gastric contents and associated complications during GA. The reported incidence of aspiration among patients undergoing elective procedural sedation ranges between ~1 in 825 and ~1 in 30,037 cases, whereas single-institution data have shown that those undergoing emergency procedures under GA have an incidence of ~1 in 373 cases versus ~1 in 4544 for those undergoing elective GA.[4,13] The American Society of Anesthesiologists recommends a fasting period of 2 hours for clear fluids, 4 hours for human milk, 6 hours for nonhuman/formula milk, and 6 hours for a light meal.[4]

Under GA, patients undergo cardiorespiratory depression, therefore needing airway support and close monitoring.[5] Strict compliance with MR imaging safety protocols of all appliances

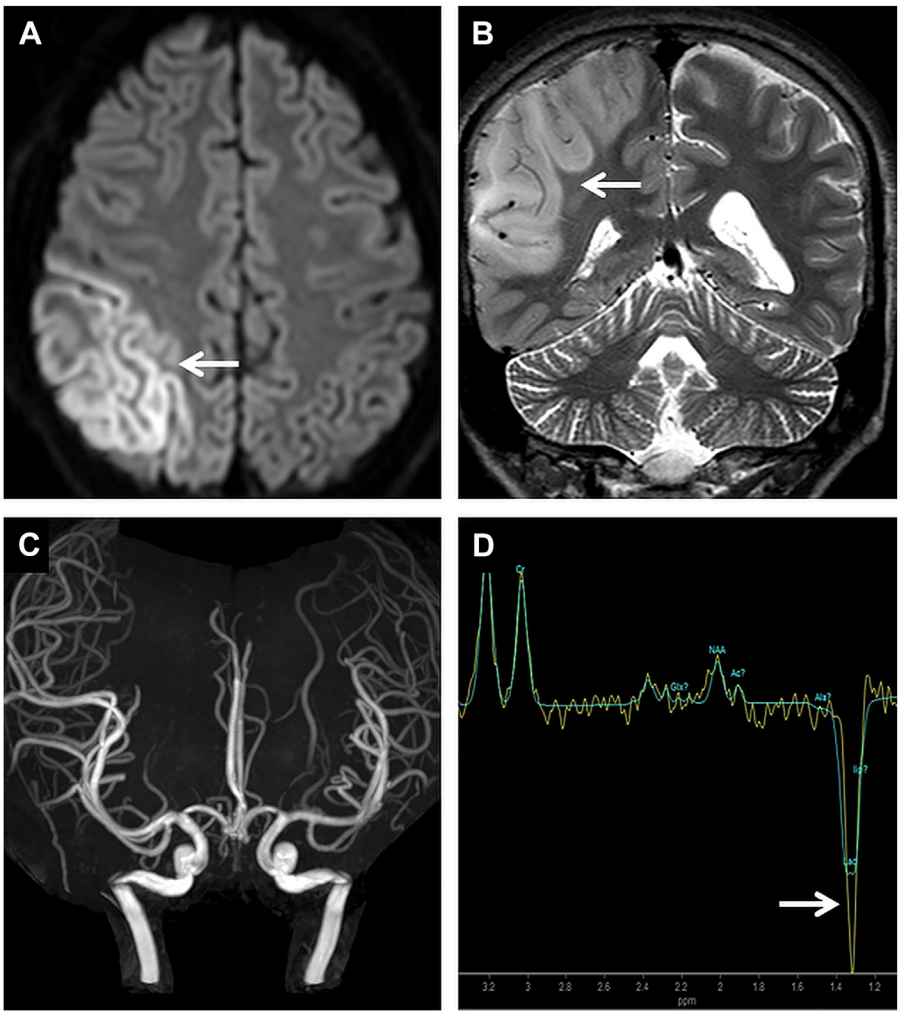

Fig. 3. Mitochondrial encephalomyopathy with lactic acidosis and strokelike episodes, an imaging and clinical mimic of stroke, diagnosed in a 9-year-old presenting with new onset of left-sided weakness. Axial DWI (*A*) reveals an area of restricted diffusion predominantly involving the right parietal lobe (*arrow*). Coronal T2W image (*B*) demonstrates corresponding gyriform T2-hyperintense swelling of the right parietal lobe (*arrow*), within the corresponding anterior circulation. Maximum intensity projection (MIP) of the TOF-MRA (C) reveals no large vessel occlusion or flow limiting stenosis along the anterior circulation. Single-voxel MR spectroscopy (TE 144; *D*) obtained from the affected right parietal lobe reveals a large lactate peak at 1.3 ppm (*arrow*).

used for monitoring patients under GA is critical, because the powerful pull of the magnetic field of the MR imaging machine can transform ferrous-containing appliances into a projectile object causing severe injury to the patient and personnel as well as hardware damage.[3]

Pediatric Arterial Ischemic Stroke Imaging: Computed Tomography versus Magnetic Resonance Imaging Considerations

Stroke accounts for 10% to 25% of all children presenting to the emergency department.[14] Pediatric stroke is differentiated into the broad categories of perinatal stroke (occurring between 20 weeks of intrauterine life and the 28th day of postnatal life) and childhood stroke (occurring beyond 29 days of life until 18 years of age).[14] In this section, only childhood stroke is discussed because perinatal stroke is best imaged only on MR imaging and hyperacute stroke therapies are not warranted in this age group.[15] The article by Flieva and colleagues in this issue provides a comprehensive overview of arterial ischemic stroke in children.

In pediatric stroke, CT as the initial line of imaging investigation is often reserved due to concerns of

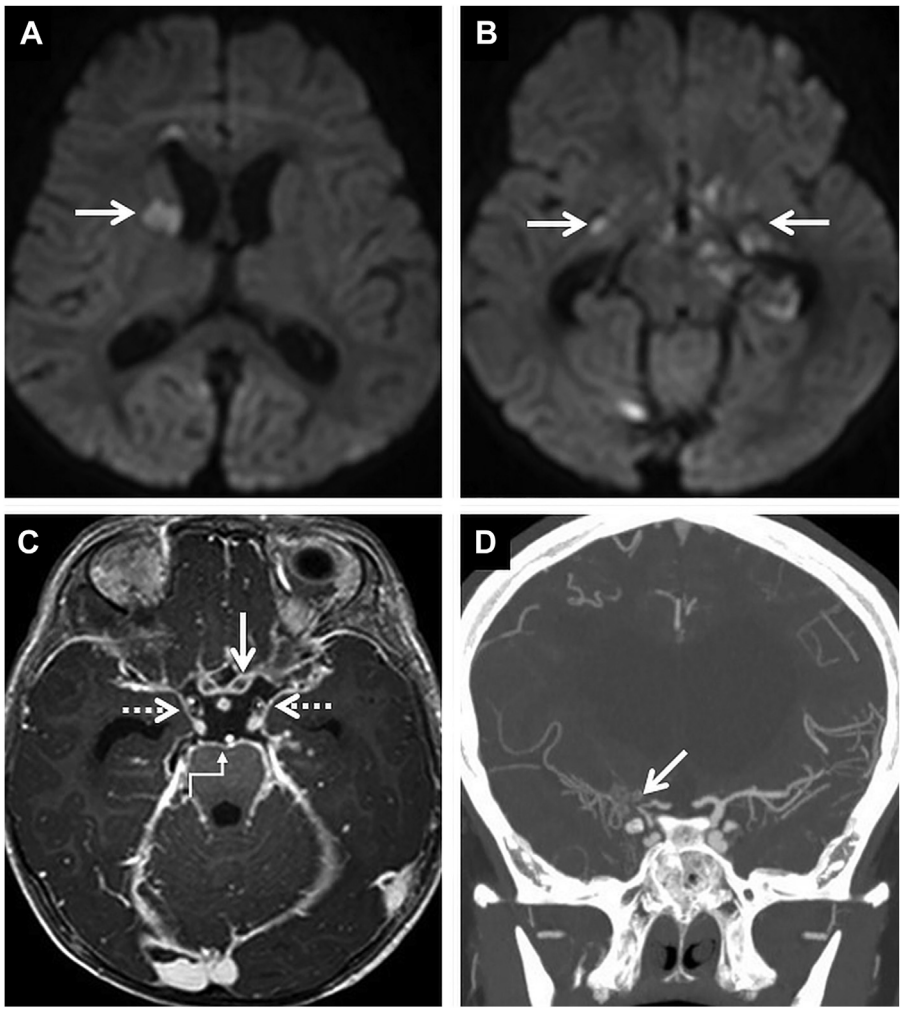

Fig. 4. Tuberculous vasculitis in an 8-year-old patient presenting with fever, seizures, and fluctuating levels of consciousness. Axial DWI (*A*, *B*) reveals multiple acute infarcts, predominantly in the perforator territories (*arrows* in *A, B*). Contrast-enhanced axial 3D T1 image (*C*) demonstrates extensive, thick, leptomeningeal enhancement/basal exudates coating the optic chiasm (*arrow*), mesial temporal lobes (*dotted arrows*), and the pial surface of the pons (*stepped arrow*). Follow-up CTA (*D*) reveals steno-occlusion of the right ICA with multiple lenticulostriate collaterals (*arrow*). Hydrocephalus was also noted on follow-up CT (not shown).

ionizing radiation.[14] CT has limited sensitivity and high false-negative rates in the detection of arterial ischemic stroke and may not detect as much as 47% of acute arterial ischemic strokes.[16–18] Despite these limitations, CT cannot be excluded from the armamentarium of pediatric stroke imaging. CT may be used in centers without MR imaging capabilities, if MR imaging is unavailable, if S/GA would substantially delay MR imaging, or if contraindications to MR imaging are identified (eg, cardiac devices)[14,16] (**Fig. 1**). In addition, CT is reasonable when the pretest probability of a large vessel occlusion is high (eg, following cardiac catheterization procedures or known cardiomyopathies) for thrombectomy candidature. Owing to quick image acquisition, CT is often used to monitor expansion, evolution, and hemorrhagic transformation of infarction.[14] Hence, efforts must be made to ensure achieving doses as low as reasonably achievable, without compromise of diagnostic output. Techniques such as reduced rotation time, lowered kilovoltage and tube current, reducing unnecessary z-axis coverage, and dose modulation allow reduction in radiation dose without compromising image resolution.[14]

Craniocervical CT angiography (CTA) poses challenges with respect to accurate timing of contrast injection through a rather narrow intravenous line in children and dynamic changes in circulatory physiology related to age. In a study

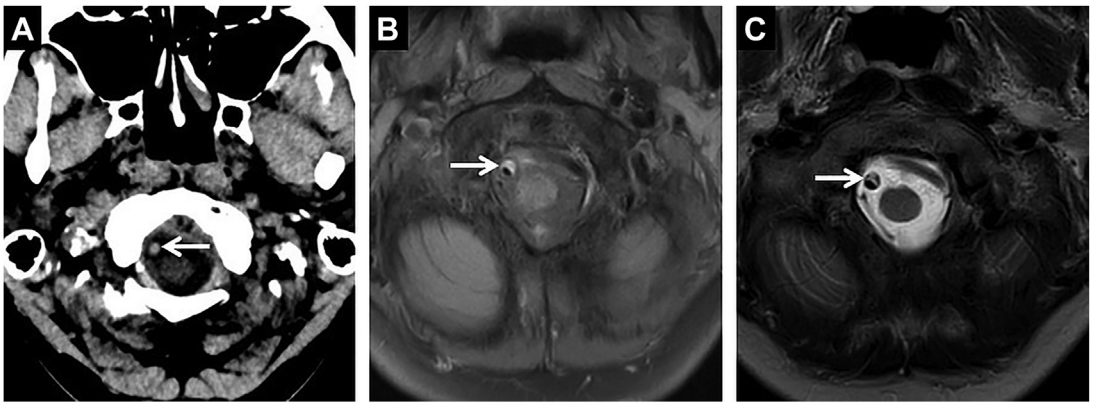

Fig. 5. VWI in a 17-year-old patient presenting with tearing neck pain. Axial unenhanced CT (*A*) reveals no acute brain parenchymal abnormality. However, a focal hyperdense attenuation of the right V4-vertebral artery (*arrow*) was suspected and MR imaging was suggested. MR imaging using the routine stroke protocol did not reveal an infarction. VWI (*B*, *C*) was performed the next day. Axial fat-saturated T1W image (*B*) and axial high-resolution T2W image (*C*) confirms an eccentric mural hematoma along the right V4-vertebral artery (*arrows* in *B, C*), in keeping with dissection.

evaluating image quality in pediatric cerebrovascular CTA, an objective improvement of contrast opacification was noted with higher flow rates (2.5–4 mL/s), thereby emphasizing the importance of larger-bore venous access (Poiseuille law).[19] In a survey conducted on Society of Pediatric Radiology (SPR) members, 44% of participants (30 of 68) confirmed a rate of injection greater than 3 mL/s for iodinated contrast for head/neck CTA examinations.[20] The American College of Radiology - American Society of Neuroradiology - Society for Pediatric Radiology (ACR-ASNR-SPR) consortium suggests dosing of contrast in children according to weight with a general guideline of 4 mL/s in any patient weighing 50 kg or more, reaching up to 6 mL/s for larger patients.[21] In infants, a 2-mL/s injection rate may be reasonable.[21]

Often patients may have venous access only via central lines. According to ACR guidelines, power injection of contrast media via a nonimplanted central venous catheter can be safely performed provided intravascular location of its tip is confirmed and venous backflow is tested.[20] Large-bore (9.5F–10F) central venous catheters can be injected using a flow rate of only up to 2.5 mL/s.[20] In the same survey by SPR, most responders preferred hand injection (54%) or a combination of hand and power injection (35%).[20] Although safe, a theoretic risk of catheter damage exists, especially during hand injections, which obviously is undesirable from a patient safety standpoint, particularly in the time-sensitive context of stroke.[20]

Substantial age- and physiology-dependent variations in circulation time mandate an appropriate delay following contrast injection, to ensure optimal arterial opacification for CTA. Accurate triggering of the scan can be achieved if the imaging is started as soon as contrast is visible in the region (artery) of interest, which in turn relies on the radiographer's skill and expertise.[19] Manual triggering has largely been replaced by automated triggering software based on real-time attenuation monitoring of vessels of interest (great neck vessel or arch of the aorta) using low-dose scans after the initiation of the contrast media injection; imaging is automatically triggered when enhancement reaches a predetermined attenuation.[21]

Last, CT contrast is associated with the potential risk of allergic and allergiclike reactions. In a study by Dillman and colleagues,[22] 11,306 pediatric intravenous administrations of low-osmolality nonionic iodinated contrast material revealed acute allergiclike reactions in 20 (0.18%) patients. Sixteen (80%) of these were categorized as mild, whereas 1 (5%) and 3 (15%) were categorized as moderate and severe, respectively.[22] Patients with known contrast allergies require premedication with steroids and antihistamines.

Accounting for these concerns and variables during CT imaging, better spatial resolution, and capability of vascular evaluation without injected contrast, MR imaging is the favored modality in the imaging workup of pediatric stroke.[14] MR imaging is also superior to CT scan in the diagnosis of alternate etiologies presenting with acute focal neurologic deficits.[14] MR imaging of a child with

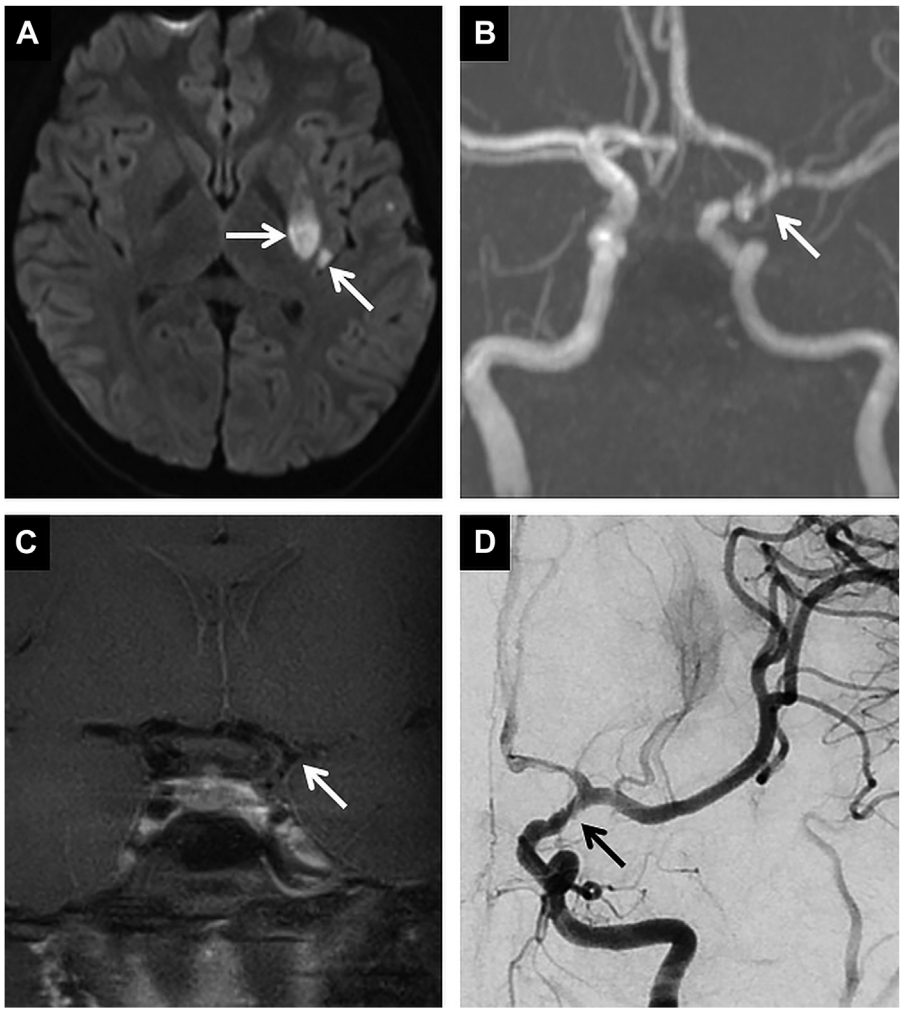

Fig. 6. VWI in a 5-year-old patient with inflammatory focal cerebral arteriopathy. Axial DWI (*A*) reveals focal striatocapsular acute infarcts (*arrows*) in the left MCA territory. MIP reconstruction of the TOF-MRA (*B*) reveals attenuation, and flow irregularity, involving the left supraclinoid ICA (*arrow*), extending into the left A1-anterior cerebral artery (ACA) and M1-MCA segments. Contrast-enhanced coronal black blood T1W VWI (*C*) reveals concentric wall enhancement along the affected left ICA (*arrow*) and the T-junction. Frontal projection of left ICA catheter-directed digital subtraction angiogram (*D*) reveals an irregular beaded appearance of the intradural left ICA (*arrow*).

suspected acute stroke comprises diffusion-weighted imaging (DWI) and apparent diffusion coefficient maps to detect acute parenchymal infarction, with susceptibility-weighted imaging (SWI) or gradient echo (GRE) sequences to assess for hemorrhage and intravascular thrombus and fluid-attenuated inversion recovery (FLAIR) imaging to assess subacute/chronic parenchymal changes.[16] Time-of-flight (TOF) MR angiography (MRA) of the craniocervical arteries is always performed to locate sites of arterial occlusion and identify evidence of arteriopathy[14] (**Fig. 2**). TOF-MRA uses short radio frequency pulses that saturate (lose signal) stationary spins, whereas newly entering unsaturated spins within vessels impart a signal. Appropriate saturation bands are used to null out venous flow so that an angiogram depicting only arteries can be obtained.[23] In scenarios where hyperacute stroke therapy is not indicated, or where an imaging mimic of stroke is identified, a full-brain imaging protocol may be used for comprehensive characterization (**Figs. 3** and **4**).

Safe MR imaging relies on thorough knowledge of implanted hardware and medical devices, before the scan. These hardware and devices may interact

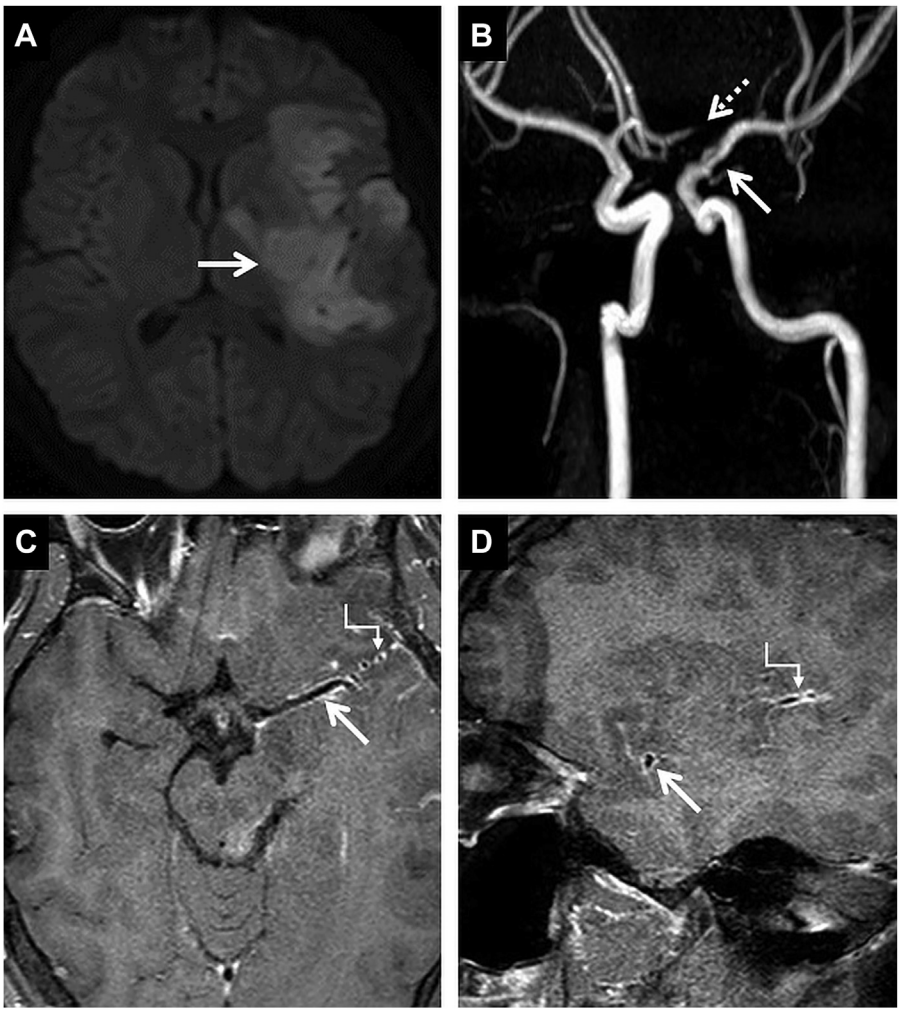

Fig. 7. Role of VWI in an 8-year-old patient presenting with acute right hemiplegia. Axial DWI (*A*) demonstrates acute infarction involving the left MCA territory (*arrow*). MIP reconstruction of the TOF-MRA (*B*) demonstrates mild attenuation, and flow irregularity, involving the left M1-MCA segment (*arrow*). Additionally, there is loss of flow signal in the proximal left A1-ACA (*dotted arrow*). Given that there was no thrombo-occlusion, VWI was performed. Contrast-enhanced axial (*C*) and sagittal (*D*) black blood T1W sequences reveal concentric enhancement of the left M1-MCA (*arrows* in *C, D*) and its cortical branches (*stepped arrows* in *C, D*) suggestive of an inflammatory arteriopathy.

with the magnetic fields causing susceptibility artifacts that limit visualization of the anatomy, or even worse, these interactions can lead to device heating, device movement, or device failure. Orthodontic hardware/dental braces are relevant in a pediatric setting, often distorting brain and MRA images.[24] Commercially available orthodontic braces may contain stainless steel (SS), ceramic, or titanium brackets.[24] As a consensus, SS brackets cause the most image distortion, requiring removal before MR imaging.[24] If needed, imaging on lower field strengths (1.5T), with signal-to-noise ratio (SNR) sacrifice, and use of sequences relatively less insensitive to susceptibility artifacts (turbo spin echo rather than GRE sequences) may be considered if braces cannot be removed.[14,24]

Perfusion-weighted imaging and flow-sensitive imaging in pediatric stroke

Although penumbral imaging in adults with arterial ischemic stroke is most often performed with CT or MR imaging-based contrast-enhanced perfusion-weighted imaging, flow-sensitive arterial spin labeling (ASL) technique is typically used to create cerebral blood flow maps in pediatric stroke imaging.[16] ASL uses endogenous flow tracers

(magnetically labeled arterial blood water), without contrast agents. For ASL imaging, 2 sets of images are obtained: first a baseline brain image followed by imaging after labeling/tagging blood arterial water protons within the cervical arteries. The second set is obtained after a delay, allowing tagged protons to enter the imaging slice. Subsequent subtraction of the datasets allows quantification of the blood entering the brain.[23] Various types of tagging are available (continuous ASL, pulsed ASL, pseudocontinuous ASL), the discussion of which is beyond the scope of this article.

Vessel wall imaging in pediatric stroke

Black blood vessel wall imaging (VWI) is a technique in which high-resolution images of the intracranial or cervical arterial walls are obtained, distinct from the lumen.[23] Signals from blood are suppressed using long turbo spin echo readout or using an inversion recovery to null the longitudinal component of the blood-water magnetization.[17] VWI is often performed using a T1-weighted sequence due to the background cerebrospinal fluid suppression and the potential to perform contrast-enhanced imaging to detect vessel wall enhancement.[23] Owing to the need for high-resolution and thin-section

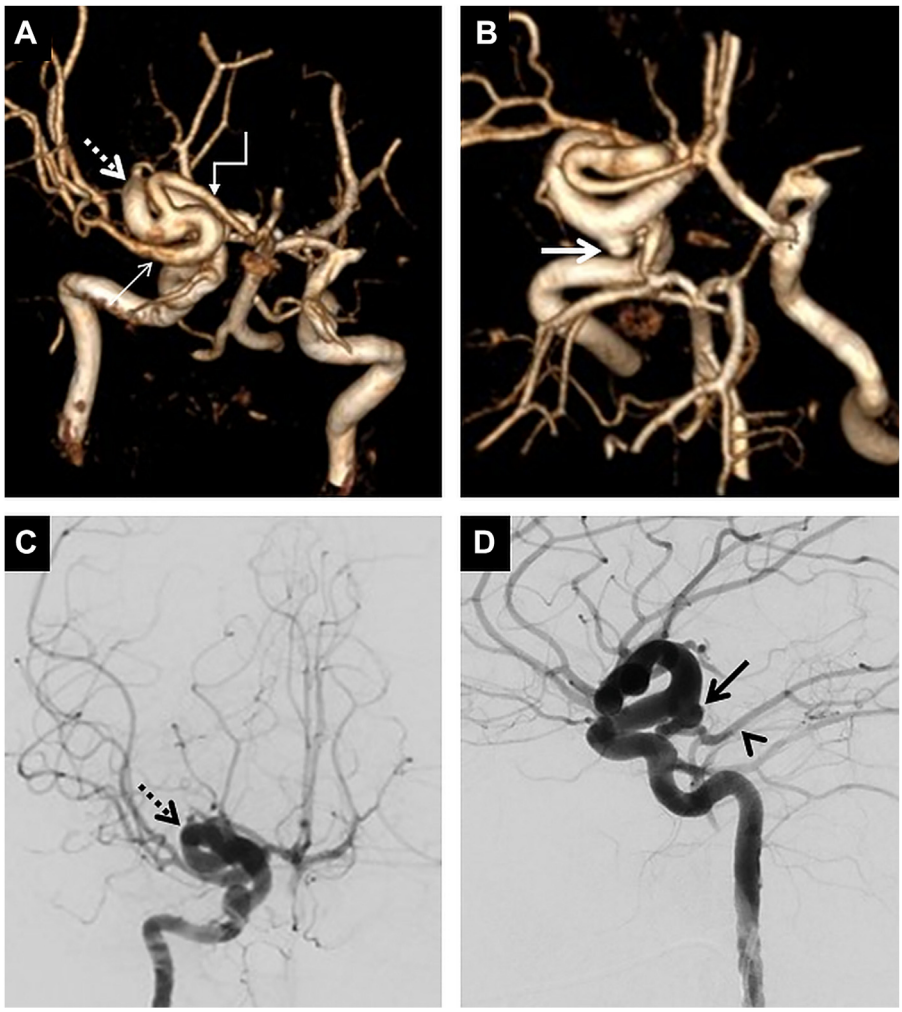

Fig. 8. Incidental aneurysm in a 12-year-old patient presenting with headache. 3D-volume reconstruction of a TOF-MRA (*A*, *B*) reveals marked dolichoectasia of the right supraclinoid ICA (*dotted arrow* in *A*). The right A1-ACA (*stepped arrow* in *A*) arises from the carotid terminus. The proximal right M1-MCA (*thin arrow* in *A*) demonstrates diffuse fusiform dilatation. Note the posteriorly directed saccular daughter aneurysm arising at the level of the right posterior communicating artery origin (*arrow* in *B*). Frontal (*C*) and lateral (*D*) projections of the right ICA catheter-directed digital subtraction angiogram confirms dolichoectasia of the intradural right ICA (*dotted arrow* in *C*) and associated posteriorly directed saccular daughter aneurysm (*arrow* in *D*); the latter is seen incorporating the right posterior communicating artery (*arrowhead*).

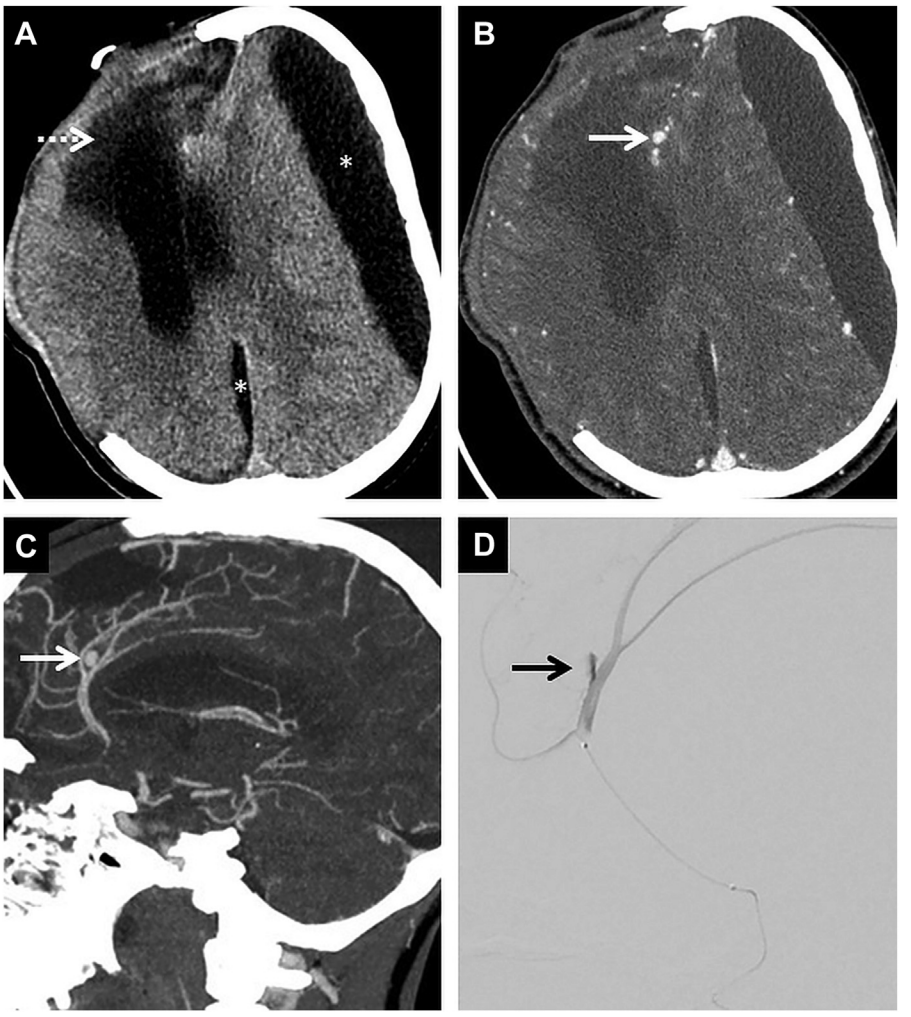

Fig. 9. Saccular aneurysm in a 9-year-old patient initially presenting with traumatic head injury. CT on presentation (not shown) revealed multifocal parenchymal hematomas and a large right frontal subdural hematoma warranting emergent evacuation and a decompressive right hemicraniectomy. CTA on presentation (not shown) revealed no significant intracranial or extracranial arterial injury. Unenhanced CT image (*A*) obtained 3 weeks postsurgery reveals extensive encephalomalacia involving the right frontal lobe (*dotted arrow*) along with hypodense subdural hygromas (*asterisk*) along the left cerebral convexity and the right posterior parafalcine region. Follow-up axial CTA image (*B*) and corresponding sagittal MIP reconstruction (*C*) reveals interval development of a traumatic saccular aneurysm/pseudoaneurysm (*arrows* in *B, C*) involving the right A2-ACA segment. Lateral projection microcatheter digital subtraction angiogram of right A2-ACA (*D*) showing the pseudoaneurysm (*arrow*) along the pericallosal ACA. This was coil embolized.

imaging, reduced SNR is a major trade-off. Hence, VWI is often performed on high-field MR imaging systems given their higher intrinsic SNR.[23] VWI has great promise in the detection of arterial dissections. In this setting, an unenhanced VWI sequence may depict a T1-hyperintense intramural hematoma[16,17] (**Fig. 5**). Contrast-enhanced VWI is also useful in the characterization of arteriopathies. Wall enhancement is presumed to reflect inflammation and increased flow within the vasa vasora of large arteries[16,17,25] (**Figs. 6 and 7**).

Pediatric Intracranial Aneurysms

A comprehensive overview of intracranial arterial aneurysms in the pediatric population is given in the article in this issue by Kartik D. Bhatia and Carmen Parra-Farinas's article, "Intracranial Arterial Aneurysms in Childhood," in this issue. For noninvasive imaging of intracranial arterial aneurysms in children, CTA, in conjunction with an unenhanced CT scan of the head, is widely used for initial workup. This approach is

Fig. 10. MR appearance of an infundibulum in a 12-year-old presenting with focal seizures. Oblique axial (*A*) and oblique sagittal (*B*) MIP reconstructions of a TOF-MRA reveal an incidental conical, posteriorly directed outpouching (*arrows*) along the right P1-posterior cerebral artery segment in keeping with an infundibulum.

particularly favored in patients presenting with nontraumatic subarachnoid hemorrhage.[26,27] The sensitivity for detecting aneurysms less than 2 mm is 53%, improving to 95% for aneurysms larger than 7 mm.[28,29] CTA comes with the inherent limitations of calculating appropriate contrast dosage and timing of the CTA, but these are outweighed by the sensitivity and speed of imaging acquisition. MRA is often reserved only for follow-up imaging[28] **Fig. 8**.

Intracranial aneurysms may be encountered in children under specific clinical circumstances. Aneurysms following a traumatic brain injury account for approximately 5% to 10% of all pediatric intracranial aneurysms (PIAs) and often occur on the distal anterior cerebral artery (40%), on arteries crossing the skull base (35%), or on distal cortical branch arteries (25%)[30] (**Fig. 9**). Notably, traumatic aneurysms involving the petrocavernous internal carotid artery are frequently associated with direct carotid-cavernous sinus fistula. Nontraumatic dissecting aneurysms account for up to 50% of all aneurysms among neonates, infants, and young children.[30] These aneurysms are frequently circumferential or fusiform and may be associated with focal tortuosity or adjacent stenoses. Infectious (mycotic) aneurysms often involve distal cortical branch arteries.[30]

Infundibular dilations (also known as infundibula) are conical or funnel-shaped dilatations at arterial ostia, with the arterial mainstem seen extending from the apex[31] (**Fig. 10**). These structures mimic aneurysms but can be distinguished based on their morphology (ie, lack of neck or asymmetric outpouching).[32] In a study on pediatric infundibula, Dmytriw and colleagues[32] found infundibula are commonly located along the left P1-posterior cerebral artery (35%). Largely, infundibula are considered benign; however, adult literature has reported evolution into true aneurysms, attributed to flow-related wall shear stress, with histopathological studies confirming changes in the arterial media.[32] In the study by Dmytriw and colleagues,[32] none of the infundibula showed aneurysmal evolution over the pediatric age spectrum (total follow-up period of 86 patient-years; mean of 32.3±35.7 months). Nevertheless, an increased incidence was noted in patients with sickle cell disease, which is a known association with PIAs.[32] Fenestration variants. which are commonly found at the vertebrobasilar junction and at the anterior communicating artery complex, can lead to unusual appearances that mimic aneurysms on cross-sectional imaging. In addition, arterial loops that are at the limit of cross-sectional imaging can mimic aneurysms, as can small arteries that turn out of the imaging plane in a TOF-MRA sequence.

Noninvasive Imaging of Intracranial Arteriovenous Shunts in Children

Numerous articles in this issue have content that address childhood hemorrhagic stroke and intracranial vascular malformations of childhood. To avoid redundancy, this article focuses specifically on principles of noninvasive cross-sectional imaging that are complementary to the other articles. A focused overview of intracranial vascular malformations of childhood including arteriovenous malformations

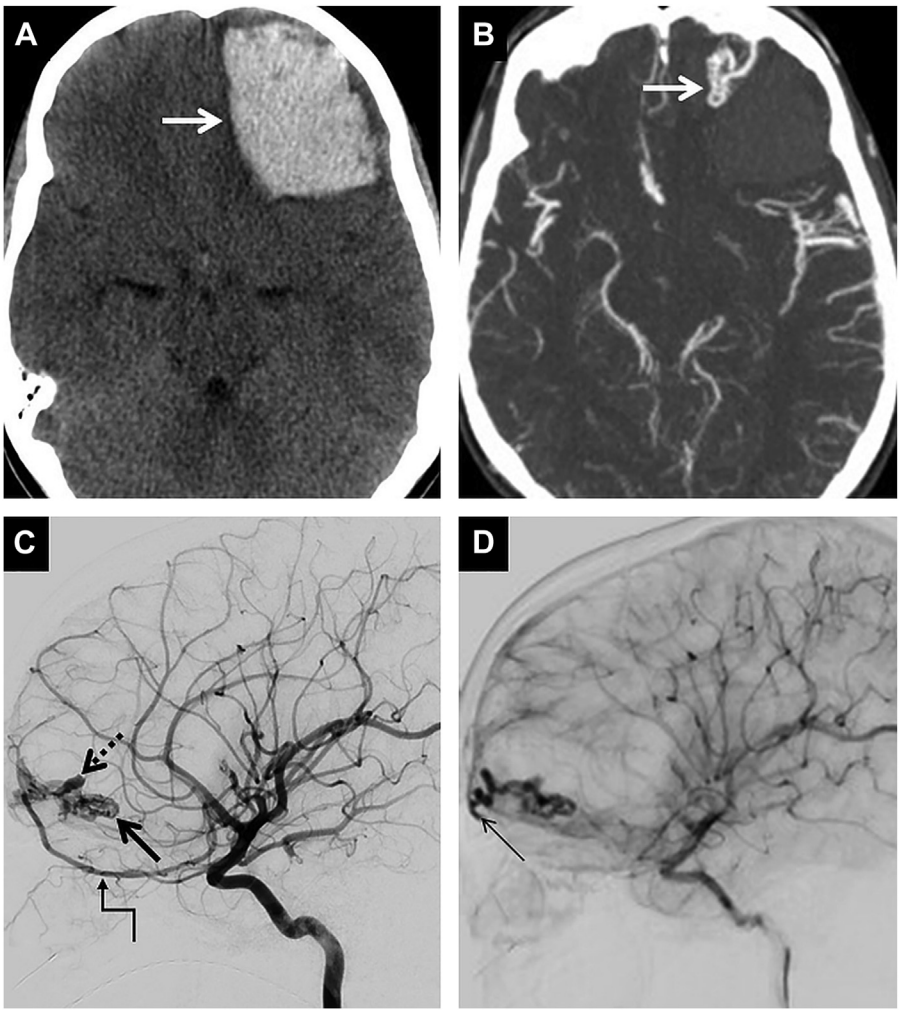

Fig. 11. Imaging appearances of a ruptured AVM with superficial venous drainage in a 16-year-old patient presenting with acute onset of headache. Axial unenhanced CT image (*A*) reveals a large, hyperdense, acute lobar hematoma in the left frontal lobe (*arrow*) exerting mass effect and a rightward midline shift. Axial MIP reconstruction of a CTA (*B*) reveals a small AVM nidus located along the anteromedial aspect of the hematoma (*arrow*). Lateral projections of the left ICA catheter-directed digital subtraction angiogram in early arterial (*C*) and capillary phases (*D*) confirm the AVM nidus in the basal left frontal lobe (*arrow* in *C*) supplied from the orbitofrontal branch of the left ACA (*stepped arrow* in *C*). A small superiorly directed pseudoaneurysm is also noted (*dotted arrow* in *C*). The AVM is drained via a superficial cortical vein (*thin arrow* in *D*) into the anterior aspect of the superior sagittal sinus.

(AVMs) is given Karim and colleagues' article, "Intracranial Vascular Malformations in Children," in this issue. Fetal vascular malformations (vein of Galen malformations, non-Galenic choroidal arteriovenous fistulae, pial arteriovenous fistulae, and dural sinus malformations) are covered in Qureshi and colleagues' article, "Neurovascular Malformations in the Fetus and Neonate," in this issue. Neuroimaging of childhood hemorrhagic stroke is presented in the Leach and colleagues' article, "Imaging of Hemorrhagic Stroke in Children," in this issue. The initial imaging evaluation of hemorrhagic stroke in children is often done using CT/CTA[33,34] (**Figs. 11** and **12**). The lack of temporal resolution and the inability to detect micro-AVMs are a technical limitation of this technique. In patients with hereditary hemorrhagic telangiectasia, contrast-enhanced and ASL sequences are useful in detecting micro-AVMs and capillary malformations (**Fig. 13**). MR imaging/MRA is useful in the evaluation of both ruptured and unruptured AVM and arteriovenous fistula (AVF) (**Figs. 14–17**).

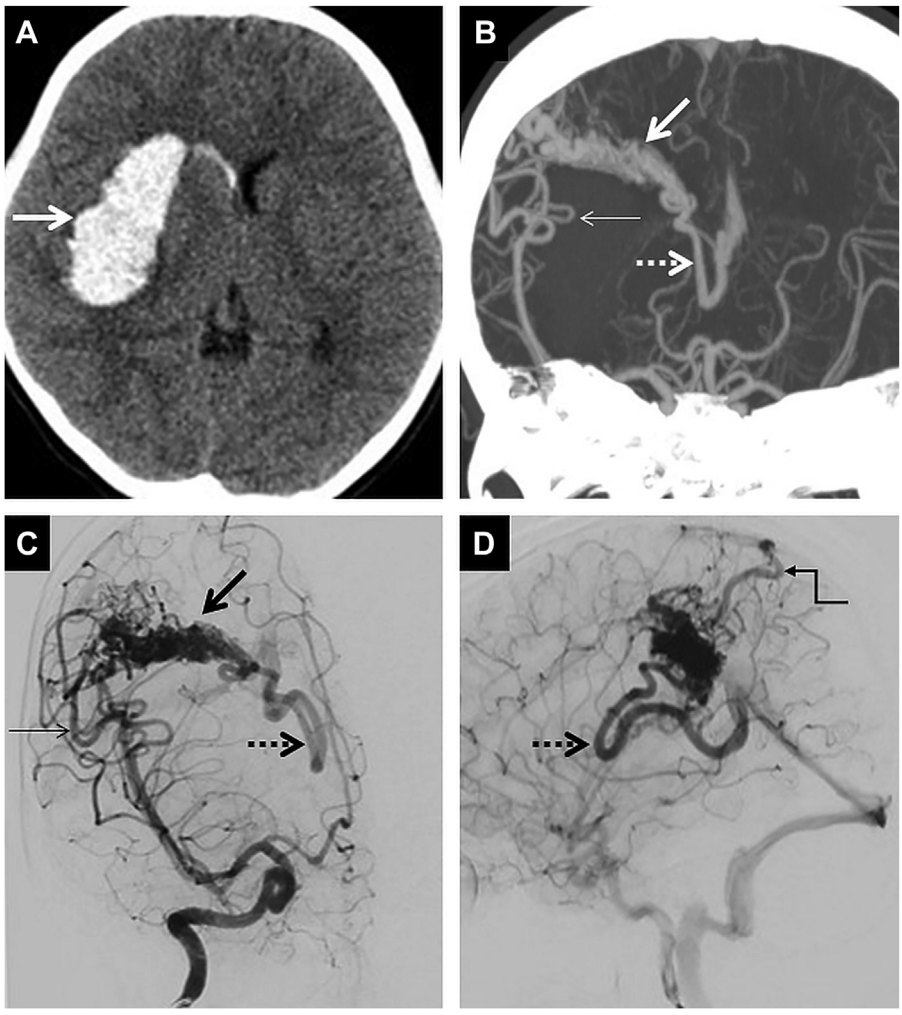

Fig. 12. Imaging appearances of a ruptured AVM with deep and superficial venous drainage in an 11-year-old patient presenting with left-sided weakness. Axial unenhanced CT image (*A*) reveals a large, hyperdense acute hematoma in the right external capsule (*arrow*). Note the marked mass effect exerted by the hematoma with resultant compression of the right lateral ventricle and a midline shift toward the left. A small amount of hemorrhage dissecting into the right frontal horn is also seen. Coronal oblique MIP reconstruction of a CTA (*B*) reveals a large AVM nidus located along the superior aspect of the hematoma (*arrow*), supplied by the distal cortical branches of the right MCA (*thin arrow*) and drained via the right thalamostriate vein into the right internal cerebral vein (*dotted arrow*). Frontal (*C*) and lateral (*D*) projections of the follow-up right ICA catheter-directed digital subtraction angiogram confirm a compact AVM nidus in the in the right frontoparietal lobe (*arrow* in *C*) supplied by arteries distributed by the right MCA (*thin arrow* in *C*) and drained by the right thalamostriate vein (*dotted arrows* in *C, D*) into the corresponding internal cerebral vein along with superficial drainage via a single cortical vein (*stepped arrow* in *D*) into the midportion of the superior sagittal sinus.

Catheter-directed digital subtraction angiography (DSA) is the gold-standard for imaging intracranial arteriovenous shunts. A detailed overview of catheter-directed neuroangiography in children is presented in the Tierradentro-Garcia and colleagues' article, "Catheter-directed Cerebral and Spinal Angiography in Children," in this issue. Exceptional spatial (0.08 mm × 0.08–0.2 mm) and temporal (up to 24 frames per second) resolution is achieved with DSA.[35] Superselective microcatheter angiography and 3D rotational reconstructions allow detailed evaluation of AVM angioarchitecture.[35] C-arm cone-beam CT (CBCT) imaging is performed with a C-arm-mounted flat-panel detector system and provides fast, high-resolution volumetric imaging. This

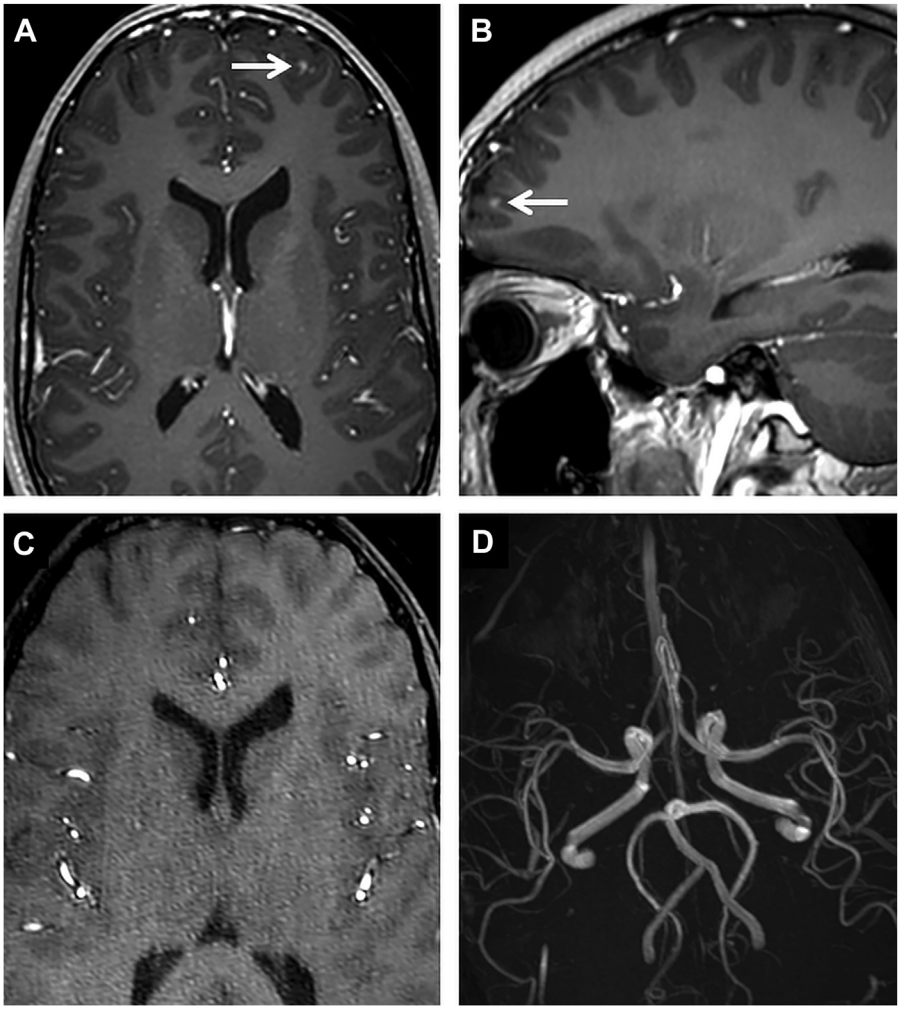

Fig. 13. Capillary malformation in a 5-year-old patient with hereditary hemorrhagic telangiectasia. Axial contrast-enhanced 3D T1 image (*A*) and its sagittal reconstruction (*B*) reveal a punctate focus of enhancement in the left frontal cortex (*arrows* in *A, B*). Axial TOF-MRA (*C*) and its MIP reconstruction (*D*) reveal no flow signal/nidus in this region or elsewhere intracranially. The findings favor capillary malformation over micro-AVM given the absence of discrete macrovascular structures forming a central nidus. No arteriovenous shunting was observed on catheter-directed digital subtraction angiography.

imaging has been found to provide morphologic characteristics and anatomic relations of contrast-injected vessels with excellent spatial resolution (0.1–0.2 mm voxels).[35] CBCT also permits multiplanar and 3D volume reconstructions using a single acquisition dataset. However, despite these advantages, CBCT increases radiation dosage. Data from adult literature suggest that a 20-second CBCT angiogram acquisition is associated with 0.2 Gy radiation dose versus a 5-second 3D rotational angiography, which provides an exposure of 0.065 Gy. In comparison, a standard catheter-directed DSA run is associated with 0.15 Gy of radiation exposure.[36] Doses for 3D rotational pediatric neuroangiography can be significantly reduced to about 15% of a standard DSA run by tailoring protocols for effectiveness and dose optimization.[36]

Although TOF-MRA is a flow-sensitive MR imaging sequence that conveys some information about flow, it lacks hemodynamic information needed for adequate characterization of intracranial arteriovenous shunts.[23] Contrast-enhanced time-resolved MR angiography (CE TR-MRA), a modification of bolus-chase MRA, enables rapid acquisition of vascular flow data. Along with short repetition time, low spatial resolution, parallel imaging, and partial Fourier acquisition, this technique performs multiple, sequential, rapid acquisitions of the entire imaging volume following intravenous contrast bolus administration. The

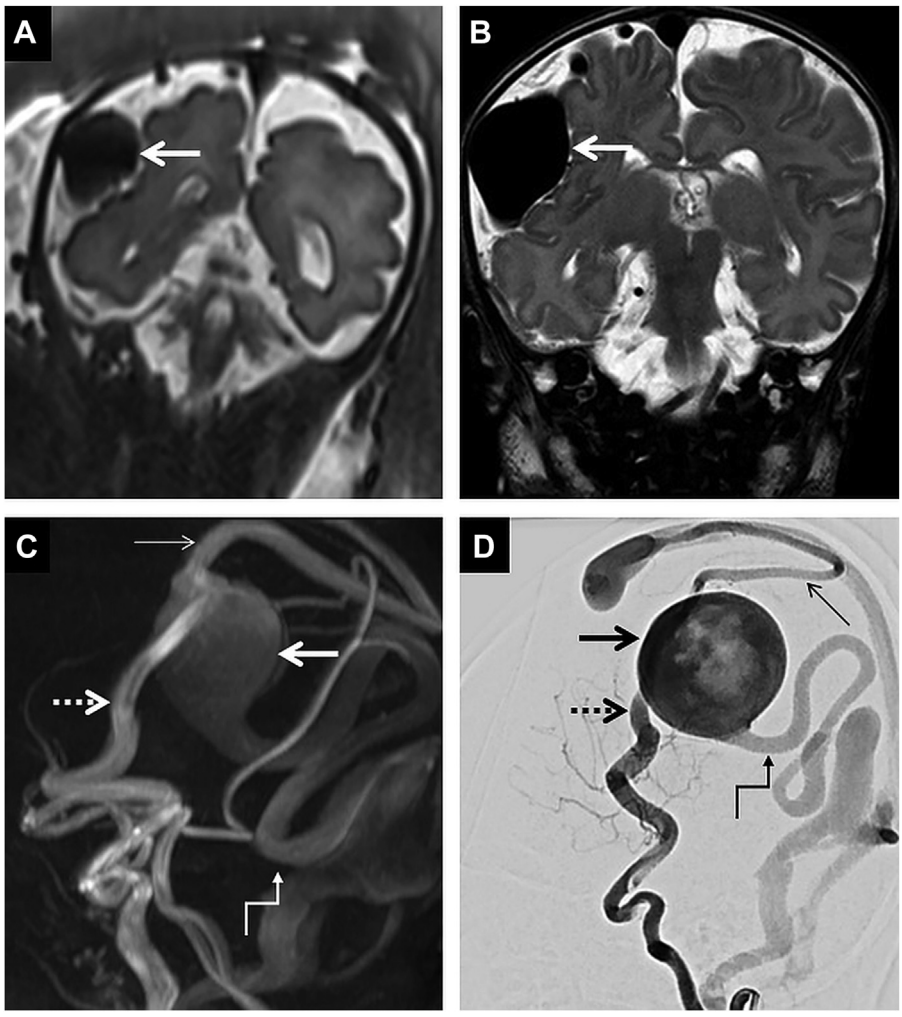

Fig. 14. Neonate with a single-hole pial arteriovenous fistula (PAVF). Coronal T2 image (*A*) obtained antenatally reveals a large venous pouch (*arrow*) along the right parietal lobe. Follow-up coronal T2 image (*B*) obtained a few hours following birth reveals an unchanged venous pouch (*arrow*) along the right parietal lobe. MIP reconstruction of a TOF-MRA (*C*) and lateral projection of the right ICA catheter-directed digital subtraction angiogram (*D*) confirm a PAVF supplied by a parietal branch of the right MCA (*dotted arrows* in *C, D*) with a large venous pouch (*arrows* in *C, D*). The arterialized venous pouch is drained via 2 venous structures, one draining superomedially toward the superior sagittal sinus (*thin arrows* in *C, D*) and the other via a posteriorly directed vein (*stepped arrows* in *C, D*) draining into the right transverse sinus.

acquisitions serve as snapshots of contrast transit and can be summed as maximum intensity pixel projections to be displayed as time-resolved "movies."[23] Temporal imaging enables assessment of intracranial hemodynamics and the venous drainage patterns for shunting lesions.[37] There is little literature on time-resolved MRA use in the pediatric age group, but experience from adult literature is encouraging. In a study by Machet and colleagues,[38] CE TR-MRA was able to detect 17 of 19 AVMs confirmed by catheter-directed DSA and found good agreement between the 2 techniques when evaluating nidus size and venous drainage (k = 0.75, 0.77) along with moderate agreement (k = 0.44) when evaluating arterial feeders. Furthermore, Farb and colleagues[39] reported that CE TR-MRA accurately identified and assigned Borden classification for 93% of adult-type dural arteriovenous fistula.

Vascular Anatomy and Variants

Selective ophthalmic artery infusion chemotherapy

Retinoblastoma is the most common pediatric primary ocular malignancy, affecting 1 in 15,000

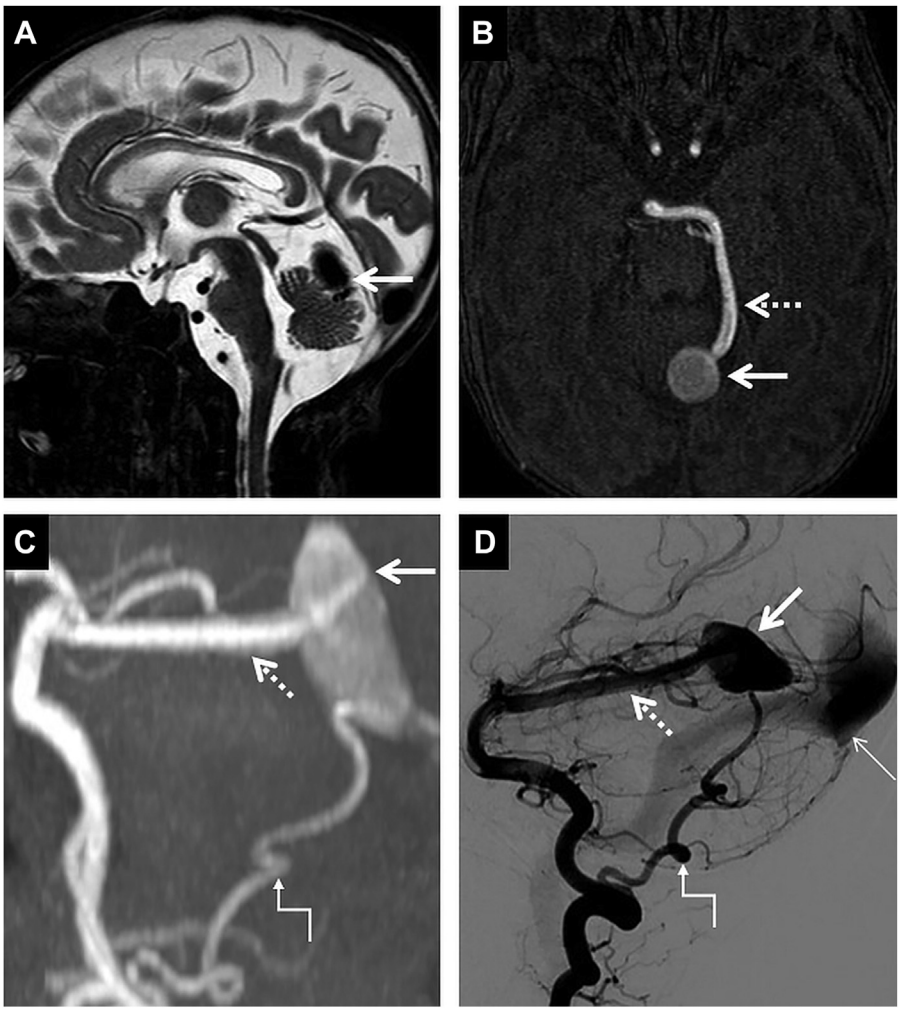

Fig. 15. Multihole PAVF in a neonate. Sagittal T2W image (*A*) reveals a venous pouch in the supravermian cistern (*arrow*). Axial TOF-MRA (*B*) reveals arterialized flow within the venous pouch (*arrow*) supplied by a hypertrophied left superior cerebellar artery (*dotted arrow*). MIP reconstruction of the TOF-MRA (*C*) and lateral projection of the left vertebral catheter-directed digital subtraction angiogram (*D*) confirm the multihole PAVF with a solitary venous pouch (*arrows* in *C, D*), supplied by the left superior cerebellar artery (*dotted arrows* in *C, D*) and left posterior inferior cerebellar artery (*stepped arrows* in *C, D*). The postfistulous venous drainage is noted via the torcula (*thin arrow* in *D*).

to 20,000 live births. Two-thirds of all cases are diagnosed before age 2 years and 95% before the age 5 years.[40,41] Treatment options in patients with retinoblastomas have evolved over the years from enucleation and external beam radiotherapy to more targeted chemotherapeutic drug delivery via the superselective catheterization of the ophthalmic artery (intra-arterial chemotherapy [IAC]).[42]

At our institution, all patients who are candidates for selective ophthalmic artery infusion chemotherapy undergo MR imaging of the brain and orbits, along with TOF-MRA to assess the OA. We use the results of TOF-MRA for neuroendovascular surgical treatment planning to improve procedural workflow efficiency. When a small caliber of the OA, variant OA origin, or unfavorable angulation of the proximal OA stem suggests that direct catheterization of the OA will be difficult or impossible, an alternative approach is formulated in advance. In such cases, chemotherapy can be administered directly into the orbital branch of the middle meningeal artery or into the infraophthalmic internal carotid artery during concurrent balloon occlusion of the supraophthalmic internal carotid artery. Advanced planning of this nature can reduce the number of vessel catheterizations, reduce patient radiation

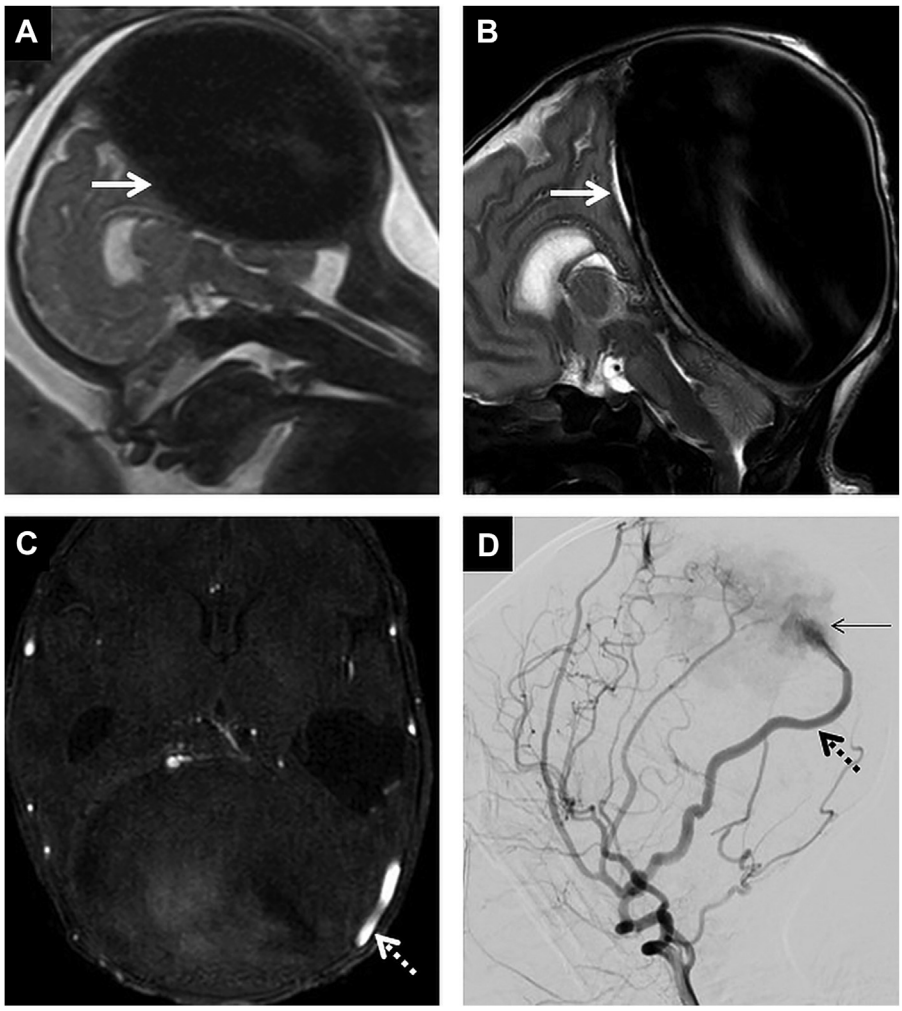

Fig. 16. Dural sinus malformation with dural arteriovenous fistulae. Sagittal T2W image obtained prenatally (*A*) and sagittal T2 image obtained within the first few hours postnatally (*B*) reveal a large venous pouch created by massive enlargement of the posterior segment of the superior sagittal sinus and contiguous torcula (*arrows* in *A, B*). Note the marked mass effect exerted over the posterior aspects of the cerebral hemispheres and the posterior fossa structures. Axial TOF-MRA (*C*) and lateral projection of the left external carotid artery (ECA) catheter-directed digital subtraction angiogram (*D*) reveal an arteriovenous macrofistula (*thin arrow in D*) between the venous pouch and the posterior division of the left middle meningeal artery (MMA) (*dotted arrows*). Arterial supply via the contralateral MMA and the dural branches of the posterior cerebral arteries was also noted (not shown).

exposure, reduce contrast load, and ensure that all necessary equipment is available at the time of neuroendovascular treatment.[43,44] (**Fig. 18**)

Wada test

Despite significant advances in functional brain MR imaging, the Wada test remains an important part of the preoperative evaluation of patients with medically refractory seizures who are under consideration for temporal lobectomy. This test typically entails slow injection of sodium amobarbital (100–500 mg) into the cervical ICA. This injection anesthetizes the ipsilateral cerebral hemisphere for almost 5 to 10 minutes, during which memory and language function can be evaluated in awake patients.[45] In patients with persistent primitive carotid-vertebrobasilar anastomoses (ie, trigeminal artery), a modified superselective Wada test involving microcatheter-directed infusion of amytal directly into the intracranial internal carotid artery is necessary to prevent amytal-induced respiratory depression and loss of consciousness[46] (**Fig. 19**). Recognition and reporting of persistent primitive carotid-vertebrobasilar anastomoses can

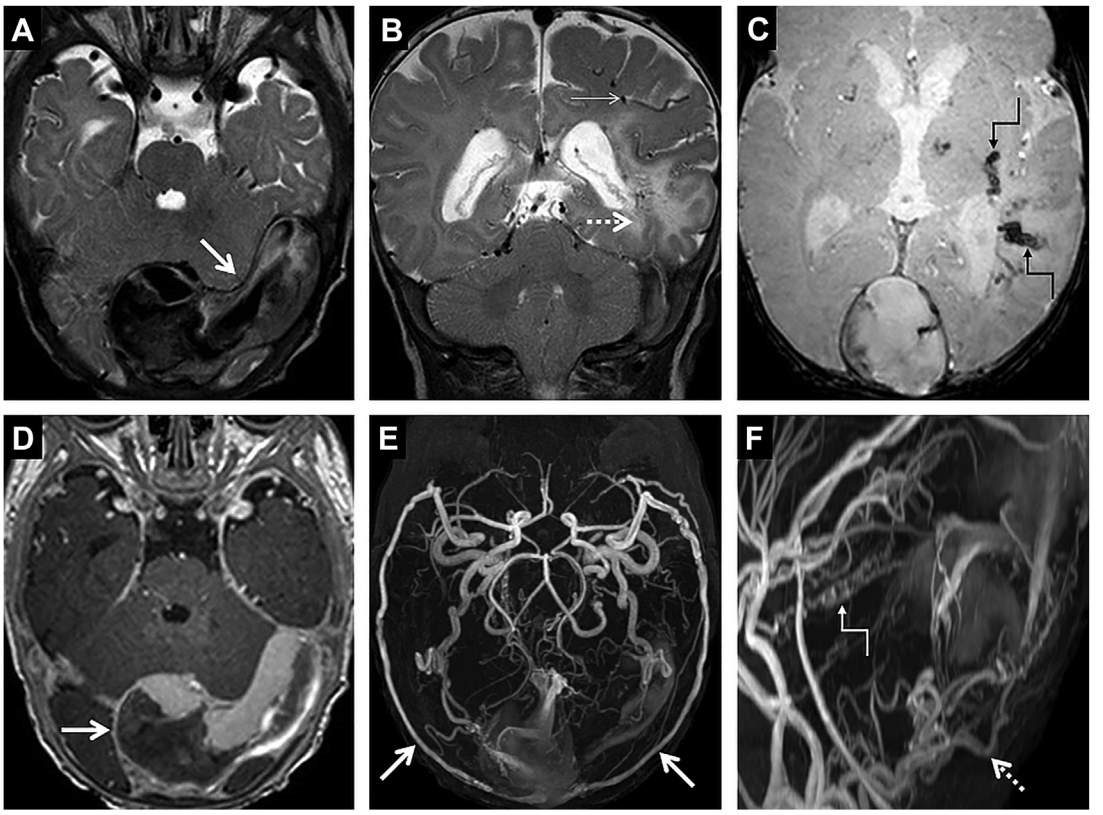

Fig. 17. Partially thrombosed dural sinus malformation (DSM) in a 3-month-old patient presenting with seizures. Axial T2W image (*A*) reveals marked ectasia of the left transverse sinus and torcula in keeping with a DSM (*arrow*). Coronal T2W image (*B*) reveals confluent T2 hyperintensity (*dotted arrow*) in the left temporal lobe along with distended cortical veins (*thin arrow*) in the left parietal region representing changes of chronic venous congestion. Axial multiplanar gradient recalled acquisition (MPGR) (*C*) demonstrates tubular foci of T2 hypointensity (*stepped arrows*) corresponding to thrombosed cortical veins and/or hemorrhage in the affected left temporal lobe. Axial contrast-enhanced 3D T1W image (*D*) reveals a large filling defect (*arrow*) within the DSM in keeping with partial thrombosis. MIP reconstructions of a TOF-MRA (*E*, *F*) reveal dominant arterial supply arising from the middle meningeal arteries (*arrows* in *E*), the occipital arteries (*dotted arrow* in *F*), and the meningohypophyseal arteries (*stepped arrow* in *F*).

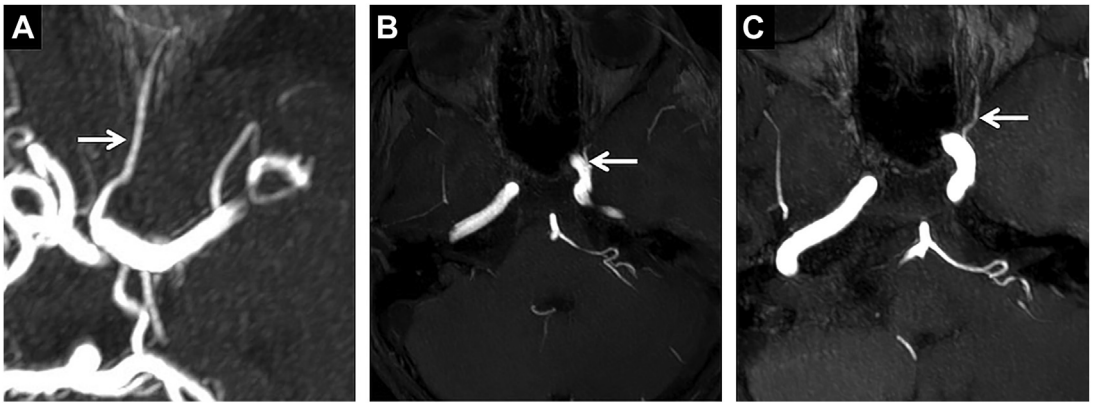

Fig. 18. Normal and variant appearances of the ophthalmic artery (OA). Axial MIP reconstruction of a TOF-MRA (*A*) reveals normal takeoff of the left OA (*arrow*) arising from the intradural paraclinoid segment of the left ICA (*A*). Axial (*B*) and oblique (*C*) 2D-MIP reconstructions of a TOF-MRA in another patient reveals dorsal variant anatomy of the left OA (*arrows* in *B, C*) arising from the lateral aspect of the cavernous left traversing the left superior orbital fissure.

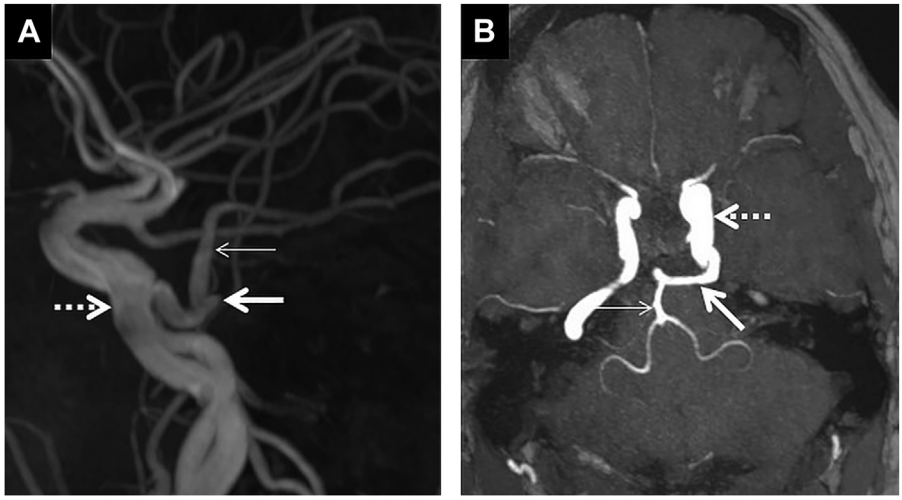

Fig. 19. Appearances of a persistent trigeminal artery. Lateral (*A*) and axial (*B*) MIP reconstructions reveal a persistent trigeminal artery (*arrows*) arising from the cavernous segment of the left ICA (*dotted arrows*) and supplying the distal basilar trunk (*thin arrows*). Note that the basilar artery caudad to the trigeminal artery is hypoplastic.

therefore improve procedural workflow efficiency for patients undergoing Wada testing. Although many such variants are well demonstrated on conventional brain MR imaging studies, TOF-MRA may be valuable for detection of less-conspicuous variants that influence the distribution of drug infused into the cervical internal carotid artery.

Cerebral Sinovenous Thrombosis: Pearls and Pitfalls

Cerebral sinovenous thrombosis (CSVT) refers to thrombo-occlusion of the dural venous sinuses, cortical veins, and/or deep cerebral veins. CSVT is a neurologic emergency with an incidence of 0.25 to 0.67 per 100,000 children per year and 0.82 to 12 per 100,000 neonates per year.[47] The associated mortality rate and risk of permanent neurologic damage range between 8% to 19% and 38% to 48.1%, respectively.[47] Patients may present with a wide spectrum of symptoms (headache, seizures, altered mentation, lethargy, and/or focal neurologic deficits).[48] Dehydration, infection, trauma, cancer, anticancer treatment, prothrombotic states (antiphospholipid syndrome, prothrombin G20210A mutation, antithrombin III deficiency, elevated homocysteine), lupus, and nephrotic syndrome are reported causes of CSVT in children.[48,49]

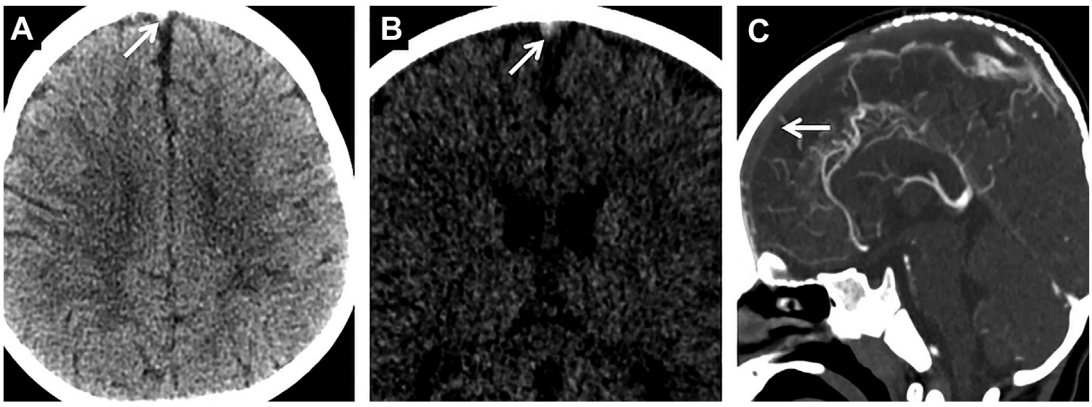

Fig. 20. CT appearances of sinovenous thrombosis in an 18-month-old patient. Axial unenhanced CT image (*A*) reveals hyperdensity within the superior sagittal sinus (*arrow*); however, this may be overlooked due to inadequate window settings. Axial unenhanced CT image viewed using a narrow window setting (*B*) accentuates the hyperdense attenuation of the superior sagittal sinus (*arrow*). CT venography (*C*) performed subsequently confirms the occlusive thrombus within the superior sagittal sinus (*arrow*).

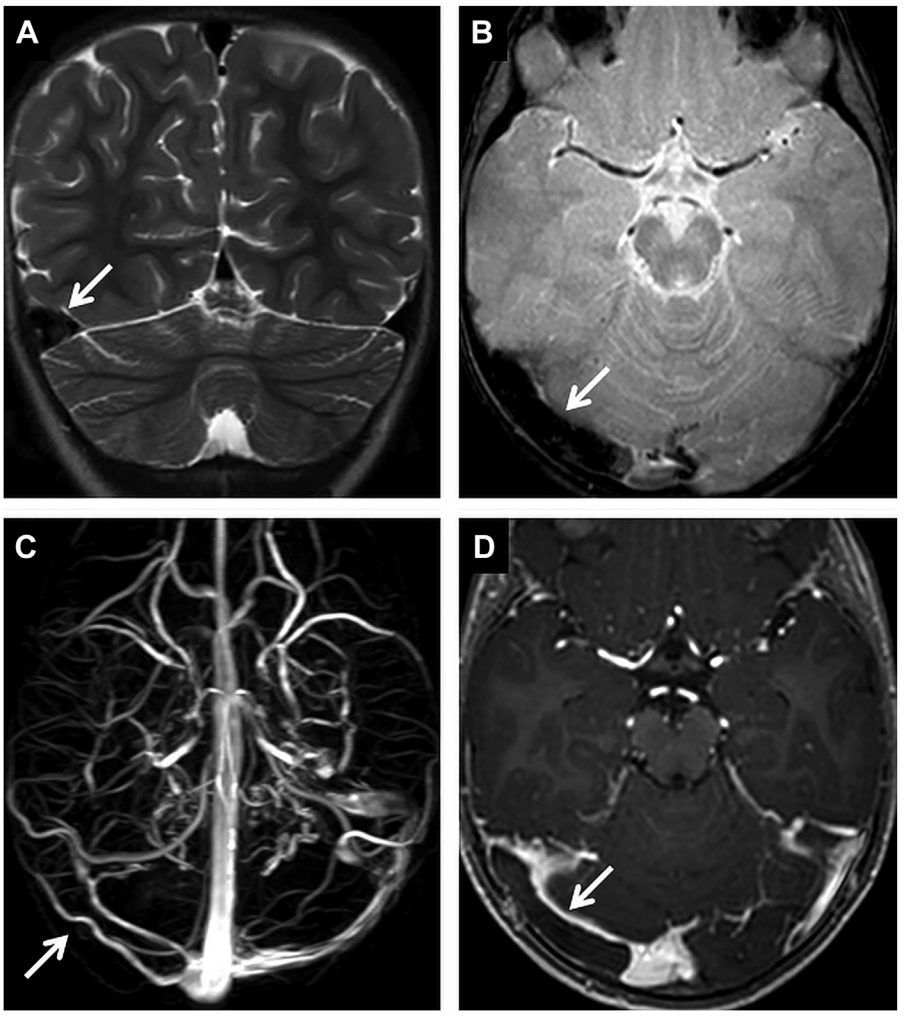

Fig. 21. Typical appearances of an acute CSVT in a 2-year-old patient. Coronal T2W image (*A*) reveals marked distention of the right transverse sinus (*arrow*), due to a T2-hypointense thrombus mimicking a flow void. Axial MPGR sequence (*B*) reveals abnormal susceptibility within the occluded right transverse sinus (*arrow*). MIP reconstruction of the phase contrast MRV (*C*) confirms complete loss of flow signal within the right transverse sinus (*arrow*) and the right sigmoid sinus. Contrast-enhanced 3D T1W image (*D*) reveals a large filling defect within the right transverse sinus (*arrow*).

Neuroimaging is essential to diagnose/confirm CSVT, identify the extent of cerebral venous compromise, and evaluate for secondary complications (venous ischemia, hemorrhage, and so on).[49] CT and MR imaging, with venographic techniques, are the mainstay of imaging a patient with known or suspected CSVT.[49] In this section the imaging features and pitfalls of CSVT imaging on CT and MR imaging are discussed. The important role of CSVT as a cause of pediatric hemorrhagic stroke and related neuroimaging issues is presented in Leach and colleagues' article, "Imaging of Hemorrhagic Stroke in Children," in this issue.

On CT imaging the intraluminal thrombus of CSVT appears hyperdense in the acute phase due to low water and high hemoglobin concentrations. This situation persists for 1 to 2 weeks, after which the clot evolves to become isodense and later hypodense. It is imperative to ensure adequate window settings when evaluating the dural venous sinuses on unenhanced CT because narrow window settings make differentiation between the sinus and the adjacent bone difficult. Beam-hardening artifacts at the skull base may obscure the venous system. Diffuse venous hyperdensity must also be evaluated with caution

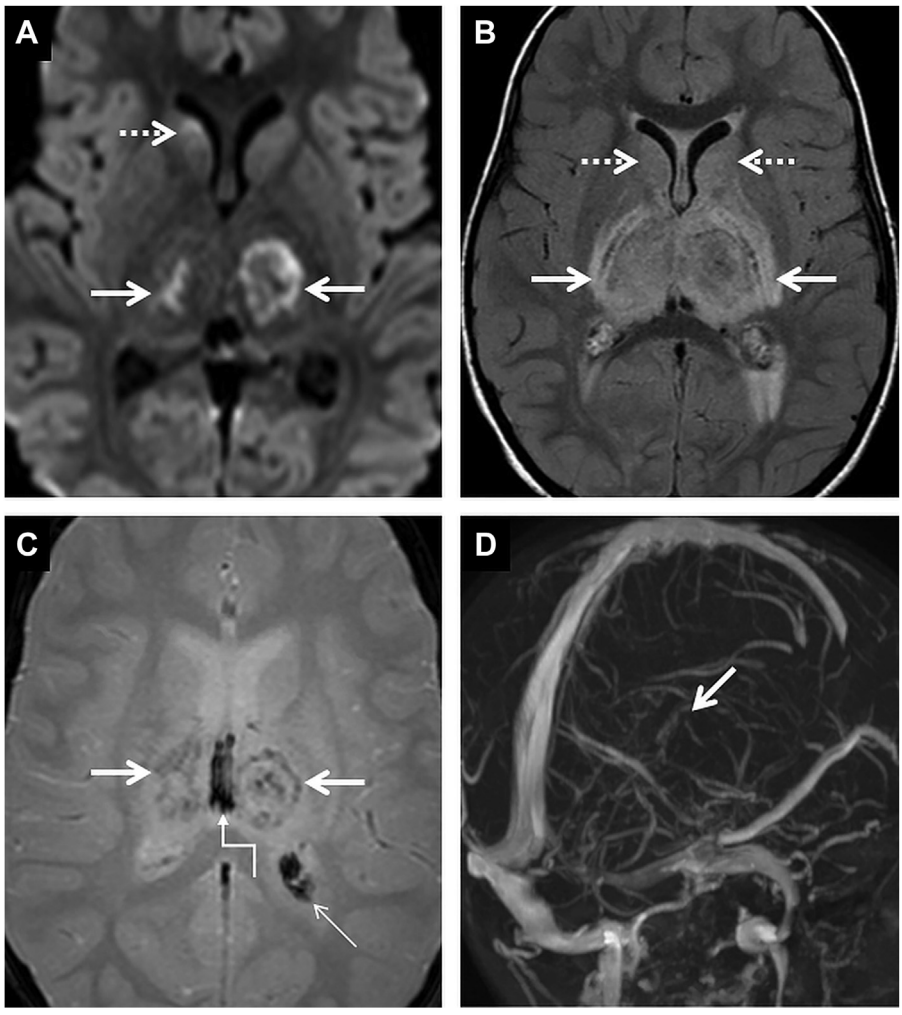

Fig. 22. Deep venous thrombosis in a 6-year-old patient presenting with altered mentation. Axial DWI (*A*) reveals bilateral, asymmetric areas of restricted diffusion in the thalami (*arrows*), more extensive on the left. Subtle restricted diffusion is also seen in the right caudate nucleus (*dotted arrow*). Axial FLAIR (*B*) reveals marked hyperintense swelling of the thalamocapsular regions (*arrows*). Subtle similar signal is also noted in the caudate nuclei (*dotted arrows*). Axial MPGR (*C*) reveals foci of hemorrhage within the involved thalami (*arrow*) along with abnormal susceptibility within the internal cerebral veins (*stepped arrow*). Some hemorrhage along the glomus of the left choroid plexus is also seen (*thin arrow*). Oblique MIP reconstruction of a TOF-MRV (*D*) reveals complete absence of flow signal within the deep cerebral venous system (*arrow*).

because this finding may be due to physiologic polycythemia (eg, in neonates).[47] On CT venography, intraluminal clot is seen as a filling defect within the sinus or vein[47] (**Fig. 20**).

The appearance of intraluminal venous clot on MR imaging varies with the stage of its evolution. In the acute phase, the clot is isointense on T1 but hypointense on T2/FLAIR sequences. As the clot evolves into the subacute phase, the degradation of deoxyhemoglobin to methemoglobin imparts a hyperintense signal on T1 sequences initially, with hyperintensity seen on T2/FLAIR sequences in the late subacute phase (extracellular methemoglobin). SWI/GRE is reliable at these stages because the degradation of hemoglobin causes a blooming artifact (hypointense signal) (**Figs. 21** and **22**). A chronic thrombus may be variable in signal intensity but usually hypointense on T1 and T2 sequences. Flow voids within a partially recanalized thrombus may be noted. SWI in the chronic phase is not as reliable because ferritin and hemosiderin (superparamagnetic substances) are removed by macrophages.[47] In a study on 37 patients with CSVT, Wagner and colleagues[49] concluded that 96% of cases could be identified on T1 and T2 sequences (74 of 77) and 88% (68 of 77) were detected on

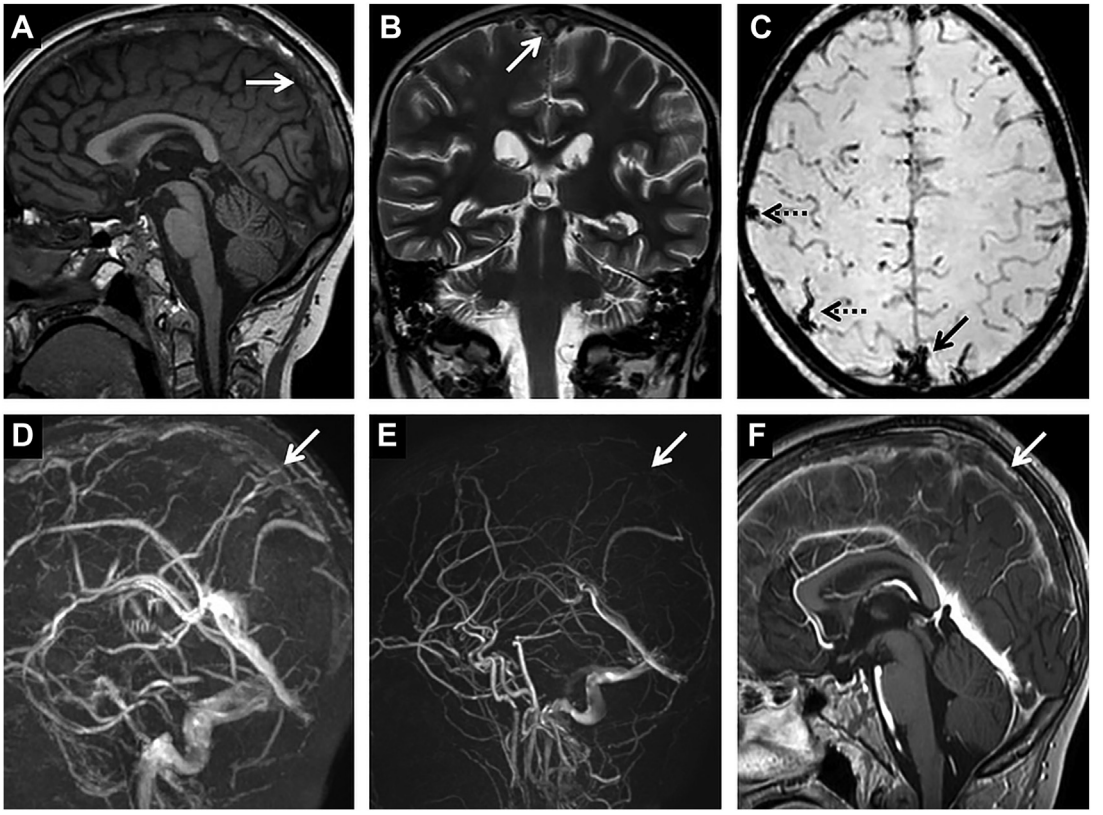

Fig. 23. MR imaging of sinovenous thrombosis in a 9-year-old patient with a known history of T-cell acute lymphoblastic leukemia on pegylated L-asparaginase. Sagittal T1W image (*A*) reveals hyperintense thrombosis extensively involving the superior sagittal sinus (*arrow*). Coronal T2W image (*B*) reveals corresponding loss of the expected flow void within the midportion of the superior sagittal sinus (*arrow*). Axial SWI (*C*) reveals abnormal susceptibility within the superior sagittal sinus (*arrow*). Also note, similar susceptibility artifacts in the cortical veins along the right frontoparietal convexity (*dotted arrows*), suggestive of concomitant cortical venous thrombosis. MIP reconstruction of a TOF-MRV (*D*) reveals apparent faint signal within the superior sagittal sinus (*arrow*), due to thrombus shine through effect; this could potentially mimic normal flow signal. PC-MRV (*E*) confirms absent flow in the superior sagittal sinus (*arrow*). Sagittal contrast-enhanced 3D T1W image (*F*) confirms a filling defect (*arrow*) extensively involving the superior sagittal sinus in keeping with thrombosis.

FLAIR images. Although 94% of thrombi within the dural venous sinuses were revealed by DWI/Diffusion tensor imaging (DTI) (72 of 77), only 40% showed restricted diffusion.[49]

Although these sequences help in the initial identification of CSVT, they are not enough to delineate the site and extent of the thrombus. TOF-MR venography (TOF-MRV) is useful in detecting defects in flow within the venous sinuses. Saturation of mobile spins, depicted as flow gaps, due to parallel orientation of the vessel and the imaging plane may mimic an occlusion. Thrombus shine through effect due to the native T1 hyperintensity of a clot, resulting in apparent flow signals in the lumen, is another important pitfall. This pitfall can be mitigated by correlating with spin echo sequences and phase contrast MRV (PC-MRV).[47,50]

PC-MRV uses bipolar gradients to induce a phase shift of mobile spins and restore it to generate a signal. A velocity-encoding gradient (VENC) is then applied to filter out the flow within the vascular structure of choice (veins in this case). Hence use of the correct VENC is critical to obtain robust intraluminal flow signals with PC-MRV. Flow velocity outside the VENC is not displayed and hence may erroneously be interpreted as occlusion. This phenomenon is more common at sites where flow is faster or turbulent, for example, around an arachnoid granulation or along the stenotic distal transverse sinuses in the setting of idiopathic intracranial hypertension.[47,50]

Contrast-enhanced MRV is a technique that uses intravenous gadolinium to cause intraluminal T1 shortening, thereby producing a lumenogram.

This technique provides better spatial resolution and is devoid of the effects of in-plane saturation or the need for application of a velocity-based gradient. Thrombi, including those with T1 hyperintensity, are seen as filling defects. (**Fig. 23**) However, chronic thrombi may enhance due to replacement of thrombus with organized connective tissue and capillary proliferation (granulation tissue).[47,50]

SUMMARY

Cross-sectional neuroimaging rests on 2 major pillars, that is, CT and MR imaging. These technologies have revolutionized the evaluation of children with neurovascular pathology, by improving the delineation of neurovascular lesions and illuminating diverse mechanisms of disease pathogenesis. The addition of catheter-directed angiographic techniques and hemodynamic imaging enables a deeper and complementary characterization of pediatric neurovascular pathologies. Expert interpretation of cross-sectional and catheter-directed neuroimaging data empowers neuropediatric specialists to formulate optimal patient-oriented treatment strategies across the full range of clinical neurovascular pathology. Despite the advantages that neuroimaging has brought to pediatrics, there are limitations and trade-offs that interpreting radiologists must be cognizant of to avoid erroneous diagnostic evaluations.

CLINICS CARE POINTS

- MRI with abbreviated stroke specific sequences is the modality of imaging modality of choice in patients presenting with clinical features of stroke. However, stroke mimics are frequent. Hence active monitoring during image acquisition is warranted so that further imaging sequences, as necessary, may be obtained.
- AV shunts in pediatric patients are different in terms of pathophysiology and angioarchitecture compared to adults. Most shunts which cause high output cardiac failure may be detected in utero. In those who present in the post-natal MRI and CT both play a complimentary role in evaluating the shunting lesion as well as its effects on the brain parenchyma.
- Sinovenous thrombosis in children may be due to underlying prothrombotic causes, complication of an intracranial pathology (e.g., infection) or idiopathic. The dural venous sinuses are an important review area in clinical practice. Understanding the physics, advantages and limitations of the various imaging sequences available is extremely important in order to avoid a mis- or missed diagnosis.

DISCLOSURE

The authors have nothing to disclose.

REFERENCES

1. Hetts SW, Meyers PM, Halbach VV, et al. Anomalies of the cerebral vasculature: diagnostic and endovascular considerations. In: Barkovich AJ, Raybaud C, editors. Pediatric neuroimaging. 6th edition. Philadelphia: Wolters Kluwer; 2019.
2. Montaser A, Smith ER. Intracranial vascular abnormalities in children. Pediatr Clin 2021;68(4):825–43.
3. Choudhary P, Neha B. Sedation and general anesthesia in diagnostic pediatric imaging. Indographics 2022;01:101–9.
4. Coté CJ, Wilson S. Guidelines for monitoring and management of pediatric patients before, during, and after sedation for diagnostic and therapeutic procedures. Pediatrics 2019;143(6):e20191000.
5. Fawole C, Webber A. Approaches to sedation in pediatric neuroimaging: what the radiologist should know. J Pediatr Neurol 2017;16(02):056–60.
6. Barkovich MJ, Xu D, Desikan RS, et al. Pediatric neuro MRI: tricks to minimize sedation. Pediatr Radiol 2018;48(1):50–5.
7. Carter AJ, Greer MLC, Gray SE, et al. Mock MRI: reducing the need for anaesthesia in children. Pediatr Radiol 2010;40(8):1368–74.
8. Khan J, Donnelly L, Koch B. A program to decrease the need for pediatric sedation for CT and MRI. Appl Radiol 2007;36:30–3.
9. Pappas JN, Donnelly LF, Frush DP. Reduced frequency of sedation of young children with multisection helical CT. Radiology 2000;215(3):897–9.
10. Callahan MJ, Cravero JP. Should I irradiate with computed tomography or sedate for magnetic resonance imaging? Pediatr Radiol 2021;52(2):340–4.
11. Arlachov Y, Ganatra RH. Sedation/anaesthesia in paediatric radiology. Br J Radiol 2012;85(1019):e1018–31.
12. Sammons HM, Edwards J, Rushby R, et al. General anaesthesia or sedation for paediatric neuroimaging: current practice in a teaching hospital. Arch Dis Child 2010;96(1):114.
13. Warner MA, Warner ME, Warner DO, et al. Perioperative pulmonary aspiration in infants and children. Anesthesiology 1999;90(1):66–71.

14. Jiang B, Mackay MT, Stence NV, et al. Neuroimaging in pediatric stroke. Semin Pediatr Neurol 2022;43:100989.
15. Ferriero DM, Fullerton HJ, Bernard TJ, et al. Management of stroke in neonates and children: a scientific statement from the American heart association/American stroke association. Stroke 2019;50(3). https://doi.org/10.1161/str.0000000000000183.
16. Mirsky DM, Beslow LA, Amlie-Lefond C, et al. Pathways for neuroimaging of childhood stroke. Pediatr Neurol 2017;69:11–23.
17. Donahue MJ, Dlamini N, Bhatia A, et al. Neuroimaging advances in pediatric stroke. Stroke 2019;50(2):240–8.
18. McGlennan C, Ganesan V. Delays in investigation and management of acute arterial ischaemic stroke in children. Dev Med Child Neurol 2008;50(7):537–40.
19. Thust SC, Chong WKK, Gunny R, et al. Paediatric cerebrovascular CT angiography-towards better image quality. Quant Imag Med Surg 2014;4(6):469–74.
20. Callahan MJ, Servaes S, Lee EY, et al. Practice patterns for the use of iodinated IV contrast media for pediatric CT studies: a survey of the society for pediatric radiology. Am J Roentgenol 2014;202(4):872–9.
21. American College of Radiology. ACR-ASNR-SPR practice parameter for the performance and interpretation of cervicocerebral computed tomography angiography (CTA). Revised. 2020. Available at: acr.org/-/media/ACR/Files/Practice-Parameters/CervicoCerebralCTA.pdf?la=en. Accessed February 28, 2024.
22. Dillman JR, Strouse PJ, Ellis JH, et al. Incidence and severity of acute allergic-like reactions to IV nonionic iodinated contrast material in children. Am J Roentgenol 2007;188(6):1643–7.
23. Vossough A. Cerebrovascular diseases in infants and children: general imaging principles. Springer eBooks; 2016. p. 1–48.
24. Poorsattar-Bejeh Mir A, Rahmati-Kamel M. Should the orthodontic brackets always be removed prior to magnetic resonance imaging (MRI)? J Oral Biol Craniofac Res 2016;6(2):142–52.
25. Dlamini N, Yau I, Muthusami P, et al. Arterial wall imaging in pediatric stroke. Stroke 2018;49(4):891–8.
26. de Aguiar GB, Ozanne A, Elawady A, et al. Intracranial aneurysm in pediatric population: a single-center experience. Pediatr Neurosurg 2022;57(4):270–8.
27. Xu R, Xie ME, Yang W, et al. Epidemiology and outcomes of pediatric intracranial aneurysms: comparison with an adult population in a 30-year, prospective database. J Neurosurg Pediatr 2021;28(6):685–94.
28. Chung C, Peterson RB, Howard BM, et al. Imaging intracranial aneurysms in the endovascular era: surveillance and posttreatment follow-up. Radiographics 2022;42(3):789–805.
29. Sanchez S, Hickerson M, Patel RR, et al. Morphological characteristics of ruptured brain aneurysms: a systematic literature review and meta-analysis. Stroke 2023;3(2). https://doi.org/10.1161/svin.122.000707.
30. Krings T, Geibprasert S, terBrugge KG. Pathomechanisms and treatment of pediatric aneurysms. Child's Nerv Syst 2009;26(10):1309–18.
31. Kameda-Smith M, Plessis J, Bhattacharya JJ. First demonstration of resolution of an infundibulum by direct treatment of the arterial wall with Pipeline flow-diverting stent. Neuroradiology 2013;56(1):35–9.
32. Dmytriw AA, Bisson DA, Phan K, et al. Locations, associations and temporal evolution of intracranial arterial infundibular dilatations in children. J Neurointerventional Surg 2019;12(5):495–8.
33. El-Ghanem M, Kass-Hout T, Kass-Hout O, et al. Arteriovenous malformations in the pediatric population: review of the existing literature. Interv Neurol 2016;5(3–4):218–25.
34. Garzelli L, Shotar E, Blauwblomme T, et al. Risk factors for early brain AVM rupture: cohort study of pediatric and adult patients. Am J Neuroradiol 2020;41(12):2358–63.
35. Mossa-Basha M, Chen J, Gandhi D. Imaging of cerebral arteriovenous malformations and dural arteriovenous fistulas. Neurosurgery Clinics of North America 2012;23(1):27–42.
36. Safain MG, Rahal JP, Raval A, et al. Use of cone-beam computed tomography angiography in planning for gamma knife radiosurgery for arteriovenous malformations. Neurosurgery 2014;74(6):682–96.
37. Grossberg JA, Howard BM, Saindane AM. The use of contrast-enhanced, time-resolved magnetic resonance angiography in cerebrovascular pathology. Neurosurg Focus 2019;47(6):E3.
38. Machet A, Portefaix C, Kadziolka K, et al. Brain arteriovenous malformation diagnosis: value of time-resolved contrast-enhanced MR angiography at 3.0T compared to DSA. Neuroradiology 2012;54(10):1099–108.
39. Farb RI, Agid R, Willinsky RA, et al. Cranial dural arteriovenous fistula: diagnosis and classification with time-resolved MR angiography at 3T. Am J Neuroradiol 2009;30(8):1546–51.
40. Chen Q, Zhang B, Dong Y, et al. Comparison between intravenous chemotherapy and intra-arterial chemotherapy for retinoblastoma: a meta-analysis. BMC Cancer 2018;18(1). https://doi.org/10.1186/s12885-018-4406-6.
41. Rauschecker AM, Patel CV, Yeom KW, et al. High-resolution MR imaging of the orbit in patients with retinoblastoma. Radiographics 2012;32(5):1307–26.
42. Fabian ID, Onadim Z, Karaa E, et al. The management of retinoblastoma. Oncogene 2018;37(12):1551–60.

43. Manjandavida FP, Stathopoulos C, Zhang J, et al. Intra-arterial chemotherapy in retinoblastoma – a paradigm change. Indian J Ophthalmol 2019;67(6):740–54.
44. Klufas MA, Gobin YP, Marr B, et al. Intra-arterial chemotherapy as a treatment for intraocular retinoblastoma: alternatives to direct ophthalmic artery catheterization. Am J Neuroradiol 2012;33(8):1608–14.
45. Loring DW, Meador KJ, Westerveld M. The Wada test in the evaluation for epilepsy surgery. Neurosciences (Riyadh, Saudi Arabia) 2000;5(4):203–8.
46. Manraj KSH, Abruzzo T. Diagnostic cerebral angiography and the Wada test in pediatric patients. Tech Vasc Interv Radiol 2011;14(1):42–9.
47. Bracken J, Barnacle A, Ditchfield M. Potential pitfalls in imaging of paediatric cerebral sinovenous thrombosis. Pediatr Radiol 2012;43(2):219–31.
48. Heller C, Heinecke A, Junker R, et al. Cerebral venous thrombosis in children. Circulation 2003;108(11):1362–7.
49. Wagner MW, Bosemani T, Oshmyansky A, et al. Neuroimaging findings in pediatric cerebral sinovenous thrombosis. Child's Nerv Syst 2015;31(5):705–12.
50. VP20. Pai V, Khan I, Sitoh YY, et al. Pearls and pitfalls in the magnetic resonance diagnosis of dural sinus thrombosis: a comprehensive guide for the trainee radiologist. J Clin Imaging Sci 2020;10:77.

ARTICLE

Spectrum of cerebral arteriopathies in children with arterial ischemic stroke

Mubeen F. Rafay, MBBS, MSc, Kevin A. Shapiro, MD, Ann-Marie Surmava, MBA, Gabrielle A. deVeber, MD, MSc, Adam Kirton, MD, Heather J. Fullerton, MD, Catherine Amlie-Lefond, MD, Bernhard Weschke, MD, Nomazulu Dlamini, MBBS, Jessica L. Carpenter, MD, Mark T. Mackay, MBBS, PhD, Michael Rivkin, MD, Alexandra Linds, MSc, and Timothy J. Bernard, MD, for the International Pediatric Stroke Study (IPSS) Group

Correspondence
Dr. Rafay
mubeen.rafay@utoronto.ca

Neurology® 2020;94:e2479-e2490. doi:10.1212/WNL.0000000000009557

Abstract

Objective

To determine that children with arterial ischemic stroke (AIS) due to an identifiable arteriopathy are distinct from those without arteriopathy and that each arteriopathy subtype has unique and recognizable clinical features.

Methods

We report a large, observational, multicenter cohort of children with AIS, age 1 month to 18 years, enrolled in the International Pediatric Stroke Study from 2003 to 2014. Clinical and demographic differences were compared by use of the Fisher exact test, with linear step-up permutation min-p adjustment for multiple comparisons. Exploratory analyses were conducted to evaluate differences between cases of AIS with and without arteriopathy and between arteriopathy subtypes.

Results

Of 2,127 children with AIS, 725 (34%) had arteriopathy (median age 7.45 years). Arteriopathy subtypes included dissection (27%), moyamoya (24.5%), focal cerebral arteriopathy–inflammatory subtype (FCA-i; 15%), diffuse cerebral vasculitis (15%), and nonspecific arteriopathy (18.5%). Children with arteriopathic AIS were more likely to present between 6 and 9 years of age (odds ratio [OR] 1.93, $p = 0.029$) with headache (OR 1.55, $p = 0.023$), multiple infarctions (OR 2.05, $p < 0.001$), sickle cell anemia (OR 2.9, $p = 0.007$), and head/neck trauma (OR 1.93, $p = 0.018$). Antithrombotic use and stroke recurrence were higher in children with arteriopathy. Among arteriopathy subtypes, dissection was associated with male sex, older age, headache, and anticoagulant use; FCA-i was associated with hemiparesis and single infarcts; moyamoya was associated with seizures and recurrent strokes; and vasculitis was associated with bilateral infarctions.

Conclusion

Specific clinical profiles are associated with cerebral arteriopathies in children with AIS. These observations may be helpful indicators in guiding early diagnosis and defining subgroups who may benefit most from future therapeutic trials.

From the Section of Pediatric Neurology (M.F.R.), Department of Pediatrics and Child Health, University of Manitoba, Children's Hospital Research Institute of Manitoba, Winnipeg, Canada; Department of Neurology and Pediatrics (K.A.S., H.J.F.), University of California, San Francisco; University of Toronto (A.-M.S.); Division of Neurology (G.A.d.V., N.D., A.L.), The Hospital for Sick Children, University of Toronto, Ontario; Department of Pediatrics and Clinical Neurosciences (A.K.), Cumming School of Medicine, University of Calgary, Alberta, Canada; Department of Neurology (C.A.-L.), University of Washington, Seattle; Department of Neuropediatrics (B.W.), Charité University Medicine Berlin, Germany; Department of Neurology (J.L.C.), George Washington University, Washington, DC; Department of Neurology (M.T.M.), Royal Children's Hospital Melbourne, Murdoch Children's Research Institute and University of Melbourne, Australia; Boston Children's Hospital (M.R.), Harvard Medical School, Boston, MA; and Division of Child Neurology (T.J.B.), Department of Pediatrics and the Hemophilia and Thrombosis Center, University of Colorado, Denver.

Go to Neurology.org/N for full disclosures. Funding information and disclosures deemed relevant by the authors, if any, are provided at the end of the article.

Coinvestigators are listed at links.lww.com/WNL/B92.

Glossary

AIS = arterial ischemic stroke; **CI** = confidence interval; **FCA** = focal cerebral arteriopathy; **FCA-i** = focal cerebral arteriopathy, inflammatory type; **IPSS** = International Pediatric Stroke Study; **OR** = odds ratio; **PSOM** = Pediatric Stroke Outcome Measure; **VIPS** = Vascular Effects of Infection in Pediatric Stroke.

Cerebral arteriopathies are reported in 30% to 50% of all children with arterial ischemic stroke (AIS).[1,2] Most childhood cerebral arteriopathies are characterized either by dissection or by stenosis and irregularity of the intracranial arteries such as moyamoya and focal cerebral arteriopathy (FCA) of childhood. FCA is characterized by acute, unilateral, segmental stenosis of ≥1 large arteries of the anterior circulation[2–5] and is presumed to be inflammatory in origin,[2–4,6] although the angiographic appearance can be mimicked by intracranial dissection.[7] One-third of cases of FCA may demonstrate initially progressive arterial narrowing, but by definition, arterial narrowing does not progress beyond 3 to 6 months after stroke.[8] Most important, childhood cerebral arteriopathies are associated with a 5-fold higher risk of stroke recurrence[9] and poor outcome.[10] Therefore, their improved understanding is crucial to the development of immediate and preventive treatment strategies.

The difficulty in identifying and classifying childhood cerebral arteriopathies is a major limitation, relating often to the imaging technique, inability to consistently and accurately identify the diagnosis at presentation, and lack of standardized terminology and diagnostic criteria.[1,2,8,11,12] Recent cohorts of cerebral arteriopathy have come from the International Pediatric Stroke Study (IPSS),[1] in which arteriopathies are classified using gradually developed and refined consensus-based definitions.[1,5] Recently, a substudy of the IPSS rereviewed neurovascular imaging of their arteriopathic cases and noted that a substantial proportion (up to 30%) of arteriopathies in their cohort remained challenging to classify.[2] Such challenges are a frequent occurrence in clinical practice, suggesting that a clinical fingerprint may be helpful in the diagnosis and classification of childhood cerebral arteriopathies, especially early in the disease course when the arteriopathy has not declared its clinical course (progression, stabilization, improvement). We hypothesized that children with AIS due to an identifiable arteriopathy are distinct from those without arteriopathy and that the arteriopathy subtypes are distinct.

Methods

Study design

The IPSS is a prospective, multicenter, observational registry that enrolls and follows up children with ischemic stroke and related conditions. The IPSS currently comprises >300 investigators (representing 24 countries across 5 continents) and a web-based master database housed at the study coordinating center, The Hospital for Sick Children, Toronto, Ontario, Canada.[13] The IPSS design has been previously published.[1,10] The present analysis includes children with AIS with and without an underlying cerebral arteriopathy who were enrolled between January 2003 and July 2014 (including previously reported 667 cases enrolled from 2003 to 2007 in the IPSS[1] and 355 cases from 2010 to 2014 coenrolled in the IPSS and an IPSS substudy, the Vascular Effects of Infection in Pediatric Stroke [VIPS][2]).

Standard protocol approvals, registrations, and patient consents

As per IPSS policy, each site investigator obtained and maintained research ethics approval according to that investigator's institutional policy to enroll and study eligible cases.

Study Population

Inclusion criteria were age from 1 month to 18 years and AIS presenting with acute onset of neurologic deficit and a radiologic pattern consistent with arterial territory ischemia. Arteriopathy was defined a priori as any abnormality on vascular imaging (stenosis, irregularity, banding, pseudoaneurysm, dissection flap) except isolated vessel occlusion, which may be due to an embolus rather than a primary blood vessel abnormality.[9] Children without arteriopathy had either idiopathic AIS (no obvious risk factor or etiology) or well-described nonarteriopathic risk factor for AIS (e.g., cardioembolic stroke). The presence of arteriopathy and its subtype were determined by the enrolling IPSS site investigators and clinicians involved in the child's care using the IPSS consensus-based definitions.[5] Because a centralized review of radiographic films could not be performed due to the lack of an imaging repository in the IPSS dataset, we validated the arteriopathy diagnosis and subtype classification on the basis of the radiographic data available through the free text comment boxes in the IPSS dataset. In cases with unclear descriptions, more data were requested and obtained from the submitting IPSS site investigators (figure 1A). The authors further refined the arteriopathy classification referencing recent literature[14] through consensus at 3 teleconferences and 1 face-to-face meeting.

The refined arteriopathy subtypes included 5 mutually exclusive subtypes: (1) FCA, inflammatory type (FCA-i), which included idiopathic or presumed inflammatory FCA, transient cerebral arteriopathy, and postvaricella arteriopathy cases[2,3,5,6,15]; (2) dissection (extracranial, intracranial); (3) moyamoya (primary moyamoya disease, moyamoya syndrome secondary to

Figure 1 Study population

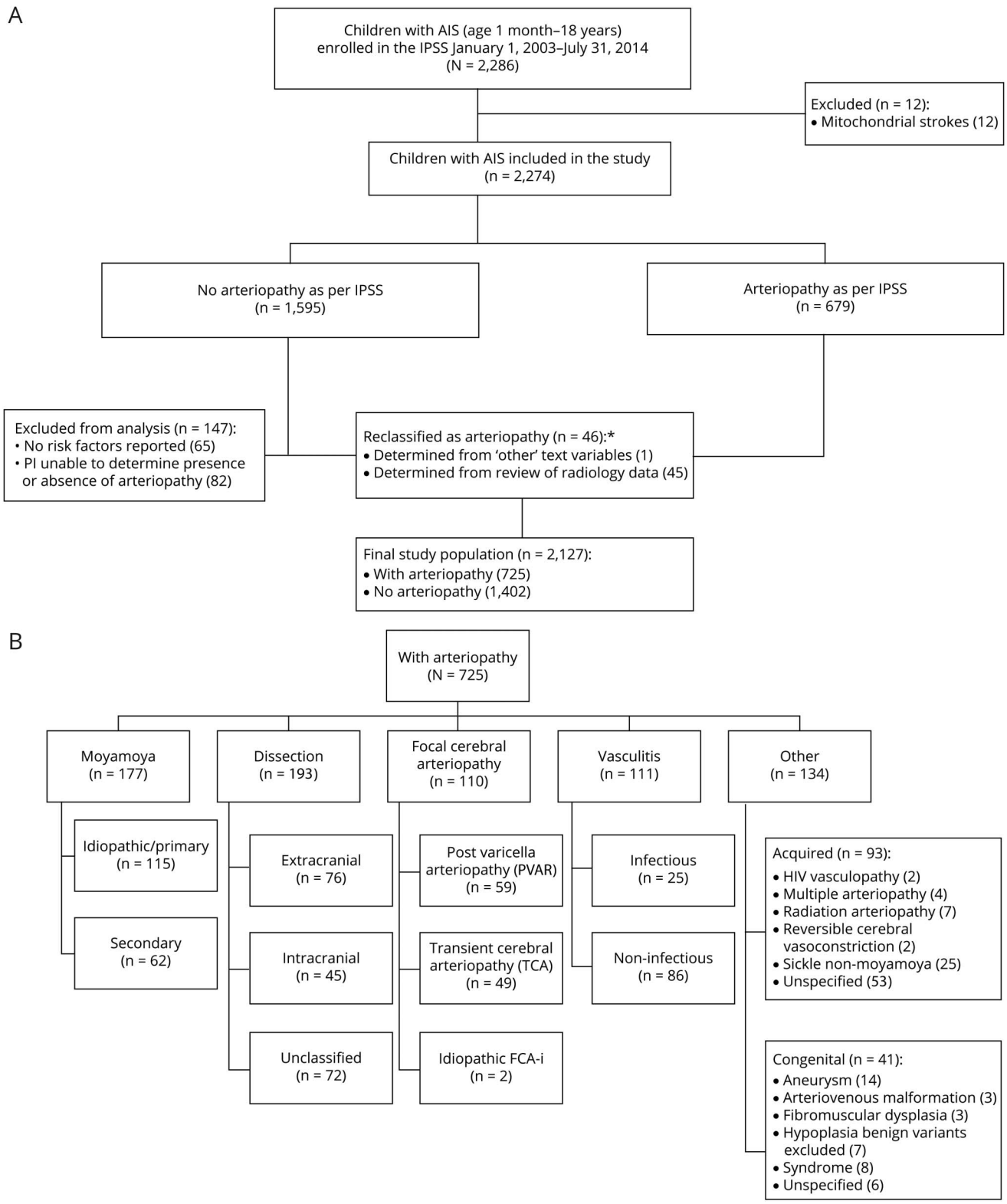

(A) International Pediatric Stroke Study (IPSS) cohort of children with arterial ischemic stroke (AIS) and cerebral arteriopathies. (B) IPSS cohort of children with AIS associated with arteriopathy. FCA-i = focal cerebral arteriopathy–inflammatory subtype.

other conditions); (4) diffuse cerebral vasculitis (infectious, noninfectious); and (5) nonclassifiable/nonspecific arteriopathies labeled as other arteriopathy (congenital, acquired) (figure 1B). Lack of sufficiently detailed vascular imaging limited our ability to further subcategorize vasculitis. We excluded children with arteriopathy but without stroke.

Data collection and abstraction

Study data were collected at each site by the IPSS site investigators and entered into the web-based IPSS database. The variables studied included demographic data (age at stroke diagnosis, sex, geographic region, race), clinical features (hemiparesis, visual field deficit, speech deficit, ataxia, decreased level of consciousness, headache, seizures, prior/concurrent thromboembolic event), radiographic information (circulation, stroke laterality, number of infarcts, hemorrhage), risk factors for stroke (cardiac disorder, underlying chronic disease, acute systemic disease, acute and chronic head/neck disease, family history of stroke), neuroimaging features (location and number of infarcts), antithrombotic treatments (classified as antiplatelet or anticoagulant agents), and outcomes. Management decisions for each case were guided by the published pediatric stroke management guidelines[16] but varied according to the treating physician's preferences and local institutional protocols. Outcomes included neurologic deficits at discharge, stroke recurrence, case fatality, and standardized stroke outcomes at 1 year and last follow-up visit that were collected through a parental Recurrence and Recovery Questionnaire[17,18] (mean duration 2.3 years), and Pediatric Stroke Outcome Measure (PSOM)[17,18] (mean duration 2.5 years). Poor outcome was defined as a PSOM score >1.

Statistical methods

Analyses were performed with SAS version 9.4 statistical software (SAS Institute, Cary, NC). Descriptive analysis, including proportions, means, and frequencies, was used to define participant characteristics. Intracranial dissection, extracranial dissection, FCA-i, moyamoya, and vasculitis were included in the subtype comparison exploratory analyses. Cases with multiple arteriopathies or missing data were excluded from the analysis. Cases with dissection that could not be classified as either intracranial or extracranial dissection were excluded from the arteriopathy subtype analysis. Multiple comparisons (arteriopathy- vs non–arteriopathy-associated AIS, arteriopathy subtypes) were performed with the Fisher exact test with linear step-up permutation min-p adjustment. Values of $\alpha \leq 0.05$ were considered significant. Significant variables were included in a stepwise multiple logistic regression analysis. Poisson regression was used to test the difference of treatment over time, and logistic regression and χ^2 tests were used as necessary to describe and measure associations involving multilevel categorical variables.

Data availability

All data used for analysis are presented in the tables and figures in this article. Data will be shared after ethics approval if requested by other investigators for purposes of replicating the results.

Results

A total of 4,294 children were enrolled in the IPSS during the study period. We identified 2,274 (53%) children, 1 month to 18 years of age, with AIS. Of these, 2,127 (93%) children fulfilled the current study inclusion criteria. Of this cohort, 725 (34%) children were identified as having AIS due to arteriopathy, and 1,402 (66%) children had AIS due to nonarteriopathic causes (figure 1A and table 1). In 2,127 children with AIS, nonarteriopathic risk factors (either single or multiple in a study participant) included cardioembolic disorders (29%), chronic diseases (31%), acute systemic illnesses (26%), acute head or neck infections/trauma (21%), chronic head or neck disorders (8%), and family history of stroke (14%) (table 2). In 725 children with arteriopathy, arteriopathy subtypes were categorized as craniocervical dissection in 193 (27%), moyamoya in 177 (24%), FCA-i in 110 (15%), diffuse cerebral vasculitis in 111 (15%), and other arteriopathy in 134 (19%) (figure 1B). Although dedicated vascular imaging was reported in 1,409 of 2,127 (66%) cases (74% noncardiac and 26% cardiac AIS), this number is underreported due to the missing data in the dataset. Of the 718 (34%) cases with no vascular imaging

Table 1 Demographic profile of children with AIS with and without arteriopathy

Variables	Arteriopathy, n (%)	No arteriopathy, n (%)
Age at index stroke, median (IQR), y[a,b]	7.45 (3.68–12.76)	4.6 (1.11–12.18)
0–3	146/725 (20)	573/1,399 (41)
3–6	145/725 (20)	203/1,399 (14)
6–9	137/725 (19)	130/1,399 (9)
9–12	88/725 (12)	135/1,399 (10)
12–15	113/725 (16)	161/1,399 (11)
15–18	96/725 (13)	197/1,399 (14)
Male sex	423/725 (58)	806/1,402 (57)
Geographic region		
Africa	0/725 (0)	3/1,402 (<1)
Asia	22/725 (3)	91/1,402 (6)
Australia	38/725 (5)	65/1,402 (5)
Europe	129/725 (18)	219/1,402 (16)
North America[a]	506/725 (70)	923/1,402 (66)
South America	30/725 (4)	101/1,402 (7)
Race		
Black[a]	73/492 (15)	86/993 (9)
White	321/492 (65)	648/993 (65)
Other	98/492 (20)	259/993 (26)

Abbreviations: AIS = arterial ischemic stroke; IQR = interquartile range.
[a] Fisher exact test showed statistically significant association with the presence of arteriopathy before multiple-comparisons adjustment.
[b] Significant association of age and arteriopathy: age as continuous variable ($p < 0.0001$, odds ratio [OR] 1.04 per unit increase) and as categorical variable (using 15–18 years as reference, those 0–3 years old are less likely to have arteriopathy [$p < 0.0001$, OR 0.52] and those 6–9 years old are more likely to have arteriopathy [$p < 0.0001$, OR 2.16]).

Table 2 Clinical profile of children with AIS with and without arteriopathy

Variables	Arteriopathy, n (%)	No arteriopathy, n (%)
Hemiparesis[a]	573/707 (81)	991/1,321 (75)
Visual field deficit	76/568 (13)	141/1,032 (14)
Dysarthria[a]	163/639 (25)	193/1,155 (17)
Ataxia[a]	77/705 (11)	82/1,349 (6)
Altered consciousness	252/685 (37)	514/1,298 (40)
Headache[a]	285/637 (45)	324/1,092 (30)
Seizures	158/691 (23)	439/1,313 (33)
Prior/concurrent thromboembolism[a]	123/629 (19)	142/1,233 (11)
Anterior circulation involvement	434/645 (67)	810/1,224 (66)
Posterior circulation involvement	141/645 (22)	278/1,224 (23)
Both circulation involvement	70/645 (11)	136/1,224 (11)
Right-sided infarction[a]	251/639 (39)	412/1,218 (34)
Left-sided infarction	232/639 (36)	559/1,218 (46)
Bilateral infarction[a]	156/639 (25)	247/1,218 (20)
Multiple infarcts[a]	309/578 (53)	415/1,097 (38)
Single infarcts	269/578 (47)	682/1,097 (62)
Hemorrhagic infarct	55/566 (10)	178/1,085 (16)
Cardiac disease	98/723 (13)	512/1,402 (37)
Underlying chronic disease	242/723 (33)	415/1,402 (30)
Connective tissue disease[a]	17/723 (2)	17/1,402 (1)
Malignancy	9/723 (1)	23/1,402 (2)
Sickle cell anemia[a]	60/723 (8)	37/1,402 (3)
Presence of syndrome	49/723 (7)	86/1,402 (6)
Prothrombotic state	66/723 (9)	131/1,402 (9)
Acute systemic disease	147/723 (20)	405/1,402 (29)
Acute head and neck disease[a]	168/723 (23)	275/1,402 (20)
Significant infection[b]	18/723 (2)	59/1,402 (4)
Noniatrogenic trauma[a]	85/723 (12)	100/1,402 (7)
Chronic head and neck disorder	53/723 (7)	110/1,402 (8)
Family history of stroke	100/687 (14)	173/1,303 (13)
Treatment with anticoagulant agent	229/694 (33)	393/1,331 (30)
Treatment with antiplatelet agent	270/694 (39)	467/1,331 (35)
Treatment with both anticoagulant and antiplatelet agents	52/694 (7)	66/1,331 (5)
Unspecified antithrombotic treatment	44/694 (6)	59/1,331 (4)

Abbreviation: AIS = arterial ischemic stroke.
[a] Fisher exact test showed statistically significant association with the presence of arteriopathy before multiple-comparisons adjustment.
[b] Significant infection defined as meningitis or mastoiditis; nonsignificant infections included sinusitis, otitis media, and pharyngitis.

indicated in the IPSS dataset, 164 (23%) were labeled as having an arteriopathy by the site investigators. As stated in the Methods section, arteriopathy cases with insufficient information or unclear diagnosis were rereviewed by the study investigators for any radiology information in the dataset, and those with no radiologic data to support the arteriopathy diagnosis were sent to the reporting site investigator for review of their radiology information to confirm the diagnosis and type of arteriopathy (figure 1A).

Tables 1 and 2 lists the demographic and clinical features of AIS and specifies all variables that were significantly associated with arteriopathy ($p \leq 0.05$) before multiple-comparison adjustment. Results (p values and odds ratios [ORs]) from multivariable analysis are stated in the section below (table 3).

Arteriopathic vs nonarteriopathic AIS

Children with arteriopathy-associated AIS were older compared to children with nonarteriopathic causes (median age 7.45 years [interquartile range 3.68–12.76] vs 4.6 years [interquartile range 1.11–12.18 years], $p < 0.0001$ [$z = 7.05$]), with the highest likelihood of AIS due to an arteriopathic cause occurring in 6- to 9-year-old children ($p = 0.029$, OR 1.93, 95% confidence interval [CI] 1.1–3.5) (figure 2A). There were equal proportions of boys (58% [423 of 725] arteriopathic AIS vs 57% [806 of 1,402] nonarteriopathic

Table 3 Demographic and clinical associations with arteriopathy in childhood AIS[a]

	Available data	Univariate analysis		Multivariable analysis[b]	
Variables	**No.**	**OR (CI)**	***p* Value**	**OR (CI)**	***p* Value**
Age (ref = 15–18 y), y[c]	2,124				
0–<3		0.52 (0.39–0.71)	<0.0001	0.93 (0.51–1.69)	0.810
3–<6		1.47 (1.06–2.03)	0.020	1.72 (0.97–3.04)	0.063
6–<9		2.16 (1.54–3.04)	<0.0001	1.93 (1.07–3.51)	0.029
9–12		1.34 (0.93–1.92)	0.116	1.81 (0.97–3.36)	0.061
12–<15		1.44 (1.02–2.03)	0.036	1.70 (0.92–3.14)	0.087
Race (ref = other)	1,485				
Black		2.24 (1.52–3.31)	<0.0001		
White		1.31 (1.00–1.71)	0.049		
Hemiparesis (ref = none)	2,028				
Bilateral		1.01 (0.59–1.75)	0.960		
Unilateral		1.45 (1.15–1.81)	0.001		
Speech deficit (ref = none)	1,794				
Aphasia		1.25 (0.98–1.60)	0.073		
Dysarthria		1.83 (1.43–2.34)	<0.0001		
Both		1.27 (0.58–2.81)	0.552		
Headache	1,729	1.92 (1.57–2.35)	<0.0001	1.55 (1.06–2.25)	0.023
Prior/concurrent thromboembolism	1,862	1.87 (1.43–2.43)	<0.0001		
Multiple infarction	1,675	1.89 (1.54–2.31)	<0.0001	2.05 (1.45–2.91)	<0.0001
Non iatrogenic trauma (ref = none)	2,125	1.74 (1.29–2.36)	0.0004	1.93 (1.12–3.31)	0.018
Sickle cell anemia	2,125	3.34 (2.19–5.08)	<0.0001	2.90 (1.32–6.34)	0.007
Treated with antithrombotic agent	2,025	2.11 (1.65–2.70)	<0.0001	1.87 (1.11–3.15)	0.018
Deficit at discharge	1,864	1.45 (1.14–1.83)	0.002		
Stroke recurrence	1,819	3.17 (2.38–4.21)	<0.0001	2.37 (1.46–3.84)	0.0004

Abbreviation: AIS = arterial ischemic stroke; CI = confidence interval; OR = odds ratio; ref = referent.
[a] Multiple logistic regression analysis. Includes significantly associated variables after multiple-comparisons adjustment.
[b] Area under the curve 70%.
[c] Age, as either continuous or categorical variable, was significant in univariate analysis. In multivariable analysis, age as categorical variable was used due to the nonlinear relationship between age and many of the other variables. For example, trauma history is more common in young children, lower in middle childhood, and then higher again in teenagers (U-shaped curve relationship).

Figure 2 Association of age

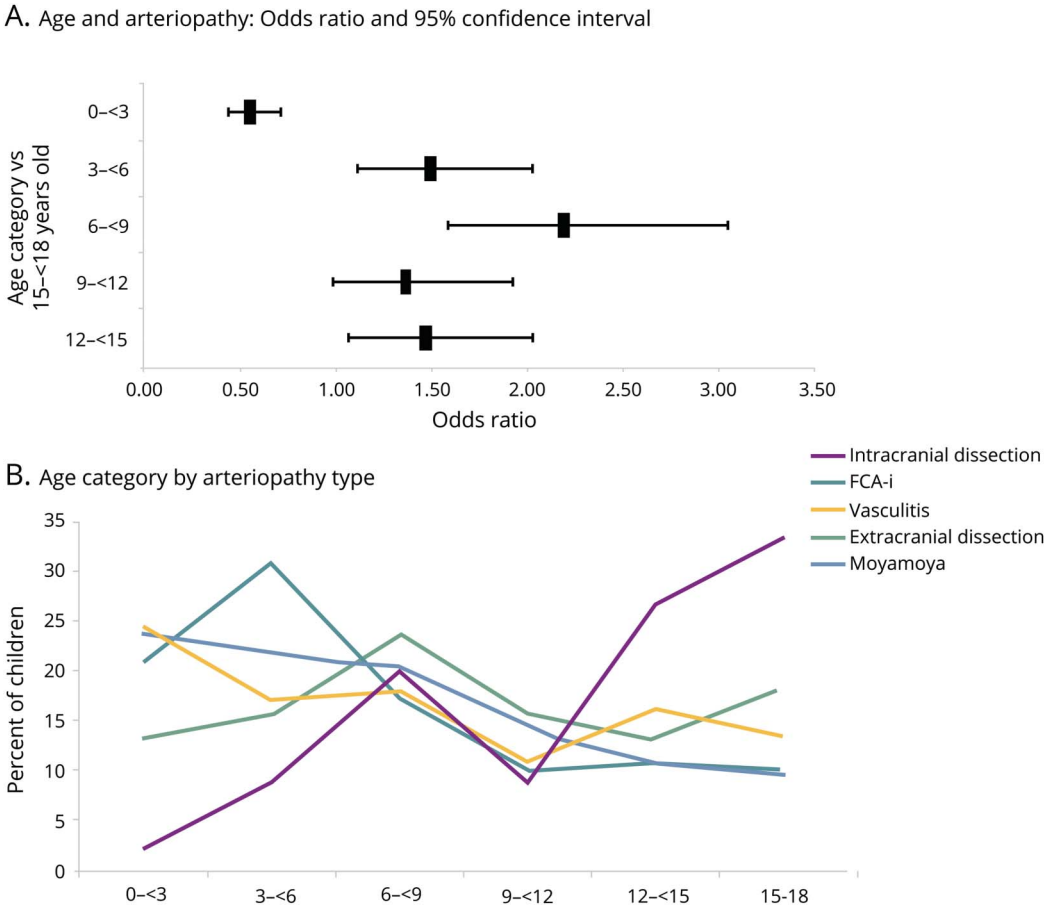

(A) Association of age and arteriopathy in children with arterial ischemic stroke (AIS). (B) Age distribution in children with AIS by arteriopathy type. FCA-i = focal cerebral arteriopathy–inflammatory subtype.

AIS) and whites (65% [321 of 725] arteriopathic AIS vs 65% [648 of 993] nonarteriopathic AIS) in each group (table 1). Geographic differences were observed, with Asia (19%) and South America (23%) having smaller proportions of arteriopathic AIS compared to other continents (35%–37%, $p < 0.0003$ [$\chi^2 = 21$, $df = 4$]) (figure 3). However, these geographic differences were not significant on multivariable analysis.

Children with arteriopathy associated AIS were more likely to present with headache ($p = 0.023$, OR 1.55, 95% CI 1.0–2.2) and multiple infarctions ($p < 0.0001$, OR 2.05, 95% CI 1.4–2.9) than those with nonarteriopathic AIS. Sickle cell anemia ($p = 0.007$, OR 2.9, 95% CI 1.3–6.3) and head or neck trauma ($p = 0.018$, OR 1.93, 95% CI 1.1–3.3) were risk factors for AIS associated with arteriopathy (table 3).

Children with arteriopathy-associated AIS were more likely to be treated with antithrombotic treatment (86% [595 of 694] arteriopathic vs 74% [985 of 1,331] nonarteriopathic AIS, $p = 0.018$, OR 1.87). Although not statistically significant, an increase in the use of antithrombotic treatment over time was noted (73% in 2003–2006, 78% in 2007–2010, and 83% in 2011–2014, $p = 0.082$) (table 3). We observed significant differences in treatment patterns between geographic regions/continents in arteriopathic AIS ($p = 0.006$ [$\chi^2 = 14$, $df = 4$]). The proportion of cases of AIS with arteriopathy receiving antithrombotic treatment was highest in Australia (97%), Europe (87%), and North America (86%) compared to Asia (74%) and South America (65%) (figure 3).

Discharge outcome was available in 88% and longitudinal outcomes were available in 37% of cases (mean duration 2.4 years, range 3 months–12.1 years). Children with arteriopathy-associated AIS had a higher likelihood of deficits at discharge (82% [538 of 659] arteriopathic vs 75% [909 of 1,205] nonarteriopathic AIS, $p = 0.002$). Longitudinal outcomes, measured by the PSOM, were not different between the 2 groups both at 1 year (52% [63 of 121] arteriopathic vs 51% [109 of 214] nonarteriopathic AIS) and at last measured PSOM (57% [159 of 279] vs 52% [266 of 510]). Overall ischemic stroke recurrence risk was 12% (226 of 1,819), with significantly higher risk in arteriopathic compared to nonarteriopathic AIS (21% [131 of 614] arteriopathic vs 8% [95 of 1,205] nonarteriopathic AIS, $p = 0.0004$, OR 2.37, 95% CI 1.5–3.8) (table 3).

Figure 3 Distribution of arteriopathy and first reported treatment of arteriopathy by geographic region

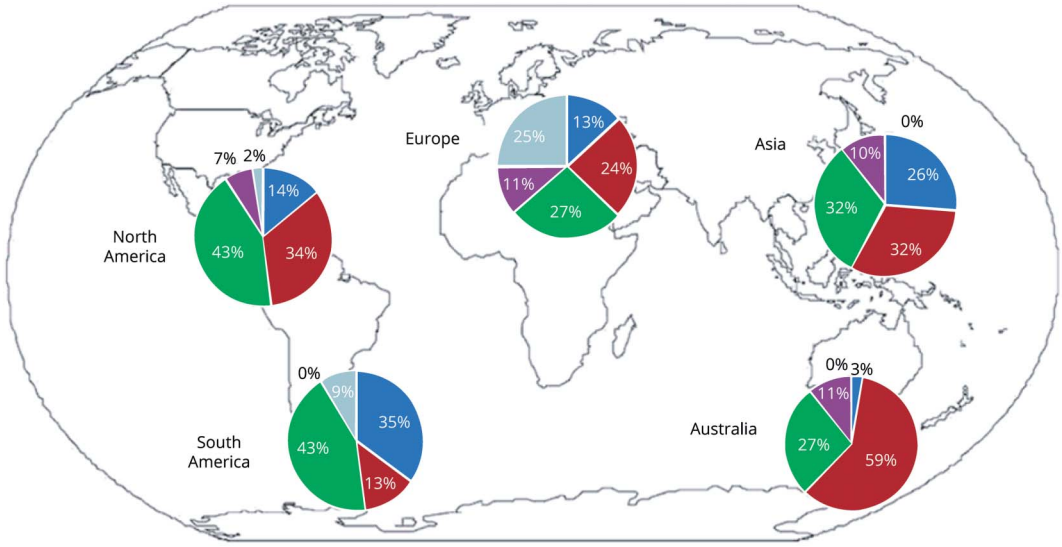

Treatment of patients with arteriopathy (N = 694/725) (96%)

- None
- Anticoagulation
- Antiplatelet
- Both anticoagulation and antiplatelet
- Unspecified antithrombotic type

Number of centers and study population by region*

	N. America	Europe	Australia	S. America	Asia
Total study population	1,429	348	103	131	113
Arteriopathy cases	506	129	38	30	22
Numbers of centers	51	15	2	7	6

AIS characteristics by arteriopathy subtype

Each arteriopathy subtype demonstrated interesting differences compared to other arteriopathies (figure 2B and tables e-1 and e-2, doi.org/10.5061/dryad.7d7wm37r3). Cases with intracranial dissection were typically >15 years of age (27%, $p = 0.035$, OR 2.3, 95% CI 1.1–5.1), while extracranial dissection was associated with male sex (80%, $p = 0.001$, OR 3.17, 95% CI 1.6–6.4). With age as a continuous variable, a per-unit increase in age was associated with an increased risk for intracranial dissection ($p < 0.0001$, OR 1.18), FCA-i ($p = 0.015$, OR 0.95), or moyamoya ($p = 0.026$, OR 0.96). Black race was common with moyamoya (24% vs 3%–11%, $p = 0.002$, OR 3.81, 95% CI 1.6–8.8) and white race with FCA-i (81% vs 49%–77%, $p = 0.009$, OR 2.79, 95% CI, 1.3–6.0).

In univariate analysis, statistically significant variations in geographic distribution of arteriopathy subtypes were observed. Post hoc analysis looking at proportion of subtypes within each region was conducted to account for the variability in the number of sites enrolling in IPSS per region (of 86 sites: South America 9 [10%], North America 54 [63%], Europe 15 [17%], Australia 2 [2%], and Asia 6 [7%]). Compared to other subtypes, FCA-i diagnosis was highest in Europe (37 of 82 [45%], $p < 0.0001$ [$\chi^2 = 47$, $df = 4$]) and Australia (16 of 35 [45%], $p = 0.001$ [$\chi^2 = 18$, $df = 4$]), and moyamoya diagnosis was highest in North America (138 of 364 [38%], $p < 0.0001$ [$\chi^2 = 45$, $df = 4$]). No significant differences in the proportion of subtypes were observed in South America and Asia (table e-1, doi.org/10.5061/dryad.7d7wm37r3).

In a comparison of arteriopathy subtypes (table e-2, doi.org/10.5061/dryad.7d7wm37r3), clinical presentations that were more prevalent with a specific arteriopathy subtype included head or neck trauma with both intracranial (38%, $p < 0.0003$, OR 4.19, 95% CI 1.9–9.0) and extracranial (37%, $p < 0.0001$, OR 5.02, 95% CI 2.5–10.3) dissection; headache (78%, $p = 0.0004$, OR 4.20, 95% CI 1.9–9.2) with intracranial dissection; posterior circulation involvement (52%, $p < 0.0001$, OR 3.65, 95% CI 1.9–6.7) with extracranial dissection; seizures (31%, $p = 0.004$, OR 2.62, 95% CI 1.3–5.1), bilateral infarction (37%, $p < 0.0004$, OR 3.97, 95% CI 1.9–8.4), and anterior circulation involvement (80%, $p < 0.0007$, OR 3.5, 95% CI 1.7–7.2) with moyamoya; unilateral hemiparesis (88%, $p = 0.02$, OR 2.95, 95% CI 1.1–7.5) and single infarcts (76%, $p < 0.0001$, OR 5.31, 95% CI 2.6–10.8) with FCA-i; and bilateral infarction (36%, $p = 0.03$, OR 1.71, 95% CI 1.0–2.8) and acute systemic findings (37%, $p < 0.0001$, OR 3.58, 95% CI 2.2–5.9) with vasculitis.

A higher proportion of cases with dissection were treated with an anticoagulation (62% extracranial [$p = 0.0008$, OR 2.79, 95% CI 1.5–5.1] and 53% intracranial dissection [$p = 0.02$ significant only in univariate analysis] vs 15%–39% other arteriopathy subtypes), whereas a higher proportion of cases with moyamoya received antiplatelet treatment (55% moyamoya [$p = 0.001$, OR 2.80, 95% CI 1.1–4.1] vs 29%–37% other arteriopathy subtypes).

Both discharge and long-term outcomes were not statistically different among the arteriopathy subtypes, except

that moyamoya arteriopathy was associated with the highest odds of having recurrent ischemic strokes (33%, $p = 0.01$, OR 2.17, 95% CI 1.1–4.1). In cases with moyamoya, stroke recurrence may have been affected by the timing of revascularization surgery. However, dates of surgery were inconsistently available, and this information could not be presented.

Discussion

We present the largest series of childhood AIS patients with and without arteriopathy, comparing their presentation, risk factors, treatments, and outcome. The proportion of children with arteriopathic AIS in our sample, both total and across geographic regions, is largely similar to what has previously been reported.[1,19] Lower frequencies of arteriopathic AIS in Asia and South America may have been due to underdiagnosis because MRI and other vascular imaging techniques are less available in these regions, although this finding might be an artifact of limited sites participating in the IPSS and needs further evaluation. Higher prevalences of young children with arteriopathy and male sex in childhood AIS have been previously reported[1,20] and are confirmed by this study. Recently, VIPS investigators reanalyzed their 355 cases with AIS and found 127 (36%) children with a radiologically confirmed arteriopathy. In their cohort, moyamoya disease more frequently affected children <8 years of age, FCA-i affected children between 8 and 15 years of age, and dissection affected all ages.[19] In the current IPSS cohort of children (including VIPS cases), cases with FCA-i were more likely to present between 3 and 6 years of age and cases with dissection were more common at >12 years of age, differing somewhat from the smaller VIPS dataset. In total, the bimodal distribution seen in all arteriopathies may be secondary to an increased prevalence of FCA-i and moyamoya among younger children and intracranial dissection among older children. These findings may be particularly important in future outcome studies because recovery from stroke is likely modified by age due to the location-specific vulnerability and plasticity in the developing brain.[21,22]

Many previously described clinical features and observations are confirmed by the current IPSS dataset, including the frequent occurrence of deficits at discharge, stroke recurrence, and multiple ischemic infarctions in children with arteriopathy.[9,10] The last is likely accounted for by arteriopathic involvement of multiple arteries or arterial segments and recurrent artery-to-artery thromboembolism. In addition, in children with sickle cell anemia, the sickle-associated arteriopathy combines with an increased baseline recurrent stroke risk from sickle cell anemia. Other study findings included frequent involvement of anterior circulation with moyamoya arteriopathy[23] and posterior circulation with extracranial dissection.[24,25] Furthermore, the finding of a high proportion of cases with seizures and bilateral infarction in children with moyamoya is also not entirely surprising because moyamoya arteriopathy involves bilateral arterial territories and causes varying ages of ischemic strokes as the disease slowly progresses.[23,26] On the same note, the presence of single infarcts with resultant hemiparesis in cases with FCA-i and bilateral infarction and acute systemic findings in cases with vasculitis can be explained by their etiopathologic involvement (typical unilateral focal arterial involvement in cases with FCA-i and bilateral diffuse arterial involvement in association with infectious or inflammatory conditions in cases with vasculitis).

Considering the large multinational IPSS dataset, the findings of the current study are generalizable to and highly representative of the childhood AIS population. While male sex and black race have previously been reported as risk factors for dissection and childhood AIS in general,[20,27] to the best of our knowledge, the very high percentage of male patients with extracranial dissection (80%) in our study is the highest reported to date. This finding may be secondary to increased head trauma in male patients,[27] although biological sex differences may also have contributed. A study comparing cases of pediatric ischemic stroke to controls has demonstrated a 1.3-fold increase in the risk for cerebral thromboembolism with each 1-nmol/L increase in testosterone in boys.[28] Furthermore, recent descriptions of V3 vertebral dissections in an exclusively male cohort[29] also suggest increased susceptibility to extracranial dissections among male patients. The proportion of cases of FCA in our cohort is smaller than reported previously (15% vs up to 25%)[2] and may be due to a lack of vascular imaging in all our patients. Geographic differences noted in this study are also interesting. Moyamoya diagnosis had the highest proportion in North America, whereas FCA-i diagnosis had the highest proportion in Europe and Australia. These findings may be related to the association between moyamoya and sickle cell anemia ($p < 0.0001$) and between sickle cell anemia and black race ($p < 0.0001$) in conjunction with the higher number of black children in North America (of 371 with AIS with race and region data, 45 of 48 [94%] of black children were in North America). The association of moyamoya and black race does not hold while controlling for the presence of sickle cell anemia. Of 25 patients with sickle cell anemia AIS with race data, 5 of 5 (100%) with vasculitis and 18 of 20 (90%) with moyamoya were black children (Fisher exact test $p = 0.99$).

The association of headache with arteriopathic childhood AIS is a clinically relevant finding in the current cohort.[30] While headache in childhood stroke has been reported, particularly with craniocervical arterial dissection,[24,30] this study demonstrates that the association is broad (across arteriopathic stroke types) and robust, with very high rates of headache in both extracranial (63%) and intracranial (78%) dissections. On the basis of these data, it is important for clinicians to consider and exclude dissection early in children with AIS who present with significant headache.[30]

The high rate of antithrombotic use acutely in children with arteriopathic AIS noted in the current cohort is similar to the previously reported increased use of antithrombotic

treatment over time.[10,31] This finding is largely reflective of current clinical practice and is likely driven by the increased awareness of high recurrence risk in cases with arteriopathy. The high rate of anticoagulation use acutely in children with extracranial dissection is reflective of the pediatric stroke management guidelines in use during the study period.[16,30] The high rate of anticoagulation use in intracranial dissection (53%) is surprising, however, and may be based on a few studies that suggested that anticoagulation is safe in cases of childhood arteriopathy.[32] Of note, despite published management guidelines for childhood stroke, ≈20% of cases of AIS received no acute antithrombotic treatment. It is unclear from these data whether this finding is due to a lack of adherence to published guidelines or, more likely, the withholding of antithrombotic therapy in circumstances when therapy may not be clearly indicated such as brain tumor, several intracranial infections, or sickle cell disease–associated strokes. This indicates an area in which further research, education, and outreach are required.

Despite the significant association between arteriopathy and risk for recurrent strokes, we found no statistically significant difference in short- and long-term outcomes between arteriopathic and nonarteriopathic AIS. The large amount of missing outcome data and the lack of longer follow-up duration to see the impact of stroke recurrence likely contributed to these nonsignificant results.

Limitations of this study include those typically associated with large cohort studies. Data may have been overreported or underreported. This finding is particularly germane to our follow-up results in that patients with a higher degree of medical impairment are more likely to seek medical care and may be overrepresented in follow-up data. These study participants were enrolled at academic centers, likely leading to referral bias; for example, AIS due to cardiac disease may be overrepresented due to the concentration of children with congenital heart disease at those centers.

In this study, few variables had significant amounts of missing data; namely, race was missing in 63% and PSOM data were missing in 37%. However, for most variables as listed in tables 1 and 2, the percentage of missing data in the current dataset is within the acceptable ranges for a large dataset (median 4.8%, mean 7.9%, range 0%–24.8%). While the large patient volume is strength of our cohort, all radiographic data are based on available radiology reports and the site investigator's interpretation, without centralized confirmation. Because the interrater reliability is only modest among trained raters,[11] imprecise classification of the AIS etiology and arteriopathy subtypes may have confounded our results. Furthermore, although the numbers are small, dedicated vascular imaging was not performed in all noncardiac cases of AIS. Other problems with validity and reliability may exist in these data.

Children with arteriopathic stroke have differentiating features compared to those without arteriopathic stroke and between each arteriopathy subtype. These observations may be helpful in guiding clinicians in managing arteriopathic cases of AIS by choosing appropriate investigations (e.g., head and neck vascular imaging) and treatment strategies. The evaluation of arteriopathy subtypes in our analysis may be particularly useful because initial radiographic diagnosis of arteriopathy does not always accurately determine the final classification; indeed, almost one-third of arteriopathies are challenging to classify. Among the 355 VIPS cases with AIS, 127 (35.7%) had definite arteriopathy and 34 (9.5%) had possible arteriopathy. Of those with definite arteriopathy, only 109 (30.7%) cases could be classified with high certainty into an arteriopathy subtype.[2] Another example, intracranial dissection, may be diagnosed on conventional angiogram performed outside of the acute phase of stroke, and 6% of patients with initial diagnosis of FCA progress to the diagnosis of moyamoya.[8] Therefore, these observations may assist clinicians in the earlier diagnoses of specific arteriopathy subtypes and appropriate treatment strategies. The results will also serve to define patient subgroups who are at higher risk for adverse outcomes and are likely to benefit most from future therapeutic trials. Specifically, these findings may assist in identifying pediatric patients for inclusion in steroid trials in the FCA-i population, studies evaluating the efficacy of antithrombotic management in extracranial dissection (in particular, utility of anticoagulant therapy because pediatric patients reportedly have higher rates for recurrent stroke compared to adult patients),[25] and trials examining the role of long-term transfusion in sickle cell disease.

Acknowledgment

The authors are extremely thankful to all the children with AIS and their families who participated in the International Pediatric Stroke Study and feel privileged to be able to provide medical care to them.

Study funding

Mubeen F. Rafay is supported by a research operating grant from the Children Hospital Research Institute of Manitoba. Dr. Timothy J. Bernard is supported by the Health Resources and Services Administration (HRSA) of the US Department of Health and Human Services (HHS) under grant 2H30MC24049, Mountain States Hemophilia Network. This information or content and conclusions are those of the author and should not be construed as the official position or policy of, nor should any endorsements be inferred by, HRSA, HHS, or the US government. Dr. Gabrielle deVeber and Dr. Heather J. Fullerton are supported by NIH R01 NS062820. Dr. Bernhard Weschke has received funding from the European Community's Seventh Framework Program (FP7/2007-2013) under grant 602391 (epistop.eu). The IPSS is graciously supported by The Auxilium Foundation.

Disclosure

The authors report no disclosures relevant to the manuscript. Go to Neurology.org/N for full disclosures.

Publication history

Received by *Neurology* July 4, 2019. Accepted in final form November 25, 2019.

Appendix 1 Authors

Name	Location	Contribution
Mubeen F. Rafay, MBBS, MSc	University of Manitoba, Winnipeg, Canada	Designed and conceptualized the study, enrolled cases and acquired data as site investigator (n = 151), validated and analyzed the data and developed the statistical methodology for the current study, interpreted the data, and drafted, edited, and finalized the manuscript for intellectual content
Kevin A. Shapiro, MD	University of California, San Francisco	Contributed to the acquisition of data and participated in drafting, revising and editing the manuscript for intellectual content
Ann-Marie Surmava, MBA	University of Toronto, Ontario, Canada	Data cleaning and validation, statistical methodology and analysis, and critical review and editing of the manuscript for the intellectual content
Gabrielle A. deVeber, MD, MSc	University of Toronto, Ontario, Canada	Original IPSS investigator and site investigator: contributed to the conceptualization, design, and establishment of IPSS, enrollment of cases (n = 427), and acquisition of the data; for the current study, contributed to the validation, analysis, and interpretation of the data and critical review and revision of the manuscript for intellectual content
Adam Kirton, MD	University of Calgary, Alberta, Canada	Contributed to the enrollment of cases (n = 110) and acquisition of the data as site investigator and critical review and revision of the manuscript for intellectual content
Heather J. Fullerton, MD	University of California, San Francisco	Contributed to the enrollment of cases (n = 71) and acquisition of the data as site investigator and critical review and revision of the manuscript for intellectual content
Catherine Amlie-Lefond, MD	University of Washington, Seattle	Contributed to the enrollment of cases (n = 28) and acquisition of the data as site investigator and critical review and revision of the manuscript for intellectual content
Bernhard Weschke, MD	Charité University Medicine Berlin, Germany	Contributed to the acquisition of the data and critical review and revision of the manuscript for intellectual content
Nomazulu Dlamini, MBBS	University of Toronto, Ontario, Canada	Contributed to the enrollment of cases (n = 427) and acquisition of the data as site investigator and critical review and revision of the manuscript for intellectual content
Jessica L. Carpenter, MD	George Washington University, Washington, DC	Contributed to the enrollment of cases (n = 105) and acquisition of the data as site investigator and critical review and revision of the manuscript for intellectual content
Mark T. Mackay, MBBS, PhD	University of Melbourne, Australia	Contributed to the enrollment of cases (n = 215) and the acquisition of the data as site investigator and critical review and revision of the manuscript for intellectual content
Michael Rivkin, MD	Harvard Medical School, Boston, MA	Contributed to the enrollment of cases (n = 97) and the acquisition of the data as site investigator and critical review and revision of the manuscript for intellectual content
Alexandra Linds, MSc	University of Toronto, Ontario, Canada	Contributed to the data validation and critical review of the manuscript for intellectual content
Timothy J. Bernard, MD	University of Colorado, Denver	Contributed to the study design, enrolled cases (n = 185), and acquired the data as site investigator; for the current study, interpreted the data and critically reviewed, edited, and supervised the manuscript for intellectual content

Appendix 2 coinvestigators

Coinvestigators are listed at [SDC link to supplemental file links.lww.com/WNL/B92].

References

1. Amlie-Lefond C, Bernard TJ, Sebire G, et al. Predictors of cerebral arteriopathy in children with arterial ischemic stroke: results of the International Pediatric Stroke Study. Circulation 2009;119:1417–1423.
2. Wintermark M, Hills NK, deVeber GA, et al. Arteriopathy diagnosis in childhood arterial ischemic stroke: results of the Vascular Effects of Infection in Pediatric Stroke Study. Stroke 2014;45:3597–3605.
3. Chabrier S, Rodesch G, Lasjaunias P, Tardieu M, Landrieu P, Sebire G. Transient cerebral arteriopathy: a disorder recognized by serial angiograms in children with stroke. J Child Neurol 1998;13:27–32.
4. Fullerton HJ, Stence N, Hills NK, et al. Focal cerebral arteriopathy of childhood. Stroke 2018;49:2590–2596.
5. Sebire G, Fullerton H, Riou E, DeVeber G. Toward the definition of cerebral arteriopathies of childhood. Curr Opin Pediatr 2004;16:617–622.
6. Sebire G, Meyer L, Chabrier S. Varicella as a risk factor for cerebral infarction in childhood: a case-control study. Ann Neurol 1999;45:679–680.
7. Dlamini N, Freeman JL, Mackay MT, et al. Intracranial dissection mimicking transient cerebral arteriopathy in childhood arterial ischemic stroke. J Child Neurol 2011;26:1203–1206.
8. Braun KP, Bulder MM, Chabrier S, et al. The course and outcome of unilateral intracranial arteriopathy in 79 children with ischaemic stroke. Brain 2009;132:544–557.
9. Fullerton HJ, Wintermark M, Hills NK, et al. Risk of recurrent arterial ischemic stroke in childhood: a prospective international study. Stroke 2016;47:53–59.
10. Goldenberg NA, Bernard TJ, Fullerton HJ, Gordon A, DeVeber G. Antithrombotic treatments, outcomes, and prognostic factors in acute childhood-onset arterial ischaemic stroke: a multicentre, observational, cohort study. Lancet Neurol 2009;8:1120–1127.

11. Bernard TJ, Beslow LA, Manco-Johnson MJ, et al. Inter-rater reliability of the CASCADE criteria: challenges in classifying arteriopathies. Stroke 2016;47:2443–2449.
12. Braun KP, Rafay MF, Uiterwaal CS, Pontigon AM, DeVeber G. Mode of onset predicts etiological diagnosis of arterial ischemic stroke in children. Stroke 2007;38:298–302.
13. Database for Stroke in Infants and Children. 18 A.D. Available at: clinicaltrials.gov/ct2/show/NCT00084292?cond=pediatric+stroke&rank=5. Accessed May 16, 2020.
14. Bernard TJ, Manco-Johnson MJ, Lo W, et al. Towards a consensus-based classification of childhood arterial ischemic stroke. Stroke 2012;43:371–377.
15. Sebire G. Transient cerebral arteriopathy in childhood. Lancet 2006;368:8–10.
16. Roach ES, Golomb MR, Adams R, et al. Management of stroke in infants and children: a scientific statement from a special Writing Group of the American Heart Association Stroke Council and the Council on Cardiovascular Disease in the Young. Stroke 2008;39:2644–2691.
17. Kitchen L, Westmacott R, Friefeld S, et al. The Pediatric Stroke Outcome Measure: a validation and reliability study. Stroke 2012;43:1602–1608.
18. Lo WD, Ichord RN, Dowling MM, et al. The Pediatric Stroke Recurrence and Recovery questionnaire: validation in a prospective cohort. Neurology 2012;79:864–870.
19. Wintermark M, Hills NK, deVeber GA, et al. Clinical and imaging characteristics of arteriopathy subtypes in children with arterial ischemic stroke: results of the VIPS study. AJNR Am J Neuroradiol 2017;38:2172–2179.
20. Golomb MR, Fullerton HJ, Nowak-Gottl U, DeVeber G. Male predominance in childhood ischemic stroke: findings from the International Pediatric Stroke Study. Stroke 2009;40:52–57.
21. Allman C, Scott RB. Neuropsychological sequelae following pediatric stroke: a non-linear model of age at lesion effects. Child Neuropsychol 2013;19:97–107.
22. Westmacott R, Askalan R, MacGregor D, Anderson P, DeVeber G. Cognitive outcome following unilateral arterial ischaemic stroke in childhood: effects of age at stroke and lesion location. Dev Med Child Neurol 2010;52:386–393.
23. Rafay MF, Armstrong D, Dirks P, MacGregor DL, DeVeber G. Patterns of cerebral ischemia in children with moyamoya. Pediatr Neurol 2015;52:65–72.
24. Fullerton HJ, Johnston SC, Smith WS. Arterial dissection and stroke in children. Neurology 2001;57:1155–1160.
25. Rafay MF, Armstrong D, DeVeber G, Domi T, Chan A, MacGregor DL. Craniocervical arterial dissection in children: clinical and radiographic presentation and outcome. J Child Neurol 2006;21:8–16.
26. Smith ER, Scott RM. Moyamoya: epidemiology, presentation, and diagnosis. Neurosurg Clin N Am 2010;21:543–551.
27. Hills NK, Johnston SC, Sidney S, Zielinski BA, Fullerton HJ. Recent trauma and acute infection as risk factors for childhood arterial ischemic stroke. Ann Neurol 2012;72:850–858.
28. Normann S, de Veber G, Fobker M, et al. Role of endogenous testosterone concentration in pediatric stroke. Ann Neurol 2009;66:754–758.
29. Rollins N, Braga B, Hogge A, Beavers S, Dowling M. Dynamic arterial compression in pediatric vertebral arterial dissection. Stroke 2017;48:1070–1073.
30. Billinghurst L, Hills N, Jastrzab L, et al. Headache presentation in childhood arterial ischemic stroke differs by arteriopathy subtype. Stroke 2017;48:A174.
31. DeVeber G, Kirton A, Booth FA, et al. Epidemiology and outcomes of arterial ischemic stroke in children: the Canadian Pediatric Ischemic Stroke Registry. Ann Neurol 2017;69:58–70.
32. Bernard TJ, Goldenberg NA, Tripputi M, Manco-Johnson MJ, Niederstadt T, Nowak-Gottl U. Anticoagulation in childhood-onset arterial ischemic stroke with non-moyamoya arteriopathy: findings from the Colorado and German (COAG) Collaboration. Stroke 2009;40:2869–2871.

Endovascular thrombectomy for childhood stroke (Save ChildS Pro): an international, multicentre, prospective registry study

Peter B Sporns, Kartik Bhatia, Todd Abruzzo, Lisa Pabst, Stuart Fraser, Melissa G Chung, Warren Lo, Ahmed Othman, Sebastian Steinmetz, Ulf Jensen-Kondering, Stefan Schob, Daniel P O Kaiser, Wolfgang Marik, Christina Wendl, Ilka Kleffner, Hans Henkes, Hermann Kraehling, Thi Dan Linh Nguyen-Kim, René Chapot, Umut Yilmaz, Furene Wang, Muhammad Ubaid Hafeez, Flavio Requejo, Nicola Limbucci, Birgit Kauffmann, Markus Möhlenbruch, Omid Nikoubashman, Peter D Schellinger, Patricia Musolino, Ali Alawieh, Jenny Wilson, Dominik Grieb, Alexandra S Gersing, Thomas Liebig, Martin Olivieri, Jaroslava Paulasova Schwabova, Ales Tomek, Panagiotis Papanagiotou, Grégoire Boulouis, Olivier Naggara, Christine K Fox, Kirill Orlov, Alexandra Kuznetsova, Carmen Parra-Farinas, Prakash Muthusami, Robert W Regenhardt, Adam A Dmytriw, Tanja Burkard, Mesha Martinez, Daniel Brechbühl, Maja Steinlin, Lisa R Sun, Ameer E Hassan, André Kemmling, Sarah Lee, Heather J Fullerton, Jens Fiehler, Marios-Nikos Psychogios, Moritz Wildgruber**

Lancet Child Adolesc Health 2024; 8: 882–90

Published Online October 11, 2024 https://doi.org/10.1016/S2352-4642(24)00233-5

See Comment page 844

*Contributed equally

Department of Neuroradiology, University Hospital Basel, Basel, Switzerland (P B Sporns MD MHBA, Prof M-N Psychogios MD); Department of Diagnostic and Interventional Neuroradiology, University Medical Center Hamburg-Eppendorf, Hamburg, Germany (P B Sporns, Prof J Fiehler MD); Department of Radiology and Neuroradiology, Stadtspital Zürich, Zürich, Switzerland (P B Sporns, T D L Nguyen-Kim MD); Department of Medical Imaging, Children's Hospital at Westmead, Sydney, NSW, Australia (K Bhatia MD); Children's Hospital at Westmead Clinical School, Faculty of Medicine and Health, University of Sydney, Sydney, NSW, Australia (K Bhatia); Department of Neurosurgery, Barrow Neurological Institute, Phoenix, AZ, USA (Prof T Abruzzo MD); Department of Radiology, Phoenix Children's Hospital, Phoenix, AZ, USA (Prof T Abruzzo); Division of Pediatric Neurology, Department of Pediatrics, University of Utah School of Medicine, Salt Lake City, UT, USA (L Pabst MD); Division of Child and Adolescent Neurology, Department of Pediatrics, The University of

Summary

Background Emerging evidence suggests that endovascular thrombectomy is beneficial for treatment of childhood stroke, but the safety and effectiveness of endovascular thrombectomy has not been compared with best medical treatment. We aimed to prospectively analyse functional outcomes of endovascular thrombectomy versus best medical treatment in children with intracranial arterial occlusion stroke.

Methods In this prospective registry study, 45 centres in 12 countries across Asia and Australia, Europe, North America, and South America reported functional outcomes for children aged between 28 days and 18 years presenting with arterial ischaemic stroke caused by a large-vessel or medium-vessel occlusion who received either endovascular thrombectomy plus best medical practice or best medical treatment alone. Intravenous thrombolysis was considered part of best medical treatment and therefore permitted in both groups. The primary outcome was the difference in median modified Rankin Scale (mRS) score between baseline (pre-stroke) and 90 days (±10 days) post-stroke, assessed by the Wilcoxon rank test (α=0·05). Efficacy outcomes in the endovascular thrombectomy and best medical treatment groups were compared in sensitivity analyses using propensity score matching. The Save ChildS Pro study is registered at the German Clinical Trials Registry, DRKS00018960.

Findings Between Jan 1, 2020, and Aug 31, 2023, of the 241 patients in the Save ChildS Pro registry, 208 were included in the analysis (115 [55%] boys and 93 [45%] girls). 117 patients underwent endovascular thrombectomy (median age 11 years [IQR 6–14]), and 91 patients received best medical treatment (6 years [3–12]; p<0·0001). The median Pediatric National Institutes of Health Stroke Scale (PedNIHSS) score on admission was 14 (IQR 10–19) in the endovascular thrombectomy group and 9 (5–13) in the best medical treatment group (p<0·0001). Both treatment groups had a median pre-stroke mRS score of 0 (IQR 0–0) at baseline. The change in median mRS score between baseline and 90 days was 1 (IQR 0–2) in the endovascular thrombectomy group and 2 (1–3) in the best medical treatment group (p=0·020). One (1%) patient developed a symptomatic intracranial haemorrhage (this patient was in the endovascular thrombectomy group). Six (5%) patients in the endovascular thrombectomy group and four (5%) patients in the best medical treatment group had died by day 90 (p=0·89). After propensity score matching for age, sex, and PedNIHSS score at hospital admission (n=79 from each group), the change in median mRS score between baseline and 90 days was 1 (IQR 0–2) in the endovascular thrombectomy group and 2 (1–3) in the best medical treatment group (p=0·029). Regarding the primary outcome for patients with suspected focal cerebral arteriopathy, endovascular thrombectomy (n=18) and best medical treatment (n=33) showed no difference in 90-day median mRS scores (2 [IQR 1–3] *vs* 2 [1–4]; p=0·074).

Interpretation Clinical centres tended to select children with more severe strokes (higher PedNIHSS score) for endovascular thrombectomy. Nevertheless, endovascular thrombectomy was associated with improved functional outcomes in paediatric patients with large-vessel or medium-vessel occlusions compared with best medical treatment. Future studies need to investigate whether the positive effect of endovascular thrombectomy is confined to older and more severely affected children.

Funding None.

Research in context

Evidence before this study

We searched Pubmed (MEDLINE) for randomised controlled trials published between Jan 1, 2000, and Dec 31, 2023, using terms "EVT" and "ischemic stroke". Several randomised trials found a positive treatment effect of endovascular thrombectomy for adult patients with acute ischaemic stroke and large-vessel occlusion. Even though randomised trials would be the gold standard to determine the benefit of endovascular thrombectomy in children with intracranial arterial occlusion, conducting a randomised trial remains infeasible due to the rarity of the disease. Therefore, the best possible approach is a prospective cohort study of children with large-vessel occlusion stroke comparing functional outcomes after endovascular thrombectomy versus best medical treatment alone.

Added value of this study

We report an international multicentre registry study of 208 paediatric patients with arterial ischemic stroke caused by a large-vessel or medium-vessel occlusion treated with endovascular thrombectomy or best medical treatment. Despite higher stroke severity in the endovascular thrombectomy group at baseline, we found better functional outcomes in the endovascular thrombectomy group than in the best medical treatment group, as measured with the modified Rankin Scale and Pediatric Stroke Outcome Measure at 90 days after the stroke and decrease in the Pediatric National Institutes of Health Stroke Scale score from hospital admission to discharge. This effect was maintained after propensity score matching for age, sex, and initial stroke severity. These findings suggest that endovascular thrombectomy is associated with improved functional outcomes in paediatric patients with large-vessel or medium-vessel occlusions compared with best medical treatment alone.

Implications of all the available evidence

In the absence of randomised controlled trial data, the findings from this multinational prospective registry study with propensity score matching provide strong support for endovascular thrombectomy in children with arterial ischaemic stroke and medium or large arterial occlusion, which will inform future guidelines.

Introduction

Arterial ischaemic stroke affects 1·3–1·6 per 100 000 children every year in high-income countries,[1] and outcomes are potentially severe, with 70% of paediatric strokes resulting in long-term neurological deficits, 20% in recurrent strokes, and 10% in death.[2–4] In adult stroke care, endovascular thrombectomy has revolutionised the treatment of arterial ischaemic stroke caused by large-vessel occlusion.[6,22,23] Several randomised clinical trials published since 2015 have shown the efficacy and safety of endovascular recanalisation for large-vessel occlusions, with large effect size.[6] However, the accumulated experience and evidence from adult stroke research cannot be directly extrapolated to children. Aside from the immense challenges of recruiting and enrolling children with acute stroke into prospective studies, the aetiology of paediatric stroke is fundamentally different from adult stroke. Whereas atherosclerosis is a major risk factor for adult stroke, cardioembolic causes and arteriopathies are dominating factors in paediatric stroke.[1,14] Moreover, the paediatric brain might better compensate for ischaemic stroke than the adult brain due to the greater neuronal plasticity,[1,24] and leptomeningeal collaterals might be more efficient in children.[25] The benefit of recanalisation might therefore be reduced in children. Although technically feasible even in newborn infants,[26] thrombectomy devices are not designed for the small artery diameters needed for mechanical recanalisation in very young children. In addition, the exact time of the stroke ictus cannot be established in neonates, whose strokes present with encephalopathy or seizures rather than focal neurological deficits. The potential risk of damaging the cerebral vasculature, with subsequent arterial dissection or thrombosis, is a major concern for endovascular thrombectomy uptake.[9,11,14]

After several paediatric case series,[7] the retrospective Save ChildS study provided the first systematic evidence for the safety and effectiveness of endovascular thrombectomy in children.[8–10] Although outcomes were generally favourable, and recanalisation and adverse events in the Save ChildS study were comparable with those reported in large randomised controlled trials with adults, the major weakness of the retrospective cohort study design (the absence of a control patient group) limited the conclusions that could be drawn.[11] However, the conclusions were subsequently confirmed in the French KidClot study.[12] Outcomes of endovascular thrombectomy did not differ by sex, but remaining questions include whether the findings are reproducible in prospective multicentre settings, whether endovascular thrombectomy is possible in even younger children, and what are the effects of specific aetiologies, such as cerebral arteriopathies, on the safety and effectiveness of endovascular thrombectomy.[8,13,14]

Confident interpretation of the existing paediatric data has been hindered by an absence of population-based reporting of the natural history of stroke in children caused by large-vessel occlusions. According to a 2022 population-based cohort study of paediatric patients with arterial ischaemic stroke, where nearly a quarter of patients had large-vessel occlusions, outcomes of conservative treatment were significantly worse among those patients with large-vessel occlusions than those with non-large-vessel occlusion arterial ischaemic stroke.[15] In a matched case–control study of

Texas McGovern Medical School, Houston, TX, USA (S Fraser MD); **Division of Critical Care Medicine and Division of Pediatric Neurology, Department of Pediatrics, Nationwide Children's Hospital and The Ohio State University, Columbus, OH, USA** (M G Chung MD); **Department of Pediatrics and Department of Neurology, Nationwide Children's Hospital and The Ohio State University, Columbus, OH, USA** (Prof W Lo MD); **Department of Neuroradiology, University Medical Center of the Johannes Gutenberg University, Mainz, Germany** (Prof A Othman MD, S Steinmetz MD); **Department of Radiology and Neuroradiology, University Medical Center Schleswig-Holstein, Kiel, Germany** (U Jensen-Kondering MD); **Department of Neuroradiology, University Medical Center Schleswig-Holstein, Lübeck, Germany** (U Jensen-Kondering); **Department of Radiology and Neuroradiology, University Hospital Halle, Halle, Germany** (S Schob MD); **Institute of Neuroradiology, Medical Faculty and University Hospital Carl Gustav Carus, Dresden University of Technology, Dresden, Germany** (D P O Kaiser MD); **Department of Neuroradiology, Medical University of Vienna, Vienna, Austria** (W Marik MD); **Institute of Radiology, University Hospital Regensburg, Regensburg, Germany** (Prof C Wendl MD); **Department of Neurology, University Hospital Knappschaftskrankenhaus, Ruhr University Bochum, Bochum, Germany** (I Kleffner MD); **Neuroradiological Clinic, Katharinenhospital, Klinikum Stuttgart, Stuttgart, Germany** (Prof H Henkes MD); **Clinic for Radiology, Department for Interventional Neuroradiology, University of Münster, Münster, Germany** (H Kraehling MD); **Department of Neuroradiology, Alfried-Krupp-Krankenhaus, Essen, Germany** (Prof R Chapot MD); **Department of Neuroradiology, Saarland University Hospital, Homburg, Germany** (U Yilmaz MD);

Department of Paediatrics, Khoo Teck Puat-National University Children's Medical Institute, National University Hospital, Singapore (F Wang MD)**; Department of Neurology, Baylor College of Medicine, Houston, TX, USA** (M U Hafeez MD)**; Department of Neuroradiology, Hospital de Pediatría J.P. Garrahan, Buenos Aires, Argentina** (F Requejo MD)**; Department of Interventional Neuroradiology, Careggi University Hospital, Florence, Italy** (N Limbucci MD)**; Department of Pediatrics and Adolescent Medicine, Eltern-Kind-Zentrum Prof Hess, Klinikum Bremen Mitte, Bremen, Germany** (B Kauffmann MD)**; Department of Neuroradiology, Heidelberg University Hospital, Heidelberg, Germany** (Prof M Möhlenbruch MD)**; Department of Neuroradiology, Aachen University, Aachen, Germany** (Prof O Nikoubashman MD)**; Department of Neurology and Neurogeriatrics, University Clinic of the Ruhr-Universität Bochum, Minden, Germany** (Prof P D Schellinger MD)**; Department of Neurology** (P Musolino MD) **and Neuroendovascular Program** (R W Regenhardt MD, A A Dmytriw MD)**, Massachusetts General Hospital, Harvard Medical School, Boston, MA, USA; Department of Neurosurgery, Emory University School of Medicine, Atlanta, GA, USA** (A Alawieh MD)**; Division of Pediatric Neurology, Oregon Health & Science University, Portland, OR, USA** (J Wilson MD)**; Department of Radiology and Neuroradiology, Sana Kliniken Duisburg, Duisburg, Germany** (D Grieb MD)**; Department of Diagnostic and Interventional Neuroradiology, Medical School Hannover, Hannover, Germany** (D Grieb)**; Department of Neuroradiology** (Prof A S Gersing MD, Prof T Liebig MD) **and Department of Radiology** (T Burkard MD MSc, Prof M Wildgruber MD PhD)**, LMU University Hospital, LMU Munich, Munich, Germany; Pediatric Thrombosis and Hemostasis Unit, Dr von Hauner Children's Hospital, LMU Munich,**

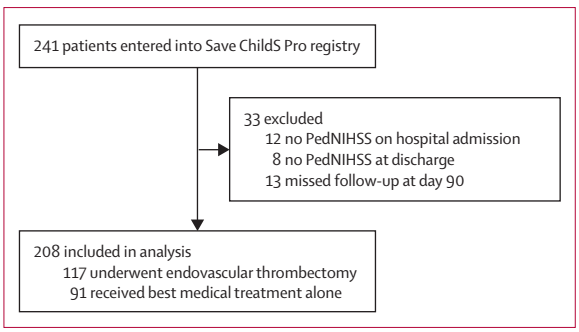

Figure 1: **Flow chart for Save ChildS Pro registry inclusion**
PedNIHSS=Pediatric National Institutes of Health Stroke Scale.

52 patients aged 2–18 years with anterior circulation large-vessel occlusion stroke,[16] clinical outcomes were better with endovascular thrombectomy than with medical management alone, even when applying a hierarchal matching system for site of occlusion, age group, side of occlusion, and sex.

Additional barriers to implementing reperfusion therapies in paediatric stroke care include slow triage and imaging pathways.[17] Historic beliefs also maintain that children with large-vessel occlusions present too late for reperfusion[18] and have better outcomes with conservative treatment than adults do.[19] Considering the difficulties of conducting a randomised trial in paediatric patients with stroke (eg, difficulties with recruitment led to the premature termination of the prospective Thrombolysis in Pediatric Stroke trial[5]), and the large treatment effect of endovascular thrombectomy in adults, a randomised trial of recanalisation treatments in children is unlikely to succeed. A prospective multicentre registry was therefore considered the best option to generate evidence regarding hyperacute recanalisation treatments in children with arterial ischaemic stroke. Drawing on data accumulated in the prospective Save ChildS Pro registry, the aim of this study was to compare functional outcomes of endovascular thrombectomy and best medical treatment in children presenting with arterial ischaemic stroke.

Methods

Study design and participants

Save ChildS Pro is an international prospective cohort study of children who presented with acute arterial ischaemic stroke across 53 centres in Europe, North America, South America, Asia, and Australia.[13] Participating centres are listed in the appendix (pp 8–14). 45 centres contributed eligible patient data that were included in this analysis.

Registry inclusion criteria were age 28 days to 18 years, a clinical diagnosis of arterial ischaemic stroke, confirmed diagnosis of intracranial arterial occlusion consistent with symptoms including occlusion of terminal internal carotid artery, middle cerebral artery (M1, M2 segments), basilar artery, vertebral artery (V4 segment), anterior cerebral artery (A1, A2 segments), posterior cerebral artery (P1, P2 segments), and proximal superior cerebellar artery. Neonates with stroke were excluded.

Procedures

All patients included in the Save ChildS Pro registry received best medical treatment, including systemic thrombolysis, platelet inhibition, and anticoagulation The endovascular thrombectomy group included all patients in whom endovascular thrombectomy was attempted (ie, patients with groin puncture initiated and all cases in which endovascular thrombectomy failed or was interrupted). The best medical treatment group included patients in whom endovascular thrombectomy was not attempted.

Local study teams recorded patient demographics and disease characteristics at time of hospital admission, treatment, 24–48 h after treatment, hospital discharge, and 90 days (±10 days) after the stroke (collected variables are listed in the appendix pp 15–16). To ensure accuracy, completeness, and exhaustivity of collected data, all centres committed to collecting these predefined patient variables and all variables were checked for plausibility by the study team. Patient outcome measures were regarded as essential for registry inclusion, so patients or datasets without outcome measures were not included. Local teams also completed standard aetiological investigations according to the Childhood AIS Standardized Classification and Diagnostic Evaluation (CASCADE) classification,[20,21] and patient sex was obtained from clinical records. Modified Rankin Scale (mRS) scores and Pediatric Stroke Outcome Measure (PSOM) were measured by local clinical teams during routine clinical care. Details of the collected variables are provided in the appendix (pp 15–16). In summary, patient data, medical history, mRS, PedNIHSS, and imaging findings were recorded at time of admission. Details of treatment (time and dose of intravenous tissue plasminogen activator for patients in the best medical treatment group; and time, anaesthesia type, morphological appearance, type of treatment and device, and treatment-related complications for patients in the endovascular thrombectomy group) were recorded. At 24 h after admission, PedNIHSS, imaging findings, and adverse events were recorded. At time of hospital discharge, patient logistics, PedNIHSS, mRS, PSOM, stroke aetiology, and adverse events were recorded. Finally, mRS, PSOM, and adverse events, were recorded at day 90 (±10).

Save ChildS Pro is registered at the German Clinical Trials Registry (DRKS00018960) and was approved by the ethics committee of the University of Münster (Münster, Germany; 2019-677-f-S), in accordance with the Declaration of Helsinki, with waiver for informed consent. The participating centres also obtained local ethics approvals and waivers for informed consent.

	Endovascular thrombectomy (n=117)	Best medical treatment (n=91)	p value
Age, years	11 (6–14)	6 (3–12)	<0·0001
Sex	..	..	0·43
Female	55 (47%)	38 (42%)	..
Male	62 (53%)	53 (58%)	..
PedNIHSS score at hospital arrival*	14 (10–19)	9 (5–13)	<0·0001
Pre-stroke mRS score†	0 (0–0)	0 (0–0)	0·95
Known time of symptom onset	91 (78%)	66 (73%)	0·28
Referral from other hospital	36 (31%)	43 (47%)	0·013
Medical history (selected)			
Cardiac anomaly	46 (39%)	16 (18%)	..
Hypertension	5 (4%)	0	..
Diabetes	0	1 (1%)	..
Sickle cell disease	0	2 (2%)	..
Other	22 (19%)	27 (30%)	..
None	54 (46%)	52 (57%)	..
Occlusion site	..	..	..
Internal carotid artery	37/127 (29%)	16/97 (16%)	..
Middle cerebral artery, M1 segment	53/127 (42%)	48/97 (49%)	..
Middle cerebral artery, M2 segment	12/127 (9%)	16/97 (16%)	..
Anterior cerebral artery, A1 segment	4/127 (3%)	3/97 (3%)	..
Anterior cerebral artery, A2 segment	1/127 (1%)	0/97	..
Basilar artery	15/127 (12%)	3/97 (3%)	..
Posterior cerebral artery, P1 segment	3/127 (2%)	5/97 (5%)	..
Posterior cerebral artery, P2 segment	0/127	3/97 (3%)	..
Vertebral artery, V4 segment	2/127 (2%)	2/97 (2%)	..
Superior proximal superior cerebellar artery	0/127	1/97 (1%)	..
Imaging method used for enrolment			
CT	70 (60%)	44 (48%)	..
MRI	47 (40%)	47 (52%)	..
ASPECTS baseline‡	8 (6–9)	8 (5–10)	0·38
Intravenous alteplase administered	20 (17%)	25 (27%)	0·086
Time between symptom onset and hospital admission for strokes with known onset, min	130 (51–273)	229 (79–424)	0·046
Time between symptom onset and recanalisation, min	388 (277–545)	..	..
Time between symptom onset and first recanalisation pass, min	340 (243–506)	..	..
Anaesthesia performed	..	..	..
Conscious sedation or none	15 (13%)	..	..
General anaesthesia	102 (87%)	..	..
Type of device used for thrombectomy	..	..	..
Aspiration catheter alone	31 (26%)	..	..
Stent retriever alone	72 (62%)	..	..
Both aspiration catheter and stent retriever	14 (12%)	..	..
Attempts for thrombectomy	2 (1–3)	..	..
CASCADE classification (aetiology)	..	..	<0·0001
1 (small vessel arteriopathy)	0	0	..
2 (focal cerebral arteriopathy)	19 (16%)	35 (38%)	..
3 (bilateral cerebral arteriopathy)	1 (1%)	7 (8%)	..
4 (aortic or cervical arteriopathy)	7 (6%)	5 (5%)	..
5 (cardioembolic)	51 (44%)	15 (16%)	..
6 (other)	32 (27%)	24 (26%)	..
7 (multifactorial)	7 (6%)	5 (5%)	..

Data are median (IQR), n (%), or n/N (%). ASPECTS=Alberta Stroke Program Early CT Score. CASCADE=Childhood AIS Standardized Classification and Diagnostic Evaluation. mRS=modified Rankin Scale. PedNIHSS=Pediatric National Institutes of Health Stroke Scale. *Scores on the PedNIHSS range from 0 to 42, with higher scores indicating greater neurological deficit. †Scores on the mRS range from 0 to 6, with higher scores indicating greater disability. ‡ASPECTS values range from 0 to 10, with lower values indicating larger infarction.

Table 1: **Demographic and clinical characteristics at baseline and treatment**

Outcomes

The primary outcome was the difference between mRS scores recorded before the stroke (pre-stroke) and at 90 days after the stroke. Secondary outcomes were the differences between Pediatric National Institutes of Health Stroke Scale (PedNIHSS) scores recorded at hospital admission and at discharge, the 90-day PSOM, and safety outcomes (symptomatic or non-symptomatic intracranial haemorrhage, peri-interventional vasospasm, and arterial dissection during treatment and 90-day mortality). Primary and secondary outcomes were analysed separately for patients with focal cerebral arteriopathy (CASCADE subtype 2).

Munich, Germany (M Olivieri MD); **Department of Paediatric Neurology** (J P Schwabova MD) **and Department of Neurology** (J P Schwabova, A Tomek MD), **Comprehensive Stroke Center, Second Faculty of Medicine, Charles University and Motol University Hospital, Prague, Czech Republic; Department of Diagnostic and Interventional Neuroradiology, Hospital Bremen-Mitte/Bremen-Ost, Bremen, Germany** (Prof P Papanagiotou MD); **First Department of Radiology, School of Medicine, National & Kapodistrian University of Athens, Areteion Hospital, Athens, Greece** (Prof P Papanagiotou); **Diagnostic and Interventional Neuroradiology Department, University Hospital of Tours, Tours, France** (G Boulouis MD); **French Center for Pediatric Stroke, Paris, France** (G Boulouis, O Naggara MD); **Department of Pediatric Radiology, Faculté de Médecine, Necker Children's Hospital, Université Paris Descartes, Sorbonne Paris Cité, Paris, France** (O Naggara); **Department of Neurology and Department of Pediatrics, University of California San Francisco, San Francisco, CA, USA** (C K Fox MD, Prof H J Fullerton MD); **Research Center of Endovascular Neurosurgery, Federal Center of Brain Research and Neuro Technologies of FMBA, Moscow, Russia** (K Orlov MD); **Morozov Moscow Children Clinical Hospital, Moscow, Russia** (K Orlov, A Kuznetsova MD); **Division of Neuroradiology and Division of Neurointervention, Hospital for Sick Children, University of Toronto, Toronto, ON, Canada** (A Kuznetsova, C Parra-Farinas MD, P Muthusami MD); **Neurovascular Centre, Divisions of Therapeutic Neuroradiology and Neurosurgery, St Michael's Hospital, University of Toronto, ON, Canada** (A A Dmytriw); **University Hospital, LMU Munich, Germany; Department of Radiology, Texas Children's Hospital, Baylor College of Medicine, Houston, TX, USA** (M Martinez MD); **Division of Neuropaediatrics, Development and**

Rehabilitation, Department of Paediatrics, Inselspital, Bern University Hospital, University of Bern, Bern, Switzerland (D Brechbühl MD, Prof M Steinlin MD); **Graduate School for Health Sciences, University of Bern, Bern, Switzerland** (D Brechbühl); **Department of Neurology, Johns Hopkins School of Medicine, Baltimore, MD, USA** (L R Sun MD); **Department of Neurology, University of Texas Rio Grande Valley, Harlingen, TX, USA** (A E Hassan DO); **Department of Neuroradiology, University of Marburg, Marburg, Germany** (Prof A Kemmling MD); **Division of Child Neurology, Department of Neurology, Stanford University, Stanford, CA, USA** (Prof S Lee MD)

Correspondence to: Dr Peter Sporns, Department of Neuroradiology, University Hospital Basel, 4031 Basel, Switzerland
peter.sporns@hotmail.de

See Online for appendix

	Endovascular thrombectomy (n=117)	Best medical treatment (n=91)	p value
90-day mRS*	1 (0 to 2)	2 (1 to 3)	0·039
Difference between 90-day and pre-stroke mRS scores*	1 (0 to 2)	2 (1 to 3)	0·020
90-day PSOM†	1 (0 to 2)	2 (1 to 3)	<0·0001
Difference between hospital admission and discharge PedNIHSS scores‡	−9 (−13 to −3)	−3 (−5 to 0)	<0·0001
Hospital discharge PSOM†	1 (0 to 2)	2 (1 to 4)	0·0030
Successful recanalisation (mTICI 2b or better)	104 (89%)	..	..
Near-complete recanalisation (mTICI 2c or better)	64 (55%)	..	..
Complete recanalisation (mTICI 3)	49 (42%)	..	..

Data are median (IQR) or n (%). Successful reperfusion was defined as grade 2b to 3 on the mTICI system ranging from 0 to 3, with higher grades indicating increased reperfusion; grade 2b indicates reperfusion of 50% or more of the occluded cerebral artery territory; and grade 3 indicates reperfusion of 100% of the occluded cerebral artery territory at the end of the thrombectomy procedure. mRS=modified Rankin Scale. mTICI=modified thrombectomy in cerebral infarction. PedNIHSS=Pediatric National Institutes of Health Stroke Scale. PSOM=Pediatric Stroke Outcome Measure. *Scores on the mRS range from 0 to 6, with higher scores indicating greater disability. †Scores on the PSOM range from 0 to 10 in 0·5 steps, with higher scores indicating greater disability. ‡Scores on the PedNIHSS range from 0 to 42, with higher scores indicating greater neurological deficit.

Table 2: **Efficacy outcomes**

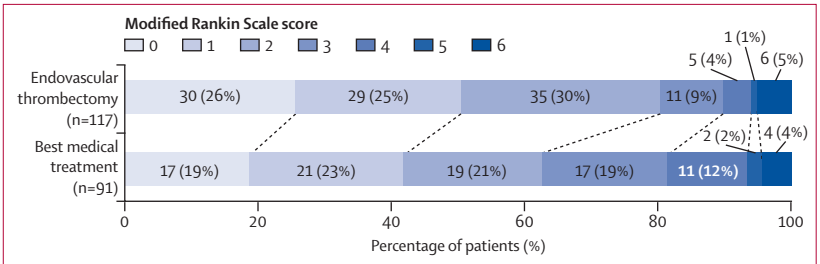

Figure 2: **Distribution of modified Rankin Scale scores at 90 days after the stroke**
Scores on the modified Rankin Scale range from 0 to 6, with higher scores indicating greater disability.

Statistical analysis

The primary outcome was compared between treatment groups by the Wilcoxon rank test (α=0·05). Secondary outcomes and baseline demographics were compared between treatment groups by the χ^2 test (or Fisher's exact test where appropriate) for categorical variables and the *t* test (or Mann–Whitney *U* test, when appropriate) for continuous variables.

To account for possible confounding factors, additional ordinal regression analyses were performed for primary and secondary outcomes on all variables that differed significantly between the treatment groups. For the assessment of effect size, *r* values were calculated as the Z value (from the Mann–Whitney *U* test) divided by the square root of n, where n is the total patient number per group. For interpretation, an *r* value greater 0·1 indicated a weak effect whereas *r* values less than 0·3 or greater than 0·5 indicated moderate and strong effects, respectively.

For sensitivity analysis, propensity score matching was used to adjust for differences in baseline parameters between treatment groups. Each patient's propensity score to receive endovascular thrombectomy or best medical treatment was determined using a multivariable logistic regression model that included covariates with a significant effect on the primary outcome. Optimised propensity score matching (SAS macro psmatch_multi) was used to match patients from each group 1:1. For matching, an absolute difference between propensity scores of 0·10 was allowed.

An α value of 0·05 was used to determine significance for all analyses. Statistical analyses were performed with SAS (version 9.4).

Role of the funding source

There was no funding source for this study.

Results

41 patients were entered into the Save ChildS Pro registry between Jan 1, 2020, and Aug 31, 2023. 208 patients met inclusion criteria for this analysis, of whom 117 underwent endovascular thrombectomy and 91 received best medical treatment only (figure 1). Baseline characteristics, including location of arterial occlusion and CASCADE classification, are listed in table 1. The median age of patients in the endovascular thrombectomy was higher than in the best medical treatment group (p<0·0001). The youngest patient to be treated with endovascular thrombectomy was aged 3 months. The median PedNIHSS score upon hospital admission was higher in the endovascular thrombectomy group than in the best medical treatment group (p<0·0001). Intravenous thrombolysis was used in both treatment groups.

Efficacy outcomes are shown in table 2. In the endovascular thrombectomy group, 104 (89%) of 117 patients had successful reperfusion (modified treatment in cerebral infarction 2b or better), and 49 patients (42%) had complete reperfusion. The difference between median pre-stroke mRS score and 90-day mRS score was 1 (IQR 0–2) in the endovascular thrombectomy group and 2 (1–3) in best medical treatment alone (p=0·020; table 2; figure 2; *r*=0·14).

Median 90-day PSOM scores are compared in table 2. The change in median PedNIHSS scores between time of hospital admission and discharge are compared in table 2 and figure 3 (*r*=0·44). The comparison of median discharge and 90-day PSOM scores is shown in the appendix (p 1; *r*=0·21).

Ordinal regression analyses revealed a significant effect of age (p=0·0029), PedNIHSS score at hospital admission (p=0·0017), and treatment group (p=0·020),

whereas no other parameter showed an effect on the primary and secondary outcomes (data not shown).

Safety outcomes are shown in table 3. Six (5%) of 117 patients in the endovascular thrombectomy group and four (5%) of 91 patients in the best medical treatment group had a 90-day mRS score of 6, indicative of death (p=0·89). In the endovascular thrombectomy group, 17 (15%) patients had transient vasospasm during the intervention, which resolved in all cases, either spontaneously or after administration of intra-arterial nimodipine. Two (2%) patients had catheterisation -associated non-flow-limiting arterial dissections. During treatment, non-symptomatic intracranial haemorrhage affected nine (8%) of 117 patients in the endovascular thrombectomy group and six (7%) of 91 patients in the best medical treatment group (p=0·79). One case of symptomatic intracranial haemorrhage was seen, and this was in the endovascular thrombectomy group. Furthermore, the prevalence of persistent arterial occlusions was significantly lower in the endovascular thrombectomy group than in the best medical treatment group (18 [15%] *vs* 49 [54%], p<0·0001; table 3). Further CASCADE classification of patients with persistent occlusion revealed suspected focal cerebral arteriopathy aetiology in eight (44%) of 18 patients in the endovascular thrombectomy group and 19 (39%) of 49 patients in the best medical treatment group.

A comparison of outcomes between patients with focal cerebral arteriopathy (CASCADE subtype 2) and patients with other aetiologies showed no difference in 90-day median mRS scores among those who underwent endovascular thrombectomy and best medical treatment (p=0·074; appendix pp 2, 6). The change in median PedNIHSS score from hospital admission to discharge was –10 (IQR –18 to –2) in the endovascular thrombectomy group and –4 (–4 to 0) in the best medical treatment group (p<0·0001; appendix pp 3–4, 6). The median 90-day PSOM score was 1·0 (IQR 0·5 to 1·5) in the endovascular thrombectomy group and 1·5 (1·0 to 2·5) in the best medical treatment group (p<0·0001; appendix pp 5–6).

79 patients from the endovascular thrombectomy group were propensity score matched 1:1 based on age, sex, and PedNIHSS score at hospital admission to 79 patients from the best medical treatment group (appendix p 7). Median age among matched patients was 10 years (IQR 7 to 13) in the endovascular thrombectomy group and 7 years (4 to 11) in the best medical treatment group. The median PedNIHSS score at hospital admission was 12 (IQR 8 to 15) in the endovascular thrombectomy group and 9 (7 to 12) in the best medical treatment group. In these patients, median pre-stroke mRS score was 0 (IQR 0 to 0) in both treatment groups and increased to 1 (0 to 2) at day 90 among patients treated with endovascular thrombectomy compared with 2 (1 to 3) among patients with best medical treatment (p=0·029). The median change in the PedNIHSS score from hospital admission to discharge was –8 (IQR –12 to –3) in the endovascular thrombectomy group and –2 (–6 to 0) in the best medical treatment group (p<0·0001). The median 90-day PSOM score was 1 (IQR 0 to 2) in the endovascular thrombectomy group and 2 (1 to 3) in the best medical treatment group (p=0·0020). No sex-specific differences were observed with respect to clinical outcome measures (data not shown).

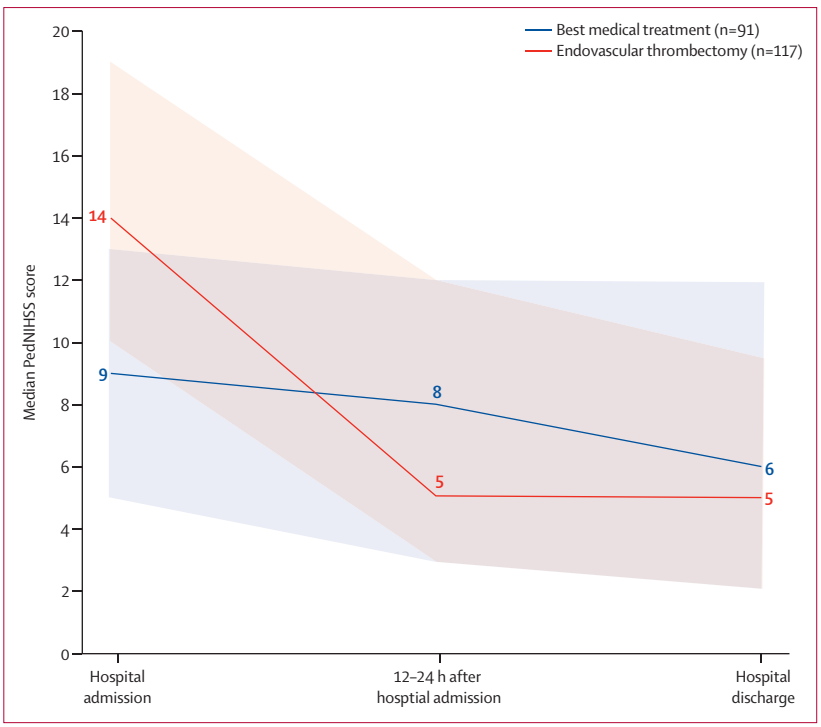

Figure 3: **Change in median PedNIHSS score between hospital admission and discharge**
Scores on the PedNIHSS range from 0 to 42, with higher scores indicating greater neurological deficit. Shaded areas indicate the IQR. PedNIHSS=Pediatric National Institutes of Health Stroke Scale.

	Endovascular thrombectomy (n=117)	Best medical treatment (n=91)	p value
Death (mRS score of 6)*	6 (5%)	4 (4%)	0·89
Symptomatic intracranial haemorrhage†‡	1 (1%)	0	1·0
Non-symptomatic intracranial haemorrhage‡	9 (8%)	6 (7%)	0·79
Transient vasospasm‡	17 (15%)	..	..
Arterial dissection‡	2 (2%)	..	..
Persistent or recurrent arterial occlusion‡	18 (15%)	49 (54%)	<0·0001

Data are n (%). mRS=modified Rankin Scale. PedNIHSS=Pediatric National Institutes of Health Stroke Scale. *Death was determined at 90 (±10) days after stroke. †Symptomatic intracranial haemorrhage was defined as an increase in the PedNIHSS score of at least 4 points with presence of parenchymal haemorrhage. ‡Recorded within 24 h of hospital admission.

Table 3: **Safety outcomes**

Discussion

The Save ChildS Pro registry study shows superior outcomes in children with large-vessel and medium-vessel occlusion treated with endovascular thrombectomy compared with best medical treatment alone. The primary outcome, defined as the change in median mRS score from pre-stroke baseline to day 90, and the secondary outcomes (change in the PedNIHSS score from hospital admission to discharge and 90-day PSOM score) were significantly better in the endovascular thrombectomy group than in the best medical care group. The consistency of these findings after propensity score matching for age, sex, and initial stroke severity emphasises the value of endovascular thrombectomy and represents a high-quality approach to analysing observational registry data in the absence of a randomised trial. These improved outcomes align with the results of a recent matched case–control study,[16] in which clinical outcomes for paediatric patients with anterior circulation large-vessel occlusion stroke were better with endovascular thrombectomy than with best medical treatment alone. The benefits of endovascular thrombectomy are more compelling in light of recent findings that outcomes of children with arterial ischaemic stroke due to large-vessel occlusion treated with medical management alone might not be as benign as for children who do not present with large-vessel occlusion.[15] Similar to previous studies, the efficacy outcomes of the endovascular thrombectomy procedure were high, with successful recanalisation (defined as modified treatment in cerebral infarction 2b or better) in 89% of patients and a median of two attempts per endovascular thrombectomy procedure. The decision of whether to perform endovascular thrombectomy should not be based on one single parameter (eg, the PedNIHSS), but always as a combination of multiple parameters (eg, the PedNIHSS, occlusion location, the Alberta Stroke Program Early CT Score [ASPECTS], pre-existing neurological deficits, and potentially salvageable tissue), because parameters such as the PedNIHSS and ASPECTS have limitations, such as potentially fluctuating symptoms, the lower representation of posterior circulation symptoms, or high inter-rater variability.[28]

Age and PedNIHSS score at baseline showed a significant effect on patient outcome. The interplay between age and symptom severity at presentation might present important selection criteria for or against endovascular thrombectomy in children. Although more severely affected children might benefit more from endovascular thrombectomy, the existing data up to now do not justify dedicated cutoff values for or against selecting children for endovascular thrombectomy. For the current analysis, the cohort size was too small to allow the formation of subgroups of younger and less severely affected children. Thus, it is currently possible that the observed positive treatment effect for endovascular thrombectomy is confined to older and more severely affected children. Larger studies including children with different symptom severities at presentation across all age groups will help to determine whether a potential benefit for endovascular thrombectomy similarly exists in younger and less severely affected children, and thereby create more detailed treatment recommendations.

Concerning safety, we found similar mortality rates in patients receiving endovascular thrombectomy and best medical treatment compared with patients who received best medical treatment alone. Only one patient had a symptomatic intracerebral haemorrhage in the endovascular thrombectomy group, and rates of non-symptomatic intracranial haemorrhage were similar in both treatment groups. A small number of patients who underwent endovascular thrombectomy had procedure-related adverse events: arterial dissections (2%) and radiographic vasospasm (15%). However, the dissections were not flow limiting, and the vasospasm resolved in all cases after intra-arterial administration of nimodipine and without any radiographic or clinical signs of ischaemia. More than half of all patients (54%) in the best medical treatment group had a persistent or recurrent vessel occlusion at 24 h follow-up imaging, a much higher proportion than the 15% in the endovascular thrombectomy group. Further characterising this subgroup, eight (44%) of 18 patients in the endovascular thrombectomy group with persistent occlusion and 19 (39%) of 49 patients in the best medical treatment group had a suspected focal cerebral arteriopathy aetiology. Recent studies in adults have shown that the administration of intravenous thrombolysis works in a synergistic way with endovascular thrombectomy and should therefore be administered if no contraindications are present.[29] By contrast, there is observational data that intravenous thrombolysis will fragment thrombi and cause thrombus migration and fragmentation which will be more difficult to remove mechanically and could potentially result in lower rates of complete recanalisation.[30]

A major concern is the safety and efficacy of endovascular thrombectomy procedures in patients with arteriopathies.[11,14] In the Save ChildS Pro registry, patients with arteriopathies had similar outcomes to those with other aetiologies when treated with endovascular thrombectomy. Furthermore, patients treated with endovascular thrombectomy had greater improvement of the PedNIHSS score as well as the PSOM score at day 90 regardless of the underlying aetiology. Although the primary outcome measure (difference in mRS from pre-stroke to day 90) was not significantly different for patients with focal cerebral arteriopathy between the endovascular thrombectomy and best medical treatment groups (p=0·075), the secondary outcomes were significantly improved in the endovascular thrombectomy group. Thus, regarding the primary outcome, there was equipoise for patients with suspected focal cerebral arteriopathy for endovascular thrombectomy and best medical treatment. This might reflect the smaller sample

size and heterogeneity of this focal cerebral arteriopathy subgroup, or potentially a more subtle yet still clinically relevant effect of endovascular thrombectomy in patients with focal cerebral arteriopathy. Of note, these results show that more severely affected patients with suspected focal cerebral arteriopathy will potentially benefit from endovascular thrombectomy, whereas patients with focal cerebral arteriopathy with milder stroke might not benefit in the same way. Yet, it is important to note that the mRS does not capture cognitive and academic deficits, which are more likely to be captured by the PSOM. Therefor, we chose to collect both parameters plus the PedNIHSS, with the mRS being the primary outcome because it the most widely used outcome parameter in stroke trials.[31]

Finally, regarding the translation of our findings to clinical practice, this study adds to the growing evidence that children with large-vessel occlusion stroke have superior outcomes when treated with endovascular thrombectomy.[8,15,16] Adequate training of all physicians involved in acute stroke care, development of clear selection criteria for endovascular thrombectomy, and standardisation of interventional procedures are crucial to maintain these positive treatment effects. This is especially the case for neurointerventionists, as navigation through the smaller vessels and successful technical outcome of the thrombectomy procedure itself require dedicated training and continuous practice, which depends on the case load of the centre in performing neurointerventional procedures in children and adults.[14] Because thrombectomy procedures in distal intracranial arteries are increasingly being performed in adults, neurointerventionists are gaining more experience with navigation in smaller vessels and likewise smaller and softer devices are continuously being developed, also providing tailored approaches for children. It is reassuring that in our study even children with suspected focal cerebral arteriopathies who presented with large-vessel occlusion stroke appeared to benefit from the endovascular restoration of blood flow. However, in patients presenting with classic imaging features of focal cerebral arteriopathy, such as arterial banding and narrowing of the terminal segment of the internal carotid artery, even greater caution must be applied. It should be noted that diagnosis of the inflammatory subtype of focal cerebral arteriopathy is difficult if the initial presentation is with complete arterial occlusion; most commonly focal cerebral arteriopathy presents subacutely with stenosis rather than complete acute occlusion. As such, in some cases, the diagnosis is made retrospectively on the basis of the presence of residual or progressive stenosis in the affected vessel after clot retrieval of a superimposed acute thrombus. Such retrospective diagnosis can be confounded by iatrogenic stenosis caused by intimal injury that can occur after use of a stent retriever for endovascular thrombectomy. Therefore, the CASCADE 2 stroke subtype (focal cerebral arteriopathy) is a group of patients in whom a definitive diagnosis is difficult to establish.

Our prospective study has limitations. First, given that this study is not a randomised trial, a potential selection bias has to be assumed because the selected treatment was at the discretion of the participating centre. Patients were nested under centres and centre-specific effects could potentially bias the results. Because most of the centres included an average of fewer than five patients (and only five centres reported treatment of more than ten patients), it currently cannot be concluded whether high-volume centres create different outcomes compared with lower-volume centres. In general, sites appeared to select for endovascular thrombectomy preferentially in the children with greater PedNIHSS scores. The impact of this selection bias might be less pronounced because some centres that do not offer endovascular thrombectomy participated, thus only including patients with best medical treatment alone. Second, patients in the endovascular thrombectomy group were older. However, in the propensity score matched analysis, the treatment effect was still maintained across all outcome variables. Third, children in the best medical treatment group more often had arteriopathies, whereas those in the endovascular thrombectomy group more often presented with cardioembolic aetiologies, probably reflecting the reluctance of treating physicians to refer children with arteriopathic changes for endovascular thrombectomy. However, the outcome of children with suspected arteriopathies who did receive endovascular thrombectomy was better than that of those treated with best medical treatment alone in this study. Fourth, there were no restrictive selection criteria regarding time from symptom onset and infarct size on admission imaging for this study. This also aligns with recent trials in adults, which have all shown that absolute and relative infarct size as well as the time from onset are less important as long as there is salvageable tissue on advanced imaging and a mismatch between clinical deficit and infarct.[6,22,23,32] Fifth, time from symptom onset to admission was comparably short in the Save ChildS Pro cohort and even though comparable to similar studies[12] it might be longer in less specialised centres, which might affect patient outcomes. Last, the clinicians performing the outcomes measurements were not masked to treatment, which might also have introduced bias. Although the largest cohort of children with endovascular thrombectomy compared with best medical treatment is reported in this study, the cohort size was too small for more detailed subanalyses, such as investigating different outcomes with respect to age and sex. Larger patient cohorts will provide more detailed insights in outcomes after endovascular thrombectomy with respect to different aetiologies and in children with different age, sex, and demographics.

In conclusion, in this prospective, registry-based, multicentre study, endovascular thrombectomy plus best medical treatment was associated with improved functional outcomes in paediatric patients with large and medium intracranial occlusions compared with best medical treatment alone. Future studies are needed to investigate whether the positive treatment effect of endovascular thrombectomy is confined to older and more severely affected children.

Contributors

PBS, M-NP, and MW directly accessed and verified the data, conducted the analyses, and wrote the manuscript. TB conducted the statistical analyses. All other authors contributed data, provided feedback on the manuscript, and accept responsibility for the decision to submit for publication.

Declaration of interests

We declare no competing interests.

Data sharing

The study data are available from the corresponding author on reasonable request from the moment of publication and with a signed data access agreement.

Acknowledgments

PBS received a grant for this research from the Novartis Foundation for Medical-Biological Research.

References

1 Sporns PB, Fullerton HJ, Lee S, et al. Childhood stroke. *Nat Rev Dis Primers* 2022; **8:** 12.
2 Ganesan V, Prengler M, McShane MA, Wade AM, Kirkham FJ. Investigation of risk factors in children with arterial ischemic stroke. *Ann Neurol* 2003; **53:** 167–73.
3 Fullerton HJ, Chetkovich DM, Wu YW, Smith WS, Johnston SC. Deaths from stroke in US children, 1979 to 1998. *Neurology* 2002; **59:** 34–39.
4 Krishnamurthi RV, deVeber G, Feigin VL, et al. Stroke Prevalence, mortality and disability-adjusted life years in children and youth aged 0–19 years: data from the Global and Regional Burden of Stroke 2013. *Neuroepidemiology* 2015; **45:** 177–89.
5 Rivkin MJ, deVeber G, Ichord RN, et al. Thrombolysis in pediatric stroke study. *Stroke* 2015; **46:** 880–85.
6 Goyal M, Menon BK, van Zwam WH, et al. Endovascular thrombectomy after large-vessel ischaemic stroke: a meta-analysis of individual patient data from five randomised trials. *Lancet* 2016; **387:** 1723–31.
7 Bhatia K, Kortman H, Blair C, et al. Mechanical thrombectomy in pediatric stroke: systematic review, individual patient data meta-analysis, and case series. *J Neurosurg Pediatr* 2019; **24:** 558–71.
8 Sporns PB, Sträter R, Minnerup J, et al. Feasibility, safety, and outcome of endovascular recanalization in childhood stroke: the Save ChildS study. *JAMA Neurol* 2020; **77:** 25–34.
9 Sporns PB, Straeter R, Minnerup J, et al. Does device selection impact recanalization rate and neurological outcome? An analysis of the Save ChildS study. *Stroke* 2020; **51:** 1182–89.
10 Sporns PB, Psychogios MN, Straeter R, et al. Clinical diffusion mismatch to select pediatric patients for embolectomy 6 to 24 hours after stroke: an analysis of the Save ChildS study. *Neurology* 2021; **96:** e343–51.
11 Chabrier S, Ozanne A, Naggara O, Boulouis G, Husson B, Kossorotoff M. Hyperacute recanalization strategies and childhood stroke in the evidence age. *Stroke* 2021; **52:** 381–84.
12 Kossorotoff M, Kerleroux B, Boulouis G, et al. Recanalization treatments for pediatric acute ischemic stroke in France. *JAMA Netw Open* 2022; **5:** e2231343.
13 Sporns PB, Kemmling A, Lee S, et al. A prospective multicenter registry on feasibility, safety, and outcome of endovascular recanalization in childhood stroke (Save ChildS Pro). *Front Neurol* 2021; **12:** 736092.
14 Sporns PB, Fullerton HJ, Lee S, Kirton A, Wildgruber M. Current treatment for childhood arterial ischaemic stroke. *Lancet Child Adolesc Health* 2021; **5:** 825–36.
15 Bhatia KD, Briest R, Goetti R, et al. Incidence and natural history of pediatric large vessel occlusion stroke: a population study. *JAMA Neurol* 2022; **79:** 488–97.
16 Bhatia KD, Chowdhury S, Andrews I, et al. Association between thrombectomy and functional outcomes in pediatric patients with acute ischemic stroke from large vessel occlusion. *JAMA Neurol* 2023; **80:** 910–18.
17 Harrar DB, Salussolia CL, Kapur K, et al. A stroke alert protocol decreases the time to diagnosis of brain attack symptoms in a pediatric emergency department. *J Pediatr* 2020; **216:** 136–41.
18 deVeber GA. Delays in the timely diagnosis of stroke in children. *Nat Rev Neurol* 2010; **6:** 64–66.
19 Lagman-Bartolome AM, Pontigon AM, Moharir M, et al. Basilar artery strokes in children: good outcomes with conservative medical treatment. *Dev Med Child Neurol* 2013; **55:** 434–39.
20 Bernard TJ, Manco-Johnson MJ, Lo W, et al. Towards a consensus-based classification of childhood arterial ischemic stroke. *Stroke* 2012; **43:** 371–77.
21 Böhmer M, Niederstadt T, Heindel W, et al. Impact of Childhood Arterial Ischemic Stroke Standardized Classification and Diagnostic Evaluation classification on further course of arteriopathy and recurrence of childhood stroke. *Stroke* 2019; **50:** 83–87.
22 Sporns PB, Fiehler J, Ospel J, et al. Expanding indications for endovascular thrombectomy—how to leave no patient behind. *Ther Adv Neurol Disord* 2021; **14:** 1756286421998905.
23 Bendszus M, Fiehler J, Subtil F, et al. Endovascular thrombectomy for acute ischaemic stroke with established large infarct: multicentre, open-label, randomised trial. *Lancet* 2023; **402:** 1753–63.
24 Wittenberg GF. Neural plasticity and treatment across the lifespan for motor deficits in cerebral palsy. *Dev Med Child Neurol* 2009; **51** (suppl 4)**:** 130–33.
25 Lee S, Jiang B, Wintermark M, et al. Cerebrovascular collateral integrity in pediatric large vessel occlusion: analysis of the Save ChildS study. *Neurology* 2022; **98:** e352–63.
26 Stracke CP, Meyer L, Schwindt W, Ranft A, Straeter R. Case report: successful mechanical thrombectomy in a newborn with basilar artery occlusion. *Front Neurol* 2022; **12:** 790486.
27 Sporns PB, Kemmling A, Hanning U, et al. Thrombectomy in childhood stroke. *J Am Heart Assoc* 2019; **8:** e011335.
28 van Horn N, Kniep H, Broocks G, et al. ASPECTS interobserver agreement of 100 investigators from the TENSION study. *Clin Neuroradiol* 2021; **31:** 1093–100.
29 Majoie CB, Cavalcante F, Gralla J, et al. Value of intravenous thrombolysis in endovascular treatment for large-vessel anterior circulation stroke: individual participant data meta-analysis of six randomised trials. *Lancet* 2023; **402:** 965–74.
30 Tan Z, Zhang L, Huang L, et al. Thrombus migration in patients with acute ischaemic stroke undergoing endovascular thrombectomy. *Stroke Vasc Neurol* 2024; **9:** 126–33.
31 Feldman SJ, Beslow LA, Felling RJ, et al. Consensus-based evaluation of outcome measures in pediatric stroke care: a toolkit. *Pediatr Neurol* 2023; **141:** 118–32.
32 Nogueira RG, Jadhav AP, Haussen DC, et al. Thrombectomy 6 to 24 hours after stroke with a mismatch between deficit and infarct. *N Engl J Med* 2018; **378:** 11–21.

Neurotherapeutics (2023) 20:633–654
https://doi.org/10.1007/s13311-023-01373-5

REVIEW

Advances in the Diagnosis and Treatment of Pediatric Arterial Ischemic Stroke

Lisa R. Sun[1] · John K. Lynch[2]

Accepted: 21 March 2023 / Published online: 18 April 2023

Abstract

Though rare, stroke in infants and children is an important cause of mortality and chronic morbidity in the pediatric population. Neuroimaging advances and implementation of pediatric stroke care protocols have led to the ability to rapidly diagnose stroke and in many cases determine the stroke etiology. Though data on efficacy of hyperacute therapies, such as intravenous thrombolysis and mechanical thrombectomy, in pediatric stroke are limited, feasibility and safety data are mounting and support careful consideration of these treatments for childhood stroke. Recent therapeutic advances allow for targeted stroke prevention efforts in high-risk conditions, such as moyamoya, sickle cell disease, cardiac disease, and genetic disorders. Despite these exciting advances, important knowledge gaps persist, including optimal dosing and type of thrombolytic agents, inclusion criteria for mechanical thrombectomy, the role of immunomodulatory therapies for focal cerebral arteriopathy, optimal long-term antithrombotic strategies, the role of patent foramen ovale closure in pediatric stroke, and optimal rehabilitation strategies after stroke of the developing brain.

Keywords Pediatric stroke · Childhood stroke · Sickle cell · Thrombectomy

Background

Cerebrovascular disorders are an important cause of mortality and chronic morbidity in children. Here, we review the most recent literature on the epidemiology, risk factors, evaluation, outcome, and treatment of pediatric arterial ischemic stroke (AIS).

Definition

The case definition for pediatric stroke has varied widely in the literature. Differences in age of onset, time at diagnosis, and cerebrovascular disorders to include have led to variability in incidence rates across studies. Perinatal stroke develops between 20 weeks gestation and 1 month of age, but it may be diagnosed months later, and it includes a diverse group of cerebrovascular disorders [1]. AIS is the most common type of cerebrovascular disorder to occur in the perinatal period. Childhood stroke develops later, between 30 days and 18 years of age, and includes AIS, hemorrhagic stroke, and sinovenous thrombosis.

Incidence

The incidence of perinatal stroke is estimated as high as one per 1100 live births [2], but lower rates have been reported [3–6]. Most estimates are based on small samples over short periods of time, with variable ascertainment methods. The rate of AIS is reported to be much higher in the perinatal period than in childhood [7]. The first population-based study of stroke in children from the 1970s found an incidence of 1 per 40,000 children for all stroke types [8]. More recent studies in Canada [9], the USA [3], the UK [10], and Sweden [11] have found similar rates. The incidence of stroke is higher in boys than girls and among Black, Asian, and Hispanic children compared to white children [10, 12]. In a community-based study of cerebrovascular disease in Texas, the incidence rate of

Invited Review: Advances in Stroke Diagnostics and Therapeutics.

✉ Lisa R. Sun
lsun20@jhmi.edu

[1] Divisions of Pediatric Neurology and Cerebrovascular Neurology, Department of Neurology, Johns Hopkins University School of Medicine, 200 N. Wolfe Street, Ste 2158, Baltimore, MD 21287, USA

[2] Acute Stroke Research Section, Stroke Branch (SB), National Institute of Neurological Disorders and Stroke, Bethesda, MD, USA

stroke was found to be higher in Mexican American children than non-Hispanic whites [13].

Clinical Presentation

The clinical presentation of AIS is related to the age of the child and location of the stroke. Infants with stroke typically present with seizures or other diffuse neurologic deficits. Some infants with stroke are not identified acutely, but are diagnosed retrospectively, when neurologic symptoms, such as emerging hemiparesis or seizures, leads to neuroimaging [5]. In contrast, children with stroke typically present with focal neurologic deficits, usually hemiplegia and/or focal seizures. Signs and symptoms of stroke in children are often misinterpreted to be other common neurologic or systemic disorders. Emergency rooms physicians are less accurate at detecting stroke in children than adults [14]. Several stroke screening tools have been shown to be highly sensitive in adults [15] but are less accurate in children [16]. Symptoms of focal weakness, seizures, ataxia, speech, or walking difficulties have been shown to discriminate stroke from migraine, a common stroke mimic in children [17]. Better screening tools to assist providers may help to alleviate delays in diagnosis that impact the study and use of acute therapies in children with stroke.

Classification and Mechanism

Identifying the cause of stroke is helpful for explaining stroke mechanism to patients, determining future stroke risk, selecting secondary prevention strategies, and stroke research. Several adult stroke classification systems have been developed and have exhibited good reliability and discriminative validity [18]. Adult classification systems have limited use in children since the causes of stroke are so different. The Childhood Arterial Ischemic Stroke Standardized Classification and Diagnostic Evaluation (CASCADE) system was developed by the International Pediatric Stroke Study (IPSS) investigators to categorize childhood strokes according to the underlying cause [19]. The CASCADE system classifies childhood AIS into seven discrete subtypes and has moderate interobserver agreement when used by experienced raters. The CASCADE subtypes include (1) small vessel arteriopathy, (2) unilateral focal cerebral arteriopathy (FCA), (3) bilateral cerebral arteriopathy, (4) aortic/cervical arteriopathy, (5) cardioembolic, (6) other, and (7) multifactorial [19]. A recent study evaluated the predictive value of the CASCADE criteria and found an association with risk of recurrent stroke and progression of arteriopathy [20].

Causes of Stroke in Children

The causes of stroke in children have varied widely among registry studies [21–23]. Most of these studies have been retrospective, without a uniform diagnostic approach or classification system, and relevant risk factors may not have been identified or recorded. The most frequently reported risk factors for AIS in children are arteriopathies, cardiac disorders, infection, hematological and metabolic disorders, and other rare causes. In many children with stroke, the cause is thought to be multifactorial [24], possibly a combination of environmental triggers and hereditary or acquired disorders that increase the risk of stroke.

Arteriopathies

The expanded use of vessel imaging has enhanced our understanding of stroke in children. Extracranial and intracranial arteriopathies are a common cause of stroke in children. Arteriopathies were identified in 53% of children in the IPSS [24]. In studies with limited use of vessel imaging, other causes are more common, which may be related to detection bias [21]. Arteriopathies lead to stroke through a variety of mechanisms including decreased blood flow and local thrombus formation.

Arterial dissections are the most common cause of extracranial arteriopathies in children. Arterial dissection is due to a tear in the intimal layer or rupture of the vasa vasorum and hemorrhage into the medial layer [25]. Intracranial dissection occurs more frequently in older children (median age 14 years) compared to extracranial dissection (median age 8 years) [26]. Arterial dissection is more common in boys, and they typically present with symptoms of hemiplegia and headache [27]. Arterial dissection has been associated with a variety of conditions, but most cases are due to trauma. Recurrent AIS occurs in up to 19% of children with arterial dissection [28].

Intracranial arteriopathies account for almost half of all childhood strokes [29] and represent a heterogenous group of disorders that can be difficult to diagnose and classify. Intracranial arteriopathies identified most often in children with AIS include inflammatory FCA, moyamoya, and arterial dissection. The vascular effects of infection in pediatric stroke (VIPS) investigators defined FCA as “unifocal and unilateral stenosis/irregularity of the large intracranial arteries of the anterior circulation” [30]. FCA can be classified into different subtypes based on the underlying etiology; these include inflammatory (FCA-i) and dissection (FCA-d) types.

Inflammatory FCA (FCA-i) is a subtype of FCA due to an inflammatory or infectious process. FCA-i has been

associated with both active and post-infectious disorders, including post-varicella arteriopathy [31]. Varicella (chicken pox) is associated with an increased risk of stroke in children [32]. Post-varicella arteriopathy can develop from a current infection or several months after infection [33]. There have been several recent reports of other infectious agents associated with FCA and stroke in children. A recent case–control study from the VIPS cohort found an increased rate of parvovirus B19 infection among cases compared to controls [34]. Dengue fever has also been reported in association with FCA and stroke [35]. An international study of children with SARS-CoV2 and AIS identified several children with vasculitis and FCA [36].

Moyamoya is a chronic non-inflammatory steno-occlusive intracranial arteriopathy that accounts for about 8% of AIS in children [37]. Moyamoya *disease* is characterized by an angiographic pattern of stenosis of the supraclinoid internal carotid artery with secondary development of an extensive collateral network that gives a radiographic appearance of a "puff of smoke". Moyamoya *syndrome* is a secondary complication of other medical disorders (Down syndrome, sickle cell disease, neurofibromatosis) that lead to this unique arteriopathy. The progressive steno-occlusive arteriopathy of moyamoya can lead to decreased blood flow, diminished cerebrovascular reserve, and ischemic stroke. Hemorrhage can also occur and is due to the rupture of vessels in the fragile collateral network or associated aneurysms [38]. The incidence of moyamoya disease is highest in Asia, predominantly in Japan. The disease is more common among females and peaks in children around 5–9 years of age [39]. The cause of moyamoya disease is unclear, but the high prevalence in Asian populations and familial clustering suggests a genetic disorder. Around 10–15% of cases are familial, mostly affecting siblings compared to a parent or offspring. Linkage studies have identified several genetic loci, such as *RNF213*, associated with moyamoya disease, but these have not been consistent across populations [40]. Children with moyamoya typically present with transient ischemic attacks (TIAs) or AIS but may develop other symptoms like headache or seizures. Some children with moyamoya are identified incidentally on brain imaging and have a lower risk of stroke after diagnosis than those with prior ischemic symptoms [41]. The risk of stroke in patients with moyamoya increases with disease progression. The incidence of stroke also varies according to moyamoya disease genotype and underlying cause of moyamoya syndrome [42]. Revascularization surgery is recommended to prevent the progression of the disease and risk of stroke. The primary indications for surgical intervention include clinical symptoms (stroke, TIA, or cognitive decline) or imaging evidence of progression and decreased cerebral blood flow or cerebral perfusion reserve [43]. Revascularization is associated with a decrease in symptomatic progression, headaches, and ischemic and hemorrhagic stroke [44].

Cardiac Disorders

Stroke is a well-recognized complication of cardiac disease in both children and adults. Cardiac disorders associated with stroke include congenital heart disease, intracardiac defects, cardiac procedures, cardiomyopathy, arrhythmias, infective endocarditis, and ventricular assist devices [45]. These disorders can lead to the development of thrombi within the heart, on an infected valve, or through a right to left shunt, which can embolize to the brain.

The rate of stroke among children with cardiac disease has varied widely among studies due to differences in case definitions, brain imaging, and cardiac disorders studied. A study of children with cardiac disease in the northwest US found a rate of stroke of one in 750 children [46], but higher rates have been reported among children who undergo cardiac procedures and catheterization [45]. While the incidence of stroke overall is low in children with cardiac disease, these disorders are common among registries of children with stroke. Cardiac disorders were identified in 30% of children in the IPSS [24].

Congenital heart disease (CHD) is the most common birth defect in newborns [47] and a common cause of cardioembolic stroke in children. In the IPSS, 60% of children with cardiac-related stroke had CHD. Children with CHD can be affected by a wide range of cyanotic and acyanotic heart disorders and have a 19-fold risk of stroke when compared to controls [48]. The risk of stroke is related to the underlying heart disorder, its comorbidities, and other factors including cardiac procedures and the use of mechanical support devices [49]. AIS occurs most often among children with cyanotic heart disease [45]. Children who undergo surgery for CHD have a 13-fold increased risk of stroke when compared to controls [48]. An imaging study of infants that underwent surgery for CHD identified stroke in 10% of patients, most of which were clinically silent [50]. Among infants who undergo surgery for CHD, younger postnatal age at the time of surgery and selective cerebral perfusion are associated with AIS in the post-operative period [51]. In children who undergo surgery, other risk factors for stroke may be present and likely play a role. A study of children with CHD and AIS from South Korea found that most strokes occurred during the periprocedural period, and almost half had an additional risk factor for thromboembolism [52].

Patent foramen ovale (PFO), especially if associated with high-risk features such as atrial septal aneurysm, is associated with an increased risk of stroke in adults [53]. Randomized clinical trials have shown a benefit of closure

in carefully selected high-risk PFO patients [54–57]. The relationship between incident and recurrent stroke and PFO in children is unclear. A large observational study found an increased rate of PFO in children with cryptogenic stroke compared to children with stroke of known etiology and children without stroke [58].

Hematologic Disorders

Blood disorders have shown stronger risk associations with stroke in children compared to adults. Blood disorders documented in children with AIS include genetic and acquired coagulation abnormalities and sickle cell disease (SCD). Prothrombotic disorders were identified in 13% of children in the IPSS but have been reported at much higher rates in other studies of children with stroke [24, 59]. Prothrombotic disorders can lead to abnormal venous and arterial thromboses.

SCD is a group of inherited disorders caused by mutations in hemoglobin and is a major risk factor for AIS in children. SCD causes abnormally shaped (sickled) red blood cells with increased fragility that interact with the vascular endothelium and cause vaso-occlusion [60]. Two major cerebrovascular manifestations of SCD are large artery intracranial occlusive disease and silent cerebral infarction (SCI). Large artery steno-occlusive disease is thought to develop from endothelial hyperplasia and intraluminal thrombosis from recurrent sickling [61]. The large vessel changes typically develop within the distal internal carotid, middle cerebral, and anterior cerebral arteries and may progress to an angiographic pattern of moyamoya. SCI is defined as chronic ischemic changes at least 3 mm in size on T2-weighted magnetic resonance imaging (MRI) without neurologic signs or symptoms related to the lesion [62]. The mechanism for SCI in SCD is unclear but thought to be related to changes in perfusion and oxygenation [63].

Children with SCD (HbSS) have a risk of AIS over 200 times that of healthy children, and 10% percent will develop symptomatic AIS before 15 years of age [60]. While symptomatic AIS is common, 32% percent of children with SCD have evidence of silent infarction [64].

Genetic prothrombotic factors likely play a greater role in individuals presenting with AIS in childhood compared to onset in later years [65]. Several genetic and acquired prothrombotic abnormalities have been evaluated in children with AIS, but the rate of these abnormalities have varied among different age groups, stroke subtypes, and international populations studied [66]. Prevalence differences are likely due to the extent and timing of investigations, small sample sizes, and population admixture and stratification [67]. Coagulation abnormalities tend to be more common in European-derived populations compared to other ethnic and racial groups. Case–control studies, utilizing hospital-based adult and population-based child controls, have shown an association between many of these abnormalities and AIS [68–71], while other studies have been negative or too small to show a difference [72–74]. The presence of a prothrombotic abnormality has also been shown to increase the risk of recurrent stroke in children [75].

Infectious Disorders

Several infectious agents have been reported in association with AIS in children. Infection can lead to cerebral ischemia through multiple mechanisms, including activation of the coagulation cascade, thrombosis from a systemic inflammatory response, septic emboli, and direct invasion of the endothelium. During serious infection, there is a rapid destruction of protein C and antithrombin III, both of which normally inhibit coagulation. Infection also produces endothelial injury and a release of inflammatory cytokines, which lead to the downregulation of thrombomodulin. Decreased levels of activated protein C and increased levels of D-dimer and C4b binding protein have also been observed in patients with AIS [76]. The timing of infection also seems to play a role in the risk of stroke and may be related to infection-related activation of the coagulation system. A population-based case–control study found that a recent infectious visit ≤ 3 days prior was associated with a 12-fold increased risk in stroke [77]. Infections were identified in 24% of children in the IPSS [24], but studies in China [22] and Turkey [78] found much higher rates in children with stroke.

Childhood AIS has been reported as a complication of bacterial infection from meningitis, encephalitis, brain abscess, sinusitis, and sepsis. The prevalence of AIS in infants and children with bacterial meningitis has ranged from 24 to 71% [79–81]. A recent population-based study in Canada found that 37% of children with bacterial meningitis developed stroke. In this study, children with meningitis plus stroke had higher rates of morbidity and mortality than children without stroke [82]. A study of children with tuberculous meningitis in South Africa identified a stroke in 71% of children at admission. Risk factors associated with stroke at admission included young age (< 3 years), seizures, and hydrocephalus [81].

Viral infections have also been linked to childhood AIS and include varicella [32], HIV [83], parvovirus B19 [34], Zika [84], Dengue viruses [85], herpes simplex [86], Epstein Barr [87], CMV [88], and COVID-19 [36]. Studies of varicella zoster virus (VZV) have provided the most evidence supporting a link between a viral infection and AIS in children [88, 89]. A case–control study of children with AIS found a history of VZV infection within the last 9 months in 64% of cases and 9% of controls [32]. A cohort study in Canada discovered a threefold increase in the frequency of

a prior VZV infection in children with AIS compared to published controls [90]. In children with VZV, the rate of AIS has been estimated at 1/26,000 children [91].

VZV infection can produce a large vessel granulomatous angiitis with multinucleated cells that affects the distal internal carotid and proximal cerebral arteries and may lead to endothelial injury and AIS. The path in which VZV infects cerebral vessels may be related to afferent fibers from the trigeminal ganglia to the circle of Willis. During VZV infection, the virus can pass into the trigeminal ganglion and enter a latent state; upon reactivation, the virus could then travel through afferent fibers that innervate the intracranial vessels and cause a focal vasculitis and ischemic stroke [92]. A recent theory on the pathogenesis of varicella arteriopathy is that infection causes adventitial fibroblasts to transform into myofibroblasts, resulting in proliferation and migration that contributes to arterial remodeling, along with endothelial activation by VZV microparticles [93]. The recurrence rate of TIA and AIS among children with VZV-related AIS has been reported as high as 45% [90].

Several other viruses and microbial infections have been reported in association with stroke in children. The rate of parvovirus B19 and herpes simplex virus was higher in cases of children with stroke compared to controls in the VIPS (Vascular Effects of Infection in Pediatric Stroke) study [34, 94]. Recently, there have been several reports of stroke in children infected with the SARS-CoV2 virus [36, 95–97]. Multisystem inflammatory syndrome is observed in children after acute infection with severe SARS-CoV2 and has been associated with stroke. A large international registry of children with stroke and SARS-CoV2 found that inflammatory arteriopathies were the most common cause of stroke [36]. Other infections, including rickettsial infections, have also been associated with stroke in children [98, 99].

Cancer-Related Stroke

Over the last 40 years, there has been an increase in the incidence of childhood cancer in the USA [100]. Despite these changes, survival rates for children with cancer continue to improve. Children with cancer can develop neurologic complications from their disease as well as acute, chronic, and late effects from cancer therapy. Cancer is a risk factor for incident and recurrent stroke [101]. Several cancer types have been associated with stroke in children and include acute lymphoblastic leukemia, Hodgkin disease, and brain tumors. The mechanisms that typically lead to stroke in cancer patients include radiation-induced cerebrovascular disease, compression of intracranial vessels, cancer-related coagulopathy, cardioembolism, infection, and complications from chemotherapy. Cancer or tumor was present in 3% of children in the IPSS. In children who developed cancer-related AIS, 88% had a brain or hematological cancer [101]. The cause of cancer-related AIS in this cohort was most often due to arteriopathy or cardioembolism [101].

Rare Causes of Stroke in Children

Stroke has been reported with over 100 medical disorders in children, many of which are rare but have been reported in the literature more recently. Bow Hunter's syndrome (BHS), or rotational vertebral arteriopathy, is due to compression and or dissection of the vertebral artery with head turning [102]. The underlying cause is thought to be due to abnormal osteophytes, fibrous bands or lateral disc herniation with neck rotation or extension [103]. Children with BHS can develop vertebral dissection and stroke, but there is no consensus on treatment and prevention. Surgical treatment with C1/C2 fusion has been performed in children with BHS, but whether this treatment is more effective than medical therapy is unknown [104]. Similar to BHS, thoracic outlet syndrome (TOS) is related to compression of neurovascular structures. TOS can occur from compression of the subclavian artery from a bony structure (such as a cervical rib) and can lead to thrombus formation and stroke. Risk factors for TOS include activities that involve repetitive movement of extreme abduction and external rotation of the shoulders [105]. The mechanism through which TOS leads to stroke is unclear. One theory is that subclavian compression can lead to trauma and thrombus formation, and retrograde propagation or propulsion of the thrombus can lead to embolization in the vertebral or common carotid arteries [106]. Similar to BHS, the optimal prevention strategy is unclear, but most patients reported in the literature have undergone thoracic outlet decompression surgery as opposed to medical therapy [106].

Outcomes of Stroke in Children

The morbidity and mortality from AIS have varied among studies due to differences in functional outcome measures, stroke type, duration of follow-up, and cohort studied. Most studies have focused on motor recovery as opposed to language, vision, cognition, quality of life, or other neurologic deficits. A review of pooled data from early studies of AIS in children from 1977 to 2004 ($N = 1364$) revealed that on average 30% of children were neurologically normal, 61% developed cognitive or motor problems, and 9% died by the outcome evaluation period [107]. More recent prospective studies that used standardized functional measures found similar rates. A study of the Swiss NeuroPediatric Stroke Registry found that in children with AIS, 26% were neurologically normal, 63% developed neurologic disability, and 11% died by 6 months [108]. A study of children with AIS from the IPSS found that 74% had a neurologic deficit at

discharge and 3% died from their stroke [109]. A study from the Canadian Pediatric Stroke Registry ($N=681$) found that among infants and children with AIS, 69% died or had a neurologic deficit at a mean follow-up time of 3 years [9]. Few studies have reported long-term outcomes. An outcome study from the IPSS found that 54% of children were neurologically normal and 46% had mild, moderate, or severe disability at 2 years. The study also found that 46% of children demonstrated recovery over the 2-year follow-up period [110]. A study of children with AIS from Switzerland found that 56% of children followed for a median of 6.9 years had a favorable outcome, as defined by a modified Rankin scale score of 0–1 [111].

Several outcome predictors have been reported in children with AIS and include age at onset, clinical presentation, lesion location and volume, post-stroke seizures, and etiology of stroke [110, 112–115]. Stroke onset in childhood is associated with a poorer outcome compared to stroke in the neonatal period [110, 113, 116]. Studies of children with stroke from Canada, the USA, Israel, the UK, and the Netherlands found an association between children who present with altered levels of consciousness and/or seizures with poor outcome [9, 117–120]. Stroke volume and location have been shown to impact both motor and cognitive function [112, 121, 122]. Large lesions (defined differently in different studies), involvement of both the subcortical and cortical regions, and Wallerian degeneration within the corticospinal tract have been shown to be associated with poor motor outcome [112, 116, 123–126]. Post-stroke seizures are more common in children than adults, with a cumulative incidence of 30% at 10 years [127]. Children who develop epilepsy post-stroke have worse neurologic outcomes than children without epilepsy [119, 128]. The underlying cause of stroke has been associated with both outcome and recurrence in children. Children with arteriopathy- and cardiac-related stroke have worse outcomes than other stroke subtypes [9, 109, 129–132].

Recurrent Stroke and Death

The reported recurrence rate of AIS in children ranges from 6 to 30% [133, 134], and most recurrences develop in the first 6 months after incident stroke [135, 136]. The recurrence rate of AIS is highest among children with TIA, cardiac disease, arteriopathies, metabolic and coagulation abnormalities, and posterior circulation strokes. A population-based study of children with stroke found a high rate of recurrent stroke among children with arteriopathy [137]. The presence of arteriopathy increased the risk of recurrent stroke fivefold in the VIPS study [28]. A study that compared the rate of recurrent AIS among children with anterior and posterior circulation stroke found much higher rates in children with posterior circulation strokes [138]. The presence of a thrombophilia or combination of coagulation abnormalities is also associated with an increased risk of recurrent stroke [134, 136].

Case fatality rates for AIS in children have ranged from 0 to 28% depending on the population studied, but recent studies have shown lower rates than in the past [8, 120, 139]. Mortality rates for AIS are highest among children less than 1 year of age. The death rate from cerebrovascular diseases in children peaks at 2.7 per 100,000 in infants, subsequently declines, and does not exceed the infant mortality rate until 35–44 years of age [140]. The mortality rate in children due to AIS is higher in males than females and in black children compared to white children [141].

Diagnostic Evaluation

Consensus guidelines have provided some guidance on the evaluation of stroke in children, but several controversies and knowledge gaps exist [43, 142–144]. The evaluation should identify the etiology and rule out other non-vascular causes that mimic stroke in children (postictal paralysis, migraine, hypoglycemia, and alternating hemiplegia). While there is limited evidence to support the use of acute therapies (intravenous [IV] tissue plasminogen activator [tPA] or mechanical thrombectomy [MT]) in children, a rapid stroke evaluation and neuroimaging seems reasonable to determine whether a favorable profile exists for hyperacute treatments. The history should include questions regarding head and neck trauma, unexplained fever or recent infection (varicella in last 12 months), drug ingestion, developmental delay, blood disorders, and associated headache. A careful family and birth history should also be taken, with special attention to neurologic disease, premature vascular disease, hematologic disease, and developmental disorders.

Acute Diagnosis of Stroke

Significant delays in the acute diagnosis of stroke in children have likely restricted access to acute therapies. Several factors have contributed to these delays including delays in arrival to medical care, diverse clinical presentations, accuracy of diagnosis among ED providers, lack of effective stroke screening tools, an absence of pediatric "code stroke" protocols, and use of imaging that is insensitive to acute ischemia [143, 145]. The American Heart Association (AHA) recommends that centers establish systems and pathways for hyperacute pediatric stroke care [43]. Standardized institutional stroke protocols have been found to improve the time to diagnosis of stroke in children [146–148]. These protocols have typically consisted of the following components: a stroke screening tool in the ED (based on time of onset and

symptoms), a code stroke activation process, a dedicated stroke responder, and a triage process for acute MRI [146, 149, 150].

Neuroimaging

MRI is the preferred imaging modality for acute stroke in children because it allows for early differentiation of stroke from mimics; this is critically important due to the high rate of stroke mimics in children. MRI is better than CT for the detection of acute ischemia and can also detect acute and chronic hemorrhage [151]. A consensus-based statement from members of the IPSS recommended the following sequences for stroke in children: DWI, FLAIR, GRE or SWI, T1 and T2 (optional sequences include T1 contrast and arterial spin labeling) [152]. Recently, several other rapid sequence MRI protocols have been recommended for stroke in children. These have included similar sequences with the addition of a time-of-flight MRA [153, 154]. Perfusion imaging is helpful in determining stroke core and penumbra and selecting patients for acute therapies. Dynamic susceptibility contrast MR perfusion is an IV contrast (gadolinium)-based perfusion technique that is commonly used in adults but seldom in children with stroke. Concerns regarding an IV bolus of contrast and gadolinium accumulation in the brain have limited its use in children. Arterial spin labeling (ASL) is a non-contrast perfusion technique that is commonly used in children with stroke. Several ASL techniques have been developed to evaluate cerebral perfusion. These techniques involve the use of radiofrequency pulses to magnetically tag arterial blood in the skull base, which is then imaged as the blood flows into the brain. A cerebral blood flow map is derived from the imaged blood as it flows into various brain regions. ASL is more useful in children than adults, since it does not require IV contrast and has better signal to noise ratio in children compared to adults [155]. Overall, the use of MRI in children with stroke has been limited due to institutional (MRI availability, anesthesia availability, lack of rapid sequence protocols) and patient-related factors [156].

Etiologic Investigations

A comprehensive evaluation of children with stroke should include cardiac, hematologic, metabolic, inflammatory, and brain and vessel imaging studies, as evidence suggests that children with stroke may have multiple risk factors [43]. Advanced studies should be considered for children with cryptogenic or recurrent stroke. The primary goal is to utilize an iterative approach to identify the cause of stroke for secondary prevention and to determine prognosis. The AHA guidelines for the management of stroke in neonates and children recommend a baseline evaluation for all children with stroke (Table 1) [43]. Depending on the clinical context, advanced diagnostic studies can be considered when the stroke remains cryptogenic and/or recurs (Table 2).

Table 1 Standard basic evaluation of childhood stroke

Standard diagnostic studies	Stroke etiology
MRI head	Rule out stroke mimics
TTE with bubble study, EKG	PFO, cardiac arrhythmias, identification of intracardiac thrombus
MRA brain and neck or CTA head and neck	Dissection, arteriopathies
Coagulation studies	Inherited or acquired thrombophilias
ESR, CRP, ANA	Inflammatory disorders

TTE transthoracic echocardiogram, *EKG* electrocardiogram, *MRA* magnetic resonance angiography, *CTA* computed tomography angiography, *ESR* erythrocyte sedimentation rate, *CRP* C-reactive protein, *ANA* antinuclear antibody

The approach to diagnostic evaluation of perinatal stroke differs from childhood stroke, as most perinatal strokes occur due to a convergence of multiple risk factors specific to the perinatal period [157]. Transthoracic echocardiography and neurovascular imaging can be performed to rule out intracardiac thrombus, abnormal cardiac anatomy, and cerebrovascular abnormalities. Several recent studies have shown that thrombophilia testing is low yield and does not typically predict recurrence risk or change management [74, 158], so these extensive laboratory studies can be reserved for children with concerning family histories or recurrent thromboembolic events.

Evidence Gaps and Diagnostic Testing

There are limited studies regarding the indications, utility, and cost-effectiveness of diagnostic studies for stroke in children. For example, a study examining the diagnostic yield of various studies in young adults (18–45 years old) with stroke showed that Holter monitoring, vasculitis panels, and toxicology screening were low yield studies [159]. The diagnostic yield of these and other studies in childhood stroke is unknown.

The role of PFO in the pathogenesis of stroke in children is unclear, as discussed below. The need for additional studies beyond standard transthoracic echocardiography with agitated saline, such as transesophageal echocardiography or transcranial Doppler (TCD) ultrasound with agitated saline, to identify and characterize PFO is also uncertain.

Several genetic and acquired prothrombotic abnormalities have been evaluated in children with AIS, and the rates of these abnormalities have varied widely among studies. Many of these abnormalities, including antithrombin deficiency, protein C deficiency, elevated lipoprotein(a), and antiphospholipid antibodies, have been associated with

Table 2 Advanced diagnostic evaluation of childhood stroke

Advanced diagnostic studies	Stroke etiology
Holter monitoring	Arrhythmia
Cerebral angiography	Moyamoya, FCA, covert dissection
Lumbar puncture	Infectious/inflammatory FCA, meningitis/encephalitis, primary angiitis of the central nervous system
Artery biopsy	Fibromuscular dysplasia
Genetic/metabolic studies	HHT, Moyamoya, arteriopathies, thrombophilia, inflammatory disorders, Fabry's, MELAS, POLG1, connective tissue disorders, DADA2
Brain biopsy	Angiography-negative childhood primary angiitis of the central nervous system
Dynamic CTA or DSA neck	Bow Hunter's syndrome

FCA focal cerebral arteriopathy, *HHT* hereditary hemorrhagic telangiectasia, *MELAS* mitochondrial encephalopathy, lactic acidosis, and stroke like episodes, *POLG1* DNA polymerase subunit gamma 1, *DADA2* deficiency of adenosine deaminase 2, *CTA* computed tomography angiography, *DSA* digital subtraction angiography

incident stroke in children, but further studies are needed to determine the risk of recurrent stroke [71]. Prothrombotic abnormalities tend to be more common in European-derived populations compared to other ethnic and racial groups, and whether these tests should be performed in all children with stroke is unknown.

MRI vessel wall imaging (VWI) is a diagnostic tool that utilizes special MR sequences to suppress the signal in areas within and around a blood vessel (flowing blood and CSF) to image the vessel wall. VWI requires a high spatial resolution and is typically performed on 3 T or higher scanners and with higher channel head coils. Imaging in multiple planes (2D and 3D) is required for optimal resolution of the vessel wall. Most protocols include pre- and post-contrast T-1 weighted studies to evaluate for enhancement within the vessel wall. The most common sequence used for blood and CSF suppression is a 3D turbo spin-echo sequence with variable flip angle refocusing pulses, which varies among vendors. VWI should be interpreted by individuals with experience in vessel wall imaging as age related, flow, and anatomical variation can sometimes mimic disease [160, 161]. MRI VWI has been shown to be helpful in the differentiation of intracranial arteriopathies [162]. Vessel wall enhancement is considered a marker of inflammatory vasculitis. A study by Dlamini and colleagues evaluated 26 children with AIS and found that distinct VWI patterns were associated with specific types of arteriopathy [163]. A study of 16 children with AIS found that strong vessel enhancement on VWI was associated with progressive arteriopathy [164]. However, a more recent study of 9 children with AIS and FCA who underwent VWI did not find an association with vessel enhancement and progression [165]. VWI studies can be long and require contrast agent and may therefore not be suitable for all children. Further studies are needed to determine the utility of VWI in children with AIS [165].

Finally, the role for genetic testing in pediatric stroke is expanding. Elucidation of the genetic cause of stroke can inform counseling, recurrence risk, and prognosis. It may also drastically change management strategies. For example, a diagnosis of deficiency of adenosine deaminase 2 (DADA2) may prompt discontinuation of antiplatelet therapies and initiation of TNF inhibitors [166, 167], as detailed below.

Therapeutics

Acute Therapies

IV Thrombolysis

The transformation of adult stroke care at the end of the twentieth century with the approval of IV thrombolysis for acute stroke and concurrent implementation of integrated stroke systems of care led to questions about the appropriateness of IV thrombolytics for childhood stroke. Several a priori considerations suggest that extrapolation from adult data may be inappropriate. Specifically, stroke etiologies differ between children and adults, with certain common childhood stroke etiologies not being clearly amenable to treatment with thrombolytic agents. Additionally, developmental changes in the coagulation cascade, termed "developmental hemostasis," should be considered, as younger children have lower levels of endogenous tPA and higher levels of plasminogen activator inhibitor-1 (PAI-1) compared with older children and adults [168–170], suggesting that different thrombolytic dosing may be needed based on age. Finally, as outcome after childhood stroke is generally better than after adult stroke in the absence of treatment, the risk–benefit balance may differ based on age.

The Thrombolysis In Pediatric Stroke (TIPS) trial was a multicenter prospective safety and dose-finding study of IV tPA in childhood stroke which unfortunately closed prematurely due to lack of participant accrual [171]. Nonetheless, TIPS resulted in important infrastructure development in participating sites, including protocols that allow for rapid, systematic diagnosis

and treatment of pediatric stroke [172]. TIPS also led to the TIPSTER study, which retrospectively analyzed the safety of IV thrombolysis for acute stroke in 26 children at prior TIPS sites [173]. The analysis yielded an estimated 2.1% rate of symptomatic intracranial hemorrhage after thrombolysis in children, suggesting IV thrombolysis for acute stroke is at least as safe in children when compared to adults [174].

Currently, IV thrombolytic agents are administered in 5–7% of cases of childhood stroke in the USA [175, 176]. A recent serial cross-sectional study of admissions for childhood AIS identified using the Kids' Inpatient Database showed that IV tPA utilization in the USA significantly increased from 2.5 to 6.5% between 2005 and 2019 [176]. An analysis of the National Inpatient Sample similarly showed an increase in IV thrombolysis use from 1.6% between 2010 and 2015 to 5.5% between 2016 and 2019 [175]. Despite the increased use of thrombolytics for acute childhood stroke, the true benefit conferred by tPA in children, the ideal weight-based dosing, and the optimal time window for administration of IV tPA in children all remain unknown.

Mechanical Thrombectomy

Mounting observational data suggest that MT for acute stroke has a good safety profile in children. In the SaveChildS study, a recent retrospective cohort study of 73 children who underwent MT for acute AIS, only 1 patient developed symptomatic intracranial hemorrhage [177]. Given the concern about high rates of large vessel arteriopathies in childhood stroke, with theoretical increased risk of dissection, vasospasm, or vessel rupture in such cases, the authors noted that none of the 14 children with arteriopathies in SaveChildS experienced these complications [177]. A similar excellent safety profile was reported in an analysis of the National Inpatient Sample, which reported that in 190 children treated with MT, no patient suffered contrast-induced kidney injury nor periprocedural iatrogenic ischemia or hemorrhage [175].

While a growing body of evidence supports the feasibility and safety of MT in children, the efficacy remains less clear. For example, in the Save ChildS study, there was no control group to account for potential natural history of improvement. Nonetheless, children in the study who underwent MT had a reduction in median pediatric National Institutes of Health Stroke Scale Score (pedNIHSS) from 14 at admission to 4 at discharge. At 6 months from stroke, patients in this study had favorable neurologic outcomes, with 87% achieving a modified Rankin scale score (mRS) of 0–2. The results from the SaveChildS study are concordant with a meta-analysis of 113 children who were treated with MT for acute stroke [178]. In that analysis, over 90% of patients had favorable neurologic outcomes, though the role of publication bias must be considered.

More recently, a retrospective, population-based cohort study of childhood ischemic stroke in Australia demonstrated that children with large vessel occlusions who were treated with MT ($n = 13$, with or without IV-tPA) had better functional outcomes compared with children with large vessel occlusions who were managed conservatively ($n = 26$) [179]. The authors point out, importantly, that the absence of randomization or standardized MT selection criteria likely led to selection bias, and children who were treated with MT were older than those children managed conservatively, which may have driven, at least in part, the differences in outcomes.

In another recent analysis using the National Inpatient Sample by Dicpinigaitis and colleagues, 55.3% of children with acute ischemic stroke treated with MT had favorable outcomes at discharge [175], though the authors defined favorable as discharge to home or acute rehabilitation, which likely encompasses a broad range of functional outcomes. After propensity adjustment to address confounding by indication, patients treated with MT had higher rates of favorable functional outcomes compared to medically managed patients, though this did not reach statistical significance. Patients with greater dysfunction (NIHSS > 11) received a larger benefit from thrombectomy compared with controls, though this also did not reach statistical significance [175].

MT use is increasing in the USA, with recent data demonstrating that 3–4% of children admitted with acute AIS are treated with MT [175, 176]. Cross-sectional data derived from the Kids' Inpatient Database showed that MT was used in 1.2% of children admitted for AIS in 2009 and in 3.0% of similar children in 2019 [176]. A recent analysis of the National Inpatient Sample likewise showed an increase in MT utilization from 1.7% prior to publication of the landmark adult thrombectomy trials (2010–2015) to 4.0% in the post-thrombectomy era (2016–2019). In an Australian study of childhood ischemic stroke conducted between 2010 and 2019, a third of children with large vessel occlusion were treated with MT, with or without IV-tPA.

The boundaries of MT use in children have not yet been established. The time window to safely perform thrombectomy is generally extrapolated from adult data, but differences in collateral vasculature or other pediatric-specific factors may modify the time window in children. In a secondary analysis of 20 children in the SaveChildS study, MT between 7.8 and 16.2 h from symptom onset in the setting of a mismatch between clinical deficit and radiographic infarction was safe and associated with neurologic improvement, with reduction of pedNIHSS from 12 on admission to 2 at day 7 [180]. Several case reports even demonstrate good outcomes after MT when performed after 24 h from stroke onset [181–184]. Nonetheless, selection criteria for late-window MT are not yet well-established, and extrapolation from adult parameters may not be appropriate given concerns about differing penumbral thresholds in children compared with adults [185].

Similarly, the minimum age for MT eligibility in pediatric stroke is controversial [186, 187]. As there are no stent retrieval or aspiration devices designed specifically for children, questions frequently arise regarding the compatibility of devices designed for adults with the smaller pediatric cervicocerebral vasculature. While the head and neck vessels approximate adult size by the age of 5 years [188], access through the femoral arterial diameter may be more limiting [189]. Nonetheless, MT has been reported with good outcome in many children below 5 years of age [190], though very preliminary data suggest younger children may receive less benefit from thrombectomy compared with their older counterparts [177]. Other technical modifications related to tolerance of blood loss and safety of contrast and radiation exposure in young children should be considered [189]. Notably, thrombectomy in neonates is generally discouraged by pediatric stroke specialists, particularly given the inability in most cases to establish a clear time of stroke ictus and likelihood of higher risk of MT due to smaller vasculature [187].

As there are no randomized controlled data that allow for clear recommendations about when to proceed with MT in children, potential risks and benefits must be carefully weighed based on each individual patient's degree of disability, age, size, stroke etiology, comorbidities, and neuroimaging characteristics.

Acute Therapies in Special Populations

Moyamoya Disease Moyamoya disease is a progressive steno-occlusive arteriopathy of the intracranial vasculature beginning with the distal internal carotid arteries with compensatory collateral vessel formation. It can occur in isolation or with an associated condition including sickle cell disease, neurofibromatosis, and Down syndrome [42]. Moyamoya accounts for about 8% of childhood AIS and is associated with high rates of stroke recurrence [37]. The perioperative period is a particularly high-risk epoch for moyamoya-related stroke, which remains a challenge in moyamoya care due to the need for angiography and surgical management [191, 192]. While long-term stroke prophylaxis may include antiplatelet therapies and/or surgical revascularization, acute stroke is typically managed with augmentation of cerebral perfusion pressure with fluids and flat head of bed. Consideration can be given to vasopressors in the right clinical context, such as if the patient is hypotensive or there are other indicators of cerebral hypoperfusion [193]. Pain and agitation control is of paramount importance, as hyperventilation can lead to cerebral vasoconstriction, thereby exacerbating cerebral hypoperfusion [191]. Maintenance of normocarbia and normoglycemia and minimization of metabolic demand through normothermia and prompt seizure control are also important neuroprotective measures. The role of antiplatelet therapy and red blood cell transfusion in acute stroke in children with moyamoya needs further investigation. IV thrombolysis is contraindicated due to high risk of intracranial hemorrhage due to fragile collateral vasculature. Similarly, MT is typically not performed in children with moyamoya given increased risks of introducing a catheter into diseased vessels and low likelihood of benefit.

Sickle Cell Disease SCD is a major risk factor for childhood ischemic stroke [194]. The highest risk time for SCD-associated stroke is in the first decade of life [60]. By 20 years of age, 11% of individuals with SCD will experience a clinically evident stroke, and nearly a quarter of individuals with SCD have a stroke by age 45 years in the absence of preventative measures [60]. Recurrent stroke is also common in patients with SCD [195].

Any person with SCD presenting with acute neurologic deficits should be treated with an emergent blood transfusion, ideally an exchange transfusion when possible [196]. The role of IV thrombolysis and MT in children with SCD is less well-studied. In an analysis of the AHA/ASA Get With The Guidelines Stroke Registry, in adults with acute stroke who received thrombolytic therapy, rates of symptomatic intracranial hemorrhage were not higher in patients with SCD, and coexistent SCD did not impact the discharge outcome [197], suggesting that IV-tPA should not be withheld from adults with SCD. In adults with SCD and acute stroke, thrombolysis and thrombectomy should be considered, as they are for patients without SCD, followed by red blood cell exchange transfusion [198]. However, most pediatric stroke protocols exclude children with SCD from consideration for IV-tPA due to perceived high risk of intracranial hemorrhage related to high rates of moyamoya syndrome and intracranial hemorrhage in this population [199], particularly in the absence of proven benefit in children. The American Society of Hematology recommends against IV tPA for children with SCD [196]. There are no data on the risks or benefits of MT in children with SCD. It is the view of the authors that eligibility for MT should be considered using standard guidelines in children with SCD and large vessel occlusion, though special consideration must be made due to high rates of cerebral arteriopathies and moyamoya syndrome in children with SCD.

Systems of Care for Delivery of Acute Stroke Interventions

With increasing utilization of both IV thrombolysis and MT [175, 176], implementation of acute pediatric stroke protocols is critical to be able to deliver these interventions rapidly, safely, and effectively. Prior to the TIPS trial, which was initially funded in 2010, centers interested in pediatric stroke lacked systematic readiness to rapidly diagnose and

treat childhood stroke [172]. In defining staffing, neuroimaging, and ordering criteria necessary to administer IV tPA, TIPS set standards that led to the emergence of the primary pediatric stroke center [172]. More recently, a survey of pediatric stroke specialists showed that at least 41 pediatric centers in the USA and Canada have established acute stroke protocols [200]. Another survey demonstrated that most pediatric hospitals surveyed have stroke protocols to be able to deliver IV tPA and thrombectomy, but respondents did not agree on precisely what the protocols should contain and how they should be actualized [201]. That survey study also highlighted the need for development of standardized pre-hospital screening tools for pediatric stroke.

Multiple acute pediatric stroke protocols and accompanying data on time to stroke diagnosis have been published [146–148, 202–204], with average time from presentation to neuroimaging/diagnosis ranging from 1.3 to 10.5 h. This starkly contrasts to adult data, which boasts median door-to-needle times of around an hour for the past decade [205, 206]. An analysis from a US hospital showed that the major source of pediatric stroke diagnostic delays was late presentation to the emergency department, suggesting that future interventions aimed improving community recognition of stroke symptoms could help alleviate these delays [203]. Though ongoing improvements in time to pediatric stroke diagnosis are needed, a recent Australian study of pediatric large vessel occlusions showed that the majority presented early enough to be eligible for MT (69% presented within 6 hours of symptom onset and 90% within 24 hours) [179].

Neuroprotection

Most children with stroke will not be candidates for IV thrombolysis or thrombectomy; however, prompt stroke diagnosis remains critical so neuroprotective measures can be implemented early. Neuroprotective measures aim to salvage penumbral tissue through optimization of oxygen and glucose delivery to at-risk tissue and minimization of metabolic demand through prompt fever and seizure control. Though there are limited data to support specific neuroprotective measures in children, strategies are generally adopted from the adult stroke literature [43].

In a retrospective multivariate analysis of modifiable physiologic parameters in 98 children with acute AIS, hyperglycemia was associated with worse neurologic outcomes, but fever and hypertension were not [121]. Based on this study as well as extrapolation from adult data, a recent scientific statement from the AHA/American Stroke Association (ASA) recommends treatment of hyperglycemia to achieve blood glucose < 180 mg/dL as well as avoidance of hypoglycemia [43].

Another retrospective study of 53 children with AIS showed that hypertension in the first 72 hours after stroke ictus was associated with higher in-hospital mortality, but not with neurologic disability [207]. The association between hypertension and childhood ischemic stroke and in-hospital mortality was supported by an analysis that identified children with ischemic stroke and hypertension using ICD codes in a large national database [208]. Importantly, hypertension may not be directly harmful but instead may be a compensatory mechanism to support cerebral perfusion in children with more severe presentations including large vessel occlusions and cerebral arteriopathies. Optimal blood pressure management in children after stroke remains an important knowledge gap [43].

Stroke Prevention

Stroke Prevention in Sickle Cell Disease

Primary Prevention Development of evidence-based primary prevention measures in childhood SCD has been incredibly successful. Without implementation of preventative measures, 11% of individuals with SCD will experience an overt stroke by 20 years of age [60]. Stroke risk in SCD can be stratified using TCD, a non-invasive bedside test that measures cerebral blood flow velocities [209]. In the 1998 Stroke Prevention Trial in Sickle Cell Anemia (STOP) trial, treatment of high-risk children (as stratified by TCD) with chronic transfusion therapy resulted in a 92% reduction in stroke risk compared with standard care [210]. Annual TCD screening is therefore recommended for screening all children with HbSS disease or HbSβ^0 thalassemia between the ages of 2 and 16 years [196, 211]. For children who meet TCD criteria for high stroke risk, monthly blood transfusions are recommended to maintain HbS level < 30% and hemoglobin > 9.0 g/dL. In environments where regular blood transfusion therapy and chelation therapy are not available or practical, hydroxyurea therapy can be considered as an alternative [196]. A retrospective trend analysis of the Nationwide Inpatient Sample and Kids' Inpatient Database showed that incidence rates of hospitalization for stroke in children with SCD decreased by 45% after publication of the STOP trial and hydroxyurea licensure in 1998, suggesting that these measures had been effective in primary stroke prevention in SCD [212].

Chronic transfusion therapy is associated with serious long-term morbidity, including alloimmunization, transfusion reaction, iron overload, and infection risk. High associated costs and burden to families and patients also limit adherence. Therefore, studies subsequent to STOP have examined when and how transfusions can be safely discontinued. In 2005, the STOP2 trial evaluated children with SCD with high stroke risk based on TCD screening but without severe

cerebral arteriopathy who had normalized cerebral blood flow velocities after at least 30 months on transfusion therapy [213]. Participants were randomized to either continue or discontinue transfusion therapy. Discontinuation of transfusions resulted in high rates of reversion to abnormal TCD readings (14 of 41 participants who had transfusion discontinued) and overt stroke (2 of 41 participants, mean 4.5 months after last transfusion) [213]. Subsequently, the 2015 TCD With Transfusions Changing to Hydroxyurea (TWiTCH) trial was a randomized, open label, non-inferiority trial that enrolled children 2–16 years old with abnormal TCD results but without severe cerebral arteriopathy who had received transfusion therapy for at least a year [214]. Participants were randomized to either continue transfusion therapy or transition to hydroxyurea. There were no differences in 24-month TCD velocities between the groups, suggesting that in children with SCD without cerebral arteriopathy, hydroxyurea may be a reasonable substitute for chronic transfusions after at least 1 year of transfusions [214]. Notably, participants in the study were on transfusion therapy for an average of 4 years, so the optimal duration of transfusion therapy prior to transition to hydroxyurea remains unknown.

Silent cerebral infarctions in children with SCD have been associated with cognitive impairment, recurrent silent infarction, and progression to overt stroke [62]. In the silent cerebral infarct (SIT) trial, children with silent cerebral infarcts who were treated with transfusion therapy, as opposed to standard observation, had lower rates of subsequent overt stroke or recurrent silent infarction [215]. Therefore, the American Society of Hematology recommends obtaining a screening brain MRI at least once in early school age children with HbSS or HbSβ^0 thalassemia once they are able to tolerate the imaging without sedation [196]. If silent cerebral infarcts are identified, secondary prevention measures, such as chronic transfusion therapy or hematopoietic stem cell transplantation, as well as neuropsychological evaluation, can be considered.

Despite effective and safe screening and prevention methods, there are substantial barriers to the widespread use of these measures. According to Medicaid claims data from 2010 to 2011, less than 25% of children in Maryland received the recommended annual TCD screening [216]. A recent national survey of SCD clinicians found only a 46% adherence to TCD screening guidelines, and low adherence was associated with practice barriers including lack of support staff or time [217]. Another study found that 22% of caregivers of children with SCD had no knowledge of TCD screening and that 42% were unaware that screenings were recommended annually [218]. Additionally, the lack of sufficient specialty SCD clinics impedes access to SCD-specific care for many individuals [219]. Importantly, as SCD affects largely Black Americans, racial disparities may play a role in poor access to care, with prior studies suggesting that differences in insurance coverage and systemic racism, among other factors, may play a role [220, 221].

Finally, there are emerging data that initiation of hydroxyurea in asymptomatic SCD patients may have a role in stroke prevention, though further investigation is needed. The BABY HUG trial demonstrated that early initiation of hydroxyurea mitigated the rise of cerebral blood flow velocities on TCD [222]. In the SCATE study, fewer children on hydroxyurea, compared with standard care, had conversion from conditional to abnormal TCD velocities [223], though the study was concluded prematurely due to slow patient accrual.

Secondary Prevention After incident stroke, two-thirds of individuals with SCD will have recurrent stroke [195]. Chronic transfusions are standard of care for secondary stroke prevention, but long-term transfusion therapy confers significant risks. In one study of 10 patients with SCD whose transfusions were halted an average of 9.5 years after stroke, 50% of participants had an ischemic event within 12 months of transfusion discontinuation [224]. In 2012, the Stroke With Transfusions Changing to Hydroxyurea (SWiTCH) trial investigated hydroxyurea plus phlebotomy as an alternative to transfusions with chelation therapy for recurrent stroke prevention in participants with SCD, prior clinical stroke, and iron overload [225]. SWiTCH was unfortunately terminated early due to statistical futility for the composite endpoint, as there was equivalent liver iron content in the two groups. Though the stroke endpoint was within the non-inferiority margin, there were no strokes in the 66 participants in the transfusion group, but 10% of the 67 participants in the hydroxyurea group experienced stroke [225]. Transfusions with chelation therefore remain standard of care for prevention of stroke recurrence in children with SCD.

Optimization of other stroke risk factors is also an important component of stroke prevention in children with SCD. Of note, the role of antiplatelet therapy in stroke recurrence prevention in patients with SCD remains unclear, and other stroke risk factors as well as the presence of arteriopathy must be considered when making decisions about antithrombotic therapy initiation.

Antithrombotic Therapies

The decision to start antithrombotic therapy, choice of agent, timing of initiation, and duration of therapy are highly dependent on the cause of the stroke and patient-specific factors such as age and comorbid conditions. After perinatal stroke, antithrombotic therapy is rarely indicated, as the stroke risk factors that converge to cause the vast majority of perinatal strokes are generally confined to the perinatal

period. In contrast, antithrombotic therapy is a mainstay of secondary prevention after childhood stroke [157].

The type of antithrombotic therapy chosen after childhood stroke varies both by stroke etiology and geographic region [226]. When the stroke etiology is determined to be cardioembolic or due to a thrombophilia, anticoagulation is typically recommended [43]. In the case of cervical arterial dissection, there are no pediatric data to guide the choice of antithrombotic agent, and there remains equipoise in adults as well [227, 228]. The presence of an intraluminal thrombus may prompt the clinician to opt for anticoagulation, while a large associated stroke may make antiplatelet therapy more appropriate. Antiplatelet agents are typically recommended for cryptogenic stroke and moyamoya. However, in the absence of strong evidence supporting a specific antithrombotic agent choice for most causes of pediatric stroke, optimal stroke prevention strategies remain unknown.

In the setting of acute stroke, the general approach is to initiate antithrombotic therapy only after the risk of recurrent stroke exceeds the risk of hemorrhagic transformation of the infarcted tissue. When anticoagulation is deemed necessary, initiation of a heparin infusion with neuroimaging once therapeutic to evaluate for hemorrhagic transfusion before transition to a longer-acting anticoagulant is reasonable. The choice of anticoagulant, which includes low molecular weight heparin, warfarin, or direct oral anticoagulants, should be based on stroke etiology and patient-specific factors. Antiplatelet agents, including aspirin and clopidogrel, can generally be initiated earlier than anticoagulation after incident stroke.

Duration of antithrombotic therapy depends on the stroke cause. In cryptogenic childhood stroke, expert consensus is to continue antithrombotic therapy for 2 years, as most stroke recurrences occur within this time frame [43].

Immunomodulatory Therapies

Steroids and other immunomodulatory therapies may play a role in stroke prevention in children with inflammatory, infectious/post-infectious, and genetic arteriopathies [229]. The most accepted use of these therapies is in primary central nervous system (CNS) angiitis, though specific regimens vary between institutions [230, 231]. In children with FCA, some evidence suggests that corticosteroids may improve outcomes when added to antithrombotic therapy [232]. This is an area of interest given emerging evidence of inflammation in the pathogenesis of FCA, though the pathophysiology of FCA is an area of ongoing investigation [165, 233]. Several studies are currently ongoing to evaluate the role of steroids in the treatment of FCA.

Anti-TNF therapy is the mainstay of therapy in children with DADA2, which is a genetic small and medium size vasculitis that results in early lacunar strokes in addition to manifestations of systemic vasculitis [166]. Available data suggest that TNF inhibition may be effective in reducing the risk of stroke in children with DADA2 [166, 167]. Importantly, patients with DADA2 are at risk for hemorrhagic stroke, and thus, antithrombotic therapy is generally not recommended.

PFO Closure

The pathophysiologic role of PFO in childhood stroke remains undetermined, but multiple recent adult studies showed that PFO closure reduces recurrent stroke risk in a subset of young adults with cryptogenic strokes when compared with medical management alone [54–57]. Based on these studies, the American Academy of Neurology 2020 practice advisory suggests that PFO closure can be considered for patients under 60 years old with a PFO and embolic-appearing infarct in the absence of another stroke mechanism [234]. In a recent prospective observational single-center study, children with cryptogenic stroke had a higher frequency of PFO compared with children with stroke of known etiology and with children who had echocardiograms for benign cardiac concerns, which hints at a potential causative relationship between PFO and childhood stroke [58]. Nonetheless, which children would benefit from PFO closure after cryptogenic stroke remains unknown, and further investigation is necessary [235].

Surgical Revascularization in Moyamoya Arteriopathy

Children with moyamoya are at high risk of occurrent and recurrent stroke [28, 37, 137]. The mainstay of long-term stroke prevention in moyamoya is revascularization surgery, which can be done via a direct anastomotic bypass or via an indirect non-anastomotic approach, the latter of which is more commonly performed in children. In a retrospective analysis of 174 children with moyamoya enrolled in the IPSS, children who had revascularization surgery were less likely to experience stroke recurrence [37]. Observational single-center data also suggest that revascularization surgery confers protection from ischemic stroke in children with moyamoya [236, 237].

Though revascularization surgery decreases the long-term risk of stroke, there is a risk of perioperative complications, especially ischemic stroke and TIA. Reported incidence of perioperative ischemic events for children with moyamoya undergoing revascularization surgery ranges from 4 to 20% [192, 237–240]. Therefore, selecting patients in whom these risks are outweighed by the long-term benefits of surgery is critical. Some data suggest that radiographic progression and the presence of biomarkers such as the ivy sign may help stratify risk of clinical disease progression and identify patients likely to benefit from surgery [241,

242]. The ivy sign is characterized by leptomeningeal fluid-attenuated inversion recovery (FLAIR) hyperintensity or contrast enhancement on T1-weighted images that looks like ivy growing along the sulci and subarachnoid space [243]. It represents engorgement of the pial vasculature and/or slow flow in leptomeningeal collateral vessels and is thought to indicate cerebral hypoperfusion and elevated stroke risk. Common comorbid conditions may also modify stroke risk, with recent data demonstrating that children with neurofibromatosis type 1 generally have milder disease, while associated Down syndrome and SCD portend a more aggressive course [42, 244].

Increasingly, patients are being diagnosed with moyamoya before they experience stroke or TIA. This occurs typically when patients with commonly associated conditions, such as neurofibromatosis and SCD, are screened with neuroimaging, or when patients present with non-ischemic symptoms such as headache. In two distinct single-center retrospective studies, 12–14% of asymptomatic children with moyamoya developed clinical ischemic stroke over an average follow-up time of 5–6 years, though more children (36–54%) developed radiographic progression [41, 241]. Therefore, the role and most optimal timing of surgery in children with asymptomatic moyamoya remain unclear.

Once appropriate patients are selected for surgery, identification of high-risk patients and meticulous perioperative management, which includes rigorous blood pressure management and maintenance of normocarbia, is critical to minimizing risk of perioperative infarction [191, 192]. When revascularization is performed at high-volume moyamoya centers, length of stay and costs are decreased without more complications [245].

Rehabilitation and Management of Stroke Sequelae

Rehabilitation is a critical aspect of stroke treatment that targets the physical, occupational, language, cognitive, and behavioral sequelae of stroke and aims to optimize function and independence [246, 247]. Unlike after adult stroke, strategies for pediatric rehabilitation differ by age and depend on the child's developmental level and degree of brain maturation. Concepts such as neuroplasticity and emerging deficits must be considered when evaluating optimal timing, dose, and intensity of therapies [248].

Constraint-induced movement therapy (CIMT) is a therapeutic approach in which the less impaired limb is restrained, promoting functional use of the more-impaired side. Several small studies in children with hemiparesis demonstrate improvements in spontaneous use, efficiency, and dexterity of the more impaired arm after CIMT [249, 250]. Bimanual therapy has also been evaluated with promising results and may be able to achieve benefits comparable to CIMT [251, 252]. Optimal timing of CIMT and bimanual therapy initiation after perinatal stroke are areas of active investigation.

Non-invasive brain stimulation is another area of active investigation [253]. Several small, randomized trials of repetitive transcranial magnetic stimulation (rTMS) in children with chronic stroke have demonstrated benefits of this technique compared with sham controls, particularly when paired with other therapeutic techniques [254–257]. In the largest pediatric rTMS trial to date, the combination of rTMS and CIMT together with intensive therapy provided the greatest benefit compared with intensive therapy paired with either rTMS or CIMT [256]. A randomized controlled trial evaluating the effect of the addition of transcranial direct current stimulation (tDCS) to intensive therapy on motor function in children with perinatal stroke-related hemiparesis failed to demonstrate a benefit in objective motor function, but subjective gains were evident 1 week after intervention [258]. Before non-invasive brain stimulation techniques can be used clinically, optimal modalities, stimulation parameters, and timing of therapy, as well as concurrent therapies and patient selection criteria, need to be established.

The best evidence supporting these novel therapies in children after stroke is primarily aimed at improving motor outcomes. Nonetheless, monitoring for language, cognitive, and behavioral dysfunction after stroke is critical. When deficits are identified, implementation of therapies, educational resources, and school accommodations can help optimize school function. For example, children with a history of stroke are at risk for attention-deficit/hyperactivity disorder (ADHD) [259]. ADHD can be medically managed when identified, thereby limiting the impact on a child's daily life. Emerging evidence is beginning to elucidate a potential role for non-invasive brain stimulation as an adjunct therapy for post-stroke aphasia in adults, though the use of brain stimulation to treat aphasia after childhood stroke is limited to case reports [260, 261].

Post-stroke care should also entail monitoring for fatigue, depression, and anxiety, all of which may interfere with participation in therapies as well as quality of life. Though data on post-stroke fatigue after childhood stroke are limited, fatigue is common in young adults after stroke and is associated with worse functional outcomes [262]. Post-traumatic stress disorder and depression are also common in parents of children who suffer stroke [263]; assessing the family unit for mental health consequences of stroke could lead to improved long-term care after childhood stroke.

Epilepsy is common after perinatal and childhood stroke, and development of epilepsy in the first year after stroke is associated with worse neurologic outcomes [127, 128, 264]. Development of epilepsy is also associated with poorer quality of life after childhood stroke [128]. Optimal epilepsy management is critical, as seizure freedom is

associated with higher likelihood of functional independence after childhood stroke [128].

Conclusions and Future Directions

Diagnostic and therapeutic advances in pediatric stroke have led to improved care for infants and children with stroke, but important knowledge gaps persist. Further advances in neuroimaging techniques, such as VWI and arterial spin labeling MRI, may provide better diagnostic capabilities in the future. Therapeutically, feasibility and safety data for IV thrombolysis and MT for childhood stroke are mounting, but high-quality evidence for efficacy of these therapies is lacking. Optimal dosing and type of thrombolytic agents and selection criteria for IV thrombolysis and MT have yet to be defined. Great advancements have been made in stroke prevention in children with SCD, but the optimal transfusion-sparing regimen remains undefined. Other knowledge gaps in stroke prevention include the role of immunomodulatory therapies for FCA, ideal long-term antithrombotic strategies, and the role of PFO closure in pediatric stroke. Finally, further evaluation of rehabilitation strategies including non-invasive brain stimulation and constraint-based therapies may allow for improved outcomes after pediatric stroke.

Supplementary Information The online version contains supplementary material available at https://doi.org/10.1007/s13311-023-01373-5.

Acknowledgements The authors thank Noah Burton for assistance with reference management.

Required Author Forms Disclosure forms provided by the authors are available with the online version of this article.

References

1. Raju TNK, Nelson KB, Ferriero D, Lynch JK, NICHD-NINDS Perinatal stroke, workshop participants. Ischemic perinatal stroke: summary of a workshop sponsored by the National Institute of Child Health and Human Development and the National Institute of Neurological Disorders and Stroke. Pediatrics. 2007;120(3):609–16.
2. Dunbar M, Mineyko A, Hill M, Hodge J, Floer A, Kirton A. Population based birth prevalence of disease-specific perinatal stroke. Pediatrics. 2020;146(5).
3. Lehman LL, Khoury JC, Taylor JM, Yeramaneni S, Sucharew H, Alwell K, et al. Pediatric stroke rates over 17 years: report from a population-based study. J Child Neurol. 2018;33(7):463–7. PMC5935572.
4. Leon RL, Kalvacherla V, Andrews MM, Thomas JM, Mir IN, Chalak LF. Placental pathologic lesions associated with stroke in term neonates. Front Endocrinol (Lausanne). 2022;13:920680. PMC9492924.
5. Xia Q, Yang Z, Xie Y, Zhu Y, Yang Z, Hei M, et al. The incidence and characteristics of perinatal stroke in Beijing: a multicenter study. Front Public Health. 2022;10:783153. PMC8987304.
6. Agrawal N, Johnston SC, Wu YW, Sidney S, Fullerton HJ. Imaging data reveal a higher pediatric stroke incidence than prior US estimates. Stroke. 2009;40(11):3415–21. PMC3387270.
7. Oleske DM, Cheng X, Jeong A, Arndt TJ. Pediatric acute ischemic stroke by age-group: a systematic review and meta-analysis of published studies and hospitalization records. Neuroepidemiology. 2021;55(5):331–41. PMC8491514.
8. Schoenberg BS, Mellinger JF, Schoenberg DG. Cerebrovascular disease in infants and children: a study of incidence, clinical features, and survival. Neurology. 1978;28(8):763–8.
9. deVeber GA, Kirton A, Booth FA, Yager JY, Wirrell EC, Wood E, et al. Epidemiology and outcomes of arterial ischemic stroke in children: the Canadian Pediatric Ischemic Stroke Registry. Pediatr Neurol. 2017;69:58–70.
10. Mallick AA, Ganesan V, Kirkham FJ, Fallon P, Hedderly T, McShane T, et al. Childhood arterial ischaemic stroke incidence, presenting features, and risk factors: a prospective population-based study. Lancet Neurol. 2014;13(1):35–43.
11. Christerson S, Stromberg B. Childhood stroke in Sweden I: incidence, symptoms, risk factors and short-term outcome. Acta Paediatr. 2010;99(11):1641–9.
12. Fullerton HJ, Wu YW, Zhao S, Johnston SC. Risk of stroke in children: ethnic and gender disparities. Neurology. 2003;61(2):189–94.
13. Zahuranec DB, Brown DL, Lisabeth LD, Morgenstern LB. Is it time for a large, collaborative study of pediatric stroke? Stroke. 2005;36(9):1825–9.
14. Mackay MT, Yock-Corrales A, Churilov L, Monagle P, Donnan GA, Babl FE. Accuracy and reliability of stroke diagnosis in the pediatric emergency department. Stroke. 2017;48(5):1198–202.
15. Zhelev Z, Walker G, Henschke N, Fridhandler J, Yip S. Prehospital stroke scales as screening tools for early identification of stroke and transient ischemic attack. Cochrane Database Syst Rev. 2019;4:CD011427. PMC6455894.
16. Mackay MT, Churilov L, Donnan GA, Babl FE, Monagle P. Performance of bedside stroke recognition tools in discriminating childhood stroke from mimics. Neurology. 2016;86(23):2154–61.
17. Mackay MT, Lee M, Yock-Corrales A, Churilov L, Donnan GA, Monagle P, et al. Differentiating arterial ischaemic stroke from migraine in the paediatric emergency department. Dev Med Child Neurol. 2018;60(11):1117–22.
18. Arsava EM, Helenius J, Avery R, Sorgun MH, Kim GM, Pontes-Neto O, et al. Assessment of the predictive validity of etiologic stroke classification. JAMA Neurol. 2017;74(4):419–26. PMC5470360.
19. Bernard TJ, Manco-Johnson M, Lo W, MacKay MT, Ganesan V, DeVeber G, et al. Towards a consensus-based classification of childhood arterial ischemic stroke. Stroke. 2012;43(2):371–7. PMC3312781.
20. Bohmer M, Niederstadt T, Heindel W, Wildgruber M, Strater R, Hanning U, et al. Impact of childhood arterial ischemic stroke standardized classification and diagnostic evaluation classification on further course of arteriopathy and recurrence of childhood stroke. Stroke. 2018:STROKEAHA118023060.
21. Ndiaye M, Lengue F, Sagna SD, Sow AD, Fogany Y, Deme H, et al. Childhood arterial ischemic stroke in Senegal (West Africa). Arch Pediatr. 2018;25(6):351–4.
22. Cao Q, Yang F, Zhang J, Liang H, Liu X, Wang H. Features of childhood arterial ischemic stroke in China. Fetal Pediatr Pathol. 2019;38(4):317–25.
23. Suppiej A, Gentilomo C, Saracco P, Sartori S, Agostini M, Bagna R, et al. Paediatric arterial ischaemic stroke and cerebral sinovenous thrombosis. First report from the Italian Registry of Pediatric Thrombosis (R. I. T. I., Registro Italiano Trombosi Infantili). Thromb Haemost. 2015;113(6):1270–7.

24. Mackay MT, Wiznitzer M, Benedict SL, Lee KJ, Deveber GA, Ganesan V, et al. Arterial ischemic stroke risk factors: the International Pediatric Stroke Study. Ann Neurol. 2011;69 (1):130–40.
25. Blum CA, Yaghi S. Cervical artery dissection: a review of the epidemiology, pathophysiology, treatment, and outcome. Arch Neurosci. 2015;2(4). PMC4604565.
26. Rafay MF, Shapiro KA, Surmava AM, deVeber GA, Kirton A, Fullerton HJ, et al. Spectrum of cerebral arteriopathies in children with arterial ischemic stroke. Neurology. 2020;94(23):e2479–90. PMC7455362.
27. Fullerton HJ, Johnston SC, Smith WS. Arterial dissection and stroke in children. Neurology. 2001;57(7):1155–60.
28. Fullerton HJ, Wintermark M, Hills NK, Dowling MM, Tan M, Rafay MF, et al. Risk of recurrent arterial ischemic stroke in childhood: a prospective international study. Stroke. 2016;47(1):53–9. PMC4696877.
29. Wintermark M, Hills N, deVeber G, Barkovich A, Elkind M, Sear K, et al. Arteriopathy diagnosis in childhood arterial ischemic stroke: results of the vascular effects of infection in pediatric stroke study. Stroke. 2014;45(12):3597–605.
30. Wintermark M, Hills NK, DeVeber GA, Barkovich AJ, Bernard TJ, Friedman NR, et al. Clinical and imaging characteristics of arteriopathy subtypes in children with arterial ischemic stroke: results of the VIPS study. AJNR Am J Neuroradiol. 2017;38(11):2172–9. PMC5985237.
31. Oesch G, Perez FA, Wainwright MS, Shaw DWW, Amlie-Lefond C. Focal cerebral arteriopathy of childhood: clinical and imaging correlates. Stroke. 2021;52(7):2258–65.
32. Sebire G, Meyer L, Chabrier S. Varicella as a risk factor for cerebral infarction in childhood: a case-control study. Ann Neurol. 1999;45(5):679–80.
33. Danchaivijitr N, Cox TC, Saunders DE, Ganesan V. Evolution of cerebral arteriopathies in childhood arterial ischemic stroke. Ann Neurol. 2006;59(4):620–6.
34. Fullerton HJ, Luna JM, Wintermark M, Hills NK, Tokarz R, Li Y, et al. Parvovirus B19 infection in children with arterial ischemic stroke. Stroke. 2017;48(10):2875–7. PMC5614850.
35. Sasidharan S, Krishnasree KS. Transient focal cerebral arteriopathy of childhood following dengue fever. J Postgrad Med. 2020;66(3):172–3. PMC7542054.
36. Beslow LA, Agner SC, Santoro JD, Ram D, Wilson JL, Harrar D, et al. International prevalence and mechanisms of SARS-CoV-2 in childhood arterial ischemic stroke during the COVID-19 pandemic. Stroke. 2022;53(8):2497–503. PMC9311284.
37. Lee S, Rivkin MJ, Kirton A, deVeber G, Elbers J. Moyamoya disease in children: results from the international pediatric stroke study. J Child Neurol. 2017;32(11):924–9.
38. Nah HW, Kwon SU, Kang DW, Ahn JS, Kwun BD, Kim JS. Moyamoya disease-related versus primary intracerebral hemorrhage: [corrected] location and outcomes are different. Stroke. 2012;43(7):1947–50.
39. Hoshino H, Izawa Y, Suzuki N, Research Committee on Moyamoya Disease. Epidemiological features of moyamoya disease in Japan. Neurol Med. 2012;52(5):295–8.
40. McCrea N, Fullerton HJ, Ganesan V. Genetic and environmental associations with pediatric cerebral arteriopathy. Stroke. 2019;50(2):257–65.
41. Gatti JR, Sun LR. Nonischemic presentations of pediatric moyamoya arteriopathy: a natural history study. Stroke. 2022;53(6):e219–20.
42. Gatti JR, Gonzalez Torriente A, Sun LR. Clinical presentation and stroke incidence differ by moyamoya etiology. J Child Neurol. 2020.
43. Ferriero D, Fullerton H, Bernard T, Billinghurst L, Daniels S, DeBaun M, et al. Management of stroke in neonates and children: a scientific statement from the American Heart Association/ American Stroke Association. Stroke. 2019;50(3):e51–96.
44. Dlamini N, Muthusami P, Amlie-Lefond C. Childhood moyamoya: looking back to the future. Pediatr Neurol. 2019;91:11–9.
45. Asakai H, Cardamone M, Hutchinson D, Stojanovski B, Galati J, Cheung M, et al. Arterial ischemic stroke in children with cardiac disease. Neurology. 2015;85(23):2053–9.
46. Hoffman JL, Mack GK, Minich LL, Benedict SL, Heywood M, Stoddard GJ, et al. Failure to impact prevalence of arterial ischemic stroke in pediatric cardiac patients over three decades. Congenit Heart Dis. 2011;6(3):211–8.
47. Reddy RK, McVadon DH, Zyblewski SC, Rajab TK, Diego E, Southgate WM, et al. Prematurity and congenital heart disease: a contemporary review. NeoReviews. 2022;23(7):e472–85.
48. Fox CK, Sidney S, Fullerton HJ. PMC4308424; Community-based case-control study of childhood stroke risk associated with congenital heart disease. Stroke. 2015;46(2):336–40.
49. Sinclair AJ, Fox CK, Ichord RN, Almond CS, Bernard TJ, Beslow LA, et al. Stroke in children with cardiac disease: report from the International Pediatric Stroke Study Group Symposium. Pediatr Neurol. 2015;52(1):5–15. PMC4936915.
50. Chen J, Zimmerman RA, Jarvik GP, Nord AS, Clancy RR, Wernovsky G, et al. Perioperative stroke in infants undergoing open heart operations for congenital heart disease. Ann Thorac Surg. 2009;88(3):823–9. PMC2840405.
51. Bonthrone AF, Stegeman R, Feldmann M, Claessens NHP, Nijman M, Jansen NJG, et al. Risk factors for perioperative brain lesions in infants with congenital heart disease: a European collaboration. Stroke. 2022.
52. Yeh HR, Kim EH, Yu JJ, Yun TJ, Ko TS, Yum MS. Arterial ischemic stroke in children with congenital heart diseases. Pediatr Int. 2022;64(1):e15200.
53. Rigatelli G, Zuin M, Bilato C. Atrial septal aneurysm contribution to the risk of cryptogenic stroke in patients with patent foramen ovale: a brief updated systematic review and meta-analysis. Trends Cardiovasc Med. 2022.
54. Saver JL, Carroll JD, Thaler DE, Smalling RW, MacDonald LA, Marks DS, et al. Long-term outcomes of patent foramen ovale closure or medical therapy after stroke. N Engl J Med. 2017;377(11):1022–32.
55. Mas J, Saver JL, Kasner SE, Nelson J, Carroll JD, Chatellier G, et al. Association of atrial septal aneurysm and shunt size with stroke recurrence and benefit from patent foramen ovale closure. JAMA Neurol. 2022.
56. Mas J, Derumeaux G, Guillon B, Massardier E, Hosseini H, Mechtouff L, et al. Patent foramen ovale closure or anticoagulation vs. antiplatelets after stroke. N Engl J Med. 2017;377 (11):1011–21.
57. Søndergaard L, Kasner SE, Rhodes JF, Andersen G, Iversen HK, Nielsen-Kudsk J, et al. Patent foramen ovale closure or antiplatelet therapy for cryptogenic stroke. N Engl J Med. 2017;377(11):1033–42.
58. Shih EK, Beslow LA, Natarajan SS, Falkensammer CB, Messe SR, Ichord RN. Prevalence of patent foramen ovale in a cohort of children with cryptogenic ischemic stroke. Neurology. 2021.
59. Chan AK, deVeber G. Prothrombotic disorders and ischemic stroke in children. Semin Pediatr Neurol. 2000;7(4):301–8.
60. Ohene-Frempong K, Weiner SJ, Sleeper LA, Miller ST, Embury S, Moohr JW, et al. Cerebrovascular accidents in sickle cell disease: rates and risk factors. Blood. 1998;91(1):288–94.
61. Farooq S, Testai FD. Neurologic complications of sickle cell disease. Curr Neurol Neurosci Rep. 2019;19(4):17.
62. DeBaun MR, Armstrong FD, McKinstry RC, Ware RE, Vichinsky E, Kirkham FJ. Silent cerebral infarcts: a review on a prevalent and progressive cause of neurologic injury in sickle cell anemia. Blood. 2012;119(20):4587–96. PMC3367871.

63. Fields ME, Guilliams KP, Ragan DK, Binkley MM, Eldeniz C, Chen Y, et al. Regional oxygen extraction predicts border zone vulnerability to stroke in sickle cell disease. Neurology. 2018;90(13):e1134–42. PMC5880632.
64. DeBaun MR, Sarnaik SA, Rodeghier MJ, Minniti CP, Howard TH, Iyer RV, et al. Associated risk factors for silent cerebral infarcts in sickle cell anemia: low baseline hemoglobin, sex, and relative high systolic blood pressure. Blood. 2012;119(16):3684–90. PMC3335377.
65. Omran SS, Lerario MP, Gialdini G, Merkler AE, Moya A, Chen ML, et al. Clinical impact of thrombophilia screening in young adults with ischemic stroke. J Stroke Cerebrovasc Dis. 2019;28(4):882–9. PMC6441373.
66. Lynch JK, Han CJ, Nee LE, Nelson KB. Prothrombotic factors in children with stroke or porencephaly. Pediatrics. 2005;116(2):447–53.
67. Ganesan V, Prengler M, McShane MA, Wade AM, Kirkham FJ. Investigation of risk factors in children with arterial ischemic stroke. Ann Neurol. 2003;53(2):167–73.
68. Akar N, Akar E, Deda G, Sipahi T, Orsal A. Factor V1691 G-A, prothrombin 20210 G-A, and methylenetetrahydrofolate reductase 677 C-T variants in Turkish children with cerebral infarct. J Child Neurol. 1999;14(11):749–51.
69. Simchen MJ, Goldstein G, Lubetsky A, Strauss T, Schiff E, Kenet G. Factor V leiden and antiphospholipid antibodies in either mothers or infants increase the risk for perinatal arterial ischemic stroke. Stroke. 2009;40(1):65–70.
70. Nowak-Gottl U, Strater R, Heinecke A, Junker R, Koch HG, Schuierer G, et al. Lipoprotein (a) and genetic polymorphisms of clotting factor V, prothrombin, and methylenetetrahydrofolate reductase are risk factors of spontaneous ischemic stroke in childhood. Blood. 1999;94(11):3678–82.
71. Kenet G, Lutkhoff LK, Albisetti M, Bernard T, Bonduel M, Brandao L, et al. Impact of thrombophilia on risk of arterial ischemic stroke or cerebral sinovenous thrombosis in neonates and children: a systematic review and meta-analysis of observational studies. Circulation. 2010;121(16):1838–47.
72. Bonduel M, Sciuccati G, Hepner M, Pieroni G, Torres AF, Mardaraz C, et al. Factor V Leiden and prothrombin gene G20210A mutation in children with cerebral thromboembolism. Am J Hematol. 2003;73(2):81–6.
73. McColl MD, Ellison J, Reid F, Tait RC, Walker ID, Greer IA. Prothrombin 20210 G–>A, MTHFR C677T mutations in women with venous thromboembolism associated with pregnancy. BJOG. 2000;107(4):565–9.
74. Curtis C, Mineyko A, Massicotte P, Leaker M, Jiang XY, Floer A, et al. Thrombophilia risk is not increased in children after perinatal stroke. Blood. 2017;129(20):2793–800.
75. deVeber G, Kirkham F, Shannon K, Brandao L, Strater R, Kenet G, et al. Recurrent stroke: the role of thrombophilia in a large international pediatric stroke population. Haematologica. 2019;104(10):2116. PMC6886444.
76. Lindsberg PJ, Grau AJ. Inflammation and infections as risk factors for ischemic stroke. Stroke. 2003;34(10):2518–32.
77. Hills NK, Sidney S, Fullerton HJ. Timing and number of minor infections as risk factors for childhood arterial ischemic stroke. Neurology. 2014;83(10):890–7. PMC4153847.
78. Per H, Unal E, Poyrazoglu HG, Ozdemir MA, Donmez H, Gumus H, et al. Childhood stroke: results of 130 children from a reference center in Central Anatolia. Turkey Pediatr Neurol. 2014;50(6):595–600.
79. Ouchenir L, Renaud C, Khan S, Bitnun A, Boisvert AA, McDonald J, et al. The epidemiology, management, and outcomes of bacterial meningitis in infants. Pediatrics. 2017;140(1).
80. Pryde K, Walker WT, Hollingsworth C, Haywood P, Baird J, Hussey M, et al. Stroke in paediatric pneumococcal meningitis: a cross-sectional population-based study. Arch Dis Child. 2013;98(8):647–9.
81. Solomons RS, Nieuwoudt ST, Seddon JA, van Toorn R. Risk factors for ischemic stroke in children with tuberculous meningitis. Childs Nerv Syst. 2021;37(8):2625–34.
82. Dunbar M, Shah H, Shinde S, Vayalumkal J, Vanderkooi OG, Wei XC, et al. Stroke in pediatric bacterial meningitis: population-based epidemiology. Pediatr Neurol. 2018;89:11–8.
83. Narayan P, Samuels OB, Barrow DL. Stroke and pediatric human immunodeficiency virus infection. Case report and review of the literature. Pediatr Neurosurg. 2002;37(3):158–63.
84. Landais A, Cesaire A, Fernandez M, Breurec S, Herrmann C, Delion F, et al. ZIKA vasculitis: a new cause of stroke in children? J Neurol Sci. 2017;15(383):211–3.
85. Nanda SK, Jayalakshmi S, Mohandas S. Pediatric ischemic stroke due to dengue vasculitis. Pediatr Neurol. 2014;51(4):570–2.
86. Hauer L, Pikija S, Schulte EC, Sztriha LK, Nardone R, Sellner J. Cerebrovascular manifestations of herpes simplex virus infection of the central nervous system: a systematic review. J Neuroinflammation. 2019;16(1):19. PMC6352343.
87. Gatto A, Angelici S, Soligo M, Di Giuda D, Manni L, Curatola A, et al. Pediatric cerebral stroke induced by Epstein-Barr virus infection: role of Interelukin overexpression. Acta Biomed. 2021;30(92):e2021135. PMC8142774.
88. Forbes HJ, Williamson E, Benjamin L, Breuer J, Brown MM, Langan SM, et al. Association of herpesviruses and stroke: systematic review and meta-analysis. PLoS ONE. 2018;13(11):e0206163. PMC6248930.
89. Amlie-Lefond C, Gilden D. Varicella zoster virus: a common cause of stroke in children and adults. J Stroke Cerebrovasc Dis. 2016;25(7):1561–9. PMC4912415.
90. Askalan R, Laughlin S, Mayank S, Chan A, MacGregor D, Andrew M, et al. Chickenpox and stroke in childhood: a study of frequency and causation. Stroke. 2001;32(6):1257–62.
91. Helmuth IG, Molbak K, Uldall PV, Poulsen A. Post-varicella arterial ischemic stroke in Denmark 2010 to 2016. Pediatr Neurol. 2018;80:42–50.
92. Grose C, Shaban A, Fullerton HJ. Common features between stroke following varicella in children and stroke following herpes zoster in adults : varicella-zoster virus in trigeminal ganglion. Curr Top Microbiol Immunol. 2023;438:247–72.
93. Eleftheriou D, Moraitis E, Hong Y, Turmaine M, Venturini C, Ganesan V, et al. Microparticle-mediated VZV propagation and endothelial activation: Mechanism of VZV vasculopathy. Neurology. 2020;94(5):e474–80. PMC7080289.
94. Elkind MS, Hills NK, Glaser CA, Lo WD, Amlie-Lefond C, Dlamini N, et al. Herpesvirus infections and childhood arterial ischemic stroke: results of the VIPS study. Circulation. 2016;133(8):732–41. PMC4766042.
95. Coronado Munoz A, Tasayco J, Morales W, Moreno L, Zorrilla D, Stapleton A, et al. High incidence of stroke and mortality in pediatric critical care patients with COVID-19 in Peru. Pediatr Res. 2022;91(7):1730–4. PMC8090521.
96. Scala MR, Spennato P, Cicala D, Piccolo V, Varone A, Cinalli G. Malignant cerebral infarction associated with COVID-19 in a child. Childs Nerv Syst. 2022;38(2):441–5. PMC8235910.
97. Siracusa L, Cascio A, Giordano S, Medaglia AA, Restivo GA, Pirrone I, et al. Neurological complications in pediatric patients with SARS-CoV-2 infection: a systematic review of the literature. Ital J Pediatr. 2021;47(1):123. PMC8170632.
98. Chiranth SB, Ashwini KR, Gowda VK, Sanjay KS, Ahmed M, Basavaraja GV. Profile of neurological manifestations in children presenting with rickettsial disease. Indian Pediatr. 2022;59(3):222–5.
99. Sun LR, Huisman TAGM, Yeshokumar AK, Johnston MV. Ongoing cerebral vasculitis during treatment of rocky mountain spotted fever. Pediatr Neurol. 2015;53(5):434–8.

100. No title. In: Aiuppa L, Cartaxo T, Spicer CM, Volberding PA, editors. Childhood cancer and functional impacts across the care continuum Washington (DC); 2020.
101. Sun LR, Linds A, Sharma M, Rafay M, Vadivelu S, Lee S, et al. Cancer and tumor-associated childhood stroke: results from the international pediatric stroke study. Pediatr Neurol. 2020;111:59–65.
102. Golomb MR, Ducis KA, Martinez ML. Bow Hunter's syndrome in children: a review of the literature and presentation of a new case in a 12-year-old girl. J Child Neurol. 2020;35(11):767–72.
103. Jost GF, Dailey AT. Bow hunter's syndrome revisited: 2 new cases and literature review of 124 cases. Neurosurg Focus. 2015;38(4):E7.
104. Rollins N, Braga B, Hogge A, Beavers S, Dowling M. Dynamic arterial compression in pediatric vertebral arterial dissection. Stroke. 2017;48(4):1070–3.
105. Kuril S, Chopade PR, Mandava M, Bhatia S. A rare case of stroke in an adolescent violinist due to thoracic outlet syndrome. Neurol India. 2021;69(6):1777–80.
106. Meumann EM, Chuen J, Fitt G, Perchyonok Y, Pond F, Dewey HM. Thromboembolic stroke associated with thoracic outlet syndrome. J Clin Neurosci. 2014;21(5):886–9.
107. Lynch JK, Han CJ. Pediatric stroke: what do we know and what do we need to know? Semin Neurol. 2005;25(4):410–23.
108. Steinlin M, Pfister I, Pavlovic J, Everts R, Boltshauser E, Capone Mori A, et al. The first three years of the Swiss Neuropaediatric Stroke Registry (SNPSR): a population-based study of incidence, symptoms and risk factors. Neuropediatrics. 2005;36(2):90–7.
109. Goldenberg NA, Bernard TJ, Fullerton HJ, Gordon A, deVeber G, International Pediatric Stroke Study Group. Antithrombotic treatments, outcomes, and prognostic factors in acute childhood-onset arterial ischaemic stroke: a multicentre, observational, cohort study. Lancet Neurol. 2009;8(12):1120–7.
110. Felling RJ, Rafay MF, Bernard TJ, Carpenter JL, Dlamini N, Hassanein SMA, et al. Predicting recovery and outcome after pediatric stroke: results from the international pediatric stroke study. Ann Neurol. 2020;87(6):840–52.
111. Goeggel Simonetti B, Cavelti A, Arnold M, Bigi S, Regenyi M, Mattle HP, et al. Long-term outcome after arterial ischemic stroke in children and young adults. Neurology. 2015;84(19):1941–7.
112. Ganesan V, Ng V, Chong WK, Kirkham FJ, Connelly A. Lesion volume, lesion location, and outcome after middle cerebral artery territory stroke. Arch Dis Child. 1999;81(4):295–300. 1718101.
113. Greenham M, Anderson V, Cooper A, Hearps S, Ditchfield M, Coleman L, et al. Early predictors of psychosocial functioning 5 years after paediatric stroke. Dev Med Child Neurol. 2017;59(10):1034–41.
114. Westmacott R, McDonald KP, Roberts SD, deVeber G, MacGregor D, Moharir M, et al. Predictors of cognitive and academic outcome following childhood subcortical stroke. Dev Neuropsychol. 2018;43(8):708–28.
115. Boardman JP, Ganesan V, Rutherford MA, Saunders DE, Mercuri E, Cowan F. Magnetic resonance image correlates of hemiparesis after neonatal and childhood middle cerebral artery stroke. Pediatrics. 2005;115(2):321–6.
116. Jiang B, Hills NK, Forsyth R, Jordan LC, Slim M, Pavlakis SG, et al. Imaging predictors of neurologic outcome after pediatric arterial ischemic stroke. Stroke. 2021;52(1):152–61. PMC7769865.
117. Delsing BJ, Catsman-Berrevoets C, Appel IM. Early prognostic indicators of outcome in ischemic childhood stroke. Pediatr Neurol. 2001r;24(4):283–9.
118. Keidan I, Shahar E, Barzilay Z, Passwell J, Brand N. Predictors of outcome of stroke in infants and children based on clinical data and radiologic correlates. Acta Paediatr. 1994;83(7):762–5.
119. Mallick AA, Ganesan V, Kirkham FJ, Fallon P, Hedderly T, McShane T, et al. Outcome and recurrence 1 year after pediatric arterial ischemic stroke in a population-based cohort. Ann Neurol. 2016;79(5):784–93.
120. Higgins JJ, Kammerman LA, Fitz CR. Predictors of survival and characteristics of childhood stroke. Neuropediatrics. 1991;22(4):190–3.
121. Grelli KN, Gindville MC, Walker CH, Jordan LC. Association of blood pressure, blood glucose, and temperature with neurological outcome after childhood stroke. JAMA Neurol. 2016;73(7):829–35.
122. Westmacott R, Askalan R, MacGregor D, Anderson P, Deveber G. Cognitive outcome following unilateral arterial ischaemic stroke in childhood: effects of age at stroke and lesion location. Dev Med Child Neurol. 2010;52(4):386–93.
123. Blackburn E, D'Arco F, Devito A, Ioppolo R, Lorio S, Quirk B, et al. Predictors of motor outcome after childhood arterial ischemic stroke. Dev Med Child Neurol. 2021;63(10):1171–9.
124. Long B, Anderson V, Jacobs R, Mackay M, Leventer R, Barnes C, et al. Executive function following child stroke: the impact of lesion size. Dev Neuropsychol. 2011;36(8):971–87.
125. Domi T, deVeber G, Shroff M, Kouzmitcheva E, MacGregor DL, Kirton A. Corticospinal tract pre-wallerian degeneration: a novel outcome predictor for pediatric stroke on acute MRI. Stroke. 2009;40(3):780–7.
126. Domi T, deVeber G, Mikulis D, Kassner A. Wallerian degeneration of the cerebral peduncle and association with motor outcome in childhood stroke. Pediatr Neurol. 2020;102:67–73.
127. Fox CK, Glass HC, Sidney S, Lowenstein DH, Fullerton HJ. Acute seizures predict epilepsy after childhood stroke. Ann Neurol. 2013;74(2):249–56. PMC3830669.
128. Fox CK, Jordan LC, Beslow LA, Armstrong J, Mackay MT, deVeber G. Children with post-stroke epilepsy have poorer outcomes one year after stroke. Int J Stroke. 2018;13(8):820–3.
129. Domi T, Edgell DS, McCrindle BW, Williams WG, Chan AK, MacGregor DL, et al. Frequency, predictors, and neurologic outcomes of vaso-occlusive strokes associated with cardiac surgery in children. Pediatrics. 2008;122(6):1292–8.
130. Ziesmann MT, Nash M, Booth FA, Rafay MF. Cardioembolic stroke in children: a clinical presentation and outcome study. Pediatr Neurol. 2014;51(4):494–502.
131. Vazquez Lopez M, de Castro P, Barredo Valderrama E, Miranda Herrero MC, Gil Villanueva N, Alcaraz Romero AJ, et al. Outcome of arterial ischemic stroke in children with heart disease. Eur J Paediatr Neurol. 2017;21(5):730–7.
132. Elbers J, deVeber G, Pontigon AM, Moharir M. Long-term outcomes of pediatric ischemic stroke in adulthood. J Child Neurol. 2014;29(6):782–8.
133. Chabrier S, Husson B, Lasjaunias P, Landrieu P, Tardieu M. Stroke in childhood: outcome and recurrence risk by mechanism in 59 patients. J Child Neurol. 2000;15(5):290–4.
134. Lanthier S, Carmant L, David M, Larbrisseau A, de Veber G. Stroke in children: the coexistence of multiple risk factors predicts poor outcome. Neurology. 2000;54(2):371–8.
135. Stacey A, Toolis C, Ganesan V. Rates and risk factors for arterial ischemic stroke recurrence in children. Stroke. 2018;49(4):842–7.
136. Strater R, Becker S, von Eckardstein A, Heinecke A, Gutsche S, Junker R, et al. Prospective assessment of risk factors for recurrent stroke during childhood–a 5-year follow-up study. Lancet. 2002;360(9345):1540–5.
137. Fullerton HJ, Wu YW, Sidney S, Johnston SC. Risk of recurrent childhood arterial ischemic stroke in a population-based cohort: the importance of cerebrovascular imaging. Pediatrics. 2007;119(3):495–501.
138. Uohara MY, Beslow LA, Billinghurst L, Jones BM, Kessler SK, Licht DJ, et al. Incidence of recurrence in posterior circulation childhood arterial ischemic stroke. JAMA Neurol. 2017;74(3):316–23. PMC5381719.

139. Wang LH, Young C, Lin HC, Wang PJ, Lee WT, Shen YZ. Strokes in children: a medical center-based study. Zhonghua Min Guo Xiao Er Ke Yi Xue Hui Za Zhi. 1998;39(4):242–6.
140. Xu Jiquan, Murphy SL, Kochanek KD, Arias E. Deaths: final data for 2019. Natl Vital Stat Rep. 2021;70.
141. Fullerton HJ, Chetkovich DM, Wu YW, Smith WS, Johnston SC. Deaths from stroke in US children, 1979 to 1998. Neurology. 2002;59(1):34–9.
142. Roach ES, Golomb MR, Adams R, Biller J, Daniels S, deVeber G, et al. Management of stroke in infants and children: a scientific statement from a special writing group of the American Heart Association Stroke Council and the council on cardiovascular disease in the young. Stroke. 2008;39(9):2644–91.
143. Medley TL, Miteff C, Andrews I, Ware T, Cheung M, Monagle P, et al. Australian Clinical Consensus Guideline: The diagnosis and acute management of childhood stroke. Int J Stroke. 2019;14(1):94–106.
144. Royal College of Paediatrics and Child Health, Stroke Association. Stroke in childhood: clinical guideline for diagnosis, management and rehabilitation. 2017.
145. Daverio M, Bressan S, Gregori D, Babl FE, Mackay MT. Patient and process factors associated with type of first neuroimaging and delayed diagnosis in childhood arterial ischemic stroke. Acad Emerg Med. 2016;23(9):1040–7.
146. DeLaroche AM, Sivaswamy L, Farooqi A, Kannikeswaran N. Pediatric stroke clinical pathway improves the time to diagnosis in an emergency department. Pediatr Neurol. 2016;65:39–44.
147. Shack M, Andrade A, Shah-Basak P, Shroff M, Moharir M, Yau I, et al. A pediatric institutional acute stroke protocol improves timely access to stroke treatment. Dev Med Child Neurol. 2017;59(1):31–7.
148. Harrar DB, Salussolia CL, Kapur K, Danehy A, Kleinman ME, Mannix R, et al. A stroke alert protocol decreases the time to diagnosis of brain attack symptoms in a pediatric emergency department. J Pediatr. 2020;216(136–141):e6.
149. Ganesan V, Hogan A, Shack N, Gordon A, Isaacs E, Kirkham FJ. Outcome after ischaemic stroke in childhood. Dev Med Child Neurol. 2000;42(7):455–61.
150. Wharton JD, Barry MM, Lee CA, Massey K, Ladner TR, Jordan LC. Pediatric acute stroke protocol implementation and utilization over 7 years. J Pediatr. 2020;220(214–220):e1.
151. Chalela JA, Kidwell CS, Nentwich LM, Luby M, Butman JA, Demchuk AM, et al. Magnetic resonance imaging and computed tomography in emergency assessment of patients with suspected acute stroke: a prospective comparison. Lancet. 2007;369(9558):293–8. PMC1859855.
152. Mirsky DM, Beslow LA, Amlie-Lefond C, Krishnan P, Laughlin S, Lee S, et al. Pathways for neuroimaging of childhood stroke. Pediatr Neurol. 2017;69:11–23.
153. Ramgopal S, Karim SA, Subramanian S, Furtado AD, Marin JR. Rapid brain MRI protocols reduce head computerized tomography use in the pediatric emergency department. BMC Pediatr. 2020;20(1):14. PMC6956479.
154. De Jong G, Kannikeswaran N, DeLaroche A, Farooqi A, Sivaswamy L. Rapid sequence MRI protocol in the evaluation of pediatric brain attacks. Pediatr Neurol. 2020;107:77–83.
155. Lee S, Jiang B, Heit JJ, Dodd RL, Wintermark M. Cerebral perfusion in pediatric stroke: children are not little adults. Top Magn Reson Imaging. 2021;30(5):245–52.
156. Khalaf A, Iv M, Fullerton H, Wintermark M. Pediatric stroke imaging. Pediatr Neurol. 2018;86:5–18. PMC6215731.
157. Felling RJ, Sun LR, Maxwell EC, Goldenberg N, Bernard T. Pediatric arterial ischemic stroke: epidemiology, risk factors, and management. Blood Cells Mol Dis. 2017;67:23–33.
158. Lehman LL, Beaute J, Kapur K, Danehy AR, Bernson-Leung M, Malkin H, et al. Workup for perinatal stroke does not predict recurrence. Stroke. 2017;48(8):2078–83.
159. Ji R, Schwamm LH, Pervez MA, Singhal AB. Ischemic stroke and transient ischemic attack in young adults: risk factors, diagnostic yield, neuroimaging, and thrombolysis. JAMA Neurol. 2013;70(1):51–7.
160. Leao DJ, Agarwal A, Mohan S, Bathla G. Intracranial vessel wall imaging: applications, interpretation, and pitfalls. Clin Radiol. 2020;75(10):730–9.
161. Mandell DM, Mossa-Basha M, Qiao Y, Hess CP, Hui F, Matouk C, et al. Intracranial vessel wall MRI: principles and expert consensus recommendations of the American Society of Neuroradiology. AJNR Am J Neuroradiol. 2017;38(2):218–29.
162. Mossa-Basha M, Zhu C, Wu L. Vessel wall MR imaging in the pediatric head and neck. Magn Reson Imaging Clin N Am. 2021;29(4):595–604. PMC8565599.
163. Dlamini N, Yau I, Muthusami P, Mikulis DJ, Elbers J, Slim M, et al. Arterial wall imaging in pediatric stroke. Stroke. 2018;49(4):891–8.
164. Stence NV, Pabst LL, Hollatz AL, Mirsky DM, Herson PS, Poisson S, et al. Predicting progression of intracranial arteriopathies in childhood stroke with vessel wall imaging. Stroke. 2017;48(8):2274–7.
165. Perez FA, Oesch G, Amlie-Lefond C. MRI vessel wall enhancement and other imaging biomarkers in pediatric focal cerebral arteriopathy-inflammatory subtype. Stroke. 2020;51(3):853–9.
166. Barron KS, Aksentijevich I, Deuitch NT, Stone DL, Hoffmann P, Videgar-Laird R, et al. The spectrum of the deficiency of adenosine deaminase 2: an observational analysis of a 60 patient cohort. Front Immunol. 2021;12:811473.
167. Cooray S, Omyinmi E, Hong Y, Papadopoulou C, Harper L, Al-Abadi E, et al. Anti-tumour necrosis factor treatment for the prevention of ischaemic events in patients with deficiency of adenosine deaminase 2 (DADA2). Rheumatology (Oxford). 2021;60(9):4373–8.
168. Monagle P, Barnes C, Auldist A, Crock C, Roy N, Rowlands S, et al. Developmental haemostasis Impact for clinical haemostasis laboratories. Thromb Haemost. 2006;95(2):362–72.
169. Andrew M, Vegh P, Johnston M, Bowker J, Ofosu F, Mitchell L. Maturation of the hemostatic system during childhood. Blood. 1992;80(8):1998–2005.
170. Parmar N, Albisetti M, Berry LR, Chan AKC. The fibrinolytic system in newborns and children. Clin Lab (Heidelberg). 2006;52(3–4):115.
171. Amlie-Lefond C, Chan AKC, Kirton A, deVeber G, Hovinga CA, Ichord R, et al. Thrombolysis in acute childhood stroke: design and challenges of the thrombolysis in pediatric stroke clinical trial. Neuroepidemiology. 2009;32(4):279–86.
172. Bernard T, Rivkin M, Scholz K, deVeber G, Kirton A, Gill J, et al. Emergence of the primary pediatric stroke center: impact of the thrombolysis in pediatric stroke trial. Stroke. 2014;45(7):2018–23.
173. Amlie-Lefond C, Shaw D, Cooper A, Wainwright M, Kirton A, Felling R, et al. Risk of intracranial hemorrhage following intravenous tPA (tissue-type plasminogen activator) for acute stroke is low in children. Stroke. 2020;51(2):542–8.
174. The National Institute of Neurological Disorders and Stroke rt-PA Stroke Study Group. Tissue plasminogen activator for acute ischemic stroke. N Engl J Med. 1995;333(24):1581–8.
175. Dicpinigaitis AJ, Gandhi CD, Pisapia J, Muh CR, Cooper JB, Tobias M, et al. Endovascular thrombectomy for pediatric acute ischemic stroke. Stroke. 2022;53(5):1530–9.
176. Kaur N, Patel S, Ayanbadejo MO, Hoffman H, Akano E, Anikpezie N, et al. Age-specific trends in intravenous thrombolysis and mechanical thrombectomy utilization in acute ischemic stroke in children under age 18. Int J Stroke. 2022:17474930221127538.
177. Sporns PB, Sträter R, Minnerup J, Wiendl H, Hanning U, Chapot R, et al. Feasibility, safety, and outcome of endovascular recanalization in childhood stroke. JAMA Neurol. 2019.

178. Bhatia K, Kortman H, Blair C, Parker G, Brunacci D, Ang T, et al. Mechanical thrombectomy in pediatric stroke: systematic review, individual patient data meta-analysis, and case series. J Neurosurg Pediatr. 2019;24(5):558–71.
179. Bhatia KD, Briest R, Goetti R, Webster R, Troedson C, Dale RC, et al. Incidence and natural history of pediatric large vessel occlusion stroke: a population study. JAMA Neurol. 2022;79(5):488–97.
180. Sporns P, Psychogios M, Straeter R, Hanning U, Minnerup J, Chapot R, et al. Clinical diffusion mismatch to select pediatric patients for embolectomy 6 to 24 hours after stroke: an analysis of the Save ChildS Study. Neurology. 2020.
181. Sun LR, Harrar D, Drocton G, Castillo-Pinto C, Felling R, Carpenter JL, et al. Mechanical thrombectomy for acute ischemic stroke: considerations in children. Stroke. 2020;51(10):3174–81.
182. Wilkinson DA, Pandey AS, Garton HJ, Savastano L, Griauzde J, Chaudhary N, et al. Late recanalization of basilar artery occlusion in a previously healthy 17-month-old child. BMJ Case Rep. 2017;13:2017. PMC5695390.
183. Xavier A, Kansara A, Majjhoo AQ, Norris G. CT perfusion guided delayed recanalization with favorable outcome in pediatric stroke. J Neurointerv Surg. 2012;4(6): e33.
184. Bodey C, Goddard T, Patankar T, Childs AM, Ferrie C, McCullagh H, et al. Experience of mechanical thrombectomy for paediatric arterial ischaemic stroke. Eur J Paediatr Neurol. 2014;18(6):730–5.
185. Lee S, Heit JJ, Albers GW, Wintermark M, Jiang B, Bernier E, et al. Neuroimaging selection for thrombectomy in pediatric stroke: a single-center experience. J Neurointerv Surg. 2019;11(9):940–6.
186. Wilson J, Amlie-Lefond C, Abruzzo T, Orbach D, Rivkin M, deVeber G, et al. Survey of practice patterns and preparedness for endovascular therapy in acute pediatric stroke. Childs Nerv Syst. 2019;35(12):2371–8.
187. Kirton A, Jordan LC, Orbach DB, Fullerton HJ. The case against endovascular thrombectomy in neonates with arterial ischemic stroke. Clin Neuroradiol. 2022;32(2):581–2.
188. He L, Ladner TR, Pruthi S, Day MA, Desai AA, Jordan LC, et al. Rule of 5: angiographic diameters of cervicocerebral arteries in children and compatibility with adult neurointerventional devices. J Neurointerv Surg. 2016;8(10):1067–71.
189. Sun LR, Harrar D, Drocton G, Castillo-Pinto C, Gailloud P, Pearl MS. Endovascular therapy for acute stroke in children: age and size technical limitations. J Neurointerv Surg. 2021.
190. Sun LR, Felling RJ, Pearl MS. Endovascular mechanical thrombectomy for acute stroke in young children. J Neurointerv Surg. 2019;11(6):554–8.
191. Gardner Yelton SE, Williams MA, Young M, Fields J, Pearl MS, Casella JF, et al. Perioperative management of pediatric patients with moyamoya arteriopathy. J Pediatr Intensive Care. 2021.
192. Gardner Yelton SE, Gatti J, Adil M, Guryildirim M, Tekes A, Sun LR. Risk factors and imaging biomarkers associated with perioperative stroke in pediatric moyamoya arteriopathy. J Child Neurol. 2022;21:8830738221125554.
193. Huguenard AL, Guerriero RM, Tomko SR, Limbrick DD, Zipfel GJ, Guilliams KP, et al. Immediate postoperative electroencephalography monitoring in pediatric moyamoya disease and syndrome. Pediatr Neurol. 2021;118:40–5.
194. Baker C, Grant AM, George MG, Grosse SD, Adamkiewicz TV. Contribution of sickle cell disease to the pediatric stroke burden among hospital discharges of African-Americans-United States, 1997–2012. Pediatr Blood Cancer. 2015;62(12):2076–81.
195. Powars D, Wilson B, Imbus C, Pegelow C, Allen J. The natural history of stroke in sickle cell disease. Am J Med. 1978;65(3):461–71.
196. DeBaun MR, Jordan LC, King AA, Schatz J, Vichinsky E, Fox CK, et al. American Society of Hematology 2020 guidelines for sickle cell disease: prevention, diagnosis, and treatment of cerebrovascular disease in children and adults. Blood Adv. 2020;4(8):1554–88.
197. Adams R, Cox M, Ozark S, Kanter J, Schulte P, Xian Y, et al. Coexistent sickle cell disease has no impact on the safety or outcome of lytic therapy in acute ischemic stroke: findings from get with the guidelines-stroke. Stroke. 2017;48(3):686–91.
198. Kavanagh PL, Fasipe TA, Wun T. Sickle cell disease: a review. JAMA. 2022;328(1):57–68.
199. DeBaun MR, Kirkham FJ. Central nervous system complications and management in sickle cell disease. Blood. 2016; 127(7):829–38.
200. Harrar DB, Benedetti GM, Jayakar A, Carpenter JL, Mangum TK, Chung M, et al. Pediatric acute stroke protocols in the United States and Canada. J Pediatr. 2022;242:220-227.e7.
201. Scoville J, Joyce E, Harper J, Hunsaker J, Gren L, Porucznik C, et al. A survey and analysis of pediatric stroke protocols. J Stroke Cerebrovasc Dis. 2022;31(9).
202. Ladner T, Mahdi J, Gindville M, Gordon A, Harris Z, Crossman K, et al. Pediatric acute stroke protocol activation in a children's hospital emergency department. Stroke. 2015;46(8):2328–31.
203. Catenaccio E, Riggs BJ, Sun LR, Urrutia VC, Johnson B, Torriente AG, et al. Performance of a pediatric stroke alert team within a comprehensive stroke center. J Child Neurol. 2020; 35(9):571–7.
204. Barkley T, Khalid R, Sharma M, Sherman A, Flint J. Demographics in children presenting with acute neurologic deficits concerning for stroke: an evaluation of the stroke alert process. J Child Neurol. 2022;37(5):321–8.
205. Fonarow GC, Zhao X, Smith EE, Saver JL, Reeves MJ, Bhatt DL, et al. Door-to-needle times for tissue plasminogen activator administration and clinical outcomes in acute ischemic stroke before and after a quality improvement initiative. JAMA. 2014;311(16):1632–40.
206. Xian Y, Xu H, Lytle B, Blevins J, Peterson ED, Hernandez AF, et al. Use of strategies to improve door-to-needle times with tissue-type plasminogen activator in acute ischemic stroke in clinical practice: findings from target: stroke. Circ Cardiovasc Qual Outcomes. 2017;10(1).
207. Brush LN, Monagle PT, Mackay MT, Gordon AL. Hypertension at time of diagnosis and long-term outcome after childhood ischemic stroke. Neurology. 2013;80(13):1225–30.
208. Adil MM, Beslow LA, Qureshi AI, Malik AA, Jordan LC. Hypertension is associated with increased mortality in children hospitalized with arterial ischemic stroke. Pediatr Neurol. 2015;56:25–9.
209. Adams R, McKie V, Nichols F, Carl E, Zhang DL, McKie K, et al. The use of transcranial ultrasonography to predict stroke in sickle cell disease. N Engl J Med. 1992;326(9):605–10.
210. Adams RJ, McKie VC, Hsu L, Files B, Vichinsky E, Pegelow C, et al. Prevention of a first stroke by transfusions in children with sickle cell anemia and abnormal results on transcranial doppler ultrasonography. N Engl J Med. 1998;339(1):5–11.
211. Yawn BP, Buchanan GR, Afenyi-Annan AN, Ballas SK, Hassell KL, James AH, et al. Management of sickle cell disease: summary of the 2014 evidence-based report by expert panel members. JAMA. 2014;312(10):1033–48.
212. McCavit TL, Xuan L, Zhang S, Flores G, Quinn CT. National trends in incidence rates of hospitalization for stroke in children with sickle cell disease. Pediatr Blood Cancer. 2013;60(5):823–7.
213. Adams RJ, Brambilla D. Discontinuing prophylactic transfusions used to prevent stroke in sickle cell disease. N Engl J Med. 2005;353(26):2769–78.
214. Ware RE, Davis BR, Schultz WH, Brown RC, Aygun B, Sarnaik S, et al. Hydroxycarbamide versus chronic transfusion for maintenance of transcranial doppler flow velocities in children with sickle cell anaemia—TCD With Transfusions Changing to Hydroxyurea (TWiTCH): a multicentre, open-label, phase 3, non-inferiority trial. Lancet (British edition). 2016;387(10019):661–70.

215. DeBaun MR, Gordon M, McKinstry RC, Noetzel MJ, White DA, Sarnaik SA, et al. Controlled trial of transfusions for silent cerebral infarcts in sickle cell anemia. N Engl J Med. 2014;371(8):699–710.
216. Bundy DG, Abrams MT, Strouse JJ, Mueller CH, Miller MR, Casella JF. Transcranial Doppler screening of medicaid-insured children with sickle cell disease. J Pediatr. 2015;166(1):188-190.e1.
217. Cabana MD, Kanter J, Marsh AM, Treadwell MJ, Rowland M, Stemmler P, et al. Barriers to pediatric sickle cell disease guideline recommendations. Glob Pediatr Health. 2019;6:2333794X19847026.
218. Bollinger LM, Nire KG, Rhodes MM, Chisolm DJ, O'Brien SH. Caregivers' perspectives on barriers to transcranial doppler screening in children with sickle-cell disease. Pediatr Blood Cancer. 2011;56(1):99–102.
219. Grosse SD, Schechter MS, Kulkarni R, Lloyd-Puryear MA, Strickland B, Trevathan E. Models of comprehensive multidisciplinary care for individuals in the united states with genetic disorders. Pediatrics (Evanston). 2009;123(1):407–12.
220. Lee L, Smith-Whitley K, Banks S, Puckrein G. Reducing health care disparities in sickle cell disease. Public Health Rep. 2019;134(6):599–607.
221. Desai P, Little J, Kanter J, Bridges K, Andemariam B, Lanzkron S. Kneeling was the first step for sickle cell disease. Ann Intern Med. 2021;174(7):1004–5.
222. Wang WC, Ware RE, Miller ST, Iyer RV, Casella JF, Minniti CP, et al. A multicenter randomised controlled trial of hydroxyurea (hydroxycarbamide) in very young children with sickle cell anaemia. Lancet (British edition). 2011;377(9778):1663–72.
223. Hankins JS, McCarville MB, Rankine-Mullings A, Reid ME, Lobo CLC, Moura PG, et al. Prevention of conversion to abnormal transcranial Doppler with hydroxyurea in sickle cell anemia: a phase III international randomized clinical trial. Am J Hematol. 2015;90(12):1099–105.
224. Wang WC, Kovnar EH, Tonkin IL, Mulhern RK, Langston JW, Day SW, et al. High risk of recurrent stroke after discontinuance of five to twelve years of transfusion therapy in patients with sickle cell disease. J Pediatr. 1991;118(3):377–82.
225. Ware RE, Helms RW. Stroke with transfusions changing to hydroxyurea (SWiTCH). Blood. 2012;119(17):3925–32.
226. Goldenberg NA, Bernard TJ, Fullerton HJ, Gordon A, deVeber G. Antithrombotic treatments, outcomes, and prognostic factors in acute childhood-onset arterial ischaemic stroke: a multicentre, observational, cohort study. Lancet Neurol. 2009;8(12):1120–7.
227. Markus HS, Levi C, King A, Madigan J, Norris J. Antiplatelet therapy vs anticoagulation therapy in cervical artery dissection: the cervical artery dissection in stroke study (CADISS) randomized clinical trial final results. Arch Neurol (Chicago). 2019;76(6):657–64.
228. Gill R, Biller J. Stroke prevention in cervical artery dissection. Curr Cardiol Rep. 2021;23(12):182.
229. Edwards HB, Mallick AA, O'Callaghan FJK. Immunotherapy for arterial ischaemic stroke in childhood: a systematic review. Arch Dis Child. 2017;102(5):410–5.
230. Quan AS, Brunner J, Rose B, Smitka M, Hahn G, Pain CE, et al. Diagnosis and treatment of angiography positive medium to large vessel childhood primary angiitis of central nervous system (p-cPACNS): an international survey. Front Pediatr. 2021;9:654537.
231. Keenan P, Brunner J, Quan AS, Smitka M, Hahn G, Pain CE, et al. Diagnosis and treatment of small vessel childhood primary angiitis of the central nervous system (sv-cPACNS): an international survey. Front Pediatr. 2021;9:756612.
232. Steinlin M, Bigi S, Stojanovski B, Gajera J, Regényi M, El-Koussy M, et al. Focal cerebral arteriopathy: do steroids improve outcome? Stroke. 2017;48(9):2375–82.
233. Fullerton H, Stence N, Hills N, Jiang B, Amlie-Lefond C, Bernard T, et al. Focal Cerebral Arteriopathy of childhood: novel severity score and natural history. Stroke. 2018;49(11):2590–6.
234. Messé S, Gronseth G, Kent D, Kizer J, Homma S, Rosterman L, et al. Practice advisory update summary: patent foramen ovale and secondary stroke prevention: Report of the Guideline Subcommittee of the American Academy of Neurology. Neurology. 2020;94(20):876–85.
235. Sun LR, Jordan LC. Cryptogenic pediatric ischemic stroke: what's the hole story? Neurology. 2021;97(21):973–4.
236. Riordan CP, Storey A, Cote DJ, Smith ER, Scott RM. Results of more than 20 years of follow-up in pediatric patients with moyamoya disease undergoing pial synangiosis. J Neurosurg Pediatr. 2019;23(5):1–592.
237. Scott RM, Smith JL, Robertson RL, Madsen JR, Soriano SG, Rockoff MA. Long-term outcome in children with moyamoya syndrome after cranial revascularization by pial synangiosis. J Neurosurg. 2004;100(2):142–9.
238. Iwama T, Hashimoto N, Yonekawa Y. The relevance of hemodynamic factors to perioperative ischemic complications in childhood moyamoya disease. Neurosurgery. 1996;38(6):1120–6.
239. Kim S, Choi J, Yang K, Kim T, Kim D. Risk factors for postoperative ischemic complications in patients with moyamoya disease. J Neurosurg. 2005;103(5):433–8.
240. Choi JW, Chong S, Phi JH, Lee JY, Kim H, Chae JH, et al. Postoperative symptomatic cerebral infarction in pediatric moyamoya disease: risk factors and clinical outcome. World Neurosurg. 2020;136:e158–64.
241. Lin N, Baird L, Koss M, Kopecky KE, Gone E, Ullrich NJ, et al. Discovery of asymptomatic moyamoya arteriopathy in pediatric syndromic populations: radiographic and clinical progression. Neurosurg Focus. 2011;31(6):E6.
242. Montaser AS, Lalgudi Srinivasan H, Staffa SJ, Zurakowski D, Slingerland AL, Orbach DB, et al. Ivy sign: a diagnostic and prognostic biomarker for pediatric moyamoya. J Neurosurg Pediatr. 2022;29(4):458–66.
243. Yu J, Du Q, Xie H, Chen J, Chen J. What and why: the current situation and future prospects of "ivy sign" in moyamoya disease. Ther Adv Chronic Dis. 2020;11:2040622320960004.
244. Kaseka ML, Slim M, Muthusami P, Dirks PB, Westmacott R, Kassner A, et al. Distinct clinical and radiographic phenotypes in pediatric patients with moyamoya. Pediatr Neurol. 2021;120:18–26.
245. Titsworth W, Scott R, Smith E. National analysis of 2454 pediatric moyamoya admissions and the effect of hospital volume on outcomes. Stroke. 2016;47(5):1303–11.
246. Gordon AL, di Maggio A. Rehabilitation for children after acquired brain injury: current and emerging approaches. Pediatric Neurol. 2012;46(6):339–44.
247. Ashwal S, Pearl PL, Swaiman KF, Schor NF, Finkel RS, Ferriero DM, et al. Swaiman's pediatric neurology: principles and practice. Elsevier; 2017.
248. Malone LA, Felling RJ. Pediatric stroke: unique implications of the immature brain on injury and recovery. Pediatr Neurol. 2020;102:3–9.
249. Taub E, Griffin A, Uswatte G, Gammons K, Nick J, Law CR. Treatment of congenital hemiparesis with pediatric constraint-induced movement therapy. J Child Neurol. 2011;26(9):1163–73.
250. Charles JR, Wolf SL, Schneider JA, Gordon AM. Efficacy of a child-friendly form of constraint-induced movement therapy in hemiplegic cerebral palsy: a randomized control trial. Dev Med Child Neurol. 2006;48(8):635–42.
251. Gordon AM, Schneider JA, Chinnan A, Charles JR. Efficacy of a hand–arm bimanual intensive therapy (HABIT) in children with hemiplegic cerebral palsy: a randomized control trial. Dev Med Child Neurol. 2007;49(11):830–8.
252. Gordon AM, Hung Y, Brandao M, Ferre CL, Kuo H, Friel K, et al. Bimanual training and constraint-induced movement therapy in children with hemiplegic cerebral palsy. Neurorehabil Neural Repair. 2011;25(8):692–702.

253. Hilderley A, Metzler M, Kirton A. Noninvasive neuromodulation to promote motor skill gains after perinatal stroke. Stroke. 2019;50(2):233–9.
254. Gillick BT, Krach LE, Feyma T, Rich TL, Moberg K, Thomas W, et al. Primed low-frequency repetitive transcranial magnetic stimulation and constraint-induced movement therapy in pediatric hemiparesis: a randomized controlled trial. Dev Med Child Neurol. 2014;56(1):44–52.
255. Kirton A, Chen R, Friefeld S, Gunraj C, Pontigon A, deVeber G. Contralesional repetitive transcranial magnetic stimulation for chronic hemiparesis in subcortical paediatric stroke: a randomised trial. Lancet neurology 2008;7(6):507–13.
256. Kirton A, Andersen J, Herrero M, Nettel-Aguirre A, Carsolio L, Damji O, et al. Brain stimulation and constraint for perinatal stroke hemiparesis: the PLASTIC CHAMPS trial. Neurology. 2016;86(18):1659–67.
257. Malone LA, Sun LR. Transcranial magnetic stimulation for the treatment of pediatric neurological disorders. Curr Treat Options Neurol. 2019;21(11):58.
258. Kirton A, Ciechanski P, Zewdie E, Andersen J, Nettel-Aguirre A, Carlson H, et al. Transcranial direct current stimulation for children with perinatal stroke and hemiparesis. Neurology. 2017;88(3):259–67.
259. Bolk J, Simatou E, Söderling J, Thorell LB, Persson M, Sundelin H. Association of perinatal and childhood ischemic stroke with attention-deficit/hyperactivity disorder. JAMA Netw Open. 2022;5(4):e228884.
260. Fridriksson J, Hillis AE. Current approaches to the treatment of post-stroke aphasia. J Stroke. 2021;23(2):183–201.
261. Carlson HL, Jadavji Z, Mineyko A, Damji O, Hodge J, Saunders J, et al. Treatment of dysphasia with rTMS and language therapy after childhood stroke: multimodal imaging of plastic change. Brain Lang. 2016;159:23–34.
262. Maaijwee NAMM, Arntz RM, Rutten-Jacobs LCA, Schaapsmeerders P, Schoonderwaldt HC, van Dijk EJ, et al. Post-stroke fatigue and its association with poor functional outcome after stroke in young adults. J Neurol Neurosurg Psychiatry. 2015;86(10):1120–6.
263. Lehman LL, Maletsky K, Beaute J, Rakesh K, Kapur K, Rivkin MJ, et al. Prevalence of symptoms of anxiety, depression, and post-traumatic stress disorder in parents and children following pediatric stroke. J Child Neurol. 2020;35(7):472–9.
264. Billinghurst L, Beslow L, Abend N, Uohara M, Jastrzab L, Licht D, et al. Incidence and predictors of epilepsy after pediatric arterial ischemic stroke. Neurology. 2017;88(7):630–7.

Journal of Stroke and Cerebrovascular Diseases 33 (2024) 107638

Contents lists available at ScienceDirect

Journal of Stroke and Cerebrovascular Diseases

journal homepage: www.elsevier.com/locate/jstroke

Longitudinal evaluation of cerebral perfusion evolution after revascularization surgery in moyamoya disease by CT perfusion

Huang Yingqian, MD [a,#], Wei Dan, MD [b,#], Lin Liping, MD [a,#], Lai Zhiman, BSc [a], Xie Dingxiang, BSc [a], Li Zhuhao, M.Med [a], Yang Zhiyun, PhD [a], Jiang Li, PhD, PhD [a,*], Zhao Jing, PhD [a,*]

[a] Department of Radiology, The First Affiliated Hospital, Sun Yat-sen University, No. 58 Zhongshan Road 2, Guangzhou, Guangdong 510080, China
[b] Department of Radiology, Hui Ya Hospital of The First Affiliated Hospital, Sun Yat-sen University, Huizhou, 516000, PR China

ARTICLE INFO

Keywords:
Moyamoya disease
One-stop CTP
Revascularization surgery
Cerebral perfusion evolution

ABSTRACT

Objective: To assess the longitudinal evolution of cerebral perfusion after revascularization surgery in patients with moyamoya disease (MMD) by CT perfusion (CTP).

Materials and methods: Thirty-one clinically confirmed MMD patients (12 males and 19 females, average age: 33.26 y, Suzuki stages 3 and 4: 19 and 11, respectively) who underwent revascularization surgery (bilateral (n=13) or unilateral (n=18)) were studied retrospectively. All patients underwent CTP examinations before and in the week after surgery and long-term (>3 months). CTP metrics (CBF, CBV, MTT, TTP, and delay TTP) were derived. The corresponding CTP metric values of the ROIs, which were manually drawn in the white matter (WM) and gray matter (GM), were recorded.

Results: Six patients developed a new or progressive cerebral infarction/hemorrhage. In all patients, compared with the preoperative level, the TTP of GM and WM decreased in the short term after the surgery ($P \leq 0.005$). Concurrently, the WM CBF increased significantly a week after surgery ($P = 0.02$). However, in the long-term follow-up, the CBV and CBF in the GM and WM decreased to equal to or lower than the preoperative level, especially for CBV in the WM ($P = 0.012$). Furthermore, cerebral perfusion began to decrease in the sixth month, and a continuous decline was observed over the next two months. It returned to the presurgical level after one year. In addition, the improvement in postsurgical perfusion was greater in Suzuki stage 3 patients than stage 4 patients.

Conclusion: Cerebral perfusion in patients with MMD improved shortly after surgery. However, in the long-term, brain perfusion decreased, most seriously in 6-8 months postoperatively, which might indicate that patients with MMD need timely follow-up and long-term intervention.

Introduction

Moyamoya disease (MMD) is characterized by progressive stenosis or occlusion of the supraclinoid internal carotid arteries and their branches, resulting in chronic ischemia and progressive cerebral infarction.[1] Compensatory collateralization can occur but is often insufficient.[2] Patients often present with symptoms related to ischemic or hemorrhagic stroke.[3] A synthesis of existing research suggests that cerebral revascularization surgery can restore cerebral blood flow (CBF), reduce stroke risk[3], prevent further neurocognitive decline[4,5], and decrease MMD mortality.[6-12] However, many patients still experience recurrent intracranial ischemia after surgery, and the dynamic changes and factors influencing cerebral perfusion after bypass surgery remain unknown.

How does cerebral perfusion change postoperatively? Many studies have shown that cerebral perfusion increases after surgery.[2,6,13]

Abbreviations: STA, superficial temporal artery; MCA, middle cerebral artery; MMD, moyamoya disease; NCCT, non-contrast CT; CTA, CT angiography; CTP, CT perfusion; CBF, cerebral blood flow; CBV, cerebral blood volume; MTT, mean transit time; TTP, time to peak; ROI, region of interest; MRA, MR angiography; DSA, digital subtraction angiography; CTP, CT perfusion imaging; ASL, arterial spin-labeling; EC–IC, extracranial-intracranial; TIA, transient ischemic attack; ICH, Intracerebral hemorrhage; IVH, intraventricular hemorrhage; ICA, internal carotid artery; PCA, posterior cerebral artery; EDAS, encephalo-duro-arterio-synangiosis.

* Corresponding authors.
E-mail addresses: jli@mail.sysu.edu.cn (J. Li), zhaoj23@mail.sysu.edu.cn (Z. Jing).
# Contributed equally.

https://doi.org/10.1016/j.jstrokecerebrovasdis.2024.107638
Received 1 November 2023; Received in revised form 9 February 2024; Accepted 13 February 2024
Available online 14 February 2024

However, these studies focused on relatively short postsurgical time points. Wouters et al.[7] showed that surgical intervention in MMD is associated with a decreased risk of stroke, most striking in patients presenting with hemorrhagic MMD, but not in patients with ischemic stroke.[7] Moreover, we have often observed that many patients with MMD have recurrent intracranial ischemia or ischemia after surgery. Based on this phenomenon, we suspected that, from a long-term perspective, the cerebral perfusion of patients with MMD after surgery did not primarily increase or decrease to some extent.

Imaging examinations may provide objective evidence for the evaluation of postoperative MMD outcomes.[14] Modalities such as CT angiography (CTA), MR angiography (MRA), digital subtraction angiography (DSA), CT perfusion imaging (CTP), and arterial spin labeling (ASL)[15] are often used to assess collateralization and perfusion. DSA is the current reference standard for evaluating MMD.[16,17] However, given its invasive nature and higher radiation exposure than CT, DSA is not optimal for longitudinal perfusion monitoring. DSA also does not fully reflect cerebral hemodynamic status.[18] With the development of CTP, the practicability of CT for evaluating cerebral hemodynamic changes in patients with MMD has been significantly enhanced. Compared with PET, SPECT, and MRI, CTP allows fast, semi-quantitative measurements with high reference value.[19] It can efficiently obtain multiple parameters, access the information of bypass vessels, and comprehensively assess cerebrovascular and perfusion status. Many studies have demonstrated its utility for assessing MMD.[20-22] In comparison, there are no reports on the role of CTP in dynamic long-term follow-up changes, and, to the best of our knowledge, no studies have compared quantitative CTP values in white matter and gray matter separately.

Thus, we retrospectively included 31 MMD patients with CTP data who underwent revascularization procedures in this study. All patients were followed up longitudinally (up to three years). Cerebral perfusion changes in the white and gray matter before and after surgery and during follow-up were analyzed to provide objective imaging evidence for the triage of MMD patients.

Table 1
Clinical and imaging information for included patients.

Category	Number of sides
Symptoms	
TIA	1
Headache	12
Epilepsy	0
Recurrent limb weakness	21
Others (involuntary movement)	2
Blurred vision	3
Loss of consciousness	2
NCCT lesions	
None	10
Cerebral infarction	21
ICH or IVH	2
Encephalatrophy	6
Involving terminal ICA-MCA	
Right side	1
Left side	3
Bilateral	27
Suzuki Staging	
Stage 2	1
Stage 3	19
Stage 4	11
Involving PCA	7
With other cerebral vascular malformation (e.g aneurysm)	3
Surgical side	
Right side	8
Left side	10
Bilateral	13
Surgical ways	
STA -MCA	35
STA -MCA+EDAS	9
Outcomes	
New cerebral infarction	4
Extensive infarcts	2
New cerebral hemorrhage	2

TIA: transient ischemic attack; ICH: Intracerebral hemorrhage; IVH: intraventricular hemorrhage; ICA: internal carotid artery; MCA: middle cerebral artery; PCA: posterior cerebral artery; ATA-MCA: superficial temporal artery-middle cerebral artery bypass surgery; EDAS: encephalo-duro-arterio-synangiosis

Materials and methods

Patients

We retrospectively collected the data of 31 patients (19 females, age range 6-53 y, mean age: 33.26±14.22 y) who were clinically diagnosed with MMD and underwent bypass surgery from January 2016 to January 2020. The inclusion criteria were as follows: ① met the diagnostic criteria in the "Interpretation of the 2012 Moyamoya Disease (Willis Circle Spontaneous Occlusion) Guidelines for Diagnosis and Treatment (Japan)"[4]; ② diagnosed by whole cerebral angiography (DSA); ③ underwent superficial temporal artery-middle cerebral artery bypass surgery; ④ CTP examination and clinical review were performed before and after the surgery. Patients with CTP source image artifacts that affected the evaluation of the CTP results were excluded. The clinical data of the included patients are presented in Table 1.

This study was approved by our hospital. The requirement for informed consent was waived due to the retrospective nature of the study.

CTP acquisition

One-stop CTP (NCCT (non-contrast CT) -CTA-CTP) was performed using a 640-slice multidetector CT scanner (Aquilion One; Canon Medical Systems Corporation). Whole-brain volumetric CTP was performed after excluding cerebral hemorrhage. A 50-mL bolus of iopromide (Ultravist 370; Bayer Schering Pharma, Berlin, Germany) was injected at a rate of 5 mL/s. Nineteen scan volumes, each containing 320 slices at a resolution of 0.5 mm, were acquired after a 7 s delay between 2 and 5 s apart over a period of 60 s after the injection, with a tube voltage of 80 kV, tube current of 150 mA, and an average effective dose of 5.25 mSv.

Post-processing of CTP

1) NCCT

Pre- and post-surgical NCCT images were used to observe the cerebral parenchyma and determine the presence of cerebral infarction, hemorrhage, or other abnormalities.

2) CTA

Virtual reality (VR) and maximum intensity projection (MIP) images post-processed by multiphase CTA display the anatomy of the collateral vessels from multiple angles. CTA images are mainly used to analyze the vessels after revascularization procedures and to determine the patency of the bridge vessel.

3) CTP

Dynamic volume perfusion images were further analyzed using commercial software (Vital Images VES Client 6.9.2, Vital Images, Minnetonka, MN, USA). The input artery and output vein were manually selected. The basal artery was chosen as the input artery and the superior sagittal or straight sinus was selected as the output vein. The time-density curve of the areas of interest was automatically obtained using this software. Subsequently, perfusion parameter maps including cerebral blood volume (CBV), cerebral blood flow (CBF), mean transit time (MTT), time to peak (TTP), and delayed peak time (delay time to peak,

Delay-TTP) were generated using the SVD+ deconvolution algorithm. The thickness of each perfusion parameter layer was 5 mm.

Regions of interest (ROIs) were automatically and manually selected on perfusion parameter maps to avoid abnormal brain parenchyma such as infarction, hemorrhage, surgery-related subdural effusion, and gas accumulation. For the series of CTP examinations, ROIs were placed on the gray and white matter in four consecutive layers (from the basal ganglia to the radial corona in the middle cerebral artery distribution). ROIs of the white matter regions were outlined manually. The ROIs of the gray matter regions (10-mm) were automatically drafted using post-processing software and adjusted manually, if applicable. The corresponding CTP metric values were recorded, and the average values of each CTP metric were calculated. (Fig. 1)

Statistical analysis

SPSS25 (IBM Corporation, Armonk, NY, USA) was used for statistical analysis. All data are presented as the mean ± standard error of the mean. Longitudinal changes for cohorts with complete data (cohorts with three measured time points [pre-, post-surgery within a week, and post-surgery after three months]) in the cerebral gray and white matter at different time points were determined using analysis of variance for repeated measurements, followed by Bonferroni post hoc multiple comparisons, and the *P* value was adjusted. In addition, the postsurgical and presurgical parameter ratios were calculated to observe perfusion changes over time, and ratio-time curves were plotted using GraphPad Prism software (version 8.0) to explore the time points at which brain perfusion started to decline. The data (cohorts that included at least two time points [pre- and post-surgery within a week, or pre- and post-surgery after three months]) were used to analyze the change in perfusion at different times in patients with different Suzuki stages using t-tests for paired samples followed by Bonferroni post hoc multiple comparisons, and the P value was adjusted. All statistical tests were two-sided, and $P < 0.05$ was considered statistically significant.

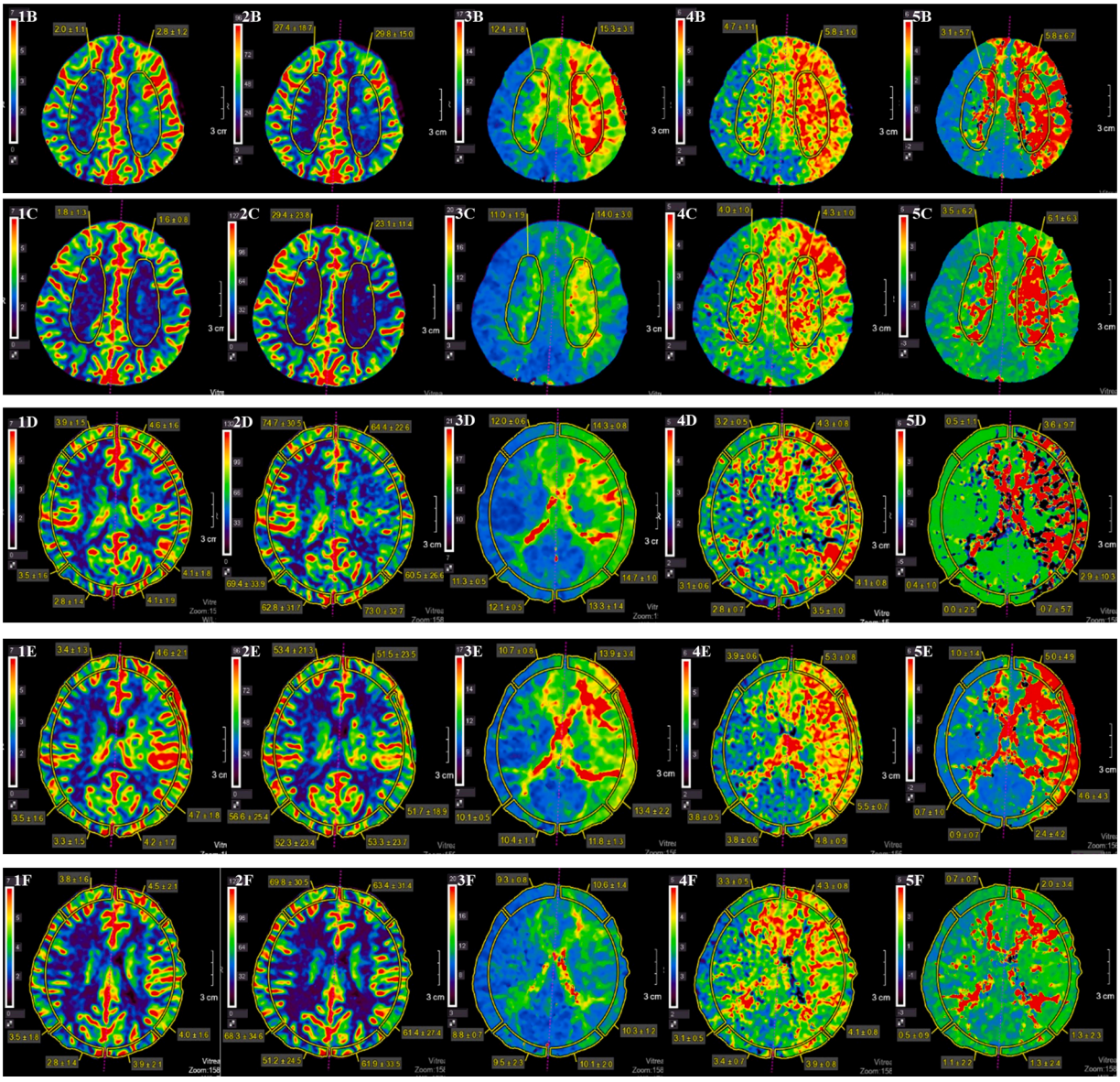

Fig. 1. An example of ROI placement. Pictures A, B and C were post-processing images of CTP for pre-surgery, post-surgery within a week, and post-surgery after three months, respectively. ROIs were manually drawn in white matter regions. Pictures D, E and F, were post-processing images of CTP for pre-surgery, post-surgery within a week, and post-surgery after three months, respectively. ROIs were manually drawn in gray matter regions. Pictures 1-5 were post-processing images of CTP (CBV, CBF, TTP, MTT and delay-TTP metrics, respectively.

Results

Clinical characteristics

Because the two cerebral hemispheres are supplied with blood separately, 31 patients with 44 sides of revascularization procedures (13 patients underwent bilateral surgery and 18 patients underwent unilateral surgery) were analyzed. Twenty-three sides had complete longitudinal data (before surgery, short-term [within a week], and long-term [>3 months] after surgery), 30 sides had short-term data (within a week), and 36 sides had long-term data (>3 months).

Presurgical NCCT showed 21 cases of cerebral infarction, 2 cases of acute cerebral hemorrhage, and 10 cases with negative NCCT results that experienced transient ischemic attack (TIA), indicating the need for further surgical treatment[23]. Postoperatively, all bridge vessels were patent. No occlusion of the bridge vessels was observed during the follow-up. Three patients developed new infarctions shortly after, and one patient had an increased infarction area with hemorrhagic transformation. All infarcts and hemorrhages occurred 5-7 days after surgery. Accompanying aneurysms were found in 3 cases of MMD on CTA. With Suzuki[1] staging, there was 1 case in stage 2, 19 in stage 3, and 11 in stage 4. By comparison, in the Matsushima[24] analysis, there were 3 cases of stage 2, 12 cases of stage 3, and 16 cases of stage 6. The detailed clinical and imaging data of the patients are presented in Table 1.

Longitudinal changes of the cerebral perfusion

Twenty-three sides with complete longitudinal data (before surgery, short-term [within a week], and long-term [>3 months] after surgery) were included for longitudinal evaluation.

1) **Perfusion evolution in the cerebral gray matter**

Significant changes in the cerebral cortex perfusion values of the TTP after surgery were detectable compared with those before surgery. TTP values decreased from 14.90±5.20 s to 11.86±2.60 s within a week after surgery and slightly increased to 12.47±2.26s after 3 months. (P = 0.016 for pre- vs. post- within a week; P = 0.155 for pre- vs. post- after 3 months). MTT values slightly decreased from 4.30±0.96 s (pre-) to 3.89 ±0.74 s within a week after surgery but increased somewhat to 4.16 ±0.61 s after 3 months. The CBV and CBF values increased slightly and decreased to even lower values than the presurgerical values in the long run. However, no significant differences were observed between groups. The delay values decreased gradually; however, no significant changes were observed. (Table 2 **and** Fig. 2).

2) **Perfusion evolution in the cerebral white matter**

TTP in the cerebral white matter compared with values before surgery significantly decreased from 15.45±5.14 s to 12.19±2.65 s within a week after surgery (P =0.008) and slightly increased in the long term follow-up. MTT values slightly dropped from 4.24±0.89 s to 4.04±0.87 s in a week and were maintained at 4.04±0.67 s after 3 months, but no significant changes were observed. CBF values increased from 36.10 to 41.62 mL/(100 g·min) just for a short time (P =0.02) and decreased to 33.61 mL/(100 g·min) in the long term. CBV values increased from 2.46 mL/100 g to 2.76 mL/100 g a short time after surgery and significantly decreased to 2.17 ml/100 g in the long term (P=0.012). The delay-TTP values gradually decreased, but no significant changes were observed. (Table 2 and Fig. 2).

Validating a time threshold for the deterioration of the cerebral perfusion

Because the follow-up time of the included patients ranged from 3 months to 3 years, we used cerebral perfusion data at the same follow-up time points on at least 3 sides. Thirty-two sides of data (3 months: 7 sides; 4 months: 4 sides; 5 months: 4 sides; 6 months: 3 sides; 8 months: 3 sides; 12 months: 7 sides; >12 months: 4 sides) were included in this part of the analysis, and mean values were calculated for each time point.

The MTT and TTP values showed similar trends, and the CBF and CBV values changed similarly. During the fourth and fifth months, the CBF ratios increased to >1, while the MTT and TTP shortened, and the ratios were <1. In the sixth month, the MTT and TTP ratios were more significant than those in the first month. The MTT ratios decreased to <1 in the eighth month and then increased slightly to approximately 1 until the 12th month. However, the TTP ratios continued to decrease and dropped to <1 in the eighth month. The CBF ratios were <1 in the sixth and eighth months and >1 in the 12th month. The CBV ratios were <1 from the sixth month until the 12th month. At long-term follow-up (>12 months), the TTP and MTT ratios and the CBF and CBV ratios remained <1. (Fig. 3)

Longitudinal changes of the cerebral perfusion in patients with different Suzuki stages

Nineteen patients with 26 sides were assigned as Suzuki stage 3 (16 sides of short-term and 22 sides of long-term post-surgical data). Eleven patients (15 sides) were assigned as Suzuki stage 4 (13 sides in the short-term and 12 sides in the long-term postsurgical data). These data were included to evaluate changes in cerebral perfusion at different Suzuki stages. A similar perfusion evolution tendency was observed in patients with MMD, irrespective of the Suzuki stage. (Table 3)

In the gray matter, significantly decreased TTP were found within a week post-surgery (13.42±3.23 s to 11.65±2.3 s) and 3 months after the surgery (11.65±2.3 s to 11.70±2.36 s) in patients with Suzuki stage 3 (P = 0.004 for pre- vs post- within a week; P = 0.013 for pre- vs post-after 3m) but not those with stage 4. Irrespective of Suzuki stage, CBF significantly increased within a week after surgery and then decreased again to the preoperative level after 3 months (pre- vs. post-surgery after

Table 2
Changes in cerebral cortex and cerebral white matter for three time points.

		Pre (n=23)	Post1 (n=23)	Post2 (n=23)	*P* values (Pre vs. post1)	*P* values (Pre vs. post2)	*P* values (post1 vs. post2)
Gray Matter	TTP	14.90±5.20	11.86±2.60	12.47±2.26	0.016*	0.155	>0.99
	MTT	4.30±0.96	3.89±0.74	4.16±0.61	0.099	>0.99	0.258
	CBF	46.81±10.95	50.49±11.59	46.12±10.88	0.487	>0.99	0.440
	CBV	3.24±0.53	3.32±0.75	3.11±0.59	>0.99	>0.99	>0.99
	delay	3.43±2.65	2.87±1.21	2.55±1.26	0.810	0.419	0.907
White Matter	TTP	15.45±5.14	12.19±2.65	13.43±2.35	0.008*	0.219	0.237
	MTT	4.24±0.89	4.04±0.87	4.04±0.67	0.635	0.190	0.147
	CBF	36.10±9.14	41.62±8.31	33.61±8.90	0.02*	0.684	0.008*
	CBV	2.46±0.67	2.76±0.76	2.17±0.55	0.139	0.012*	0.001*
	delay	3.72±2.21	3.40±1.60	3.26±1.58	>0.99	0.917	>0.99

Pre: Pre-surgery; post1: post-surgery within a week; post2: post-surgery after three months; TTP, MTT and delay were measured in seconds (s); CBF was measured in ml/(100g.min); CBV was measured in ml/100g; P values were adjusted by Bonferroni correction for multiple comparison.

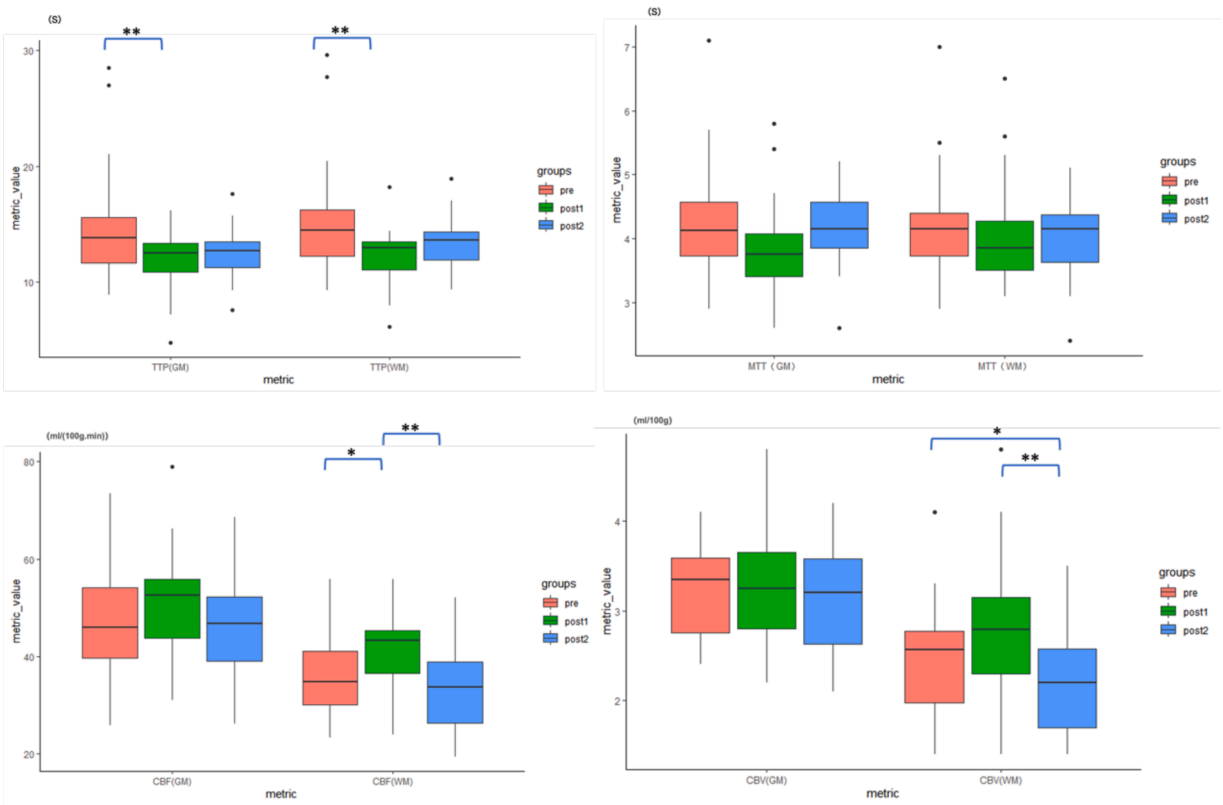

Fig. 2. Boxplots for longitudinal alterations of CTP-derived metrics TTP, MTT, CBF and CBV over times (pre: pre-surgery; post1: post-surgery within 7day; post2: postsurgery after 3month). P values indicate significant differences compared with pre (baseline) after adjustment for multiple comparisons. *=P < .05, **=P < .01.

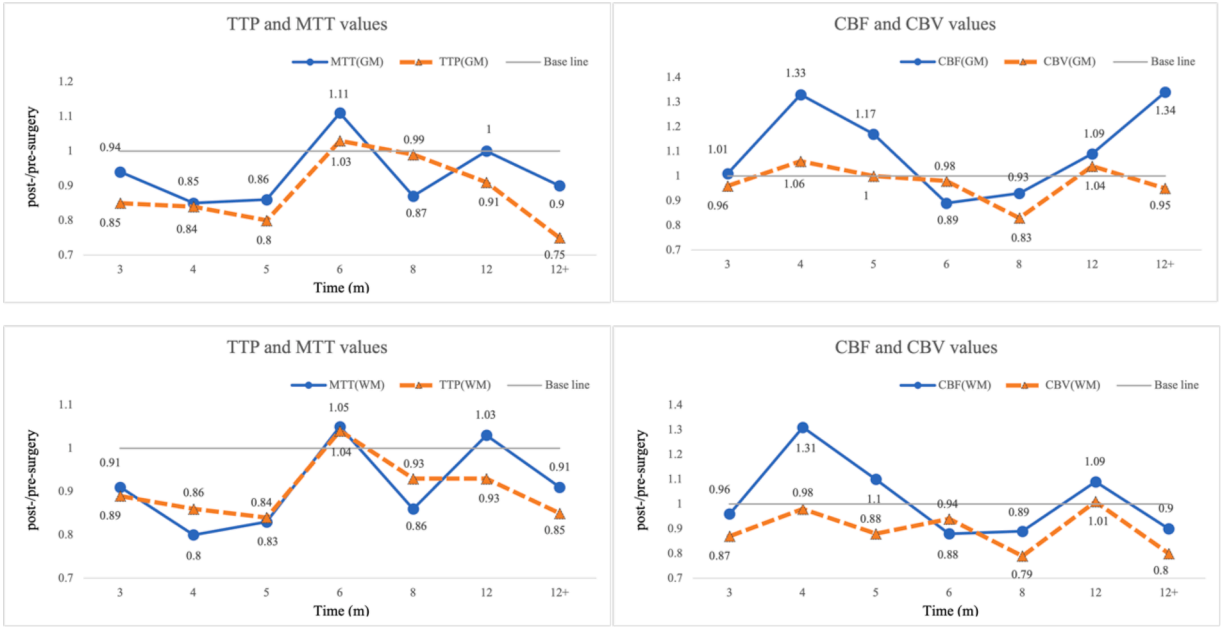

Fig. 3. Graphs show longitudinal alterations of the ratio of postsurgical and presurgical CTP-derived metrics over time.

3 months: 51.98±13.3 ml/(100 g·min) vs 52.76±10.2 ml/(100g·min), *P*=0.821). No significant changes in CBV values were observed within a week after surgery or 3 months after surgery in patients with Suzuki stage 3 or 4 MMD.

Within a week after surgery, the TTP of the white matter significantly decreased and the CBF increased considerably, irrespective of Suzuki stage. In addition, the CBV of patients with Suzuki stage 3 MMD substantially increased during short-term follow-up. Regarding long-term follow-up, the TTP of the white matter was still significantly lower than that before surgery in patients with Suzuki stage 3 MMD. Compared with presurgical values, reduced CBF and substantially lowered CBV were identified in patients with Suzuki stage 3 or 4 MMD.

Table 3
Changes in cerebral cortex and cerebral white matter for Suzuki Stage 4 and Stage 3 patients.

		Suzuki Stage 4					
		Pre (n=15)	Post1 (n=13)	Post2 (n=12)	*P* values (Pre vs. post1)	*P* values (Pre vs. post2)	*P* values (post1 vs. post2)
Gray Matter	TTP	15.87±6.57	12.14±3.87	12.00±2.96	0.077	0.068	0.445
	MTT	5.07±1.27	4.47±0.70	4.26±0.55	0.068	0.133	0.934
	CBF	43.05±9.29	49.30±11.86	43.71±10.44	0.043*	0.788	0.303
	CBV	3.55±0.92	3.64±0.91	3.04±0.56	0.660	0.143	0.305
	delay	4.53±3.34	2.75±1.25	2.71±1.12	0.060	0.177	0.841
White Matter	TTP	16.55±6.42	12.48±3.80	13.14±2.96	0.03*	0.107	0.159
	MTT	4.91±1.30	4.42±0.94	4.15±0.60	0.077	0.148	0.781
	CBF	34.98±8.11	40.51±9.26	34.36±11.63	0.05*	0.244	0.064
	CBV	2.77±0.82	2.97±0.87	2.29±0.62	0.412	0.007*	0.064
	delay	4.31±2.57	3.38±1.84	3.26±1.66	0.16	0.143	0.916
		Suzuki Stage 3					
Gray Matter	TTP	13.42±3.23	11.65±2.31	11.70±2.36	0.004*	0.013*	0.649
	MTT	4.20±0.71	3.48±0.46	4.00±0.62	0.006*	0.319	0.032*
	CBF	51.98±13.30	58.31±14.06	52.76±10.20	0.038*	0.821	0.262
	CBV	3.56±0.80	3.50±0.78	3.43±0.63	0.179	0.395	0.507
	delay	3.17±1.96	2.80±1.23	2.23±1.39	0.728	0.021*	0.275
White Matter	TTP	14.45±3.39	12.13±2.32	12.94±2.23	0.001*	0.034*	0.255
	MTT	4.24±0.73	3.75±0.75	3.98±0.81	0.106	0.068	0.671
	CBF	38.49±10.77	44.99±7.31	37.36±7.56	0.001*	0.652	0.021*
	CBV	2.72±0.92	2.79±0.62	2.41±0.72	0.003*	0.015*	<0.001*
	delay	4.21±2.18	3.80±1.55	3.23±1.49	>0.99	0.075	0.833

Pre: Pre-surgery; post1: post-surgery within a week; post2: post-surgery after three months; TTP, MTT and delay were measured in seconds (s); CBF was measured in ml/(100g.min); CBV was measured in ml/100g; p values were adjusted by Bonferroni correction for multiple comparison.

Discussion

Our study demonstrated that CTP can depict the patency of the bridge vessels and easily identify new infarcts or hemorrhages. Longitudinal CTP analysis showed that TTP in the white and gray matter decreased significantly for a short period after surgery. CBF values in the white matter increased significantly for a short time after surgery but decreased again for a long time after surgery. Furthermore, our study found that cerebral perfusion began to deteriorate in the sixth month and continued to deteriorate at 6-8 months, returning to the presurgical level after a year. In addition, the improvement in postsurgical perfusion was greater in stage 3 patients than in stage 4 patients.

Our comprehensive study found that TTP values within a week after surgery were significantly lower than those before surgery, whereas CBF increased significantly. These changes in the gray and white matter were similar, indicating marked perfusion improvement in the short-term after surgery. These results were consistent with those reported by Wang et al.[13]. This suggests that the cerebral parenchymal blood supply effectively benefited from STA-MCA surgery in a short time.[25-27] However, over time, compared with preoperative values, CBF and CBV decreased again and showed no significant improvement. The CBF and CBV of the white matter decreased to a lower level than before surgery. However, inconsistent with CBF or CBV, the TTP was still slightly lower than the presurgical TTP, with no statistical significance, suggesting that neovascularization coverage was still ongoing. This result verified the findings of Calamante et al.[28] and Shimizu et al.[29]. They suggested cerebral hemodynamics did not develop immediately because blood vessels took 3 to 4 months to form.[28,29]

Furthermore, our longitudinal study identified that cerebral perfusion began to deteriorate in the sixth month, continued to deteriorate from the sixth to eighth months, and returned to the presurgical level after a year. The results of previous studies might explain these findings. Calamante et al.[23] and Shimizu et al.[24] suggested that cerebral hemodynamics did not improve immediately after surgery because blood vessels took 3–4 months to develop, and presurgical cerebral ischemia could occur during this time. Therefore, more supportive treatment is required during this period. Zhao et al.[18] reported that neovascularization coverage for patients with MMD was not ideal 3–6 months after bypass surgery; neovascularization was generally completed at approximately 6 months, and the coverage increased significantly one year later. Our results were partially consistent with these findings, and a study with a longer (>2 years) follow-up period is warranted.

We further investigated the impact of surgery on different Suzuki stages to identify patients with MMD who may benefit from surgery. Our study showed a similar perfusion evolution tendency in patients with MMD, irrespective of Suzuki stage. CBF and TTP temporarily improved in both gray and white matter. Significantly decreased TTP in the gray matter at 3 months and substantially increased CBV in the white matter within a week after surgery were only identified in patients with Suzuki stage 3 but not those with stage 4. This suggests that in patients with MMD with Suzuki stage 4, less perfusion improvement was observed during surgery than in those with Suzuki stage 3 disease. Additionally, we found that there were no significant improvements in the long-term relevant to Suzuki stage, and CBV values in white matter regions were significantly lower than presurgical values. These results indicate that the short-term improvement effect of surgery in MMD is better than that in the long term, and the curative effect of surgery in patients was similar, irrespective of the Suzuki stage.

Surgical treatment methods for MMD include direct and indirect surgery.[23] Some researchers have indicated that direct surgery yields a larger postoperative perfusion area and more significant improvement than indirect surgery.[30] However, longitudinal studies comparing these two surgical methods and the evolution of brain perfusion are yet to be conducted. In our study, all included patients underwent direct (n=35) or direct combined with indirect (n=9) revascularization surgery. However, owing to the small sample size, the impact of different surgical methods on brain perfusion alterations in patients cannot be evaluated or applied in our study. Multicenter studies with large sample sizes are required to analyze the longitudinal perfusion changes using different revascularization techniques.

Our study has several limitations. First, radiation exposure during CTP is inevitable. CTP at our hospital significantly reduced the mean effective dose. Second, the study cohort was limited, and follow-up was inconsistently performed. There have been few long-term follow-up studies, and few studies have analyzed white and gray matter separately. However, MMD often affects different vessel territories to a different extent; in this study, we mainly focused on the overall perfusion alterations of the brain parenchyma while neglecting the impact of the different circulation regions. This problem should be solved in future

studies with larger sample sizes. Third, CTP scans were performed before and after surgery a total of three times; therefore, it was challenging to ensure that the ROIs were precisely the same all three times, which might have caused some bias. However, all brain CTP collections were standardized with high consistency.

In conclusion, CTP can be used to evaluate bridge vessels and simultaneously obtain dynamic alterations in brain parenchymal perfusion in patients with MMD after revascularization surgery. Increased cerebral perfusion was observed shortly after surgery. However, as time passed, brain perfusion began to deteriorate in the sixth month and continued to deteriorate from the sixth to eighth months. It returned to or was lower than the presurgical level after the last follow-up, which may be the leading cause of disease progression. In addition, the improvement in postsurgical perfusion was greater in Suzuki stage 3 patients than in stage 4 patients. Our results should be verified in a prospective study with a longer follow-up period.

Sources of funding

Guangdong Basic and Applied Basic Research Foundation, China (No. 2020A1515011436) Science and Technology Program of Guangzhou, China (No. 202201011244).

Guarantor

The scientific guarantor of this publication is Zhao Jing.

Statistics and biometry

One of the authors (Huang Yingqian) has significant statistical expertise (4 years of experience in statistical analysis).

Informed consent

Written informed consent was signed by all patients before enrollment in the initial study.

Ethical approval

This study was approved by the Ethics Committee of the First Affiliated Hospital of Sun Yat-sen University.

CRediT authorship contribution statement

Huang Yingqian: Writing – review & editing, Writing – original draft, Visualization, Validation, Software, Project administration, Methodology, Investigation, Formal analysis, Data curation, Conceptualization. **Wei Dan:** Writing – original draft, Validation, Software, Methodology, Investigation, Data curation, Conceptualization. **Lin Liping:** Methodology, Formal analysis, Data curation, Conceptualization. **Lai Zhiman:** Visualization, Validation, Data curation, Conceptualization. **Xie Dingxiang:** Validation, Methodology, Data curation, Conceptualization. **Li Zhuhao:** Visualization, Validation, Data curation, Conceptualization. **Yang Zhiyun:** Writing – review & editing, Visualization, Supervision, Software, Resources, Methodology, Investigation, Funding acquisition, Conceptualization. **Jiang Li:** Writing – review & editing, Visualization, Validation, Supervision, Software, Resources, Project administration, Methodology, Investigation, Funding acquisition, Formal analysis, Data curation, Conceptualization. **Zhao Jing:** Writing – review & editing, Visualization, Validation, Supervision, Software, Resources, Project administration, Methodology, Investigation, Funding acquisition, Formal analysis, Data curation, Conceptualization.

Declaration of competing interest

The authors of this manuscript declare no relationships with any companies, whose products or services may be related to the subject matter of the article.

Acknowledgments

Thanks for the support of Guangdong Stroke Association in China.

References

1. Suzuki J, Takaku A. Cerebrovascular "moyamoya" disease. Disease showing abnormal net-like vessels in base of brain. *Arch Neurol*. 1969;20(3):288–299.
2. Quon JL, et al. Arterial spin-labeling cerebral perfusion changes after revascularization surgery in pediatric moyamoya disease and syndrome. *J Neurosurg Pediatr*. 2019;23(4):486–492.
3. Golby AJ, et al. Direct and combined revascularization in pediatric moyamoya disease. *Neurosurgery*. 1999;45(1):50–58. p.discussion 58-60.
4. Baek HJ, et al. Preliminary study of neurocognitive dysfunction in adult moyamoya disease and improvement after superficial temporal artery-middle cerebral artery bypass. *J Korean Neurosurg Soc*. 2014;56(3):188–193.
5. Zeifert PD, et al. Neurocognitive performance after cerebral revascularization in adult moyamoya disease. *Stroke,*. 2017;48(6):1514–1517.
6. Miyamoto S, et al. Effects of extracranial-intracranial bypass for patients with hemorrhagic moyamoya disease: results of the Japan Adult Moyamoya Trial. *Stroke*. 2014;45(5):1415–1421.
7. Wouters A, et al. Cerebrovascular events after surgery versus conservative therapy for moyamoya disease: a meta-analysis. *Acta Neurol Belg*. 2019;119(3):305–313.
8. Arias EJ, et al. *Advances and surgical considerations in the treatment of moyamoya disease*. 74. Neurosurgery; 2014:S116–S125.
9. Funaki T, et al. Unstable moyamoya disease: clinical features and impact on perioperative ischemic complications. *J Neurosurg*. 2015;122(2):400–407.
10. Fan AP, et al. Identifying hypoperfusion in moyamoya disease with arterial spin labeling and an [(15)O]-water positron emission tomography/magnetic resonance imaging normative database. *Stroke*. 2019;50(2):373–380.
11. Gross BA, Du R. Adult moyamoya after revascularization. *Acta Neurochir (Wien)*. 2013;155(2):247–254.
12. Houkin K, et al. How does angiogenesis develop in pediatric moyamoya disease after surgery? A prospective study with MR angiography. *Childs Nerv Syst*. 2004;20(10):734–741.
13. Wang X, et al. Evaluation of hemodynamics before and after revascularization in hemorrhagic moyamoya disease: a computed tomography perfusion imaging case study. *World Neurosurg*. 2019;131:e277–e283.
14. Guo X, et al. Encephaloduroarteriosynangiosis (EDAS) treatment of moyamoya syndrome: evaluation by computed tomography perfusion imaging. *Eur Radiol*. 2021;31(11):8364–8373.
15. Wolf RL, Detre JA. Clinical neuroimaging using arterial spin-labeled perfusion magnetic resonance imaging. *Neurotherapeutics*. 2007;4(3):346–359.
16. Lee S, et al. Monitoring cerebral perfusion changes after revascularization in patients with moyamoya disease by using arterial spin-labeling MR imaging. *Radiology*. 2018;288(2):565–572.
17. Zaharchuk G, et al. Arterial spin-labeling MRI can identify the presence and intensity of collateral perfusion in patients with moyamoya disease. *Stroke*. 2011;42(9):2485–2491.
18. Kronenburg A, et al. Cerebrovascular reactivity measured with ASL perfusion MRI, ivy sign, and regional tissue vascularization in moyamoya. *World Neurosurg*. 2019;125:e639–e650.
19. Sasagawa A, et al. Characteristics of cerebral hemodynamics assessed by CT perfusion in moyamoya disease. *J Clin Neurosci*. 2018;47:183–189.
20. Kawamura K, et al. Persistent local vasogenic edema with dynamic change in the regional cerebral blood flow after STA-MCA bypass for adult moyamoya disease. *J Stroke Cerebrovasc Dis*. 2020;29(4), 104625.
21. Chen Y, et al. CT perfusion assessment of moyamoya syndrome before and after direct revascularization (superficial temporal artery to middle cerebral artery bypass). *Eur Radiol*. 2016;26(1):254–261.
22. Zhao Y, et al. Time course of neoangiogenesis after indirect bypass surgery for moyamoya disease: comparison of short-term and long-term follow-up angiography. *Clin Neuroradiol*. 2020;30(1):91–99.
23. Bao XY, Duan L. Chinese expert consensus on the treatment of MMD. *Chin Neurosurg J*. 2023;9(1):5.
24. Matsushima T, et al. Surgical treatment of moyamoya disease in pediatric patients–comparison between the results of indirect and direct revascularization procedures. *Neurosurgery*. 1992;31(3):401–405.
25. Yan J, et al. Clinical features and prognostic analysis of moyamoya disease associated with intracranial aneurysms. *Neurol Res*. 2020;42(9):767–772.
26. Tanabe N, et al. Indocyanine green visualization of middle meningeal artery before craniotomy during surgical revascularization for moyamoya disease. *Acta Neurochir (Wien)*. 2017;159(3):567–575.
27. Machida T, et al. Postoperative cerebral ischemia due to hypotension in moyamoya patient with autonomic dysfunction. *World Neurosurg*. 2018;109:204–208.

28. Calamante F, et al. MR perfusion imaging in Moyamoya Syndrome: potential implications for clinical evaluation of occlusive cerebrovascular disease. *Stroke*. 2001;32(12):2810–2816.
29. Shimizu T, et al. In reply to the letter to the editor regarding "large craniotomy increases the risk of minor perioperative complications in revascularization surgery for moyamoya disease". *World Neurosurg*. 2020;143:584.
30. Yuan X, et al. Evaluation of surgical revascularization procedure outcomes for adult Moyamoya disease: a computed tomography perfusion-based study. *Insights Imaging*. 2023;14(1):184.

Arterial Spin-Labeling MRI Can Identify the Presence and Intensity of Collateral Perfusion in Patients With Moyamoya Disease

Greg Zaharchuk, PhD, MD; Huy M. Do, MD; Michael P. Marks, MD; Jarrett Rosenberg, PhD; Michael E. Moseley, PhD; Gary K. Steinberg, MD, PhD

Background and Purpose—Determining the presence and adequacy of collateral blood flow is important in cerebrovascular disease. Therefore, we explored whether a noninvasive imaging modality, arterial spin labeling (ASL) MRI, could be used to detect the presence and intensity of collateral flow using digital subtraction angiography (DSA) and stable xenon CT cerebral blood flow as gold standards for collaterals and cerebral blood flow, respectively.

Methods—ASL and DSA were obtained within 4 days of each other in 18 patients with Moyamoya disease. Two neurointerventionalists scored DSA images using a collateral grading scale in regions of interest corresponding to ASPECTS methodology. Two neuroradiologists similarly scored ASL images based on the presence of arterial transit artifact. Agreement of ASL and DSA consensus scores was determined, including kappa statistics. In 15 patients, additional quantitative xenon CT cerebral blood flow measurements were performed and compared with collateral grades.

Results—The agreement between ASL and DSA consensus readings was moderate to strong, with a weighted kappa value of 0.58 (95% confidence interval, 0.52–0.64), but there was better agreement between readers for ASL compared with DSA. Sensitivity and specificity for identifying collaterals with ASL were 0.83 (95% confidence interval, 0.77–0.88) and 0.82 (95% confidence interval, 0.76–0.87), respectively. Xenon CT cerebral blood flow increased with increasing DSA and ASL collateral grade ($P<0.05$).

Conclusions—ASL can noninvasively predict the presence and intensity of collateral flow in patients with Moyamoya disease using DSA as a gold standard. Further study of other cerebrovascular diseases, including acute ischemic stroke, is warranted. **(*Stroke*. 2011;42:2485-2491.)**

Key Words: angiography ■ arterial spin labeling ■ cerebral blood flow ■ cerebral hemodynamics ■ cerebrovascular disease ■ collateral flow ■ neuroradiology ■ perfusion

Moyamoya disease is characterized by progressive stenosis of the supraclinoid anterior circulation.[1] By the time of diagnosis, these patients have extensively developed collateral vessels. Cerebral collateral flow is poorly understood despite its importance in maintaining the cerebral circulation during acute stroke and chronic hypoperfusion.[2,3] In acute stroke, the presence of collaterals is associated with better outcomes after thrombolytics[4,5] and appears to decrease the rate of hemorrhagic transformation.[6] A commonly accepted method of judging the presence of collateral vessels is digital subtraction angiography (DSA), which is relatively time-consuming, invasive, and costly. DSA-based grading systems described in the literature are qualitative, relying on the visual inspection of contrast transit to an ischemic region.[7–9] Other methodologies, including bolus contrast methods such as CT perfusion and MRI-based perfusion-weighted imaging, may permit evaluation of the adequacy of flow related to collaterals, although they do require the use of exogenous contrast agents. It would be helpful to have information about the collateral networks using a truly noninvasive, noncontrast tomographic approach.

Arterial spin-labeling (ASL) is a noncontrast MRI perfusion method whose greatest flaw is its exquisite sensitivity to arterial arrival delays.[10–15] However, the bright intravascular signal known as arterial transit artifact (ATA) actually contains important information about late-arriving flow. However, this complicates the calculation of quantitative cerebral blood flow (CBF),[16,17] which can be circumvented by the use of gold standard diffusible tracer methods such as stable xenon (Xe) CT.[18,19] The goal of the current study was to test

Received February 4, 2011; accepted March 31, 2011.

From the Department of Radiology (G.Z., H.M.D., M.P.M., J.R., M.E.M.) and Department of Neurosurgery (G.K.S.), Stanford University and Stanford University Medical Center, Stanford, CA.

The online-only Data Supplement is available at http://stroke.ahajournals.org/lookup/suppl/doi:10.1161/STROKEAHA.111.616466/-/DC1.

Correspondence to Greg Zaharchuk, PhD, MD, Stanford University Medical Center, 1201 Welch Road, Mailcode 5488, Stanford, CA 94305-5488. E-mail gregz@stanford.edu

***Stroke* is available at http://stroke.ahajournals.org** **DOI: 10.1161/STROKEAHA.111.616466**

whether ASL using a single postlabel delay (PLD) time could be used to reliably identify the presence of angiographic collaterals using DSA as a gold standard. Additionally, we sought to understand whether quantitative CBF measurements using stable Xe CT correlated with either DSA-based or ASL-based measures of collateral flow.

Materials and Methods

The study was approved by our institution's Committee on Human Research. DSA and ASL imaging was performed in 18 patients with newly diagnosed Moyamoya disease (5 men, 13 women; mean age, 43 years; range, 19–65 years; 11 unilateral disease, 7 bilateral disease) as part of their preoperative assessment for possible superficial temporal artery to middle cerebral artery bypass. All patients were symptomatic, with the most common symptoms including transient ischemic attacks, small deep white matter infarcts, seizures, and headache. The DSA study was acquired within 4 days of the MRI study in all cases.

DSA was performed using a dedicated biplane cerebral angiographic system (Axiom Artis dBA Twin; Siemens Medical Systems). Images of bilateral internal and external carotid artery and at least 1 vertebral artery injection were acquired and stored. Imaging through the entire arterial and venous phases was performed to evaluate slowly flowing collateral vessels.

All MRI studies were performed at 1.5 T. In addition to the anatomic imaging, which is part of the clinical routine at our institution, we acquired pulsed continuous ASL using a repetition time of 5500 ms, echo time of 2.5 ms, labeling period of 1500 ms, and a PLD of 2000 ms, with a total acquisition time of 6 minutes. Readout was accomplished with a 3-dimensional background-suppressed fast spin-echo method, with in-plane and through-plane spatial resolution of 3 mm and 4 mm, respectively.

In 15 of these patients (83%), stable Xe CT CBF measurements were also performed. CT was performed using a GE Lightspeed 8 detector scanner integrated with a stable Xe enhancer system (Diversified Diagnostic Products). The Xe CT protocol imaged 4 contiguous 10-mm slices (80 kVp, 240 mA), with the lowest slice at the level of the basal ganglia. Eight sets of images were acquired at 45-second intervals. The first 2 time points were acquired during room air inhalation, whereas the remaining 6 time points were acquired during 28% Xe gas inhalation. End-tidal Xe concentration was assumed equal to arterial Xe concentration, a reasonable approximation except in patients with severe respiratory disease. CBF was calculated using the Kety autoradiographic method by the manufacturer's commercial software,[20] yielding CBF maps with a 1-mm nominal and 2 to 3 mm true in-plane spatial resolution. Rigid body rotation based on mutual information using SPM5 (University College of London, available at www.fil.ion.ucl.ac.uk/spm/software/spm5) was used to coregister the ASL CBF images to the Xe CT images.

Two interventional neuroradiologists (M.P.M. and H.Y.D.) separately evaluated the DSA studies using a 4-point collateral grading scale describing the intensity of collateral flow.[7] It incorporates specific comparison locations between regions identified on DSA and tomographic images based on 2 slices corresponding with the Alberta Stroke Programme Early Computed Tomography Score (ASPECTS) locations. This scale is as follows: 0, no collaterals visible (absence of any capillary blush); 1, mild to moderate collaterals; 2, robust collateral flow; and 3, normal antegrade flow. This grading was performed in 20 regions in each patient, as described in Figure 1. We chose to focus only on cortical regions because of the difficulties in visualizing capillary blush on DSA and signal on ASL imaging in the white matter. Disagreements were resolved by consensus. ASL images were evaluated by 2 additional neuroradiologists (G.Z. and N.J.F.) blinded to the DSA studies and grading results. These were scored in the same regions of interests using a similar 4-point scale (0, no or minimal ASL signal; 1, moderate ASL signal with ATA; 2, high ASL signal with ATA; and 3, normal perfusion without ATA). To improve the robustness of this score, several slices immediately above and below the precise ASPECTS slice were mentally summed to be more comparable with the DSA measurement.[21] An example of the ASL collateral grading scale is shown in Figure 2. Disagreements were resolved by consensus.

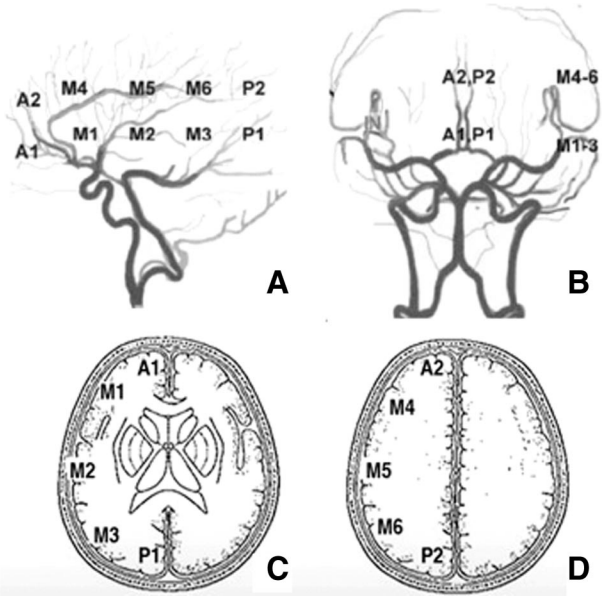

Figure 1. Collateral grading scales. Regions on digital subtraction angiography (**A**, **B**) are compared with corresponding regions on cross-sectional images (**C**, **D**). Figure modified with permission from Kim JJ, Fischbein NJ, Lu Y, Pham D, Dillon WP. Regional angiographic grading system for collateral flow: correlation with cerebral infarction in patients with middle cerebral artery occlusion. *Stroke*. 2004;35:1340–1344.

Agreement, linear-weighted κ values, Kendall τ-b measure of correlation, and the exact Bowker test of symmetry (to determine any tendency for disagreements to be predominantly in 1 direction) were calculated for both the individual inter-reader scores and intermodality consensus scores. Also, the scores were dichotomized between 0 and 2 (collateral flow) and 3 (antegrade flow) and were compared using unweighted κ, the Kruskal-Goodman γ measure of correlation, and the exact Bowker test of symmetry. The consensus DSA reading was considered the gold standard and, based on this, specificity, positive predictive value, and negative predictive value of ASL for identifying collateral flow were determined.

Quantitative Xe CT CBF was measured in the same regions-of-interest in which collaterals were assessed, using the two 10-mm slices most closely aligned with the ASPECTS system. After coregistering and reslicing the ASL CBF images to the same slice thickness and locations as the Xe CT slices (10-mm-thick), qualitative CBF values were also obtained in the same regions; the ASL measurements cannot be considered quantitative, considering the unknown effects of arterial arrival time, and are shown only for comparative purposes. The Jonckheere-Terpstra test was used to evaluate whether there was a trend for increasing CBF based on either the consensus DSA or the ASL collateral scores. All statistical analyses were performed with Stata Release 9.2.

Results

An example of a DSA image in the late venous phase and corresponding ASL images at the relevant levels in a patient with unilateral Moyamoya disease is shown as Figure 3. Note the clear depiction of arterial transit artifact on the ASL images in the right middle cerebral artery territory that also demonstrates delayed collateral flow on the DSA study. Although most cases showed good correlation, we present in

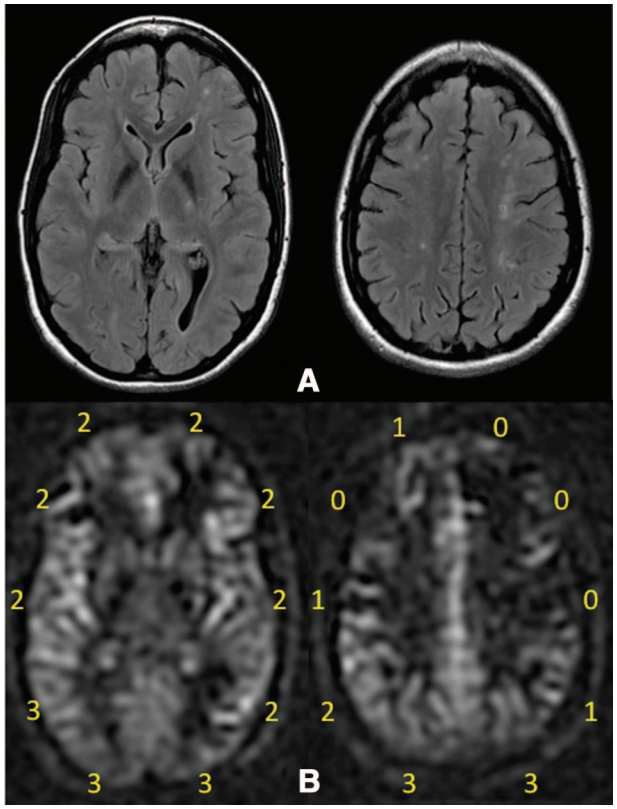

Figure 2. A 30-year-old woman with bilateral Moyamoya disease. FLAIR (**A**) and arterial spin-labeling (ASL; **B**) images at the 2 ASPECTS levels used in the current study. ASL collateral consensus scores are shown as an illustration of the grading scale (0, no or minimal ASL signal; 1, moderate ASL signal with arterial transit artifact [ATA]; 2, high ASL signal with ATA; 3, normal perfusion without ATA). FLAIR indicates fluid attenuated inversion recovery.

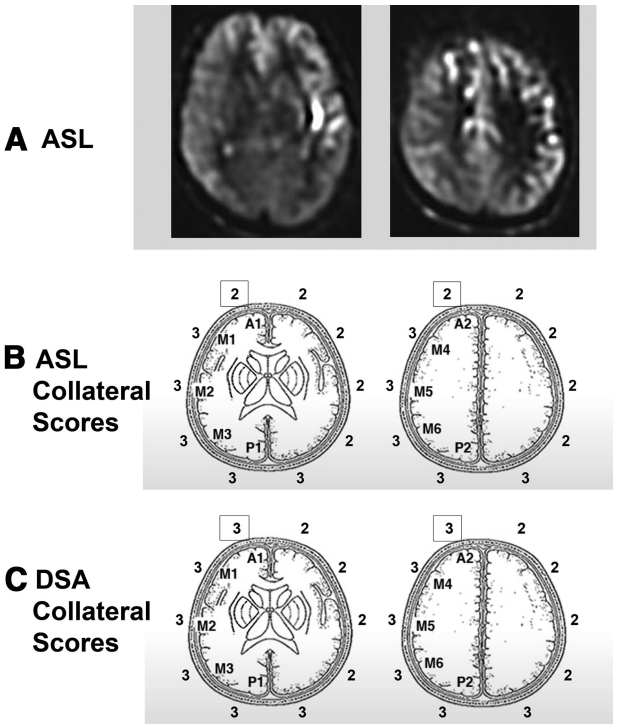

Figure 4. A 40-year-old woman with Moyamoya disease. Arterial spin-labeling CBF images (**A**) and collateral grades (**B**). **C**, Digital subtraction angiography (DSA) collateral grades. In this patient, there is good correlation except in the right A1 and A2 regions, which were called abnormal on ASL but not on DSA. Later, it was deemed that this patient had early bilateral Moyamoya disease and underwent bilateral superficial temporal artery to middle cerebral artery bypass.

Figure 4 an example of a case in which there was a discrepancy between the DSA and ASL collateral scores in which an area was deemed to be fed by collaterals on ASL but was called normal antegrade flow on DSA. Interestingly, it was later deemed that this patient had early bilateral Moyamoya based on clinical and angiographic features and underwent bilateral superficial temporal artery to middle cerebral artery bypass.

Overall, there was good agreement between the 2 readers for each modality as shown in the Table. It was more common for the ASL readers to agree regarding the exact

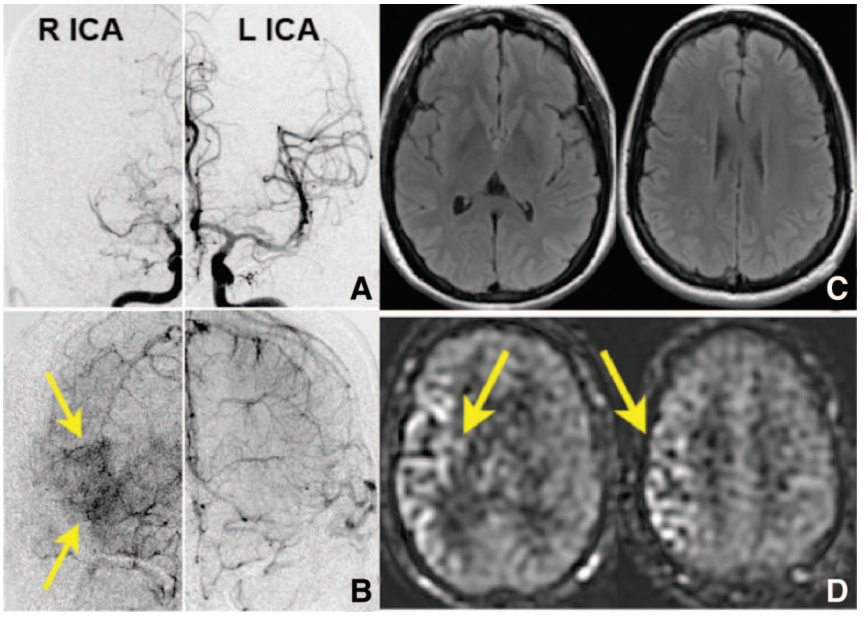

Figure 3. Comparison between digital subtraction angiography and MRI findings in a 41-year-old woman with unilateral Moyamoya disease. Anterior projections from right and left internal carotid artery injections in the (**A**) arterial and (**B**) venous phases demonstrate delayed capillary blush in the middle cerebral artery (MCA) territory (arrows), which corresponds to the MCA regions on ASPECTS. FLAIR (**C**) and arterial spin-labeling (**D**; ASL) images in the same patient corresponding to the 2 ASPECTS levels. ASL images demonstrate clear abnormality in the M1–M3 and M5–M6 regions. The arterial transit artifact signal on the ASL images in the affected territories reflects flow arriving via collateral routes. FLAIR indicates fluid attenuated inversion recovery.

Table. Inter-Reader and Intermodality Agreement of Collateral Scores

Full 4-Point Score	Weighted κ	95% CI	Kendall τ-b	Symmetry Test *P*	
DSA1 vs DSA2	0.52	0.47–0.56	0.78	<0.0001	DSA1>DSA2
ASL1 vs ASL2	0.79	0.74–0.84	0.85	<0.0001	ASL2>ASL1
ASLc vs DSAc	0.58	0.52–0.64	0.67	0.0013	DSAc>ASLc
Dichotomized Scores (Collateral vs Antegrade Perfusion)	κ	95% CI	Kruskal γ	Symmetry Test *P*	
DSA1 vs DSA2	0.86	0.80–0.91	0.99	0.009	DSA1>DSA2
ASL1 vs ASL2	0.87	0.82–0.92	0.99	0.541	
ASLc vs DSAc	0.65	0.56–0.72	0.91	0.450	

ASL indicates arterial spin-labeling; CI, confidence interval; DSA, digital subtraction angiography.
DSA1: DSA scored by reader 1.
DSA2: DSA scored by reader 2.
DSAc: DSA score based on consensus read of readers 1 and 2.
ASL1: ASL scored by reader 1.
ASL2: ASL scored by reader 2.
ASLc: ASL score based on consensus read of readers 1 and 2.
DSA1>DSA2 reflects that the average scores for reader 1 were higher than those of reader 2.

score as compared with the DSA readers (83% versus 65%, respectively). This is also reflected in a higher-weighted κ for the ASL readers (κ=0.79; 95% confidence interval [CI], 0.74–0.84) compared with the DSA readers (κ=0.52; 95% CI, 0.47–0.56). Weighted κ for the agreement between the consensus DSA and ASL scores was 0.58 (95% CI, 0.52–0.64). Using a dichotomized scale (ie, collateral flow [score, 0–2] versus normal flow [score 3]), the κ value was even higher (0.65; 95% CI, 0.56–0.72), which can be considered as substantial agreement.[22] Based on DSA consensus scores, 46% of the regions assessed where deemed to be fed by collaterals. For the consensus ASL and DSA collateral scores, sensitivity, specificity, positive predictive value, and negative predictive value were 0.83 (95% CI, 0.77–0.88), 0.82 (95% CI, 0.76–0.87), 0.80 (95% CI, 0.73–0.86), and 0.85 (95% CI, 0.79–0.90), respectively. The nonsignificant exact Bowker test (P=0.45) indicated that was no tendency toward false-positive results over false-negative results. Supplemental Table I (http://stroke.ahajournals.org) shows the breakdown of the various collateral scores using the entire 4-point scale.

Figure 5 shows the results of the Xe CT and ASL CBF measurements as a function of either increasing DSA or increasing ASL collateral scores. The Xe CT CBF measurements increase with increasing collateral score, regardless of the method used, but the trend is more pronounced for the ASL collateral score compared with the DSA collateral score (ASL collateral score: J*=8.00; for DSA collateral score: J*=6.16; Supplemental Table II). ASL CBF shows that the regions with robust collaterals (score=2) had higher apparent CBF than those with anterograde perfusion (score=3). This is likely attributable to artifacts associated with delayed arterial arrival and high ASL signal in the feeding arteries that perfuse more distal tissue.

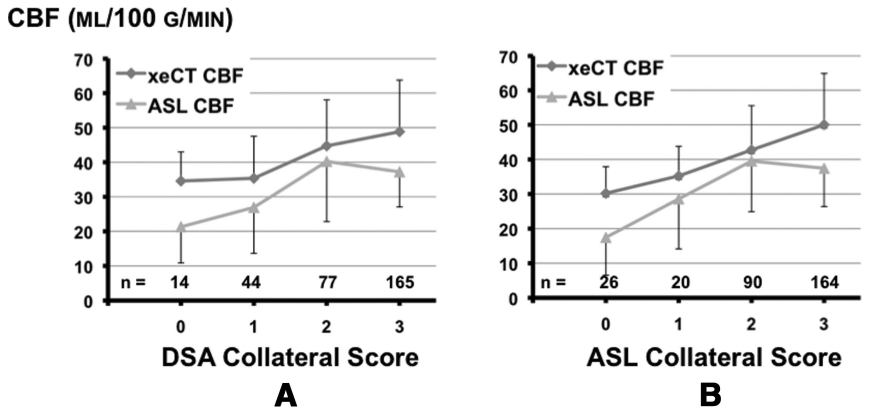

Figure 5. Mixed-cortical cerebral blood flow (CBF) measured with a gold standard method (xenon CT [Xe CT]) and arterial spin-labeling (ASL) in the same regions assessed for collaterals, as a function of either (**A**) digital subtraction angiography (DSA)-based consensus collateral score or (**B**) ASL-based consensus collateral score. Xe CT CBF increased with both DSA-based and ASL-based collateral scores, but the trend was more pronounced for the ASL-based collateral score. Data shown are from the 15 patients who had both Xe CT and ASL performed. The number of regions in which the measurements were made is shown under the data points. Error bars represent standard deviation of the respective method. These are shown only on the upper half of the Xe CT and the lower half of the ASL data for clarity. No significant difference between the CBF measurement types for any of the collateral scores was present.

Discussion

Collateral blood flow plays a critical role in supporting the cerebral circulation in the setting of acute and chronic cerebral ischemia.[3,23,24] In response to a decrease in local perfusion pressure, there is recruitment of flow from both circle of Willis and leptomeningeal anastomoses, which compensate for the lack of anterograde flow.[3] Patients with the same vascular occlusion may have significantly different outcomes based on their ability to recruit collateral pathways to restore flow to the ischemic region during the minutes and hours after an acute event.[25,26] The eventual failure of collateral pathways is thought to lead to infarct growth and is ultimately responsible for the decreasing efficacy of stroke therapy with time.[27] Timely knowledge about the status of collaterals affects the decision-making process regarding acute therapy in individual patients with ischemic stroke.[23,27] For example, Kucinski et al[25] demonstrated that the best predictor of favorable outcome in the retrospective series of patients undergoing intra-arterial thrombolysis was the presence of good collateral flow as judged by the initial DSA study. For all these reasons, having the ability to assess the location and amount of collateral perfusion using a noninvasive test such as MRI would be desirable.

Given its sensitivity to arrival time and its ability to quantify CBF, ASL combines features of both angiography and perfusion. Previous studies have shown good correlation with gold standard CBF imaging of gray matter in healthy subjects,[28] but it is likely that it underestimates CBF in regions with delayed arterial arrival times. This is because the label decays with the blood T1, which is on the same order as arterial arrival delays in patients with Moyamoya disease.[29] However, this drawback for quantitation may be turned to advantage for visualizing collaterals. With ASL, late-arriving flow appears as serpiginous high ASL signal within cortical vessels, which has been termed ATA.[11,30] ATA was seen frequently in a small group of acute ischemic stroke patients and was associated with tissue survival and improved clinical outcome.[31] Also, patients with chronic hypoperfusion and ATA had poor cerebrovascular reserve in response to acetazolamide.[11] ATA is dependent on several sequence parameters, particularly the labeling time and the PLD. Only a single PLD was used in this study; ASL sequences with a range of PLD times exist and can be helpful for quantifying CBF[32–34] but require longer imaging times for equivalent signal-to-noise ratio. There is some evidence that choosing a single PLD in a range that is highly sensitive to delay can increase the sensitivity for identifying pathology.[12,35]

This study shows that an ASL sequence with a single moderately long PLD can identify regions with collateral flow and can differentiate between poor and robust collateral flow, as determined using a DSA-based collateral grading scale. In particular, the agreement between consensus ASL and DSA scores for the distinction of normal perfusion versus collateral flow was quite good. Also, there was no evidence of a systematic bias in the ASL scoring compared with the consensus DSA. These findings are consistent with a previous study[36] that used a high-field (3-T) multiple PLD ASL method that also used perfusion territory imaging, an ASL method that can separate flow contributions from different cerebral arteries. These investigators examined a population of patients with a variety of cerebrovascular disease, some of whom had Moyamoya disease, and found a κ value of 0.72 for distinguishing collateral from antegrade perfusion, similar to that in the current study (κ=0.65). In addition to validating these general results, the current study also examines how well different readers agree on both the DSA and ASL grading scales, showing that agreement is higher with the ASL method. Furthermore, we suggest that high-field imaging, perfusion territory imaging, and multiple PLD ASL imaging are not required to identify collateral flow with a similar degree of accuracy. This is important because these modifications to the ASL experiment required additional imaging time (10 minutes for the ASL and 4 minutes for the 3-dimensional time-of-flight angiogram that is required to plan the ASL sequence). The current study demonstrates good performance using a faster ASL imaging protocol (6 minutes), making it more feasible in the clinical setting.

We also undertook understanding the relationship between collateral scores and CBF. Previous reports have suggested that identification of collaterals on DSA was not a good predictor of the adequacy of cerebral perfusion based on oxygen extraction fraction measurements using positron emission tomography.[37,38] Our findings show that gold standard Xe CT-based CBF increases as collateral score increases for both DSA-based and ASL-based consensus collateral scores. This effect was more pronounced with the ASL-based scores than the DSA-based scores (Supplemental Table II). Interestingly, the highest correlation was for Xe CT CBF based on ASL collateral score. ASL CBF also increased with increasing collateral score but is unreliable in the presence of known long arterial arrival delays. This likely explains why the ASL CBF measurements are highest in regions rated to have robust collaterals (score=2), because this flow is destined for more distal slices. Bolus perfusion-weighted imaging, using either CT or MRI, also can be used to estimate CBF, cerebral blood volume, mean transit time, and normalized bolus arrival time and could be used for this application. However, it is challenging to acquire quantitative CBF measurements using such nondiffusible intravascular tracers, particularly in patients with Moyamoya disease.[29,39] Delay-corrected algorithms[40] may mitigate problems associated with pure delays, but not with dispersion.[41] We performed perfusion-weighted imaging measurements in a subset of these patients, but we do not present these data because the acquisition parameters were not standardized, and the imaging planes did not completely cover the regions of interest interrogated in the remainder of the study. To our knowledge, few methods using bolus perfusion-weighted imaging to distinguish normal from collateral flow have been reported,[42] and we hope to explore this more thoroughly in a prospectively recruited study. This ASL method may be particularly amenable for use in patients who cannot receive gadolinium-containing contrast agents or who may need multiple studies (either in a single or consecutive sessions) to assess either cerebrovascular reserve or effects of treatment.

The limitations of this study include the difficulties of applying the DSA collateral grading system,[7] initially developed for acute ischemic stroke as part of the PROACT 2

study, to a chronic cerebrovascular disease such as Moyamoya disease. Also, perfusion territory imaging using vessel-selective ASL was not used,[36,43,44] which may further help identify regions fed via collateral pathways. Such a method would allow one to distinguish slow antegrade flow attributable to a high-grade stenosis from leptomeningeal or other retrograde-type collateral flow, which was not possible with the current study. Historically, such methods have required additional scan time, but newer techniques have been described that achieve vessel selectivity without the scan time penalties.[45] It is probable that such methods would prove even more accurate. Also, we do not report quantitative CBF using the ASL method. Given the long arterial arrival delays in Moyamoya patients,[29] it is likely that some degree of CBF underestimation occurs in the regions perfused by collaterals. Finally, we recognize that the use of a consensus reading from 2 separate readers for each modality allows only a limited evaluation of the variability related to multiple readers, which is reported in the Table.

Conclusions

This study shows that ASL can noninvasively evaluate the presence and intensity of collateral flow in patients with Moyamoya disease when compared to DSA. Further study of other cerebrovascular diseases, including acute ischemic stroke, is warranted.

Sources of Funding

The authors were funded by NIH R01NS66506-1 and R01NS047607. G.Z. was supported by the Neuroradiology Education and Research Foundation Scholar Award, which enabled this work.

Disclosures

G.Z. is a member of the Neuroradiology Advisory Board and receives research support from GE Healthcare.

References

1. Suzuki J, Takaku A. Cerebrovascular "moyamoya" disease: Disease showing abnormal net-like vessels in base of brain. *Arch Neurol*. 1969; 20:288–299.
2. Powers WJ. Cerebral hemodynamics in ischemic cerebrovascular disease. *Ann Neurol*. 1991;29:231–240.
3. Liebeskind DS. Collateral circulation. *Stroke*. 2003;34:2279–2284.
4. von Kummer R, Holle R, Rosin L, Forsting M, Hacke W. Does arterial recanalization improve outcome in carotid territory stroke? *Stroke*. 1995; 26:581–587.
5. Christoforidis GA, Mohammad Y, Kehagias D, Avutu B, Slivka AP. Angiographic assessment of pial collaterals as a prognostic indicator following intra-arterial thrombolysis for acute ischemic stroke. *AJNR Am J Neuroradiol*. 2005;26:1789–1797.
6. Christoforidis GA, Karakasis C, Mohammad Y, Caragine LP, Yang M, Slivka AP. Predictors of Hemorrhage Following Intra-Arterial Thrombolysis for Acute Ischemic Stroke: The Role of Pial Collateral Formation. *AJNR Am J Neuroradiol.* 2008.
7. Kim JJ, Fischbein NJ, Lu Y, Pham D, Dillon WP. Regional angiographic grading system for collateral flow: correlation with cerebral infarction in patients with middle cerebral artery occlusion. *Stroke*. 2004;35: 1340–1344.
8. Higashida RT, Furlan AJ, Roberts H, Tomsick T, Connors B, Barr J, et al. Trial design and reporting standards for intra-arterial cerebral thrombolysis for acute ischemic stroke. *Stroke*. 2003;34:e109–e137.
9. Qureshi AI. New grading system for angiographic evaluation of arterial occlusions and recanalization response to intra-arterial thrombolysis in acute ischemic stroke. *Neurosurgery.* 2002;50:1405–1414; discussion 1414–1405.
10. Detre JA, Leigh JS, Williams DS, Koretsky AP. Perfusion imaging. *Magn Reson Med*. 1992;23:37–45.
11. Detre JA, Samuels OB, Alsop DC, Gonzalez-At JB, Kasner SE, Raps EC. Noninvasive magnetic resonance imaging evaluation of cerebral blood flow with acetazolamide challenge in patients with cerebrovascular stenosis. *J Magn Reson Imaging*. 1999;10:870–875.
12. Zaharchuk G, Bammer R, Straka M, Shankaranarayan A, Alsop DC, Fischbein NJ, et al. Arterial spin-label imaging in patients with normal bolus perfusion-weighted MR imaging findings: pilot identification of the borderzone sign. *Radiology*. 2009;252:797–807.
13. Deibler AR, Pollock JM, Kraft RA, Tan H, Burdette JH, Maldjian JA. Arterial spin-labeling in routine clinical practice, part 1: technique and artifacts. *AJNR Am J Neuroradiol*. 2008;29:1228–1234.
14. Deibler AR, Pollock JM, Kraft RA, Tan H, Burdette JH, Maldjian JA. Arterial spin-labeling in routine clinical practice, part 2: hypoperfusion patterns. *AJNR Am J Neuroradiol*. 2008;29:1235–1241.
15. Deibler AR, Pollock JM, Kraft RA, Tan H, Burdette JH, Maldjian JA. Arterial spin-labeling in routine clinical practice, part 3: hyperperfusion patterns. *AJNR Am J Neuroradiol*. 2008;29:1428–1435.
16. Alsop DC, Detre JA. Reduced transit-time sensitivity in noninvasive magnetic resonance imaging of human cerebral blood flow. *J Cereb Blood Flow Metab*. 1996;16:1236–1249.
17. Campbell AM, Beaulieu C. Pulsed arterial spin labeling parameter optimization for an elderly population. *J Magn Reson Imaging*. 2006;23: 398–403.
18. Drayer BP, Wolfson SK, Reinmuth OM, Dujovny M, Boehnke M, Cook EE. Xenon enhanced CT for the analysis of cerebral intergrity, perfusion, and blood flow. *Stroke*. 1978;9:123–130.
19. Yonas H, Darby JM, Marks EC, Durham SR, Maxwell C. CBF measured by Xe-CT: approach to analysis and normal values. *J Cereb Blood Flow Metab*. 1991;11:716–725.
20. Johnson DW, Stringer WA, Marks MP, Yonas H, Good WF, Gur D. Stable xenon CT cerebral blood flow imaging: rationale for and role in clinical decision making. *AJNR Am J Neuroradiol*. 1991;12:201–213.
21. Puetz V, Dzialowski I, Coutts SB, Hill MD, Krol A, O'Reilly C, et al. Frequency and clinical course of stroke and transient ischemic attack patients with intracranial nonocclusive thrombus on computed tomographic angiography. *Stroke*. 2009;40:193–199.
22. Landis JR, Koch GG. The measurement of observer agreement for categorical data. *Biometrics*. 1977;33:159–174.
23. Astrup J, Siesjö BK, Symon L. Thresholds in cerebral ischemia - the ischemic penumbra. *Stroke*. 1981;12:723–725.
24. Yuh WT, Ueda T, White M, Schuster ME, Taoka T. The need for objective assessment of the new imaging techniques and understanding the expanding roles of stroke imaging. *AJNR Am J Neuroradiol*. 1999; 20:1779–1784.
25. Kucinski T, Koch C, Eckert B, Becker V, Krömer H, Heesen C, et al. Collateral circulation is an independent radiological predictor of outcome after thrombolysis in acute ischaemic stroke. *Neuroradiology*. 2003;45: 11–18.
26. Bang OY, Saver JL, Buck BH, Alger JR, Starkman S, Ovbiagele B, et al. Impact of collateral flow on tissue fate in acute ischaemic stroke. *J Neurol Neurosurg Psychiatry*. 2008;79:625–629.
27. Liebeskind DS. Collaterals in acute stroke: beyond the clot. *Neuroimaging Clin North Am.* 2005;15:553–573, x.
28. Ye FQ, Berman KF, Ellmore T, Esposito G, van Horn JD, Yang Y, et al. H(2)(15)O PET validation of steady-state arterial spin tagging cerebral blood flow measurements in humans. *Magn Reson Med*. 2000;44: 450–456.
29. Calamante F, Ganesan V, Kirkham FJ, Jan W, Chong WK, Gadian DG, et al. MR perfusion imaging in Moyamoya Syndrome: potential implications for clinical evaluation of occlusive cerebrovascular disease. *Stroke*. 2001;32:2810–2816.
30. Wolf RL, Alsop DC, McGarvey ML, Maldjian JA, Wang J, Detre JA. Susceptibility contrast and arterial spin labeled perfusion MRI in cerebrovascular disease. *J Neuroimaging*. 2003;13:17–27.
31. Chalela JA, Alsop DC, Gonzalez-Atavales JB, Maldjian JA, Kasner SE, Detre JA. Magnetic resonance perfusion imaging in acute ischemic stroke using continuous arterial spin labeling. *Stroke*. 2000;31:680–687.
32. Hendrikse J, van Osch MJ, Rutgers DR, Bakker CJ, Kappelle LJ, Golay X, et al. Internal carotid artery occlusion assessed at pulsed arterial spin-labeling perfusion MR imaging at multiple delay times. *Radiology*. 2004;233:899–904.

33. Petersen ET, Lim T, Golay X. Model-free arterial spin labeling quantification approach for perfusion MRI. *Magn Reson Med*. 2006;55: 219–232.
34. MacIntosh BJ, Pattinson KT, Gallichan D, Ahmad I, Miller KL, Feinberg DA, et al. Measuring the effects of remifentanil on cerebral blood flow and arterial arrival time using 3D GRASE MRI with pulsed arterial spin labelling. *J Cereb Blood Flow Metab*. 2008;28:1514–1522.
35. Xie J, Gallichan D, Gunn RN, Jezzard P. Optimal design of pulsed arterial spin labeling MRI experiments. *Magn Reson Med*. 2008;59:826–834.
36. Chng SM, Petersen ET, Zimine I, Sitoh YY, Lim CC, Golay X. Territorial arterial spin labeling in the assessment of collateral circulation: comparison with digital subtraction angiography. *Stroke*. 2008;39: 3248–3254.
37. Derdeyn CP, Yundt KD, Videen TO, Carpenter DA, Grubb RL Jr, Powers WJ. Increased oxygen extraction fraction is associated with prior ischemic events in patients with carotid occlusion. *Stroke*. 1998;29:754–758.
38. Powers WJ, Press GA, Grubb RL Jr, Gado M, Raichle ME. The effect of hemodynamically significant carotid artery disease on the hemodynamic status of the cerebral circulation. *Ann Intern Med*. 1987;106:27–34.
39. Zaharchuk G, Bammer R, Straka M, Newbould RD, Rosenberg J, Olivot JM, et al. Improving dynamic susceptibility contrast MRI measurement of quantitative cerebral blood flow using corrections for partial volume and nonlinear contrast relaxivity: A xenon computed tomographic comparative study. *J Magn Reson Imaging*. 2009;30:743–752.
40. Wu O, Østergaard L, Weisskoff RM, Benner T, Rosen BR, Sorensen AG. Tracer arrival timing-insensitive technique for estimating flow in MR perfusion-weighted imaging using singular value decomposition with a block-circulant deconvolution matrix. *Magn Reson Med*. 2003;50: 164–174.
41. Calamante F, Gadian DG, Connelly A. Delay and dispersion effects in dynamic susceptibility contrast MRI: simulations using singular value decomposition. *Magn Reson Med*. 2000;44:466–473.
42. Christensen S, Calamante F, Hjort N, Wu O, Blankholm AD, Desmond P, et al. Inferring origin of vascular supply from tracer arrival timing patterns using bolus tracking MRI. *J Magn Reson Imaging*. 2008;27: 1371–1381.
43. Zaharchuk G, Ledden PJ, Kwong KK, Reese TG, Rosen BR, Wald LL. Multislice perfusion and perfusion territory imaging in humans with separate label and image coils. *Magn Reson Med*. 1999;41:1093–1098.
44. Hendrikse J, van der Grond J, Lu H, van Zijl PC, Golay X. Flow territory mapping of the cerebral arteries with regional perfusion MRI. *Stroke*. 2004;35:882–887.
45. Wong EC. Vessel-encoded arterial spin-labeling using pseudocontinuous tagging. *Magn Reson Med*. 2007;58:1086–1091.